



MONASH University

Modelling interactions of novel anti-cancer therapeutics with DNA

Gwee Shu Hui Eunice

School of Chemistry

Faculty of Science

A thesis submitted for the degree of Doctor of Philosophy at

Monash University in 2021

Contents

Copyright notice	xi
Abstract	xiii
Declaration	xvii
Acknowledgements	xix
Abbreviations	xxi
1 Introduction	1
1.1 What is DNA?	1
1.2 Platinum-Based Anti-Cancer Drugs	2
1.3 Methods used to study biological systems and binding events	6
1.4 RNA: A possible drug target?	15
1.5 Overview	16
1.6 References	19
2 Selecting the appropriate level of theory to study the Infrared Spectra of Pt complexes	37
2.1 Introduction	37
2.2 Influence of DFT Functionals and Solvation Models on the Prediction of Far-Infrared Spectra of Pt-Based Anticancer Drugs: Why Do Different Complexes Require Different Levels of Theory?	39
3 Effects of explicit solvation on the hydrolysis mechanism of the Pt complexes.	55
3.1 Introduction	55
3.2 Theoretical Procedures	63
3.3 Results and Discussion	68
3.4 Conclusions	83
3.5 References	85
4 Effects of fragmentation schemes and solvation model on geometries of DNA building blocks	97
4.1 Introduction	97
4.2 Theoretical Procedures	109

4.3	Influence of Fragmentation schemes and Solvation Models	113
4.4	Conclusions	133
4.5	References	137
5	Interactions between Pt-complexes and DNA/RNA building blocks	145
5.1	Introduction	145
5.2	Theoretical Procedures	155
5.3	Results and Discussion	161
5.4	Conclusion	201
5.5	References	205
6	Conclusions	219
6.1	Future Works	223
	Appendices	225
A	Additional stuff	227
A.1	Selecting the appropriate level of theory to study the Infrared Spectra of Pt complexes - Supporting Information	227
A.2	Selecting the appropriate level of theory to study the Infrared Spectra of Pt complexes - Supporting Information	228

List of Figures

1.1	Pt-based anti-cancer drugs: cisplatin (A), carboplatin (B), oxaliplatin (C) and nedaplatin (D).	2
1.2	DNA replication fork.	3
1.3	Hydrolysis mechanism of cisplatin to form either the mono- or di-aquated equivalent. ^{26,35–37}	5
1.4	Jacob's ladder: A categorisation of DFT functionals.	7
1.5	Schematic of Fragment Molecular Orbital Theory.	11
3.1	Hydrolysis of cisplatin, resulting in either the mono- (left) or di-aquated (right) complexes.	56
3.2	Examples of anti-cancer Pt-based complexes with decreased hydrolysis. ¹¹ . . .	57
3.3	Models of cisplatin (top left), carboplatin (top right), oxaliplatin (bottom left) and nedaplatin (bottom right) solvated with explicit water molecules. The Pt metal ion is shown in red and explicit water molecules in white.	64
3.4	Dissociation reaction involving Pt metal from the WCCR10 benchmark set. Experimental dissociation energies are given under each reaction in kJ mol^{-1} . ^{31,79,80}	65
3.5	Step-wise hydrolysis and di-hydrolysis processes for cisplatin (1) and carboplatin (2).	67
3.6	Relaxed scans of the first step of hydrolysis of cisplatin (blue), carboplatin (orange), oxaliplatin (green) and nedaplatin (pink).	69
3.7	Box and whiskers plot of Hydrogen bonding between water molecules and leaving groups at either equilibrium or at 1 Å away. The length of the box plot indicates the spread of the H bonding between the water molecules and the leaving groups.	72
3.8	Relaxed scans of first and second step of hydrolysis and di-hydrolysis of cisplatin, carboplatin, oxaliplatin and nedaplatin.	73
3.9	Charges of water molecule within a 4 Å radius of either the Pt metal ion or the leaving group.	77
3.10	Energy profile diagram of hydrolysis of cisplatin.	82
4.1	3 different modes of fragmentation explored by Komeiji <i>et al.</i> ⁴⁸	106

4.2	The two different fragmentation modes that were investigated in this study. The bond fragmentation occurs about the bond highlighted in black and the bond detached atom (BDA) is highlighted in orange, whereas the bond attached atom (BAA) is highlighted in blue.	107
4.3	Single and double stranded models.	110
4.4	Scheme used to compare the optimised geometries. The arrows indicate the comparison between the re-optimised geometries with the original full system calculations.	113
4.5	Comparison of the dGMP optimised geometries between full system optimisations (blue) and Fragmentation scheme II (white) using the PBE-D3 functional and SMD solvation model.	116
4.6	Optimised geometries of dGMP and dAMP between full system (blue) and FMO (white) optimisations with Fragmentation scheme II and SMD solvation model.	117
4.7	Optimised geometries of dGMP from full system (left) or Fragmentation scheme II (right) optimisations. Dashed lines show distances from C-H on guanine to O on phosphate.	118
4.8	Dihedral angles between phosphate-sugar (left) and base-sugar (right) used in analysis.	118
4.9	Optimised geometries of d(GpG) using full system optimisation (grey) and Fragmentation scheme II optimisation (pink) in gas phase.	122
4.10	Tilt angle between the two Guanine units in the stacked d(GpG) model.	123
4.11	π - π stacking between the two guanine units in the d(GpG) structure optimised with Fragmentation scheme II and the PBE functional in the gas phase.	124
4.12	Optimised geometries of the double stranded dGMP-dCMP model optimised as the full system (grey) and Fragmentation scheme I (pink) with CPCM solvation model and either PBE-D3 (left) or SRS-MP2 (right).	129
4.13	Bonding distances in the dGMP-dCMP model.	129
4.14	Mean absolute deviation between the optimised geometries obtained from both full system and FMO calculations to previously published experimental data.[72]	131
4.15	Difference in optimised geometries between full system optimisation (pink) and Fragmentation scheme I optimisation (blue).	133
5.1	Mono- and di-aquated complexes of cisplatin. ⁴	146
5.2	Oxaliplatin, oxalato-(1,2-cyclohexanediamine)Pt(II), a Pt-based anti-cancer drug with oxalate as the leaving group. ^{3,8,9}	147
5.3	Binding mode of fully dissociated cisplatin (left) and oxaliplatin (right) to dGMP.	148
5.4	Different RNA conformations formed with Watson.	149
5.5	Activated forms of Pt drugs considered in the study.	156
5.6	DNA and RNA building blocks	157
5.7	Dissociation reactions used for benchmarking purposes. The numbers represents previously published experimental values in kJ mol ⁻¹	158

5.8	Starting geometries of cisplatin in its various aquated state with dGMP	158
5.9	Schematic explaining the calculation of interaction energy between the activated form of Pt-based drug (blue) and the building block (pink).	160
5.10	Interaction energy of activated cisplatin with either dGMP, GMP, dAMP or AMP.	162
5.11	Electrostatic and correlation components to the interaction between activated cisplatin with either dGMP or GMP.	163
5.12	Interaction of <i>CPPT</i> -1 with dGMP (left) or GMP (right).	165
5.13	Optimised structures of activated mono-aquated complex of cisplatin with dGMP (left) and GMP (right).	166
5.14	Optimised structures of activated di-aquated complex of cisplatin with dGMP (left) and GMP (right).	167
5.15	HOMO-LUMO gaps (eV) of the Pt-building blocks as calculated with SRS-MP2 and ω B97X-D3.	168
5.16	Root mean square deviation of either dGMP or GMP before and after binding event.	169
5.17	Difference in geometries of dGMP (left) and GMP (right) before (pink) and after (blue) binding to <i>CPPT</i> -1.	170
5.18	Deformation energy (kJ mol^{-1}) of either dGMP or GMP due to the binding of Pt complex.	171
5.19	Electrostatic and correlation components to interaction energy in complexes between activated forms of cisplatin and dAMP/AMP.	172
5.20	Optimised structures of complexes between <i>CPPT</i> -1, <i>CPPT</i> -2 and <i>CPPT</i> -3 and dAMP or AMP.	174
5.21	HOMO-LUMO (eV) gap of dAMP and AMP calculated with SRS-MP2 and ω B97X-D3.	175
5.22	Root mean square deviation of either dAMP or AMP before and after binding event.	176
5.23	Deformation energy (kJ mol^{-1}) of dAMP and AMP upon binding to the activated forms of cisplatin.	177
5.24	Difference in geometry of dAMP (left) and AMP (right) before (pink) and after (blue) binding of <i>CPPT</i> -1 with Conf3 of AMP/dAMP.	177
5.25	Comparison of interaction energies and Gibbs free energies of solvation (ΔG_{soln} (kJ mol^{-1})) of activated forms of cisplatin (<i>CPPT</i> -1, <i>CPPT</i> -2 and <i>CPPT</i> -3) with dGMP, GMP, dAMP and AMP.	179
5.26	Interaction energies of activated forms of oxaliplatin with dGMP, GMP, dAMP and AMP	180
5.27	Electrostatic and correlation components to the interaction between activated oxaliplatin with either dGMP or GMP.	181
5.28	Optimised structures of <i>OXPT</i> -1 with dGMP (left) and GMP (right).	183
5.29	Optimised structures of <i>OXPT</i> -1 and dGMP building block. Conf1 (left) and Conf3 (right)	183

5.30	Optimised structures of dGMP or GMP with <i>OXPT</i> -2.	184
5.31	Optimised structures of dGMP or GMP with <i>OXPT</i> -3.	185
5.32	HOMO-LUMO (eV) gap of dGMP and GMP calculated with SRS-MP2 and ω B97X-D3.	186
5.33	RMSD values of dGMP and GMP building blocks after binding to either <i>OXPT</i> -1, <i>OXPT</i> -2 or <i>OXPT</i> -3.	187
5.34	Deformation energies (kJ mol ⁻¹) of the dGMP and GMP building after binding to either <i>OXPT</i> -1, <i>OXPT</i> -2 or <i>OXPT</i> -3.	188
5.35	Geometric changes of dGMP (left) and GMP (right) before (pink) and after (blue) binding to <i>OXPT</i> -1.	189
5.36	Geometric changes of GMP after interacting with Conf2 (left) and Conf3 (right) of <i>OXPT</i> -1. The structure in pink and blue are before and after binding to <i>OXPT</i> -1, respectively.	189
5.37	Electrostatic and correlation components to the interaction between oxaliplatin with either dAMP or AMP.	190
5.38	Optimised structures between <i>OXPT</i> -1 and dAMP (left) and AMP (right). . .	192
5.39	Visual geometric changes in dAMP (left) and AMP (right) before (pink) and after (blue) binding to <i>OXPT</i> -1	193
5.40	Optimised structures of dAMP and AMP with <i>OXPT</i> -2	193
5.41	Optimised structures of dAMP and AMP with <i>OXPT</i> -3	194
5.42	HOMO-LUMO (eV) gaps of dAMP and AMP calculated with SRS-MP2 and ω B97X-D3.	195
5.43	RMSD values of dAMP and AMP building blocks after binding to <i>OXPT</i> -1, <i>OXPT</i> -2 and <i>OXPT</i> -3.	196
5.44	Deformation energies (kJ mol ⁻¹) of the dAMP and AMP building block after binding to either <i>OXPT</i> -1, <i>OXPT</i> -2 or <i>OXPT</i> -3.	197
5.45	Interaction energies and Gibbs free energies of solvation (ΔG_{solv} , kJ mol ⁻¹) of complexes between activated forms of oxaliplatin (<i>OXPT</i> -1, <i>OXPT</i> -2 and <i>OXPT</i> -3) and dGMP, GMP, dAMP or AMP.	198
5.46	Strongest interaction energies calculated between DNA/RNA building blocks and activated forms of cisplatin and oxaliplatin.	199
5.47	RMSD values of DNA/RNA building blocks after interacting with activated forms of cisplatin and oxaliplatin.	200

List of Tables

3.1	Raw errors (in kJ mol^{-1}) of M06-2X and ω B97XD with varying Dunning's basis sets on VDZ- and VTZ-optimised complexes. Opt represents geometry optimisation calculations. SP represents single point energy calculation on a given optimised geometry.	66
3.2	ChelpG partial atomic charges of cisplatin, carboplatin, oxaliplatin and nedaplatin in their equilibrium geometries optimised using implicit (CPCM) and explicit solvation approaches.	70
3.3	ChelpG partial atomic charges of cisplatin, carboplatin, oxaliplatin and nedaplatin optimised with the Pt-Cl/Pt-O bonds fixed at 2 Å within the explicit solvation approach.	79
3.4	Comparison of ΔG_{solv} calculated using the thermodynamic cycle and implicit solvation and ΔE_{solv} calculated from the relaxed scans. All values are given in kJ mol^{-1}	80
4.1	Energy differences (kJ mol^{-1}) of deoxyguanosine monophosphate (dGMP) and deoxyadenosine monophosphate (dAMP) between full system and FMO calculations.	114
4.2	RMSD values (in Å) of geometries optimised with Fragmentation schemes I and II.	116
4.3	Energy differences (kJ mol^{-1}) of d(GpG) between full system and FMO optimisations.	119
4.4	Differences in electrostatic (HF energy) and dispersion (correlation energy) components (kJ mol^{-1}) of optimised geometries of d(GpG).	120
4.5	RMSD values (in Å) of d(GpG) FMO optimised geometries compared to full system optimisations.	121
4.6	Tilt ($^{\circ}$) between guanine bases in d(GpG).	123
4.7	Inter-base distance (Å) between the two guanine bases in d(GpG).	124
4.8	Total energy differences (ΔE , kJ mol^{-1}) and differences in electrostatic and dispersion components (kJ mol^{-1}) of FMO-optimised d(GpG) model. All comparisons are made with respect to full system optimisations.	125
4.9	Energy differences (kJ mol^{-1}) between full system and FMO optimisations in the double stranded (G-C) model.	126
4.10	RMSD values (in Å) of double stranded (G-C) geometries obtained using FMO as compared to the full system optimisation.	126

4.11	Differences in electrostatic (HF) and dispersion (Corr) components (in kJ mol^{-1}) of the double stranded (G-C) system as compared to full system optimisations	128
4.12	Total energy differences (ΔE , kJ mol^{-1}) and differences in electrostatic and dispersion components (kJ mol^{-1}) of FMO-optimised dGMP-dCMP model. All comparisons are made with respect to full system optimisations.	132
5.1	Pt-N7 distance (\AA) between activated cisplatin and dGMP or GMP building blocks. Values in brackets indicate the absolute deviation from previously published Pt-N7 distance (1.992 \AA). ⁸⁶	164
5.2	Differences in predicted HOMO-LUMO gaps (eV) between SRS-MP2 and ω B97X-D3.	168
5.3	Pt-N7 distances (in \AA) between the activated forms of cisplatin and dAMP/AMP building block. Values in brackets indicate the absolute deviation from the previously published Pt-N7 distance of 2.010 \AA . ^{61,105}	173
5.4	Difference in predicted HOMO-LUMO gap (eV) between SRS-MP2 and ω B97X-D3	175
5.5	Pt-N7 distances (\AA) between activated forms of oxaliplatin and dGMP/GMP building block. Values in brackets indicate the absolute deviation from the previously reported Pt-N7 distance (1.992 \AA). ⁸⁶	182
5.6	Difference in the predicted HOMO-LUMO gaps (eV) between SRS-MP2 and ω B97X-D3	186
5.7	Pt-N7 distance (\AA) between activated oxaliplatin and dAMP or AMP building blocks. Values in brackets indicate the absolute deviation from the experimental value of 2.010 \AA . ^{61,105}	191
5.8	Differences in predicted HOMO-LUMO gap (eV) as calculated with SRS-MP2 and ω B97X-D3	195

Copyright notice

© Gwee Shu Hui Eunice (2021).

I certify that I have made all reasonable efforts to secure copyright permissions for third-party content included in this thesis and have not knowingly added copyright content to my work without the owner's permission.

Abstract

Platinum-based complexes, such as cisplatin, carboplatin, oxaliplatin and nedaplatin, have been utilised as one of the main drug classes to combat cancer. It has been suggested that these Pt-complexes produce their activated form after hydrolysis when they enter the cell cytoplasm. The hydrolysis occurs by replacing leaving groups with either one or two water molecules, to form its mono- or di-aquated species. The activated form of the complex exhibits cytotoxic characteristics as it binds to DNA, disrupting the replication process and resulting in apoptosis. However, the use of these complexes are accompanied with side effects, which lead to the motivation to design Pt-based complexes with higher cytotoxicity and lower toxicity. To achieve that, it is vital to understand the mechanism of hydrolysis and the identity of the activated form of the currently used Pt-complexes. Despite the numerous experimental studies conducted since its discovery, there is a lack of consensus on the specific activated form, with kinetic studies and in vitro studies supporting either the mono- or di-aquated species to be the active form. Computational chemistry studies have been hindered due to the presence of the Pt metal ion and dative bonds between Pt and leaving ligands. With the ability of Pt to exist in different electronic states and presence of relativistic effects, reliable computational chemistry methods are yet to be identified before further advances can be achieved

Density Functional Theory (DFT) has been shown to be a reliable approach to study both biomolecules and enzymes containing transition metals. Previously conducted studies have demonstrated their ability to accurately predict the characteristic bands of cisplatin in the far-infrared region. In order to assess the effect of leaving groups on the hydrolysis, a systematic study was conducted in this work to examine four factors affecting the prediction of characteristic bands in far IR of cisplatin and carboplatin - DFT functionals, basis sets, effective core potentials and solvation models. It was determined that different functionals were required

for the two complexes due to the different extent of charge transfer between the Pt ion and leaving ligands.

The effect of explicit solvation on the mechanism of hydrolysis of Pt complexes was additionally investigated. Using the relaxed scan approach, the energy barriers of the Pt complexes were determined and compared to experimental data. Compared to implicit solvation models, the inclusion of explicit solvation better reproduces the energy barrier, indicating the importance of explicit solvation to study the hydrolysis mechanism of such complexes. Two transition states corresponding to the replacement of each chloride anion with a water molecule were also located using explicit solvation. Thus obtained reaction barriers were compared to those from the relaxed scan also performed in explicit solvation. It was revealed that former was able to better replicate experimental trends, whereas the relaxed scans tended to overestimate these barriers. Overall, explicit solvation as shown to be critical in establishing reliable mechanisms of hydrolysis in Pt-based complexes.

Due to the large size of biomolecules, there is a need to identify a reliable computational chemistry method with reduced computational cost and chemical accuracy. Fragment Molecular Orbital (FMO) is able to divide large molecules into smaller fragments by breaking covalent bonds and calculating them in parallel. The energy of each individual fragment is calculated in the Coulomb bath of the entire system. The total energy of the system is determined by summing the energies of all fragments together with two- and three-body interactions. The geometries of DNA models obtained using the conventional full system optimisations were compared to those obtained using various fragmentations scheme within the FMO framework. Previously, only gas phase tests were performed on similar models. Here the effects of different methods (PBE, PBE-D3 and SRS-MP2) and implicit solvation models (CPCM and SMD) were studied. Depending on the fragmentation type, different geometries were obtained between FMO and full system optimisations, highlighting the importance of interfacing implicit solute-solvent interactions within the FMO framework. These interactions were also found to depend on the level of theory used suggesting that different parametrisation might be required for such implementation for each level of theory.

The interactions between Pt-drugs and DNA/RNA building blocks were also studied with the view of identifying the effect of hydrolysis in the Pt complexes on the mechanism of

binding. The mode of interaction of non- ($[\text{PtL}]^{2+}$), mono- ($[\text{PtL}(\text{H}_2\text{O})]^{2+}$) and di-aquated ($[\text{PtL}(\text{H}_2\text{O})_2]^{2+}$) species of cisplatin and oxaliplatin (where L is either two ammonia for cisplatin or 1,2-diaminocyclohexane for oxaliplatin) were modelled with deoxyguanosine monophosphate (dGMP), deoxyadenosine monophosphate (dAMP), guanosine monophosphate (GMP) and adenosine monophosphate (AMP). It has been recently suggested that cisplatin is able to interact with RNA building blocks, binding to either guanine or adenine units. The interaction energies between the three types of the potential active form of Pt complexes and DNA/RNA building blocks were analysed. The fully dissociated and non-aquated form of the $[\text{PtL}]^{2+}$ type were determined to interact the strongest. This is in good agreement with the previously published X-ray crystal structure, where the non-aquated form of the drug was found to interact with the nucleobase on DNA. Both mono-aquated equivalent of cisplatin and oxaliplatin have also demonstrated to be able to interact and form the vital Pt-N7 bond with the DNA and RNA building blocks, suggesting that they might be precursors complexes before losing the water molecule and forming a stronger bond between the Pt complex and the building block. The presence of two water molecules on the Pt^{2+} centre were identified to form H-bonding with the phosphate of the DNA/RNA model, inhibiting the interaction between the Pt ion and the N7 centre of the nucleobase. The interaction energies also revealed that the fully dissociated cisplatin interacts stronger than the fully dissociated oxaliplatin. However, larger DNA/RNA models need to be studied to better understand the relationship between the strength and mode of interaction between active forms of Pt-complexes and their effects on DNA and RNA.

Declaration

I hereby declare that this thesis contains no material which has been accepted for the award of any other degree or diploma at any university or equivalent institution and that, to the best of my knowledge and belief, this thesis contains no material previously published or written by another person, except where due reference is made in the text of the thesis.

This thesis includes one original paper published in peer reviewed journal. The core theme of the thesis is model the interactions between Pt anti-cancer drugs and DNA/RNA models. The ideas, development and writing up of all the papers in the thesis were the principal responsibility of myself, the student, working within the Faculty of Science graduate research programme under the supervision of A/Prof. Ekaterina I. Izgorodina and Prof. Bayden R. Wood.

The inclusion of co-authors reflects the fact that the work came from active collaboration between researchers and acknowledges input into team-based research.

In the case of chapter two, my contribution to the work involved the following:

LIST OF TABLES

Thesis chapter	Publication title	Status (published, in press, accepted or returned for revision)	Nature and % of student contribution	Co-author name(s), nature and % of co-author's contribution	Co-author(s), Monash student Y/N
2	Influence of DFT Functionals and Solvation Models on the Prediction of Far-Infrared Spectra of Pt-Based Anti-cancer Drugs: Why Do Different Complexes Require Different Levels of Theory?	Published	75% - Data collection, analysis and manuscript	1. Zoe L. Seeger - Analysis - 5%; 2. Dominique Appadoo - Data collection - 5%; 3. Bayden R. Wood - Supervision - 5%; 4. Ekaterina I. Izgorodina - Supervision, concept and editing - 10%	Y, N, N, N

I have / have not renumbered sections of submitted or published papers in order to generate a consistent presentation within the thesis.

Student name: Gwee Shu Hui Eunice

Student signature:

Date:

Supervisor name:

Supervisor signature:

Date:

Acknowledgements

To the Family A 'thank you' will never be able to convey my gratitude. The support and patience I've received from you is unparalleled and I would never have gotten this far without you. Thank you for putting up with my frustrations and wilfulness. I no longer have an excuse for my bad temper. You have your daughter and your sister back. To my grandfather. Thank you for believing in me. I hope I made you proud.

To the Friends My F4Ls, Yooyoung, Weihui, Yueshi, Leow, Keith and Tak. Thank you for always picking up the phone and letting me vent, no matter how late it is. Thank you Keith and Leow for spoiling me so. Emma, Yanling and Peggy. My safety net. You guys are always there to catch me and be my constants. To RD, thank you for watching over me. My JJBs. The friends that embarked on the same journey in different locations. We did it! To Miggy and Jess. The most amazing housemates that one could ask for. We've made it through the trial of fire. To Geena, my absolute constant in life. Your love and support is unparalleled. To Caesar, you are the best work/couch buddy. Your warmth and love is definitely a blessing. To the le douche. You made this year significantly more bearable. Thank you for being so understanding and may our dreams become reality. And to everyone else who came along for the journey. Thank you.

To the Pas and Wood Group The people that maintained my sanity and made this experience so enjoyable. You guys made me want to go to the office everyday and made the late nights less gruelling. The mid day coffee breaks and the food runs are memories that I hold very close to my heart. To Zoe, Nicole, Fi, Tom, Kaycee, Ivan and Anh, thank you for aiding me so along the way. To Abhi, Su and Sam, thank you for being so reassuring. There is always a light at the end of the tunnel. To Peter, Luke and Michael, thank you for being office buddies. To Nathan,

coffee buddies for life. To Miggy, Liz, Zack, Kamila, David, Khansa and Supti, thank you for helping me out with all my spectroscopy needs!

To the Supervisors It has been a great honor to work with you. Its definitely been a journey of ups and downs but I'm glad that I have the two of you to guide me along the way. To Katya and Bayden, I've learnt so much from the two of us over the years and it was an absolute pleasure.

To everyone who did not believe in me Thank you for the negativity. And where are you now?

To You You've got to the end. Despite all the doubts over the years, you got to the end. Remember the moments of imposter syndrome. Remember the numerous tears. Remember the days and nights where you were so close to throwing in the towel. Remember all those struggles. You never thought this journey was so arduous and demanded so much. But you've got to the end. Believe in yourself and your ability to work hard. When you pull this thesis off your shelf, remember how resilient you were and you are capable of more than you think.

Abbreviations

^1H - ^{15}N HSQC	^1H - ^{15}N heteronuclear single quantum coherence
A	Adenine
AFO	Adaptive Frozen Orbital
AMP	Adenosine Monophosphate
ATR-FTIR	Attenuated Total Reflection Fourier Transform Infrared
BAA	Bond Attached Atom
BBD	Branch-Bulge Domain
BDA	Bond Detached Atom
BDE	Bond Dissociation Energy
BSSE	Basis Set Superposition Error
C	Cytosine
CBS	Complete Basis Set
CCSD(T)	Coupled Cluster With Single, Double and Perturbative Triple Excitations
CDM	Continuum Dielectric Model
ChelpG	Charges From Electrostatic Potentials Using A Grid-Based Method
COSMO	Conductor-like Screening Solvation Model
CP	Counterpoise
CPCM	Car-Parrinello Molecular Dynamics
CPMD	Continuum Dielectric Model
dAMP	Deoxyadenosine Monophosphate
dCMP	Deoxycytosine Monophosphate
dGMP	Deoxyguanosine Monophosphate
DNA	Deoxyribonucleic Acid

DFT	Density Functional Theory
DFT-D	Dispersion Corrected DFT functional
DFT-D3	DFT-D Version Three
ECP	Effective Core Potential
ERs	Estrogen Receptors
FMO	Fragment Molecular Orbital
G	Guanine
GAMESS-US	General Atomic And Molecular Electronic Structure Systems
GGA	Generalised Gradient Approximation
GMP	Guanosine Monophosphate
HF	Hartree-Fock
HOMO	Highest Occupied Molecular Orbital
HPLC	High Pressure Liquid Chromatography
HOP	Hybrid Operator Projection
IR	Infrared
IEFPCM	Integral Equation Formalism Polarisable Continuum Model
ICP-MS	Inductively Coupled Plasma Mass Spectrometry
LBD	Ligand Binding Domain
LG	Leaving Group
IFIE	Inter-Fragment Interaction Energy
LSDA	Local Spin-Density Approximation
LUMO	Lowest Unoccupied Molecular Orbital
MAD	Mean Absolute Deviation
MD	Molecular Dynamics
MEP	Molecular Electrostatic Potential
MM	Molecular Mechanics
MP2	Second Order Moller-Plesset Perturbation Theory
mRNA	Messenger Ribonucleic Acid
NMR	Nuclear Magnetic Resonance
PCM	Polarisable Continuum Model

PrP	Prion Protein
QM	Quantum Mechanics
RAL	Raloxifene
RBA	Relative Binding Affinities
RIXS	In Situ Inelastic X-ray Scattering
RMSD	Root Mean Square Deviation
RNA	Ribonucleic Acid
rRNA	Ribosomal Ribonucleic Acid
SCRF	Self-Consistent Reaction Field
SMD	Solvent Model Based On Density
SCS-MP2	Generalised Spin-Component Scaled MP2
SRS-MP2	Generalised Spin-Ratio Scaled MP2
T	Thymine
TAM	Tamoxifen
TMs	Transition Metals
tRNA	Transport Ribonucleic Acid
TST	Transition State Theory
U	Uracil
UBF	Upstream Binding Factor
UEG	Uniform Electron Gas
VDZ	Correlation-Consistent Polarized Double Zeta
VTZ	Correlation-Consistent Polarized Triple Zeta
VQZ	Correlation-Consistent Polarized Quadruple Zeta
ZPVE	Zero Point Vibrational Energy

Chapter 1

Introduction

1.1 What is DNA?

Deoxyribonucleic acid (DNA), one of the building blocks of life, is essential for a myriad of biological functions. DNA has been the one of the main focal drug targets since its structure has been determined by Watson and Crick, with the help of Rosalind Franklin.¹⁻⁵ Consisting of 4 bases, guanine (G), adenine (A), cytosine (C) and thymine (T), phosphate and a deoxyribose, DNA is known to contain genetic information due to the irregularity of base sequencing.^{1,4,6-8} DNA consists of two helix strands with a phosphodiester backbone, with the bases positioned on the inside of the helix.^{1,9} The bases, exhibiting a complementary nature where G will bind to C and A will bind to T, maintain the double helix structure via a network of hydrogen bonding between the purines and pyrimidines.^{1,4}

DNA is very robust and able to exist in various different conformations, with A-, B- and Z-DNA known to be the three biologically relevant conformations of DNA, the former two consisting of a right-handed helix and the latter consisting of a left-hand helix.¹⁰ The difference in conformations arises from changing conditions: base composition, water concentration and presence of counter ions.¹¹⁻¹⁵ It has been established that B-DNA is able to undergo conformational changes to form A-DNA when the concentration of water decreases below 75%.^{11,16} The transformation in conformation is the result of the interaction of water with either the base or phosphate groups present in DNA.^{11,17,18} It has been established that A-DNA has a

large major groove and a narrow minor groove, with water molecules well-ordered around the phosphate groups, increasing its structural stability by bridging the phosphate groups across the major groove.^{11,17,18} B-DNA, on the other hand, is significantly more hydrated than A-DNA, with water molecules arranged in the minor groove, rich with dA-dT sequences.^{11,17,18} Higher hydration levels present in B-DNA result in additional water molecules interacting with the already present water molecules thus forming an organised matrix of water molecules. The difference in conformations due to water molecules resulted in different biological activities due to their ability to bind to specific proteins.^{11,19–22}

1.2 Platinum-Based Anti-Cancer Drugs

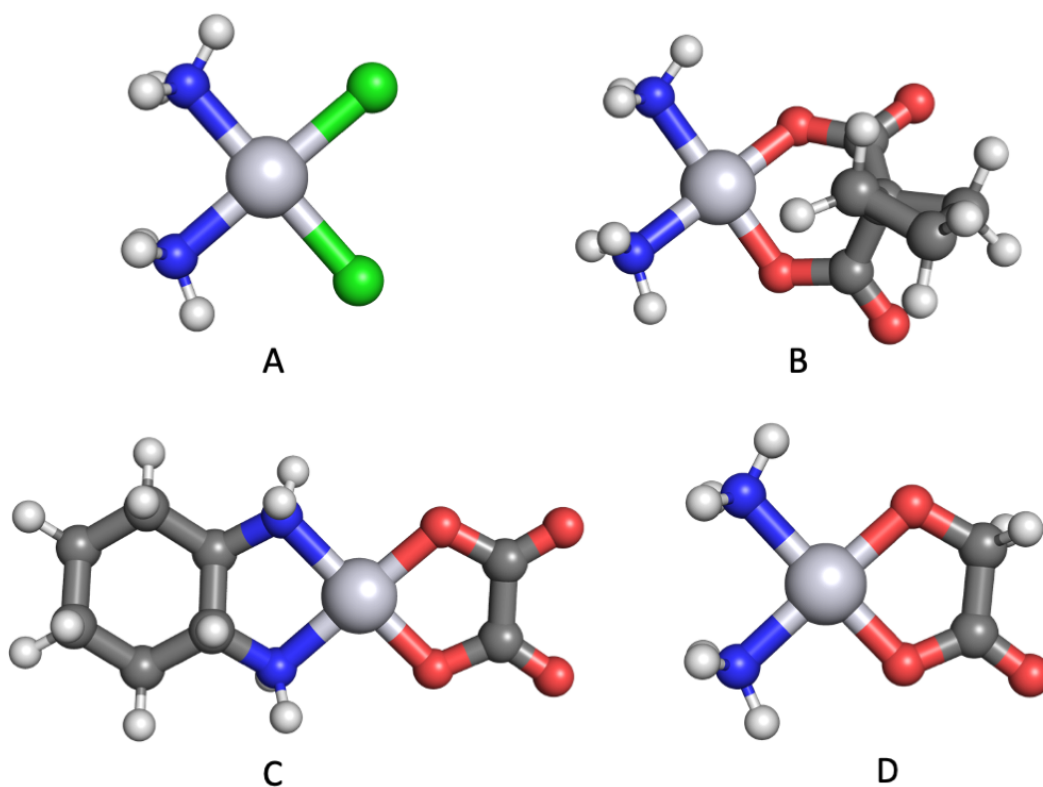


Figure 1.1: *Pt-based anti-cancer drugs: cisplatin (A), carboplatin (B), oxaliplatin (C) and nedaplatin (D).*

Platinum-based anti-cancer drugs continue to play a significant role in cancer treatment ever since their discovery more than 50 years ago.^{23–25} Cisplatin, carboplatin and oxaliplatin are the three most commonly used Pt(II) drugs during chemotherapy (Fig: 1.1).^{26–34} Nedaplatin, a

fourth generation Pt drug, is currently undergoing clinical trials (Fig: 1.1).²⁸ These Pt complexes are ideal as they are neutrally charged, which aids in diffusing the complex through the lipid bilayer before it enters the cell.³¹ In the case of cisplatin, the change in environment as it passes from the blood plasma into the cell cytoplasm encourages the loss of the chloride anion, undergoing hydrolysis to produce $cis-[Pt(NH_3)_2(H_2O)Cl]^+$ or $cis-[Pt(NH_3)_2(H_2O)_2]^{2+}$. The hydrated forms of the Pt complexes are known as the activated forms of the drugs that bind to DNA to form 1,2-intrastrand adducts.^{26,35–37} These adducts compromise the structural integrity of DNA by inducing an unwinding of the helix and bending it towards the major groove.^{26,35–38} The unwinding of the helix disrupts the DNA replication process by interfering with the progression of the replication fork in the S and G₂ phase of the cell cycle.^{26,35,39,40} The activated form of Pt drug bound to DNA delays the progress of the replication fork thus enabling the activation of other reaction pathways that lead to apoptosis (Fig: 1.2).^{41,42} An example of such reaction pathways is the activation of the p53 protein, a tumor suppressor, that inhibits DNA synthesis.^{42,43} In addition, the influx of cisplatin in the cell results in the accumulation of the p73 protein, a pro-apoptotic protein.⁴¹ The accumulation of the p73 protein promotes a mismatch repair protein dependent apoptosis.⁴¹ With these mechanisms in place, the binding of Pt-based anti-cancer drugs are able to result in the successful programmed cell death of cancer cells.^{26,35,41,42}

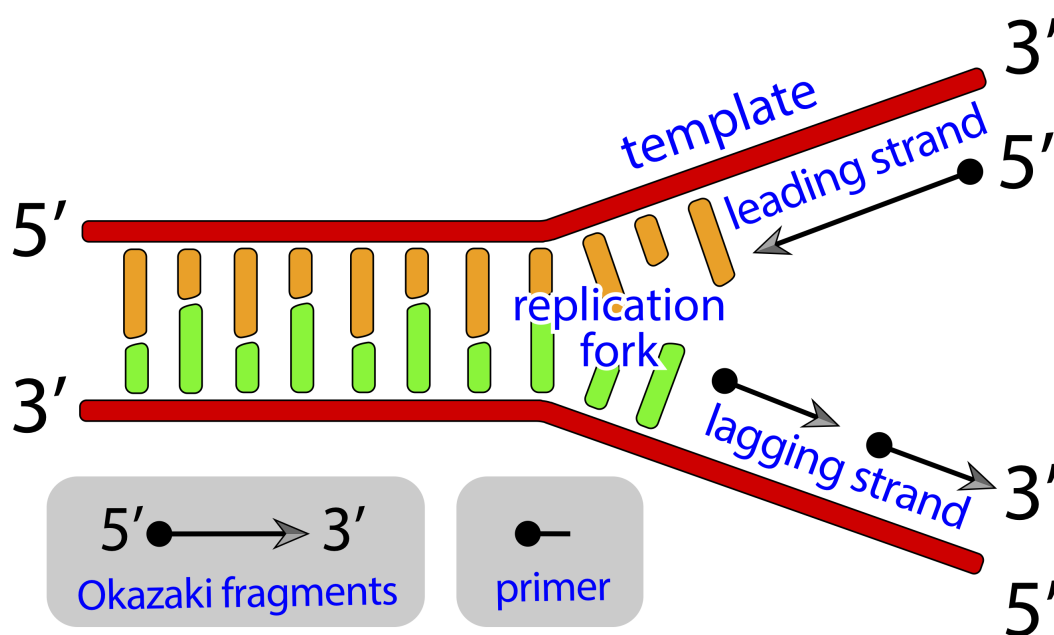


Figure 1.2: DNA replication fork.

While cisplatin is extremely effective for a variety of cancers, including ovarian, testicular and neck cancer, it is also accompanied by complications from side effects, such as nephrotoxicity and neurotoxicity, loss of hearing and resistance.^{29,30,44–49} The main mode of elimination of Pt-complexes in the human body is through urine. The accumulation of cisplatin in the kidney results is significant, with an accumulation of 720 mg after the 6th chemotherapy session of a dosage of 75 mg/m².^{30,50} A toxicity study conducted by Weiner *et al.* has demonstrated that the nephrotoxicity of cisplatin is site-specific, specifically on the outer stripe of the medulla.⁵¹ The damage caused by cisplatin is evident after 3 days, resulting in cell swelling and tubular necrosis.⁵¹ The use of cisplatin also results in the loss of hearing due to the accumulation of the Pt drug in the cochlea.⁴⁴ With the use of inductively coupled plasma mass spectrometry (ICP-MS), Cunningham *et al.* determined the accumulation of cisplatin in murine tissues and human cochleae after administration over a course of 42 days.⁴⁴ Whilst other organs, such as liver and lungs, are able to eliminate cisplatin, ICP-MS revealed the accumulation of cisplatin in the cochlea after each treatment and likely to be the cause of hearing loss.⁴⁴ The emergence of resistance is also another concern in the use of cisplatin.⁵² Davey *et al.* made use of cellular models and determined that there is a positive correlation between chemotherapy with cisplatin and accumulation of glutathione.⁵² Though not directly related to resistance, glutathione was hypothesised to participate in resistance to other drugs and radiotherapy.⁵²

Due to the adverse effects of cisplatin, carboplatin and oxaliplatin were designed to decrease the toxicity whilst maintaining their cytotoxicity.^{32,33,53,54} Interestingly, the introduction of different leaving groups also resulted in different effectiveness to treat different types of cancer.^{32,33,53,54} Replacing the Cl[−] with cyclobutanedicarboxylate and oxalate, more complicated leaving groups, to give carboplatin and oxaliplatin enables them to be more effective against ovarian and colon cancer, respectively.^{24,35,55} The introduction of different leaving groups also curbed the issue of toxicity due to the accumulation of plasma free Pt complex through the decrease of the rate of hydrolysis.^{24,35,55}

With the introduction of the relatively more stable cyclobutanedicarboxylate group, carboplatin exhibits much lower toxicity as compared to cisplatin.^{56–58} On top of demonstrating similar effectiveness to treatment of testicular cancer as cisplatin, carboplatin is also a suitable

candidate to treat bronchogenic carcinoma.^{56,59} However, a higher dosage of carboplatin is required due to the slower rate of forming adducts with DNA, approximately 45 times slower.^{34,60} Oxaliplatin, on the other hand, requires the same dosage as cisplatin and is a suitable candidate to treat melanoma and breast cancer as well, giving rise to a 33% and 20% response rate, respectively.⁶⁰ Despite the improvements, oxaliplatin induces periphery neuropathy.⁶¹ Currently, nedaplatin, an analogue of cisplatin with a 2-oxidoacetate group, is undergoing clinical trials to investigate its suitability to treat small lung and cervical cancer.^{28,62,63} The specificity to target different types of cancer suggests that the leaving groups may play more than just the role of a counter ion through altering the rate of hydrolysis (Fig: 1.1).

However, despite the multiple studies (discussed later) conducted on these Pt-based anti-cancer drugs, a clear conclusion has yet to be drawn over the activated form of the drugs: mono- or di-aquated (Fig: 1.3).^{36,64,65} The inability to arrive at a consensus on the hydrolysis pathway of the Pt complexes and the subsequent binding mechanism to DNA has motivated this study. The overall aim of this study is to gain a better understanding of the hydrolysis mechanism of the different Pt-based anti-cancer drugs. The energy barriers of the stepwise and simultaneous hydrolysis mechanisms influenced by leaving groups will be examined. This study also aims to investigate the interaction of the activated form of the Pt- based anti-cancer drugs with DNA and RNA building blocks. While it is well established that the Pt complex interacts with N7 on the nucleobase, the interactions between mono- and di-aquated complexes and nucleobases have yet to be determined. The following segments will elaborate on the previously used methods, both computational and experimentally, as well as the challenges involved in studying such complexes and reactions.

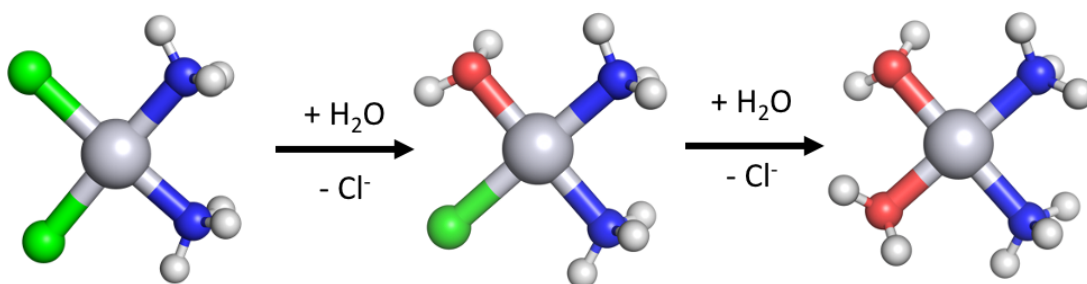


Figure 1.3: Hydrolysis mechanism of cisplatin to form either the mono- or di-aquated equivalent.^{26,35–37}

1.3 Methods used to study biological systems and binding events

1.3.1 Computational studies

1.3.2 Density Functional Theory

Density Functional Theory (DFT) is a quantum mechanical approach that utilises the electron density of a system to predict its physical and chemical properties, such as dissociation energies, vibrational spectra, ground state energies and many others.^{66,67} It has been demonstrated that DFT is a viable technique to study the properties of Pt-based anti-cancer drugs.^{36,68–74} DFT is a cheaper and equally accurate alternative to the wavefunction-based method.^{66,75} This significantly decreases computational cost compared to wavefunction-based methods which scale N^n where $n \geq 5$ with increasing system size.^{66,75} DFT is capable of determining the electronic energy of a chemical system by utilising the electronic structure theory and the Born-Oppenheimer approximation.^{66,75}

$$E_e[\rho(r)] = T[\rho(r)] + V_{en}[\rho(r)] + J[\rho(r)] + Q[\rho(r)] \quad (1.1)$$

where $T[\rho(r)]$ is the kinetic energy term describing electrons, $V_{en}[\rho(r)]$ describes the attractive energy between nuclei and electrons, $J[\rho(r)]$ and $Q[\rho(r)]$ are the terms describing electron-electron repulsion and electron-correlation energies, respectively.^{66,75} Whilst the second and third term can be solved exactly, the first and fourth terms remain the key to improve the performance of DFT functionals.^{66,75}

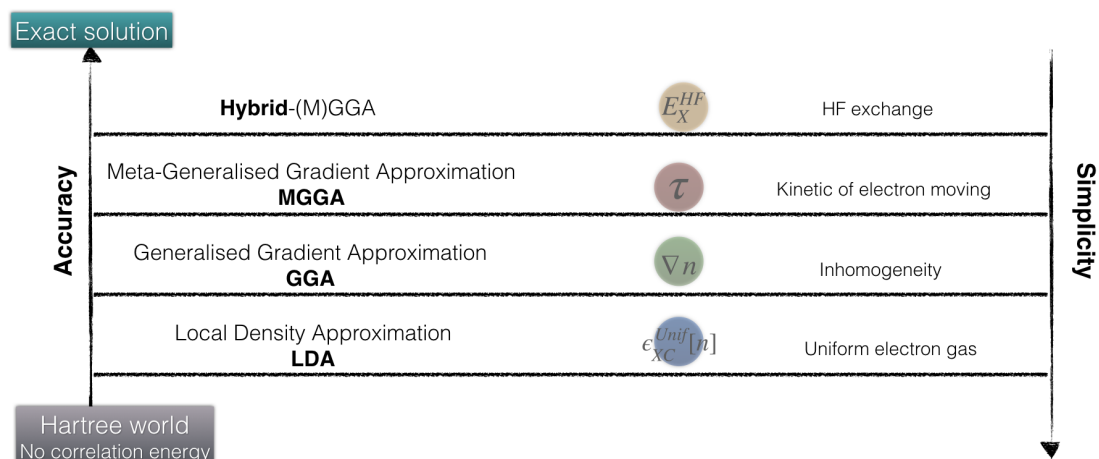


Figure 1.4: *Jacob's ladder: A categorisation of DFT functionals.*

Over time, adjustments have been made to improve the kinetic energy term and the electron-electron interaction energy.^{66,75} Gradient corrections and nonlocality have been introduced to better describe electron densities of systems.^{66,75} However, as DFT functionals cannot be improved systematically, the Jacob's ladder (Fig: 1.4) has been introduced and contains five rungs, categorising different formulations.^{66,75} The five different categories are local spin-density approximation (LSDA), generalised gradient approximation (GGA), meta-GGA, hybrid GGA and double hybrid functionals.^{66,75} Where LSDA is exact for the uniform electron gas (UEG), it is not reliable to describe chemical systems.^{66,75} GGA, on the other hand, makes use of both the function and gradient of electron density to describe the exchange-correlation energy, making it more flexible to describe chemical bonds.^{66,75} Meta-GGA functionals, the third rung of the ladder, includes either the laplacian of the density or the kinetic energy density of the system to improve accuracy by increasing the flexibility of the functional.^{66,75} The fourth rung introduces Hartree-Fock (HF) exchange energy to either a GGA or meta-GGA functional, giving rise to hybrid functionals, that have been demonstrated to improve accuracy in predicting chemical properties, such as atomisation energies and bond lengths.^{36,66,75,76} Last but not least, the fifth rung of the ladder represents double hybrid functionals that include both HF exchange and an additional term to treat non-local electron correlation and other components from the fourth rung.^{66,75,77}

Despite the plethora of DFT functionals available, the involvement of a metal ion throws a wrench in the mix due to its ability to exist in multiple electronic states with low energy barriers between different electronic states and long-range charge separation.⁷⁸ Another concern is relativistic effects that arise from modelling heavy atoms, resulting from the shielding and stabilising effects on the s and p shells.^{78–80} The increase in atomic mass results in the stabilising of s and p orbitals and destabilisation of the d and f orbitals.⁸⁰ Due to the issues that arise with the presence of metal ions, it is necessary to identify the suitable method to study complexes containing Pt metal ions.

In previously conducted studies, DFT has been shown to be a suitable approach to study the reaction profile and spectra prediction of Pt complexes. Luo *et al.* and Wysokinski *et al.* are amongst the few groups who have successfully shown that DFT is a suitable method to predict the far infrared spectra of Pt complexes, specifically their characteristic stretching and bending vibrations.^{71,74} Due to the presence of dative bonds, metal-ligand vibrations appear below 600 cm^{-1} . The donor-acceptor nature of the metal and its ligand, differing from covalent bonds, adds another challenge to predicting IR spectra.^{69,74,81,82} Santos *et al.*, Eriksson *et al.*, Burda *et al.* and Lippard *et al.* have also taken advantage of DFT to study the hydrolysis reaction pathway of Pt complexes.^{83–86} With the use of DFT, specifically the combination of either B3P86 or B3PW91 functional, 6-31G(d) basis set for non-Pt atoms and the LANL2DZ effective core potential (ECP) for the Pt ion within an implicit solvation model, Santos was able to predict the activation Gibbs free energy of the second hydrolysis step of *cis*-dichloro(ethylene)diammineplatinum(II), with an error of 1.42 kJ mol^{-1} .⁸³ By including explicit water molecules in addition to implicit solvation models, Eriksson *et al.* showed a significant role that explicit solvation played during the hydrolysis reaction of cisplatin.⁸⁴ The addition of explicit H_2O molecules made it a more realistic model, predicting a more accurate Gibbs energy of activation with respect to experiment.⁸⁴

1.3.3 Previously reported computational chemistry studies

Leszczynski *et al.* examined the hydrolysis of *cis*- and *trans*-platin, specifically their reaction kinetics and thermodynamics, via DFT.^{85,87} While Leszczynski *et al.* used the HF method when studying the hydrolysis of the two Pt complexes, B3LYP was the functional of choice

when implicit solvation was modelled using the Conductor-like screening solvation model (COSMO).^{85,87} The combination of B3LYP, COSMO, 6-31+G(d) basis set and Stuttgart–Dresden effective core potential (ECPs) for Cl and Pt atoms was used to optimise cis- and trans-platin.⁸⁷ CCSD(T), 6-31++G(d,p), COSMO and Stuttgart–Dresden ECPs were used for single point energy calculations to obtain more accurate energies.⁸⁷ With the model consisting of the Pt complex and one explicit water molecule, the hydrolysis reaction was considered as a two step reaction, replacing one Cl^- with H_2O at a time.⁸⁷ Kinetic properties were determined using the Eyring's Transition State Theory (TST).⁸⁷ When compared to its gas phase counterpart, the inclusion of COSMO solvation model decreases the reaction energies.⁸⁷ The calculated kinetic rates were also in agreement with previously published experimental data.⁸⁷ The method used was able to accurately predicting the kinetic rate of the first dechlorination step to be $1.3 \times 10^{-4} \text{ s}^{-1}$, in accordance to the $1.9 \times 10^{-4} \text{ s}^{-1}$ determined by Mauristo *et al.*^{87,88}

Platts *et al.* made use of DFT to investigate the interaction between water and cisplatin.⁸⁹ With the combination of PW91 functional and Stuttgart–Dresden basis set, Platts *et al.* located three energy minima for a system consisting of cisplatin and water (1:1 ratio).⁸⁹ Differing by a maximum of 27.0 kJ mol^{-1} , all three conformations display interactions between Cl and N-H.⁸⁹ Molecular electrostatic potential (MEP), a method to identify the strength of hydrogen bonding, revealed the ability of cisplatin to play the role of both a hydrogen bond acceptor and donor.⁸⁹ The most stable conformation is obtained when the water molecule forms hydrogen bonding with both the NH_3 and Cl on cisplatin.⁸⁹ Subsequently, a total of 10 water molecules were positioned around cisplatin, resulting in an increase in stabilisation energy of 10 kJ mol^{-1} as compared to the previous 1:1 model.⁸⁹ The presence of explicit water molecules also resulted in a longer Pt-Cl bond, increasing it by 0.1 \AA .⁸⁹ Interestingly, the opposite was observed for the Pt-N bond where the increase in solvation decreased the bond distance by 0.1 \AA .⁸⁹ The effects of explicit solvation when predicting the transition state of the first hydrolysis step of cisplatin was also investigated. Significantly different geometries were obtained with and without explicit solvation, indicating that the presence of explicit solvation plays an important role in describing such reactions.⁸⁹

1.3.4 Fragmentation techniques

Usually molecular mechanics (MM), which employs force fields, is utilised to study large systems.⁹⁰ Armed with the theory that molecules are essentially individual atoms linked together via harmonic forces, MM offers the option to calculate large systems at a much lower cost than quantum mechanical methods with a trade-off in accuracy.^{90,91} In addition, MM is also unable to provide accurate information of intermolecular interactions.^{90,91} Hence, the need to identify a method that is both computationally cheap and able to provide accurate interaction energies is required. Fortunately, many different fragmentation techniques within ab initio theory have been developed: divide and conquer methods, systematic fragmentation methods and methods based on many-body interactions.^{92–95} Whilst the divide and conquer methods divide the electron density of the system into smaller subunits, accounting for interactions with neighbouring subunits using a buffer region, the systematic fragmentation method divides large systems into smaller fragments and accounts for interactions via overlapping sections (Fig: 1.5).^{92,94,96} An example of methods based on many-body interactions is the Fragment Molecular Orbital (FMO) method. With the ability to divide large systems into smaller fragments, the total energy can be calculated by summing up the energies of each individual fragment and adding the two- and/or three-body energy corrections with respect to all other fragments.^{92,97,98} Either using the hybrid operator projection (HOP) or adaptive frozen orbital (AFO) method, bonds are fragmented and each fragment is treated accordingly.⁹² HOP allocates both electrons involved in bonding to one atom, known as the bond attached atom (BAA), and projects the electron orbital of the other atom, known as the bond detached atom (BDA), out to ensure that electron density from the BDA does not occupy the bond region.⁹² AFO, on the other hand, describes the fragmented bond by using predetermined parameters of model systems and freezes the electron density of the fragmented bond.⁹² While HOP allows for electron density of the system to be flexible, AFO restricts the fluidity of the electron density that is involved in the fragmented bond.⁹² Due to the difference in treatment of the fragmented bond, different fragmentation methods are more applicable to studying different systems. For example, while AFO produces more accurate results when studying polypeptides and molecular surfaces, HOP is the better choice when investigating polar systems.⁹²

As FMO constructs a coulomb bath by summing the coulomb field of each fragment, the energies of each monomer is calculated while being exposed to the coulomb bath.^{92,97,98} Previously, Komeiji made use of FMO to study DNA models in gas phase, investigating the appropriate fragmentation mode of DNA.⁹⁹ Three different fragmentation modes were studied and the appropriate fragmentation point of a DNA monomer was determined to be between the base and the sugar, giving rise to two fragments per monomer.⁹⁹

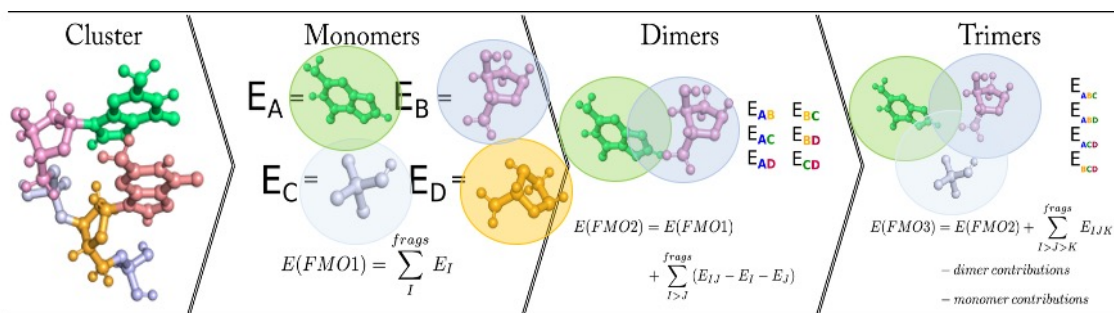


Figure 1.5: Schematic of Fragment Molecular Orbital Theory.

Kitaura *et al.*, Nakano *et al.* and Kuwata *et al.* have employed the use of FMO to study large systems with much success.^{100–104} Kuwata *et al.* investigated the interactions of a protein, a prion protein (PrP), and a small molecule (2-pyrrolidin-1-yl-N-[4-[4-(2-pyrrolidin-1-ylacetyl-amino)-benzyl]-phenyl]-acetamide, also known as GN8).¹⁰² PrP is a protein that plays a part in prion diseases when it converts from its cellular form to its scrapie form, resulting in distorted proteins.^{102,105,106} It was found that the inhibition of GN8 to the cellular form of PrP will impede the conversion to its scrapie form, giving rise to the need to study the interaction of PrP with suitable drug candidates.^{102,107} Before conducting QM calculations, Kuwata *et al.* conducted molecular dynamics (MD) calculations on the structure obtained from the Protein Data Bank (1AG2) with the AMBER99SB force field.^{102,108–110} Kuwata *et al.* decided to utilise FMO on the obtained 20 geometries from MD, specifically the in-built inter-fragment interaction energy (IFIE) function of FMO, to study the interaction of the large protein and GN8, treating each amino acid as a fragment, with the exception of C179 and C214 where they are fragmented together due to the presence of the S-S bond, and GN8 is divided into 4 individual fragments.¹⁰² As interaction energies are usually overestimated due to the artificial stabilisation arising from basis set superposition error (BSSE), counterpoise (CP) correction was implemented resulting in BSSE values of 63 and 146 kJ mol⁻¹ for HF and MP2, respectively.¹⁰² Interaction energies

obtained from the 20 structures obtained from MD, ranged from -175.7 to -301.2 kJ mol⁻¹ due to geometric differences.¹⁰² However, with the use of IFIE, Kuwata *et al.* determined the crucial amino acids that interact strongly with GN8, specifically N159, Q160, K194, and E196.¹⁰²

Nakano *et al.* also made use of FMO to study the interactions between human estrogen receptors (ERs) and ligands, such as raloxifene (RAL) and tamoxifen (TAM) to understand their role in regulating tissue growth.¹⁰⁴ The binding of some compounds to the ligand binding domain (LBD) have resulted in a hormone-like effect, making it a drug target.¹⁰⁴ Similar to the approach taken by Kitaura, Nakano first optimised the complexes with MD, specifically the CHARMM force field.¹⁰⁴ After which, the model is condensed to include the ER-ligand and water molecules interacting via hydrogen bonding. The condensed system was optimised with HF/6-31G(d) level of theory with the PCM solvation model.¹⁰⁴ Smaller models were then constructed and single point energy calculations were performed using FMO-HF/STO-3G level of theory to analyse the binding energies of the various ligands.¹⁰⁴ Nakano *et al.* specifically investigated the binding energies of various ligands to 17 β -estradiol and plotted it to the relative binding affinities (RBA). With an overall correlation of 0.837 and 0.035 for FMO and MD, respectively, FMO-HF is unsurprisingly the better method to investigate binding energies.¹⁰⁴

However, the study was conducted in gas phase and the effects of implicit solvation on FMO energies and optimised geometries is yet to be determined, especially in DNA models, and the validity of this method will be further investigated in this study.

1.3.5 Computational studies

Unsurprisingly, a significant amount of effort has been put in to understand the Pt complexes experimentally. Though armed with an arsenal of different techniques, such as high pressure liquid chromatography (HPLC) and *in situ* resonant inelastic X-ray scattering (RIXS) spectroscopy, a conclusion has yet to be drawn on the hydrolysis mechanism of these complexes.¹¹¹⁻¹²⁵

With ¹H-¹⁵N heteronuclear single quantum coherence (¹H-¹⁵N HSQC) nuclear magnetic resonance (NMR) spectroscopy, Hambley *et al.* attempted to determine the rate of reactions of the hydrolysis reactions under specific conditions over a time period of 40 hours.⁶⁴ Both the mono- and di-hydrated equivalent of ¹⁵N-cisplatin were detected after 2 and 3.5 hours,

respectively.⁶⁴ The kinetic rates of the reactions were calculated via the relative concentrations of *cis*-[Pt(¹⁵NH₃)₂]²⁺ at specific time points.⁶⁴ It was reported that the formation of di-hydrated equivalent of ¹⁵N-cisplatin resulted in a decrease of pH, from 6.6 to 4.9.⁶⁴ With the mono-hydrated equivalent of ¹⁵N-cisplatin determined to be the major product after 40 hours, the pK_as of the first and second step of the hydrolysis were determined to be 2.07 and 3.49, respectively.⁶⁴ Subsequently, the binding event between ¹⁵N-cisplatin and a DNA oligomer (5'-d(AATTGGTACCAATT)-3' prepared in a phosphate buffer solution of pH 6%) was investigated.⁶⁴ Accompanied with ¹H NMR, a chemical shift of $\delta = 6.5 - 9.2$ ppm for the aromatic protons was observed.⁶⁴ ¹H-¹⁵N HSQC NMR measurements were collected over a span of 350 hours.⁶⁴ It was observed that the mono-hydrated equivalent of ¹⁵N-cisplatin was no longer detectable after 20 hours.⁶⁴ The mono-hydrated equivalent formed mono-functional adducts with the DNA oligomer and ring closes to form bi-functional adducts with the oligomer.⁶⁴ The di-hydrated equivalent was not observed at all.⁶⁴

Chottard *et al.* made use of HPLC to study rate constants of the binding event of three derivatives of hydrated cisplatin to either δ (TATGGTATT₄ATACCATA) (-GG-) or δ (TATAGTATT₄ATACTATA) (-AG-) in a solution of 0.1M NaClO₄ with a pH of 4.5: *cis*-[PtCl(NH₃)₂H₂O]⁺, *cis*-[Pt(NH₃)₂(H₂O)₂]²⁺ and *cis*-[Pt(NH₃)₂(OH)(H₂O)]²⁺.⁶⁵ However, due to the tendency of the mono-hydrated equivalent to form the di-hydrated species in acidic reactions, different conditions were implemented to investigate their respective rate constant.⁶⁵ By comparing the rate constants of the respective species, it was discovered that other than the mono-hydrated species, there is a clear preference of the *cis*-[Pt(NH₃)₂(H₂O)₂]²⁺ and *cis*-[Pt(NH₃)₂(OH)(H₂O)]²⁺ to bind to GG instead of AG.⁶⁵ It was also determined that the di-hydrated equivalent will form adducts with GG and AG in a ratio of 3:1, the known adduct ratio formed in vivo studies.^{65,126}

Previously, IR spectroscopy has also been used to study Pt-based anti-cancer drugs.^{116,127-132} It is established that IR spectra of cells are a combination of all molecules present in the cell.¹³² Any changes in spectra due to incubation with drugs will be attributed to changes in chemical bonding to molecules in the cell.^{129,132}

Michalska *et al.* demonstrated that IR is a viable technique to identify different Pt complexes.⁷⁴ Focusing on the far IR region, between the 600 - 50 cm⁻¹, Michalska *et al.* was able to identify

characteristic bands for carboplatin.⁷⁴ For example, the 348 and 351 cm^{-1} bands are assigned to be $\nu(\text{Pt-O})$ and 450 cm^{-1} is assigned to be $\nu_s(\text{N-Pt-N})$.⁷⁴ Wood *et al.* was also able to characterise the distinct far IR bands for cisplatin.¹³³ With access to the Australian Synchrotron, Wood *et al.* assigned the 155, 201 and 323 cm^{-1} bands to be $\gamma(\text{N-Pt-N}) + \gamma(\text{Cl-Pt-Cl})$, $\alpha(\text{N-Pt-N}) + \alpha(\text{Cl-Pt-Cl})$ and $\nu_s(\text{Cl-Pt-Cl}) + \nu_{\text{asym}}(\text{Cl-Pt-Cl})$, respectively.¹³³

Spiccia *et al.* took advantage of vibrational spectroscopy as being a nondestructive method and measured the vibrational spectra of *trans,trans,trans*-[Pt(N₃)₂(OH)₂(py)₂] (C1), a promising anti-cancer prodrug.¹²⁹ Producing either *trans*-[Pt(N₃)₂(py)₂] (C2) or *trans*-[PtCl₂(py)₂] (C3) after being exposed to UV-A and visible light irradiation, attenuated total reflection Fourier transform infrared (ATR-FTIR), Raman and far-IR spectra were measured and vibrational modes were assigned with the use of DFT.¹²⁹ By better understanding the changes of the complex, specifically the metal - ligand binding modes, it gives a better understanding of the mechanism of *trans,trans,trans*-[Pt(N₃)₂(OH)₂(py)₂] upon activation.¹²⁹ After spectra were collected, a systematic approach was taken to calculate the infrared spectra using DFT. Geometry optimisations were performed using either M06-2X or PBE functional with cc-pVDZ basis set, cc-pVDZ-PP (VDZ-PP) ECP and conductor-like polarisable continuum model (CPCM) with water as the solvent.¹²⁹ Subsequently, a full conformation screening was conducted by using the tree search approach to identify all the local minima geometries.^{129,134} Calculated geometries were compared to that of crystal structure and the spectra corresponding to the most similar geometry were compared to that of experimental spectra and characteristic bands were assigned.¹²⁹ The bands at 545 and 541 cm^{-1} were assigned to be $\nu_{\text{asym}}(\text{OH-Pt-OH})$ while the band at 540 cm^{-1} was assigned to be $\nu_{\text{sym}}(\text{OH-Pt-OH})$. Based on the far-IR spectra, it is also possible to distinguish between the complexes. For example, while four $\nu_{\text{asym}}(\text{N}_3\text{-Pt-N}_3)$ bands were identified for C1 (417, 413, 407 and 395 cm^{-1}), only two bands were identified for C2 (408 and 400 cm^{-1}). The activation of C1 due to irradiation could also be witnessed in the Raman spectra, for example the change in intensity of the 406 cm^{-1} band after C1 was dissolved in water.¹²⁹

Currently, there is still a lack of far IR data for other Pt complexes due to limitations such as the low sensitivity of benchtop IR spectrometers. Access to facilities, such as the Australian Synchrotron, are required for far IR measurements where it is able to adequately measure

the weaker far IR bands.^{133,135,136} Coupled with the low solubility issue of the complexes, a consensus of the mechanism and identity of the activated complexes has yet to be reached.

1.4 RNA: A possible drug target?

Over the past few years, ribonucleic acid (RNA) has emerged as an important drug target for a few ailments, such as hepatitis C and cancer.^{137–155} Similar to DNA, RNA is significant in maintaining biological functions, such as the regulation of genes, in cells.¹⁵⁶ Consisting of G, A, C and uracil (U), RNA is a single stranded molecule but folds and interacts with itself via Watson-Crick hydrogen bonding to give rise to different secondary structures, the helices, loops, junctions and bulge.^{139,156} Different types of RNA have been shown to play very specific biological roles, *e.g.* messenger RNA (mRNA) determines the amino acid sequence of the newly synthesised protein and transfer RNA (tRNA) is responsible for transporting the amino acids where it links to the ribosomal RNA (rRNA).^{139,156,157}

Several different features of RNA make it a potential drug target. Firstly, it was suggested that its ability to alter its conformation plays a vital role in several biological functions.^{152,154} This gives rise to the opportunity of designing a compound to prevent conformational changes to impede certain processes.^{152,154} The direct relationship between the amino acid sequence in RNA and the binding pockets formed aids in the design of molecules to bind to specific RNA.^{152,154,158} This is useful as different types of RNA are likely to result in different types of folding, for *e.g.* tRNA is likely to form a conformation with three loops.¹⁵⁸ This enables the specific targeting of the RNA of interest.¹⁵⁸ Unlike DNA, where the targeting sites are either the major or minor grooves, the ideal drug targeting sites are formed due to the mismatch base pairs in RNA and usually has a electronegative charge.¹⁵⁸ So far, this has been explored as a target for antibacterial and antiviral treatments.¹⁵⁸

Recently, RNA has been the focal point in the hopes to identify a new cancer treatment.^{138,159–164} Pt-based anti-cancer drugs have demonstrated to be able to affect regulation and expression of RNA.¹⁵⁹ Polikanov *et al.* were able to identify the 70S RNA-cisplatin binding event.¹⁴² With a x-ray crystal structure solved at 2.6 Å resolution, nine cisplatin molecules were found to interact with RNA.¹⁴² Interestingly, five and three cisplatin molecules were found to bind to the N7 of G and A, respectively.¹⁴² The last cisplatin molecule was found to bind to the N-terminus of a

protein.¹⁴² It was also noticed that the binding sites revealed some conformational similarities. While binding to G, cisplatin was found to interact strongly with the phosphate group as well as bind to A, it has to be positioned immediately before G.¹⁴² This specificity in interaction with cisplatin indicates that RNA has the potential to be an important drug target for cancer treatment.

Similar to studies conducted on DNA, a consensus of the identity of the Pt drug that binds to RNA is currently unknown. In addition, the selectivity of Pt drugs for DNA and RNA is currently up for debate as well. A study conducted by Mezencev found that cisplatin is more likely to bind to RNA than DNA in human cervical adenocarcinoma HeLa cells.¹⁶⁵ In addition, an ex vivo study conducted by DeRose *et al.* has indicated that cisplatin is more likely to bind to DNA than RNA, by approximately 3 times more over twelve hours.¹⁴⁹

Despite the growing interest as a new drug target, there is a lack of understanding from a computational viewpoint and a preliminary studies of Pt-complexes binding to either RNA or DNA will be explored.

1.5 Overview

The main aim of this thesis is to gain a better understanding of the hydrolysis mechanism of the various Pt-based anti-cancer drugs and their interactions with DNA and RNA building blocks. In order to achieve this goal, a step-by-step approach was undertaken to:

- 1) Identify a suitable level of theory to predict far IR spectra of Pt-based anti-cancer drugs;
- 2) Investigate the importance of explicit solvation when studying the mechanism of hydrolysis of Pt-based anti-cancer drugs;
- 3) Evaluate the application of the FMO approach to study models of DNA using implicit solvation models;
- 4) Study the strength and mode of binding of active forms of Pt-based anti-cancer drugs to DNA and RNA building blocks.

Chapter 2 aims to identify the appropriate level of theory to predict the far IR (FIR) spectra of Pt-based anti-cancer drugs. Cisplatin and carboplatin were the two complexes of interest

due to the availability of experimental data. The performance of four DFT functionals such as PBE, PBE0, M06-L and M06-2X were investigated. In addition, the effect of basis sets on the non-Pt atoms (VDZ, VTZ, aVDZ and aVTZ), effective core potentials on the Pt (VDZ-pp, VTZ-pp, aVDZ-pp and aVTZ-pp) and solvation models (IEFPCM, CPCM and SMD) were also considered. The predicted FIR spectra were compared to available experimental results, specifically for the bands characteristic of the Pt-ligand dative bonds. With the aid of the partial charge analysis, the dative bonds present in the two complexes were found to possess different characteristics - partially covalent in cisplatin and predominantly ionic in carboplatin. The different types of bonding explained why different DFT functionals were needed to best predict the FIR spectra for the two complexes.

Chapter 3 investigates the importance of explicit solvation on the hydrolysis mechanism of the Pt complexes. The energetics of the hydrolysis was performed using a relaxed scan approach with both implicit and explicit solvation models. The addition of an explicit solvation shell has a stabilising effect on the dissociation of the ligands, evident from the ChelpG analysis performed. The water molecules form hydrogen bonds with the respective leaving groups, redistributing the charge in the system. The Gibbs' free energy (ΔG_{solv}), obtained from the thermodynamic cycle with an implicit solvation model, and energy differences (ΔE_{solv}), obtained from the relaxed scans with explicit solvation, were compared for their validity to study the dissociation reactions. It was concluded that whilst ΔG_{solv} indicates that the dissociations are thermodynamically feasible, it does not take into consideration the formation of a contact ion pair between the metal ion and the leaving groups. This could result in an artificial effect that might increase the activation barrier. Though computationally more expensive, ΔE_{solv} is able to reflect a more realistic activation barrier. Through the relaxed scans, it was also concluded that whilst a two-step hydrolysis reaction is the likely hydrolysis reaction for the four Pt complexes, the first and second step of the hydrolysis have similar rates and the second step will occur quickly after the first step. In the case of cisplatin, these results were compared to the reaction barriers obtained from locating two transition states (one for each leaving group) using explicit solvation. The latter better reproduced experimental barriers, thus highlighting the importance of explicit solvation. The relaxed scans with explicit solvation were found to

overestimate barriers, thus providing the upper bound kinetics for the hydrolysis of Pt-based complexes.

Chapter 4 focuses on the geometry optimisations of DNA building blocks such as dAMP and dGMP using the FMO approach. Single stranded systems such as dGMP and dAMP and their double stranded and stacked models were considered in the study. The geometries and energies obtained with various types of fragmentation schemes within the FMO framework were compared to those of the full system optimisations. The influence of different methods (PBE, PBE-D3 and SRS-MP2) and solvation models (CPCM and SMD) were also considered. Geometries obtained from full system and FMO optimisations were significantly different, indicating when fragmentation is used within the FMO approach, the location of a different local minimum was achieved. The differences in optimised geometries increased with increasing complexity in the system. Both stacked and hydrogen-bonded models of the two building blocks had significantly larger difference when combined with implicit solvation models. This suggests the need to improve the interfacing of solute-solvent interactions within the FMO approach for a given level of theory.

Chapter 5 investigates the binding mode of three potential activated forms of Pt-based anti-cancer drugs, non- ($[\text{PtL}]^{2+}$), mono- ($[\text{PtL}(\text{H}_2\text{O})]^{2+}$) and di-aquated ($[\text{PtL}(\text{H}_2\text{O})_2]^{2+}$) species, with building blocks of DNA and RNA, specifically dGMP, dAMP, GMP and AMP. In addition, the changes in the geometries of the DNA/RNA building blocks upon the binding of these forms were evaluated by analysing the deformation energies after the binding event.

Lastly, *Chapter 6* will conclude this thesis and reiterate the overall findings of this work and its contributions to the field of computational chemistry. Further works required will also be discussed.

1.6 References

- [1] James D Watson, Francis HC Crick, et al. Molecular structure of nucleic acids. *Nature* **171**(4356) (1953), 737–738.
- [2] JD Watson and FHC Crick. Molecular structure of nucleic acids. *Landmarks in Medical Genetics: Classic Papers with Commentaries* **171**(51) (2004), 216.
- [3] Albino Bacolla, David N Cooper, and Karen M Vasquez. DNA structure matters. *Genome Medicine* **5**(6) (2013), 51.
- [4] Andrew Travers and Georgi Muskhelishvili. DNA structure and function. *The FEBS Journal* **282**(12) (2015), 2279–2295.
- [5] Michelle G Gibbons. Reassessing discovery: Rosalind Franklin, scientific visualization, and the structure of DNA. *Philosophy of Science* **79**(1) (2012), 63–80.
- [6] Francis Harry Compton Crick and James Dewey Watson. The complementary structure of deoxyribonucleic acid. *Proceedings of the Royal Society of London. Series A. Mathematical and Physical Sciences* **223**(1152) (1954), 80–96.
- [7] Petter Portin. The birth and development of the DNA theory of inheritance: sixty years since the discovery of the structure of DNA. *Journal of Genetics* **93**(1) (2014), 293–302.
- [8] Eric T Kool, Juan C Morales, and Kevin M Guckian. Mimicking the structure and function of DNA: insights into DNA stability and replication. *Angewandte Chemie International Edition* **39**(6) (2000), 990–1009.
- [9] Linus Pauling and Robert B Corey. Structure of the nucleic acids. *Nature* **171**(4347) (1953), 346–346.
- [10] Zippora Shakked and Dov Rabinovich. The effect of the base sequence on the fine structure of the DNA double helix. *Progress in Biophysics and Molecular Biology* **47**(3) (1986), 159–195.
- [11] Bayden R Wood. The importance of hydration and DNA conformation in interpreting infrared spectra of cells and tissues. *Chemical Society Reviews* **45**(7) (2016), 1980–1998.
- [12] E Taillandier and J Liquier. “Infrared spectroscopy of DNA”. In: *Methods in Enzymology*. Vol. 211. 1992, pp.307–335.

- [13] Daniel Svozil, Jan Kalina, Marek Omelka, and Bohdan Schneider. DNA conformations and their sequence preferences. *Nucleic Acids Research* **36**(11) (2008), 3690–3706.
- [14] J Brahms, J Pilet, Tran-Thi Phuong Lan, and LR Hill. Direct evidence of the C-like form of sodium deoxyribonucleate. *Proceedings of the National Academy of Sciences* **70**(12) (1973), 3352–3355.
- [15] Zippora Shakked, Gali Guerstein-Guzikevich, Miriam Eisenstein, Felix Frolow, and Dov Rabinovich. The conformation of the DNA double helix in the crystal is dependent on its environment. *Nature* **342**(6248) (1989), 456.
- [16] G Burckhardt, Ch Zimmer, and G Luck. Conformation and reactivity of DNA V. pH-dependent conformational changes of DNA in complexes with poly-L-histidine: Transitions from B-to A-form and to a condensed state. *FEBS Letters* **30**(1) (1973), 35–39.
- [17] Richard E Dickerson, Horace R Drew, Benjamin N Conner, Richard M Wing, Albert V Fratini, and Mary L Kopka. The anatomy of a-, b-, and z-dna. *Science* **216**(4545) (1982), 475–485.
- [18] Tao Lan and Larry W McLaughlin. Minor groove functional groups are critical for the B-form conformation of duplex DNA. *Biochemistry* **40**(4) (2001), 968–976.
- [19] Delphine Flatters, Matthew Young, David L Beveridge, and Richard Lavery. Conformational properties of the TATA-box binding sequence of DNA. *Journal of Biomolecular Structure and Dynamics* **14**(6) (1997), 757–765.
- [20] Markus C Wahl, Sambhorao T Rao, and Muttaiya Sundaralingam. Crystal structure of the B-DNA hexamer d (CTCGAG): model for an A-to-B transition. *Biophysical Journal* **70**(6) (1996), 2857–2866.
- [21] Gali Guzikevich-Guerstein and Zippora Shakked. A novel form of the DNA double helix imposed on the TATA-box by the TATA-binding protein. *Nature Structural Biology* **3**(1) (1996), 32.
- [22] Alfredo Jacobo-Molina, Jianping Ding, Raymond G Nanni, Arthur D Clark, Xiaode Lu, Chris Tantillo, Roger L Williams, Greg Kamer, Andrea L Ferris, and Patrick Clark. Crystal structure of human immunodeficiency virus type 1 reverse transcriptase complexed

- with double-stranded DNA at 3.0 Å resolution shows bent DNA. *Proceedings of the National Academy of Sciences* **90**(13) (1993), 6320–6324.
- [23] Barnett Rosenberg, Loretta Vancamp, James E Trosko, and Virginia H Mansour. Platinum compounds: a new class of potent antitumour agents. *Nature* **222**(5191) (1969), 385–386.
- [24] Markus Galanski and Bernhard K Keppler. Searching for the magic bullet: anticancer platinum drugs which can be accumulated or activated in the tumor tissue. *Anti-Cancer Agents in Medicinal Chemistry (Formerly Current Medicinal Chemistry-Anti-Cancer Agents)* **7**(1) (2007), 55–73.
- [25] Timothy C Johnstone, Kogularamanan Suntharalingam, and Stephen J Lippard. The next generation of platinum drugs: targeted Pt (II) agents, nanoparticle delivery, and Pt (IV) prodrugs. *Chemical Reviews* **116**(5) (2016), 3436–3486.
- [26] Zahid H Siddik. Cisplatin: mode of cytotoxic action and molecular basis of resistance. *Oncogene* **22**(47) (2003), 7265–7279.
- [27] Archie W Prestayko, JC D’aoust, BF Issell, and ST Crooke. Cisplatin (cis-diamminedichloroplatinum II). *Cancer Treatment Reviews* **6**(1) (1979), 17–39.
- [28] Kazuo Ota. Nedaplatin. *Gan to Kagaku Ryoho. Cancer & chemotherapy* **23**(3) (1996), 379–387.
- [29] Ana-Maria Florea and Dietrich Büsselberg. Cisplatin as an anti-tumor drug: cellular mechanisms of activity, drug resistance and induced side effects. *Cancers* **3**(1) (2011), 1351–1371.
- [30] Shaloam Dasari and Paul Bernard Tchounwou. Cisplatin in cancer therapy: molecular mechanisms of action. *European Journal of Pharmacology* **740** (2014), 364–378.
- [31] Nasma D Eljack, Ho-Yu M Ma, Janine Drucker, Clara Shen, Trevor W Hambley, Elizabeth J New, Thomas Friedrich, and Ronald J Clarke. Mechanisms of cell uptake and toxicity of the anticancer drug cisplatin. *Metallomics* **6**(11) (2014), 2126–2133.
- [32] Renzo Canetta, Marcel Rozenzweig, and Stephen K Carter. Carboplatin: the clinical spectrum to date. *Cancer Treatment Reviews* **12** (1985), 125–136.

- [33] Robert W Hay and Sian Miller. Reactions of platinum (II) anticancer drugs. Kinetics of acid hydrolysis of cis-diammine (cyclobutane-1, 1-dicarboxylato) platinum (II)“Carboplatin”. *Polyhedron* **17**(13-14) (1998), 2337–2343.
- [34] G Mathe, Y Kidani, M Segiguchi, M Eriguchi, G Fredj, G Peytavin, JL Misset, S Brienza, F De Vassals, E Chenu, et al. Oxalato-platinum or 1-OHP, a third-generation platinum complex: an experimental and clinical appraisal and preliminary comparison with cis-platinum and carboplatinum. *Biomedicine & Pharmacotherapy* **43**(4) (1989), 237–250.
- [35] Alice V Klein and Trevor W Hambley. Platinum drug distribution in cancer cells and tumors. *Chemical Reviews* **109**(10) (2009), 4911–4920.
- [36] Johan Raber, Chuanbao Zhu, and Leif A Eriksson. Theoretical study of cisplatin binding to DNA: the importance of initial complex stabilization. *The Journal of Physical Chemistry B* **109**(21) (2005), 11006–11015.
- [37] R.M. Wing, P. Pjura, H.R. Drew, and R.E. Dickerson. The primary mode of binding of cisplatin to a B-DNA dodecamer: C-G-C-G-A-A-T-T-C-G-C-G. *The EMBO Journal* **3**(5) (1984), 1201–1206. DOI: [10.1002/j.1460-2075.1984.tb01951.x](https://doi.org/10.1002/j.1460-2075.1984.tb01951.x). eprint: <https://www.embopress.org/doi/pdf/10.1002/j.1460-2075.1984.tb01951.x>.
- [38] Deborah B. Zamble and Stephen J. Lippard. Cisplatin and DNA repair in cancer chemotherapy. *Trends in Biochemical Sciences* **20**(10) (1995), 435–439. DOI: [https://doi.org/10.1016/S0968-0004\(00\)89095-7](https://doi.org/10.1016/S0968-0004(00)89095-7).
- [39] L Galluzzi, L Senovilla, I Vitale, J Michels, I Martins, O Kepp, M Castedo, and G Kroemer. Molecular mechanisms of cisplatin resistance. *Oncogene* **31**(15) (2012), 1869–1883.
- [40] Dana Branzei and Marco Foiani. The DNA damage response during DNA replication. *Current Opinion in Cell Biology* **17**(6) (2005), 568–575.
- [41] Satoshi Tanida, Tsutomu Mizoshita, Keiji Ozeki, Hironobu Tsukamoto, Takeshi Kamiya, Hiromi Kataoka, Daitoku Sakamuro, and Takashi Joh. Mechanisms of cisplatin-induced apoptosis and of cisplatin sensitivity: potential of BIN1 to act as a potent predictor of cisplatin sensitivity in gastric cancer treatment. *International Journal of Surgical Oncology* **2012** (2012).

- [42] Kohji Hizume and Hiroyuki Araki. Replication fork pausing at protein barriers on chromosomes. *FEBS Letters* **593**(13) (2019), 1449–1458.
- [43] Michael B Kastan, Onyinye Onyekwere, David Sidransky, Bert Vogelstein, and Ruth W Craig. Participation of p53 protein in the cellular response to DNA damage. *Cancer Research* **51**(23 Part 1) (1991), 6304–6311.
- [44] Andrew M Breglio, Aaron E Rusheen, Eric D Shide, Katharine A Fernandez, Katie K Spielbauer, Katherine M McLachlin, Matthew D Hall, Lauren Amable, and Lisa L Cunningham. Cisplatin is retained in the cochlea indefinitely following chemotherapy. *Nature Communications* **8**(1) (2017), 1–9.
- [45] Bernard Desoize and Claudie Madoulet. Particular aspects of platinum compounds used at present in cancer treatment. *Critical Reviews in Oncology/Hematology* **42**(3) (2002), 317–325.
- [46] Neel Shah and Don S Dizon. New-generation platinum agents for solid tumors (2009).
- [47] Dennis Alexander Günes, Ana-Maria Florea, Frank Splettstoesser, and Dietrich Büsselberg. Co-application of arsenic trioxide (As₂O₃) and cisplatin (CDDP) on human SY-5Y neuroblastoma cells has differential effects on the intracellular calcium concentration ([Ca²⁺] i) and cytotoxicity. *Neurotoxicology* **30**(2) (2009), 194–202.
- [48] Ana-Maria Florea and Dietrich Büsselberg. Occurrence, use and potential toxic effects of metals and metal compounds. *Biometals* **19**(4) (2006), 419–427.
- [49] Roger Y Tsang, Turki Al-Fayea, and Heather-Jane Au. Cisplatin overdose. *Drug Safety* **32**(12) (2009), 1109–1122.
- [50] Istvan Arany and Robert L Safirstein. Cisplatin nephrotoxicity. In: *Seminars in Nephrology*. Vol. 23. 5. Elsevier. 2003, pp.460–464.
- [51] D C Dobyan, J Levi, C Jacobs, J Kosek, and M W Weiner. Mechanism of cis-platinum nephrotoxicity: II. Morphologic observations. *Journal of Pharmacology and Experimental Therapeutics* **213**(3) (1980), 551–556. eprint: <http://jpet.aspetjournals.org/content/213/3/551.full.pdf>.

- [52] Britta Stordal and Mary Davey. Understanding cisplatin resistance using cellular models. *IUBMB Life* **59**(11) (2007), 696–699. DOI: [10.1080/15216540701636287](https://doi.org/10.1080/15216540701636287). eprint: <https://iubmb.onlinelibrary.wiley.com/doi/pdf/10.1080/15216540701636287>.
- [53] Jörg Thomas Hartmann and Hans-Peter Lipp. Toxicity of platinum compounds. *Expert Opinion on Pharmacotherapy* **4**(6) (2003), 889–901. DOI: [10.1517/14656566.4.6.889](https://doi.org/10.1517/14656566.4.6.889). eprint: <https://doi.org/10.1517/14656566.4.6.889>.
- [54] Urban Frey, John D Ranford, and Peter J Sadler. Ring-opening reactions of the anticancer drug carboplatin: NMR characterization of cis-[Pt (NH₃)₂ (CBDCA-O)(5'-GMP-N7)] in solution. *Inorganic Chemistry* **32**(8) (1993), 1333–1340.
- [55] Irena Kostova. Platinum complexes as anticancer agents. *Recent Patents on Anti-Cancer Drug Discovery* **1**(1) (2006), 1–22.
- [56] AH Calvert, DR Newell, K Balmano, AD Pearson, L Price, and M Kier. “Pharmacokinetics of carboplatin in children and the development of a paediatric dose equation”. In: *Platinum and Other Metal Coordination Compounds in Cancer Chemotherapy*. 1991, pp.335–343.
- [57] Miles P Hacker, Evan B Douple, and Irwin H Krakoff. *Platinum Coordination Complexes in Cancer Chemotherapy: Proceedings of the Fourth International Symposium on Platinum Coordination Complexes in Cancer Chemotherapy Convened in Burlington, Vermont by the Vermont Regional Cancer Center and the Norris Cotton Cancer Center, June 22–24, 1983*. Vol. 17. 2012.
- [58] WJF Van der Vijgh and I Klein. Protein binding of five platinum compounds. *Cancer Chemotherapy and Pharmacology* **18**(2) (1986), 129–132.
- [59] IE Smith, SJ Harland, BA Robinson, BD Evans, LC Goodhart, AH Calvert, J Yarnold, JP Glees, J Baker, and HT Ford. Carboplatin: a very active new cisplatin analog in the treatment of small cell lung cancer. *Cancer Treatment Report* **69**(1) (1985), 43–46.
- [60] Kenneth C Micetich, Diane Barnes, and Leonard C Erickson. A comparative study of the cytotoxicity and DNA-damaging effects of cis-(diammino)(1, 1-cyclobutanedicarboxylato)-platinum (II) and cis-diamminedichloroplatinum (II) on L1210 cells. *Cancer Research* **45**(9) (1985), 4043–4047.

- [61] Francis Lévi, Gérard Metzger, Claire Massari, and Gerard Milano. Oxaliplatin. *Clinical Pharmacokinetics* **38**(1) (2000), 1–21.
- [62] Satoshi Igawa, Sakiko Otani, Yoshiro Nakahara, Shinichiro Ryuge, Yasuhiro Hiyoshi, Tomoya Fukui, Hisashi Mitsufuji, Masaru Kubota, Masato Katagiri, Yuichi Sato, et al. Phase I study of Nedaplatin, a platinum based antineoplastic drug, combined with nab-paclitaxel in patients with advanced squamous non-small cell lung cancer. *Investigational New Drugs* **36**(1) (2018), 45–52.
- [63] Marta E Alberto, Maria Fatima A Lucas, Matej Pavelka, and Nino Russo. The second-generation anticancer drug Nedaplatin: a theoretical investigation on the hydrolysis mechanism. *The Journal of Physical Chemistry B* **113**(43) (2009), 14473–14479.
- [64] Murray S Davies, Susan J Berners-Price, and Trevor W Hambley. Slowing of cisplatin aquation in the presence of DNA but not in the presence of phosphate: improved understanding of sequence selectivity and the roles of mono-aquated and diaquated species in the binding of cisplatin to DNA. *Inorganic Chemistry* **39**(25) (2000), 5603–5613.
- [65] Franck Legendre, Véronique Bas, Jiří Kozelka, and Jean-Claude Chottard. A complete kinetic study of GG versus AG platination suggests that the doubly aquated derivatives of cisplatin are the actual DNA binding species. *Chemistry—A European Journal* **6**(11) (2000), 2002–2010.
- [66] Christopher J Cramer. *Essentials of computational chemistry: theories and models*. 2013.
- [67] P Hohenberg and WJPR Kohn. Density functional theory (DFT). *Physical Review* **136** (1964), B864.
- [68] Ana M Amado, Sónia M Fiuza, Maria PM Marques, and Luis AE Batista de Carvalho. Conformational and vibrational study of platinum (II) anticancer drugs: cis-diamminedichloroplatinum (II) as a case study. *The Journal of Chemical Physics* **127**(18) (2007), 11B612.
- [69] Magdalena Malik and Danuta Michalska. Assessment of new DFT methods for predicting vibrational spectra and structure of cisplatin: Which density functional should we

- choose for studying platinum (II) complexes? *Spectrochimica Acta Part A: Molecular and Biomolecular Spectroscopy* **125** (2014), 431–439.
- [70] I Georgieva, N Trendafilova, N Dodoff, and D Kovacheva. DFT study of the molecular and crystal structure and vibrational analysis of cisplatin. *Spectrochimica Acta Part A: Molecular and Biomolecular Spectroscopy* **176** (2017), 58–66.
- [71] Yang Wang, Qingzhu Liu, Ling Qiu, Tengfei Wang, Haoliang Yuan, Jianguo Lin, and Shineng Luo. Molecular structure, IR spectra, and chemical reactivity of cisplatin and transplatin: DFT studies, basis set effect and solvent effect. *Spectrochimica Acta Part A: Molecular and Biomolecular Spectroscopy* **150** (2015), 902–908.
- [72] Juliana Fedoce Lopes, Victor Ströele de A. Menezes, Hélio A Duarte, Willian R Rocha, Wagner B De Almeida, and Hélio F Dos Santos. Monte Carlo simulation of cisplatin molecule in aqueous solution. *The Journal of Physical Chemistry B* **110**(24) (2006), 12047–12054.
- [73] Amrit Sarmah and Ram Kinkar Roy. Understanding the preferential binding interaction of aqua-cisplatins with nucleobase guanine over adenine: a density functional reactivity theory based approach. *RSC advances* **3**(8) (2013), 2822–2830.
- [74] Rafał Wysokiński, Janina Kuduk-Jaworska, and Danuta Michalska. Electronic structure, Raman and infrared spectra, and vibrational assignment of carboplatin. Density functional theory studies. *Journal of Molecular Structure: THEOCHEM* **758**(2-3) (2006), 169–179.
- [75] Narbe Mardirossian and Martin Head-Gordon. Thirty years of density functional theory in computational chemistry: an overview and extensive assessment of 200 density functionals. *Molecular Physics* **115**(19) (2017), 2315–2372.
- [76] Enrico Clementi and Subhas J Chakravorty. A comparative study of density functional models to estimate molecular atomization energies. *The Journal of Chemical Physics* **93**(4) (1990), 2591–2602.
- [77] Stefan Grimme. Semiempirical hybrid density functional with perturbative second-order correlation. *The Journal of Chemical Physics* **124**(3) (2006), 034108.

- [78] Antonín Vlček Jr and Stanislav Zálaiš. Modeling of charge-transfer transitions and excited states in d6 transition metal complexes by DFT techniques. *Coordination Chemistry Reviews* **251**(3-4) (2007), 258–287.
- [79] Lan Cheng, Jürgen Gauss, and John F Stanton. Treatment of scalar-relativistic effects on nuclear magnetic shieldings using a spin-free exact-two-component approach. *The Journal of Chemical Physics* **139**(5) (2013), 054105.
- [80] Pekka Pyykkö. Relativistic effects in chemistry: more common than you thought. *Annual Review of Physical Chemistry* **63** (2012), 45–64.
- [81] Thomas M Gilbert. Tests of the MP2 Model and Various DFT Models in Predicting the Structures and B- N Bond Dissociation Energies of Amine- Boranes (X3C) m H3-m B- N (CH3) n H3-n (X= H, F; m= 0- 3; n= 0- 3): Poor Performance of the B3LYP Approach for Dative B- N Bonds. *The Journal of Physical Chemistry A* **108**(13) (2004), 2550–2554.
- [82] Elizabeth L Smith, Daniel Sadowsky, James A Phillips, Christopher J Cramer, and David J Giesen. A short yet very weak dative bond: structure, bonding, and energetic properties of N2- BH3. *The Journal of Physical Chemistry A* **114**(7) (2010), 2628–2636.
- [83] Luiz Antônio S Costa, Willian R Rocha, Wagner B De Almeida, and Hélio F Dos Santos. The solvent effect on the aquation processes of the cis-dichloro (ethylenediammine) platinum (II) using continuum solvation models. *Chemical Physics Letters* **387**(1-3) (2004), 182–187.
- [84] Johan Raber, Chuanbao Zhu, and Leif A Eriksson*. Activation of anti-cancer drug cis-platin—is the activated complex fully aquated? *Molecular Physics* **102**(23-24) (2004), 2537–2544.
- [85] Jaroslav V Burda, Michal Zeizinger, and Jerzy Leszczynski. Activation barriers and rate constants for hydration of platinum and palladium square-planar complexes: An ab initio study. *The Journal of Chemical Physics* **120**(3) (2004), 1253–1262.
- [86] Mu-Hyun Baik, Richard A Friesner, and Stephen J Lippard. Theoretical study of cisplatin binding to purine bases: why does cisplatin prefer guanine over adenine? *Journal of the American Chemical Society* **125**(46) (2003), 14082–14092.

- [87] Jaroslav V Burda, Michal Zeizinger, and Jerzy Leszczynski. Hydration process as an activation of trans- and cisplatin complexes in anticancer treatment. DFT and ab initio computational study of thermodynamic and kinetic parameters. *Journal of Computational Chemistry* **26**(9) (2005), 907–914.
- [88] Jorma Arpalahti, Marjaana Mikola, and Sari Mauristo. Kinetics and mechanism of the complexation of cis-diamminedichloroplatinum (II) with the purine nucleoside inosine in aqueous solution. *Inorganic Chemistry* **32**(15) (1993), 3327–3332.
- [89] Arturo Robertazzi and James A Platts. Hydrogen bonding, solvation, and hydrolysis of cisplatin: a theoretical study. *Journal of Computational Chemistry* **25**(8) (2004), 1060–1067.
- [90] Edward M Engler, Joseph D Andose, and Paul VR Schleyer. Critical evaluation of molecular mechanics. *Journal of the American Chemical Society* **95**(24) (1973), 8005–8025.
- [91] N Claude Cohen. *Guidebook on molecular modeling in drug design*. 1996.
- [92] Mark S Gordon, Dmitri G Fedorov, Spencer R Pruitt, and Lyudmila V Slipchenko. Fragmentation methods: A route to accurate calculations on large systems. *Chemical Reviews* **112**(1) (2012), 632–672.
- [93] Weitao Yang. Direct calculation of electron density in density-functional theory. *Physical Review Letters* **66**(11) (1991), 1438.
- [94] Michael A Collins and Vitali A Deev. Accuracy and efficiency of electronic energies from systematic molecular fragmentation. *The Journal of Chemical Physics* **125**(10) (2006), 104104.
- [95] Kazuo Kitaura, Eiji Ikeo, Toshio Asada, Tatsuya Nakano, and Masami Uebayasi. Fragment molecular orbital method: an approximate computational method for large molecules. *Chemical Physics Letters* **313**(3-4) (1999), 701–706.
- [96] Heather M Netzloff and Michael A Collins. Ab initio energies of nonconducting crystals by systematic fragmentation. *The Journal of Chemical Physics* **127**(13) (2007), 134113.
- [97] Dmitri G Fedorov. The fragment molecular orbital method: theoretical development, implementation in GAMESS, and applications. *Wiley Interdisciplinary Reviews: Computational Molecular Science* **7**(6) (2017), e1322.

- [98] Dmitri G Fedorov, Kazuo Kitaura, Hui Li, Jan H Jensen, and Mark S Gordon. The polarizable continuum model (PCM) interfaced with the fragment molecular orbital method (FMO). *Journal of Computational Chemistry* **27**(8) (2006), 976–985.
- [99] Kaori Fukuzawa, Chiduru Watanabe, Ikuo Kurisaki, Naoki Taguchi, Yuji Mochizuki, Tatsuya Nakano, Shigenori Tanaka, and Yuto Komeiji. Accuracy of the fragment molecular orbital (FMO) calculations for DNA: total energy, molecular orbital, and inter-fragment interaction energy. *Computational and Theoretical Chemistry* **1034** (2014), 7–16.
- [100] Dmitri G Fedorov, Toyokazu Ishida, Masami Uebayasi, and Kazuo Kitaura. The fragment molecular orbital method for geometry optimizations of polypeptides and proteins. *The Journal of Physical Chemistry A* **111**(14) (2007), 2722–2732.
- [101] Shinji Amari, Masahiro Aizawa, Junwei Zhang, Kaori Fukuzawa, Yuji Mochizuki, Yoshio Iwasawa, Kotoko Nakata, Hiroshi Chuman, and Tatsuya Nakano. VISCANA: Visualized cluster analysis of protein- ligand interaction based on the ab initio fragment molecular orbital method for virtual ligand screening. *Journal of Chemical Information and Modeling* **46**(1) (2006), 221–230.
- [102] Takeshi Ishikawa, Takakazu Ishikura, and Kazuo Kuwata. Theoretical study of the prion protein based on the fragment molecular orbital method. *Journal of Computational Chemistry* **30**(16) (2009), 2594–2601.
- [103] Dmitri G Fedorov and Kazuo Kitaura. The three-body fragment molecular orbital method for accurate calculations of large systems. *Chemical Physics Letters* **433**(1-3) (2006), 182–187.
- [104] Kaori Fukuzawa, Kazuo Kitaura, Masami Uebayasi, Kotoko Nakata, Tsuguchika Kaminuma, and Tatsuya Nakano. Ab initio quantum mechanical study of the binding energies of human estrogen receptor α with its ligands: an application of fragment molecular orbital method. *Journal of Computational Chemistry* **26**(1) (2005), 1–10.
- [105] Stanley B Prusiner. Novel proteinaceous infectious particles cause scrapie. *Science* **216**(4542) (1982), 136–144.
- [106] Stanley B Prusiner. Prions. *Proceedings of the National Academy of Sciences* **95**(23) (1998), 13363–13383.

- [107] Kazuo Kuwata, Noriyuki Nishida, Tomoharu Matsumoto, Yuji O Kamatari, Junji Hosokawa-Muto, Kota Kodama, Hironori K Nakamura, Kiminori Kimura, Makoto Kawasaki, Yuka Takakura, et al. Hot spots in prion protein for pathogenic conversion. *Proceedings of the National Academy of Sciences* **104**(29) (2007), 11921–11926.
- [108] Roland Riek, Simone Hornemann, Gerhard Wider, Martin Billeter, Rudi Glockshuber, and Kurt Wüthrich. NMR structure of the mouse prion protein domain PrP (121–231). *Nature* **382**(6587) (1996), 180–182.
- [109] David A Case, TA Darden, Thomas E Cheatham III, CL Simmerling, Junmei Wang, Robert E Duke, Ray Luo, Kenneth M Merz, David A Pearlman, Mike Crowley, et al. AMBER 9. *University of California, San Francisco* **45** (2006).
- [110] Viktor Hornak, Robert Abel, Asim Okur, Bentley Strockbine, Adrian Roitberg, and Carlos Simmerling. Comparison of multiple Amber force fields and development of improved protein backbone parameters. *Proteins: Structure, Function, and Bioinformatics* **65**(3) (2006), 712–725.
- [111] Koert NJ Burger, Rutger WHM Staffhorst, Hanke C de Vijlder, Maria J Velinova, Paul H Bomans, Peter M Frederik, and Ben de Kruijff. Nanocapsules: lipid-coated aggregates of cisplatin with high cytotoxicity. *Nature Medicine* **8**(1) (2002), 81–84.
- [112] Ewelina Lipiec, Joanna Czapla, Jakub Szlachetko, Yves Kayser, Wojciech Kwiatek, Bayden Wood, Glen B Deacon, and Jacinto Sá. Novel in situ methodology to observe the interactions of chemotherapeutical Pt drugs with DNA under physiological conditions. *Dalton Transactions* **43**(37) (2014), 13839–13844.
- [113] Jacinto Sá, Joanna Czapla-Masztafiak, Ewelina Lipiec, Yves Kayser, Wojciech Kwiatek, Bayden Wood, Glen B Deacon, Gilles Berger, François Dufrasne, Daniel LA Fernandes, et al. The use of Resonant X-ray Emission Spectroscopy (RXES) for the electronic analysis of metal complexes and their interactions with biomolecules. *Drug Discovery Today: Technologies* **16** (2015), 1–6.
- [114] Joanna Czapla-Masztafiak, Juan J Nogueira, Ewelina Lipiec, Wojciech M Kwiatek, Bayden R Wood, Glen B Deacon, Yves Kayser, Daniel LA Fernandes, Mariia V Pavliuk, Jakub Szlachetko, et al. Direct determination of metal complexes' interaction with DNA by

- atomic telemetry and multiscale molecular dynamics. *The Journal of Physical Chemistry Letters* **8**(4) (2017), 805–811.
- [115] Theophile Theophanides. Fourier transform infrared spectra of calf thymus DNA and its reactions with the anticancer drug cisplatin. *Applied Spectroscopy* **35**(5) (1981), 461–465.
- [116] Rukshani Haputhanthri, Ruchika Ojha, Ekaterina I Izgorodina, Si-Xuan Guo, Glen B Deacon, Don McNaughton, and Bayden R Wood. A spectroscopic investigation into the binding of novel platinum (IV) and platinum (II) anticancer drugs with DNA. *Vibrational Spectroscopy* **92** (2017), 82–95.
- [117] Peter Larkin. *Infrared and Raman spectroscopy: principles and spectral interpretation*. 2017.
- [118] A Rygula, Katarzyna Majzner, Katarzyna M Marzec, Agnieszka Kaczor, Marta Pilarczyk, and M Baranska. Raman spectroscopy of proteins: a review. *Journal of Raman Spectroscopy* **44**(8) (2013), 1061–1076.
- [119] Katrin Kneipp, Harald Kneipp, Irving Itzkan, Ramachandra R Dasari, and Michael S Feld. Ultrasensitive chemical analysis by Raman spectroscopy. *Chemical Reviews* **99**(10) (1999), 2957–2976.
- [120] JL Lippert, D Tyminski, and PJ Desmeules. Determination of the secondary structure of proteins by laser Raman spectroscopy. *Journal of the American Chemical Society* **98**(22) (1976), 7075–7080.
- [121] Warner L Peticolas. “[17] Raman spectroscopy of DNA and proteins”. In: *Methods in Enzymology*. Vol. 246. 1995, pp.389–416.
- [122] KA1 Okotrub, NV Surovtsev, VF Semeshin, and LV Omelyanchuk. Raman spectroscopy for DNA quantification in cell nucleus. *Cytometry Part A* **87**(1) (2015), 68–73.
- [123] Catarina Costa Moura, Rahul S Tare, Richard OC Oreffo, and Sumeet Mahajan. Raman spectroscopy and coherent anti-Stokes Raman scattering imaging: prospective tools for monitoring skeletal cells and skeletal regeneration. *Journal of The Royal Society Interface* **13**(118) (2016), 20160182.
- [124] T Kitagawa and AT Tu. *Introduction to Raman spectroscopy*. 1988.

- [125] Stephen C Erfurth, Ernest J Kiser, and Warner L Peticolas. Determination of the backbone structure of nucleic acids and nucleic acid oligomers by laser Raman scattering. *Proceedings of the National Academy of Sciences* **69**(4) (1972), 938–941.
- [126] Franck Legendre, Jiří Kozelka, and Jean-Claude Chottard. GG versus AG platination: A kinetic study on hairpin-stabilized duplex oligonucleotides. *Inorganic Chemistry* **37**(16) (1998), 3964–3967.
- [127] Theophile Theophanides. Fourier Transform Infrared Spectra of Calf Thymus DNA and its Reactions with the Anticancer Drug Cisplatin. *Applied Spectroscopy* **35**(5) (1981), 461–465.
- [128] Alberto De Petris, Alessandra Ciavardini, Cecilia Coletti, Nazzareno Re, Barbara Chiavarino, Maria Elisa Crestoni, and Simonetta Fornarini. Vibrational signatures of the naked aqua complexes from platinum (II) anticancer drugs. *The Journal of Physical Chemistry Letters* **4**(21) (2013), 3631–3635.
- [129] Robbin R Vernooij, Tanmaya Joshi, Evyenia Shaili, Manja Kubeil, Dominique RT Appadoo, Ekaterina I Izgorodina, Bim Graham, Peter J Sadler, Bayden R Wood, and Leone Spiccia. Comprehensive vibrational spectroscopic investigation of trans, trans, trans-[Pt (N3) 2 (OH) 2 (py) 2], a Pt (IV) diazido anticancer prodrug candidate. *Inorganic Chemistry* **55**(12) (2016), 5983–5992.
- [130] Deepak K Jangir, Gunjan Tyagi, Ranjana Mehrotra, and Suman Kundu. Carboplatin interaction with calf-thymus DNA: a FTIR spectroscopic approach. *Journal of Molecular Structure* **969**(1-3) (2010), 126–129.
- [131] Gilles Berger, Régis Gasper, Delphine Lamoral-Theys, Anja Wellner, Michel Gelbcke, Ronald Gust, Jean Nève, Robert Kiss, Erik Goormaghtigh, and François Dufrasne. Fourier transform infrared (FTIR) spectroscopy to monitor the cellular impact of newly synthesized platinum derivatives. *International Journal of Oncology* **37**(3) (2010), 679–686.
- [132] Alix Mignolet, Allison Derenne, Margarita Smolina, Bayden R Wood, and Erik Goormaghtigh. FTIR spectral signature of anticancer drugs. Can drug mode of action be identified? *Biochimica et Biophysica Acta (BBA)-Proteins and Proteomics* **1864**(1) (2016), 85–101.

- [133] PRAVINDYA RUKSHANI HAPUTHANTHRI. A Spectroscopic investigation into the binding of novel Platinum(IV) and Platinum(II) anticancer drugs with DNA and cells (2017). DOI: [10.4225/03/590fb381acb41](https://doi.org/10.4225/03/590fb381acb41).
- [134] Ekaterina I Izgorodina, Ching Yeh Lin, and Michelle L Coote. Energy-directed tree search: an efficient systematic algorithm for finding the lowest energy conformation of molecules. *Physical Chemistry Chemical Physics* **9**(20) (2007), 2507–2516.
- [135] Don McNaughton and Bayden R Wood. Synchrotron infrared spectroscopy of cells and tissue. *Australian Journal of Chemistry* **65**(3) (2012), 218–228.
- [136] Paul Dumas, Ganesh D Sockalingum, and Josep Sule-Suso. Adding synchrotron radiation to infrared microspectroscopy: what’s new in biomedical applications? *Trends in Biotechnology* **25**(1) (2007), 40–44.
- [137] ROSCOE KLINCK, ERIC WESTHOE, STEPHEN WALKER, MOHAMMAD AFSHAR, ADAM COLLIER, and FAREED ABOUL-ELA. A potential RNA drug target in the hepatitis C virus internal ribosomal entry site. *RNA* **6**(10) (2000), 1423–1431.
- [138] Alethia A Hostetter, Erich G Chapman, and Victoria J DeRose. Rapid cross-linking of an RNA internal loop by the anticancer drug cisplatin. *Journal of the American Chemical Society* **131**(26) (2009), 9250–9257.
- [139] Ignacio Tinoco Jr and Carlos Bustamante. How RNA folds. *Journal of Molecular Biology* **293**(2) (1999), 271–281.
- [140] Jason R Thomas and Paul J Hergenrother. Targeting RNA with small molecules. *Chemical Reviews* **108**(4) (2008), 1171–1224.
- [141] Katherine Deigan Warner, Christine E Hajdin, and Kevin M Weeks. Principles for targeting RNA with drug-like small molecules. *Nature Reviews Drug Discovery* **17**(8) (2018), 547–558.
- [142] Sergey V Melnikov, Dieter Söll, Thomas A Steitz, and Yury S Polikanov. Insights into RNA binding by the anticancer drug cisplatin from the crystal structure of cisplatin-modified ribosome. *Nucleic Acids Research* **44**(10) (2016), 4978–4987.

- [143] José Gallego and Gabriele Varani. Targeting RNA with small-molecule drugs: therapeutic promise and chemical challenges. *Accounts of Chemical Research* **34**(10) (2001), 836–843.
- [144] Katja Michael and Yitzhak Tor. Designing novel RNA binders. *Chemistry—A European Journal* **4**(11) (1998), 2091–2098.
- [145] C Frank Bennett and Eric E Swayze. RNA targeting therapeutics: molecular mechanisms of antisense oligonucleotides as a therapeutic platform. *Annual Review of Pharmacology and Toxicology* **50** (2010), 259–293.
- [146] K Asish Xavier, Paul S Eder, and Tony Giordano. RNA as a drug target: methods for biophysical characterization and screening. *Trends in Biotechnology* **18**(8) (2000), 349–356.
- [147] Elizabeth Iorns, Christopher J Lord, Nicholas Turner, and Alan Ashworth. Utilizing RNA interference to enhance cancer drug discovery. *Nature Reviews Drug Discovery* **6**(7) (2007), 556–568.
- [148] Carolyn Shasha, Robert Y Henley, Daniel H Stoloff, Kevin D Rynearson, Thomas Hermann, and Meni Wanunu. Nanopore-based conformational analysis of a viral RNA drug target. *ACS Nano* **8**(6) (2014), 6425–6430.
- [149] Alethia A Hostetter, Maire F Osborn, and Victoria J DeRose. RNA-Pt adducts following cisplatin treatment of *Saccharomyces cerevisiae*. *ACS Chemical Biology* **7**(1) (2012), 218–225.
- [150] Takuya Kumazawa, Kazuho Nishimura, Naohiro Katagiri, Sayaka Hashimoto, Yuki Hayashi, and Keiji Kimura. Gradual reduction in rRNA transcription triggers p53 acetylation and apoptosis via MYBBP1A. *Scientific Reports* **5**(1) (2015), 1–13.
- [151] Sylvie Chenavas, Thibaut Crépin, Bernard Delmas, Rob WH Ruigrok, and Anny Slama-Schwok. Influenza virus nucleoprotein: structure, RNA binding, oligomerization and antiviral drug target. *Future Microbiology* **8**(12) (2013), 1537–1545.
- [152] Quentin Vicens and Eric Westhof. RNA as a drug target: the case of aminoglycosides. *ChemBioChem* **4**(10) (2003), 1018–1023.

- [153] Thomas Hermann and Eric Westhof. RNA as a drug target: chemical, modelling, and evolutionary tools. *Current Opinion in Biotechnology* **9**(1) (1998), 66–73.
- [154] Neil D Pearson and Catherine D Prescott. RNA as a drug target. *Chemistry & Biology* **4**(6) (1997), 409–414.
- [155] David N Frick. The hepatitis C virus NS3 protein: a model RNA helicase and potential drug target. *Current Issues in Molecular Biology* **9**(1) (2007), 1.
- [156] Harry F Noller. RNA structure: reading the ribosome. *Science* **309**(5740) (2005), 1508–1514.
- [157] Geoffrey M Cooper and Robert E Hausman. *The cell: Molecular approach*. 2004.
- [158] Yitzhak Tor. Targeting RNA with small molecules. *ChemBioChem* **4**(10) (2003), 998–1007.
- [159] Peter Jordan and Maria Carmo-Fonseca. Cisplatin inhibits synthesis of ribosomal RNA in vivo. *Nucleic Acids Research* **26**(12) (1998), 2831–2836.
- [160] Christophe N N'soukpoé-Kossi, Caroline Descôteaux, Eric Asselin, Joseph Bariyanga, Heidar-Ali Tajmir-Riahi, and Gervais Bérubé. Transfer RNA bindings to antitumor estradiol-platinum (II) hybrid and cisplatin. *DNA and Cell Biology* **27**(6) (2008), 337–343.
- [161] V Cepero, B Garcia-Serrelde, V Moneo, F Blanco, AM Gonzalez-Vadillo, A Alvarez-Valdes, C Navarro-Ranninger, and A Carnero. Trans-platinum (II) complexes with cyclohexylamine as expectator ligand induce necrosis in tumour cells by inhibiting DNA synthesis and RNA transcription. *Clinical and Translational Oncology* **9**(8) (2007), 521–530.
- [162] Gerald A LeBlanc, Scott S Sundseth, Georg F Weber, and David J Waxman. Platinum anticancer drugs modulate P-450 mRNA levels and differentially alter hepatic drug and steroid hormone metabolism in male and female rats. *Cancer Research* **52**(3) (1992), 540–547.
- [163] Evyenia Shaili, Marta Fernández-Giménez, Savina Rodríguez-Astor, Albert Gandioso, Lluís Sandín, Carlos García-Vélez, Anna Massaguer, Guy J Clarkson, Julie A Woods, Peter J Sadler, et al. A photoactivatable platinum (IV) anticancer complex conjugated

- to the RNA ligand Guanidinoneomycin. *Chemistry–A European Journal* **21**(50) (2015), 18474–18486.
- [164] Jürgen Boer, Kenneth F Blount, Nathan W Luedtke, Lev Elson-Schwab, and Yitzhak Tor. RNA-selective modification by a platinum (II) complex conjugated to amino- and guanidinoglycosides. *Angewandte Chemie International Edition* **44**(6) (2005), 927–932.
- [165] Roman Mezencev. Interactions of cisplatin with non-DNA targets and their influence on anticancer activity and drug toxicity: the complex world of the platinum complex. *Current Cancer Drug Targets* **14**(9) (2014), 794–816.

Chapter 2

Selecting the appropriate level of theory to study the Infrared Spectra of Pt complexes

2.1 Introduction

To better understand the mechanism and activation of Pt-based anti-cancer drugs prior to binding to DNA, it is important to first identify a single level of theory is able to accurately describe the bonding in Pt complexes with different ligands appropriately. Infrared spectroscopy, specifically the Far Infrared (FIR) region ($0 - 600 \text{ cm}^{-1}$), has enabled us to identify the different nature of the donor-acceptor bonds present in cisplatin and carboplatin.^{1,2} These bonds, a special type of covalent bonds, have been demonstrated to be a challenge for quantum chemical methods.³⁻⁵ Despite the shortcomings of Density Functional Theory (DFT), it is still the most feasible approach to study these bonds. This approach represents a good balance between computational cost and accuracy to predict the FIR spectra of the Pt complexes. With a vast range of Density Functional Theory (DFT) functionals (PBE, PBE0, M06-L and M06-2X), basis sets (VDZ, VTZ, aVDZ and aVTZ), effective core potentials (ECPs) (VDZ-pp, VTZ-pp, aVDZ-pp and aVTZ-pp) and solvation models (IEFPCM, CPCM and SMD) available, it is necessary to identify the suitable level of theory to predict the bonding in Pt-based complexes, which

manifests itself in the FIR region. In addition, with the presence of different ligands, this study aimed to determine if one level of theory was sufficient to study both cisplatin and carboplatin.

A publication from *ACS Omega* is presented, demonstrating a systematic study that investigates the effects of different combinations of DFT functionals, basis sets, ECPs and solvation models on the prediction of FIR spectra of cisplatin and carboplatin. The aim of the study was to identify an appropriate level of theory that is able to predict the characteristic FIR bands of cisplatin (155, 201 and 323 cm^{-1}) and carboplatin (194, 348, 351, 441, 475 and 573 cm^{-1}). Geometry optimisations and frequency calculations were performed using different levels of theory and the predicted spectra were compared to previously published experimental spectra. An algorithm was written in Wolfram Mathematica[®] to determine the optimal level of theory to predict the experimental spectra. Lastly, Charges from Electrostatic Potentials Grid Method (ChelpG) was utilised to investigate the difference of electrostatic potential of the two Pt complexes.

Upon analysing the differences in the predicted spectra, the different basis set and ECPs resulted in insignificant deviation from the experimental spectra, resulting in a maximum mean absolute deviation of 4.0 cm^{-1} . The choice of DFT functional and solvation model plays a more significant role in predicting the spectra and two different levels of theory demonstrated to be optimal for the two Pt complexes. Whereas the combination of PBE and SMD was optimal to predict the characteristic bands of cisplatin, M06-L and either IEFPCM or CPCM was found to be optimal for carboplatin. This was explained by the different nature of Pt-ligand bonds present in the two complexes. Pt-Cl, found in cisplatin, was determined to possess more covalent characteristics than the Pt-O bond in carboplatin.

Vibrational frequencies corresponding to different bonds were found to be either over- or underestimated. For example, the Pt-Cl stretching vibration for cisplatin was usually overestimated, whereas the Pt-O stretching vibration for carboplatin was found to be either under- or overestimated. This study concludes that different levels of theory, due to the presence of diverse bond characteristics, should be determined to study different Pt complexes.

Influence of DFT Functionals and Solvation Models on the Prediction of Far-Infrared Spectra of Pt-Based Anticancer Drugs: Why Do Different Complexes Require Different Levels of Theory?

Eunice S. H. Gwee,[†] Zoe L. Seeger,[†] Dominique R. T. Appadoo,[‡] Bayden R. Wood,[§] and Ekaterina I. Izgorodina^{*,†}

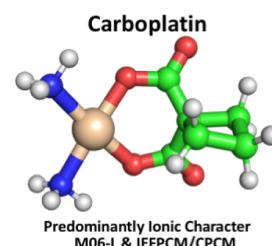
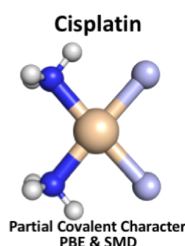
[†]Monash Computational Chemistry Group, School of Chemistry and [§]Centre for Biospectroscopy, School of Chemistry, Monash University, 17 Rainforest Walk, Clayton, Victoria 3800, Australia

[‡]Australian Synchrotron, 800 Blackburn Road, Clayton, Victoria 3168, Australia

Supporting Information

ABSTRACT: Computational modeling was applied to far-infrared (FIR) spectra of Pt-based anticancer drugs to study the hydrolysis of these important molecules. Here, we present a study that investigates the influence of different factors—basis sets on non-Pt atoms, relativistic effective core potentials (RECPs) on the Pt atom, density functional theory (DFT) functionals, and solvation models—on the prediction of FIR spectra of two Pt-based anticancer drugs, cisplatin and carboplatin. Geometry optimizations and frequency calculations were performed with a range of functionals (PBE, PBE0, M06-L, and M06-2X), Dunning's correlation-consistent basis sets (VDZ, VTZ, aVDZ, and aVTZ), RECPs (VDZ-pp, VTZ-pp, aVDZ-pp, and aVTZ-pp), and solvation models (IEFPCM, CPCM, and SMD). The best combination of the basis set/DFT functional/solvation model was identified for each anticancer drug by comparing with experimentally available FIR spectra. Different combinations were established for cisplatin and carboplatin, which was rationalized by means of the partial atomic charge scheme, ChelpG, that was utilized to study the charge transfer between the Pt ion and ligands in both cisplatin and carboplatin.

Prediction of Far IR Spectra



INTRODUCTION

Since its discovery by Rosenberg, cisplatin (Figure 1) has become one of the most commonly used anticancer drugs.^{1,2}

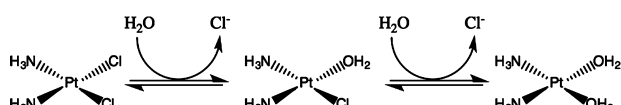


Figure 1. Hydrolysis of cisplatin to produce products that would form either a mono- or bifunctional adduct with DNA.

The chloride ion in cisplatin helps to stabilize the drug before activation.³ After absorption via diffusion, cisplatin is activated by hydrolysis, whereby the chloride ions are replaced with water molecules (Figure 1).⁴ The hydrolysis occurs as the drug passes from the blood plasma to the cell cytoplasm, where the concentration of chloride decreases.⁵ The activated form of cisplatin interacts with the purine base on guanine of the DNA sequence to form either mono- or bifunctional adducts, mostly by binding to two neighboring guanines (G) or neighboring guanine and adenine (A).^{4–6} These adducts form cross-links between base pairs on the same helical chain, resulting in the localized unwinding of the helix and increasing the width of the

minor groove.^{4,5,7} This disruption in structure thus interrupts the process of cell replication and initiates apoptotic cell death.^{4,7} Currently, there are uncertainties about the identity of the active form of cisplatin and in particular whether it is mono- or diaquated. Kinetic studies have indicated that the mono-aquated complex is the active form; however, in vitro studies have shown that the diaquated complex should be the active form instead.⁵

The use of cisplatin in cancer treatments is accompanied with a number of harmful side effects, such as diminishing hearing ability, nephrotoxicity, and neurotoxicity, which results from the accumulation of the active form of the drug in the body.^{2,8} This has motivated the discovery of other Pt-based compounds with less side effects to act as a substitute for cisplatin, like carboplatin (Figure 2).^{2,4} Carboplatin has more complex functional groups based on cyclobutane, and hence, it hydrolyzes at a slower rate compared to cisplatin (at least 2 orders of magnitude slower), thus decreasing the rate of accumulation and is therefore less toxic.² The mechanism of

Received: December 10, 2018

Accepted: February 25, 2019

Published: March 13, 2019

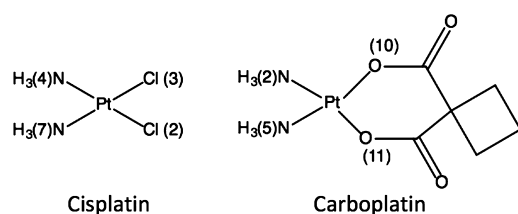


Figure 2. Platinum-based anticancer drugs. Cisplatin (left) and carboplatin (right). Number on the complexes reflects the identity of the ligands that are given in Tables 3 and 4.

carboplatin, unlike cisplatin, involves a two-step ring opening of the cyclobutanedicarboxylate group.⁹

Currently, there are still uncertainties with respect to the mechanism of how cisplatin and its derivatives hydrolyze prior to their binding to DNA. There is evidence that the hydrolysis of cisplatin might be a two-step process.^{6,10} Hambley et al. used [¹H, ¹⁵N] heteronuclear single quantum coherence two-dimensional nuclear magnetic resonance spectroscopy to study the kinetics of hydrolysis of cisplatin and its binding to a 14 base pair oligonucleotide (5'-d(AATTAGTACTAATT)-3').⁶ They identified that cisplatin hydrolyzed first to the mono-aquated form that subsequently formed a covalent bond with the guanine base of the oligonucleotide before it hydrolyzed to the diaquated form.⁶

Far-infrared (FIR) spectroscopy has the potential to unravel the mechanistic detail of this process and is particularly useful for investigating low-energy metal–ligand bonds. The FIR spectrum of cisplatin and carboplatin allows us to understand the nature of the donor–acceptor bonds whose stretching and bending vibrations can only be detected between 10 and 600 cm^{−1}.^{11,12} In addition, the FIR region can provide an insight into changes of metal–ligand interactions and hence, their activity.^{4,12,13} This, in itself, has been a challenge as reliable detection of the FIR region requires a bright light source, normally absent in conventional benchtop instruments because of less sensitive detectors, such as deuterated triglycine sulfate detectors.¹⁴ Because of this limitation, the FIR region of both cisplatin and carboplatin was measured with a synchrotron source that achieves high quality of spectra as the high brightness of FIR protons provides a high signal-to-noise ratio in the FIR region.¹⁵

The characteristic FIR vibrations of cisplatin and carboplatin have been identified previously by comparing the experimental spectra to those predicted with density functional theory (DFT).^{14,16,17} Wood et al. assigned main experimental bands to be 155, 201, and 323 cm^{−1} for cisplatin and 194, 348, 351, 441, 475, and 573 cm^{−1} for carboplatin.¹⁴ The presence of the heavy Pt cation increases the difficulty of assignment of all the vibrations in the FIR region because of band splitting.^{14,18–20} The heavy metal ion causes factor group splitting, a phenomenon that arises from vibrational coupling interactions in molecules or crystals, affecting the Pt–N vibrations.^{18–21} In addition, the presence of intermolecular hydrogen bonding between the complex molecules may also contribute to splitting of the stretching Pt–Cl and Pt–N bands.¹¹

The two Pt-based complexes—cisplatin and carboplatin—studied here possess donor–acceptor bonds between the Pt(II) ion and ligands, with Pt playing the role of an acceptor. These bonds are different from normal covalent bonds. The study by Wysocki et al. reported results of the natural bond orbital (NBO) analysis for both cisplatin and carboplatin. It

was found that the lone pair on the donor N atoms of cisplatin exhibits at least 85.3% p-type character and has occupancy of 1.719e, whereas the N atoms on carboplatin exhibit 81.5% p-type character.²² This indicates that there is a partial π -back donation to Pt orbitals, which is more apparent in carboplatin.²²

Luo et al. applied LC- ω PBE, mPW1PW, and PBE0 functionals, specifically DFT, to conduct structural, IR, and molecular orbital studies of two conformations of Pt-(NH₃)₂Cl₂—cisplatin and transplatin.²³ Analysis of the electrostatic potential on the two complexes revealed that cisplatin was more susceptible to nucleophilic attack compared to transplatin.²³ This conclusion further supports the observation that transplatin was inactive as an anticancer drug, on top of the inability of transplatin to form bifunctional adducts with DNA.^{24–26} Wysocki et al. compared the calculated spectra of carboplatin, using mPW1PW91 and MP2 methods with either LanL2DZ, D95V(d,p), and D95V++(d,p) basis sets in gas, to experimental data and identified the characteristic stretching and bending modes of carboplatin.²⁷ It was concluded that the mPW1PW91/LanL2DZ level of theory predicted the experimental spectra to be the best out of the combinations studied.²⁷ In addition, a study conducted by Barone et al. indicates the validity of DFT as a tool to study the Raman spectroscopy of cisplatin.²⁸ IR spectra calculated with the B3PW91-D3 and B2PLYP-D3 functionals were compared with the experimental spectra.²⁸ Mean absolute deviations (MADs) of 41 and 45 cm^{−1} were reported for these functionals.²⁸ The MAD decreased to 15 cm^{−1} when an anharmonic force field was used. It should be pointed out that in this case, MADs were applied to the full spectrum. On closer inspection of the data, the harmonic oscillator performed equally well in the FIR region.²⁸ Moreover, the results were computed in the gas phase, thus additionally affecting the quality of the prediction.²⁸

Since donor–acceptor bonds are special types of covalent bonds, accurate quantum chemical methods are required to predict their properties.^{14,27,29–31} The Pt–N bond in cisplatin has been proven to be difficult to model in previous studies, with B3LYP resulting in a longer Pt–N bond length and thus underestimating the stretching frequency.^{29–31} For example, DFT functionals, such as B3LYP and B3PW91, have been shown to produce inconsistent results in determining geometries and bond dissociation energy (BDE) of the B→N dative bond.²⁹ The study also demonstrated that MPW1K, a hybrid functional, consistently underestimated the BDE of the B→N bond by a root-mean-square deviation (rmsd) of 4.1 kcal mol^{−1} on average, producing the best results out of the tested functionals (PBE and mPW1PW91 giving rise to RMSDs of 4.5 and 5.1 kcal mol^{−1}, respectively).²⁹ Another study by Philips et al. indicated that it was challenging to identify a suitable DFT functional to predict IR spectra of a nitrile→BH₃ complex because of the presence of the dative bond.³⁰

Despite these shortcomings, DFT still represents the most computationally feasible approach to studying these bonds. FIR spectroscopy represents the most definitive indirect technique in probing the mode of donor–acceptor bonding in Pt-based anticancer drugs and thus, aid in unraveling their mechanism of action in the cell. Therefore, it is important to know limitations of current DFT functionals in the prediction of FIR spectra of these drugs. To date, no systematic study has been performed on the accuracy of DFT functionals for the prediction of stretching and bending vibrations of Pt–ligand

bonds. It is particularly important to establish which DFT functionals are reliable for the prediction of stretching vibrations as these are more likely to be affected by the accuracy of the selected functional as well as the inclusion of solvent effects, whereas bending vibrations might not be as sensitive.^{32,33} The dependency of stretching vibrations on the chosen functional was demonstrated in a study conducted by Wysokiński and Michalska, in which different DFT functionals resulted in underestimation of Pt–N stretching vibrations in cisplatin.³³ Although a number of theoretical strategies have been applied to offset systematic errors in the predicted frequencies (e.g., the application of scaling factors), different strategies might need to be applied for stretching and bending vibrations in the case of Pt–ligand dative bonds.^{34,35} In particular, electrostatic effects of the bulk on predicted spectra were not considered in the reported studies on Pt-based anticancer drugs.

In this work, we have performed a systematic study analyzing the accuracy and reliability of a series of DFT functionals (PBE, PBE0, M06-L, and M06-2X), Dunning's correlation consistent basis sets (VDZ, VTZ, aVDZ, and aVTZ), relativistic effective core potentials (RECPs) for Pt (VDZ-pp, VTZ-pp, aVDZ-pp, and aVTZ-pp), and solvation models (IEFPCM, CPCM, and SMD) for the prediction of experimental FIR spectra of cisplatin and carboplatin. The M06-L functional with no contribution from exact Hartree–Fock (HF) exchange was selected as it was originally designed to study transition metal complexes,³⁶ whereas PBE is traditionally used for studying metal surfaces.³⁷ Instead of Grimme's empirical dispersion correction,³⁸ the use of hybrid functionals such as PBE0 and M06-2X was adopted as the inclusion of the exact HF exchange was shown to reliably treat noncovalent interactions.^{39,40} Although there are a number of RECPs available,^{41–45} RECPs developed by Peterson et al.⁴⁶ were selected for the Pt atom because of their superior description of the valence electrons. These potentials showed excellent performance against the benchmark method, CCSDTQ, for the atomic properties of 5d elements.⁴⁶ Geometry optimizations and frequency calculations were performed on cisplatin and carboplatin, respectively, using different combinations of the DFT functionals, basis sets, and solvation models. The previously characteristic experimental peaks of both platinum complexes were used as a reference to the predicted spectra. The optimal combination of the functional, basis set, and solvation model to predict the experimental spectra was identified. In addition, the effect of each factor was also analyzed to determine the extent of its influence on the predicted spectra and stretching vibrations of Pt–ligand bonds in particular. Last, charges from electrostatic potentials grid method (ChelpG) analysis were performed on both cisplatin and carboplatin to study the electrostatic potential of the Pt metal ion and ligands and the differences between the two different complexes.

THEORETICAL PROCEDURES

All molecular orbital calculations were performed using the Gaussian 09 quantum chemical package. Both complexes of interest, cisplatin and carboplatin, were subjected to geometry optimization, followed by a frequency calculation. For both complexes, the Pt cation center has a square planar (C_{2v}) symmetry.^{31,33,34} Carboplatin has a similar geometry, with the Cl^- anions being replaced with the cyclobutanedicarboxylate group.^{1,2,27}

Four different DFT functionals were chosen for this study: PBE,³⁷ M06-L,³⁶ PBE0,³⁹ and M06-2X.⁴⁰ PBE is a generalized gradient approximation (GGA) functional developed by Perdew, Burke, and Ernzerhof.³⁷ PBE0, a hybrid functional developed by Adamo, builds on the PBE functional to include 25% HF exchange energy.³⁹ HF exchange energy improves the accuracy of chemical property predictions, for example, atomization energies and ionization potentials, of small- to medium-sized systems, especially for noncovalent interactions and excited states.^{47–49} Upon the addition of the 25% HF exchange energy, PBE0 is comparable to other more heavily parameterized functionals for the prediction of structures and molecular properties, such as kinetic and thermodynamic properties.^{39,49} M06-L and M06-2X are Minnesota functionals, with the former being a meta-GGA functional and the latter being a hybrid meta-GGA functional.^{36,40} M06-L, a local density functional, takes into consideration the local spin density, the local spin gradient, as well as the spin kinetic energy density.^{31,36} This allows M06-L to provide higher efficiency for larger systems, specifically to study the thermodynamics of transition metal complexes.³⁶ In addition, being a local density functional, M06-L has been successfully benchmarked for the MLBE21/05 database containing organometallic and inorganometallic complexes, such as $CrCH_3^+$ and $Fe(CO)$, to reproduce the benchmark data within 5.4 kcal mol^{−1} on average for transition metal–ligand bond energies. M06-L has also been benchmarked for intermolecular hydrogen bonds using the HB6/04 database, which contains hydrogen-bonded complexes such as dimers of ammonia and water, with M06-L predicting the smallest mean unsigned error of 0.36 kcal mol^{−1}.³⁶ M06-2X contains 54% of HF exchange and was formulated to meet five different criteria, including the description of noncovalent interactions, transition metal bonding, and electronic spectroscopy predictions.⁴⁰ M06-2X has also been successfully benchmarked for the π TC13 and TME53 databases consisting of varying complexes with π – π stacking interactions and ionization potentials, producing mean unsigned errors of 1.40 and 2.54 kcal mol^{−1}, respectively.⁴⁰

The two complexes of interest were studied using different implicit solvation models: integral equation formalism polarizable continuum model (IEFPCM),⁵⁰ conductor-like polarizable continuum model (CPCM),⁵¹ and solute model based on density (SMD),⁵² with water as the solvent. These implicit solvation models place the molecule of interest into a cavity, whose surface charge is stabilized in accordance with the dielectric constant of the selected solvent, thus simulating the effect of the solute being exposed to the solvent.^{52,53} Both IEFPCM and CPCM apply the dielectric permittivity, ϵ , of the solvent as a uniform medium with the solute placed in a cavity.^{50,51,54} The difference between IEFPCM and CPCM lies in the method used to define the cavity. IEFPCM makes the use of connected spheres to model the solute, with radii of the spheres matching those of solute atoms.^{50,54} The uniform dielectric permittivity of the solvent acts on the wavefunction of the modeled solute.⁵⁰ CPCM, on the other hand, makes the use of unique, small regions on these connected spheres called tesserae.⁵¹ These tesserae are defined by their individual position and interaction with the dielectric constant.⁵¹ Partial charges are then assigned to each of the tesserae based on the electrostatic potential. SMD is a model that makes use of a smooth continuous model to assign charges on the molecular surface of the solute.⁵² For SMD, the solute is polarizable by

the charge density of the solvent and the interaction between the solute and solvent can be determined via the charge density of the former and the electric polarization field of the latter.⁵² In addition, SMD has proven to be an effective solvation model for use in both charged and uncharged systems and is able to predict accurate solvation energies for various different functional groups, achieving an average of mean absolute error of 4 kcal mol⁻¹ for ions.⁵²

RECPs were employed on the Pt atom to model the inner core electrons to reduce computational costs.^{46,55} Developed by Peterson et al., these RECPs were taken from multi-configuration Dirac–Hartree–Fock calculations for 5d elements that also explicitly included relativistic effects.⁴⁶ RECPs are regularly used to model heavy atoms as they aid to decrease computational costs and already take relativistic effects into consideration.^{41,56} In a study conducted by Xu and Truhlar, a range of RECPs, cc-pVxZ-pp (x = D, T, Q, 5), LANL2DZ, and MDF28, were utilized to investigate the dissociation energy of diatomic molecules, for example, As₂ and AsFe.⁴¹ They determined that the relativistic ECPs developed by Peterson et al. performed the best, with VTZ-pp producing an average mean unsigned error of 1.1 kcal mol⁻¹.⁴¹ In this study, the RECPs used for the Pt metal ion are VDZ-pp, VTZ-pp, aVDZ-pp, and aVTZ-pp.

A series of Dunning's basis sets—VDZ, VTZ, aVDZ, and aVTZ—were chosen for this study, enabling the systematic approximation to the complete basis set (CBS) limit.⁵⁷ Augmented basis sets, aVDZ and aVTZ, were also considered because of their superior treatment of induction interactions.⁵⁷

This study aims to identify the optimal combination of the functional, basis set for the non-Pt atoms, RECP for the Pt metal ion, and solvation model to predict the experimental FIR spectra of Pt complexes. The statistical tools used in this study are the mean deviation, denoted as mean, standard deviation (SD), and the MAD. The mean denotes how accurate the predicted spectra are to the experimental spectra. MAD is calculated with eq 1 and indicates the spread of the peaks calculated in the predicted spectra when compared to the experimental spectra. SD is calculated with eq 2.

$$\text{MAD} = \frac{\sum_i |v_i - \omega_i|}{n} \quad (1)$$

$$\text{SD} = \sqrt{\frac{\sum (v_i - \omega_i)^2}{n - 1}} \quad (2)$$

where v_i and ω_i are experimental and calculated wavenumber values, respectively, and n is the number of peaks compared.

In the following figures, the MAD is represented by the horizontal line in the box plot, as seen in Figure 3. The MAD is

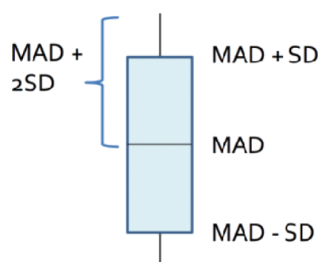


Figure 3. Box plot, representing MAD and SD to indicate the deviation of the predicted peaks to the experimental peaks.

used to demonstrate the deviation of predicted peaks to the experimental peaks. The upper and lower quantile of the box is the SD about the MAD, and the whiskers represent the spread of twice the SD about the MAD. In this analysis, it is preferred that MAD to be as close to zero as possible and the box to be as narrow as possible.

RESULTS AND DISCUSSION

The calculated results in this study are compared to the previously experimentally measured spectra.^{14,31} Tables 1 and 2 present the characteristic peaks of both cisplatin and carboplatin, respectively. Each peak is assigned to a specific type of vibration observed in the FIR region.

Table 1. Comparison of Experimental and Predicted (Gas-Phase PBE/VDZ with VDZ-pp RECP on Pt) Characteristic FIR Peaks of Cisplatin

experimental wavenumber (cm ⁻¹)	predicted wavenumber (cm ⁻¹)	assignment ^a
155 ^{14,31}	156	$\gamma(\text{N-Pt-N}) + \gamma(\text{Cl-Pt-Cl})$
201 ^{14,31}	223	$\alpha(\text{N-Pt-N}) + \alpha(\text{Cl-Pt-Cl})$
323 ^{14,31}	339/350	$\nu_{\text{asym}}(\text{Pt-Cl}) + \nu_{\text{sym}}(\text{Pt-Cl})$

^a γ —out-of-plane bending; α —scissoring; ν_{sym} —symmetric stretching; ν_{asym} —asymmetric stretching.

Table 2. Experimental and Predicted (Gas-Phase PBE/VDZ with VDZ-pp RECP on Pt) Characteristic FIR Peaks of Carboplatin

experimental wavenumber (cm ⁻¹)	predicted wavenumber (cm ⁻¹)	assignment ^a
194 ^{14,27}	192	$\alpha(\text{N-Pt-N})$
348 ^{14,27}	341	$\nu(\text{Pt-O})$
351 ^{14,27}	352	$\nu(\text{Pt-O})$
441 ^{14,27}	450	$\nu_{\text{sym}}(\text{Pt-N})$
475 ^{14,27}	465	$\alpha(\text{O-Pt-O}) + \nu_{\text{sym}}(\text{Pt-N})$
573 ^{14,27}	565	$\alpha(\text{O-Pt-O})$

^a α —scissoring; ν —stretching; ν_{sym} —symmetric stretching; ν_{asym} —asymmetric stretching. Differences between the calculated and experimental peaks were calculated for each combination of the DFT functional/basis set/solvent model.

In order to make an unbiased assignment of the predicted spectra to experimental bands, for each predicted peak the differences to all experimental wavenumber values were calculated. The smallest difference dictated the assignment of the predicted band to the corresponding experimental band. An independent assignment was performed this way for four varying conditions—DFT functional, basis set on non-Pt atoms, RECP basis set on Pt, and solvent model. An example of predicted and experimental band alignment is shown in Figure 4, in which the RECP basis set varied from VDZ-pp to aVTZ-pp. In order to assess the performance of each DFT functional/basis set/solvent model combination, mean and MAD values were computed. Additionally, these statistical measures were used to ensure that the correct band assignment was achieved.

In the case of cisplatin, two predicted peaks would manifest in the 335–355 cm⁻¹ region, with the peak with the lower wavenumber corresponding to $\nu_{\text{asym}}(\text{Pt-Cl})$ and the higher wavenumber corresponding to $\nu_{\text{sym}}(\text{Pt-Cl})$.^{14,17} In the

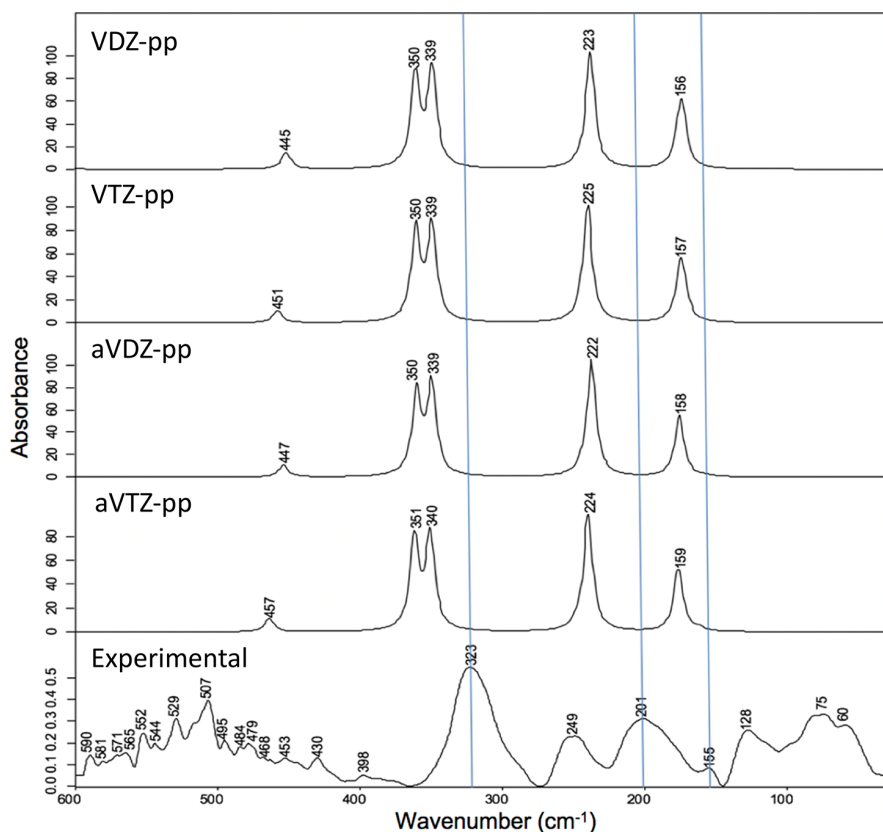


Figure 4. Example of alignment of the three characteristic peaks of cisplatin to predicted spectra. Spectra were obtained with the PBE functional in the gas phase combined with the VDZ basis set on non-Pt atoms. RECPs on Pt are given on the left top corner of each spectrum.

experimental data, only one broad peak was detected, an overlapping of both the symmetric and asymmetric Pt–Cl stretch.^{14,17} In this case, the closer predicted peak out of the two (symmetric and asymmetric) was taken into consideration for peak allocation. Despite being represented by one broad peak in the experimental data, the two different types of stretching—symmetric and asymmetric—manifest at slightly different wavenumber values.

The 249 cm^{-1} peak that is found in the experimental spectra was initially assigned to the $\text{NH}_3\text{--Pt--NH}_3$ bending vibration arising from the cisplatin dimer.¹⁷ In this study, we focus on the vibrations that represent the Pt-based complex monomers and, therefore, this peak was not considered.

The same assignment process was performed for carboplatin, as shown in Figure 5. It was noted that there are a few weak peaks detected at 230, 248, and 320 cm^{-1} . Some of these peaks were originally assigned to bending/stretching vibrations of the carboxylate groups. For example, the band located at 320 cm^{-1} was assigned to a rocking vibration of the cyclobutanedicarboxylate group.²⁷ It was outside the scope of this study to investigate these types of vibrations, and therefore, these peaks were not considered.

Further in the text, we look at each of the four criteria for both cisplatin and carboplatin separately to identify the best combination to predict FIR spectra for each compound.

Selection of Effective Core Potential on Pt and Basis Set on Non-Pt Atoms for Cisplatin. The SD values calculated for the four DFT functionals in the gas phase are shown in Figure 6 by varying the basis sets applied for both Pt and non-Pt atoms. Analysis of Figure 6 reveals that apart from

the PBE0 functional, the SD values fall in a narrow range of 13.5–23.0 cm^{-1} . PBE0 produces slightly larger errors of up to 35.0 cm^{-1} . On the other hand, the effect of the basis sets of both Pt and non-Pt atoms appears to be very minimal. This was studied by taking the maximum difference in both MAD and SD (labeled as \pm further in the text) when different RECP and basis sets were applied. For example, the maximum difference in MAD when the VDZ basis set was applied for the non-Pt atoms is $19.0 \pm 19.2 \text{ cm}^{-1}$ and the maximum difference when VDZ-pp RECP was applied for the Pt ion is $18.7 \pm 20.31 \text{ cm}^{-1}$. The maximum differences of the different basis sets and RECPs were 4.0 ± 4.25 and $2.0 \pm 3.6 \text{ cm}^{-1}$, respectively. The VTZ-pp RECP basis set for Pt was found to produce the smallest MAD values in the range of 15.6–21.5 cm^{-1} , for all functionals except PBE0, regardless of the choice of basis set on non-Pt atoms.

In order to select the best-performing basis set for non-Pt atoms, the performance of the four DFT functionals was compared while keeping the VTZ-pp RECP basis set constant for the Pt atom. The corresponding MAD and SD values are presented in a box and whisker plot in Figure 7. These box and whisker plots give an indication of the spread of the calculated peaks about the characteristic experimental peaks. Ideally, a combination of the MAD close to zero and a narrow distribution in SD indicates the best performance of the method.

Analysis of Figure 7 reveals that the increasing basis set on non-Pt atoms does not alter the performance of the DFT functionals, with triple- ζ quality basis sets giving marginally larger errors compared to double- ζ ones. Out of these, the

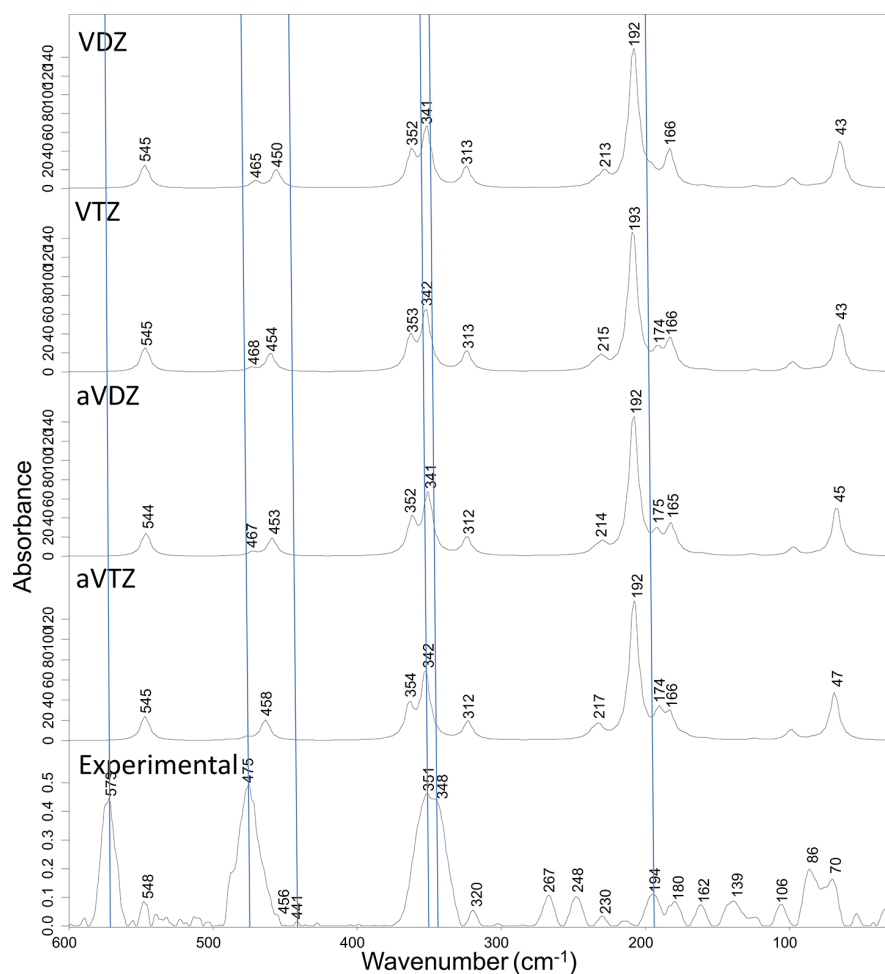


Figure 5. Example of alignment of the five characteristic peaks of carboplatin to predicted spectra. Spectra were obtained with the PBE functional in the gas phase combined with the VDZ basis set on non-Pt atoms. RECPs on Pt are given on the left top corner of each spectrum.

PBE0 functional was found to exhibit the largest MAD and SD values of 25.0 and 33.3 cm^{-1} , respectively. The MAD and SD values of PBE, M06-L, and M06-2X functionals are as follows: 15.0 ± 21.5 , 11.0 ± 20.0 , and 11.0 ± 18.4 cm^{-1} . Out of the four functionals, M06-L and M062X give the MAD values closer to zero, with the former producing slightly smaller SD values of 15.6 cm^{-1} for the VDZ basis set. To this end, the VDZ basis set was established to be the optimal basis set for non-Pt atoms in the gas phase regardless of the DFT functional. Further in the text, only results calculated with the VDZ basis set on non-Pt atoms and the VTZ-pp RECP basis set on Pt are discussed for cisplatin.

The effect of solvent model is shown in a box and whisker plot in Figure 8, in which the VDZ basis set was used for non-Pt atoms and the VTZ-pp RECP basis set for Pt. Analysis of these results reveals that the choice of functionals and solvation models plays a significant role in the prediction of the characteristic FIR wavenumbers of cisplatin. Some functionals are affected more than the others. For example, the PBE0 functionals show the largest reduction in the MAD and SD values going from the gas phase to SMD. The MAD and SD values for PBE0 decreased from 24.3 ± 32.6 to 5.0 ± 9.3 cm^{-1} from the gas phase to SMD. The Minnesota functionals undergo the least changes, with M062X giving the largest MAD errors of 19.7 and 20.7 cm^{-1} in combination with the

IEFPCM and CPCM models, respectively. The SMD model appears to produce the lowest MAD and SD errors for all four DFT functionals, with PBE showing the MAD value as low as 5.7 cm^{-1} . These results identify the importance of selecting an optimal combination of solvent model and DFT functional for studying donor–acceptor bonds in Pt-based complexes because of their polar properties⁵⁸ as well as the π -back donation of lone pairs on N/Cl atoms to unoccupied orbitals on Pt.⁵⁹ It was previously hypothesized that the π -back donation could dictate the characteristic of the Pt–N bond.⁵⁹ It has been shown previously that increasing the polarity of the solvent (from C_6H_6 to CH_3CN) has a stabilizing effect on the donor–acceptor bond in the previously studied compounds such as polyenes.^{58,60,61}

Out of the three FIR bands identified from the experimental spectrum of cisplatin, there is only one stretching vibration observed at 323 cm^{-1} . It has been previously reported that both stretching and bending vibrations are usually overestimated when calculated using HF or DFT methods in the gas phase.⁶² This was also previously observed in a cisplatin study conducted by Wang et al., where the IR spectra were calculated in the gas phase using LC- ω PBE functional, 6-311++G** basis set on the non-Pt atoms, and SDD ECP on the Pt ion in both the gas phase and SMD solvation model with water as the solvent.²³ A calculation performed in the gas phase

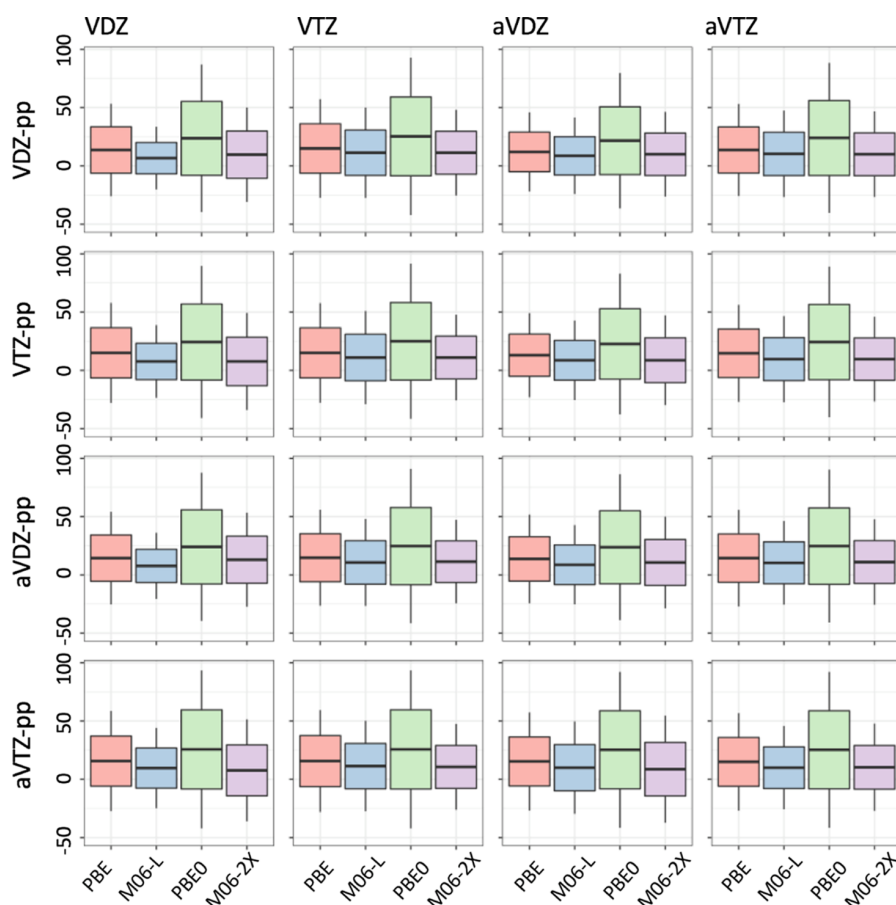


Figure 6. Effect of RECPs on the Pt atom (y-axis) and basis sets on the non-Pt atoms (x-axis) on the MAD (horizontal line) and SD values (upper and lower quantile of box) of PBE, M06-L, PBE0, and M06-2X DFT functionals used on gas-phase optimized geometries of cisplatin. All values given in cm^{-1} .

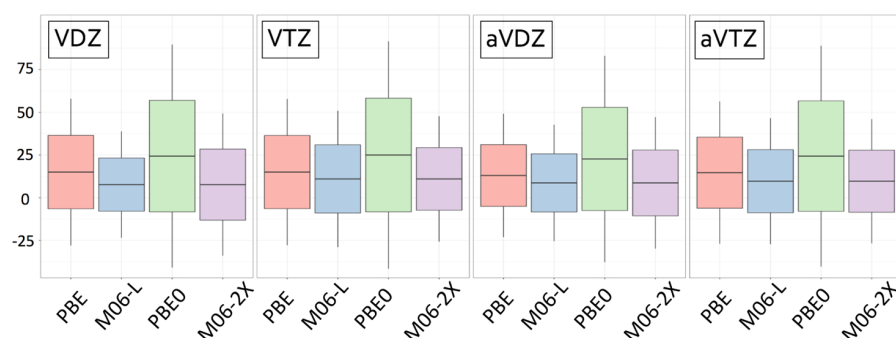


Figure 7. Box and whisker plots depicting the effect of basis sets (x-axis) on non-Pt atoms on the performance of DFT functionals using gas-phase optimized geometries of cisplatin and the VTZ-pp RECP basis set on Pt. All values given in cm^{-1} .

predicted that the Pt–Cl bond length is shorter by 0.035 Å and the Pt–N bond length is longer by 0.076 Å compared with the experimental data.²³ Both Pt–Cl and Pt–N stretching vibrations were overestimated, and a scaling factor of 0.95 was applied to the spectra.²³ As the SMD solvation model was utilized in the optimization of cisplatin, it decreases the error in predicted bond lengths—Pt–N is 0.037 Å and Pt–Cl is 0.006 Å longer than the experimental data.²³ The absence of the solvation field has proven to decrease the accuracy in predicting the geometry of cisplatin and, therefore, the IR spectrum.²³ Stretching vibrations also appear to be more

sensitive to the choice of level of theory because of their increased strength compared to that of bending ones.⁶² As expected, the stretching vibration is overestimated by 32 cm^{-1} for the combination of PBE0 and the gas phase. This stretching vibration becomes underestimated with the inclusion of solvation models by as much as 33 cm^{-1} with M06-2X and CPCM solvation model, with two exceptions (PBE0 functional with IEFPCM and SMD solvation model where the stretching vibration is overestimated by 5 and 1 cm^{-1} , respectively). The bending vibrations were usually overestimated, with PBE0 functional in the gas phase giving the largest SD of 33.2 cm^{-1} .

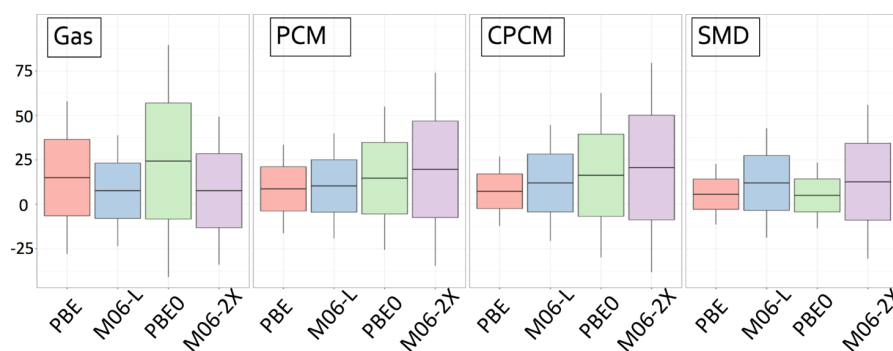


Figure 8. Box and whisker plots depicting the effect of solvent models (x -axis) on the performance of DFT functionals of cisplatin using the VTZ-pp RECP basis set on Pt and VDZ basis set on the non-Pt atoms. All values given in cm^{-1} .

It was observed that γ bending vibrations were consistently overestimated when compared to the 155 cm^{-1} experimental peak, with the largest deviation of 15 cm^{-1} being produced with the PBE functional and the IEFPCM. α bending vibrations, an in-plane scissoring vibration that is represented by the 201 cm^{-1} experimental peak, is considerably less consistent as compared to the prediction of γ bending, which is an out-of-plane bending vibration, with a combination of both over- and underestimation. The largest underestimation and overestimation of the α bending vibrations resulted with PBE0 in gas (32 cm^{-1}) and M06L with SMD (13 cm^{-1}), respectively. In the case of cisplatin, the absolute deviations of the only stretching vibration in cisplatin are shown in Figure 9. Upon

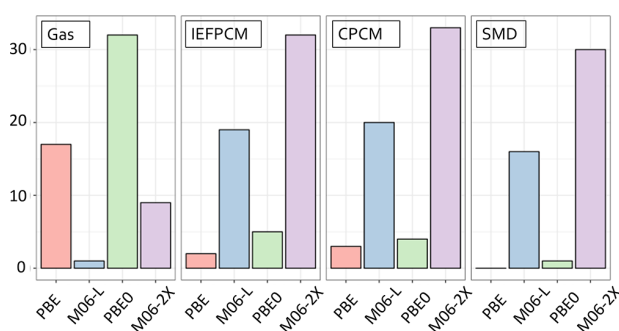


Figure 9. Absolute errors (in cm^{-1}) of solvation models and functionals for the prediction of the cisplatin stretching vibration at 323 cm^{-1} .

comparison of Figures 8 and 9, the main contribution of MAD in Figure 8 is due to the MAD that arose from the stretching vibration. For example, the use of PBE0 in conjunction with the gas phase resulted in the large MAD of stretching vibration, 32.0 cm^{-1} , and a large overall MAD, of 24.3 cm^{-1} , when all three experimental peaks were compared. In other cases, with M06-2X functional and solvation models, the MAD recorded for the stretching vibration is between 30.0 and 33.0 cm^{-1} . The stretching vibration has the biggest contribution to the MAD when compared to all three experimental peaks. Overall, the PBE and PBE0 functionals reproduce the stretching vibration in cisplatin within as low as 1 cm^{-1} when combined with the SMD solvation model. The MAD values for these functionals (see Figure 8) come entirely from overestimation of the two bending vibrations.

In the case of cisplatin, the combination of the SMD solvation model and the PBE functional appears to be the optimal combination to predict its FIR spectrum.

Selection of Effective Core Potential on Pt and Basis Set on Non-Pt Atoms for Carboplatin. As in the case of cisplatin, the effect of the basis set applied for non-Pt atoms was found to be minimal (see Figure 10). The PBE0 functional has been demonstrated to give rise to the larger range of SD values, a minimum of 20.0 cm^{-1} , among the four functionals. Excluding PBE0, the SD values of the other three functionals lie between a smaller range of 8.7 – 15.7 cm^{-1} . The maximum SD values were found to be 14.5 cm^{-1} for the aVDZ basis set on the non-Pt atoms and 13.9 cm^{-1} with the aVTZ-pp RECP on the Pt ion. The change in SD values across basis sets and RECPs was 0.8 and 0.4 cm^{-1} , respectively. The maximum MAD values were found to be 11.4 and 13.0 cm^{-1} for the aVTZ basis set and aVTZ-pp RECP, respectively. The variation in MAD values across basis sets and RECPs fell in the region of 1.6 and 2.7 cm^{-1} . As for cisplatin, the effect of the RECP basis set on Pt on the carboplatin vibrations was small, with VTZ-pp showing the best trade-off between accuracy and cost as demonstrated in Figure 11 (MAD values between 5.8 and 9.8 cm^{-1} excluding PBE0). The VDZ basis set was again sufficient for non-Pt atoms, where the VTZ-pp RECP was the best option for the Pt atom.

In the case of carboplatin, it is evident that the influence of solvation model and functional (see Figure 12) is different when compared to that of cisplatin. Out of all combinations tested, the M06-L functional together with CPCM produced the least MAD and SD values of 6.8 and 9.1 cm^{-1} , respectively. Surprisingly, the PBE0 functional in combination with the SMD model generated the largest errors, with MAD and SD being 19.0 and 30.5 cm^{-1} , respectively, which is in contrast to the trend found in cisplatin. M06-2X produced second best results, apart from the SMD model. Overall, the Minnesota functionals performed better for carboplatin than for cisplatin. This striking difference might be attributed to the differences between the description of the donor–acceptor bonds present in the two complexes: Pt–Cl bond versus the Pt–O bond. Analysis of the atomic charges fitted to reproduce the electrostatic potential using the ChelpG, it was confirmed that the Pt–Cl bond had more covalent characteristics compared to the Pt–O bond. For gas-phase optimized geometries, the predicted charges on the Cl atoms in cisplatin and O atoms in carboplatin are approximately $-0.7e$ and $-1.5e$, respectively. This trend is further supported by the charges on Pt atoms, which were predicted to be $1.8e$ and $2.1e$

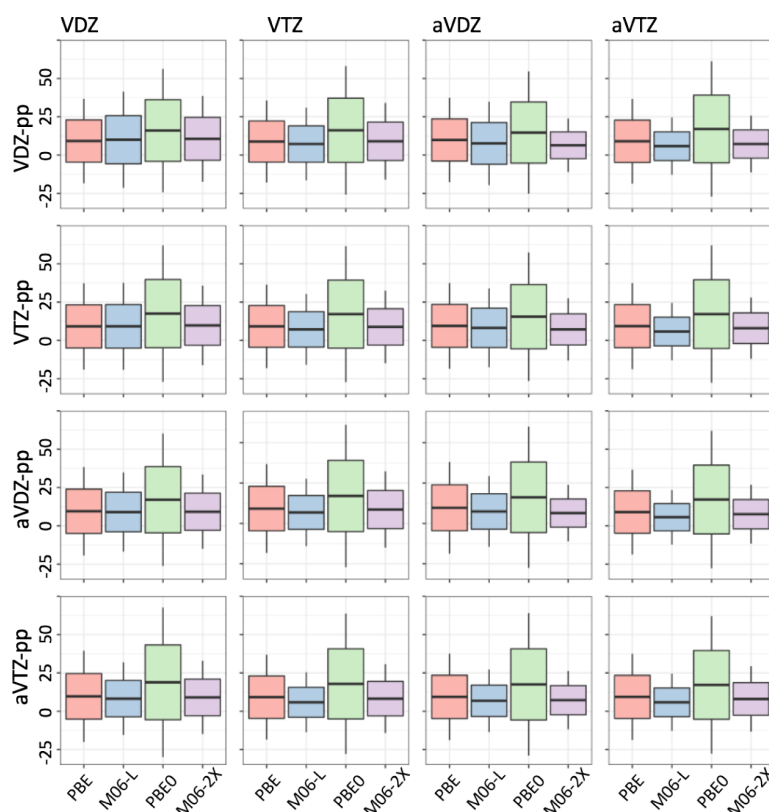


Figure 10. Effects of RECPs on the Pt atom (y-axis) and basis sets on the non-Pt atoms (x-axis) on the MAD (horizontal line) and SD values (upper and lower quantile of box) of PBE, M06-L, PBE0, and M06-2X functionals used on gas-phase optimized geometries of carboplatin. All values given in cm^{-1} .

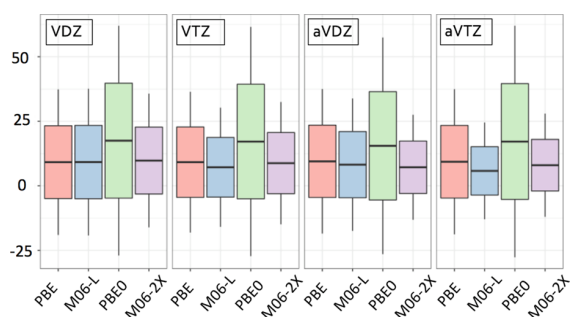


Figure 11. Box and whisker plots depicting the effect of basis set (x-axis) on non-Pt atoms on the performance of DFT functionals using gas-phase optimized geometries of carboplatin and VTZ-pp RECP basis set carboplatin. All values given in cm^{-1} .

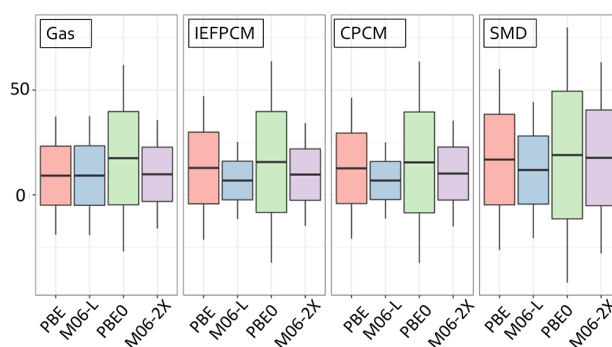


Figure 12. Box and whisker plots depicting the effect of solvent models (x-axis) on the performance of DFT functionals of carboplatin using the VTZ-pp RECP basis set on Pt and VDZ basis set on non-Pt atoms. All values given in cm^{-1} .

for cisplatin and carboplatin, respectively. Solvent-phase optimized geometries produced similar trends as discussed below. The partial charge on the chloride and charge on Pt $< 2.0e$ in cisplatin clearly demonstrate a charge transfer on the Pt–Cl bond of $0.3e$. In the case of carboplatin, there does not seem to be a charge transfer between the Pt and O atoms. This observation explains why M06-L performs better for carboplatin and PBE performs better for cisplatin. The outstanding performance of M06-L is expected as the functional was developed for treating transition metal complexes.³⁶ As mentioned before, PBE is a GGA functional that is an improvement to the local density approximation and

is able to better describe covalent bonds compared to M06-L.^{36,37,63}

In the carboplatin case, there are three pure stretching vibrations out of six (located at 348, 351, and 441 cm^{-1}) and a peak (located at 475 cm^{-1}) that has both stretching and bending contributions assigned experimentally in the FIR region. The MAD and SD values for the stretching vibrations are given in Figure 13. The stretching vibrations of carboplatin are not as consistently underestimated as compared to those cisplatin, noting that these vibrations usually manifest as a mixture of vibrations. For example, the theoretical bands at 341 and 352 cm^{-1} assigned to the $\nu(\text{Pt}–\text{O})$ vibration are usually

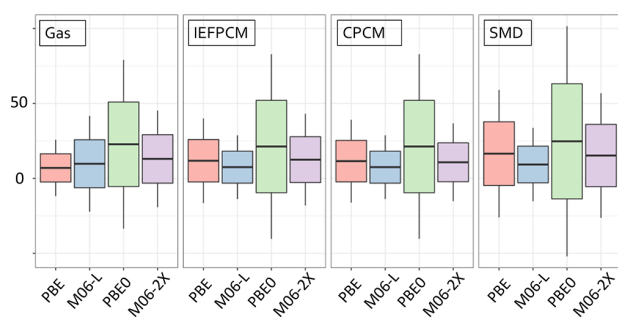


Figure 13. Absolute errors (in cm^{-1}) of solvation models and functionals for the prediction of the carboplatin stretching vibrations at 348, 351, 441, and 475 cm^{-1} .

coupled with bending vibrations of the cyclobutanedicarboxylate side group. The experimental peak at 441 cm^{-1} that has been assigned to a pure Pt–N symmetric vibration is usually accompanied by a Pt–O bending vibration. These mixtures of vibrations resulted in the inconsistent over- and underestimation of the measured peaks, with the exception for the PBE0 functional that always results in an overestimation of all four characteristic peaks in the range of 85 cm^{-1} with the CPCM/IEFPCM solvation model to 99 cm^{-1} with the SMD solvation model. With the exception of PBE0, $\nu(\text{Pt–O})$ is more prone to be underestimated as compared to $\nu(\text{Pt–N})$. Both $\nu(\text{Pt–O})$ experimental peaks (348 and 351 cm^{-1}) were only overestimated with the M06-2X functional in the gas phase. $\nu(\text{Pt–N})$ experimental peaks at 441 and 475 cm^{-1} , on the other hand, were found to be overestimated with a few exceptions. For example, M06-L and M06-2X functionals in the gas phase underestimate the 441 cm^{-1} experimental peak by 26 and 7 cm^{-1} , respectively. As one can see, the MAD and SD values practically reflect those in Figure 12, identifying a similar trend observed for cisplatin, with larger errors arising from stretching vibrations. The M06-L functional produces the least errors when combined with the IEFPCM and CPCM models, whereas the PBE0 functional gives the largest errors regardless of the solvent model used.

In addition, the bending vibrations of carboplatin and the experimental wavenumber of 194 and 573 cm^{-1} were also studied. The peaks at 194 and 573 cm^{-1} were assigned to $\alpha(\text{N–Pt–N})$ and $\alpha(\text{O–Pt–O})$, respectively. Interestingly, the O–Pt–O bending vibration at 573 cm^{-1} was underestimated regardless of the functional and solvation model, with the PBE and SMD combination giving rise to the largest deviation of 31 cm^{-1} . The smallest deviation of 2 cm^{-1} was obtained with the M06-2X functional in the gas phase. This could be due to the absence of a pure bending vibration. The presence of a more complex cyclobutanedicarboxylate group in carboplatin appears to play a role in these predictions.

Comparison of the predicted stretching vibrations of cisplatin and carboplatin, excluding the PBE0 functional that consistently produces large MAD and SD values, shows a range of MAD values from 0 cm^{-1} with the PBE functional and the SMD solvation model to 33 cm^{-1} with the M06-2X functional and the CPCM solvation model for cisplatin. For carboplatin, the MAD and SD (denoted as $\text{MAD} \pm \text{SD}$) values are 7.0 ± 9.4 and $16.5 \pm 21.3 \text{ cm}^{-1}$ both with PBE functional in the gas phase and SMD, respectively. These results highlight that a different scaling factor is needed not only for each DFT functional but also for their combination with a solvent model.

Analysis of bending vibrations of both complexes was compared. The range of MAD and SD for bending vibrations of both cisplatin and carboplatin is significantly narrower compared to that of stretching vibrations. The range of MAD and SD values for cisplatin lies between 4 ± 5.8 and $22.5 \pm 32.5 \text{ cm}^{-1}$ for cisplatin and between 4.0 ± 7.1 and $17.5 \pm 31.3 \text{ cm}^{-1}$ for carboplatin. As mentioned above, the γ bending vibrations present in cisplatin were always overestimated, and the prediction of α bending vibrations was less consistent. Therefore, universal scaling factors cannot be obtained if both stretching and two types of bending vibrations are to be accurately predicted.

Correlation between Pt–Ligand Bond Length and FIR Vibrations. It is well-known that there exists a direct correlation between the bond length and its strength.⁶⁴ Figure 14 presents the relationship between the predicted Pt–Cl bond length and corresponding stretching vibration.

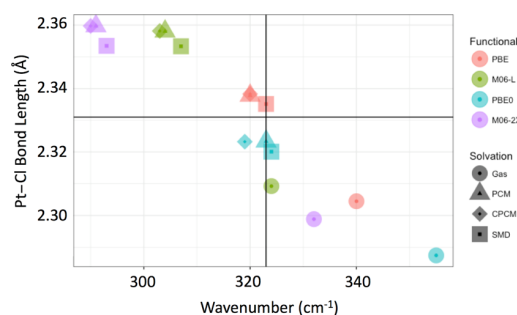


Figure 14. Relationship between the Pt–Cl bond length and the predicted Pt–Cl stretching vibration. The vertical line represents the Pt–Cl stretching experimental peak (323 cm^{-1}) and the horizontal line represents the Pt–Cl bond length determined using X-ray data (2.331 Å).

Analysis of Figure 14 confirms a linear relationship between the Pt–Cl bond length and the predicted wavelength. It has become very evident that the gas phase makes the bond shorter in a very narrow range of 2.29 – 2.36 Å for the four functionals studied. Inclusion of a solvent model stretched the bond by 0.034 Å on average for the PBE and PBE0 functionals and by 0.053 Å on average for the Minnesota functionals. The latter produce the longest Pt–Cl bond. The nature of the solvent model varies the bond length only slightly. The PBE and PBE0 functionals in combination with all three solvent models seem to find a nice fit to produce accurate prediction for the Pt–Cl stretching vibration, whereas the Minnesota functionals seem to underestimate it. These results further support the previous finding that in this case each DFT functional/solvent combination requires its individual scaling coefficient. Moreover, the gas phase results overestimate the stretching vibration in the range of 1 cm^{-1} for the M06-L functional and 32 cm^{-1} for the PBE0 functional as a result of a rather short Pt–Cl bond, thus highlighting the importance of inclusion of a solvent model for Pt-based complexes.

In the case of carboplatin data shown in Figure 15, one can see that while the prediction of both Pt–O1 and Pt–O2 wavenumber values does not deviate significantly (in the range of 332 – 361 cm^{-1} for Pt–O1 and 343 – 372 cm^{-1} for Pt–O2), the prediction of the Pt–O bond lengths is generally underestimated by 0.061 Å on average. Both wavenumber values and Pt–N bond lengths are mostly overestimated up to

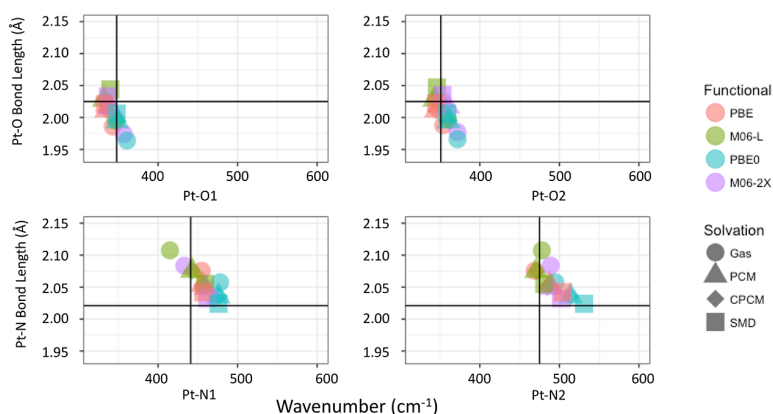


Figure 15. Relationship between the Pt–O and Pt–N bond lengths and theoretical stretching vibrations in carboplatin. Vertical black lines on graphs correspond to experimental wavenumbers of stretching vibrations for the Pt–O1, Pt–O2, Pt–N1, and Pt–N2 bonds (348, 351, 441, and 475 cm^{-1} , respectively). Horizontal black lines show the Pt–O and Pt–N bond lengths (2.025 and 2.021 Å, respectively) taken from X-ray data. Reported Pt–N bond lengths are the average of both Pt–N bonds.

Table 3. ChelpG Fitted Partial Atomic Charges for Cisplatin and Carboplatin

		Cisplatin				
gas/solvation model	functional	Pt	Cl(2)	Cl(3)	N(4)	N(7)
gas	PBE	1.786	−0.707	−0.707	−2.652	−2.652
	PBE0	1.819	−0.707	−0.707	−2.766	−2.766
	M06-L	1.859	−0.721	−0.721	−2.734	−2.734
	M06-2X	1.473	−0.658	−0.658	−2.128	−2.128
IEFPCM	PBE	1.783	−0.700	−0.700	−2.71	−2.710
	PBE0	1.818	−0.694	−0.694	−2.866	−2.866
	M06-L	1.771	−0.701	−0.701	−2.675	−2.675
	M06-2X	1.764	−0.694	−0.694	−2.751	−2.751
CPCM	PBE	1.781	−0.696	−0.696	−2.744	−2.744
	PBE0	1.748	−0.685	−0.685	−2.744	−2.744
	M06-L	1.773	−0.708	−0.701	−2.681	−2.681
	M06-2X	1.754	−0.674	−0.702	−2.798	−2.588
SMD	PBE	2.074	−0.733	−0.733	−3.289	−3.289
	PBE0	1.86	−0.698	−0.698	−2.96	−2.96
	M06-L	2.035	−0.727	−0.727	−3.228	−3.228
	M06-2X	2.104	−0.734	−0.734	−3.412	−3.412
		Carboplatin				
gas/solvation model	functional	Pt	O(10)	O(11)	N(2)	N(5)
gas	PBE	2.118	−1.479	−1.509	−2.439	−2.217
	PBE0	2.161	−1.514	−1.528	−2.489	−2.339
	M06-L	2.063	−1.426	−1.457	−2.412	−2.13
	M06-2X	2.139	−1.506	−1.508	−2.521	−2.236
IEFPCM	PBE	1.987	−1.22	−1.282	−2.482	−2.202
	PBE0	1.986	−1.212	−1.267	−2.509	−2.274
	M06-L	2.008	−1.248	−1.275	−2.504	−2.178
	M06-2X	2.12	−1.302	−1.362	−2.629	−2.325
CPCM	PBE	1.987	−1.222	−1.284	−2.479	−2.202
	PBE0	1.986	−1.211	−1.267	−2.511	−2.272
	M06-L	2.008	−1.247	−1.275	−2.504	−2.178
	M06-2X	2.048	−1.27	−1.332	−2.496	−2.271
SMD	PBE	1.964	−1.169	−1.24	−2.509	−2.199
	PBE0	2.092	−1.226	−1.299	−2.688	−2.378
	M06-L	2.229	−1.247	−1.304	−2.924	−2.533
	M06-2X	2.033	−1.224	−1.258	−2.594	−2.303

99 cm^{-1} and 0.0865 Å, respectively. Similar to cisplatin, both Pt–O and Pt–N bond lengths are predicted to be short when calculated in the gas phase, with a range of 1.96–2.00 Å for Pt–O and 2.08–2.11 Å for Pt–N. With the inclusion of

solvation models, the bond lengths increased slightly by 0.030 Å on average for Pt–O with PBE and PBE0 functionals and 0.043 Å on average with the Minnesota functionals. However, the Pt–N bond decreased by 0.026 Å with PBE and PBE0

Table 4. Electrostatic Potential Obtained from ChelpG Calculations of Ligands of the Two Complexes

		Cisplatin		
gas/solvation model	functional	N(4)H ₃	N(7)H ₃	
gas	PBE	−0.186	−0.186	
	PBE0	−0.202	−0.202	
	M06-L	−0.208	−0.208	
	M06-2X	−0.078	−0.078	
IEFPCM	PBE	−0.192	−0.192	
	PBE0	−0.215	−0.215	
	M06-L	−0.185	−0.185	
	M06-2X	−0.188	−0.188	
CPCM	PBE	−0.195	−0.195	
	PBE0	−0.189	−0.189	
	M06-L	−0.186	−0.186	
	M06-2X	−0.222	−0.156	
SMD	PBE	−0.304	−0.304	
	PBE0	−0.233	−0.233	
	M06-L	−0.290	−0.290	
	M06-2X	−0.318	−0.318	
		Carboplatin		
gas/solvation model	functional	N(2)H ₃	N(5)H ₃	cyclobutanedicarboxylate
gas	PBE	−0.069	−0.013	−2.036
	PBE0	−0.070	−0.032	−2.059
	M06-L	−0.068	0.001	−1.995
	M06-2X	−0.076	−0.015	−2.048
IEFPCM	PBE	−0.116	−0.043	−1.828
	PBE0	−0.117	−0.055	−1.814
	M06-L	−0.122	−0.041	−1.846
	M06-2X	−0.142	−0.063	−1.914
CPCM	PBE	−0.116	−0.043	−1.829
	PBE0	−0.118	−0.055	−1.813
	M06-L	−0.122	−0.041	−1.845
	M06-2X	−0.116	−0.052	−1.879
SMD	PBE	−0.129	−0.047	−1.788
	PBE0	−0.164	−0.080	−1.847
	M06-L	−0.218	−0.117	−1.894
	M06-2X	−0.144	−0.064	−1.825

functionals and 0.039 Å with the Minnesota functionals. The inclusion of solvation better predicted the Pt–ligand bond lengths when compared to X-ray data. Although the choice of functionals and solvation model does not affect the prediction of the Pt–O stretching vibrations significantly, it plays a larger role for the Pt–N stretching vibrations. For example, the PBE0 functional in conjunction with SMD overestimates both Pt–N vibrations by a minimum of 26 cm^{−1}. M06-L and either IEFPCM or CPCM reproduce the Pt–N experimental peaks the closest within 7 cm^{−1}, supporting the above conclusion that the Minnesota functionals perform well for systems containing transition metals.^{36,40}

Analysis of Partial Atomic Charges with ChelpG. NBO analysis, as mentioned above, is a definitive tool in providing information about the electronic charge distribution, type of bond, and charge transfer in a molecular system.^{65,66} However, the application of the NBO method proved to be an issue in this study because of the orbital inversion that was attributed to incorrect reading of the RECPs used. Instead, the ChelpG analysis, combined with the HF method VDZ basis set on non-Pt atoms and VTZ-pp on Pt, was used to study partial atomic charges by fitting these to reproduce the electrostatic potential of complexes.^{67–70} ChelpG developed by Cox and William was demonstrated the ability of atomic charge assignment to

explain molecular properties such as dipole moments.⁶⁸ ChelpG, a grid-based method, utilizes points spaced by 0.3–0.8 Å, placed at the center of the atoms, to imitate the electrostatic potential surface of a molecular system.^{68–70} ChelpG removes any points that are located in the van der Waals radius of all atoms because of the influence of being in close proximity to the nucleus. The ionic radius selected for Pt(II) was 0.8 Å.⁷¹ The van der Waals radii used for the other atoms are the default values defined in the ChelpG scheme.^{69,70} Table 3 shows partial atomic charges calculated for cisplatin and carboplatin, whereas Table 4 presents the overall charges on the ligands. In cisplatin, the charges on the Cl anion were found to be significantly less negative than those of the N atom. For example, when calculated with PBE in the gas phase, the atomic charges of Cl and N were computed to be −0.707e and −2.652e, respectively. The overall charge of the NH₃ ligand was found to be −0.184e, indicating that the ligand is more likely to draw the electron density from the Pt center. This is in agreement with the predicted charge of 1.786e on the Pt ion. Considering the nominal charge of +2.0 on the Pt ion, these numbers demonstrate a charge transfer of 0.293e from the chloride anion to Pt and then a charge transfer of 0.186e to the ammonia ligand. With a larger extent of the charge transfer between Pt and Cl, the Pt–Cl bond experiences

a bigger orbital overlap than the Pt–NH₃ bond.^{72,73} This finding also indicates that the Pt–Cl bond exhibits more covalent characteristics.⁷³ Table 3 also demonstrates that apart from the SMD solvation model, the charge flows away from the Pt metal ion in the range from 0.252e for the PBE0/CPCM combination to 0.181e for the PBE0/gas combination. The M06-2X functional in the gas phase as well as all DFT functionals with SMD produces slightly elevated charge-transfer values, further supporting the above established conclusion that both the DFT functional and inclusion of solvent model are important in the prediction of accurate vibrations in Pt-based complexes.

In contrast to cisplatin, the charges on the oxygen atoms in carboplatin are more negative than $-1.0e$ by at least $0.2e$ regardless of the functional/solvent model combination. In addition, the atomic charge on O is computed to be more negative when calculated in the gas phase, which is in agreement with the above results that solvation plays a role in charge transfer for carboplatin. This finding highlights that the Pt–O bond is clearly more ionic than the Pt–Cl bond, with the charge on the Pt ion being slightly higher than the nominal $+2.0$ charge. The largest difference of $0.229e$ was observed for M06-L with SMD, indicating the charge transfer from the Pt atom to the ligands.

In addition, by comparing the charges of ligands in carboplatin and cisplatin, the direction of charge transfer could potentially give an insight into the different rates of hydrolysis. Using the calculations conducted with PBE and gas phase as an example, a charge transfer of $0.293e$ from the chloride anion to Pt and then a charge transfer of $0.184e$ to the ammonia ligand in cisplatin. For carboplatin, charge transfer occurs from Pt to both the O atoms on the cyclobutanedicarboxylate in the amount of $0.479e$, whereas the ammonia ligands experience charge transfer to a much lesser extent. This redistribution of the electron density about the ligands for carboplatin could play a pivotal role in the different rates of hydrolysis and, hence, the different levels of toxicity of the two Pt drugs.

The overall charges of NH₃ groups in cisplatin and carboplatin have also been analyzed. As in Table 4, the overall charges of NH₃ in cisplatin are found to be equivalent for all but one calculation, M06-2X and CPCM solvation model, where one NH₃ is $0.066e$ more negative than the other NH₃ ligand. This gives an indication that the two NH₃ ligands result in the same extent of charge transfer from the Pt metal ion. This is, however, not the case for carboplatin. The overall charge of the two NH₃ ligands in carboplatin is significantly different, for example, -0.069 and $0.013e$ with PBE functional and gas. This difference implies that there is an imbalance of charge transfer from the metal ion and a larger extent of orbital overlap for N(3)H₃ than N(5)H₃. Across the different combinations of functional and solvation models, the overall charge of NH₃ is more negative in cisplatin than that of carboplatin, indicating a stronger interaction in the Pt–NH₃ bond in cisplatin.

Merz–Kollman (MK) partial charge analysis was also performed to study the atomic charges of cisplatin and carboplatin.⁶⁷ The results are presented in the Supporting Information and not discussed here as the findings further support the trends from the ChelpG analysis, whereby the Pt–O bond in carboplatin is found to exhibit a stronger ionic character compared to the Pt–Cl bond in cisplatin. MK analysis is included in the Supporting Information.

CONCLUSIONS

This study shows that the accuracy of theoretical vibrational frequencies in the FIR region of the two Pt complexes depends on the choice of both DFT functional and solvation model. In the case of cisplatin, the combination of PBE and SMD was found to be the best for the prediction of experimentally measured characteristic bands with a MAD and SD of 5.7 ± 8.5 cm⁻¹, whereas the M06-L and IEFPCM or CPCM combination is the best choice for carboplatin, with a MAD and SD of 6.8 ± 9.2 and 6.8 ± 9.1 cm⁻¹, respectively. These findings were attributed to the differences in the covalent nature of Pt–ligand bonds present in the complex of interest. As the Pt–Cl bond was found to exhibit more covalent characteristics than the Pt–O bond in carboplatin, it is not surprising that PBE performs better for cisplatin because it was designed to treat covalent bonds.³⁷ This is indicated by a charge transfer of $0.293e$ from the chloride anion to Pt in cisplatin and the reduced charge on Pt below the nominal $+2.0$ charge. Instead, the Pt–O bonds were more of ionic nature, with the Pt charge being slightly higher than the nominal $+2.00$ charge and a charge transfer of 0.036 and $0.013e$ to the cyclobutanedicarboxylate and NH₃ groups. Therefore, M06-L was found to perform better for carboplatin because it was designed for ionic systems.³⁶ Projecting these findings to other Pt-based complexes such as oxaliplatin and nedaplatin with Pt–O bonds, the M06-L functional with SMD is recommended as the best choice.

As expected, stretching vibrations are usually overestimated when calculated in gas phase as they produce shorter Pt–ligand bonds when calculated with a solvation model. With the inclusion of the solvation model, stretching vibrations are usually found to be overestimated in cisplatin, with the exception of the PBE0 functional in combination with both IEFPCM and SMD. For carboplatin, the stretching vibrations are less accurate because of the mixing of stretching and bending vibrations. While Pt–O stretching vibrations can be found to be either under- or overestimated, Pt–N vibrations are mostly overestimated. This further affirms the conclusion that the appropriate functional–solvation model combination should be determined to study such complexes with diverse bond characteristics. In addition, the different scaling factors are required not only for pure bending and stretching vibrations but also for mixed stretching and bending vibrations.

ASSOCIATED CONTENT

Supporting Information

The Supporting Information is available free of charge on the ACS Publications website at DOI: 10.1021/acsomega.8b03455.

Optimized geometries of both cisplatin and carboplatin using different combinations of functionals, basis sets, RECPs, and solvation models (ZIP)

AUTHOR INFORMATION

Corresponding Author

*E-mail: katya.pas@monash.edu.

ORCID

Eunice S. H. Gwee: 0000-0002-7599-1086

Bayden R. Wood: 0000-0003-3581-447X

Ekaterina I. Izgorodina: 0000-0002-2506-4890

Author Contributions

The manuscript was written through contributions of all authors. All authors have given approval to the final version of the manuscript.

Notes

The authors declare no competing financial interest.

ACKNOWLEDGMENTS

The authors gratefully acknowledge a generous allocation of computer resources through the Monash eResearch Centre and the National Computational Infrastructure. This work was generously supported by the Australian Research Council through a Discovery Project Grant and a Future Fellowship for E.I.I. E.S.H.G. is grateful to the Faculty of Science and School of Chemistry in Monash University for the Dean's Postgraduate Research Scholarship and the Dean's International Postgraduate Research Scholarship. B.R.W. would like to acknowledge funding from an Australian Research Council Discovery Grant DP140102504. The authors are also grateful to the use of Far Infrared Beamline of the Australian Synchrotron.

ABBREVIATIONS

FIR, far-infrared; RECP, relativistic effective core potential; DFT, density functional theory; G, guanine; A, adenine; NBO, natural bond orbital method; BDE, bond dissociation energy; GGA, generalized gradient approximation; HF, Hartree–Fock; IEFPCM, integral equation formalism polarizable continuum model; CPCM, conductor-like polarizable continuum model; SMD, solvent model based on density; CBS, complete basis set; SD, standard deviation; MAD, mean absolute deviation; ChelpG, charges from electrostatic potential grid method

REFERENCES

- (1) Barnett, R.; Loretta, V.; James, E. T.; Virginia, H. M. Platinum Compounds: a New Class of Potent Antitumour Agents. *Nature* **1969**, *222*, 385–386.
- (2) Galanski, M.; Keppler, B. Searching for the Magic Bullet: Anticancer Platinum Drugs Which Can Be Accumulated or Activated in the Tumor Tissue. *Anti-Cancer Agents Med. Chem.* **2007**, *7*, 55–73.
- (3) Goodsell, D. S. The Molecular Perspective: Cisplatin. *Oncologist* **2006**, *11*, 316–317.
- (4) Klein, A. V.; Hambley, T. W. Platinum drug distribution in cancer cells and tumors. *Chem. Rev.* **2009**, *109*, 4911–4920.
- (5) Raber, J.; Zhu, C.; Eriksson, L. A. Theoretical study of cisplatin binding to DNA: The importance of initial complex stabilization. *J. Phys. Chem. B* **2005**, *109*, 11006–11015.
- (6) Davies, M. S.; Berners-Price, S. J.; Hambley, T. W. Rates of Platination of AG and GA Containing Double-Stranded Oligonucleotides: Insights into Why Cisplatin Binds to GG and AG but Not GA Sequences in DNA. *J. Am. Chem. Soc.* **1998**, *120*, 11380–11390.
- (7) Siddik, Z. H. Cisplatin: mode of cytotoxic action and molecular basis of resistance. *Oncogene* **2003**, *22*, 7265–7279.
- (8) Florea, A.-M.; Büsselfeld, D. Cisplatin as an Anti-Tumor Drug: Cellular Mechanisms of Activity, Drug Resistance and Induced Side Effects. *Cancers* **2011**, *3*, 1351–1371.
- (9) Frey, U.; Ranford, J. D.; Sadler, P. J. Ring-opening reactions of the anticancer drug carboplatin: NMR characterization of cis-[Pt(NH₃)₂(CBDCA-O)(S'-GMP-N7)] in solution. *Inorg. Chem.* **1993**, *32*, 1333–1340.
- (10) Davies, M. S.; Berners-Price, S. J.; Hambley, T. W. Slowing of cisplatin aquation in the presence of DNA but not in the presence of phosphate: Improved understanding of sequence selectivity and the roles of monoaquated and diaquated species in the binding of cisplatin to DNA. *Inorg. Chem.* **2000**, *39*, 5603–5613.

- (11) Cioslowski, J.; Liu, G.; Mosquera Castro, R. A. Badger's rule revisited. *Chem. Phys. Lett.* **2000**, *331*, 497–501.
- (12) Knözinger, E. Fourier Spectroscopy as a Method for Structure Determination in Chemistry. *Angew. Chem., Int. Ed. Engl.* **1976**, *15*, 25–39.
- (13) Umapathy, P. The Chemical and Biochemical Consequences of the Binding of the Antitumor Drug Cisplatin and other Platinum-Group Metal-Complexes to DNA. *Coord. Chem. Rev.* **1989**, *95*, 129–181.
- (14) Haputhanthri, P. A *Spectroscopic Investigation into the Binding of Novel Platinum(IV) and Platinum(II) Anticancer Drugs with DNA and Cells*; Monash University, 2017.
- (15) Medcraft, C.; Thompson, C. D.; Robertson, E. G.; Appadoo, D. R. T.; McNaughton, D. The far-infrared rotational spectrum of ethylene oxide. *Astrophys. J.* **2012**, *753*, 18.
- (16) Orto, M.; Pantazis, D.; Neese, F. *Density Functional Theory*; Springer Science & Business Media: Dordrecht, 2009; Vol. 102, pp 443–453.
- (17) Georgieva, I.; Trendafilova, N.; Dodoff, N.; Kovacheva, D. DFT study of the molecular and crystal structure and vibrational analysis of cisplatin. *Spectrochim. Acta, Part A* **2017**, *176*, 58–66.
- (18) Vernooij, R. R.; Joshi, T.; Shaili, E.; Kubeil, M.; Appadoo, D. R. T.; Izgorodina, E. I.; Graham, B.; Sadler, P. J.; Wood, B. R.; Spiccia, L. Comprehensive Vibrational Spectroscopic Investigation of trans,trans-Pt(N₃)₂(OH)₂(py)₂, a Pt(IV) Diazo Anticancer Prodrug Candidate. *Inorg. Chem.* **2016**, *55*, 5983–5992.
- (19) Forster, D.; Horrocks, W. D. Synthesis and Vibrational Spectra of [Co(N₃)₄]·2-,[Zn(N₃)₄]·2-, and [Sn(N₃)₆]·2. *Inorg. Chem.* **1966**, *5*, 1510–1514.
- (20) Schmidtke, H.-H.; Garthoff, D. The Electronic Spectra of Some Noble Metal Azide Complexes. *J. Am. Chem. Soc.* **1967**, *89*, 1317–1321.
- (21) Durman, R.; Jayasooriya, U. A.; Kettle, S. F. A.; Mahasuverachai, S.; Mortimer, R.; Norrby, L. J. Factor group splitting and dispersion on internal vibrational modes: A qualitative discussion. *J. Chem. Phys.* **1984**, *81*, 5247–5251.
- (22) Wysokiński, R.; Hernik, K.; Szostak, R.; Michalska, D. Electronic structure and vibrational spectra of cis-diammine-(orotato)platinum(II), a potential cisplatin analogue: DFT and experimental study. *Chem. Phys.* **2007**, *333*, 37–48.
- (23) Wang, Y.; Liu, Q.; Qiu, L.; Wang, T.; Yuan, H.; Lin, J.; Luo, S. Molecular structure, IR spectra, and chemical reactivity of cisplatin and transplatin: DFT studies, basis set effect and solvent effect. *Spectrochim. Acta, Part A* **2015**, *150*, 902–908.
- (24) Hemminki, K.; Ludlum, D. B. Covalent modification of DNA by antineoplastic agents. *J. Natl. Cancer. Inst.* **1984**, *73*, 1021–1028.
- (25) Cohen, G. L.; Ledner, J. A.; Bauer, W. R.; Ushay, H. M.; Caravana, C.; Lippard, S. J. Sequence dependent binding of cis-dichlorodiammineplatinum(II) to DNA. *J. Am. Chem. Soc.* **1980**, *102*, 2487–2488.
- (26) Coluccia, M.; Natile, G. Trans-Platinum Complexes in Cancer Therapy. *Anti-Cancer Agents Med. Chem.* **2007**, *7*, 111–123.
- (27) Wysokiński, R.; Kuduk-Jaworska, J.; Michalska, D. Electronic structure, Raman and infrared spectra, and vibrational assignment of carboplatin. Density functional theory studies. *J. Mol. Struct.: THEOCHEM* **2006**, *758*, 169–179.
- (28) Tasinato, N.; Puzzarini, C.; Barone, V. Correct Modeling of Cisplatin: a Paradigmatic Case. *Angew. Chem., Int. Ed.* **2017**, *56*, 13838–13841.
- (29) Gilbert, T. M. Tests of the MP2 model and various DFT models in predicting the structures and B–N bond dissociation energies of amine-boranes (X₃C)(sub m)H(sub 3-m)B–N(CH₃)(sub n)H(sub 3-n) (X=H, F; m=0–3; n=0–3): Poor performance of the B3LYP approach for dative B–N bonds. *J. Phys. Chem. A* **2004**, *108*, 2550–2554.
- (30) Smith, E. L.; Sadowsky, D.; Phillips, J. A.; Cramer, C. J.; Giesen, D. J. A short yet very weak dative bond: structure, bonding, and energetic properties of N(2)–BH(3). *J. Phys. Chem. A* **2010**, *114*, 2628–2636.

- (31) Malik, M.; Michalska, D. Assessment of new DFT methods for predicting vibrational spectra and structure of cisplatin: which density functional should we choose for studying platinum(II) complexes? *Spectrochim. Acta, Part A* **2014**, *125*, 431–439.
- (32) Barth, A. Infrared spectroscopy of proteins. *Biochim. Biophys. Acta, Bioenerg.* **2007**, *1767*, 1073–1101.
- (33) Wysokiński, R.; Michalska, D. The performance of different density functional methods in the calculation of molecular structures and vibrational spectra of platinum(II) antitumor drugs: Cisplatin and carboplatin. *J. Comput. Chem.* **2001**, *22*, 901–912.
- (34) Amado, A. M.; Fiuza, S. M.; Marques, M. P. M.; Batista de Carvalho, L. A. E. Conformational and vibrational study of platinum(II) anticancer drugs: cis -diamminedichloroplatinum (II) as a case study. *J. Chem. Phys.* **2007**, *127*, 185104.
- (35) Scott, A. P.; Radom, L. Harmonic vibrational frequencies: An evaluation of Hartree-Fock, Moller-Plesset, quadratic configuration interaction, density functional theory, and semiempirical scale factors. *J. Phys. Chem.* **1996**, *100*, 16502–16513.
- (36) Zhao, Y.; Truhlar, D. A new local density functional for main-group thermochemistry, transition metal bonding, thermochemical kinetics, and noncovalent interactions. *J. Chem. Phys.* **2006**, *125*, 194101–194118.
- (37) Perdew, J. P.; Burke, K.; Ernzerhof, M. Generalized Gradient Approximation Made Simple. *Phys. Rev. Lett.* **1996**, *77*, 3865–3868.
- (38) Grimme, S.; Antony, J.; Ehrlich, S.; Krieg, H. A consistent and accurate ab initio parametrization of density functional dispersion correction (DFT-D) for the 94 elements H–Pu. *J. Chem. Phys.* **2010**, *132*, 154104.
- (39) Adamo, C.; Barone, V. Toward reliable density functional methods without adjustable parameters: The PBE0 model. *J. Chem. Phys.* **1999**, *110*, 6158–6170.
- (40) Zhao, Y.; Truhlar, D. G. The M06 suite of density functionals for main group thermochemistry, thermochemical kinetics, non-covalent interactions, excited states, and transition elements: two new functionals and systematic testing of four M06-class functionals and 12 other functionals. *Theor. Chem. Acc.* **2008**, *120*, 215–241.
- (41) Xu, X.; Truhlar, D. G. Accuracy of Effective Core Potentials and Basis Sets for Density Functional Calculations, Including Relativistic Effects, As Illustrated by Calculations on Arsenic Compounds. *J. Chem. Theory Comput.* **2011**, *7*, 2766–2779.
- (42) Paranthaman, S.; Moon, J.; Kim, J.; Kim, D. E.; Kim, T. K. Performance of Density Functional Theory and Relativistic Effective Core Potential for Ru-Based Organometallic Complexes. *J. Phys. Chem. A* **2016**, *120*, 2128–2134.
- (43) Weigend, F.; Ahlrichs, R. Balanced basis sets of split valence, triple zeta valence and quadruple zeta valence quality for H to Rn: Design and assessment of accuracy. *Phys. Chem. Chem. Phys.* **2005**, *7*, 3297–3305.
- (44) Hay, P. J.; Wadt, W. R. Ab initio effective core potentials for molecular calculations. Potentials for the transition metal atoms Sc to Hg. *J. Chem. Phys.* **1985**, *82*, 270–283.
- (45) Roy, L. E.; Hay, P. J.; Martin, R. L. Revised Basis Sets for the LANL Effective Core Potentials. *J. Chem. Theory Comput.* **2008**, *4*, 1029–1031.
- (46) Figgen, D.; Peterson, K. A.; Dolg, M.; Stoll, H. Energy-consistent pseudopotentials and correlation consistent basis sets for the S d elements Hf–Pt. *J. Chem. Phys.* **2009**, *130*, 164108.
- (47) Clementi, E.; Chakravorty, S. J. A comparative study of density functional models to estimate molecular atomization energies. *J. Chem. Phys.* **1990**, *93*, 2591–2602.
- (48) Perdew, J. P.; Ernzerhof, M.; Burke, K. Rationale for mixing exact exchange with density functional approximations. *J. Chem. Phys.* **1996**, *105*, 9982–9985.
- (49) Becke, A. D. Density functional thermochemistry. III. The role of exact exchange. *J. Chem. Phys.* **1993**, *98*, 5648–5652.
- (50) Cammi, R. *Molecular Response Functions for the Polarizable Continuum Model: Physical Basis and Quantum Mechanical Formalism*; Springer, 2013.
- (51) Takano, Y.; Houk, K. N. Benchmarking the Conductor-like Polarizable Continuum Model (CPCM) for Aqueous Solvation Free Energies of Neutral and Ionic Organic Molecules. *J. Chem. Theory Comput.* **2005**, *1*, 70–77.
- (52) Marenich, A. V.; Cramer, C. J.; Truhlar, D. G. Universal Solvation Model Based on Solute Electron Density and on a Continuum Model of the Solvent Defined by the Bulk Dielectric Constant and Atomic Surface Tensions. *J. Phys. Chem. B* **2009**, *113*, 6378–6396.
- (53) Barone, V.; Cossi, M. Quantum Calculation of Molecular Energies and Energy Gradients in Solution by a Conductor Solvent Model. *J. Phys. Chem. A* **1998**, *102*, 1995–2001.
- (54) Cancès, E.; Mennucci, B.; Tomasi, J. A new integral equation formalism for the polarizable continuum model: Theoretical background and applications to isotropic and anisotropic dielectrics. *J. Chem. Phys.* **1997**, *107*, 3032–3041.
- (55) Labello, N. P.; Ferreira, A. M.; Kurtz, H. A. Correlated, relativistic, and basis set limit molecular polarizability calculations to evaluate an augmented effective core potential basis set. *Int. J. Quantum Chem.* **2006**, *106*, 3140–3148.
- (56) Whittleton, S. R.; Boyd, R. J.; Grindley, T. B. Evaluation of Effective Core Potentials and Basis Sets for the Prediction of the Geometries of Alkyltin Halides. *J. Phys. Chem. A* **2006**, *110*, 5893–5896.
- (57) Woon, D. E.; Dunning, T. H. Gaussian basis sets for use in correlated molecular calculations. IV. Calculation of static electrical response properties. *J. Chem. Phys.* **1994**, *100*, 2975–2988.
- (58) Corni, S.; Cappelli, C.; Del Zoppo, M.; Tomasi, J. Prediction of solvent effects on vibrational absorption intensities and Raman activities in solution within the polarizable continuum model: a study on push-pull molecules. *J. Phys. Chem. A* **2003**, *107*, 10261.
- (59) Baik, M.-H.; Friesner, R. A.; Lippard, S. J. cis-[Pt(NH₃)₂(L)]²⁺ (L = Cl, H₂O, NH₃) Binding to Purines and CO: Does π -Back-Donation Play a Role? *Inorg. Chem.* **2003**, *42*, 8615–8617.
- (60) Zuliani, P.; Del Zoppo, M.; Castiglioni, C.; Zerbi, G.; Marder, S. R.; Perry, J. W. Solvent effects on first-order molecular hyperpolarizability: A study based on vibrational observables. *J. Chem. Phys.* **1995**, *103*, 9935–9940.
- (61) Duchesne, J. *Electrical, Optical, and Magnetic Properties of Nucleic Acids and Components*; Academic Press: London, New York, 1973.
- (62) Quack, M.; Merkt, F. d. r. *Handbook of High-Resolution Spectroscopy*; Wiley: Hoboken, N.J., 2011.
- (63) Mardirossian, N.; Head-Gordon, M. Thirty years of density functional theory in computational chemistry: an overview and extensive assessment of 200 density functionals. *Mol. Phys.* **2017**, *115*, 2315–2372.
- (64) Badger, R. M. A Relation Between Internuclear Distances and Bond Force Constants. *J. Chem. Phys.* **1934**, *2*, 128–131.
- (65) Frenking, G.; Fröhlich, N. The Nature of the Bonding in Transition-Metal Compounds. *Chem. Rev.* **2000**, *100*, 717–774.
- (66) Glendening, E. D.; Landis, C. R.; Weinhold, F. Natural bond orbital methods. *Wiley Interdiscip. Rev.: Comput. Mol. Sci.* **2012**, *2*, 1–42.
- (67) Singh, U. C.; Kollman, P. A. An approach to computing electrostatic charges for molecules. *J. Comput. Chem.* **1984**, *5*, 129–145.
- (68) Rigby, J.; Izgorodina, E. I. Assessment of atomic partial charge schemes for polarisation and charge transfer effects in ionic liquids. *Phys. Chem. Chem. Phys.* **2013**, *15*, 1632–1646.
- (69) Breneman, C. M.; Wiberg, K. B. Determining atom-centered monopoles from molecular electrostatic potentials. The need for high sampling density in formamide conformational analysis. *J. Comput. Chem.* **1990**, *11*, 361–373.
- (70) Chirlian, L. E.; Francl, M. M. Atomic charges derived from electrostatic potentials: A detailed study. *J. Comput. Chem.* **1987**, *8*, 894–905.
- (71) Shannon, R. D. Revised effective ionic radii and systematic studies of interatomic distances in halides and chalcogenides. *Acta*

Crystallogr., Sect. A: Cryst. Phys., Diff., Theor. Gen. Crystallogr. **1976**, 32, 751–767.

(72) de Oliveira, B. G.; Araújo, R.; Chagas, F.; Carvalho, A.; Ramos, M. The electronic structure of the C₂H₄O...2HF tri-molecular heterocyclic hydrogen-bonded complex: a theoretical study. *J. Mol. Model.* **2008**, 14, 949–955.

(73) Salafranca, J.; Rincón, J.; Tornos, J.; León, C.; Santamaria, J.; Dagotto, E.; Pennycook, S. J.; Varela, M. Competition between covalent bonding and charge transfer at complex-oxide interfaces. *Phys. Rev. Lett.* **2014**, 112, 196802.

Chapter 3

Effects of explicit solvation on the hydrolysis mechanism of the Pt complexes.

3.1 Introduction

Platinum based anticancer drugs, such as cisplatin, continue to play a vital role in cancer treatment.¹ The current understanding in the field suggests that cisplatin must undergo hydrolysis and form either a mono- or di-aquated complex before reaching the cell (Fig: 3.1).² These complexes, usually referred to as activated forms of the drug, are understood to interact with the guanine base of DNA and form intra-strand mono- or di-functional adducts that result in the localized unwinding and hence, increasing the width of minor groove of the DNA helix.²⁻⁴ The disruption to the structural integrity of DNA leads to disruption of the cell replication process in the early stages and apoptosis in later stages.^{2,3} Cisplatin has both chloride anions in the cis position and this has been attributed to its ability to form intra-strand adducts and act as an anti-cancer drug. Transplatin, on the other hand, was shown to be unable to form intra-strand adducts due to the chloride anions in the trans position, thus rendering it inactive as an anti-cancer drug.^{5,6}

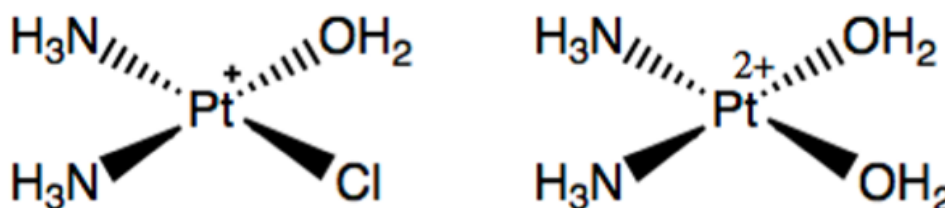


Figure 3.1: Hydrolysis of cisplatin, resulting in either the mono- (left) or di-aquated (right) complexes.

Crystallographic data on the binding mechanism of cisplatin to DNA indicates the chloride anions must be preferred leaving groups because only ammonia ligands were found to be bound to the Pt cation in X-ray crystallographic experiments.^{7,8} For example, Takahara *et al.* reported structural changes in the double-stranded deoxyoligonucleotide, a mimic of DNA, before and after the binding of cisplatin via X-ray crystallography.⁹ The X-ray crystal structures were resolved at 2.6 Å resolution.⁹ It was noted that after cisplatin binds to the nucleotide, the structure of the dodecamer becomes significantly distorted by a minimum of 8°.⁹ The width of the minor grooves were also measured to lie between 9.2 and 11.2 Å, deviating significantly from that of 5.7 Å found in B-DNA, one of the biologically relevant conformations of DNA.⁹ In addition, upon cisplatin binding, the hydrogen bonding between nucleobases is disrupted, decreasing the rotation angle between two neighbouring guanine fragments from the original 80° to 54°.⁹ Despite numerous crystallographic studies, definitive details about the hydrolysis mechanism of cisplatin have not been reported.

The use of cisplatin in anti-cancer treatments is accompanied by several side effects, such as diminished hearing ability, hair loss, nephrotoxicity and neurotoxicity, toxicity to kidney and peripheral nervous system, respectively; all of which were attributed to the accumulation of the activated form of the drug due to its fast hydrolysis in the body.^{10,11} These effects have thus motivated the development of analogous Pt-based complexes to decrease their rate of hydrolysis and subsequent accumulation, leading to lower toxicity.¹¹ Replacement of chloride

with additional functional groups such as dicarboxylate and glycolate was shown to reduce side effects in Pt-based drugs such as carboplatin, oxaliplatin and nedaplatin (Fig: 3.2).¹¹

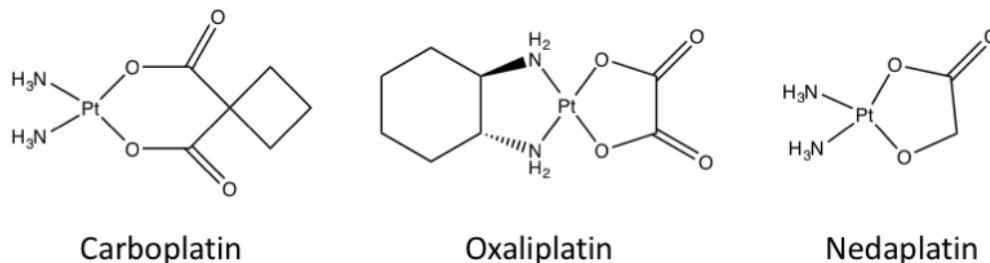


Figure 3.2: Examples of anti-cancer Pt-based complexes with decreased hydrolysis.¹¹

The nephrotoxicity of cisplatin is thought to arise from the accumulation of plasma free Pt complexes in the body due to continuous administration.^{12,13} As reported by Harrington *et al.*, the elimination of cisplatin from the body has proven to be an issue, with only 25% being secreted 24 hours after administration. The drug appeared to be accumulated mainly in liver, kidney, stomach and intestine.¹³ It was reported that cisplatin was able to interact with biomolecules in the kidneys, rendering its function as a mutagen.¹⁴ Drugs such as carboplatin, oxaliplatin and nedaplatin with more complex leaving groups were also designed to be eliminated from the body more efficiently. For example, at least 50% of the administered carboplatin was found to be secreted after 24 hours, effectively decreasing the accumulation of Pt complexes in the body,^{14,15} whereas 50% of nedaplatin was secreted already after 8 hours of administration.¹⁶ Carboplatin was also designed to specifically decrease the nephrotoxicity that was not induced with a dosage of up to 400 mg/m².^{14,17,18} Oxaliplatin was shown to further suppress the abnormal tissue growth.¹⁹ Saijo *et al.* compared the pharmacokinetics of cisplatin, carboplatin and nedaplatin and discovered that the half-lives were 2880, 840 and 768 mins, respectively, indicating that introducing cyclo-groups decreased the half-lives of Pt-complexes significantly.^{16,20}

Despite the numerous experiments conducted to study the side effects of Pt-based complexes, little is understood about the role of varying ligands on the hydrolysis rate. This is mainly due to significant limitations present in both computational and experimental approaches. Experimentally, studies have been hindered due to low solubility of these Pt compounds.²¹

As a result, the emphasis of experimental studies was given towards generation of possible hydrolysed species of Pt complexes by varying the pH of the solution and subsequent analysis of their binding to nucleobases.

Chottard *et al.* conducted kinetic studies on the platination of 1,2-d(GpG) and 1,2-d(ApG) by cisplatin using high pressure liquid chromatography (HPLC).²² Acidic conditions of experiments varied to produce three unique hydrolysed states of cisplatin: *cis*-[Pt(NH₃)₂Cl₂], *cis*-[Pt(NH₃)₂Cl(H₂O)]⁺ and *cis*-[Pt(NH₃)₂(H₂O)₂]²⁺.²² The mono- and di-hydrolysed states were prepared separately, with *cis*-[Pt(NH₃)₂Cl(H₂O)]⁺ being isolated with ClO₄⁻ as a counter-ion and *cis*-Pt(NH₃)₂(H₂O)₂]²⁺ being prepared with the addition of stoichiometric amounts of AgNO₃.^{23,24} Although previous studies suggested that DNA platination was concurrent with the first hydrolysis step, in which one chloride anion was replaced with a water molecule.^{25,26} Chottard *et al.* could not conclude which species participated in binding with DNA *in vivo*.²² The main difficulty was associated with maintaining the stability of the oligonucleotides under varying acidic conditions.²² It was established that a pH of 4.5 was required to hydrolyse cisplatin forming both *cis*-[Pt(NH₃)₂Cl(H₂O)]⁺ and *cis*-[Pt(NH₃)₂(H₂O)₂]²⁺.²² *cis*-[Pt(NH₃)₂(H₂O)₂]²⁺ was found to be the most reactive out of the three plausible species, binding approximately three times faster with the 1,2-d(GpG) oligonucleotide compared with that of the 1,2-d(ApG) oligonucleotide.²² Based on these results, Chottard *et al.* concluded that the *cis*-[Pt(NH₃)₂(H₂O)₂]²⁺ was the likely activated species of cisplatin.²²

Further studies established that the binding of Pt-based complexes to DNA was found to be kinetically driven.^{27,28} Hambley *et al.* made use of ¹H and ¹⁵N heteronuclear single-quantum coherence (HSQC) 2D nuclear magnetic resonance (NMR) to study the rate of binding between the two forms of cisplatin - *cis*-[Pt(NH₃)₂Cl₂] and *cis*-[Pt(NH₃)₂(H₂O)₂]²⁺ - and a 14-base pair oligonucleotide, 5'-d(AATTGATATCAATT)-3'.²⁷ *cis*-[Pt(NH₃)₂(H₂O)₂]²⁺ was prepared with AgNO₃ in dimethylformamide and extracted via centrifuge.²⁷ Upon studying the reaction of *cis*-[Pt(NH₃)₂Cl₂] with the oligonucleotide, they were able to detect the presence of *cis*-[Pt(NH₃)₂Cl(H₂O)]⁺.²⁷ They determined that the rate of binding of the mono-aquated form of cisplatin to the guanine (G) nucleobase was approximately four times faster than that to the adenine (A) nucleobase.²⁷ It was also reported that the di-aquated form of cisplatin still formed a bi-functional adduct with the oligonucleotide via a two-step mechanism.²⁷ The

mono-hydrated form was found to bind to G on the oligonucleotide > 20 times slower than the di-hydrated form, indicating the preference for the di-aquated form to almost instantly bind to DNA.²⁷

From the theoretical point of view, difficulties in studying hydrolysis of Pt-based complexes arise from the lack of thorough benchmarking and assessment studies. Presence of both main group elements and transition metals present in the system poses an issue because these two classes may require different functionals of Density Functional Theory (DFT).^{29,30} There is a general lack of transition metal databases that can be used to assess the performance of DFT functionals for studying hydrolysis and binding mechanisms of Pt-based complexes.³¹ Early studies of 20 complexes of main group elements, for example H₂, NH₃ and Cl₂ demonstrates that PBE, a DFT functional of the second rung on the Jacob's ladder, overestimated their atomisation energies with a mean absolute error of 33.1 kJmol⁻¹ when compared to experimental results.³²⁻³⁴ On the other hand, GGA functionals such as G96LYP, XLYP and BLYP were shown to perform better for systems containing transition metals (TMs).^{29,35-37} Truhlar *et al.* studied the bond dissociation energies of the transition metal complexes in the MLBE21/05 database, containing a range of metal ions from Be²⁺, Co²⁺ and Fe²⁺, with a range of local spin density approximation (LSDA) functionals, GGA, hybrid GGA, meta GGA and hybrid meta GGA functionals.²⁹ The mean unsigned error (MUE) of the LDA, GGA, hybrid GGA, meta-GGA and hybrid meta GGA with TZQ basis set is as follows: 128.4, 40.6, 31.0, 44.8 and 31.8 kJmol⁻¹, respectively.²⁹ Schultz *et al.* undertook a systematic approach to investigate the accuracy of 5 different types of DFT functionals corresponding to five rungs of Jacob's ladder for the existing three databases containing transition metal complexes - TMBL8/05, TMAE9/05 and TMAE4/05.³⁸ Upon investigation of the different types of DFT functionals with TMBL8/05, containing bond lengths of 8 metal dimers, for example Ag₂, Cu₂ and CuAg, GGA functionals reproduced the smallest MUE of 0.05 Å, with the HCTH functional producing the largest MUE of 0.16 Å.³⁸ TMAE9/05, consisting of atomisation energies of the 8 dimers in TMBL8/05 and the atomisation energy of ZrV, also revealed that GGA functionals produced the smallest MUE of 29.7 kJ mol⁻¹, out of the different rungs of Jacob's ladder, with LSDA and surprisingly hybrid meta-GGA functionals producing the largest MUE of 127.2 and 84.1 kJ mol⁻¹, respectively.³⁸ Lastly, results from the TMAE4/05 database, a subset of TMAE9/05, containing Cr₂, Cu₂, V₂

and Zr_2 , supported the conclusion from TMAE9/05, with GGA functionals reproducing the smallest MUE of 30.5 kJ mol^{-1} .³⁸ Inclusion of 21% of the exact Hartree-Fock exchange in the B97-2 functional led to the smallest average MUE of 5.3 kJ mol^{-1} for atomisation energies of the TMAE9/05 database, whereas GGA functionals, such as G96LYP, performed consistently better than hybrid ones for atomisation energies of metal dimer systems.³⁸

To date, only a handful of computational chemistry studies have been conducted to investigate the hydrolysis mechanism in Pt-based anti-cancer drugs.^{39–43} It was computationally established that during the initial stage of hydrolysis cisplatin underwent an S_N2 reaction proceeding via a trigonal bipyramidal transition state and the water molecule paying the role of a nucleophile.^{39,44–47} However, the effect of Pt-based complexes hydrolysis with either implicit solvation models or inclusion of explicit water molecules has only been explored to a certain extent.^{39–43,48} Santos *et al.* conducted a study on the second step of *cis*-dichloro(ethylene)diammineplatinum(II) (*cis*-DEP) hydrolysis using a thermodynamic cycle.⁴⁰ Gas phase and implicit polarisable continuum model (PCM) real cavities and self-consistent reaction field (SCRF) spherical cavities were used in combination with the HF, MP2, B3P86 and B3PW91 levels of theory coupled with the 6-31G(d) basis set for non-Pt atoms and the LANL2DZ effective core potential (ECP) for the Pt ion.⁴⁰ The MP2 activation Gibbs free energy of the second step of hydrolysis was calculated to be 125.77 , 97.65 and $98.95 \text{ kJ mol}^{-1}$ in gas phase, SCRF and PCM, respectively, which was found to be the closest to the experimental value of $96.23 \pm 25 \text{ kJ mol}^{-1}$.^{40,49,50}

The overestimation of $29.54 \text{ kJ mol}^{-1}$ when calculated in gas phase highlighted the importance of solvation models for the prediction of reliable energetics.^{40,49,50} The MP2 method in combination with the SCRF and PCM approaches predicted the rate constant of $4.84 * 10^{-5}$ and $2.87 * 10^{-5} \text{ M}^{-1}\text{s}^{-1}$, respectively, which were found to be the closest to the experimental value of $4.4 \pm 0.6 * 10^{-5} \text{ M}^{-1}\text{s}^{-1}$.^{40,49,50} Gas phase calculation produced a significantly slower rate of hydrolysis of $1.92 * 10^{-11} \text{ M}^{-1}\text{s}^{-1}$, indicating that solvation models played a vital role in the prediction of hydrolysis rates of Pt-based complexes.⁴⁰

Eriksson *et al.* contrasted the energetics of the cisplatin step-wise hydrolysis using an implicit solvation model, IEF-PCM and an explicit solvation approach with the inclusion of 6 water

molecules.⁴⁴ B3LYP,^{35,51} LanL2DZ ECP,⁵² 6-311+G(d,p) basis set⁵³ were employed for geometry optimisations and electronic energies were improved by performing single point energy calculations with a larger basis set, 6-311+G(2d,2p) basis set⁵³ and including the IEF-PCM⁵⁴ solvation model.⁴⁴ The importance of explicit water molecules to stabilise the electrostatic interactions in the Pt-Cl bond manifested itself by lowering the Gibbs energy of activation of both the first and second hydrolysis steps by 6.7 and 29.3 kJ mol⁻¹, respectively.⁴⁴ The explicit solvation approach predicted the Gibbs free energy of activation for the first hydrolysis step to be 95.8 kJ mol⁻¹, which was in better agreement with the reported experimental values of 81.6-90.0 kJ mol⁻¹.⁵⁵ The activation Gibbs free energy for the second step of hydrolysis was within 6.7 kJ mol⁻¹ of the experimentally measured barrier of chloride anation of the fully hydrolysed Pt complex.⁵⁶ This further emphasized the importance of explicit solvation in investigating such hydrolysis reactions. In the study of Burda *et al.* the level of theory was also identified as critical for the accurate prediction of activation barriers.⁵⁷

You *et al.* studied the effects that implicit solvation model, the Onsager SCRF model, on the step-wise hydrolysis of cisplatin, in particular its influence on the optimised geometry and the thermodynamics of the reaction.⁴² The Pt-Cl and Pt-O bond lengths obtained with implicit solvation is usually longer than that obtained in gas phase, by an average of 0.13 and 0.02 Å.⁴² Gibbs Free energies of the first and second step of hydrolysis were reported to be 15.6 and 15.9 kJ mol⁻¹, supporting the previously published experimental observation.^{42,58-60}

Lippard also made use of B3LYP functional, 6-31G** basis set and Los Alamos LACVP** basis for Pt,⁶¹ to examine the thermodynamics and kinetics of the formation of the mono- and dehydrated equivalents of cisplatin and their binding to either guanine or adenine.⁶² Single point energies were performed using cc-pVTZ(-f) basis set for non-metal atoms and LACV3P** basis for Pt.⁶² Solvation effects were investigated by incorporating SCRF based on Poisson-Boltzmann equation on the geometries optimised in gas phase.⁶² To study the binding event, the optimised geometries of both Pt complex and base were placed at Pt-N(base) at a distance of 4.0 Å and decreasing the distance by an increment of 0.1 Å until the distance of 2.0 Å was reached.⁶² Guanine was found to be energetically preferred for platination of the hydrolysed Pt complexes.⁶² Compared to the mono-aquated complex, the di-aquated complex was found

to be both thermodynamically and kinetically preferred for platanation to guanine.⁶² This was attributed to the involvement of one of the ammine ligands in hydrogen bonding.⁶²

However, a study conducted by Deubel *et al.* has demonstrated limitations of DFT to study hydrolysis reactions when coupled with implicit solvation models.⁶³ Deubel *et al.* studied the step-wise hydrolysis of cisplatin and recorded the pK_a values of the Pt complexes with the B3LYP functional, a continuum dielectric model (CDM), the LANL2DZ effective core potential for Pt and the 6-31G(d,p) basis set for non-metal atoms.⁶³ The activation free energy for the first and second hydrolysis was found to be 125.5 and 129.7 kJ mol⁻¹, respectively, in which the activation free energy was 25.1 kJ mol⁻¹ higher than the previously reported experimental values.⁶³ The pK_a of the complexes were calculated using a thermodynamic cycle, resulting in an overestimation of pK_a compared to experimental by 1.4 and 2.9 pK_a units for mono- and di-hydrated equivalent, respectively.^{63,64} These overestimations may indicate that implicit solvation is not sufficient to describe the hydrolysis reactions.

To-date, the effect of explicit solvation was identified among the most important factors that affect the prediction of Gibbs free energy of step-wise hydrolysis and reaction mechanisms of cisplatin and its analogue. Andreoni *et al.* made use of Car-Parrinello molecular dynamics (CPMD) with the BLYP functional, alongside 35 water molecules to study the first step of the hydrolysis mechanism, replacing one Cl⁻ to form the mono-hydrated equivalent.^{65,66} They discovered that inclusion of explicit water molecules was essential to study the S_N2 reaction of replacing Cl⁻ with a H₂O, with 4 to 8 water molecules required to solvate the Cl⁻ leaving group.⁶⁵ Previously conducted kinetics experiments have indicated that the hydrolysis reaction was enthalpically driven, with a ΔH of 83.9 kJ mol⁻¹.^{55,67,68} Ensing *et al.* also applied CPMD with metadynamics and 50 explicit water molecules to investigate the free energy landscape of the step-wise hydrolysis reaction of cisplatin, in particular the activation free energies.⁶⁹ The 5 *ps* simulations revealed that an intricate hydrogen bonded water network surrounds cisplatin, with Cl⁻ and NH₃ forming an average of 1.7 and 2.9 hydrogen bonds to the surrounding water molecules, respectively.⁶⁹ The water structure did not undergo significant changes during the hydrolysis process, with the chloride preferring to be located near the Pt centre at 4.5 Å, thus forming a contact ion pair.⁶⁹ Through the simulations, 3 minima were located corresponding to the reactant, intermediate and final product.⁶⁹ Free energy profiles and total free energies of

the step-wise hydrolysis were calculated using metadynamics and compared to experimental data. They determined that the free energies of the second step was 31.4 kJ mol^{-1} lower than that of the first step, indicating the latter to be the rate determining step, which is in accordance with experimental data.⁶⁸

In summary, none of the studies contrasted the hydrolysis rate of a series of Pt-based complexes. In order to address this gap in the literature, an explicit solvation approach through inclusion of tens of water molecules was adopted in this study to obtain the thermodynamic properties such as dissociation energies of the step-wise hydrolysis of commonly used Pt-based anti-cancer drugs - cisplatin, carboplatin, oxaliplatin and nedaplatin. This was achieved by performing relaxed scan geometry optimisations by an incremental increase of the dative bond between the Pt cation and the leaving group (LG) such as chloride and ammonia in cisplatin. The results from the explicit solvation approach were compared to Gibbs free energies obtained from the classical thermodynamic cycle of the two-step hydrolysis in combination with implicit solvation models.

3.2 Theoretical Procedures

3.2.1 Geometry optimisation and relaxed scans within explicit solvation approach

An explicit solvation approach was adopted for studying the potential energy surface of the dissociation mechanism of the bond between the Pt cation and a leaving group in cisplatin, carboplatin, oxaliplatin and nedaplatin. Ammonia molecules, chloride and dicarboxylate anions were considered as leaving groups in the study. Each Pt-based complex was surrounded with explicit H_2O molecules (see Fig 3.3) - 33 for cisplatin, 48 for carboplatin, 52 for oxaliplatin, and 51 for nedaplatin to ensure that they were fully surrounded with a single solvation layer of water molecules.

All DFT calculations were performed using either Gaussian 09⁷⁰ or Gaussian 16⁷¹ quantum chemical packages. The Pt-based complexes underwent geometry optimisation and a subsequent frequency calculation in combination with the M06-2X functional,⁷² Dunning's cc-pVDZ (VDZ) basis set for the non-Pt atoms,⁷³ Dunning's cc-pVTZ-pp (VTZ-pp) ECP⁷⁴ for the Pt atom and an implicit solvent model, a conductor-like polarisable continuum model (CPCM)

solvation model⁷⁵ with water as solvent. The absence of imaginary frequencies confirmed the location of a minimum on the potential energy surface.

Relaxed scan geometry optimisations were performed by incrementally stretching the Pt–leaving group bond by 0.1 Å up to 1.0 Å, 1.2 Å, 1.4 Å and 2.0 Å away from its equilibrium length. Both a universal solvation model based on density (SMD)⁷⁶ and the CPCM were initially used to perform the relaxed scans. However, SMD geometry optimisations led to convergence issues because of the poor description of the solvent accessible surface area in some of the systems and therefore, CPCM solvation model results were used exclusively within the large explicit solvation approach.

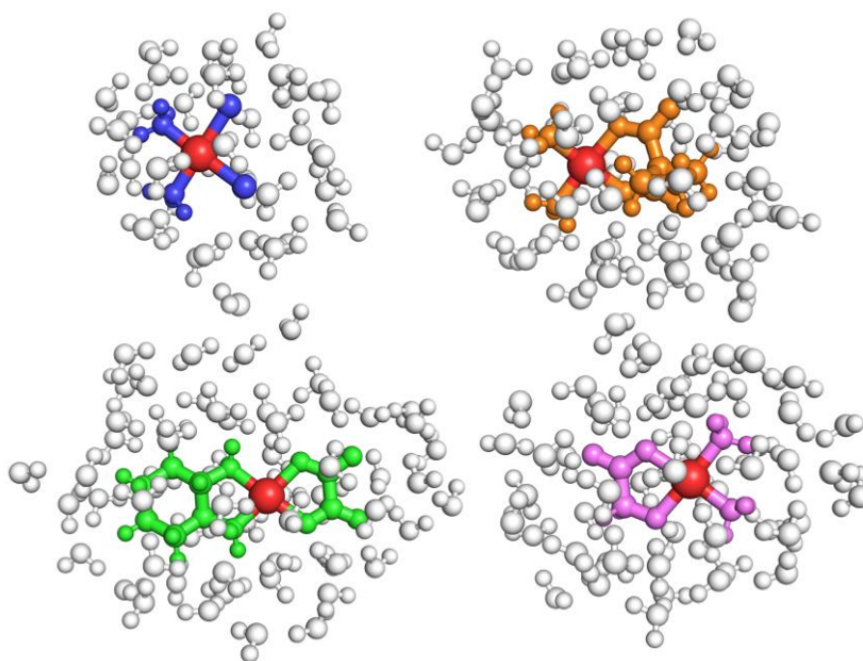


Figure 3.3: Models of cisplatin (top left), carboplatin (top right), oxaliplatin (bottom left) and nedaplatin (bottom right) solvated with explicit water molecules. The Pt metal ion is shown in red and explicit water molecules in white.

3.2.2 Assessment study for single point improved energy calculations

Recently Reiher et al. has established the WCCR10 database that contains 10 dissociation reactions of transition metal complexes, with three dissociation reactions involving the Pt metal centre.³¹ In this work two of these dissociation reactions (see Figure 3.4) were assessed with two of the most widely used DFT functionals - M06-2X⁷² and ω B97X-D.⁷⁷ M06-2X, a hybrid meta-GGA functional, was specifically designed to predict non-covalent interactions and barrier heights.⁷² ω B97X-D, a long-range corrected hybrid functional respectively, has shown superior performance for the prediction of majority of thermodynamic properties, including atomisation energies.⁷⁷ All species were optimised with both functionals combined with both VDZ and VTZ basis sets for the main group elements and VDZ-pp and VTZ-pp ECPs for the Pt metal ion, respectively.^{73,74,78} Single point energy calculations were performed with the cc-pVQZ (VQZ), aug-cc-pVTZ (aVTZ) and aug-cc-pVQZ (aVQZ) basis sets for non-Pt atoms, accompanied with the cc-pVQZ-pp (VQZ-pp), aug-pVTZ-pp (aVTZ-pp) and aug-pVQZ-pp (aVQZ-pp) ECPs, respectively, on Pt. Zero point vibrational energy (ZPVE) corrections were obtained from the optimisation step and added to the single point energies. The obtained dissociation energies was compared to that obtained experimentally^{79,80} to identify which of the two functionals was better for studying Pt-based complexes considered here. The experimentally reported dissociation energy for Reactions 1 and 2 are 120.2 ± 2.7 ⁷⁹ and 102.6 ± 2.5 kJ mol^{-1} ,⁸⁰ respectively.

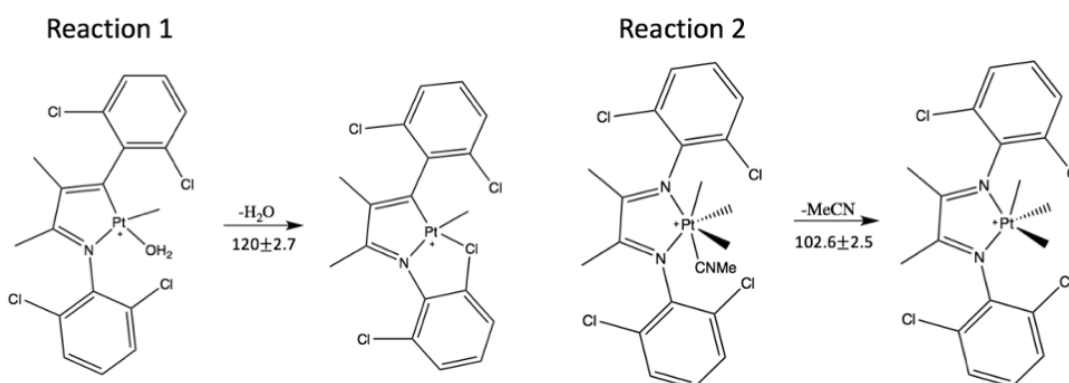


Figure 3.4: Dissociation reaction involving Pt metal from the WCCR10 benchmark set. Experimental dissociation energies are given under each reaction in kJ mol^{-1} .^{31,79,80}

Table 3.1: Raw errors (in kJ mol^{-1}) of M06-2X and ω B97XD with varying Dunning's basis sets on VDZ- and VTZ-optimised complexes. Opt represents geometry optimisation calculations. SP represents single point energy calculation on a given optimised geometry.

	Reaction 1		Reaction 2	
	M06-2X	ω B97X-D	M06-2X	ω B97X-D
Opt VDZ	21.9	23.4	-14.7	-10.0
SP VTZ	-5.5	-6.9	-18.9	-15.2
SP VQZ	-13.2	-15.3	-20.9	-17.8
SP aVTZ	-16.0	-18.5	-20.5	-17.2
SP aVQZ	-16.7	-20.0	-20.8	-18.4
Opt VDZ	-5.6	-6.9	-19.4	-17.0
SP VQZ	-13.5	-15.5	-10.8	-19.6
SP aVTZ	-16.2	-18.5	-10.2	-19.0
SP aVQZ	-17.1	-20.0	-10.7	-20.3

Analysis of the raw errors of the M06-2X and ω B97XD functionals showed systematic underestimation of the experimentally measured dissociation energies in the range of -5.5 to -20.3 kJ mol^{-1} . VDZ represented the only exception, as the errors became positive $> 22 \text{ kJ mol}^{-1}$. The downside of these meta-GGA functionals that their performance can only be considered reliable with at least a triple- ζ quality basis set. Out of the basis sets used aVTZ with the ω B97X-D functional performed consistently for both reactions. Underestimating experimental values by 18.0 kJ mol^{-1} on average. Therefore, ω B97X-D/aVTZ (with aVTZ-pp ECP used for the Pt metal) was used for all single point energy calculations unless stated otherwise.

3.2.3 Gibbs free energy calculations of step-wise hydrolysis and di-hydrolysis using implicit solvation

Gibbs free energies of step-wise hydrolysis and di-hydrolysis for all 4 complexes were predicted using a standard thermodynamic cycle. Examples of the studied thermodynamic cycles are given in Figure 3.5 for cisplatin and carboplatin. In the step-wise hydrolysis, a single water molecule replaces one or parts of the leaving group at each step. In the case of cisplatin $[\text{Pt}(\text{NH}_3)_2\text{Cl}(\text{H}_2\text{O})]^+$ and $[\text{Pt}(\text{NH}_3)_2(\text{H}_2\text{O})_2]^{2+}$ complexes are produced at step 1 and step 2, respectively. In the case of carboplatin one of the two carboxylate groups becomes liberated at step 1, whereas at step two a di-anion is produced. I-hydrolysis, on the other hand, was

considered as a simultaneous dissociation of either both chlorides in the case of cisplatin or the di-carboxylate anion in the case of carboplatin. For oxaliplatin and nedaplatin thermodynamic cycles similar to that of carboplatin were considered.

Geometry optimisations were again performed with the M06-2X functional combined with the VDZ basis set for non-metal atoms, the VTZ-pp ECP basis set for the Pt atom and the SMD solvation model. Gas phase electronic energies were improved with the ω B97X-D functional as identified above. Both Gibbs free energies in gas, ΔG_{gas} , and with implicit solvent, ΔG_{solv} , (see equations 3.1 and 3.2) were calculated using the standard physical chemistry formulae.⁸¹

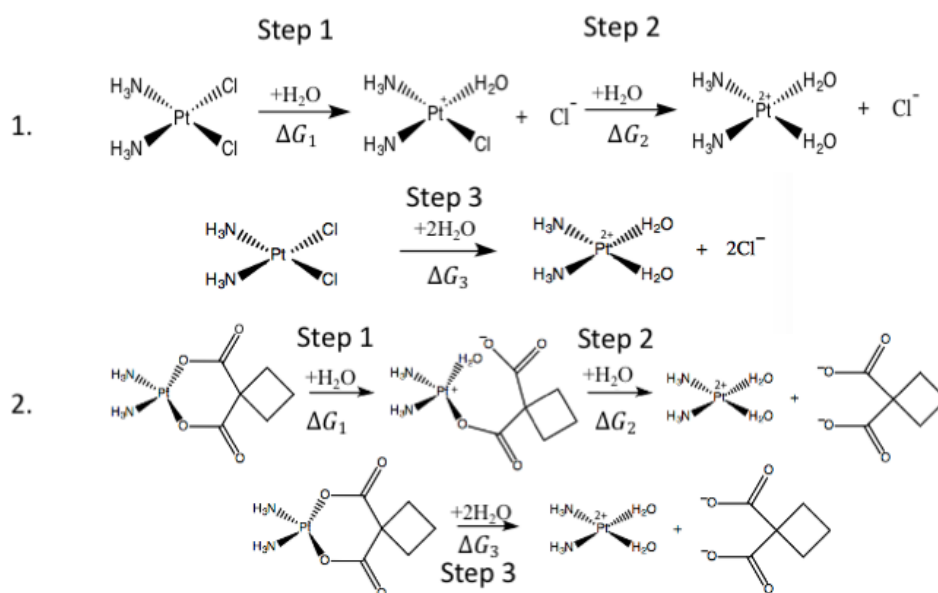


Figure 3.5: Step-wise hydrolysis and di-hydrolysis processes for cisplatin (1) and carboplatin (2).

$$\Delta G_{diss}^{solv} = \Delta H + TC - T\Delta S + \Delta(\Delta G_{solv}) \quad (3.1)$$

$$\Delta G_{diss}^{gas} = \Delta H + TC - T\Delta S \quad (3.2)$$

where ΔG_{diss}^{solv} is Gibbs free energy in implicit solvent model, ΔG_{diss}^{gas} is Gibbs free energy in gas phase, ΔH is the dissociation enthalpy in gas phase ($\Delta E + \Delta ZPVE$), E is the electronic energy,

$ZPVE$ is the zero-point vibration energy, TC is the temperature correction, and ΔS is the entropic contribution. The latter three were calculated at the geometry optimisation level of theory. ΔG_{solv} represents solvation energy of each component included in the thermodynamic cycle. ΔG_{solv} was calculated by taking the difference of single point energies of solvent (SMD) and gas at M06-2X functional, VDZ basis set and VTZ-pp ECP.

3.2.4 ChelpG partial atomic charges

ChelpG analysis is performed on the optimised geometries using the HF method, VDZ basis set on the non-Pt atoms and VTZ-pp ECP on Pt metal ion, represented with an ionic radius of 0.8 Å.⁸²

3.2.5 Energy profile calculations of step-wise hydrolysis of cisplatin in explicit solvation

Geometry optimisations were again performed with the M06-2X functional combined with the VDZ basis set for non-metal atoms, the VTZ-pp ECP basis set for the Pt atom and the CPCM solvation model. Location of minima and maxima were confirmed by performing frequency calculations, with no or one imaginary frequency, to ensure that either equilibrium or transition state was obtained.

3.3 Results and Discussion

3.3.1 Relaxed scans of the first step of hydrolysis using explicit solvation approach

Figure 3.6 shows relaxed scans of the dissociation mechanism of leaving groups in the four Pt complexes studied by incrementally increasing the Pt-leaving group dative bond from its equilibrium value, R_e . On the relaxed scans, energies are given in the form of relative energies calculated with respect to the original minimum located for each complex. Relaxed scans were performed for each unique leaving group in the complex as demonstrated in the snapshots of optimised structures for each Pt-based complex in Figure 3.6. For example, for cisplatin the Pt bond to both the ammonia molecule and the chloride anion were allowed to be stretched to generate two potential energy curves. In the case of the di-carboxylate anion present in

carboplatin and oxaliplatin, only one of the carboxylate groups was allowed to be stretched away from the Pt cation. For nedaplatin, the di-anion is based on the glycolic acid with the different chemical environment for the two oxygens in bonding with Pt. Therefore, relaxed scans were performed for both Pt-O bonds.

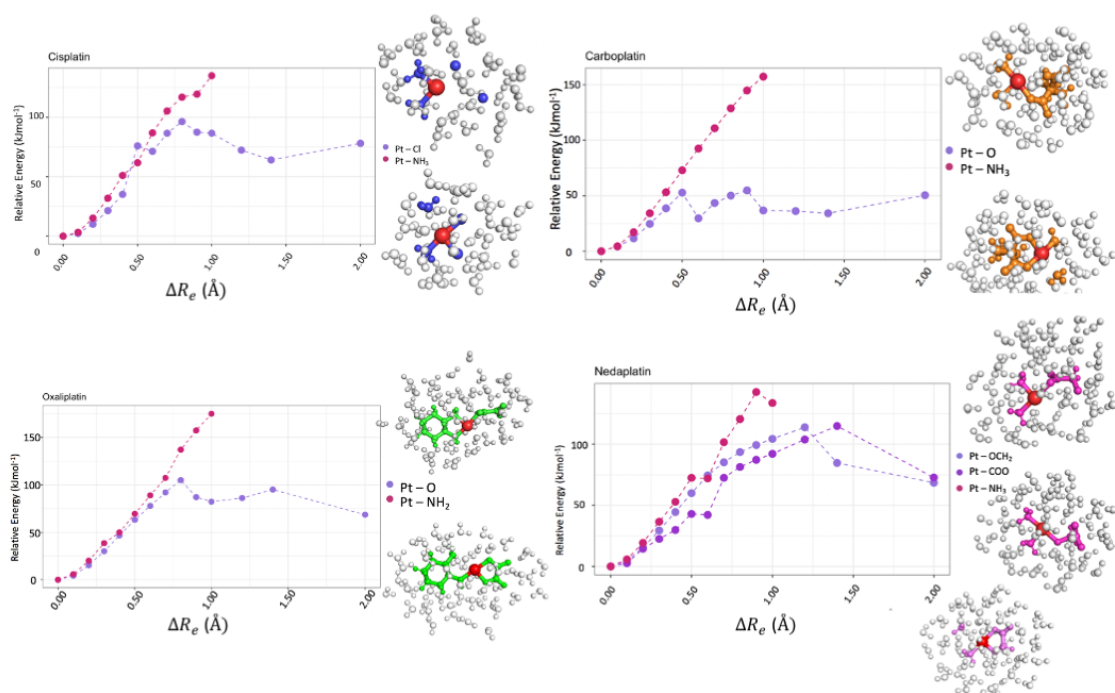


Figure 3.6: Relaxed scans of the first step of hydrolysis of cisplatin (blue), carboplatin (orange), oxaliplatin (green) and nedaplatin (pink).

Analysis of the relaxed scans has revealed that the dissociation of the Pt-anion bond lies energetically between 96.4 kJ mol⁻¹ or Pt-Cl in cisplatin and 54.8 kJ mol⁻¹ for Pt-O in carboplatin. The result for cisplatin slightly overestimates previously published experimental data, in which Gibbs free energy of activation of the first step of hydrolysis was found to lie between 81.6 and 90.0 kJ mol⁻¹.⁵⁵ It should be noted that the experimental Gibbs free energy of activation were obtained through pH adjustments and titration to ensure the anation of Cl⁻ whereas the calculations presented in this study only looks at the effects of water on the reactions. Hence, while the trends are similar, the Gibbs free energy of activation should not be compared to directly. The dissociation of NH₃ and the NH₂ group in the case of oxaliplatin has not even

peaked at 1.0 Å (with the exception of nedaplatin), with the barrier reaching 135.1 kJ mol⁻¹, thus confirming lower preference for the Pt-N bond dissociation. In the case of nedaplatin, the carboxylate group of the di-anion is more likely to dissociate first, with the dissociation of the second Pt-O bond being 12.2 kJ mol⁻¹ higher in energy when positioned 1.0 Å away from their R_e. Interestingly, upon increasing the Pt-leaving group to 1.4 Å, the dissociation of the ether group forms the more stable complex, resulting in a structure that is 30.2 kJ mol⁻¹ lower in energy. Apart from nedaplatin, the anionic leaving group dissociation from the Pt centre has reached the highest point on the potential energy surface already within 1.0 Å away - 96.5 kJ mol⁻¹ for cisplatin, 54.8 kJ mol⁻¹ for carboplatin and 105.1 kJ mol⁻¹ for oxaliplatin. This distance is still rather short for a water molecule to diffuse in and start directly interacting with the Pt cation and hence, why the formation of mono-aquated complexes was not directly observed. Compared to cisplatin, the dissociation of the carboxylate-based di-anions has a similar amount of energy, with the exception of carboplatin, for which the barrier is only 54.8 kJ mol⁻¹. These initial results indicate that the first step of hydrolysis of carboplatin, oxaliplatin and nedaplatin occurs at a similar or slightly faster rate to that of cisplatin. This finding supports the conclusion from the previously published work from our group, in which the ChelpG analysis performed on the cisplatin and carboplatin structures optimised with an implicit solvation model suggested that the Pt-O bond was more ionic in the latter and hence more likely to dissociate faster.⁸³

Table 3.2: ChelpG partial atomic charges of cisplatin, carboplatin, oxaliplatin and nedaplatin in their equilibrium geometries optimised using implicit (CPCM) and explicit solvation approaches.

	Implicit Solvation Approach				Explicit Solvation Approach			
	Pt	O or Cl	NH ₂ /NH ₃	Di-anionic LG	Pt	O or Cl	NH ₂ /NH ₃	Di-anionic LG
Cisplatin	2.104	-0.734 -0.734	-0.318 -0.318		2.599	-1.185 -0.844	-0.121 -0.172	
Carboplatin	2.102	-1.236 -1.286	-0.160 -0.090	-1.852	2.866	-2.050 -1.874	-0.232 -0.174	-0.569
Oxaliplatin	2.376	-0.957 -0.957	-1.144 -1.144	-0.637	2.827	-2.569 -1.059	-1.475 -0.908	-2.146
Nedaplatin	2.018	-0.932 -0.820	-0.225 -0.229	-1.564	3.044	-3.331 -1.896	-0.274 -0.021	-4.279

To understand whether the use of an explicit solvation approach affects the charge distribution in Pt-based complexes, ChelpG partial atomic charges were compared between structures optimised with implicit and explicit solvation approaches adopted in the study (see Table 3.2). The presence of explicit water molecules introduced significant changes to the charge distribution, especially to the positive charge on the Pt cation (up to 1 e in the case of nedaplatin) and the negative charge on the anionic leaving groups, with the charge on the ammonia molecule or the NH_2 group decreasing only slightly. The charges on the oxygen atoms in the di-anions are particularly striking in the explicit approach, especially compared to those on chlorides in cisplatin. These charges range between -1.896 e on the ether oxygen in nedaplatin and -2.569 e and -3.331 e on the carboxylic oxygen in oxaliplatin and nedaplatin, respectively.

The ChelpG charges are in excellent agreement with Gibbs solvation energies predicted for individual anions with M06-2X/VDZ and SMD. The solvation energies recalculated to *per formal charge* of each anion (-1 for chloride and -2 for di-anions) indicate that solvation of di-anions such as cyclobutanedicarboxylate (-460.9 kJ mol⁻¹), oxalate (-511.5 kJ mol⁻¹) and 2-oxidoacetate (-528.8 kJ mol⁻¹) is energetically more favourable than that of chloride (-283.9 kJ mol⁻¹) by a factor of at least 1.6. To this end, the dissociation of the carboxylate-based anions is predicted to occur at the same rate or faster than the chloride dissociation.

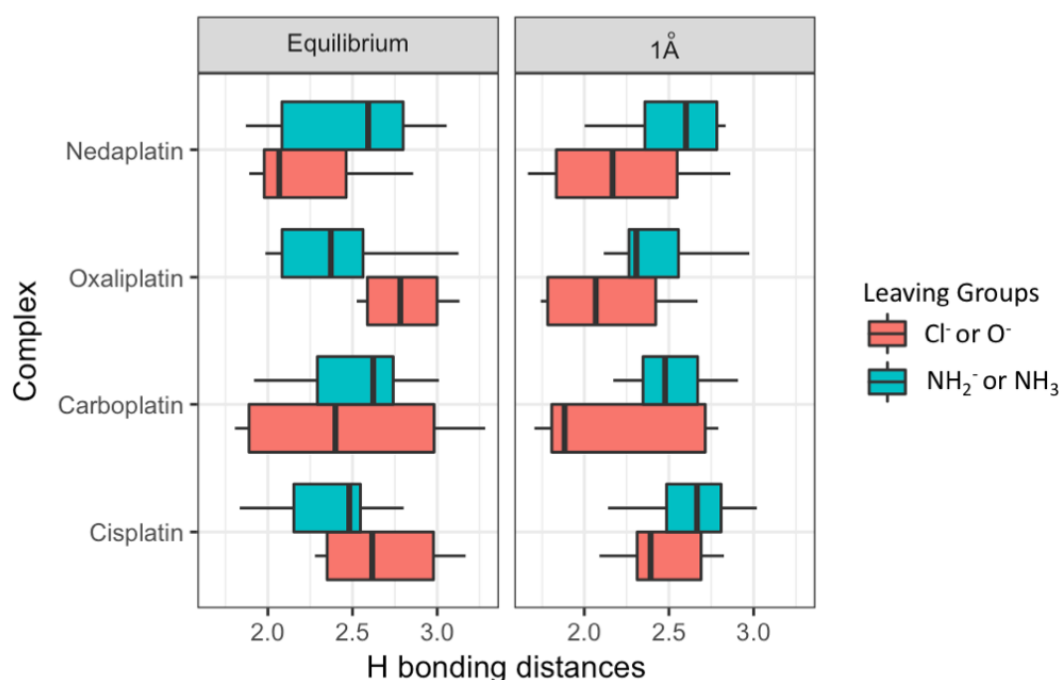


Figure 3.7: Box and whiskers plot of Hydrogen bonding between water molecules and leaving groups at either equilibrium or at 1 Å away. The length of the box plot indicates the spread of the H bonding between the water molecules and the leaving groups.

To further understand the charge distribution in explicit models, the hydrogen bonding distances between explicit water molecules and the respective leaving groups were compared in Figure 3.7. Both scenarios – the complex in the initial equilibrium geometry and the complex in which when the leaving group is located at 1 Å away from the Pt centre were considered. As the NH₂ or NH₃ group are 1 Å away from their equilibrium distance, the hydrogen bonding distance to the surrounding water molecules became longer, from a minimal increase of 0.13 Å for oxaliplatin and nedaplatin to 0.31 Å for cisplatin. This increase in hydrogen bonds to the NH₂ or NH₃ group decreases the strength of hydrogen bonding. However, the opposite can be seen when the Cl⁻ and di-anions move away by 1 Å from their equilibrium distance. The hydrogen bonding between water molecules decreases, ranging from 0.1 to 0.8 Å for carboplatin and oxaliplatin, respectively. This decrease in hydrogen bonding suggests stronger hydrogen bonding as compared to their NH₂ or NH₃ counterpart, hence better stabilisation of the system. These findings further support experimental results that chloride and di-anions

are more energetically stable leaving groups. Apart from cisplatin, the hydrogen bonding in water molecules around carboplatin, oxaliplatin and nedaplatin becomes quite short, 2.168 Å on average compared to 2.462 Å in cisplatin. This observation agrees with the energetic data in Figure 3.6 that the first step of hydrolysis in the Pt-based complexes studied are expected to be similar in rate.

3.3.2 Relaxed scans of the second step of hydrolysis and di-hydrolysis using explicit solvation approach

The second step of hydrolysis was only studied for the energetically preferred leaving groups – chlorides and di-anions. Relaxed scans were again performed in the same manner as described above for the first step of hydrolysis.

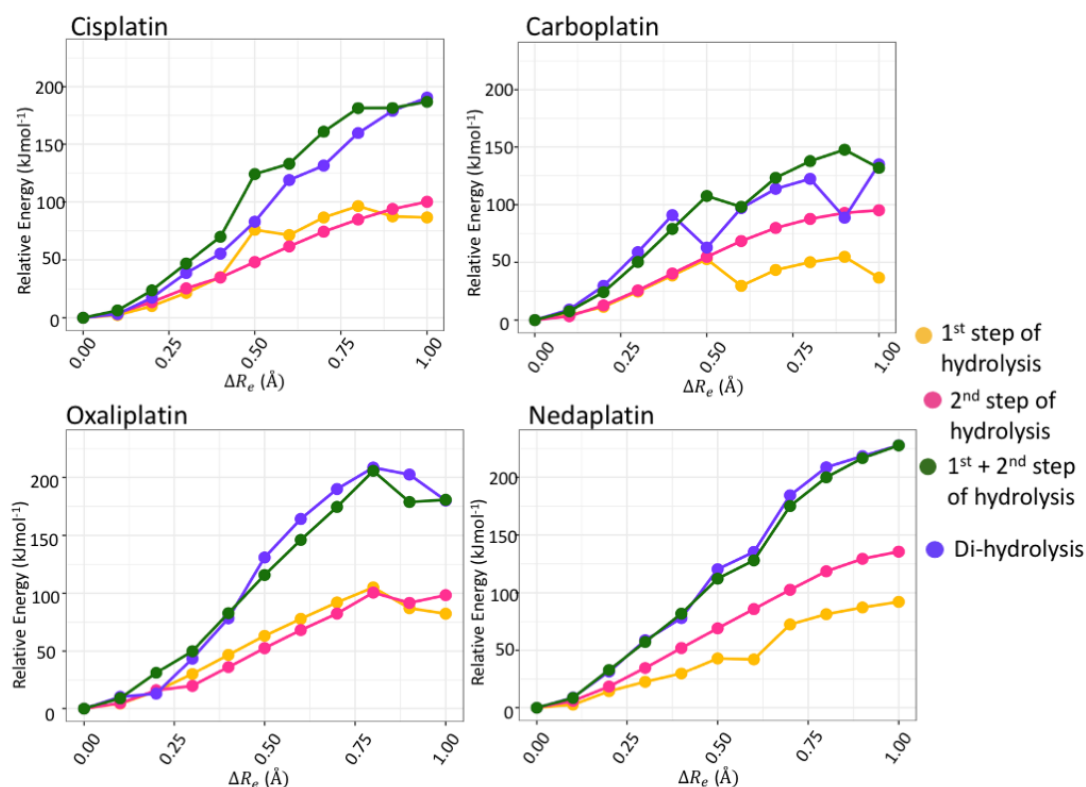


Figure 3.8: Relaxed scans of first and second step of hydrolysis and di-hydrolysis of cisplatin, carboplatin, oxaliplatin and nedaplatin.

Figure 3.8 shows the relaxed scans of the dissociation mechanism that emulates either the second step of hydrolysis or the di-hydrolysis reaction of the four Pt complexes. The two-step hydrolysis was studied by incrementally increasing the second Pt-leaving group bond from its equilibrium value, R_e , while keeping the first leaving group at 1.0 Å away from its equilibrium length. The energy of the latter was used as the reference point to calculate relative energies of the second hydrolysis step in Figure 3.8. The di-hydrolysis reaction was studied by incrementally increasing both Pt-leaving group bonds simultaneously up to 1.0 Å away from its equilibrium length. The original minimum energy structure was used as the reference point in Figure 3.8.

The activation barrier of the first and second step of the step-wise reaction and the di-hydrolysis reaction could be calculated from Figure 3.8. The activation barrier of the first and second step of the step-wise reaction for cisplatin was revealed to be 96.5 and 100.2 kJ mol⁻¹, respectively, indicating that both steps of hydrolysis is likely to occur at a similar rate. This was also confirmed by a [¹H, ¹⁵N] heteronuclear multiple-quantum correlation (HMQC) NMR spectroscopy study conducted by Kozelka *et al.*, who measured the rate of hydrolysis of the first hydrolysis and the rate of anation of the di-hydrolysed equivalent of cisplatin.⁸⁴ Kozalka *et al.* determined the rate of hydrolysis to be 1.6×10^{-5} and 1.2×10^{-5} s⁻¹, respectively.⁸⁴ This is similar for the other Pt-complexes, with the exception of carboplatin, with the first and second step energy barrier to be 105.1 and 100.6 kJ mol⁻¹ for oxaliplatin and 114.9 and 135.6 kJ mol⁻¹ for nedaplatin. For carboplatin, however, there is a large energetic difference of 40.4 kJ mol⁻¹. This is supported by previously conducted acid hydrolysis studies on cisplatin, where the first order rate constants for the first and second step of the step-wise hydrolysis to be 2.5 and 3.3×10^{-5} s⁻¹ at 25°C.⁶⁷ The higher energy barrier of the second step for carboplatin is also supported by a much slower rate constant (3.96×10^{-4} and 9.05×10^{-5} for the first and second step, respectively) reported by Hay et al, where the dissociation of cyclobutanedicarboxylate was studied in 1 mol dm⁻³ of HClO₄.⁸⁵

The dissociation of the second step of hydrolysis has not peaked at 1.0 Å, other than oxaliplatin, with the barrier reaching > 131.9 kJ mol⁻¹. In the case of oxaliplatin, the second step of hydrolysis peaked on the energy surface when the second Pt-O bond is 0.8 Å away from R_e , with a relative energy of 183.0 kJ mol⁻¹ when compared to the original minimum located.

Similar to the first hydrolysis step, the increase of 1.0 Å is too short for a water molecule to diffuse and interact with the Pt metal centre and the di-hydrolysed species were not witnessed.

Upon comparing the energy barrier of the di-hydrolysis reactions, it is highly unlikely that Pt- complex will undergo that reaction pathway. With the energy barrier of the di-hydrolysis reaction to be 190.60, 134.94, 208.54 and 227.82 kJ mol⁻¹ for cisplatin, carboplatin, oxaliplatin and nedaplatin, respectively, they are nearly twice as energetically demanding as compared to the first step of the step-wise hydrolysis. This much higher energy barrier also suggests that if the di-hydrolysis reaction did occur, it would occur at a much slower rate than the first and second step of the step-wise hydrolysis.

The ChelpG partial atomic charges of the Pt-based complexes were compared between the original minimum located, first and second steps of the hydrolysis mechanism (see Tables 3.2 and 3.3). Upon the first step of the hydrolysis, the partial charge of Pt cation increased for all Pt-complexes, ranging between 0.002 *e* for nedaplatin and 0.312 *e* for cisplatin. The first hydrolysis step also altered the negative charge of the anionic leaving groups quite significantly, especially 2-oxidoacetate on nedaplatin (increasing the partial charge by 2.223 *e*), with the charge of the NH₂ and NH₃ groups relatively unchanged.

With the exception of cisplatin, the partial charge of the Pt cation decreases from the first to second step of hydrolysis on average by 0.190 *e*. Interestingly, the partial charge of the di-anions differed rather slightly between the first and second steps of hydrolysis. For cisplatin and oxaliplatin, the total charge on the chloride and the oxalate increased by 0.766 and 0.701 *e*, respectively. In carboplatin and nedaplatin, the charge decreased slightly by 0.320 and - 1.124 *e*. After the second step of hydrolysis, the charges on the oxygen atoms in the di-anions became significantly less negative after the second step of the hydrolysis, ranging between - 1.154 *e* on the oxygen on carboplatin and -1.743 and -2.621 *e* on oxaliplatin and nedaplatin, respectively. The overall charge on the dianions remained below -2, a formally assigned charge, with the 2-oxidoacetate anion maintaining a charge of -3.180 *e*. Contrary to this trend, the overall charge on the chlorides reduced to merely -1.359 *e* in the second step. The presented data indicate that after the second step of hydrolysis the strongly positive charge on the Pt centre (> 2.8 *e*) and the strongly negative charge on the di-anions in carboplatin, oxaliplatin and nedaplatin might lead to the formation of a contact ion pair. On the other hand, the formation of such

contact pair is less likely in the case of cisplatin contrary to what was suggested previously based on the metadynamics simulations.⁶⁹

The interaction energies of all four complexes were also calculated. The explicit water molecules were removed from the systems in both the original minima and final structure obtained after the second step of the step-wise hydrolysis. The full structures (E1) obtained after were divided into the Pt-complex without the dianion (E2) and the dianion (E3), both within the full basis set of the full complex and at ω B97XD functional, VDZ basis set, VTZ-pp ECP level of theory. E2 and E3 were also calculated with counterpoise correction to account for the basis set superposition error (BSSE). By subtracting E2 and E3 from E1 will give the interaction energies, E_{int} , respective leaving groups with the metal complex at their equilibrium geometries and when the leaving group is extended away from the metal centre. At equilibrium geometries, the E_{int} of cisplatin, carboplatin, oxaliplatin and nedaplatin were -2210.6, -2161.6, -2036.6 and -2332.8 kJ mol⁻¹, respectively, and -1679.9, -1554.8, -1451.7 and -1724.8 kJ mol⁻¹ after the step-wise hydrolysis. The difference in E_{int} between the equilibrium geometry and hydrolysed geometry ranges from -608.0 to -530.7 kJ mol⁻¹ from nedaplatin to cisplatin. With the large E_{int} , this indicates that though the leaving groups are at 2 Å away from the equilibrium Pt-LG distance, the strong interaction could be hindering the formation of a Pt-H₂O bond with an explicit water molecule.

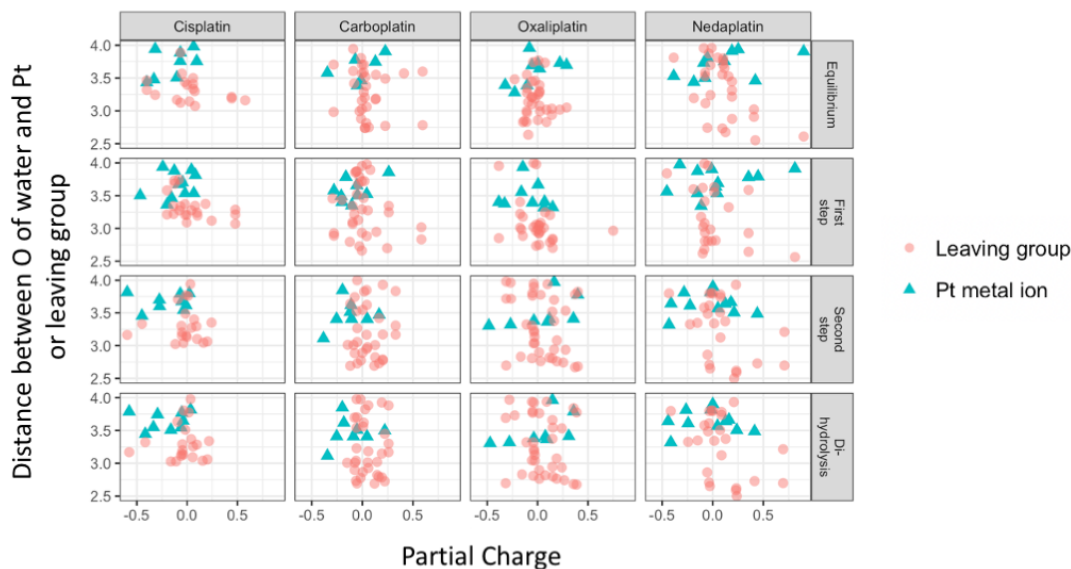


Figure 3.9: Charges of water molecule within a 4 Å radius of either the Pt metal ion or the leaving group.

Figure 3.9 demonstrates the importance of explicit water molecules to stabilise the dissociated species. Analysis of Figure 3.9 reveals tremendous capacity of water molecules to redistribute their electron density to equally stabilise positively and negatively charged products. The stabilising effect that water molecules have around the Pt metal ion can be seen even at the respective original minimum located for the Pt-complexes, ranging from -0.399 to $0.898 e$ from cisplatin to nedaplatin, respectively. The partial charges around the leaving groups ranges between -0.399 to 0.577 , -0.284 to 0.595 , -0.228 to 0.288 and -0.386 to $0.898 e$ for cisplatin, carboplatin, oxaliplatin and nedaplatin, respectively. Upon hydrolysis, the presence of the water molecules continues to play a pivotal role to stabilise the system. For example, as cisplatin undergoes the step-wise hydrolysis, the maximum partial charge of water within 4 Å of Pt and the Cl^- decreases from 0.577 to 0.084 and 0.577 to $0.479 e$, respectively. This suggests that the hydrolysis results in a charge transfer from Pt to both the Cl^- leaving group and the explicit water molecules, stabilising the reaction electronically. The minimum partial

charges of the water molecules around Pt ranges also decreases from -0.399 to -0.466 e , giving further evidence of the importance of explicit solvation to study such hydrolysis reactions. This trend can be witnessed across the various Pt-complexes, with the maximum partial charge of water molecules around Pt to decrease, with the exception of carboplatin, from 0.288 to 0.149 e and 0.898 to 0.811 e for oxaliplatin and nedaplatin. For carboplatin, it increased from 0.227 to 0.261 e . The minimum partial charge of H₂O around Pt decreased for the Pt-complexes, except carboplatin, -0.323 to -0.385 e and -0.386 to -0.454 e for oxaliplatin and nedaplatin, respectively. The minimum partial charge of H₂O around Pt increases for carboplatin from -0.347 to -0.281 e .

	Cisplatin			
	Pt	Cl	NH ₃	
First Step	2.911	-0.611	-0.259	
		-1.514	-0.161	
Second Step	2.760	-0.361	-0.036	
		-0.998	0.038	
	Carboplatin			
	Pt	O	NH ₃	Cyclobutanedi carboxylate
First Step	3.103	0.238	0.278	-2.352
		-2.782	-0.180	
Second Step	2.892	-1.725	-0.054	-2.672
		-1.154	0.031	
	Oxaliplatin			
	Pt	O	Diaminocyclohexane	Oxalate
First Step	3.134	-0.560	-0.157	-3.095
		-3.234		
Second Step	2.859	-1.743	-0.566	-2.394
		-1.750		
	Nedaplatin			
	Pt	O	NH ₃	2-oxidoacetate
First Step	3.046	0.346	-0.171	-2.056
		-3.296	-0.001	
Second Step	2.923	-1.823	-0.317	-3.180
		-2.621	-0.143	

Table 3.3: ChelpG partial atomic charges of cisplatin, carboplatin, oxaliplatin and nedaplatin optimised with the Pt-Cl/Pt-O bonds fixed at 2 Å within the explicit solvation approach.

3.3.3 Comparison of energetics between explicit and implicit solvation approaches

Table 3.4 compares Gibbs free energies, ΔG_{solv} , calculated using the thermodynamic cycle and implicit solvation (see Figure 3.5) and energy differences, ΔE_{solv} , calculated using the structures from the relaxed scans. ΔE_{solv} was calculated as the difference in electronic energy, obtained from single point energy calculations with ω B97X-D functional, aVTZ basis set, aVTZ-pp ECP and CPCM solvation model.

$$\Delta E_{solv} = E_{\omega B97X-D}^{CPCM}(Complex_{eq}) - E_{\omega B97X-D}^{CPCM}(Complex_{2A}^{\circ}) \quad (3.3)$$

where $Complex_{eq}$ is the energy of the explicitly solvated Pt-complex in its equilibrium geometry and $Complex_2$ is the maximum energy deviation of the explicitly solvated Pt-complex with one or both anionic leaving groups away from the Pt metal ion.

Table 3.4: Comparison of ΔG_{solv} calculated using the thermodynamic cycle and implicit solvation and ΔE_{solv} calculated from the relaxed scans. All values are given in kJ mol^{-1}

	Cisplatin		Carboplatin		Oxaliplatin		Nedaplatin	
	ΔG_{solv}	ΔE_{solv}	ΔG_{solv}	ΔE_{solv}	ΔG_{solv}	ΔE_{solv}	ΔG_{solv}	ΔE_{solv}
First Step	101.4	109.4	84.6	100.0	49.6	120.4	87.6	125.4
Second Step	108.1	98.0	40.9	94.6	22.7	95.7	73.5	136.8
Di-Hydrolysis	209.5	209.9	125.5	196.4	72.3	253.1	161.1	224.6

From Table 3.4, different trends can be seen when comparing the ΔG_{solv} and ΔE_{solv} quantities of the Pt-complexes. It is not that surprising to some extent as these represent different measures of the hydrolysis mechanism. ΔG_{solv} provides an insight of Gibbs free energy of stepwise and di-hydrolysis reactions based on the information of the thermodynamically preferred intermediates and final products. As already identified above, ΔE_{solv} indicates that the activation barrier of the first step of hydrolysis is energetically rather similar among the studied complexes ranging from 87.3 to 125.4 kJ mol^{-1} for nedaplatin and oxaliplatin, respectively. The ΔE_{solv} values of the second step activation barrier also indicate that, except

for nedaplatin, are also similar, with the highest barrier of 98.0 kJ mol^{-1} corresponding to cisplatin. For nedaplatin, the ΔE_{solv} of the second step is significantly higher, by 38.8 kJ mol^{-1} , than those of the other complexes. This observation is further supported by the charges created on the dissociated species during the hydrolysis, with 2-oxidoacetate anion carrying a strongly negative charge of $-3.180 e$, $> 30\%$ more negative than theoretically predicted. The increased barrier reflects strong interaction that still exists between the Pt centre and the dianion, thus leading to an increase in the activation barrier.

ΔG_{solv} decreases significantly, by at least 14.1 kJ mol^{-1} , for carboplatin, oxaliplatin and nedaplatin going from the first to the second step of hydrolysis. The ΔG_{solv} numbers of the second step are particularly small ($< 40.9 \text{ kJ mol}^{-1}$) for carboplatin and oxaliplatin. The ΔG_{solv} criterion indicates that the hydrolysis mechanism is not thermodynamically demanding and should occur at an even faster rate for carboplatin, oxaliplatin and nedaplatin than cisplatin. However, this criterion does not account for a strong possibility of the formation of a contact ion pair between the dissociated Pt-complex and the leaving dianion, which might lead to the increase of the activation barrier. In addition, less positive small ΔG_{solv} values for carboplatin, oxaliplatin and nedaplatin are influenced by a strong solvation energy of the corresponding dianions as anions tend to have much affinity towards water – -921.9 , -1023.1 and $-1057.7 \text{ kJ mol}^{-1}$ for cyclobutanedicarboxylate, oxalate, 2-oxidoacetate, respectively. As a result, the ΔG_{solv} criterion must be used with caution because it does not depict the complete picture of the hydrolysis mechanism. Therefore, explicit solvation should be considered superior despite its cost to allow one to predict correct mechanistic details of the hydrolysis of Pt-based complexes.

Lastly, the ΔE_{solv} numbers in Table 3.4 indicate that the hydrolysis reactions for the four different Pt-complexes are likely to be a consecutive two-step reaction, with both steps to be energetically rather similarly and, hence, only small variations in hydrolysis rates. In the case of cisplatin and carboplatin, the ΔE_{solv} values for the second hydrolysis are 11.4 and 5.4 kJ mol^{-1} , respectively, lower than those of the first hydrolysis step, indicating that the second step will occur even faster after the first step is complete. In the case of carboplatin, oxaliplatin and nedaplatin, a strong possibility of the contact ion pair formation points out that the complex might not undergo a complete hydrolysis and the ligand might potentially

survive the hydrolysis by keeping itself close to the Pt-centre. The contact ion pair might be even thermodynamically stable enough for the ligand to enter a damaged cell and enhance the platination to the guanine nucleobase.

3.3.4 Accuracy of explicit solvation on the reaction mechanism of cisplatin

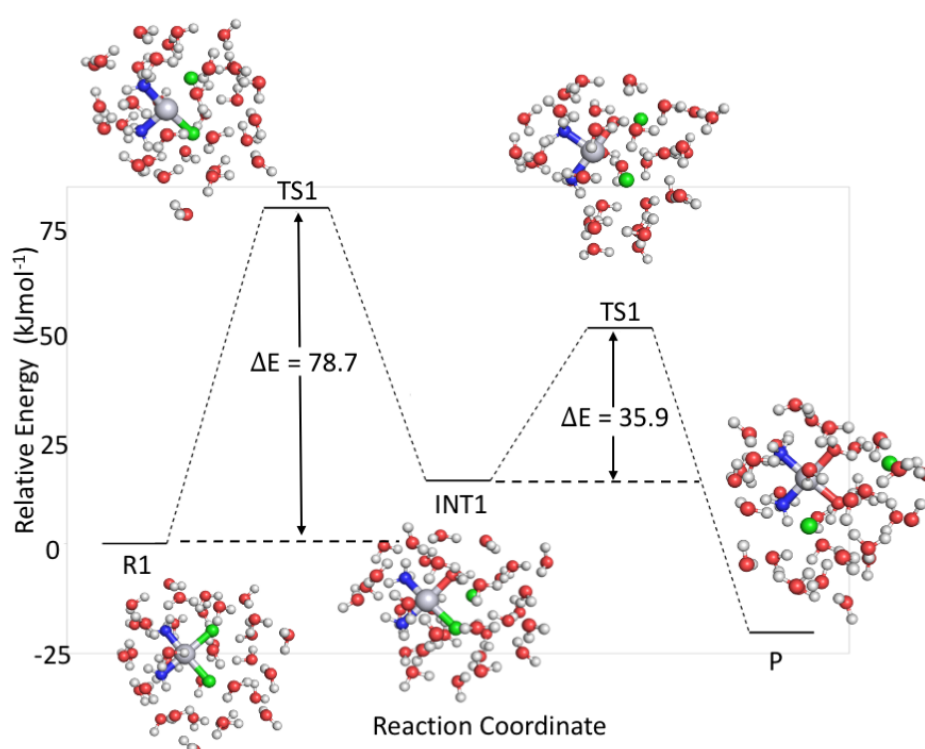


Figure 3.10: *Energy profile diagram of hydrolysis of cisplatin.*

Fig 3.10 shows the calculated energy profile of the hydrolysis of cisplatin. In the relaxed scans, the barrier heights of dechlorination of cisplatin was determined, to be 109.4 and 98.0 kJ mol⁻¹ for the first and second dissociation. By calculating the energy profile of hydrolysis, containing the same number of water molecules as the relaxed scans, the energy barriers to form transition states were compared to that obtained from the relaxed scans. The two-step hydrolysis was studied by optimising the equilibrium and transition state structures. The first transition state, TS1, was constructed by placing one water molecule approximately 2.5 Å away from the Pt metal centre and undertaking transition state optimisation. An imaginary frequency of -148 cm⁻¹ was observed for TS1. The first intermediate, INT1, was obtained by performing geometry

optimisation. The second transition state was constructed from INT1, placing another water molecule approximately 2.5 Å away from the Pt and an imaginary frequency of -142 cm^{-1} was obtained. The final product, the di-aquated complex (P), was obtained by optimising TS2.

From Figure 3.10, the activation barrier for the first and second hydrolysis steps was determined to be 78.7 and 35.9 kJ mol^{-1} , respectively. This finding is in contradiction to the energy barrier determined in Figure 3.8, where the activation barriers were revealed to be 96.45 and 100.19 kJ mol^{-1} for the first and second step, respectively. The lower activation barrier obtained from Figure 3.10 could be due to difference in modelling. Where the reaction coordinates located the transition states of cisplatin forming trigonal bipyramidal structures with the incoming H_2O molecule, it is likely to better reflect the barrier heights of the reaction. This formation of transition states and the additional Pt-OH₂ increases the Pt-Cl by at least 0.4 Å. The inclusion of explicit solvation also helps to stabilise the Cl leaving group by solvating it, with two water molecules positioned 2.1 Å away from Cl⁻ in both transition states. For INT1 and P, 4 and 5 water molecules were positioned within 2.5 Å away from Cl⁻.

The calculated 78.7 kJ mol^{-1} energy barrier for the first hydrolysis step was found to be in agreement to previously published experimental data of 81.6 to 90.0 kJ mol^{-1} .⁵⁵ Differing by a maximum of 12.3 kJ mol^{-1} , the inclusion of explicit solvation has demonstrated to be vital in reproducing experimental results.

3.4 Conclusions

This study investigates the hydrolysis reactions of four different Pt-complexes with the use of explicit solvation using a relaxed scan approach. By studying the relative energies, it was determined that Cl⁻ and di-anions are energetically favoured to be the leaving group, between 96.4 kJ mol^{-1} for cisplatin and 54.8 kJ mol^{-1} for carboplatin.

This study also shows that the inclusion of explicit solvation in studying the hydrolysis reactions of Pt-complexes is vital. Upon ChelpG analysis, the explicit water molecules play a stabilisation role in sharing the overall charge of the system, especially for nedaplatin, where 2-oxidoacetate differs significantly from its nominal -2.0 charge.

With the use of ΔG_{solv} and ΔE_{solv} , it was revealed that the Pt-complexes are likely to be activated via step-wise reaction. Similar ΔE_{solv} of the complexes indicates that they have similar rates of hydrolysis. This was witnessed in hydrolysis studies conducted in the lab and will be reported shortly. In addition, the importance of including explicit solvation in studying the hydrolysis mechanism was reiterated by producing more accurate energy barriers when compared to experimental data.

The activation barriers of the first and second step of the step-wise hydrolysis were calculated. Other than carboplatin, the activation barrier for the first and second step were similar, indicating that both steps would occur at similar rates. This was supported by previously published experimental results where the rate of hydrolysis of the first and second step of cisplatin were found to be similar. The higher energy barrier of the second step for carboplatin, by 40.4 kJ mol^{-1} , is also supported by a much slower rate constant in previously published experimental results.

In addition, the ΔE_{solv} was determined to overestimate the true energy barrier of the hydrolysis reaction. When the reaction coordinate of cisplatin was calculated with the presence of explicit solvation, it was determined that it was able to better reproduce previously published experimental data, differing by a maximum of 12.3 kJ mol^{-1} . By the formation of transition states, it was able to better predict barrier heights than the relaxed scan approach.

Di-hydrolysis reactions of the four Pt complexes were also emulated with explicit solvation. With the activation barrier ranging from 134.94 to $227.82 \text{ kJ mol}^{-1}$, it was concluded that it is unlikely that the four Pt complexes would undergo di-hydrolysis reaction as their activation barriers were nearly twice as energetically demanding as the first step of the step-wise hydrolysis. The significantly higher activation barriers of the di-hydrolysis reaction also suggests that if it took place, it would occur at a much slower rate as compared to the step-wise hydrolysis reaction.

3.5 References

- [1] Barnett Rosenberg, Loretta Van Camp, and Thomas Krigas. Inhibition of cell division in *Escherichia coli* by electrolysis products from a platinum electrode. *Nature* **205**(4972) (1965), 698–699.
- [2] Alice V Klein and Trevor W Hambley. Platinum drug distribution in cancer cells and tumors. *Chemical Reviews* **109**(10) (2009), 4911–4920.
- [3] Zahid H Siddik. Cisplatin: mode of cytotoxic action and molecular basis of resistance. *Oncogene* **22**(47) (2003), 7265–7279.
- [4] Richard M Wing, Philip Pjura, Horace R Drew, and Richard E Dickerson. The primary mode of binding of cisplatin to a B-DNA dodecamer: C-G-C-G-A-A-T-T-C-G-C-G. *The EMBO Journal* **3**(5) (1984), 1201–1206.
- [5] Kari Hemminki and David B Ludlum. *Covalent modification of DNA by antineoplastic agents*. 1984.
- [6] Gary L Cohen, Jay A Ledner, William R Bauer, H Michael Ushay, Carl Caravana, and Stephen J Lippard. Sequence dependent binding of cis-dichlorodiammineplatinum (II) to DNA. *Journal of the American Chemical Society* **102**(7) (1980), 2487–2488.
- [7] Franck Coste, Jean-Marc Malinge, Laurence Serre, Marc Leng, Charles Zelwer, William Shepard, and Michel Roth. Crystal structure of a double-stranded DNA containing a cisplatin interstrand cross-link at 1.63 Å resolution: hydration at the platinated site. *Nucleic Acids Research* **27**(8) (1999), 1837–1846.
- [8] Suzanne E Sherman, Dan Gibson, AHI Wang, and Stephen J Lippard. X-ray structure of the major adduct of the anticancer drug cisplatin with DNA: cis-[Pt (NH₃)₂ (d (pGpG))]. *Science* **230**(4724) (1985), 412–417.
- [9] Patricia M Takahara, Amy C Rosenzweig, Christin A Frederick, and Stephen J Lippard. Crystal structure of double-stranded DNA containing the major adduct of the anticancer drug cisplatin. *Nature* **377**(6550) (1995), 649–652.

- [10] Ana-Maria Florea and Dietrich Büsselberg. Cisplatin as an anti-tumor drug: cellular mechanisms of activity, drug resistance and induced side effects. *Cancers* **3**(1) (2011), 1351–1371.
- [11] Markus Galanski and Bernhard K Keppler. Searching for the magic bullet: anticancer platinum drugs which can be accumulated or activated in the tumor tissue. *Anti-Cancer Agents in Medicinal Chemistry (Formerly Current Medicinal Chemistry-Anti-Cancer Agents)* **7**(1) (2007), 55–73.
- [12] Ronald P Miller, Raghu K Tadagavadi, Ganesan Ramesh, and William Brian Reeves. Mechanisms of cisplatin nephrotoxicity. *Toxins* **2**(11) (2010), 2490–2518.
- [13] Nicolaos E Madias and John T Harrington. Platinum nephrotoxicity. *The American Journal of Medicine* **65**(2) (1978), 307–314.
- [14] Corinne Isnard-Bagnis, Vincent Launay-Vacher, Svetlana Karie, and Gilbert Deray. “Anticancer drugs”. In: *Clinical Nephrotoxins*. 2008, pp.511–535.
- [15] Stephen J Harland, David R Newell, Zahid H Siddik, Ruth Chadwick, A Hilary Calvert, and Kenneth R Harrap. Pharmacokinetics of cis-diammine-1, 1-cyclobutane dicarboxylate platinum (II) in patients with normal and impaired renal function. *Cancer Research* **44**(4) (1984), 1693–1697.
- [16] Yasutsuna Sasaki, Tomohide Tamura, Kenji Eguchi, Tetsu Shinkai, Yasuhiro Fujiwara, Masaaki Fukuda, Yuichiro Ohe, Masami Bungo, Naoya Horichi, Shigeki Niimi, et al. Pharmacokinetics of (glycolato-0, 0’)-diammine platinum (II), a new platinum derivative, in comparison with cisplatin and carboplatin. *Cancer Chemotherapy and Pharmacology* **23**(4) (1989), 243–246.
- [17] Franck Martinez, Gilbert Deray, Michèle Dubois, Hélène Beaufiles, Claude Jacquiaud, Richard Bourbouze, M Benhmida, Marie-Chantal Jaudon, and Claude Jacobs. Comparative nephrotoxicity of carboplatin and cisplatin in euvoletic and dehydrated rats. *Anti-Cancer Drugs* **4**(1) (1993), 85–90.
- [18] Renzo Canetta, Marcel Rozencweig, and Stephen K Carter. Carboplatin: the clinical spectrum to date. *Cancer Treatment Reviews* **12** (1985), 125–136.

- [19] Ali Yaghobi Joybari, Samaneh Sarbaz, Payam Azadeh, S Abbas Mirafsharieh, Ali Rahbari, Maryam Farasatinasab, and Majid Mokhtari. Oxaliplatin-induced renal tubular vacuolization. *Annals of Pharmacotherapy* **48**(6) (2014), 796–800.
- [20] Eric Teboul and Guy Chouinard. A guide to benzodiazepine selection. Part I: Pharmacological aspects. *The Canadian Journal of Psychiatry* **35**(8) (1990), 700–710.
- [21] Koert NJ Burger, Rutger WHM Staffhorst, Hanke C de Vijlder, Maria J Velinova, Paul H Bomans, Peter M Frederik, and Ben de Kruijff. Nanocapsules: lipid-coated aggregates of cisplatin with high cytotoxicity. *Nature Medicine* **8**(1) (2002), 81–84.
- [22] Franck Legendre, Véronique Bas, Jiří Kozelka, and Jean-Claude Chottard. A complete kinetic study of GG versus AG platination suggests that the doubly aquated derivatives of cisplatin are the actual DNA binding species. *Chemistry—A European Journal* **6**(11) (2000), 2002–2010.
- [23] Florence Gonnet, Franziska Reeder, Jiří Kozelka, and Jean-Claude Chottard. Kinetic analysis of the reactions between GG-containing oligonucleotides and platinum complexes. 1. Reactions of single-stranded oligonucleotides with cis-[Pt (NH₃)₂ (H₂O)₂]²⁺ and [Pt (NH₃)₃ (H₂O)]²⁺. *Inorganic Chemistry* **35**(6) (1996), 1653–1658.
- [24] Florence Gonnet, Damien Lemaire, Jiří Kozelka, and Jean-Claude Chottard. Isolation of cis-[PtCl (NH₃)₂ (H₂O)](ClO₄), the monohydrated form of the anti-tumour drug cisplatin, using cation-exchange high-performance liquid chromatography. *Journal of Chromatography A* **648**(1) (1993), 279–282.
- [25] P Horáček and J Drobnik. Interaction of cis-dichlorodiammineplatinum (II) with DNA. *Biochimica et Biophysica Acta (BBA)-Nucleic Acids and Protein Synthesis* **254**(2) (1971), 341–347.
- [26] Donald L Bodenner, Peter C Dedon, Peter C Keng, and Richard F Borch. Effect of diethyldithiocarbamate on cis-diamminedichloroplatinum (II)-induced cytotoxicity, DNA cross-linking, and γ -glutamyl transpeptidase inhibition. *Cancer Research* **46**(6) (1986), 2745–2750.
- [27] Murray S Davies, Susan J Berners-Price, and Trevor W Hambley. Rates of platination of AG and GA containing double-stranded oligonucleotides: Insights into why cisplatin

- binds to GG and AG but not GA sequences in DNA. *Journal of the American Chemical Society* **120**(44) (1998), 11380–11390.
- [28] Murray S Davies, Susan J Berners-Price, and Trevor W Hambley. Slowing of cisplatin aquation in the presence of DNA but not in the presence of phosphate: improved understanding of sequence selectivity and the roles of monoaquated and diaquated species in the binding of cisplatin to DNA. *Inorganic Chemistry* **39**(25) (2000), 5603–5613.
- [29] Nathan E Schultz, Yan Zhao, and Donald G Truhlar. Density functionals for in-organometallic and organometallic chemistry. *The Journal of Physical Chemistry A* **109**(49) (2005), 11127–11143.
- [30] Michael B Sullivan, Mark A Iron, Paul C Redfern, Jan ML Martin, Larry A Curtiss, and Leo Radom. Heats of formation of alkali metal and alkaline earth metal oxides and hydroxides: Surprisingly demanding targets for high-level ab initio procedures. *The Journal of Physical Chemistry A* **107**(29) (2003), 5617–5630.
- [31] Thomas Weymuth, Erik PA Couzijn, Peter Chen, and Markus Reiher. New benchmark set of transition-metal coordination reactions for the assessment of density functionals. *Journal of Chemical Theory and Computation* **10**(8) (2014), 3092–3103.
- [32] Jon Baker, Max Muir, Jan Andzelm, and Andrew Scheiner. “Hybrid hartree—fock density-functional theory functionals: The adiabatic connection method”. In: 1996.
- [33] Narbe Mardirossian and Martin Head-Gordon. Thirty years of density functional theory in computational chemistry: an overview and extensive assessment of 200 density functionals. *Molecular Physics* **115**(19) (2017), 2315–2372.
- [34] John P Perdew, Kieron Burke, and Matthias Ernzerhof. Generalized gradient approximation made simple. *Physical Review Letters* **77**(18) (1996), 3865.
- [35] Axel D. Becke. Density-functional thermochemistry. III. The role of exact exchange. *The Journal of Chemical Physics* **98**(7) (1993), 5648–5652. DOI: [10.1063/1.464913](https://doi.org/10.1063/1.464913). eprint: <https://doi.org/10.1063/1.464913>.

- [36] Yan Zhao and Donald G Truhlar. Design of density functionals that are broadly accurate for thermochemistry, thermochemical kinetics, and nonbonded interactions. *The Journal of Physical Chemistry A* **109**(25) (2005), 5656–5667.
- [37] Yan Zhao, Nathan E. Schultz, and D. G. Truhlar. Exchange-correlation functional with broad accuracy for metallic and nonmetallic compounds, kinetics, and noncovalent interactions. *The Journal of Chemical Physics* **123**(16) (2005).
- [38] Nathan E Schultz, Yan Zhao, and Donald G Truhlar. Databases for transition element bonding: Metal- metal bond energies and bond lengths and their use to test hybrid, hybrid meta, and meta density functionals and generalized gradient approximations. *The Journal of Physical Chemistry A* **109**(19) (2005), 4388–4403.
- [39] Andrea Melchior, Enrique Sánchez Marcos, Rafael R. Pappalardo, and José Martínez. Comparative study of the hydrolysis of a third- and a first-generation platinum anti-cancer complexes. *Theoretical Chemistry Accounts* **128**(4) (2011), 627–638.
- [40] Luiz Antônio S Costa, Willian R Rocha, Wagner B De Almeida, and Hélio F Dos Santos. The solvent effect on the aquation processes of the cis-dichloro(ethylenediammine)platinum(II) using continuum solvation models. *Chemical Physics Letters* **387**(1-3) (2004), 182–187.
- [41] Matěj Pavelka, Maria Fatima A. Lucas, and Nino Russo. On the Hydrolysis Mechanism of the Second-Generation Anticancer Drug Carboplatin. *Chemistry – A European Journal* **13**(36) (2007), 10108–10116.
- [42] Yong Zhang, Zijian Guo, and Xiao-Zeng You. Hydrolysis Theory for Cisplatin and Its Analogues Based on Density Functional Studies. *Journal of the American Chemical Society* **123**(38) (2001), 9378–9387.
- [43] Jaroslav V. Burda, Michal Zeizinger, and Jerzy Leszczynski. Hydration process as an activation of trans- and cisplatin complexes in anticancer treatment. DFT and ab initio computational study of thermodynamic and kinetic parameters. *Journal of Computational Chemistry* **26**(9) (2005), 907–914.

- [44] Johan Raber, Chuanbao Zhu, and Leif A Eriksson. Activation of anti-cancer drug cis-platin - is the activated complex fully aquated? *Molecular Physics* **102**(23-24) (2004), 2537–2544.
- [45] Jason Cooper and Tom Ziegler. A Density Functional Study of SN2 Substitution at Square-Planar Platinum(II) Complexes. *Inorganic chemistry* **41**(25) (2002), 6614–6622.
- [46] Ronald J. Cross. Ligand substitution reactions of square-planar molecules. *Chemical Society Reviews* **14**(3) (1985), 197–223.
- [47] Z. Chval and M. Sip. Pentacoordinated transition states of cisplatin hydrolysis—ab initio study. *Journal of Molecular Structure: THEOCHEM* **532**(1-3) (2000), 59–68.
- [48] Luiz Antônio Sodr  Costa, Willian R. Rocha, Wagner B. De Almeida, and H lio F. Dos Santos. The hydrolysis process of the cis -dichloro(ethylenediamine)platinum(II): A theoretical study. *The Journal of Chemical Physics* **118**(23) (2003), 10584–10592.
- [49] R.F. Coley and D.S. Martin. Kinetics and equilibria for the acid hydrolysis of dichloro(ethylenediamine)platinum(II). *Inorganica Chimica Acta* **7**(C) (1973), 573–577.
- [50] Sian E Miller, Kathryn J Gerard, and Donald A House. The hydrolysis products of cis-diamminedichloroplatinum (II) 6. A kinetic comparison of the cis-and trans-isomers and other cis-di (amine) di (chloro) platinum (II) compounds. *Inorganica Chimica Acta* **190**(1) (1991), 135–144.
- [51] Chengteh Lee, Weitao Yang, and Robert G. Parr. Development of the Colle-Salvetti correlation-energy formula into a functional of the electron density. *Physical Review B* **37**(2) (1988), 785–789.
- [52] P. Jeffrey Hay and Willard R. Wadt. Ab initio effective core potentials for molecular calculations. Potentials for K to Au including the outermost core orbitals. *The Journal of Chemical Physics* **82**(1) (1985), 299–310.
- [53] R. Ditchfield, W. J. Hehre, and J. A. Pople. Self-Consistent Molecular-Orbital Methods. IX. An Extended Gaussian-Type Basis for Molecular-Orbital Studies of Organic Molecules. *The Journal of Chemical Physics* **54**(2) (1971), 724–728.

- [54] E. Cancès, B. Mennucci, and J. Tomasi. A new integral equation formalism for the polarizable continuum model: Theoretical background and applications to isotropic and anisotropic dielectrics. *The Journal of Chemical Physics* **107**(8) (1997), 3032–3041.
- [55] Rathindra N Bose, Ronald E Viola, and Richard D Cornelius. Phosphorus-31 NMR and kinetic studies of the formation of ortho-, pyro-, and triphosphato complexes of cis-dichlorodiammineplatinum(II). *Journal of the American Chemical Society* **106**(11) (1984), 3336–3343.
- [56] Kathryn Hindmarsch, Donald A House, and Mark M Turnbull. The hydrolysis products of cis-diamminedichloroplatinum(II) 9. Chloride and bromide anation kinetics for some $[\text{Pt II}(\text{N})_2(\text{OH})_2]^{2+}$ complexes and the structures of $[\text{Pt IVBr}_4(\text{N})_2]$ ($(\text{N})_2 = \text{en, tn}$) 1. *Inorganica Chimica Acta* **257**(1) (1997), 11–18.
- [57] Jaroslav V Burda, Michal Zeizinger, and Jerzy Leszczynski. Activation barriers and rate constants for hydration of platinum and palladium square-planar complexes: an ab initio study. *The Journal of Chemical Physics* **120**(3) (2004), 1253.
- [58] Sian E Miller and Donald A House. The hydrolysis products of cis-diamminedichloroplatinum(II) 5. The anation kinetics of cis- $\text{Pt}(\text{X})(\text{NH}_3)_2(\text{OH})_2 + (\text{X} = \text{Cl, OH})$ with glycine, monohydrogen malonate and chloride. *Inorganica Chimica Acta* **187**(2) (1991), 125–132.
- [59] Ralph G. Pearson, Harry B. Gray, and Fred Basolo. Mechanism of Substitution Reactions of Complex Ions. XVI. 1 Exchange Reactions of Platinum(II) Complexes in Various Solvents 2. *Journal of the American Chemical Society* **82**(4) (1960), 787–792.
- [60] Niklaus Marti, Gaston Hui Bon Hoa, and Jiří Kozelka. Reversible hydrolysis of $[\text{PtCl}(\text{dien})]^+$ and $[\text{PtCl}(\text{NH}_3)_3]^+$. Determination of the rate constants using UV spectrophotometry. *Inorganic Chemistry Communications* **1**(11) (1998), 439–442.
- [61] P. Jeffrey Hay and Willard R. Wadt. Ab initio effective core potentials for molecular calculations. Potentials for the transition metal atoms Sc to Hg. *The Journal of Chemical Physics* **82**(1) (1985), 270–283.

- [62] Mu-Hyun Baik, Richard A Friesner, and Stephen J Lippard. Theoretical Study of Cisplatin Binding to Purine Bases: Why Does Cisplatin Prefer Guanine over Adenine? *Journal of the American Chemical Society* **125**(46) (2003), 14082–14092.
- [63] Justin Kai-Chi Lau and Dirk V Deubel. Hydrolysis of the Anticancer Drug Cisplatin: Pitfalls in the Interpretation of Quantum Chemical Calculations. *Journal of Chemical Theory and Computation* **2**(1) (2006), 103–106.
- [64] Susan J. Berners-Price, Tom A. Frenkiel, Urban Frey, John D. Ranford, and Peter J. Sadler. Hydrolysis products of cisplatin: pK_a determinations via [¹H, ¹⁵N] NMR spectroscopy. *Journal of the Chemical Society, Chemical Communications* (10) (1992), 789.
- [65] Paolo Carloni, Michiel Sprik, and Wanda Andreoni. Key Steps of the cis-Platin-DNA Interaction: Density Functional Theory-Based Molecular Dynamics Simulations. *The Journal of Physical Chemistry. B* **104**(4) (2000), 823–835.
- [66] R. Car and M. Parrinello. Unified Approach for Molecular Dynamics and Density-Functional Theory. *Physical Review Letters* **55**(22) (1985), 2471–2474.
- [67] John W Reishus and Don S Martin. cis-Dichlorodiammineplatinum(II). Acid Hydrolysis and Isotopic Exchange of the Chloride Ligands¹. *Journal of the American Chemical Society* **83**(11) (1961), 2457–2462.
- [68] Jayarama R Perumareddi and Arthur W Adamson. Photochemistry of complex ions. V. Photochemistry of some square-planar platinum(II) complexes. *Journal of Physical Chemistry* **72**(2) (1968), 414–420.
- [69] Justin Kai-Chi Lau and Bernd Ensing. Hydrolysis of cisplatin: a first-principles molecular dynamics study. *Physical Chemistry Chemical Physics* **12**(35) (2010), 10348–10355.
- [70] M. J. Frisch, G. W. Trucks, H. B. Schlegel, G. E. Scuseria, M. A. Robb, J. R. Cheeseman, G. Scalmani, V. Barone, B. Mennucci, G. A. Petersson, H. Nakatsuji, M. Caricato, X. Li, H. P. Hratchian, A. F. Izmaylov, J. Bloino, G. Zheng, J. L. Sonnenberg, M. Hada, M. Ehara, K. Toyota, R. Fukuda, J. Hasegawa, M. Ishida, T. Nakajima, Y. Honda, O. Kitao, H. Nakai, T. Vreven, J. A. Montgomery Jr., J. E. Peralta, F. Ogliaro, M. Bearpark, J. J. Heyd, E. Brothers, K. N. Kudin, V. N. Staroverov, R. Kobayashi, J. Normand, K. Raghavachari, A. Rendell, J. C. Burant, S. S. Iyengar, J. Tomasi, M. Cossi, N. Rega, J. M. Millam, M. Klene, J. E.

- Knox, J. B. Cross, V. Bakken, C. Adamo, J. Jaramillo, R. Gomperts, R. E. Stratmann, O. Yazyev, A. J. Austin, R. Cammi, C. Pomelli, J. W. Ochterski, R. L. Martin, K. Morokuma, V. G. Zakrzewski, G. A. Voth, P. Salvador, J. J. Dannenberg, S. Dapprich, A. D. Daniels, Ö. Farkas, J. B. Foresman, J. V. Ortiz, J. Cioslowski, and D. J. Fox. *Gaussian 09 Revision E.01*. Gaussian Inc. Wallingford CT 2009.
- [71] M. J. Frisch, G. W. Trucks, H. B. Schlegel, G. E. Scuseria, M. A. Robb, J. R. Cheeseman, G. Scalmani, V. Barone, G. A. Petersson, H. Nakatsuji, X. Li, M. Caricato, A. V. Marenich, J. Bloino, B. G. Janesko, R. Gomperts, B. Mennucci, H. P. Hratchian, J. V. Ortiz, A. F. Izmaylov, J. L. Sonnenberg, D. Williams-Young, F. Ding, F. Lipparini, F. Egidi, J. Goings, B. Peng, A. Petrone, T. Henderson, D. Ranasinghe, V. G. Zakrzewski, J. Gao, N. Rega, G. Zheng, W. Liang, M. Hada, M. Ehara, K. Toyota, R. Fukuda, J. Hasegawa, M. Ishida, T. Nakajima, Y. Honda, O. Kitao, H. Nakai, T. Vreven, K. Throssell, J. A. Montgomery Jr., J. E. Peralta, F. Ogliaro, M. J. Bearpark, J. J. Heyd, E. N. Brothers, K. N. Kudin, V. N. Staroverov, T. A. Keith, R. Kobayashi, J. Normand, K. Raghavachari, A. P. Rendell, J. C. Burant, S. S. Iyengar, J. Tomasi, M. Cossi, J. M. Millam, M. Klene, C. Adamo, R. Cammi, J. W. Ochterski, R. L. Martin, K. Morokuma, O. Farkas, J. B. Foresman, and D. J. Fox. *Gaussian 16 Revision C.01*. Gaussian Inc. Wallingford CT. 2016.
- [72] Yan Zhao and Donald G. Truhlar. The M06 suite of density functionals for main group thermochemistry, thermochemical kinetics, noncovalent interactions, excited states, and transition elements: two new functionals and systematic testing of four M06-class functionals and 12 other functionals.(Report). *Theoretical Chemistry Accounts: Theory, Computation, and Modeling (Theoretica Chimica Acta)* **120**(13) (2008), 215.
- [73] David E. Woon and Thom H. Dunning. Gaussian basis sets for use in correlated molecular calculations. IV. Calculation of static electrical response properties. *The Journal of Chemical Physics* **100**(4) (1994), 2975–2988.
- [74] Detlev Figgen, Kirk A. Peterson, Michael Dolg, and Hermann Stoll. Energy-consistent pseudopotentials and correlation consistent basis sets for the 5 d elements Hf–Pt. *The Journal of Chemical Physics* **130**(16) (2009).

- [75] Yu Takano and K. N Houk. Benchmarking the Conductor-like Polarizable Continuum Model (CPCM) for Aqueous Solvation Free Energies of Neutral and Ionic Organic Molecules. *Journal of Chemical Theory and Computation* **1**(1) (2005), 70–77.
- [76] Aleksandr V Marenich, Christopher J Cramer, and Donald G Truhlar. Universal Solvation Model Based on Solute Electron Density and on a Continuum Model of the Solvent Defined by the Bulk Dielectric Constant and Atomic Surface Tensions. *The journal of Physical Chemistry B* **113**(18) (2009), 6378–6396.
- [77] Jeng-da Chai and Martin Head-gordon. Long-range corrected hybrid density functionals with damped atom–atom dispersion corrections. *Physical Chemistry Chemical Physics* **10**(44) (2008), 6615–6620.
- [78] Nicholas P Labello, Antonio M Ferreira, and Henry A Kurtz. Correlated, relativistic, and basis set limit molecular polarizability calculations to evaluate an augmented effective core potential basis set. *International Journal of Quantum Chemistry* **106**(15) (2006), 3140–3148.
- [79] Loubna A Hammad, Gerd Gerdes, and Peter Chen. Electrospray Ionization Tandem Mass Spectrometric Determination of Ligand Binding Energies in Platinum(II) Complexes. *Organometallics* **24**(8) (2005), 1907–1913.
- [80] Erik P. A Couzijn, Ilia J Kobylanskii, Marc-Etienne Moret, and Peter Chen. Experimental Gas-Phase Thermochemistry for Alkane Reductive Elimination from Pt(IV). *Organometallics* **33**(11) (2014), 2889–2897.
- [81] Ekaterina I Izgorodina and Michelle L Coote. Accurate ab initio prediction of propagation rate coefficients in free-radical polymerization: Acrylonitrile and vinyl chloride. *Chemical Physics* **324**(1) (2006), 96–110.
- [82] R. D. Shannon. Revised effective ionic radii and systematic studies of interatomic distances in halides and chalcogenides. *Acta Crystallographica Section A* **32**(5) (1976), 751–767.
- [83] Eunice S. H Gwee, Zoe L Seeger, Dominique R. T Appadoo, Bayden R Wood, and Ekaterina I Izgorodina. Influence of DFT Functionals and Solvation Models on the Prediction

of Far-Infrared Spectra of Pt-Based Anticancer Drugs: Why Do Different Complexes Require Different Levels of Theory? *ACS Omega* **4**(3) (2019), 5254–5269.

- [84] Jo Vinje, Einar Sletten, and Jiří Kozelka. Influence of dT20 and [d (AT) 10] 2 on Cis-platin Hydrolysis Studied by Two-Dimensional [¹H, ¹⁵N] HMQC NMR Spectroscopy. *Chemistry–A European Journal* **11**(13) (2005), 3863–3871.
- [85] Robert W Hay and Sian Miller. Reactions of platinum(II) anticancer drugs. Kinetics of acid hydrolysis of cis-diammine(cyclobutane-1,1-dicarboxylato)platinum(II) “Carboplatin”. *Polyhedron* **17**(13-14) (1998), 2337–2343.

Chapter 4

Effects of fragmentation schemes and solvation model on geometries of DNA building blocks

4.1 Introduction

Even though experimental techniques like IR and Raman spectroscopy have been previously used to study DNA, it is still a challenge to study large biomolecules computationally using fully ab initio methods. The first challenge lies in achieving the accurate treatment of dispersion forces in molecular systems, which is one of the leading intra- and inter-molecular interactions in DNA due to the presence of π - π stacking of the nucleobase pairs and hydrogen bonding.^{1,2} Although dispersion-driven intermolecular interactions can be accurately recovered with wavefunction-based methods, their scalability of at least N^7 (where N is the number of basis functions) prohibits applications to large-sized molecules.³ The inclusion of electron correlation is required to account for dispersion forces in such systems.³⁻⁵ This is achieved with highly correlated levels of theory such as Møller-Plesset second order perturbation theory (MP2) and the “gold standard” method, coupled cluster with singles and doubles and perturbative triple excitations, CCSD(T), with the complete basis set (CBS).³⁻⁵ Although CCSD was able to describe non-interacting H_2 molecules in a lattice, the inclusion of perturbative triple

excitations in CCSD(T) allows for the accurate description of non-covalent interactions.^{6,7} While the coupled cluster methods can be improved systematically by including higher excitation operators, CCSD(T) is a good balance between computational cost and accuracy.^{6,7} In a study conducted by Hobza, and Řezáč, CCSD(T)/CBS was able to predict the interaction energies of the A24 dataset, consisting of 24 non-covalent complexes, within an average error of 0.05 kJ mol⁻¹ when compared to that of the significantly more expensive CCSDT(Q) with the 6-31G** basis set.⁶ However, due to limited computational resources, CCSD(T)/CBS is currently limited to small to medium-sized systems. This motivated the development of cheaper computational alternatives, such as the spin-component scaled MP2 (SCS-MP2) method, to decrease computational costs while retaining a high level of accuracy. SCS-MP2 scales separately the opposite- and same-spin components of the correlation energy, thus compensating overestimation of MP2 due to the same-spin component (discussed below).⁸ Head-Gordon *et al.* also developed the spin-component-scaled method, specifically used to study molecular interactions, SCS(MI)-MP2, which was parameterised specifically to improve the description of different types of intermolecular interactions and successfully tested against the S22 dataset.⁹ SCS(MI)-MP2 has been demonstrated to be able to reproduce CCSD(T), with a root mean square error of 1.3 kJ mol⁻¹.⁹ The spin-ratio scaled MP2 (SRS-MP2) method developed by the Pas group is based on the original SCS-MP2 and uses the ratio of the opposite-spin correlation interaction energy to the same-spin correlation energy to determine the scaling coefficients in the MP2 correlation energy.⁵ For dispersion driven complexes the opposite and same-spin components were found to be very close in energy, thus requiring only the scaling coefficient to correct the opposite-spin component.¹⁰ The uniqueness of SRS-MP2 lies in the fact that CCSD(T) accuracy is achieved without the need to perform counterpoise correction, thus reducing the overall computational cost.^{5,10}

Due to the delicate balance of π - π stacking and H-bonding in DNA and RNA, it is important to identify a suitable quantum chemical method to predict their molecular and energetic properties. Due to the size of DNA, the second, equally big, challenge is to identify a quantum chemical method that is cost-effective and scales linearly with increasing molecular size. This problem can be solved by developing fragmentation approaches capable of dividing

the molecular system into smaller fragments, whose calculations can be easily performed in parallel on massively parallel computers.¹¹

There are four different types of fragment-based approaches that result in a decrease of computational cost: divide-and-conquer approach,^{12–16} the systematic fragmentation method (SFM) developed by Collins,^{17,18} approaches that incorporate many-body interactions and the embedded many-body expansion approach.^{12,19–22} The main difference between these approaches lies in the description of the inter-fragment interactions.¹² The divide and conquer approach sums the electron density of each small-sized subsystem to construct the electron density of the whole system, for which a one-electron density matrix is formed from the molecular orbitals of each subsystem.¹² Inter-fragment interactions are indirectly accounted by considering the basis functions of surrounding fragments in each subsystem calculation.¹² A cut-off region, known as the buffer, can be introduced to ignore inter-fragment interactions if they are deemed too far away.¹² This decreases computational cost to scale as N_α^3 , where N_α is the number of basis functions of the subsystem and the buffer.¹² Yang *et al.* performed geometry optimisations of the RP71955 protein using the divide and conquer approach with the PM3 method in both gas and solvation phase as described with COSMO.¹⁴ The optimised geometries of smaller fragments were in agreement with those obtained using full system calculation, obtaining average root mean square differences of 0.026 Å and 2.83° in bond lengths and bond angles, respectively.¹⁴

Yang *et al.* made use of the divide-and-conquer approach to study polyglycine, by considering each glycine unit as a separate subsystem.¹⁵ The computational cost was significantly decreased, completing one self consistent field (SCF) iteration of the polypeptide consisting of 400 glycines in 213 seconds using one Cray T3E parallel machine processor.¹⁵ However, the divide-and-conquer approach is deemed to be ineffective for studying molecular systems with delocalised orbitals.^{12,23} Merz *et al.* noted limitations of the divide-and-conquer approach in its description of explicit solute-solvent interactions, resulting in overestimation of polarisation effects of solvent molecules.¹⁶ As a result, further improvements have been implemented in the divide-and-conquer approach to improve the description of different components of interaction energy, such as electrostatics, polarization and charge transfer.¹⁶ The two interacting molecules can also be divided into further smaller subunits.¹⁶ By expressing all three energy

components - electrostatics, polarization and charge transfer - in terms of Fermi energies, the interaction energy components between two subsystems can be calculated by including different conditions.¹⁶ For example, the electrostatic components can be determined by subtracting the energies of all possible interactions between the subunits of the two molecules from the total energies of all subunits.¹⁶ The polarization and charge transfer components can be determined by allowing intra- and inter-molecular charge flow.¹⁶ Such developments have enabled Merz *et al.* to describe the charge distribution in proteins, identifying the charge transfer between a fully solvated major cold shock protein A, consisting of six aspartate, two glutamate, seven lysine and one histidine, and surrounding water molecules.¹⁶

The systematic fragmentation method (SFM) approximates the energy of the system by summing the energies of each fragment.^{12,17,18,24} The difference between the SFM and the divide-and-conquer approach is how the system is divided into fragments. With the SFM approach, bonds can be fragmented to form smaller subunits.^{18,24} To fragment a molecule, the two electrons involved in bonding are assigned to the two fragments, one electron assigned to each fragment, and the bond is stretched to infinity.^{18,24} Hydrogen caps were introduced to both fragments and placed in the position of the broken bond.^{18,24} The total electronic energy of the system is calculated by summing the electronic energies of all fragments and dE , the net energy change due to fragmentation about a bond.^{17,18,24,25} To incorporate interactions of non-bonded fragments, all possible combination of dimers and trimers for the two- and three-body non-bonded interaction that are not bonded, are considered.^{12,17,24-26} The two-body interaction energy is obtained by subtracting the one-body energies of each fragment from the dimer energy of the non-bonded fragments.^{12,17,24,25} The three-body interaction energy, on the other hand, assumes that it is negligible unless two of the three fragments are bonded to each other.^{12,17,24-26} The three-body interaction energy is then obtained by subtracting the monomer energy of the non-bonded fragment, the dimer energy of the bonded fragments and the non-bonded two-body energies between the non-bonded fragments from the trimer energy of the three fragments.^{12,17,24-26} Collins *et al.* made use of the SFM approach and analysed its accuracy in describing molecular energies on different hydrocarbon systems, such as butane, pentane and hexane.²⁵ Single point energies and frequency calculations were performed using HF/6-31G level of theory and the energies obtained using the SFM method were compared to

that via full system calculation.²⁵ The errors obtained from one-, two- and three-body energy calculations decreased from 13.37 kJ mol⁻¹ to -0.17 kJ mol⁻¹, indicating the importance of including higher order body interactions.²⁵ The higher order body interactions also improved frequency calculations, decreasing the average error in frequency from 7.89 to 0.38 cm⁻¹ with the use of one- to three-body calculations.²⁵ However, the SFM approach cannot be used to fragment unsaturated bonds.^{12,17,24-26} Another limitation arises due to the addition of hydrogen caps.^{12,17,24-26} The fragmented bond should not be in close proximity and should allow for the addition of hydrogen caps.^{12,17,24-26}

Truhlar *et al.* also developed the electrostatically embedded many-body (EE-MB) method, an approach that is able to incorporate the two-body or three-body expansions to calculate the energies of molecular clusters.^{22,27} The total energy of the system can be calculated by summing the energies of all monomers and including either electrostatically embedded pairwise- or three-body interactions.^{22,27} Electrostatic embedding is incorporated by using point charges and determining the partial atomic charge for all monomers in the system, after which, the energies of the monomers and pair-wise (EE-PA) or three-body (EE-3B) interactions are calculated in the previously determined electrostatic embedding.^{22,27} Truhlar *et al.* tested the EE-MB method on water clusters of varying sizes, eight trimers, six tetramers, a cluster of 21 molecules and a pentamer, with a range of methods, BLYP, B3LYP, PBE, PBE1W and MP2, and 5 different point-charge models, AM1, AM1M, B3LYP, CM4M and TIP3P.²² The energies obtained via the EEMB method are compared to those obtained for the full system calculations with the same level of theory.²² It was determined that the inclusion of the electrostatic embedding significantly improved the accuracy for EE-PA by at least a factor of 10. EE-3B resulted in a much smaller improvement with the inclusion of electrostatic embedding, with an average improvement of error by 1.0 kJ mol⁻¹.²² The accuracy of the EE-MB approach was also tested on Zn metalloenzymes models, specifically the bond dissociation energy of the metal complex and leaving groups.²⁸ The bond dissociation energy of the NH₃ ligand from the Zn metal complexes was investigated.²⁸ With a range of Zn metalloenzyme models, for example [Zn(NH₃)₂(OH)₃]⁻ and [Zn(Imd)₃(OH)₂], the study was conducted by following four guidelines: 1) the monomer containing the metal cation should be coordinated to two ligands, 2) bonds within fragments are not dissociated, 3) only one fragment can be charged, and 4) no

trans coordination should be considered.²⁸ With those four guidelines in mind, Truhlar *et al.* compared the bond dissociation energies obtained from EE-MB calculations to full system calculations and determined that EE-3B outperformed EE-PA and was more accurate, with a maximum error of 9.2 and 38.7 kJ mol⁻¹, obtained for EE-3B and EE-PA, respectively. However, due to these guidelines, it becomes challenging to employ EE-MB to study larger biomolecules where multiple side chains might be charged.

Manby *et al.* also developed the embedded many-body expansion approach to solve the issue of computational cost when studying large systems, specifically for molecular crystal energies.²⁹ Manby *et al.* developed the embedded many-body expansion approach to decrease computational cost while predicting accurate lattice energies by improving the description of the embedding potential, which describes the electrostatic and exchange-repulsion of the system.²⁹ The improved embedding potential is able to describe the interaction between monomers and dimers with their surroundings.²⁹ The electrostatic potential was included as the summation of all electronic and nuclear charges of the system, excluding the given monomer or dimer, while the exchange-repulsion component was incorporated based on the density overlap of the two monomers established by Wheatley and Price to estimate repulsion.^{29,30} Using Wheatley and Price's formulation to estimate the exchange-repulsion energy and the effects it has on the overall embedding potential, Manby *et al.* were able to reproduce lattice energies of molecular crystals to high levels of accuracy.^{29,30} The density overlap between dimers were calculated using symmetry adapted perturbation theory (SAPT).²⁹ Tested on several different systems in a 3 x 3 x 3 unit cell, such as carbon dioxide, hydrogen fluoride and ice polymorphs, the combination of the density-fitting HF method and Dunning's aug-cc-pVQZ basis set, the embedded many-body expansion approach was shown to be an accurate method for the prediction of the cohesive energy of CO₂ molecules in a crystal, differing by 0.3 kJ mol⁻¹ when compared to periodic Hartree-Fock results.²⁹ The approach produced the cohesive energy of an ice polymorph within 5 kJ mol⁻¹ of the experimental value when using the density-fitting Hartree-Fock method and Dunning's aug-cc-pVTZ basis set.^{29,31} This small difference is achieved at a low computational cost by considering the monomer energies and two-body interactions, indicating the importance of the embedded potential to obtain accurate results.²⁹

In the present study, we employ the Fragment Molecular Orbital (FMO) approach to study the effects of different modes of fragmentation and solvation model on DNA models. The FMO approach, a different embedded approach to that developed by Manby *et al.*, divides a large molecular system into smaller fragments, that are manageable for calculations using highly correlated wavefunction-based methods (Figure 4.1).^{32–35} The electron density of each individual fragment undergoes a self consistent charge procedure until individual densities are converged.^{32–35} These converged densities are added together to form the Coulomb bath of the entire molecular system, in which the energies of the individual fragments are calculated using a method of choice.^{32–35} The sum of energies of the individual fragments provides the FMO1 energy, which also includes polarisation of each individual fragment by the entire molecular system.^{32–35} To account for the interaction between fragments, the two-body (FMO2) and/or three-body (FMO3) effects can be calculated.^{32–35} For FMO2, the pairwise interaction energy of all possible dimers are computed in the Coulomb bath.^{32–35} FMO2 is able to take into account additive electrostatic and dispersion forces between the fragments, provided a correlated level of theory (i.e. a post-HF method) is used.^{32–35} In FMO3, the interaction energy of all possible trimers are calculated in the converged Coulomb bath. When a correlated level of theory is used, FMO3 is capable to recover non-additive forces such as induction, charge transfer and the non-additive component of dispersion.^{32–35} Beyond the three-body effects higher-order terms are not required to be implemented in the FMO approach. Due to the inclusion of polarisation effects at the monomer level, the FMO3 energy converges rapidly with respect to the exact energy of the system.

The FMO approach has been demonstrated to be able to be able to study non-bonded systems.^{36–40} Studies conducted by Izgorodina *et al.* have demonstrated how invaluable the FMO method is in the calculation of large systems.^{36–40} Izgorodina *et al.* validated the use of the FMO approach to describe ionic liquid systems, defining each ion as an individual fragment.⁴¹ Geometry optimisations were performing using either FMO2 and FMO3 with the MP2 method and TZVPP basis set on 4 different ionic liquids: [NMe₄][BF₄] (tetramethylammonium tetrafluoroborate), [C₁mim][BF₄] (1,3-dimethylimidazolium tetrafluoroborate), [C₃mim][BF₄] (1-propyl-3-methylimidazolium tetrafluoroborate) and [C₄mim][BF₄] (1-butyl-3-methylimidazolium tetrafluoroborate).⁴¹ 1, 2, 4 and 8 ion pairs of the ionic liquids were also

considered to investigate the influence of many-body effects with increasing cluster sizes.⁴¹ Interaction energies of the ionic liquids were calculated and the basis set superposition error was accounted for by employing Boys and Bernardi's counterpoise approach.^{41,42} After analysing the interaction energies, it becomes clear that larger clusters are required to properly describe many-body effects.⁴¹ FMO2 has also demonstrated to be able to reproduce full system interaction energies, differing by a maximum error of 2 kJ mol⁻¹.⁴¹ The inclusion of three-body interaction of FMO3 was more accurate, giving rise to a maximum error of 0.2 kJ mol⁻¹, further emphasising the importance of many-body effects in large clusters.⁴¹

Subsequently, Izgorodina *et al.* also made use of the FMO approach to investigate the physicochemical properties of 24 ionic liquids, specifically from the imidazolium and pyrrolidinium families with either chloride, tetrafluoroborate or dicyanamide as counter ions.⁴⁰ One and two ion pairs of the ionic liquids were considered in this study to demonstrate the importance of induction and dispersion with the presence of additional ion pairs to better predict chemical and physical properties of bulk ionic liquids.⁴⁰ In addition, the effects of increasing alkyl chain lengths on the imidazolium and pyrrolidinium ions were investigated.⁴⁰ Geometry optimisations were performed using different conformations using FMO2, each ion defined as a fragment, using SRS-MP2 and cc-pVDZ (VDZ) basis set.⁴⁰ For imidazolium-based systems, the two ion pair cluster was arranged to either alternating charges or to include $\pi^+ - \pi^+$ stacking of the imidazolium rings.⁴⁰ Single point energies were calculated using the FMO3 approach, SRS-MP2 method and the cc-pVTZ (VTZ) basis set to identify all possible minima and, hence, the global minima.⁴⁰ After analysing the energies of the optimised geometries, Izgorodina *et al.* determined both the anion and the length of the alkyl chain on the cation play significant roles in determining the lowest energy configurations.⁴⁰ While the combination of imidazolium and tetrafluoroborate preferred the alternating charge arrangement (by 21 kJ mol⁻¹), the combination of imidazolium and chloride does not have a clear preference for ion arrangement as the alternating charge configuration only differed from the $\pi^+ - \pi^+$ stacking configuration by an insignificant amount.⁴⁰ Interestingly, the length of the alkyl chain affects the preferred configuration of imidazolium and dicyanamide.⁴⁰ For methyl and ethyl alkyl groups on the imidazolium ion, it is energetically favourable for the complex to adopt the

alternating charge arrangement, whereas for propane and butane alkyl groups on the imidazolium ion, the $\pi^+ - \pi^+$ is preferred.⁴⁰ For the pyrrolidinium clusters, the propane and butane alkyl groups encourage the interaction between the alkyl chain and the pyrrolidinium ring.⁴⁰ The pyrrolidinium clusters also demonstrate a strong preference for certain configurations, for example the pyrrolidinium chloride clusters resulted in two low energy configurations with a difference of 10 kJ mol⁻¹.⁴⁰ The FMO optimised geometries of the various different combinations of cations and anions were in agreement with previously published results by the Hunt group who made use of full system calculations.^{40,43,44}

Upon further development, the FMO approach enables the fragmentation of covalent bonds via either the hybrid orbital projection (HOP) or adaptive frozen orbital (AFO) approach.¹² While the former assigns both electrons involved in the bond to one fragment, the latter freezes the electron density of the bond. In a previously conducted study by Slipchenko *et al.* it was determined that AFO and HOP approaches are optimal for different systems.¹² While HOP has been demonstrated to be optimal to study polar systems, AFO has been demonstrated to be an appropriate to study polypeptide systems and molecular surfaces.¹² By fragmenting about a covalent bond, HOP assigns both electrons involved in the bond formation to one atom of the bond, labeled as the bond attached atom (BAA), and none to the other atom, labeled the bond detached atom (BDA).^{35,45,46} When this happens, the BDA is included in both fragments.⁴⁷ HOP, constructed from hybridised orbitals, projects the orbital energy corresponding to the orbital involved in the fragmented bond to a large value.^{46,47} This prevents the electron density of the BDA from occupying the bond region.^{46,47} Even though this restricts the exchange interaction between fragments at the FMO1 level, it is recovered when FMO2 and FMO3 calculations are performed.³⁵

FMO has proven to be a suitable method to study polypeptide systems. As performed by Kitaura *et al.*, the FMO two-body approach was used to calculate single point energies of α -helical model peptides of varying length of 5, 10, 15 and 20 units of glycine (Gly) and alanine (Ala).⁴⁵ FMO calculations were performed at the HF/STO-3G level of theory and the energies of the peptide models were compared with the results obtained for the full systems.⁴⁵ The largest errors of 7.1 and 10.0 kJ mol⁻¹ were obtained for the largest 20 units peptide models of glycine and alanine, respectively.⁴⁵

The FMO approach was used by Komeiji *et al.* to study the total energy, molecular orbitals and inter-fragment interaction energy of DNA in the gas phase.⁴⁸ Due to the dispersion forces present in the systems studied, specifically the π - π stacking between bases, HOP was employed as the fragmentation approach in this study. It was well established that the second order Møller-Plesser method (MP2) significantly improves the accuracy of amino acid interactions and π - π stacking of bases in DNA.⁴⁸⁻⁵⁰ However, it is well accepted that MP2 overestimates interaction energy of non-covalently bound systems, and thus Komeiji opted to use the spin consistent scaled MP2 method (SCS-MP2) instead.^{48,51,52} The effects of different types of fragmentation in the DNA model were thoroughly studied. Three different fragmentation modes were employed, all of which involve fragmenting covalent bonds, either C-N, C-C or C-O bonds, using the hybrid orbital projection (HOP) operators as shown in Figure 4.1.^{35,45,46,48} The Frag-A type was fragmented into individual bases and backbone units, whereas the Frag-B and Frag-C types were fragmented at the sugar unit and divided the atoms of the sugar unit into different fragments.⁴⁸ They discovered the importance of including Na^+ counter-ions to neutralize the charge of the phosphate group, with an average HOMO-LUMO energy gap of 1.7 eV.⁴⁸ They also determined the importance of using the optimal fragmentation for the system, where Frag-A outperformed both Frag-B and Frag-C, resulting in the largest error to be 16.7 kJ mol^{-1} .⁴⁸

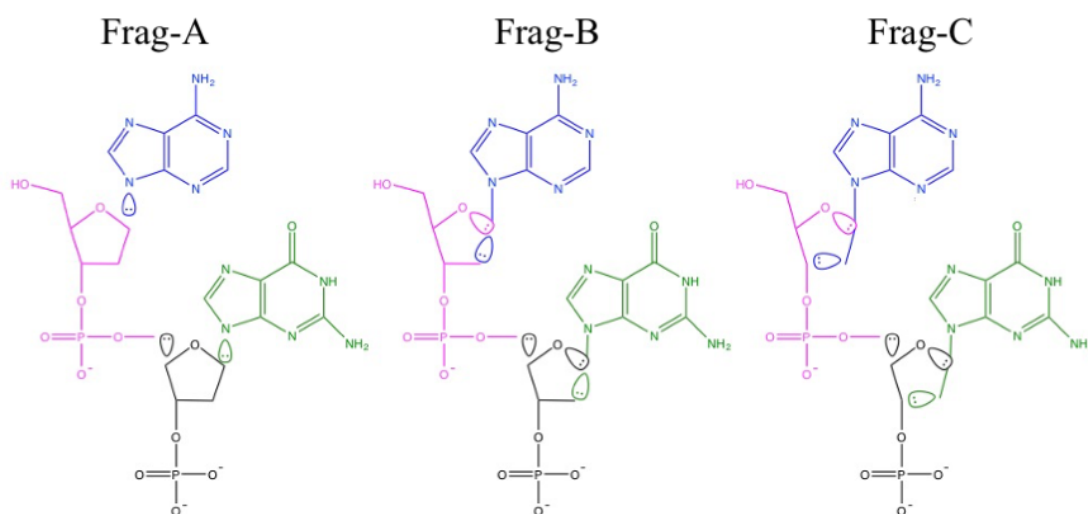


Figure 4.1: 3 different modes of fragmentation explored by Komeiji *et al.*⁴⁸

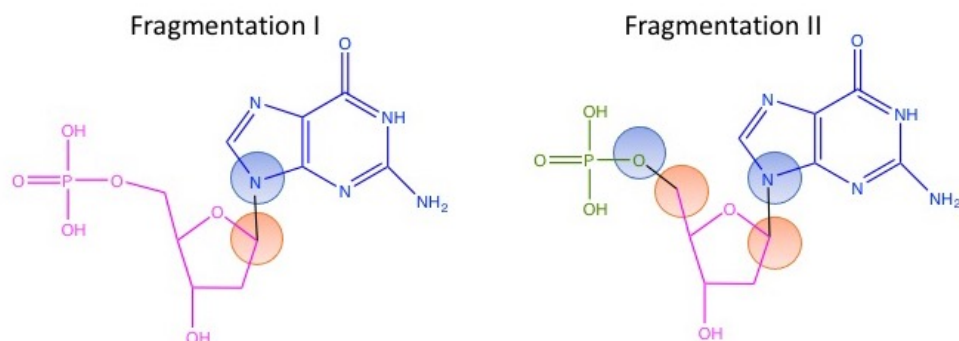


Figure 4.2: The two different fragmentation modes that were investigated in this study. The bond fragmentation occurs about the bond highlighted in black and the bond detached atom (BDA) is highlighted in orange, whereas the bond attached atom (BAA) is highlighted in blue.

The CPCM solvation model has been incorporated into the FMO approach via the FMO/PCM many-body expansion method.⁵³ Gordon *et al.* have previously determined that the many-body expansion of both the electron density of the solute and the electrostatic potential, \mathbf{V} , of the solvent is required to better understand solute-solvent interactions.⁵³ FMO/PCM allows for the fragments to be calculated once the cavity generated in PCM is introduced, including the implicit solvation effects into the coulomb bath for further calculations.⁵³ The main difference between FMO/PCM and conventional PCM lies the flexibility to incorporate many-body densities to define the overall electrostatic potential, \mathbf{V} , exerted on the cavity by the solute.⁵³

The FMO/PCM approach is further refined in FMO n /PCM[$m(l)$], where m represents the m -body expansion to obtain the \mathbf{V} potential and the apparent surface charge of each tesserae self consistently.⁵³ l represents the l -body expansion of \mathbf{V} potential to determine the apparent surface charge of each tesserae.⁵³ After determining the apparent surface charge of each tesserae, the n -body FMO calculation is obtained by using the updated apparent surface charge.⁵³ The FMO n /PCM[$m(l)$] approach, specifically FMO/PCM[2] and FMO/PCM[1(2)], was used to study both the α -helices and β -strands of alanine of various different length - 10, 20 and 40 residues. The difference between FMO/PCM[2] and FMO/PCM[1(2)] is that while the

former included dimer corrections to describe the V potential, the latter does not include dimer corrections to describe the V potential but includes a two-body expansion to determine the apparent surface charge of each tesserae.⁵³ The results were compared to those of the full system calculations with the PCM model as reference.⁵³ Fedorov *et al.* tested the FMO/PCM approach on both α and β conformations of alanine peptides, with lengths of 10, 20 and 40 alanine units.⁵³ It was found that errors could be decreased by increasing the number of residues per fragment, evident when studying both α and β conformations of a peptide consisting of 40 alanine units. In the case where each residue represented a fragment, the method resulted in errors of 13.4 and -48.1 kJ mol⁻¹ for the α and β conformations, respectively.⁵³ In the case when 2 residues were selected as a fragment, this approach produced errors of 8.8 and -25.9 kJ mol⁻¹ for the α and β conformations, respectively.⁵³ It was also determined that the errors of solvation energies for β conformations exhibited a linear relationship with the system size.⁵³ The errors for the α conformations did not scale with system size, with the largest error of 6.3 kJ mol⁻¹ resulting from the system comprising of 40 alanine units.⁵³ This was explained by the inability to fully account for the charge transfer effects of the α conformers.⁵³ Gordon *et al.* also established that FMO/PCM[2] approach is able to reproduce the smallest solvation energy errors when compared to the full system calculations using the conventional PCM scheme with a maximum error of -2.5 kJ mol⁻¹. On the other hand, FMO/PCM[1(2)] was deemed to be a suitable alternative, in terms of accuracy and computational cost and it produced a maximum error of -8.8 kJ mol⁻¹.

In this work, we used DFT functionals, PBE and PBE-D3, and the SRS-MP2 method to study the influence of varying fragmentation and implicit solvation models on geometry optimisations of the building blocks of DNA, deoxyguanosine monophosphate (dGMP) and deoxyadenosine monophosphate (dAMP). Double-stranded models such as d(GpG) and dGMP-dCMP were also considered to investigate the influence of varying the fragmentation scheme on the description of intermolecular π - π stacking and hydrogen bonding motifs. Two implicit solvation models were considered - a conductor-like polarizable continuum model (CPCM)⁵⁴ and a universal solvation model based on density (SMD).⁵⁵ Grimme introduced an empirical dispersion correction, D3, to improve the performance of non-covalent interactions.^{4,56,57} The comparison between the performance of PBE and PBE-D3 showcases whether the inclusion of

D3 improves the prediction of intra- and intermolecular interactions in DNA building blocks. Based on the previous studies described above, FMO/PCM[1(2)] was exclusively used in this study. Two types of fragmentation of the DNA model were considered: 1) Fragmentation scheme I, in which the bond between the sugar and the base units is broken and 2) Fragmentation II scheme, in which two covalent bonds are broken - between the sugar and the base units and between the sugar and the phosphate units (for more detail see Figure 4.2).

4.2 Theoretical Procedures

Geometry optimisations were performed using the General Atomic and Molecular Electronic Structure System (GAMESS-US) software.⁵⁸ The single- and double stranded models considered in this study are shown in Figure 4.3. The double stranded models consisted of a guanine-cytosine base pair with the Watson-Crick hydrogen bonding and a double guanine base pair for the stacked model. All models studied were neutral, with an additional hydrogen placed on the phosphate group to neutralize it. The two types of fragmentation explored with FMO can be seen in Figure 4.2. HOP operators were used to fragment the corresponding C-O and C-N bonds.

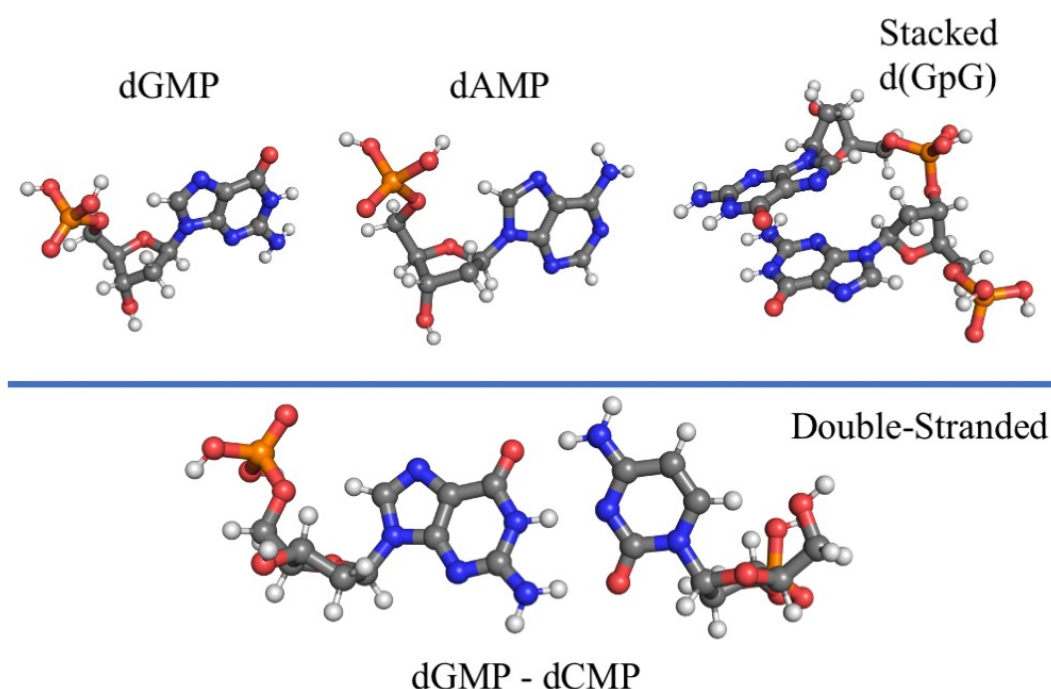


Figure 4.3: Single and double stranded models.

SCS-MP2, developed by Grimme, enables the ability to scale the same- and opposite-spin components separately⁸ as shown below:

$$E_{INT}^{corr} = c_{OS}E_{INT}^{OS} + c_{SS}E_{INT}^{SS}$$

where c_{OS} and c_{SS} are scaling coefficients.

The coefficients for SCS-MP2 were determined by comparing the reaction energies to those obtained using QCISD(T)/QZV(3d2f,2p1d) level of theory.⁸ Grimme determined the optimal coefficients of $\frac{6}{5}$ for the opposite-spin component and $\frac{1}{3}$ for the same-spin component.⁸ Upon employment of the scaling coefficients, SCS-MP2 resulted in more consistent correlation energies as compared to MP2, consistently recovering between 88.6% to 96.2% of electron correlation compared to 80.2% to 98.1% for the latter.⁸ However, it was shown that SCS-MP2 was not as reliable when applied to study the binding and interaction energies of molecular systems with non-covalent interactions.^{5,59} Tan *et al.* developed the SRS-MP2 method

to predict interaction energies of non-covalently bound molecular systems that are driven by dispersion forces and hydrogen bonding.⁵ Compared to SCS-MP2, SRS-MP2⁵ scales the same-spin (SS) and opposite-spin (OS) components based on the ratio of correlation interaction energy between the same spin and opposite spin components defined as $\epsilon_{\Delta s} = \frac{E_{INT}^{OS}}{E_{INT}^{SS}}$. When the ratio was above 1.0, only the opposite-spin component was scaled, thus improving the description of non-covalent bonds. The scaling coefficients in SRS-MP2 were fitted to reproduce CCSD(T)/CBS interaction energies of the intermolecular complexes in the S22, S66 and IL174 databases for a series of Dunning's basis sets, both cc-pVXZ and aug-cc-pVXZ (X=D,T,Q)^{5,60-63} The databases contained a diverse range of systems of three different types of interactions: electrostatic, dispersion and mixed.^{5,60-62} The systems were classified depending on the $\epsilon_{\Delta s}$: 1) systems with $\epsilon_{\Delta s} \leq 1$, of electrostatic nature, and 2) systems with $\epsilon_{\Delta s} > 1$, of dispersion nature. Different coefficients were obtained for the two ranges of $\epsilon_{\Delta s}$, producing small errors within 2 kJ/mol on average.^{5,10,64}

PBE⁶⁵ and PBE-D3⁶⁶ functionals were also employed for this study. PBE, a generalised gradient approximation (GGA) functional, where the exchange-correlation energy is dependent on both the function and density of electron spins.^{56,67} Scuseria *et al.* evaluated PBE's ability to predict atomisation energies of the G2 set, a dataset comprising of molecules such as allene, butadiene and isobutane.⁶⁷ When compared to that of previously published experimental results, PBE resulted in a mean average error of 71.5 kJ mol⁻¹, the largest error of 217.6 kJ mol⁻¹ arising from pyridine.⁶⁷ PBE-D3 includes an empirical dispersion correction, thus allowing for a better description of intermolecular interactions, especially dispersion forces.⁶⁶ The D3 correction has been demonstrated to better describe medium-range exchange and correlation effects.^{4,66} When applied to the X23 dataset, consisting of 23 crystal structure of small- to medium sized molecules (between 3 and 26 atoms), either van der Waals' or hydrogen-bonded, PBE-D3 accurately predicted their cohesive energies, producing a mean absolute deviation (MAD) of 4.2 kJ mol⁻¹ when compared to experimental results.⁶⁸

In this study two implicit solvation models were used, the conductor-like polarizable continuum model (CPCM)⁵⁴ and the solvent model based on density (SMD).⁵⁵ In general, implicit solvation models construct a cavity around the molecule with the surface charge, in accordance with the dielectric constant of the medium, representing the choice of solvent in the

calculation.⁵⁵ The molecule in the cavity is polarized by the charge density of the solvent.⁵⁵ SMD has been shown to be an effective solvation model to study the solvation energies of both charged and neutral molecular systems, achieving a mean absolute error of 16.7 kJ mol⁻¹ for ions.⁵⁵ As mentioned in the Introduction, FMO/PCM was specifically formulated to better describe solvent-solute interactions.⁵³ Along with FMO/PCM, parameters used in the previous paper were also utilised in this study. For example, the density of tesserae was defined as 240 and the simplified united atomic radii were employed to describe the van der Waals radii of atoms.⁵³ Due to the different availability of the FMO/PCM variations in GAMESS-US for DFT functionals and MP2 methods, FMO/PCM[1(2)] was utilised with PBE and PBED3, whereas FMO/PCM(1) was used for SRS-MP2.

Dunning's basis sets⁶³ such as cc-pVDZ (VDZ) and cc-pVTZ (VTZ), were used in this study, with VDZ being employed for geometry optimisations and VTZ for single point energy calculations in conjunction with SRS-MP2. The cc-pVTZ basis set was selected, as it performed exceptionally well with SRS-MP2.¹⁰

Once the geometries were optimised with various functionals/methods and solvation models, single point energy calculations were performed with SRS-MP2 and the VTZ basis set in the gas phase to compare the effects of implicit solvent models, level of fragmentation and level of theory on the optimised configurations of the DNA models used. The single point energy calculations were performed without the use of fragmentation.

Root mean square deviations (RMSD) were used to investigate the extent of difference in optimised geometries by calculating the displacement of each atom as defined below:

$$RMSD = \sqrt{\frac{1}{n}((x_i - x_j)^2 + (y_i - y_j)^2 + (z_i - z_j)^2)} \quad (4.1)$$

where n is the number of atoms, x, y and z are the coordinates of atoms i and j.

The energies of geometries optimised with two fragmentation schemes in FMO were compared to those obtained via full system calculations to compare the stability of the respective geometries. Unless otherwise stated, the energies obtained from full system calculations are used as reference. No approximations to calculate two-electron integrals were used and no cut-offs to treat two-body effects in FMO calculations were introduced. Further in the text, "full system"

calculations refer to either geometry optimisations or single point calculations performed outside the FMO framework, i.e. without fragmenting the system into smaller components.

The starting configurations of the single stranded models, dGMP, dAMP, d(GpG), and the double stranded model, dGMP-dCMP, were obtained from the previously published 1Z9C crystal structure.⁶⁹ The starting geometries then underwent optimisation using either full system calculation or the FMO approach.

$$\text{Difference in Energy} = \text{Energy}_{(FMO)} - \text{Energy}_{(Full\ system)} \quad (4.2)$$

4.3 Influence of Fragmentation schemes and Solvation Models

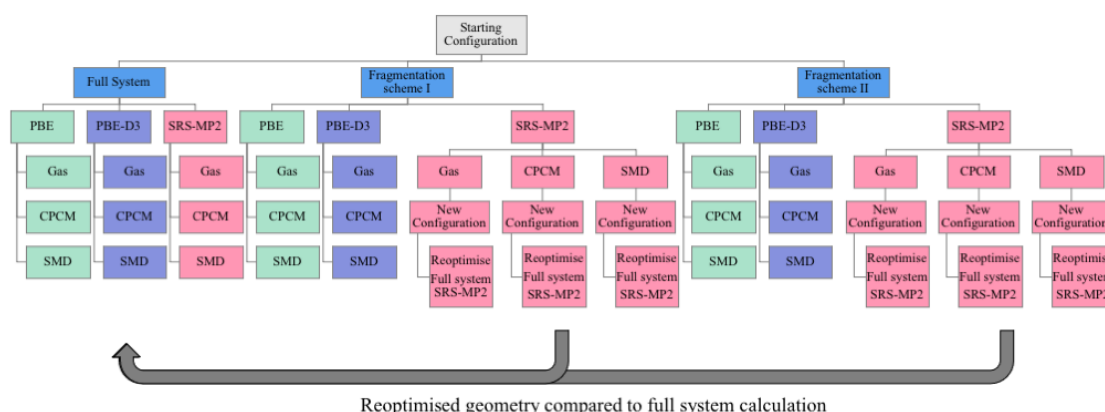


Figure 4.4: Scheme used to compare the optimised geometries. The arrows indicate the comparison between the re-optimised geometries with the original full system calculations.

Figure 4.4 shows the overall structure of the calculations performed in the study. The same starting configuration for either a single stranded or a double stranded DNA model was used for all Fragmentation schemes. The configuration was optimised as “full system” and within the Fragmentation scheme I or II in the FMO framework. The energies of the optimised structures were improved with “full system” SRS-MP2/VTZ in the gas phase to study the effect of fragmentation and implicit solvent on geometry optimisation. The comparison of resulting geometries was performed for each level of theory. For example, the SRS-MP2/VTZ energy of the geometry optimised with any of the FMO Fragmentation schemes, the PBE functional and SMD was compared to that of the full system geometry optimisation performed with the PBE

functional and SMD. This comparison allowed us to determine whether the Fragmentation scheme and the full system calculation located the same local minimum.

4.3.1 Single stranded models

Results from the geometry optimisations of the single stranded model, dGMP and dAMP (Fig: 4.3), are given in Table 4.1.

Table 4.1: Energy differences (kJ mol^{-1}) of deoxyguanosine monophosphate (dGMP) and deoxyadenosine monophosphate (dAMP) between full system and FMO calculations.

	dGMP						dAMP					
	FMO2 (Fragmentation I)			FMO2 (Fragmentation II)			FMO2 (Fragmentation I)			FMO2 (Fragmentation II)		
	Gas	CPCM	SMD	Gas	CPCM	SMD	Gas	CPCM	SMD	Gas	CPCM	SMD
PBE	0.02	1.1	23.7	4.1	1.1	7.8	-0.03	-0.6	4.0	2.7	3.6	9.5
PBE-D3	0.03	1.8	21.9	3.9	1.4	-18.1	0.1	-0.6	2.4	2.7	3.2	10.2
SRS-MP2	0.03	0.6	28.4	3.9	1.2	39.1	-0.03	0.9	3.1	2.1	6.0	9.1

From Table 4.1, the Fragmentation scheme I appears to produce smaller deviations compared to those of the Fragmentation scheme II regardless of method and solvation conditions. When the gas phase calculations were performed, the mean energetic difference of the Fragmentation I and Fragmentation II schemes fall in the range of 0.02 and 4.1 kJ mol^{-1} for dGMP and -0.03 and 2.7 kJ mol^{-1} for dAMP. The smaller energy differences indicate that the Fragmentation scheme I is able to reproduce geometries of the full system calculations better the Fragmentation scheme II. The optimised geometries of the two fragmentation schemes are compared to the full system ones via RMSD values further in the text (Table 4.2). In the gas phase, the energy difference produced for the single base systems, dGMP and dAMP (Figure 4.3), are relatively narrow, ranging from -0.03 to 0.07 kJ mol^{-1} and 2.1 to 4.1 kJ mol^{-1} for the Fragmentation schemes I and II, respectively. The narrow differences in gas phase suggest that all the methods converge to similar geometries (within 4 kJ mol^{-1}) regardless of the Fragmentation scheme, with the largest energy difference of 4.1 kJ mol^{-1} produced by the PBE functional with the Fragmentation scheme II.

With the inclusion of solvation models, it is not surprising that it generates a larger deviation as compared to the gas phase geometries. A similar trend as for the gas phase was still observed - the Fragmentation scheme I outperformed the Fragmentation scheme II within the solvation

models by converging to the same geometries as the full system calculations. The use of CPCM gave rise to a narrower range in energy difference from -0.6 to 6.0 kJ mol^{-1} compared to that of -18.1 to 39.1 kJ mol^{-1} with SMD, regardless of the nucleobase. The largest difference of 39.1 kJ mol^{-1} was observed with the combination of SRS-MP2, the SMD solvation model and the Fragmentation scheme II. This indicates that the CPCM solvation model is able to optimise to similar local minima as full system optimisations. This can be attributed to the many-body expansion formulated in the FMO/PCM method, FMO/PCM[1(2)] for PBE and PBE-D3 and FMO/PCM(1) for SRS-MP2, thus allowing for a better description of the solute-solvent interactions. Interestingly, the average energy difference produced for dGMP is larger than that of dAMP, with the former ranging from -18.1 to 39.1 kJ mol^{-1} and the latter ranging from -0.6 to 10.2 kJ mol^{-1} , regardless of functional, solvation model and Fragmentation scheme.

RMSD values of the optimised geometries were analysed to explain the energy differences obtained with the two Fragmentation schemes. It is expected that larger RMSD values result in larger energy differences. From Table 4.2, it can be seen that the RMSD values for the geometries with the largest energy differences are 1.8 and 0.3 \AA for dGMP and dAMP, respectively. Upon comparing Tables 4.1 and 4.2, it becomes apparent that a clear relationship between energy differences and RMSD values could not be established. The largest RMSD value of 2.1 \AA observed for dGMP was obtained with the combination of PBE-D3, SMD and the Fragmentation scheme II, resulting in a geometry that differed by as much as 18.1 kJ mol^{-1} when compared to the full system calculation. From Figure 4.5, this large RMSD could be explained by the displacement of the phosphate group and the sugar. It can be seen that the geometry obtained from the Fragmentation scheme II is significantly different from that obtained from the full system calculation. This is evident from the hydrogen bonding between the O-H group of the phosphate towards the N on the guanine, with a bond length of 1.59 \AA . This additional hydrogen bonding appears to stabilise the system.

Table 4.2: *RMSD values (in Å) of geometries optimised with Fragmentation schemes I and II.*

	dGMP						dAMP					
	Fragmentation I			Fragmentation II			Fragmentation I			Fragmentation II		
	Gas	CPCM	SMD	Gas	CPCM	SMD	Gas	CPCM	SMD	Gas	CPCM	SMD
PBE	0.002	0.276	1.272	0.299	0.096	1.034	0.083	0.012	0.420	0.043	0.104	0.340
PBE-D3	0.057	0.273	1.160	0.199	0.110	2.115	0.008	0.017	0.251	0.034	0.205	0.334
SRS-MP2	0.005	0.108	1.320	0.571	0.259	1.773	0.003	0.057	0.360	0.107	0.096	0.280

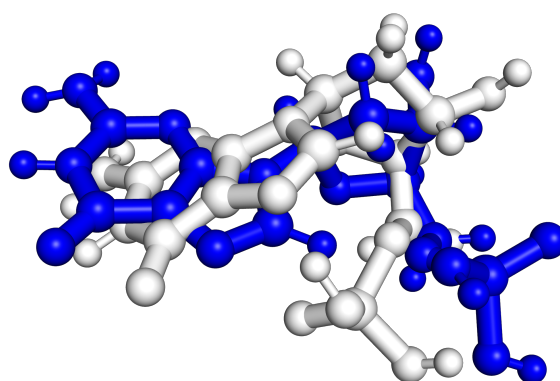


Figure 4.5: *Comparison of the dGMP optimised geometries between full system optimisations (blue) and Fragmentation scheme II (white) using the PBE-D3 functional and SMD solvation model.*

Overall, the FMO approach seems to be able to optimise geometries similar to full system optimisations in the case of dAMP, with the largest energy difference being recorded at 10.2 kJ mol⁻¹ when using the SMD solvation model. The FMO approach resulted in larger energy differences for dGMP, ranging from -18.1 to 39.1 kJ mol⁻¹ for dGMP when using the SMD solvation model. From Figure 4.6 and Table 4.2, it can be seen that smaller energetic differences reflect smaller RMSD values in the range of 0.008 and 0.420 Å. Figure 4.6 shows a typical example of how FMO-optimised structures using the Fragmentation scheme II and SMD solvation model of dGMP deviate more from full system ones compared to those of dAMP. This was evident from the longer distances between the two O atoms on the phosphate group and the C-H on the guanine as shown in Figure 4.7. For dGMP, these distances were calculated to be 4.9 and 6.4 Å when the Fragmentation scheme II was used as compared to those of 2.4 and 2.6 Å resulting from full system optimisations. Contrary to this observation, the deviation

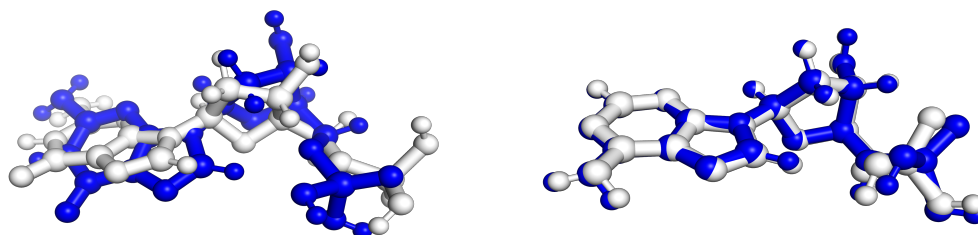


Figure 4.6: *Optimised geometries of dGMP and dAMP between full system (blue) and FMO (white) optimisations with Fragmentation scheme II and SMD solvation model.*

in geometries for dAMP were not as significant, with the distances between the C-H on the adenine to the two O atoms on the phosphate falling in the range of 2.2 and 2.6 Å when using the Fragmentation scheme II. This range is comparable with that of 2.4 and 3.2 Å obtained from the full system optimisation. The large energy differences could also be explained by measuring the dihedral angles between the phosphate group and the nucleobase and the nucleobase to the sugar unit as shown in Figure 4.8. In the case of dGMP, full system optimisations with SRS-MP2 and the SMD solvation model predicted dihedral angles between phosphate-sugar and base-sugar to be 67.3° and 61.6°, respectively. In the case of dAMP, the same angles were measured to be 66.5° and 60.3°, respectively, using the same level of theory and solvation model. The Fragmentation scheme II reproduced dihedral angle differences by an average of 11.1° and 6.8° for dGMP and dAMP, respectively. Interestingly, the larger dihedral angle differences for dGMP and dAMP came from different structural motifs. While the Fragmentation scheme II resulted in a difference of 11.7° between the sugar and the base for dGMP, the larger dihedral difference of 13.5° resulted from the phosphate-sugar motif for dAMP. These large differences in geometries when compared to the full system optimisations offer an explanation of the large energy differences obtained from FMO optimisations.

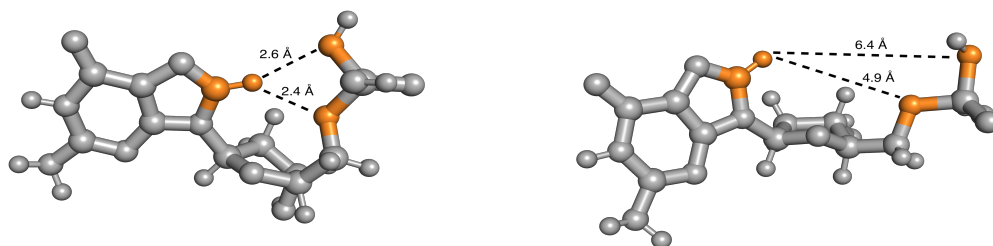


Figure 4.7: *Optimised geometries of dGMP from full system (left) or Fragmentation scheme II (right) optimisations. Dashed lines show distances from C-H on guanine to O on phosphate.*

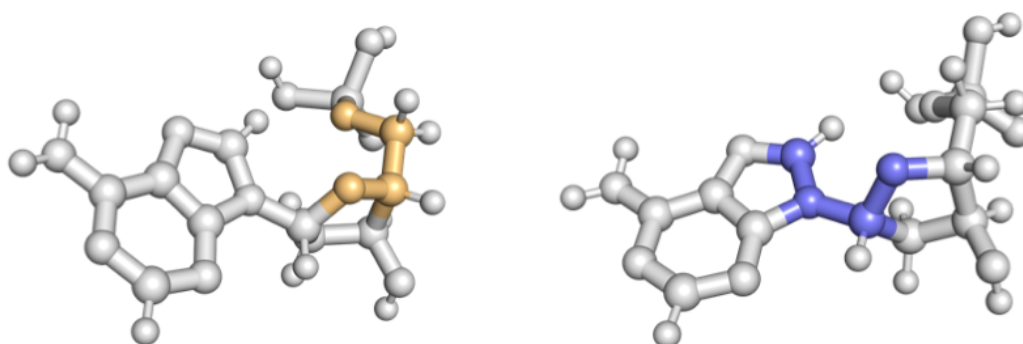


Figure 4.8: *Dihedral angles between phosphate-sugar (left) and base-sugar (right) used in analysis.*

It was also determined from Table 4.1 that the CPCM solvation and Fragmentation scheme I were able to produce geometries with smaller energy differences when compared to those of the SMD solvation model and the Fragmentation scheme II. Therefore, it is not surprising that smaller energy differences when using CPCM are reflected in lower RMSD values as shown in Table 4.2.

4.3.2 Stacked and double stranded models

The same approach was adopted to investigate the effects of fragmentation, solvation model and method on stacked and double stranded models of DNA, d(GpG) and dGMP-dCMP, as shown in Figure 4.3.

Table 4.3: Energy differences (kJ mol^{-1}) of d(GpG) between full system and FMO optimisations.

	Fragmentation I			Fragmentation II		
	Gas	CPCM	SMD	Gas	CPCM	SMD
PBE	-40.9	15.6	52.2	72.4	36.6	14.1
PBE-D3	-40.8	12.9	11.7	41.0	44.1	103.9
SRS-MP2	21.7	18.5	47.0	37.3	22.8	110.0

From Table 4.3 it can be seen that energy differences for the stacked d(GpG) model are significantly larger compared to those of the single-stranded dGMP and dAMP models, with differences ranging from -40.9 to 110.0 kJ mol^{-1} . Apart from the exception of SMD and Fragmentation scheme II, gas phase calculations gave rise to significantly large energy differences, ranging from -40.9 to 72.4 kJ mol^{-1} regardless of the Fragmentation scheme. This is in stark contrast to the trends found in single stranded systems. Compared to the narrow energy differences obtained for the single base systems, the large errors obtained for the stacked d(GpG) system suggests that when either of the two Fragmentation schemes, I or II, are used, the system becomes more flexible at adopting alternative energy configurations. In the majority of cases, higher energy configurations are more likely to be adopted. The only exception is gas phase optimisations performed with Fragmentation scheme I and the PBE or PDE-D3 functional, for which significantly lower energy configurations were located. Out of all the methods studied, SRS-MP2 resulted in smaller energy differences in the gas phase of 21.7 and 37.3 kJ mol^{-1} when using Fragmentation schemes I and II, respectively.

With respect to the gas phase, the CPCM solvation model resulted in a decrease of energy differences, ranging from 12.9 to 18.5 kJ mol^{-1} for Fragmentation scheme I and 22.8 to 44.2 kJ mol^{-1} for Fragmentation scheme II. All of the errors were found to be positive, suggesting that higher energy configurations are adopted when fragmentation is invoked. By incorporating the SMD solvation model, the range of energy differences becomes wider, ranging from 11.7 to

52.2 kJ mol⁻¹ for the Fragmentation scheme I and 14.1 to 110.0 kJ mol⁻¹ for the Fragmentation scheme II. This is similar to the single base systems, for which SMD gave rise to larger deviations, further confirming the ability of FMO/PCM to converge to configurations closer to those from full system optimisations. Interestingly, regardless of the solvation model, the combination of the Fragmentation scheme I and PBE-D3 results in the smallest deviation in energies of 12.9 and 11.7 kJ mol⁻¹ for CPCM and SMD, respectively. Overall, the combination of SRS-MP2 and CPCM produced consistently lower deviations when combined with Fragmentation scheme I.

Table 4.4: Differences in electrostatic (HF energy) and dispersion (correlation energy) components (kJ mol⁻¹) of optimised geometries of d(GpG).

	FMO2 (Fragmentation I)						FMO2 (Fragmentation II)					
	Gas		CPCM		SMD		Gas		CPCM		SMD	
	HF	Corr	HF	Corr	HF	Corr	HF	Corr	HF	Corr	HF	Corr
PBE	-39.5	-1.4	49.3	-33.8	20.6	31.6	39.4	32.9	35.3	1.2	39.2	-25.1
PBE-D3	-25.8	-14.9	58.4	-44.5	-2.4	14.2	33.4	7.7	64.2	-20.0	139.2	-35.4
SRS-MP2	-27.0	48.7	38.6	-20.2	1.5	45.5	4.7	32.6	45.5	-22.7	155.2	-45.2

The differences in two energetic components of electronic energies - electrostatic (HF energy) and dispersion (correlation energy) in the optimised geometries were further analysed (see Table 4.4). A huge range of differences clearly indicates the reason behind larger deviations found for the stacked model. At first glance the number may appear to be rather random, there are two obvious trends. The HF component is underestimated when using the Fragmentation schemes, with an average of 34.9 kJ mol⁻¹. This is subsequently reflected in the overestimation of the dispersion component, with an average of -2.7 kJ mol⁻¹. The SMD model in combination with Fragmentation scheme I and the SRS-MP2 method appears to form an outlier, for which both the electrostatic and dispersion components were found to be underestimated, by 1.5 and 45.5 kJ mol⁻¹, respectively. In addition, gas phase optimisations with Fragmentation scheme I overestimated the electrostatic component, whereas both electrostatic and dispersion components were underestimated in Fragmentation scheme II. The largest difference in the HF components, of 155.2 kJ mol⁻¹, was observed with the combination of the SRS-MP2 method, SMD model and Fragmentation scheme II. The largest difference in the dispersion component, of 48.7 kJ mol⁻¹, was observed with the combination of the SRS-MP2 method, gas phase and

Fragmentation scheme I. The smallest differences in the HF and correlation components, -2.4 and 14.2 kJ mol⁻¹, respectively, resulted from Fragmentation scheme I and the SMD solvation model when combined with the PBE-D3 functional. None of the methods and Fragmentation schemes produced small enough differences in the two energetic components. The found trends suggest that more work needs to be done in tweaking solute-solvent interactions in the implicit solvent models in the FMO formulation. These observations may also highlight the need to use three-body effects when performing FMO geometry optimisations of molecular systems consisting of more than three fragments. In the case of the stacked model used here, there were six fragments to be considered.

Table 4.5: *RMSD values (in Å) of d(GpG) FMO optimised geometries compared to full system optimisations.*

	Fragmentation I			Fragmentation II		
	Gas	CPCM	SMD	Gas	CPCM	SMD
PBE	1.560	1.354	1.235	1.216	3.650	3.668
PBE-D3	1.155	1.092	1.226	0.574	3.525	5.144
SRS-MP2	1.103	0.637	0.985	0.705	3.551	4.955

The optimised geometries were then compared in the hope to explain large discrepancies in electronic energies. The RMSD values in Table 4.5 reveal unexpectedly that both Fragmentation scheme I and II resulted in similar geometries when compared to full system optimisations. For example, the combination of Fragmentation scheme I, gas phase and PBE functional, which resulted in the energy difference of -40.9 kJ mol⁻¹, yielded an RMSD of 1.56 Å. Upon further examination, there does not seem to be a direct relationship between energetic differences and RMSD values. For example, whilst the Fragmentation scheme I and gas phase result in similar RMSD of 1.2 Å for PBE-D3 and 1.1 Å for SRS-MP2, they result in -40.8 and 21.7 kJ mol⁻¹ energy difference, respectively. Figure 4.9 reveals that, despite giving rise to similar overall RMSD values, geometries obtained with PBE-D3 using the full system optimisation and FMO-based optimisations are significantly more different than those with SRS-MP2. Despite similar RMSD values, the geometry obtained from PBE-D3 is significantly more distorted. Whilst the guanine bases are reproduced to a reasonable degree, the large discrepancy arises from the position of the phosphate group. FMO-based optimisations resulted in the formation of hydrogen

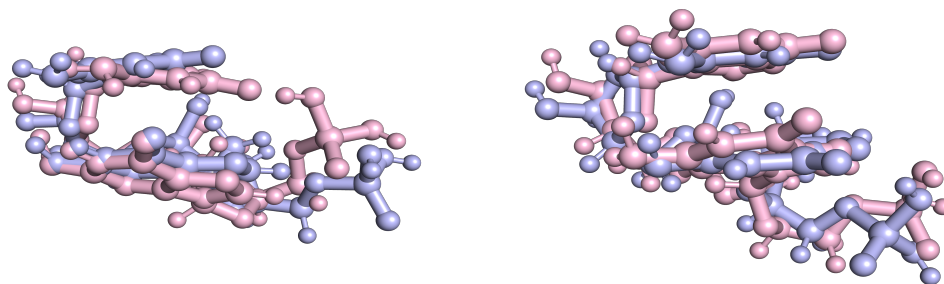


Figure 4.9: Optimised geometries of *d*(GpG) using full system optimisation (grey) and Fragmentation scheme II optimisation (pink) in gas phase.

bonding between the phosphate group and the carbonyl group on guanine. The additional intramolecular H-bonding results in a further stabilising effect and the formation of a different geometry, thus differing in energy difference when compared to the full system optimisation. The optimised geometry obtained from FMO Fragmentation scheme II reproduced the stacking of the bases sufficiently well with an RMSD of 1.1 Å, which mainly reflected the difference in the position of the phosphate groups.

The results presented in Table 4.5 motivated us to take a closer look at the tilt and inter-base distances of the guanine bases in the *d*(GpG) model. Curtis *et al.* utilised linear dichroism and determined the tilt of DNA bases while dissolved in 0.01 M Na⁺ (phosphate buffer) to be 75°. ⁷⁰ Table 4.6 presents the tilt between the two guanine bases measured as demonstrated in Figure 4.10. While the combination of PBE, CPCM and full system calculation is optimal to predict the tilt between the two guanine bases, PBE predicts an average of 81°, regardless of Fragmentation scheme and solvation. Both PBE-D3 and SRS-MP2 predicted a similar tilt angles, an average of 64° and 64°, respectively. This suggests that the energetic differences are a direct result of the distinct configurational differences obtained between the FMO-based and full system optimisations.

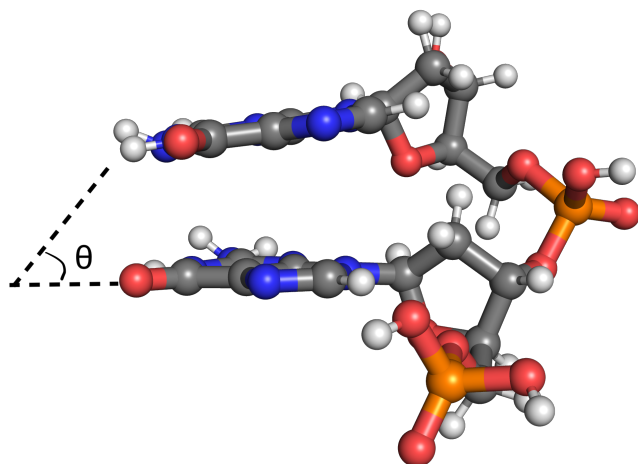


Figure 4.10: Tilt angle between the two Guanine units in the stacked $d(\text{GpG})$ model.

Table 4.6: Tilt ($^{\circ}$) between guanine bases in $d(\text{GpG})$.

	Full system			FMO2 (Fragmentation I)			FMO2 (Fragmentation II)		
	Gas	CPCM	SMD	Gas	CPCM	SMD	Gas	CPCM	SMD
PBE	64	76	70	87	72	91	87	85	79
PBE-D3	61	70	62	64	67	60	62	64	76
SRS-MP2	60	65	64	61	62	70	67	61	65

In addition, Table 4.6 demonstrates that the SRS-MP2 method is able to best replicate the geometry of the stacked system within the Fragmentation schemes. This is unsurprising that SRS-MP2 has previously demonstrated its superiority in describing $\pi - \pi$ stacking systems.^{5,10,64} When full system optimisations are concerned, SRS-MP2 predicted a tilt angle of 65° and 64° with CPCM and SMD solvation models, respectively.

Table 4.7 presents the inter-base distances between the two Guanine units in the $d(\text{GpG})$ system, taking the centre of the 6 membered ring as a reference. The inter-base distance is well reported to be 2.6 or 3.4 Å for A-DNA and B-DNA, respectively.⁷¹ Table 4.7 reveals that the PBE functional constantly overestimates the inter-base distance, by at least 0.987 and 0.187 Å, for A-DNA and B-DNA, respectively. The largest inter-base distance, of 4.969 Å, was obtained with the combination of Fragmentation scheme II and the PBE functional in the gas

phase, indicating its inability to model the π - π stacking interactions between the Guanine units as observed in the full system optimisation (see Figure. 4.11). SRS-MP2, once again, demonstrates its ability to reliably describe non-covalent interactions and is able to best predict the inter-base distance with an average of 3.336 Å with both Fragmentation schemes.

Table 4.7: *Inter-base distance (Å) between the two guanine bases in $d(\text{GpG})$.*

	Full system			Fragmentation I			Fragmentation II		
	Gas	CPCM	SMD	Gas	CPCM	SMD	Gas	CPCM	SMD
PBE	3.587	3.887	3.684	4.819	4.048	4.961	4.969	4.701	4.108
PBE-D3	3.413	3.590	3.423	3.579	3.347	3.376	3.464	3.570	4.380
SRS-MP2	3.332	3.195	3.180	3.164	3.192	3.906	3.559	3.164	3.328

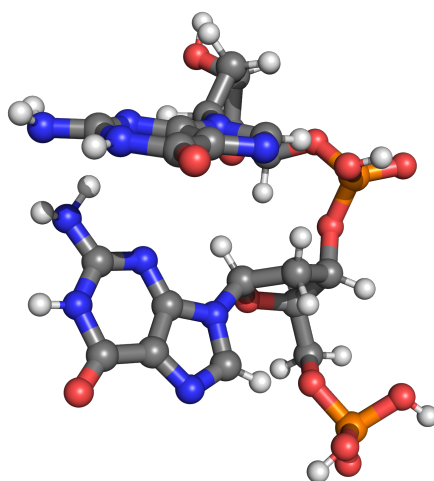


Figure 4.11: *π - π stacking between the two guanine units in the $d(\text{GpG})$ structure optimised with Fragmentation scheme II and the PBE functional in the gas phase.*

Subsequently, we posed a question of whether the re-optimisation of FMO optimised geometries using full system optimisations would result in locating the same local minima as the latter. Optimised geometries using FMO and the SRS-MP2 method were further re-optimised using full system optimisation with SRS-MP2/VDZ and either CPCM or SMD solvation model. Single point energy calculations were then performed using SRS-MP2/VTZ in the gas phase and compared to that obtained from the original full system optimisations. RMSD values were also analysed.

Table 4.8: Total energy differences (ΔE , kJ mol^{-1}) and differences in electrostatic and dispersion components (kJ mol^{-1}) of FMO-optimised $d(\text{GpG})$ model. All comparisons are made with respect to full system optimisations.

Solvation Model	Fragmentation scheme	ΔE	HF	Corr
Gas	I	-0.003	0.6	-0.6
	II	-0.080	0.1	-0.2
CPCM	I	0.3	31.2	-30.9
	II	-0.3	29.9	-30.2
SMD	I	-4.9	-7.4	2.6
	II	33.4	68.2	-34.8

Table 4.8 presents total energy differences between the re-optimised geometries as “full system” of the FMO-optimised geometries and those obtained from full system optimisations. When the re-optimisations were performed on the FMO-optimised geometries obtained in gas phase, the total energy differences between the re-optimised and full system geometries were very small averaging $-0.003 \text{ kJ mol}^{-1}$ for Fragmentation scheme I and $-0.080 \text{ kJ mol}^{-1}$ for Fragmentation scheme II. This suggests that the re-optimisation located the same local minima as the original full system optimisations. This is further supported through small differences obtained for the electrostatic and dispersion components of total electronic energies. These differences fell under 1 kJ mol^{-1} . The situation changes when the re-optimisation was performed with implicit solvation models resulting in slightly larger energy differences between -0.3 and 0.3 kJ mol^{-1} for CPCM and between -4.9 and 33.4 kJ mol^{-1} for SMD for both Fragmentation schemes. Even though the energy differences obtained from CPCM solvation model are very small, the re-optimised geometries resulted in large differences in the electrostatic and dispersion components when compared to full system optimisations. The re-optimisation resulted in an underestimation of the electrostatic component by 31.2 kJ mol^{-1} and overestimation of the dispersion component by 30.2 kJ mol^{-1} on average regardless of the Fragmentation scheme used. The re-optimisation of the geometry obtained with Fragmentation scheme I and SMD resulted in a smaller deviation in both electrostatic and dispersion components of -7.4 and 2.6 kJ mol^{-1} , respectively. However, the geometry from Fragmentation scheme II and SMD did not fare well, producing a significantly different local minimum with a large difference in total

electronic energy of 33.9 kJ mol^{-1} as well as corresponding electrostatic (62.8 kJ mol^{-1}) and dispersion ($-34.8 \text{ kJ mol}^{-1}$) components. These results suggest that the inclusion of implicit solvation models is less likely to optimise to the same local minimum as the original full system optimisation.

Further studies were conducted to investigate the reliability of FMO optimisations to study double stranded systems. In this study the double stranded G-C system was constructed as shown in Figure 4.3. Table 4.9 reports the energy difference between the optimised geometries obtained from full system and FMO calculations. From Table 4.9, there does not appear to be a clear trend. Regardless of the Fragmentation scheme, method and solvation model, the range of energy differences, ranging between -22.8 to 45.5 kJ mol^{-1} , is almost half as narrow as compared to that of d(GpG). For the double stranded system, gas phase calculations gave rise to the smallest range of errors, regardless of fragmentation scheme and method, ranging between 0.9 to 22.3 kJ mol^{-1} . The smallest error was reported when PBE-D3 and the Fragmentation scheme I were used in conjunction. Overall, regardless of method, the Fragmentation scheme I has a smaller average energy deviation of 5.1 kJ mol^{-1} compared to that of 13.7 kJ mol^{-1} found for Fragmentation scheme II.

Table 4.9: Energy differences (kJ mol^{-1}) between full system and FMO optimisations in the double stranded (G-C) model.

	FMO2 (Fragmentation I)			FMO2 (Fragmentation II)		
	Gas	CPCM	SMD	Gas	CPCM	SMD
PBE	1.9	3.3	-1.5	1.3	45.5	29.6
PBE-D3	0.9	48.1	-0.4	9.7	24.8	27.1
SRS-MP2	12.6	-22.6	45.8	22.3	18.3	35.9

Table 4.10: RMSD values (in Å) of double stranded (G-C) geometries obtained using FMO as compared to the full system optimisation.

	FMO2 (Fragmentation I)			FMO2 (Fragmentation II)		
	Gas	CPCM	SMD	Gas	CPCM	SMD
PBE	0.216	0.507	0.836	0.129	0.719	0.340
PBE-D3	0.149	6.587	1.060	0.129	0.280	0.273
SRS-MP2	0.823	0.324	0.830	0.896	0.402	0.445

With the inclusion of solvation models, the energy deviations are significantly larger than those in the gas phase, ranging between -22.6 to 48.1 kJ mol^{-1} and -1.5 to 45.8 kJ mol^{-1} for CPCM and SMD, respectively. The largest deviation for both CPCM and SMD resulted from the use of Fragmentation scheme I and PBE-D3 and SRS-MP2, respectively. Upon analysing RMSD values, the structures surprisingly deviate to a different degree. In the case of PBE-D3, as the average deviation of 6.6 Å was observed, whereas for SRS-MP2, it was only 0.8 Å. Upon investigating the optimised geometries visually, it can be seen that the structures obtained from PBE-D3 and Fragmentation scheme I are significantly different as compared to those optimised as the full system. An example of this trend is shown in Figure 4.12. For the same structure obtained from optimisation with Fragmentation scheme I and SRS-MP2, the configuration of dCMP was adequately predicted whereas the dGMP component converged to a different local minimum. These observations re-enforce the conclusion that the inclusion of an implicit solvation model is more likely to result in a different local minimum due to the lack of an accurate description of the solute-solvent interactions.

When using CPCM, the range of energy deviations becomes broader for the double stranded system compared to those of the stacked system, ranging from -22.6 to 48.1 kJ mol^{-1} for the former and 12.9 to 44.2 kJ mol^{-1} for the latter. However, the mean absolute deviations of the Fragmentation schemes I and II for the double stranded system are significantly lower than those for the stacked system. The mean absolute deviation of the Fragmentation schemes I and II for the double stranded system with CPCM is 24.7 and 29.5 kJ mol^{-1} , respectively, whereas the mean absolute deviation for the stacked system using Fragmentation scheme I and II is 15.6 and 34.5 kJ mol^{-1} , respectively. When using SMD, the range of energy deviation is significantly smaller for the double stranded system compared to those of the stacked system, ranging from -1.5 to 45.8 kJ mol^{-1} for the former and 11.7 to 110.0 kJ mol^{-1} for the latter. Similar to CPCM, the mean absolute deviations of the Fragmentation schemes I and II in conjunction with SMD for the double stranded system are also significantly lower than the stacked system. The mean absolute deviation of the Fragmentation schemes I and II for the double stranded with SMD is 15.9 and 30.9 kJ mol^{-1} , respectively, whereas the mean absolute deviation for the stacked system using Fragmentation schemes I and II is 37.0 and 76.0 kJ mol^{-1} , respectively. The present results suggest that the three hydrogen bonds between the nucleobases in the double stranded

system are better reproduced than the π - π stacking due to the directional nature of hydrogen bonding. On the other hand, the sugar and phosphate backbone has a much higher degree of flexibility. The inclusion of an implicit solvation model results in the sugar and phosphate units adopting different local minima to the full system optimisation.

Table 4.11: Differences in electrostatic (HF) and dispersion (Corr) components (in kJ mol^{-1}) of the double stranded (G-C) system as compared to full system optimisations

	Fragmentation I						Fragmentation II					
	Gas		CPCM		SMD		Gas		CPCM		SMD	
	HF	Corr	HF	Corr	HF	Corr	HF	Corr	HF	Corr	HF	Corr
PBE	2.8	-0.9	6.0	0.3	4.1	-5.5	16.1	-6.8	60.3	-14.8	39.7	-10.2
PBE-D3	1.3	-0.4	92.8	-44.7	10.1	-10.5	16.5	-6.8	34.4	-9.6	36.2	-9.1
SRS-MP2	-3.6	16.2	-37.5	14.9	65.1	-19.4	9.0	13.3	25.1	-6.8	44.9	-9.0

The differences in the energetic components of the double stranded structures optimised with FMO and as the full system are presented in Table 4.11. Once again, the Fragmentation scheme I is able to recover better the electrostatic component as compared to the Fragmentation scheme II, giving rise to an average deviation of 15.7 and 31.4 kJ mol^{-1} , respectively, regardless of method and solvation model. The average deviations of the dispersion component were found to be -5.6 and -6.6 kJ mol^{-1} for Fragmentation schemes I and II, respectively. A smaller range in both the electrostatic and dispersion component for the double stranded model explains the smaller differences in electronic energies, which represent a stark contrast to the trends found in the stacked model. Gas phase calculations resulted in the energy differences ranging from -3.6 to 16.5 kJ mol^{-1} for the electrostatic component and -6.8 to 16.2 kJ mol^{-1} for the dispersion component. In the gas phase, SRS-MP2 predicted a smaller range for both the electrostatic and dispersion components compared to those of PBE and PBE-D3. While SRS-MP2 predicted a difference of -3.6 and 9.0 kJ mol^{-1} for the electrostatic component with either Fragmentation I and II, respectively, PBE-D3 predicted a difference of 1.3 and 16.5 kJ mol^{-1} , respectively.

In general, the inclusion of a solvation model increased the range of differences in energetic components compared to the gas phase. For the electrostatic component, the inclusion of CPCM and SMD solvation models, resulted in the range of -37.5 to 92.8 kJ mol^{-1} and 4.1 to

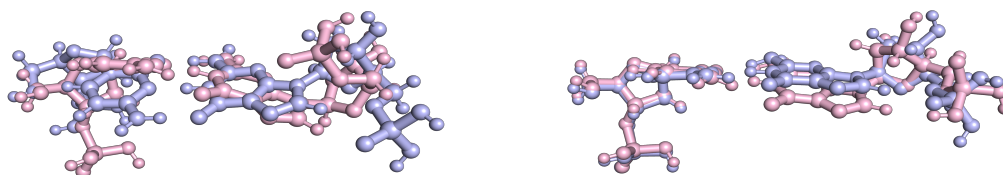


Figure 4.12: *Optimised geometries of the double stranded dGMP-dCMP model optimised as the full system (grey) and Fragmentation scheme I (pink) with CPCM solvation model and either PBE-D3 (left) or SRS-MP2 (right).*

65.1 kJ mol⁻¹, respectively. For the dispersion component, the range was smaller, namely from -44.7 to 14.9 kJ mol⁻¹ for CPCM and -19.4 to -5.5 kJ mol⁻¹ for SMD. These observations explain significantly smaller energy differences obtained with SMD when studying the double stranded model as compared to the stacked model (see Table 4.3). The inclusion of CPCM, on the other hand, resulted in larger energy deviations for the double stranded model than the stacked model. This suggests that the solvation models within FMO must be carefully parameterised to account for the presence of varying intermolecular interactions from hydrogen bonding to π - π stacking.

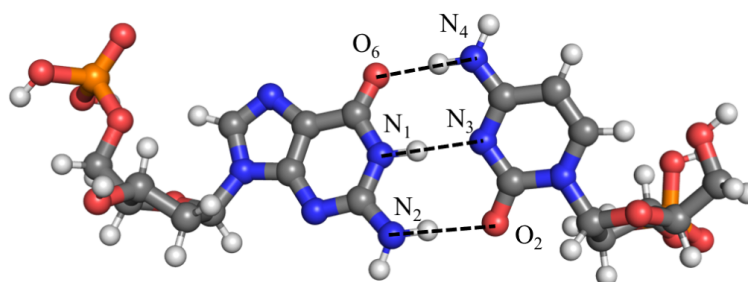


Figure 4.13: *Bonding distances in the dGMP-dCMP model.*

The calculated H-bond lengths between guanine and cytosine were measured and compared to previously measured experimental data. By utilising X-ray crystallography, Fourme *et al.* determined the distance between O6-N4, N1-N3 and N2-O2 to be 2.90, 2.92 and 2.84 Å, respectively (see Figure 4.13).⁷² Figure 4.14 shows the deviation of the calculated hydrogen bonded distances between the two nucleobases to those experimentally determined distances.⁷² The combination of SMD, SRS-MP2 and the full system calculation resulted in the smallest deviations from experimental data, deviating by as little as 0.044 Å. The largest deviation of 0.149 Å resulted from the combination of SMD, SRS-MP2 and the Fragmentation scheme I. This was also reflected in the energy difference of 45.8 kJ mol⁻¹ when compared to the full system optimised structure. Overall, the full system optimisations were able to predict the geometries slightly more consistently with experiment compared to FMO. The average deviation in hydrogen bond distances for the full system optimisations was determined to be 0.059 Å, with the Fragmentation schemes I and II yielding an average deviation of 0.076 and 0.071 Å, respectively. Excluding the outlier of SRS-MP2, SMD and the Fragmentation scheme I, SRS-MP2 was found to be the optimal method for geometry optimisations, yielding an average deviation in hydrogen bond distances of 0.06 Å regardless of fragmentation scheme and solvation models. PBE and PBE-D3 deviate slightly more, yielding an average deviation of 0.065 and 0.072 Å, respectively. This further supports the ability of SRS-MP2 to reliably predict geometries of hydrogen bonded systems.

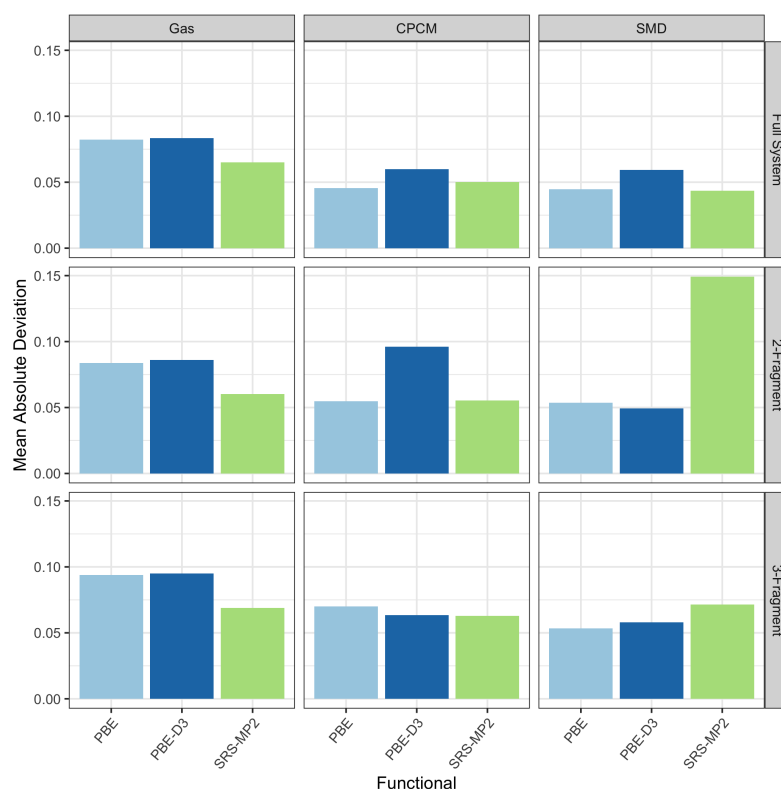


Figure 4.14: Mean absolute deviation between the optimised geometries obtained from both full system and FMO calculations to previously published experimental data.^[72]

Once again, we posed the question of whether a re-optimisation of FMO generated geometries using the full system SRS-MP2 optimisation would locate the same local minima. The same procedure as in the case of the d(GpG) model was used for the double stranded system (see Figure 4.4). Optimised geometries from the two Fragmentation schemes in combination with SRS-MP2 were re-optimised with full system SRS-MP2/VDZ and either the CPCM or SMD solvation model. Energies of thus optimised structures were improved with the SRS-MP2, VTZ basis set in the gas phase and were compared to those obtained from the original full system optimisations.

Table 4.12: *Total energy differences (ΔE , kJ mol^{-1}) and differences in electrostatic and dispersion components (kJ mol^{-1}) of FMO-optimised dGMP-dCMP model. All comparisons are made with respect to full system optimisations.*

Solvation Model	Fragmentation scheme	ΔE	HF	Corr
Gas	I	12.3	-4.0	16.3
	II	0.8	-0.8	1.7
CPCM	I	-11.7	-14.4	2.8
	II	2.5	2.6	-0.1
SMD	I	12.0	24.2	-12.3
	II	21.6	27.9	-6.3

Table 4.12 presents the total energy differences between the re-optimised geometries of the original FMO-optimised geometries and the full system optimisations. In the gas phase, the total energy differences between the re-optimised and full system geometries were found to be 12.3 and 0.8 kJ mol^{-1} for Fragmentation schemes I and II, respectively. Only the geometry from Fragmentation scheme II converged close to the original full system optimisation minimum, which is also demonstrated in small differences (well within chemical accuracy) in the electrostatic and dispersion components. The geometry from Fragmentation scheme I converged to a different local minimum which was higher in energy $> 10 \text{ kJ mol}^{-1}$. The inclusion of solvation models generally resulted in larger energy differences as compared to those in the gas phase. The difference fell between -11.7 and 2.5 kJ mol^{-1} for CPCM solvation model and between 12.0 and 21.6 kJ mol^{-1} for the SMD solvation model for both Fragmentation schemes. The re-optimisation of the geometry obtained from Fragmentation scheme II and CPCM resulted in the smallest energy difference of 2.5 kJ mol^{-1} with an underestimation of 2.6 kJ mol^{-1} for the electrostatic component and an overestimation of 0.1 kJ mol^{-1} for the correlation component. Re-optimisation of SMD-optimised geometries led to higher energy local minima, for which the electrostatic component was underestimated by 26.1 kJ mol^{-1} on average. Again, SMD did not fare as well as CPCM during full system re-optimisations and therefore, cannot be recommended to be used within the FMO framework.

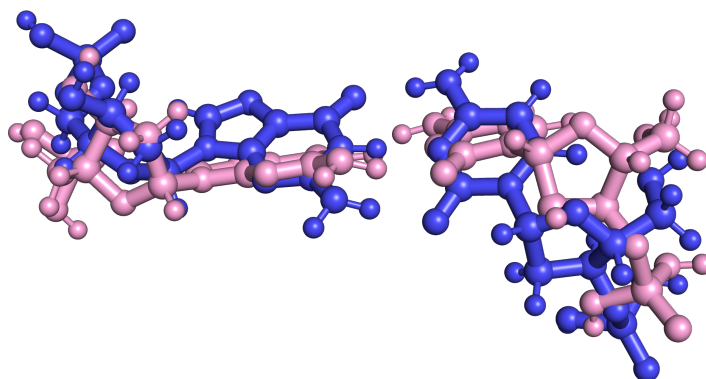


Figure 4.15: *Difference in optimised geometries between full system optimisation (pink) and Fragmentation scheme I optimisation (blue).*

Upon analysing the re-optimised geometry using the full system approach, it is clear to see that the different approaches located different minima on the potential energy surface (Figure 4.15). The flexibility of sugar and phosphate groups, due to the absence of intra-strand π - π stacking, allows for significantly different geometries.

4.4 Conclusions

In this study, the FMO approach was utilised to investigate its ability to reproduce full system optimisations when studying small DNA models with implicit solvation models, such as CPCM and SMD and three different quantum chemical methods - PBE, PBE-D3 and SRS-MP2. When geometry optimisations were performed in the gas phase for single base systems such as dAMP and dGMP, the Fragmentation scheme I outperformed the Fragmentation scheme II, producing an average energy difference of 0.02 and 3.2 kJ mol⁻¹, respectively. The incorporation of implicit solvation models resulted in significantly larger energy differences, with the largest energy difference of 39.1 kJ mol⁻¹ being observed for the combination of the Fragmentation scheme II, SRS-MP2 and the SMD solvation model. Upon analysing the respective optimised geometries and RMSD values, the large energy differences were attributed to the location of different local

minima due to the backbone flexibility of the phosphate and the sugar units in the dAMP and dGMP models.

The same approach was used to study both stacked, d(GpG), and double stranded, dGMP-dCMP, models. Unsurprisingly, the same trend was observed, whereby large energy differences were recorded for these models compared to single base models. This was explained due to the ability of larger molecular systems to adopt many more local minima as compared to the single base systems. While the largest RMSD values for dGMP and dAMP were determined to be 2.115 and 0.420 Å, respectively; the largest RMSD recorded for d(GpG) and dGMP-dCMP was 5.144 and 6.587 Å, respectively. The optimised geometries of d(GpG) and dGMP-dCMP were compared to previously determined experimental data. For d(GpG), the calculated inter-base distance and the base pair tilt were compared to experimental values. The calculated base pair tilts were usually underestimated, with a mean absolute deviation of 10°. When comparing the inter-base distance between the two guanine units in d(GpG), the predicted distances were found to be overestimated by 0.436 Å on average. The directionality of hydrogen bonds in the double stranded model significantly reduced the flexibility of the nucleobase units. Long-range π - π stacking is less directional and resulted in large differences in optimised geometries for the stacked model are not surprising. Overall, the SRS-MP2 method in combination with SMD and full system optimisations reproduced experimental in-plane hydrogen bonds in the double stranded model within 0.06 Å on average.

In the case of the dGMP-dCMP model the sugar and phosphate group backbone was found to become more flexible in the presence of implicit solvation models, thus resulting in optimisations to different local minima and hence larger differences in electronic energies when compared to those of full system optimisations. The range of energy differences, when improved with SRS-MP2/VTZ in the gas phase, was found to be smaller for the double stranded model than the stacked model. For the former, the range was found to fall between 0.9 to 22.3 kJ mol⁻¹ and for the latter between -40.9 and 72.4 kJ mol⁻¹.

When optimisations were performed in the gas phase for the stacked systems, the Fragmentation scheme I outperformed the Fragmentation scheme II, resulting in mean absolute deviations of 40.9 and 50.2 kJ mol⁻¹, respectively. While the incorporation of the CPCM solvation model decreased the mean absolute deviation, of 15.6 and 34.5 kJ mol⁻¹ for Fragmentation

schemes I and II, respectively, the SMD solvation model resulted in a larger mean absolute deviation of 76.0 kJ mol^{-1} with the use of Fragmentation scheme II. The gas phase optimisations for the double-stranded systems resulted in smaller mean absolute deviations as compared to those of the stacked system, falling in between 5.1 and 13.7 kJ mol^{-1} for Fragmentation schemes I and II, respectively. The inclusion of solvation models increased the mean absolute deviation, with the largest absolute energy difference of 45.8 kJ mol^{-1} resulting from the combination of the SRS-MP2 method, Fragmentation scheme I and the SMD solvation model. Similar to the single base system, the energy differences were attributed to locating different local minima, a result of the increased flexibility of the phosphate and sugar units due to the absence of steric hindrance of larger DNA models.

Due to the location of different minima, the geometries of the double stranded and stacked systems obtained from FMO and SRS-MP2 calculations were re-optimised using full system optimisations to determine if the same minima would be located. Upon re-optimisation, the energies differences between the re-optimised geometries and the original full system optimisations revealed that different minima were located for most of the method-solvation model combinations. Only gas phase re-optimisations for the stacked model managed to produce similar local minima as the original full system optimisation. For the stacked system, the mean absolute deviation obtained for the FMO-optimised and re-optimised geometries was 42.9 and 6.5 kJ mol^{-1} , respectively, regardless of Fragmentation scheme and solvation model used. For the double stranded system, the mean absolute deviation obtained for the FMO-optimised and re-optimised geometries was 26.3 and 10.1 kJ mol^{-1} , respectively, regardless of Fragmentation scheme and solvation model. The inclusion of implicit solvation models was found to result in larger differences in geometries when compared to the gas phase. These findings suggest the different approaches locate different minima on the potential energy surface. Moreover, the use of the SMD solvation model for geometry optimisations of DNA models beyond a single base system is not recommended within the FMO framework. In the case of CPCM, only Fragmentation scheme I can be recommended.

Overall, the inclusion of implicit solvation models into the geometry optimisation procedure within the FMO approach affected the location of similar local minima when compared with full system optimisations. All three methods used, PBE, PBE-D3 and SRS-MP2, located varying

minima. This suggests two potential issues that require solutions. Firstly, as the number of fragments increases in the system, the inclusion of three body effects might become crucial already at the optimisation level. For example, within Fragmentation scheme II the number of fragments increases from three in single base systems to six fragments in double stranded and stacked systems. Therefore, the use of FMO3 should be studied in the future. Secondly, more work needs to be done in refining solute-solvent interactions to interface implicit solvation models to be able to treat varying intermolecular interactions with similar accuracy.

4.5 References

- [1] Maylis Orio, Dimitrios A Pantazis, and Frank Neese. Density functional theory. *Photo-synthesis Research* **102**(2-3) (2009), 443–453.
- [2] Jiri Cerny, Martin Kabelác, and Pavel Hobza. Double-helical→ ladder structural transition in the B-DNA is induced by a loss of dispersion energy. *Journal of the American Chemical Society* **130**(47) (2008), 16055–16059.
- [3] Edward G Hohenstein and C David Sherrill. Wavefunction methods for noncovalent interactions. *Wiley Interdisciplinary Reviews: Computational Molecular Science* **2**(2) (2012), 304–326.
- [4] Narbe Mardirossian and Martin Head-Gordon. Thirty years of density functional theory in computational chemistry: an overview and extensive assessment of 200 density functionals. *Molecular Physics* **115**(19) (2017), 2315–2372.
- [5] Samuel Tan, Santiago Barrera Acevedo, and Ekaterina I Izgorodina. Generalized spin-ratio scaled MP2 method for accurate prediction of intermolecular interactions for neutral and ionic species. *The Journal of Chemical Physics* **146**(6) (2017), 064108.
- [6] Jan Rezac and Pavel Hobza. Describing noncovalent interactions beyond the common approximations: How accurate is the “gold standard,” CCSD (T) at the complete basis set limit? *Journal of Chemical Theory and Computation* **9**(5) (2013), 2151–2155.
- [7] Pavel Hobza. Calculations on noncovalent interactions and databases of benchmark interaction energies. *Accounts of Chemical Research* **45**(4) (2012), 663–672.
- [8] Stefan Grimme. Improved second-order Møller–Plesset perturbation theory by separate scaling of parallel-and antiparallel-spin pair correlation energies. *The Journal of Chemical Physics* **118**(20) (2003), 9095–9102.
- [9] Robert A Distasio Jr and Martin Head-Gordon. Optimized spin-component scaled second-order Møller-Plesset perturbation theory for intermolecular interaction energies. *Molecular Physics* **105**(8) (2007), 1073–1083.

- [10] Samuel YS Tan, Luke Wylie, Ivan Begic, Dennis Tran, and Ekaterina I Izgorodina. Application of spin-ratio scaled MP2 for the prediction of intermolecular interactions in chemical systems. *Physical Chemistry Chemical Physics* **19**(42) (2017), 28936–28942.
- [11] Dmitri G Fedorov, Ryan M Olson, Kazuo Kitaura, Mark S Gordon, and Shiro Koseki. A new hierarchical parallelization scheme: Generalized distributed data interface (GDDI), and an application to the fragment molecular orbital method (FMO). *Journal of Computational Chemistry* **25**(6) (2004), 872–880.
- [12] Mark S Gordon, Dmitri G Fedorov, Spencer R Pruitt, and Lyudmila V Slipchenko. Fragmentation methods: A route to accurate calculations on large systems. *Chemical Reviews* **112**(1) (2012), 632–672.
- [13] Weitao Yang. Direct calculation of electron density in density-functional theory. *Physical Review Letters* **66**(11) (1991), 1438.
- [14] Tai-Sung Lee, Darrin M York, and Weitao Yang. Linear-scaling semiempirical quantum calculations for macromolecules. *The Journal of Chemical Physics* **105**(7) (1996), 2744–2750.
- [15] Wei Pan, Tai-Sung Lee, and Weitao Yang. Parallel implementation of divide-and-conquer semiempirical quantum chemistry calculations. *Journal of Computational Chemistry* **19**(9) (1998), 1101–1109.
- [16] Arjan van der Vaart, Valentin Gogonea, Steven L Dixon, and Kenneth M Merz Jr. Linear scaling molecular orbital calculations of biological systems using the semiempirical divide and conquer method. *Journal of Computational Chemistry* **21**(16) (2000), 1494–1504.
- [17] Michael A Collins. Molecular forces, geometries, and frequencies by systematic molecular fragmentation including embedded charges. *The Journal of Chemical Physics* **141**(9) (2014), 094108.
- [18] Michael A Collins and Vitali A Deev. Accuracy and efficiency of electronic energies from systematic molecular fragmentation. *The Journal of Chemical Physics* **125**(10) (2006), 104104.

- [19] Kazuo Kitaura, Eiji Ikeo, Toshio Asada, Tatsuya Nakano, and Masami Uebayasi. Fragment molecular orbital method: an approximate computational method for large molecules. *Chemical Physics Letters* **313**(3-4) (1999), 701–706.
- [20] Erin E Dahlke and Donald G Truhlar. Electrostatically embedded many-body expansion for simulations. *Journal of Chemical Theory and Computation* **4**(1) (2008), 1–6.
- [21] Erin E Dahlke, Hannah R Leverentz, and Donald G Truhlar. Evaluation of the electrostatically embedded many-body expansion and the electrostatically embedded many-body expansion of the correlation energy by application to low-lying water hexamers. *Journal of Chemical Theory and Computation* **4**(1) (2008), 33–41.
- [22] Hannah R Leverentz and Donald G Truhlar. Electrostatically embedded many-body approximation for systems of water, ammonia, and sulfuric acid and the dependence of its performance on embedding charges. *Journal of Chemical Theory and Computation* **5**(6) (2009), 1573–1584.
- [23] Steven L Dixon and Kenneth M Merz Jr. Semiempirical molecular orbital calculations with linear system size scaling. *The Journal of Chemical Physics* **104**(17) (1996), 6643–6649.
- [24] Jonathan M Mullin, Luke B Roskop, Spencer R Pruitt, Michael A Collins, and Mark S Gordon. Systematic fragmentation method and the effective fragment potential: an efficient method for capturing molecular energies. *The Journal of Physical Chemistry A* **113**(37) (2009), 10040–10049.
- [25] Vitali Deev and Michael A Collins. Approximate ab initio energies by systematic molecular fragmentation. *The Journal of Chemical Physics* **122**(15) (2005), 154102.
- [26] Matthew A Addicoat and Michael A Collins. Accurate treatment of nonbonded interactions within systematic molecular fragmentation. *The Journal of Chemical Physics* **131**(10) (2009), 104103.
- [27] Erin E Dahlke and Donald G Truhlar. Electrostatically embedded many-body expansion for large systems, with applications to water clusters. *Journal of Chemical Theory and Computation* **3**(1) (2007), 46–53.

- [28] Elbek K Kurbanov, Hannah R Leverentz, Donald G Truhlar, and Elizabeth A Amin. Electrostatically embedded many-body expansion for neutral and charged metalloenzyme model systems. *Journal of Chemical Theory and Computation* **8**(1) (2012), 1–5.
- [29] PJ Bygrave, NL Allan, and FR Manby. The embedded many-body expansion for energetics of molecular crystals. *The Journal of Chemical Physics* **137**(16) (2012), 164102.
- [30] Richard J Wheatley and Sarah L Price. An overlap model for estimating the anisotropy of repulsion. *Molecular Physics* **69**(3) (1990), 507–533.
- [31] Lorenzo Maschio, Denis Usvyat, and Bartolomeo Civalleri. Ab initio study of van der Waals and hydrogen-bonded molecular crystals with a periodic local-MP2 method. *CrystEngComm* **12**(8) (2010), 2429–2435.
- [32] Mark S Gordon, Dmitri G Fedorov, Spencer R Pruitt, and Lyudmila V Slipchenko. Fragmentation methods: A route to accurate calculations on large systems. *Chemical Reviews* **112**(1) (2011), 632–672.
- [33] Dmitri G Fedorov. The fragment molecular orbital method: theoretical development, implementation in GAMESS, and applications. *Wiley Interdisciplinary Reviews: Computational Molecular Science* **7**(6) (2017), e1322.
- [34] Dmitri G Fedorov and Kazuo Kitaura. Pair interaction energy decomposition analysis. *Journal of Computational Chemistry* **28**(1) (2007), 222–237.
- [35] Dmitri G Fedorov and Kazuo Kitaura. “Theoretical development of the fragment molecular orbital (FMO) method”. In: *Modern methods for theoretical physical chemistry of biopolymers*. 2006, pp.3–38.
- [36] Peter Halat, Zoe L Seeger, Santiago Barrera Acevedo, and Ekaterina I Izgorodina. Trends in two-and three-body effects in multiscale clusters of ionic liquids. *The Journal of Physical Chemistry B* **121**(3) (2017), 577–588.
- [37] Dmitri G Fedorov and Kazuo Kitaura. The importance of three-body terms in the fragment molecular orbital method. *The Journal of Chemical Physics* **120**(15) (2004), 6832–6840.

- [38] Samuel YS Tan and Ekaterina I Izgorodina. Comparison of the effective fragment potential method with symmetry-adapted perturbation theory in the calculation of intermolecular energies for ionic liquids. *Journal of Chemical Theory and Computation* **12**(6) (2016), 2553–2568.
- [39] Zoe L Seeger and Ekaterina I Izgorodina. A Systematic Study of DFT Performance for Geometry Optimizations of Ionic Liquid Clusters. *Journal of Chemical Theory and Computation* **16**(10) (2020), 6735–6753.
- [40] Zoe L Seeger, Rika Kobayashi, and Ekaterina I Izgorodina. Cluster approach to the prediction of thermodynamic and transport properties of ionic liquids. *The Journal of Chemical Physics* **148**(19) (2018), 193832.
- [41] Ekaterina I Izgorodina, Jason Rigby, and Douglas R MacFarlane. Large-scale ab initio calculations of archetypical ionic liquids. *Chemical Communications* **48**(10) (2012), 1493–1495.
- [42] S F Boys and FJMP Bernardi. The calculation of small molecular interactions by the differences of separate total energies. Some procedures with reduced errors. *Molecular Physics* **19**(4) (1970), 553–566.
- [43] Richard P Matthews, Tom Welton, and Patricia A Hunt. Hydrogen bonding and π – π interactions in imidazolium-chloride ionic liquid clusters. *Physical Chemistry Chemical Physics* **17**(22) (2015), 14437–14453.
- [44] Richard P Matthews, Claire Ashworth, Tom Welton, and Patricia A Hunt. The impact of anion electronic structure: similarities and differences in imidazolium based ionic liquids. *Journal of Physics: Condensed Matter* **26**(28) (2014), 284112.
- [45] Tatsuya Nakano, Tsuguchika Kaminuma, Toshiyuki Sato, Yutaka Akiyama, Masami Uebayasi, and Kazuo Kitaura. Fragment molecular orbital method: application to polypeptides. *Chemical Physics Letters* **318**(6) (2000), 614–618.
- [46] Dmitri G Fedorov, Jan H Jensen, Ramesh C Deka, and Kazuo Kitaura. Covalent bond fragmentation suitable to describe solids in the fragment molecular orbital method. *The Journal of Physical Chemistry A* **112**(46) (2008), 11808–11816.

- [47] Takeshi Nagata, Dmitri G Fedorov, and Kazuo Kitaura. Importance of the hybrid orbital operator derivative term for the energy gradient in the fragment molecular orbital method. *Chemical Physics Letters* **492**(4-6) (2010), 302–308.
- [48] Kaori Fukuzawa, Chiduru Watanabe, Ikuo Kurisaki, Naoki Taguchi, Yuji Mochizuki, Tatsuya Nakano, Shigenori Tanaka, and Yuto Komeiji. Accuracy of the fragment molecular orbital (FMO) calculations for DNA: total energy, molecular orbital, and inter-fragment interaction energy. *Computational and Theoretical Chemistry* **1034** (2014), 7–16.
- [49] Kaori Fukuzawa, Yuji Mochizuki, Shigenori Tanaka, Kazuo Kitaura, and Tatsuya Nakano. Molecular interactions between estrogen receptor and its ligand studied by the ab initio fragment molecular orbital method. *The Journal of Physical Chemistry B* **110**(32) (2006), 16102–16110.
- [50] Kaori Fukuzawa, Yuto Komeiji, Yuji Mochizuki, Akifumi Kato, Tatsuya Nakano, and Shigenori Tanaka. Intra-and intermolecular interactions between cyclic-AMP receptor protein and DNA: Ab initio fragment molecular orbital study. *Journal of Computational Chemistry* **27**(8) (2006), 948–960.
- [51] Jiří Šponer, Jerzy Leszczynski, and Pavel Hobza. Hydrogen bonding and stacking of DNA bases: a review of quantum-chemical ab initio studies. *Journal of Biomolecular Structure and Dynamics* **14**(1) (1996), 117–135.
- [52] Trygve Helgaker, Poul Jorgensen, and Jeppe Olsen. *Molecular electronic-structure theory*. 2014.
- [53] Dmitri G Fedorov, Kazuo Kitaura, Hui Li, Jan H Jensen, and Mark S Gordon. The polarizable continuum model (PCM) interfaced with the fragment molecular orbital method (FMO). *Journal of Computational Chemistry* **27**(8) (2006), 976–985.
- [54] Yu Takano and KN Houk. Benchmarking the conductor-like polarizable continuum model (CPCM) for aqueous solvation free energies of neutral and ionic organic molecules. *Journal of Chemical Theory and Computation* **1**(1) (2005), 70–77.
- [55] Aleksandr V Marenich, Christopher J Cramer, and Donald G Truhlar. Universal solvation model based on solute electron density and on a continuum model of the solvent

- defined by the bulk dielectric constant and atomic surface tensions. *The Journal of Physical Chemistry B* **113**(18) (2009), 6378–6396.
- [56] Stefan Grimme. Semiempirical hybrid density functional with perturbative second-order correlation. *The Journal of Chemical Physics* **124**(3) (2006), 034108.
- [57] Stefan Grimme. Accurate description of van der Waals complexes by density functional theory including empirical corrections. *Journal of Computational Chemistry* **25**(12) (2004), 1463–1473.
- [58] Michael W Schmidt, Kim K Baldridge, Jerry A Boatz, Steven T Elbert, Mark S Gordon, Jan H Jensen, Shiro Koseki, Nikita Matsunaga, Kiet A Nguyen, Shujun Su, et al. General atomic and molecular electronic structure system. *Journal of Computational Chemistry* **14**(11) (1993), 1347–1363.
- [59] Jens Antony and Stefan Grimme. Is Spin-Component Scaled Second-Order Møller-Plesset Perturbation Theory an Appropriate Method for the Study of Noncovalent Interactions in Molecules? *The Journal of Physical Chemistry A* **111**(22) (2007), 4862–4868.
- [60] Petr Jurečka, Jiří Šponer, Jiří Černý, and Pavel Hobza. Benchmark database of accurate (MP2 and CCSD (T) complete basis set limit) interaction energies of small model complexes, DNA base pairs, and amino acid pairs. *Physical Chemistry Chemical Physics* **8**(17) (2006), 1985–1993.
- [61] Jan Rezáč, Kevin E Riley, and Pavel Hobza. S66: A well-balanced database of benchmark interaction energies relevant to biomolecular structures. *Journal of Chemical Theory and Computation* **7**(8) (2011), 2427–2438.
- [62] Jason Rigby and Ekaterina I Izgorodina. New SCS- and SOS-MP2 coefficients fitted to semi-coulombic systems. *Journal of Chemical Theory and Computation* **10**(8) (2014), 3111–3122.
- [63] David E Woon and Thom H Dunning Jr. Gaussian basis sets for use in correlated molecular calculations. IV. Calculation of static electrical response properties. *The Journal of Chemical Physics* **100**(4) (1994), 2975–2988.

- [64] Kaycee Low, Luke Wylie, David LA Scarborough, and Ekaterina I Izgorodina. Is it possible to control kinetic rates of radical polymerisation in ionic liquids? *Chemical Communications* **54**(80) (2018), 11226–11243.
- [65] John P Perdew, Kieron Burke, and Matthias Ernzerhof. Generalized gradient approximation made simple. *Physical Review Letters* **77**(18) (1996), 3865.
- [66] Stefan Grimme, Stephan Ehrlich, and Lars Goerigk. Effect of the damping function in dispersion corrected density functional theory. *Journal of Computational Chemistry* **32**(7) (2011), 1456–1465.
- [67] Matthias Ernzerhof and Gustavo E Scuseria. Assessment of the Perdew–Burke–Ernzerhof exchange–correlation functional. *The Journal of Chemical Physics* **110**(11) (1999), 5029–5036.
- [68] Jonas Moellmann and Stefan Grimme. DFT-D3 study of some molecular crystals. *The Journal of Physical Chemistry C* **118**(14) (2014), 7615–7621.
- [69] Minsun Hong, Mayuree Fuangthong, John D Helmann, and Richard G Brennan. Structure of an OhrR-ohrA operator complex reveals the DNA binding mechanism of the MarR family. *Molecular Cell* **20**(1) (2005), 131–141.
- [70] Stephen P Edmondson and W. Curtis Johnson. Base tilt of DNA in various conformations from flow linear dichroism. *Biochemistry* **24**(18) (1985), 4802–4806.
- [71] Bayden R Wood. The importance of hydration and DNA conformation in interpreting infrared spectra of cells and tissues. *Chemical Society Reviews* **45**(7) (2016), 1980–1998.
- [72] Eric Girard, Thierry Prange, Anne-Claire Dhaussy, Evelyne Migianu-Griffoni, Marc Lecouvey, Jean-Claude Chervin, Mohamed Mezouar, Richard Kahn, and Roger Fourme. Adaptation of the base-paired double-helix molecular architecture to extreme pressure. *Nucleic Acids Research* **35**(14) (2007), 4800–4808.

Chapter 5

Interactions between Pt-complexes and DNA/RNA building blocks

5.1 Introduction

Cisplatin, an accidental discovery by Rosenberg in 1965, has become one of the most commonly administered anti-cancer drugs.¹⁻³ Whilst conducting electrolysis studies to investigate bacterial growth, he discovered that the platinum product disrupted the process of cell division.¹ This led to an investigation of Pt complexes and their effects on tumours, especially sarcoma 180 and mouse leukaemia L1210.¹ With a sample size of 10 mice, Rosenberg successfully demonstrated that Pt complexes, such as *cis*-Pt(II)(NH₃)₂Cl₂, are able to treat tumour growth.² It was also reported that some mice remained tumour free for the following 6 months after the initial treatment.² This remarkable discovery has led to Pt complexes becoming major candidates for anti-cancer drugs. Cisplatin (Figure: 5.1) undergoes hydration as it passes into the cell cytoplasm, where either one or both Cl⁻ gets replaced with water molecules, forming either the mono- or di-aquated complexes (see Figure: 5.1).⁴ These aquated complexes inhibit DNA to form either mono- or di-functional adducts, preferentially intrastrand at 1,2-d(GpG) or 1,2-d(GpA) position at 65% and 25%, respectively.⁴ Upon inhibition, the adducts cause a localised unwinding of the helix, leading to an increase in the width of the minor groove.⁴⁻⁶ The first crystal structure of cisplatin-DNA interaction was discovered by Lippard *et al.* in

1995.⁷ $cis-[Pt(NH_3)_2]^{2+}$ was found to form intrastrand adducts between two neighbouring guanine moieties.⁷ This disruption to the structural integrity of DNA effectively interrupts the cell replication process and programs the cell death.^{5,6}

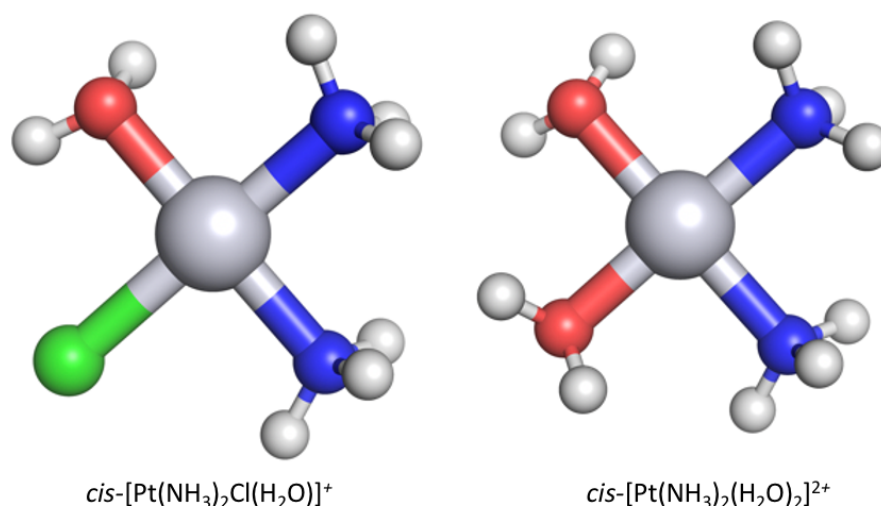


Figure 5.1: Mono- and di-aquated complexes of cisplatin.⁴

Due to the toxicity and side effects of cisplatin, other Pt-based complexes were studied. Oxaliplatin is one of these complexes (see Fig 5.2). Pt complexes are found to have similar cytotoxicity as cisplatin without the same limitations.^{3,8,9} For example, despite forming fewer cross linkages, oxaliplatin exhibits similar cytotoxicity when compared to cisplatin.^{3,8,9} Lipard *et al.* published a crystal structure of oxaliplatin interacting with DNA, forming a similar 1,2-d(GpG) adduct as cisplatin.¹⁰ Solved at 2.4 Å resolution, a bend of 30° of the DNA helix towards the major groove was induced after the binding of oxaliplatin.¹⁰ The activated oxaliplatin, as identified in the crystal structure, loses its oxalate group and while retaining the (1R,2R)-diaminocyclohexane.¹⁰ This is in agreement with the study conducted in Chapter 3 where it was determined that it is energetically favourable for the oxalate to play the role of a leaving group. The Pt metal centre in the activated oxaliplatin, similar to that of cisplatin, binds to the N7 of two neighbouring guanine moieties.¹⁰ Hydrogen bonding between the NH₂ group of the (1R,2R)-diaminocyclohexane and the O6 on guanine is absent in cisplatin-DNA binding (Figure: 5.3).¹⁰ The difference in binding could explain the different in specificity

between the two Pt complexes towards treating different types of cancer. Where cisplatin is usually administered for testicular and ovarian cancer, the combination of oxaliplatin and 5-fluorouracil is effective against colon cancer.^{9,11–15} These findings motivated this study to identify how the interaction between DNA and cisplatin/oxaliplatin occurs, and specifically whether the presence of water molecules coordinated to the Pt centre, affects the geometry of deoxyribonucleic acid (DNA) building blocks.

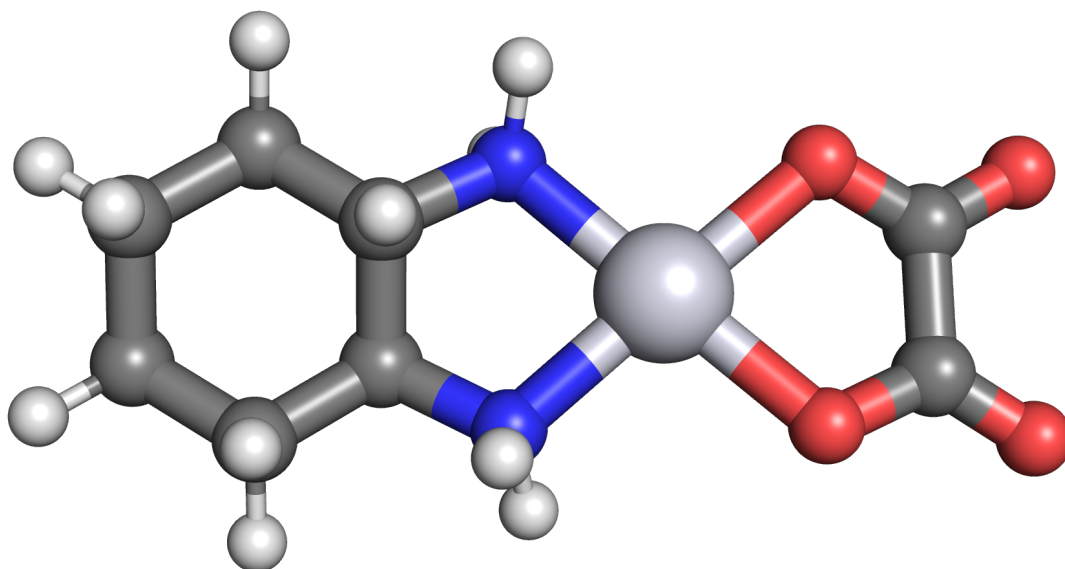


Figure 5.2: *Oxaliplatin, oxalato-(1,2-cyclohexanediamine)Pt(II), a Pt-based anti-cancer drug with oxalate as the leaving group.*^{3,8,9}

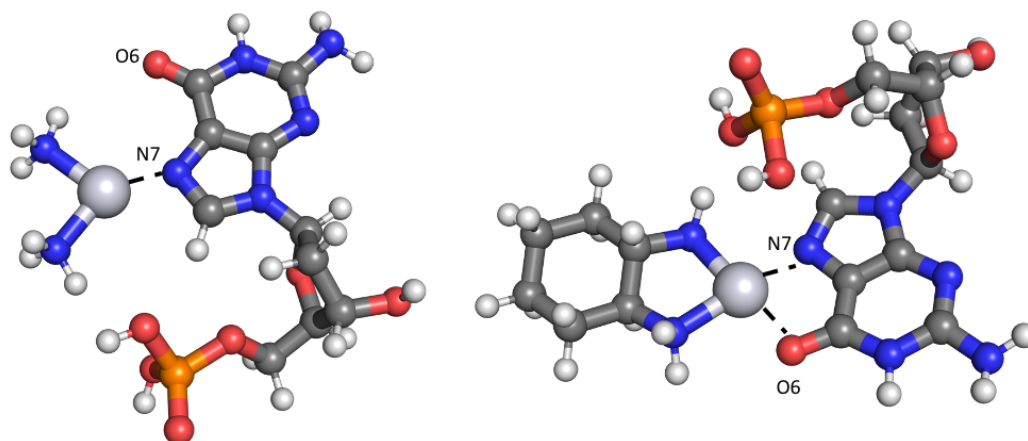


Figure 5.3: *Binding mode of fully dissociated cisplatin (left) and oxaliplatin (right) to dGMP.*

Despite extensive studies conducted on Pt-based anti-cancer drugs and DNA, there is still uncertainty about the influence of Pt drugs on ribonucleic acid (RNA).^{7,16–22} RNA is involved in the regulation and expression of genes and has become an important drug target in recent years.^{23–30} Compared to DNA, RNA is able to possess different biological functions such as translating genetic information from DNA to proteins and is a very robust molecule.^{28–31} Messenger RNA (mRNA) is involved in transmitting genetic information from DNA to the ribosome in the form of transfer RNA (tRNA).^{32–34} tRNA has an anticodon on one terminal end and an amino acid on the other that binds to the codon, a sequence of three nucleotides, on mRNA.^{32–34} The ribosomal RNA (rRNA) then acts as a catalyst that links the amino acids together to form the protein in the specific sequence dictated by mRNA.³² The biological functions of RNA makes them very attractive for small molecule targeting to modulate and regulate protein production.^{35–39}

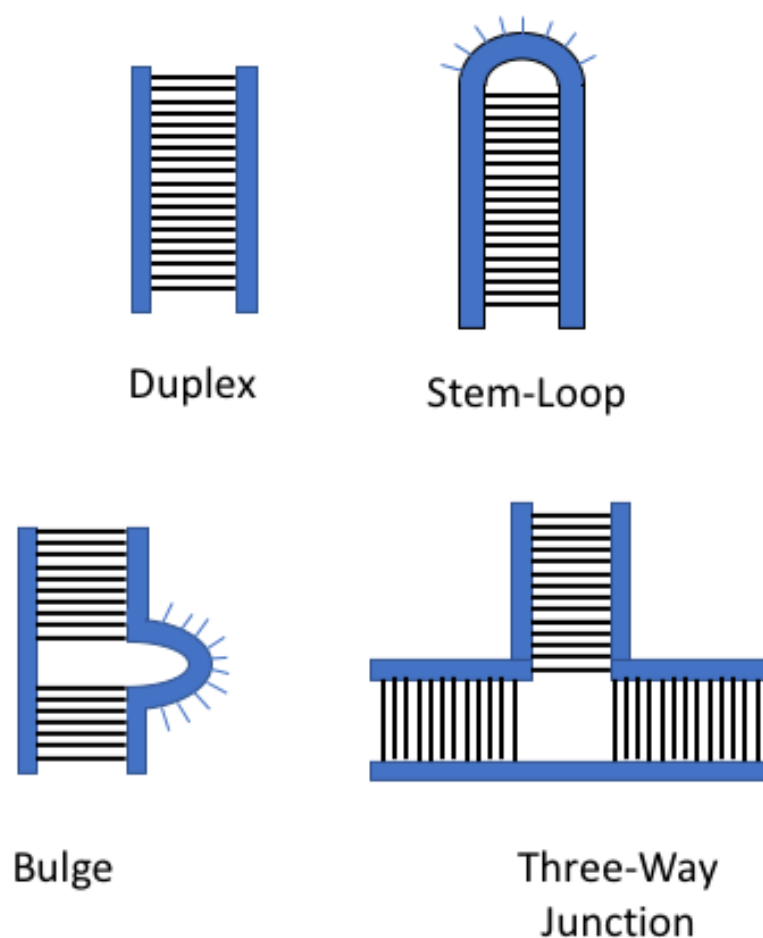


Figure 5.4: *Different RNA conformations formed with Watson.*

Despite RNA being similar to DNA, consisting of a ribose unit connected to a phosphate group and a nucleobase (one of the four - guanine (G), adenine (A), cytosine (C) and uracil (U)), there are plenty of unknowns regarding using them as drug targets.³¹ The binding pocket of RNA arises from the intrastrand folding, governed by intermolecular interactions between the nucleobases.^{30,40} As the primary structure of RNA determines its secondary structure, different functioning RNA will result in different secondary structures, such as the stem-loop and bulge conformations, and this allows for specific binding of small molecules (Figure: 5.4).³⁰ The imperfect base pair interactions within RNA occur due to the mismatch in nucleobases outside the conventional Watson-Crick hydrogen bonding types and result in the formation of binding pockets for proteins or small molecules.³⁵⁻³⁷ Imperfect base pairs, often caused by

the formation of Hoogsteen base pairs instead of Watson-Crick base pairs, result in perturbed base pairing of RNA, thus resulting in a larger solvent-exposed major groove and allowing for binding events to occur.^{31,35–37,41} The differences between Hoogsteen and Watson-Crick base pairs are their conformations, where Hoogsteen base pairs exist in the *syn* conformation, whereas Watson-Crick base pairs exist in *anti* conformation.^{41,42} The four basic secondary structures that RNA can adopt are duplexes, loops, bulges and junctions (Figure: 5.4).^{30,31,36,37,40} It was also reported that the A-form of RNA, the helical conformation, is more likely to result in a mismatch of base pairs, giving rise to the binding pockets.^{31,35} Upon binding, small molecules are able to alter the biological functions of RNA.^{35–37} For example, oligonucleotides bind to RNA and interfere with the function of RNA by either inhibiting the translation mechanism translation or degrading it.^{36,43}

Though the interest in better understanding of RNA as a drug target is rapidly gaining momentum, there are some roadblocks on the way.^{35–37} Due to the flexibility of RNA, attributed to the presence of an additional hydroxyl group on the ribose, it is able to exist in multiple low energy conformations as a single stranded molecule.^{31,36,44} Consequently there is a need to be able to design small molecules with high affinity and high specificity for the RNA targets. In particular, the understanding of how the binding to RNA can be manipulated, is needed.^{35,36,38} For RNA to be a drug target, it is first vital to understand the biological effects of binding to different regions of the molecule.³⁸ Not surprisingly, electrostatics and dispersion interactions are both important to increase affinity for RNA binding sites.³⁸ In a study conducted using aminoglycosides, including Neomycin B, butirosin B and ribostamycin, it was discovered that a number of amines significantly influenced the binding affinity of small molecules to RNA.^{35,45,46}

Cisplatin has demonstrated its ability to affect RNA, both directly and indirectly. The human upstream binding factor (UBF) is an essential component in the expression of rRNA.⁴⁷ However, UBF has been reported to bind preferentially to the intrastrand adduct formed when cisplatin binds to DNA, resulting in the suppression of rRNA synthesis.^{47,48} In addition, cisplatin also results in the redistribution of proteins, such as UBF and RNA polymerase I, in the nucleolus. While RNA polymerase I is redistributed to the fringe of the nucleolus, the activity of RNA polymerase II remains unaffected, indicating that the suppression of rRNA synthesis could

contribute to the cytotoxicity of cisplatin.⁴⁷ Furthermore, it has been reported that a decrease in rRNA expression leads to the activation of the Myb-binding protein 1A (MYBBP1A), a protein that increases p53 (tumour growth suppression protein) acetylation.^{49–52} The increased levels of p53 acetylation then results in apoptosis.⁴⁹

Cisplatin has been reported to form adducts with RNA.²⁸ Although the extent of cisplatin interaction with different types of RNA, like mRNA or tRNA, is not yet known, cisplatin has been shown to form a strong interaction with RNA.²⁸ With the use of inductively coupled plasma mass spectrometry (ICP-MS), DeRose *et al.* determined that cisplatin interacted with DNA and RNA in the ratio of 3:1 in cells.²⁸ Interestingly, *in vitro* studies showed that cisplatin bound preferentially to RNA over DNA in human cervical adenocarcinoma HeLa cells.^{26,53,54} It was also reported that the positively charge activated form of cisplatin interacted more rapidly with hairpin RNA than DNA.^{53,55} Binding to RNA could result in the disruption of RNA functions and contribute to the cytotoxicity of Pt-based drugs.⁵³ DeRose *et al.* also reported the ability of cisplatin to form intrastrand adducts with the internal branch-bulge domain (BBD), a conformation formed with the combination of a hairpin loop and a bulge caused by mismatched base pairs, thus inhibiting its biological activity.⁵⁵

Crystal structures of cisplatin binding to *Thermus thermophilus*, a Gram negative bacterium, were solved at 2.6 Å resolution by Polikanov *et al.*⁵⁶ Cisplatin was crystallized with *Thermus thermophilus* 70S ribosome containing mRNA and tRNA. Nine cisplatin-derived complexes were found to coordinate to the ribosome by studying the difference in the electron density map.⁵⁶ Cisplatin was identified to bind to adenine three times and guanine five times out of the nine possibilities identified.⁵⁶ Similarities were found among the binding sites that were targeted by cisplatin.⁵⁶ For the guanine binding sites, cisplatin also formed hydrogen bonds with the phosphate backbone through its NH₃ group.⁵⁶ On the other hand, guanine needed to be next in the RNA sequence for cisplatin to bind to adenine.⁵⁶ It was noted that cisplatin still bound to the N7 of adenine and formed hydrogen bonds with the O6 atom of the neighbouring guanine through the NH₃ group.⁵⁶ The binding of the active form of cisplatin to adenine also altered the RNA geometry by bringing the guanine moiety closer to adenine, thus resulting in a more compact structure.⁵⁶

Quantum chemical methods, such as those of density functional theory (DFT), have proven to be a reliable tool to study biomolecules and DNA in particular.^{57–61} Leszczynski *et al.* applied B3LYP, a DFT functional that incorporates Becke's 3 parameter exchange-correlation functional (B3) and Lee-Yang-Parr's correlation functional (LYP), to study the interactions between Pt-based complexes and DNA nucleobases.⁶¹ The interaction between species produced during the hydrolysis of Pt complexes such as $[\text{Pt}(\text{NH}_3)_4]^{2+}$, $[\text{Pt}(\text{NH}_3)_3(\text{H}_2\text{O})]^{2+}$ and *cis*- $[\text{Pt}(\text{NH}_3)_2(\text{H}_2\text{O})_2]^{2+}$ and a nucleobase (either guanine and adenine) was modelled.⁶¹ The Pt-complexes were modelled to bind to one or two bases, thus forming a link between these.⁶¹ Electronic energies of the optimised structures were improved with MP2.^{62,63} Analysis of the bond dissociation energies (BDE) and stabilisation energies revealed that the complexes are generally more stable when bonded to two guanine units instead of two adenine units, with the average BDE of the Pt-guanine bond being calculated to be 62.8 kJ mol^{-1} higher than that of the Pt-adenine bond.⁶¹ This supports the observation that Pt-complexes are more likely to bind between two neighbouring guanine (G) moieties than two neighbouring adenine (A) moieties.^{4,5,64} Czyżnikowska-Balcerak *et al.* utilised MP2 to study the effects of guanine π - π stacking with other DNA bases.⁵⁸ Seven different stacking models were constructed with different combinations of bases such as GG, GA, GT and GC.⁵⁸ The effects of electronic correlation, solvation effects and thermodynamic effects were explored.⁵⁸ The highest occupied molecular orbital (HOMO) and lowest unoccupied molecular orbital (LUMO) between the different bases were used to discuss the donor-acceptor characteristics contributing to π - π stacking.⁵⁸ Geometry optimisations were performed with the MP2/6-31G(d) level of theory with the initial geometries generated using the 3DNA software.⁵⁸ They discovered that π - π stacking interactions between pyrimidine rings were crucial for stabilisation of the GA stacking, with the HOMO being localised on G and LUMO localised on A.⁵⁸ It was also noted that the π - π stacking nature played a role in stabilising the structure. For example, the GA stacking was found to be by 8.4 kJ mol^{-1} more stable than the AG stacking.⁵⁸ In general, the stacking stability decreased in the following order: $\text{GC} > \text{GA} > \text{AG} > \text{CG} > \text{TG/GT}$ (C and T representing cytosine and thymine, respectively) $> \text{GG}$, with stacking pair energies ranging from -46.7 to $-20.9 \text{ kJ mol}^{-1}$.⁵⁸

Shoeib *et al.* also used DFT to investigate the interaction between Pt complexes and biomolecules such as 4-sulfocalix[4]arene.^{65,66} It was previously reported that the interactions between biomolecules, such as 4-sulfocalix[4]arene, and Pt-based anti-cancer drugs could alter their properties.⁶⁵ Shoeib *et al.* demonstrated that the binding of nedaplatin to 4-sulfocalix[4]arene is more stable through the formation of hydrogen bonds between the NH_3 of nedaplatin and the O present on 4-sulfocalix[4]arene.⁶⁵ Shoeib also investigated the interactions between cisplatin and carnosine, a dipeptide that has been detected in multiple organs, like stomach and brain, and has been shown to interact with Pt complexes, hindering their ability to bind to DNA.^{12,66} With 5 possible sites for interaction, such as the carboxylic group and the imidazole ring, carnosine is able to interact with oxaliplatin, inhibiting its ability to bind to DNA and, hence, decreasing its potency.⁶⁶ The binding modes of the three tautomers of carnosine have since been the subject of interest with various different metal ions, such as Zn^{2+} , Co^{2+} and Ru^{2+} .⁶⁶⁻⁶⁸ Shoeib *et al.* used B3LYP, LanL2DZ basis set and gas phase to identify the lowest energy conformations of carnosine and fully dissociated oxaliplatin.⁶⁶ Binding energies were also analysed in both gas phase and with the polarizable continuum solvation model.⁶⁶ The study once again emphasizes the inability of gas phase to predict non-covalently bound complexes by overestimating the Pt-O bond length by 1.3 Å when compared to typical Pt-O bond lengths of 2.0 Å in nanoparticles.⁶⁶ Binding energies of carnosine and the fully dissociated form of oxaliplatin were calculated to be -1668.6 and -372.8 kJ mol⁻¹ obtained in gas phase and PCM, respectively.⁶⁶ However, Shoeib *et al.* did not consider the possibility of the aquated species of oxaliplatin.

Platts *et al.* utilised the QM/MM approach to investigate the effect that hydrogen bonding and π - π stacking in single and double-stranded DNA have on cisplatin-DNA interactions.⁶⁹ Using DNA models consisting of di- and trinucleobases in length, Platts *et al.* investigated their interactions with either *cis*-[Pt(NH₃)₂]²⁺ or *cis*-[Pt(NH₃)₂Cl]⁺ by treating the nucleobase and cisplatin species using quantum chemical methods (BH&H functional, 6-311++G(d,p) basis set and SDD, a basis set that applies Stuttgart/Dresden effective core potentials (ECPs) for the Pt), while treating the sugar and phosphate backbone of DNA with molecular mechanics (MM) (the Amber force field).^{69,70} The optimised geometry of *cis*-[Pt(NH₃)₂]²⁺ bound to d(pGpG) were in agreement with experimental data, with an average deviation of 0.05 Å in bond length

and 2° in bond angles.⁶⁹ Comparison of calculated binding energies of cisplatin to form bifunctional adducts with d(GpG) and d(GpA) showed the energetic preference of binding to two neighbouring guanines over a guanine and adenine by approximately $113.8 \text{ kJ mol}^{-1}$, with a binding energy of $-1307.2 \text{ kJ mol}^{-1}$ for d(GpG) and $-1193.4 \text{ kJ mol}^{-1}$ for d(GpA).^{69,71} Platts *et al.* also made use of the atoms-in-molecules (AIM) approach to study the effects platination has on the H-bonding and π - π stacking interactions of the DNA model.⁶⁹ Hydrogen bonding was found to dominate over π - π stacking to stabilise the d(GpG) model, contributing 88.5 kJ mol^{-1} to the binding energy of *cis*-[Pt(NH₃)₂{dGpG}]²⁺.⁶⁹ The platination of *cis*-[Pt(NH₃)₂]²⁺ disrupts the geometry of d(GpG) by rotating the purine bases towards each other, disrupting the π - π stacking and destabilising the structure.⁶⁹

Schofield *et al.* also utilised the QM/MM to study the effect of Pt complexes, specifically cisplatin and oxaliplatin, binding to DNA.⁸ With 5'-d(CCTCAGGCCTCC)-3' as a DNA model, the extent of deformation due to cisplatin and oxaliplatin was analysed through a series of parameters: torsional angles, binding affinities, hydrogen bonding between the Pt complex and the DNA model.⁸ 20 ns simulations were ran for both cisplatin and oxaliplatin interacting with DNA. Simulations were conducted with the AMBER parm99SB force field including the TIP3P water model with a radius of 10 Å. Na⁺ ions were included as counterions.⁸ B3LYP/6-31G** and the LanL2DZ effective core potential on Pt were used to perform the partial charge analysis of the system.⁸ QM/MM calculations were performed using the ONIOM approach, with the BH&H functional, the 6-31G basis set and the LanL2DZ effective core potential on Pt for the higher layer and AMBER parm99SB force field for the lower layer.⁸ Binding energies were calculated by employing either the MM/generalized born surface area (MMGBSA) or MM/Poisson-Boltzman surface area (MMPBSA) approach.⁸ The binding energies reported with the use of MMGBSA for cisplatin and oxaliplatin were -65.1 and $-134.8 \text{ kJ mol}^{-1}$, respectively, whereas MMPBSA reported binding energies of -137.5 and $-252.8 \text{ kJ mol}^{-1}$, respectively.⁸ Both approaches suggested preferential binding of oxaliplatin to DNA over cisplatin.⁸ The binding of the Pt complex was found to significantly distort the DNA backbone.⁸ In addition, cisplatin and oxaliplatin produced different bends in the helix axis, 56.1° and 46.8° , respectively.⁸ Both resultant angles were much wider than the previously reported value of 34.3° of an undistorted DNA model.⁷²

Despite the growing interest in RNA as a potential drug target, fewer computational studies have been conducted to investigate the binding mechanism of small molecule to RNA. This study aims to investigate the difference in binding energies between Pt-based anti-cancer drugs and building blocks of RNA and DNA. Lower energy conformations of guanosine monophosphate (GMP), adenosine monophosphate (AMP), deoxyguanosine monophosphate (dGMP) and deoxyadenosine monophosphate (dAMP) were considered for binding with cisplatin and oxaliplatin. Three types of their proposed activated forms were studied: the activated form of the drug of the $[\text{PtL}]^{2+}$ type (further referred to as the non-aquated form), the mono-aquated form of the $[\text{PtL}(\text{H}_2\text{O})]^{2+}$ type and the di-aquated form of the $[\text{PtL}(\text{H}_2\text{O})_2]^{2+}$ type (where $\text{L} = (\text{NH}_3)_2$ for cisplatin and $(\text{CH}_2)_4(\text{CHNH}_2)_2$ for oxaliplatin). Geometry optimisations were performed with the M06-L functional in combination with the cc-pVDZ (VDZ) basis set on the non-Pt atoms and cc-pVTZ-pp (VTZ-pp) with a corresponding effective core potential (ECP) on the Pt atom. A universal solvation model, SMD, was applied with water as solvent. Interaction energies between the three types of activated forms and DNA/RNA building blocks were calculated with SRS-MP2 in combination with cc-pVTZ for non-Pt atoms and cc-pVTZ-pp (VTZ-pp) with a corresponding ECP on the Pt atom in gas phase. For comparison, $\omega\text{B97X-D3}$ in combination with aug-cc-pVTZ (aVTZ) basis set on non-Pt atoms and aug-cc-pVTZ-pp (aVTZ-pp) with a corresponding ECP on the Pt atom also in gas phase. Deformation energies of the RNA and DNA building blocks upon geometry optimisations were calculated to investigate the extent of structural disruption. The extent of aquation on the binding mode and bond strength was analysed.

5.2 Theoretical Procedures

All calculations were performed using of the three quantum chemical packages: Gaussian16,⁷³ the General Atomic and Molecular Electronic Structure Systems (GAMESS-US)⁷⁴ software and Orca version 4.0.1.⁷⁵ The activated forms of cisplatin and oxaliplatin (Figure: 5.5) were optimised with Gaussian 16 and in combination with the M06-L functional,⁷⁶ the cc-pVDZ (VDZ) basis set⁷⁷ on non-Pt atoms and the cc-pVTZ-pp (VTZ-pp) basis set with a corresponding effective core potential (ECP) on the Pt atom.^{78,79} The ECP decreases the computational cost of the heavy Pt metal by modelling the inner-core electrons and only calculates the outer

electron shell explicitly.^{80,81} Including both the one- and two-component potentials, the ECP is able to describe the Pauli repulsion, spin-orbital interactions and relativistic effects.^{80,81} A conductor-like polarisable continuum (CPCM) solvation model⁷⁷ with water as solvent was added to mimic the aqueous environment. This level of theory was chosen as in a previously conducted study it was demonstrated to be able to describe the ionic nature of the Pt-O bonds in Pt-based complexes such as carboplatin.⁸² The building blocks of RNA and DNA (Figure: 5.6) were initially optimised in GAMESS-US in combination with SRS-MP2, the VDZ basis set and the SMD solvation model with water as solvent.⁸³ This level of theory has been shown to replicate experimental geometries (for more detail see Chapter 4).

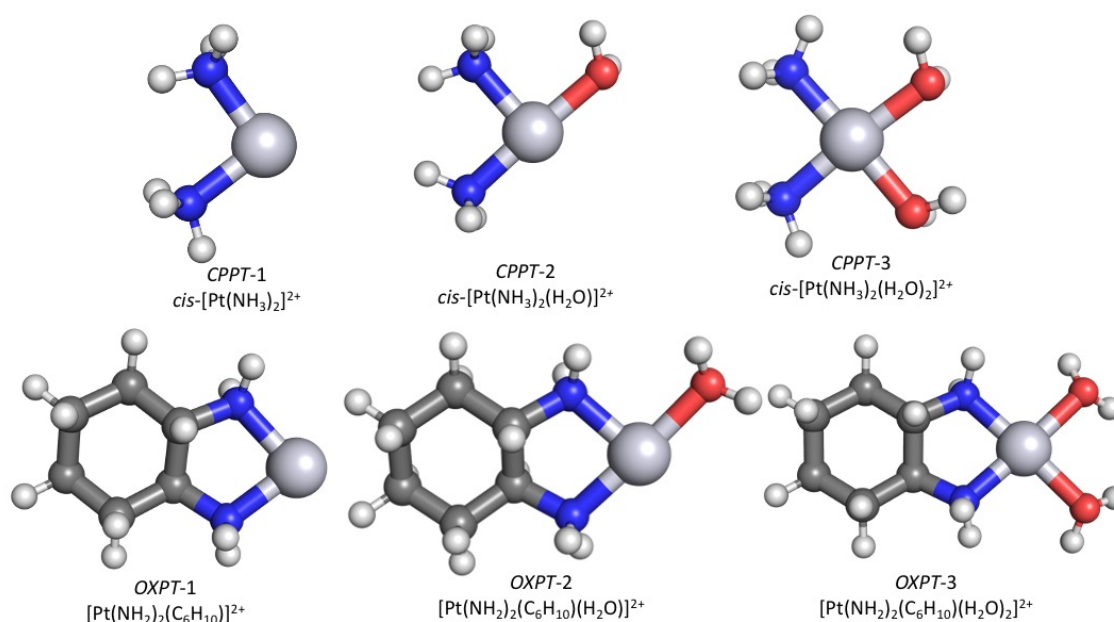


Figure 5.5: Activated forms of Pt drugs considered in the study.

The starting geometries of deoxyguanosine monophosphate (dGMP), deoxyadenosine monophosphate (dAMP), guanosine monophosphate (GMP) and adenosine monophosphate (AMP) were obtained from previously published crystal structures (Figure: 5.6).^{84,85} dGMP and dAMP were obtained from 1Z9C crystal structure, GMP and AMP were obtained from 4C2M crystal structure.^{84,85} The various different building blocks then underwent geometry optimisation before the Pt-building block complexes were constructed.

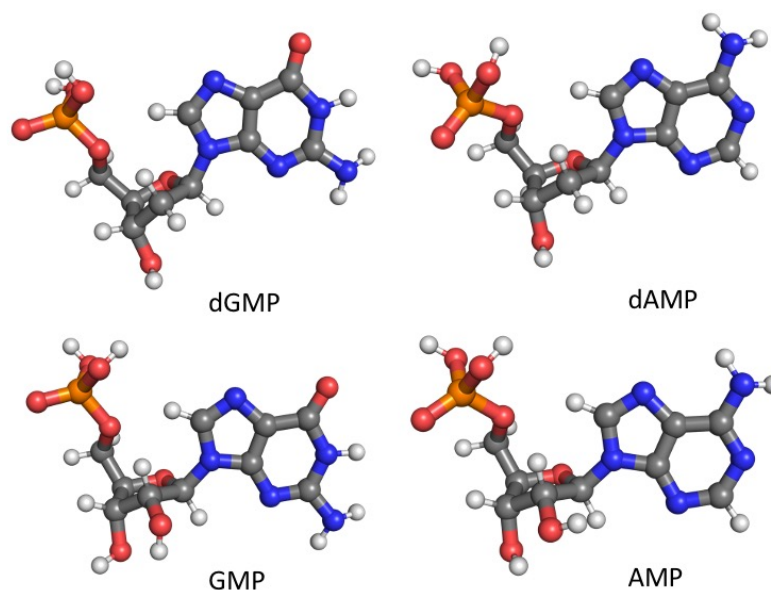


Figure 5.6: DNA and RNA building blocks

Subsequently, DNA-Pt complexes were constructed by placing the Pt centre approximately 2.0 Å away from the N7 atom on guanine of the building block. Three types of activated forms of the Pt complexes were investigated for both cisplatin and oxaliplatin: the non- ($[\text{PtL}]^{2+}$), mono- ($[\text{PtL}(\text{H}_2\text{O})]^{2+}$) and di-aquated ($[\text{PtL}(\text{H}_2\text{O})_2]^{2+}$) forms of each Pt complex (where $\text{L} = (\text{NH}_3)_2$ for cisplatin and $(\text{CH}_2)_4(\text{CHNH}_2)_2$ for oxaliplatin). The non-, mono- and di-aquated equivalent of cisplatin are labelled as *CPPT-1*, *CPPT-2* and *CPPT-3*, respectively. Similarly, the non-, mono- and di-aquated equivalent of oxaliplatin are labelled as *OXPT-1*, *OXPT-2* and *OXPT-3*, respectively. 8 different combinations of aquation modes and configurations were considered for cisplatin and oxaliplatin, respectively (Figure: 5.8). The configurations were constructed to promote the formation of the Pt-N7 bond, which has been reported to be 1.992 Å for guanine and 2.010 Å for adenine.^{61,86} In this chapter, the different configurations of each aquation mode were also investigated and labelled as Conf1, Conf2 and Conf3 representing three different starting binding modes (Figure: 5.8). These starting geometries were optimised in Orca with SRS-MP2, the VDZ basis set for non-Pt atoms, VTZ-pp ECP for the Pt atom and the SMD solvation model. Single point energy calculations were then performed with SRS-MP2, the VTZ basis set for non-Pt atoms and VTZ-pp ECP for Pt atoms in gas phase to obtain more accurate energies. Interaction energies were also calculated using $\omega\text{B97X-D3}$ for a comparison.

In a previously conducted benchmarking study, the combination of ω B97X-D and the aVTZ basis set, with aVTZ-pp ECP on Pt, was determined to predict the dissociation energies of two cationic (diimine) Pt^{2+} complexes with different ligands.⁸⁷ In chapter 3, a benchmarking study was conducted on two dissociation reactions containing the Pt^{2+} metal ion from the WCCR10 benchmark set (Figure: 5.7). The combination of ω B97X-D, aVTZ basis set, aVTZ-pp ECP on Pt was able to perform consistently for both dissociation reactions, giving rise to an average underestimation of 18 kJ mol^{-1} when compared to previously published experimental results.⁸⁷

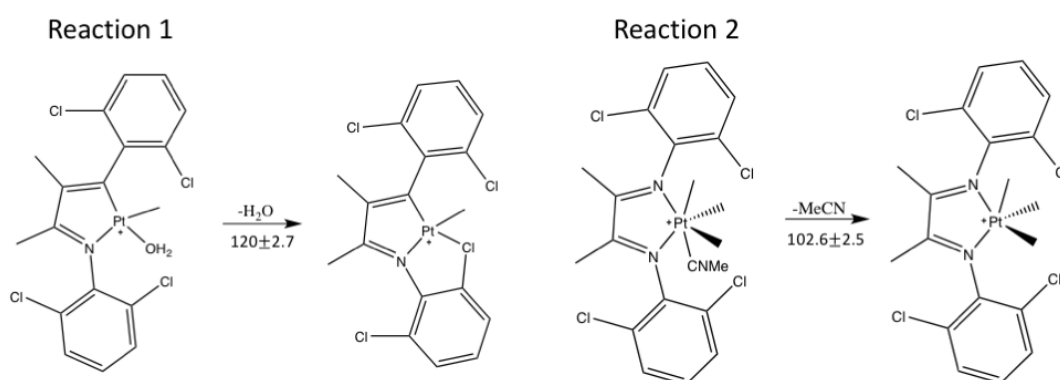


Figure 5.7: Dissociation reactions used for benchmarking purposes. The numbers represents previously published experimental values in kJ mol^{-1} .

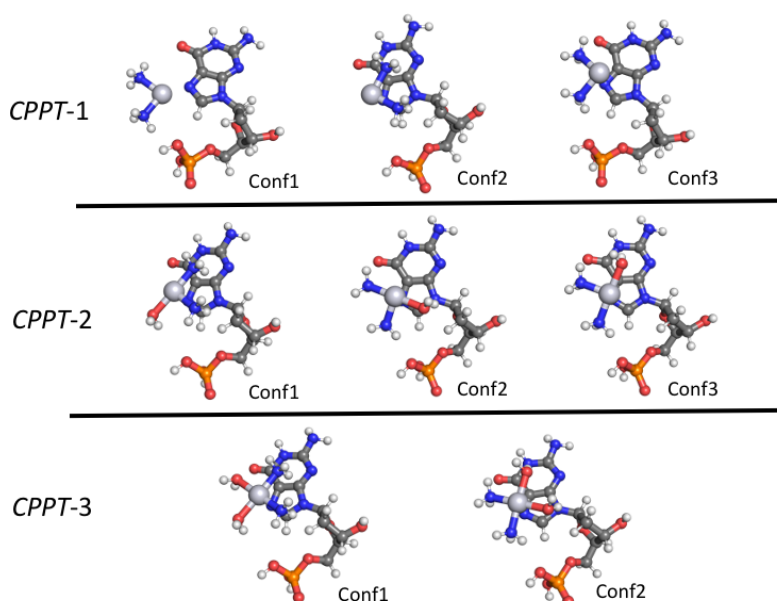


Figure 5.8: Starting geometries of cisplatin in its various aquated state with dGMP.

SRS-MP2, the spin-ratio scaled MP2 method, uses the ratio of the opposite-spin (OS) and same-spin (SS) component of the correlation energy, $\epsilon_{\Delta s} = \frac{E_{INT}^{OS}}{E_{INT}^{SS}}$.^{88,89} This allowed the interaction energy components, the same-spin (SS) and opposite-spin (OS), separately to give $E_{INT}^{corr} = c_{OS}E_{INT}^{OS} + c_{SS}E_{INT}^{SS}$, where c_{OS} and c_{SS} are the respective scaling factors.⁸⁹ It was also determined that different scaling factors are optimal for different Dunning basis sets, for example, for a system dominated by electrostatics and the $\epsilon_{\Delta s} < 1$, c_{OS} should be 1.752 or 1.640 when VDZ or VTZ basis sets were employed.⁸⁹ Upon splitting and scaling the two spin components, SRS-MP2 is able to reproduce non-covalent interactions within 4 kJ mol⁻¹ of the CCSD(T)/CBS gold standard data.⁸⁹ In addition, SRS-MP2 is able to accurately predict correlation energy without the need to correct for basis set superposition error (BSSE) and has been demonstrated to be the superior method to calculate correlation energy over DFT functionals and the original MP2 method.^{88,89}

ω B97X-D is a hybrid DFT functional based on the B97 functional has been modified to include 100% long-range and 22% short-range exact exchange.^{90,91} This functional was tested on several databases, such as G3/05 and S22, and its performance was compared with other DFT-D (B97-D, B3LYP-D and BLYP-D) and long-range corrected functionals (ω B97X and ω B97).^{90,91} ω B97X-D was demonstrated to be optimal method to study non-covalent interaction energies and reaction energies, giving rise to a mean average error of 1.93 kJ mol⁻¹.^{90,91} Due to the availability of the functional in Orca, ω B97X-D3, with Grimme's D3 dispersion correction was used in this study. While ω B97X-D was formulated to correct for the C_6R^{-6} interatomic potential, ω B97X-D3 includes an additional C_8R^{-8} term, resulting in more accurate description of systems containing heavy atoms.⁹⁰⁻⁹² When tested on the HEAVY28 dataset, systems containing lead and antimony, DFT coupled with the D3 dispersion corrections outperforms the DFT-D functionals, reducing the mean absolute deviation by at least 1.6 kJ mol⁻¹.⁹⁰⁻⁹²

Solvent model based on density (SMD) was used to determine the Gibbs free energy of solvation of the complexes between the activated forms of Pt-based anti-cancer drugs and the DNA/RNA building blocks, further referred to as building block-Pt activated form complexes. SMD was formulated to investigate the polarisation of the solute due to the influence of the solvent.⁸³ Formulated with 6 different levels of theory, SMD has been demonstrated to be an excellent solvation model in reproducing solvation energies of multiple different types

of solute, like amides and aromatic N-heterocycles, with a mean unsigned error of 16.7 kJ mol⁻¹.⁸³ The smallest unsigned error of 4.1 kJ mol⁻¹ was obtained with M05-2X/6-31G* level of theory. Within this model ΔG_{sol} , the Gibbs free energy of solvation of a solute, is defined as the difference between the electronic energy of the solute calculated in SMD and the gas phase. In this study the M06-2X/6-31G* level of theory with SMD and gas phase were used to calculate the solvation energy of the building block-Pt (bb-Pt) activated form complexes.⁹³

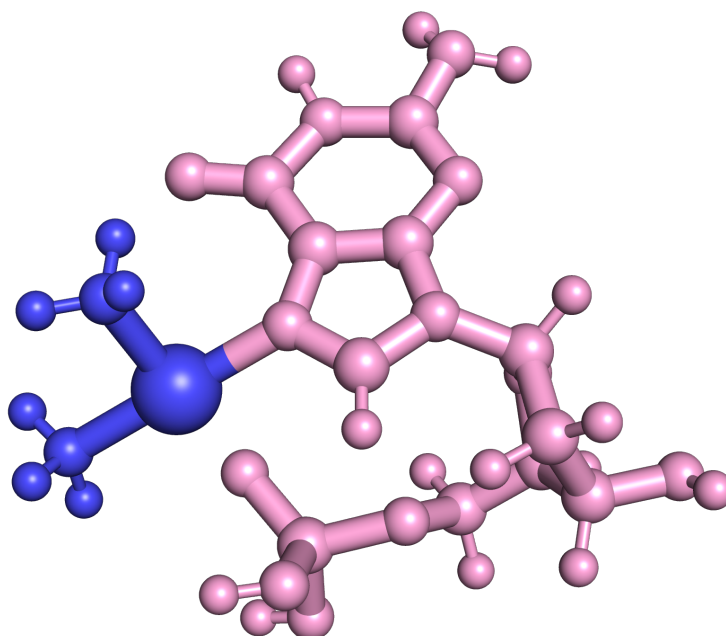


Figure 5.9: Schematic explaining the calculation of interaction energy between the activated form of Pt-based drug (blue) and the building block (pink).

Upon obtaining the optimised geometries of the bb-Pt activated form complexes, single point energy calculations were performed to determine the interaction energy between the Pt complex and DNA/RNA building blocks (Figure: 5.9). The interaction energy (E_{INT}) is defined as the difference in electronic energy of the complex and the sum of the electronic energies of the activated form of the Pt drug and the building block taken in the geometries they adopt in

the complex. The E_{INT} is split into two main components, electrostatics (Electro), the HF component of electronic energy, and dispersion (Disp), the correlation component of SRS-MP2, as follows:

$$E_{INT}^{Electro} = E_{system}^{HF} - E_{frag1}^{HF} - E_{frag2}^{HF} \quad (5.1)$$

$$E_{INT}^{Disp} = E_{system}^{SRS-MP2, Disp} - E_{frag1}^{SRS-MP2, Disp} - E_{frag2}^{SRS-MP2, Disp} \quad (5.2)$$

where $frag1$ and $frag2$ refers to either the DNA/RNA building block or the Pt complex.

The HF component of E_{INT} was corrected for basis set superposition error (BSSE) using the Boys and Bernardi counterpoise correction scheme.⁹⁴ Interaction energies were also calculated using the ω B97X-D3 functional and corrected for BSSE also using the Boys and Bernardi counterpoise correction. The interaction energies obtained with the two methods were compared.

The deformation of the building block was defined as follows:

$$E_{def} = E_{after\ binding} - E_{before\ binding} \quad (5.3)$$

where $E_{before\ binding}$ and $E_{after\ binding}$ is the electronic energy of the building block before and after the drug binding, respectively.

Root mean square deviation (RMSD) was employed to compare geometries of optimised structures and was calculated as shown below, where x , y and z represents the spatial coordinates of each atom:

$$RMSD = \sqrt{\frac{1}{n} \sum ((x_i - x_j)^2 + (y_i - y_j)^2 + (z_i - z_j)^2)} \quad (5.4)$$

5.3 Results and Discussion

5.3.1 Interaction between DNA/RNA building blocks and activated forms of cis-platin

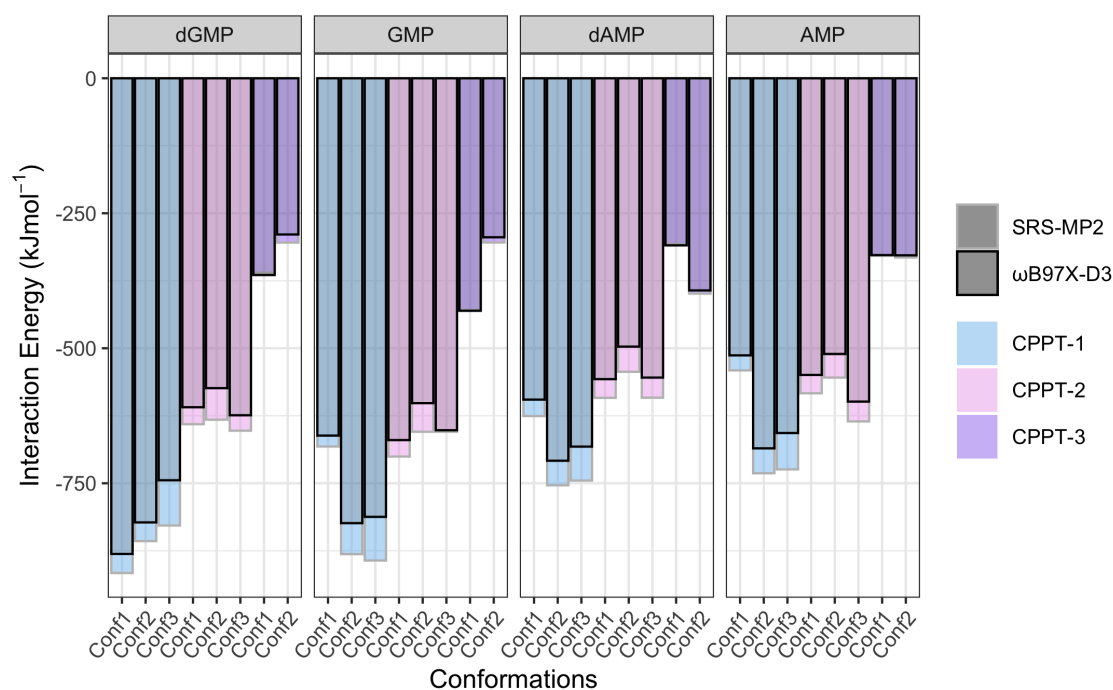


Figure 5.10: Interaction energy of activated cisplatin with either dGMP, GMP, dAMP or AMP.

Figure 5.10 shows interaction energies of activated forms of cisplatin - non-, mono- or di-aquated complexes - with dGMP, GMP, dAMP and AMP. Analysis of SRS-MP2 interaction energies demonstrated a clear preference of CPPT-1 binding to dGMP over the other building blocks, with an average interaction energy of $-867.2 \text{ kJ mol}^{-1}$. The average interaction energy between CPPT-1 and the three other building block - GMP, dAMP and AMP - were determined to be -818.8 , -708.1 and $-665.6 \text{ kJ mol}^{-1}$, respectively. The aquated equivalents of cisplatin, CPPT-2 and CPPT-3, have demonstrated to have weaker interactions with these building blocks than CPPT-1. For example, for dGMP, the average interaction energies decreased by 225.3 and $535.0 \text{ kJ mol}^{-1}$ for CPPT-2 and CPPT-3, respectively, when compared to CPPT-1. A closer look into correlating geometries and energy differences was undertaken to possibly explain the preferential binding to dGMP over the other building blocks. The strong interaction energies are a result of the overall $2+$ charge of the systems.

Comparison of the strength of binding to GMP and dGMP reveals that the interaction energy of the Pt complexes, regardless of the number of water molecules present, ranges from -304.1 to -916.2 kJ mol⁻¹. Comparing SRS-MP2 interaction energies, *CPPT*-3 interacts the weakest out of the three different hydration modes, with a mean interaction energy of -332.1 and -366.6 kJ mol⁻¹ for dGMP and GMP, respectively. The *CPPT*-1 interacts the strongest, with an average of -867.2 and -818.8 kJ mol⁻¹ for dGMP and GMP, respectively. This is expected as previously published crystal structures confirmed that *CPPT*-1 was the species that bound to both DNA and RNA.^{7,56} Interestingly, the extent of aquation of the Pt complex displays a selectivity for either dGMP or GMP depending on the number of water molecules in the Pt complexes. *CPPT*-3 would preferentially bind to GMP over dGMP while the *CPPT*-1 would preferentially bind to dGMP over GMP, interacting by 34.5 and 48.4 kJ mol⁻¹ on average stronger, respectively. Further analysis on their respective optimised geometries was conducted to understand the influence of an additional hydroxyl group on the strength and mode of interaction between the Pt complexes and DNA/RNA building blocks.

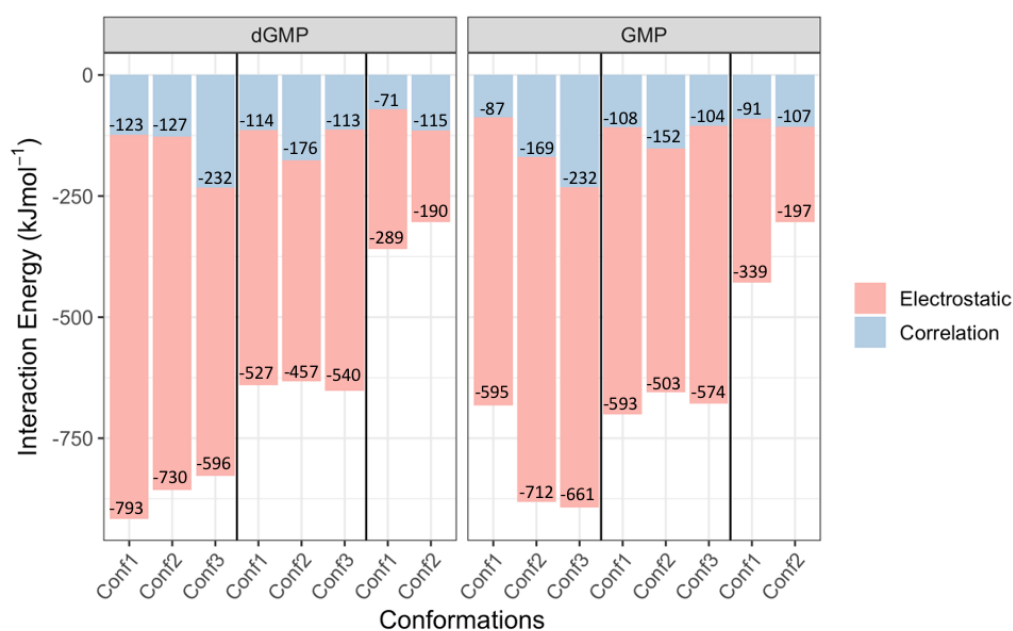


Figure 5.11: *Electrostatic and correlation components to the interaction between activated cisplatin with either dGMP or GMP.*

It is unsurprising that electrostatics dominates over correlation (dispersion) when the Pt complexes possess an overall 2+ charge. The stronger interaction between dGMP or GMP and *CPPT*-1 over *CPPT*-2 and *CPPT*-3 could be explained by the higher electrostatic interaction

(Figure: 5.11). The average electrostatic component for *CPPT*-1, *CPPT*-2 and *CPPT*-3 with dGMP is -706.3, -507.7 and -239.1 kJ mol⁻¹, respectively. The average correlation component for *CPPT*-1, *CPPT*-2 and *CPPT*-3 with dGMP is -160.9, -134.1 and -93.0 kJ mol⁻¹, respectively. Whereas the average electrostatic component for *CPPT*-1, *CPPT*-2 and *CPPT*-3 with GMP is -656.1, -556.6 and -267.8 kJ mol⁻¹ and the average correlation component is -162.7, -121.3 and -98.8 kJ mol⁻¹. Both dGMP and GMP demonstrate a more significant decrease of the electrostatics component than the decrease in correlation with an increasing number of bound water molecules, which is in direct correlation with the reduction of charge on Pt as the number of water molecules increases. The decrease in interaction energies due to the increase of Pt bound water molecules is an indication of the complex's ability to form the Pt-N7 dative bond. This was investigated by studying the Pt-N7 distances of the activated forms of cisplatin (Table: 5.1).

Table 5.1: *Pt-N7 distance (Å) between activated cisplatin and dGMP or GMP building blocks. Values in brackets indicate the absolute deviation from previously published Pt-N7 distance (1.992 Å).⁸⁶*

Activated Cisplatin	Configuration	dGMP	GMP
<i>CPPT</i> -1	1	1.998 (0.006)	1.996 (0.004)
	2	1.997 (0.005)	2.824 (0.823)
	3	2.035 (0.043)	2.039 (0.047)
<i>CPPT</i> -2	1	1.998 (0.006)	1.993 (0.001)
	2	2.881 (0.889)	2.846 (0.823)
	3	2.002 (0.010)	2.000 (0.008)
<i>CPPT</i> -3	1	3.414 (1.422)	3.492 (1.500)
	2	4.085 (2.093)	4.734 (2.742)

Table 5.1 display the Pt-N7 bond distances obtained from the optimised structures of the three different activated forms of cisplatin and dGMP or GMP building blocks. Other than *CPPT*-3, both *CPPT*-1 and *CPPT*-2 produced significantly shorter Pt-N7 distances (in the range of 1.996 to 2.035 Å on average) than the previously reported value of 1.992 Å obtained from crystal structure.⁸⁶ The three outliers that deviated significantly from the trend are Conf2 of GMP with both *CPPT*-1 and *CPPT*-2, resulting in longer distances of 2.824 and 2.846 Å, respectively, as well as Conf2 of dGMP with *CPPT*-2, resulting in a distance of 2.881 Å. *CPPT*-3 usually resulted in longer Pt-N7 distances for both dGMP and GMP, ranging from 3.414 to 4.734 Å, suggesting

that no bonds were formed. The explanation for these long Pt-N7 distances in the case of *CPPT*-3 will be discussed later.

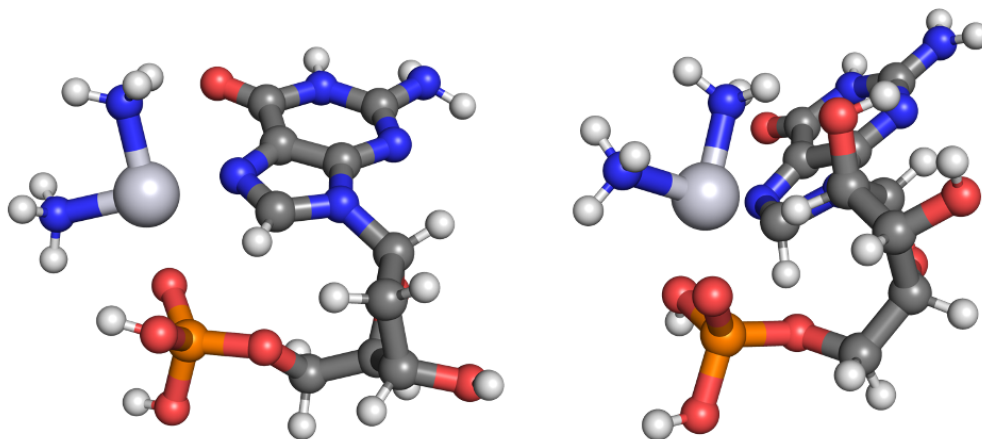


Figure 5.12: *Interaction of CPPT-1 with dGMP (left) or GMP (right).*

From Figure 5.12, it can be seen that the additional hydroxyl group on GMP results in significantly different types of interaction. Where *CPPT*-1 interacts with N7 on dGMP, a hydrogen bond forms between the NH_3 of *CPPT*-1 and the additional hydroxyl group of GMP. Hydrogen bonding results in an increase of the Pt-N7 distance in GMP to 2.8 Å, deviating from the previously published bond distance of 1.992 Å (Table 5.1).⁸⁶ In the case of dGMP, the Pt-N7 distance was found to be 2.000 Å, in agreement to the previously published Pt-N7 distance of 1.992 Å.⁸⁶ The overestimation of the Pt-N7 distance could be due to the absence of a longer oligomer chain and explicit “free” water molecules, resulting in the absence of steric hindrance and stabilising effects from other nucleobases as well as water molecules.

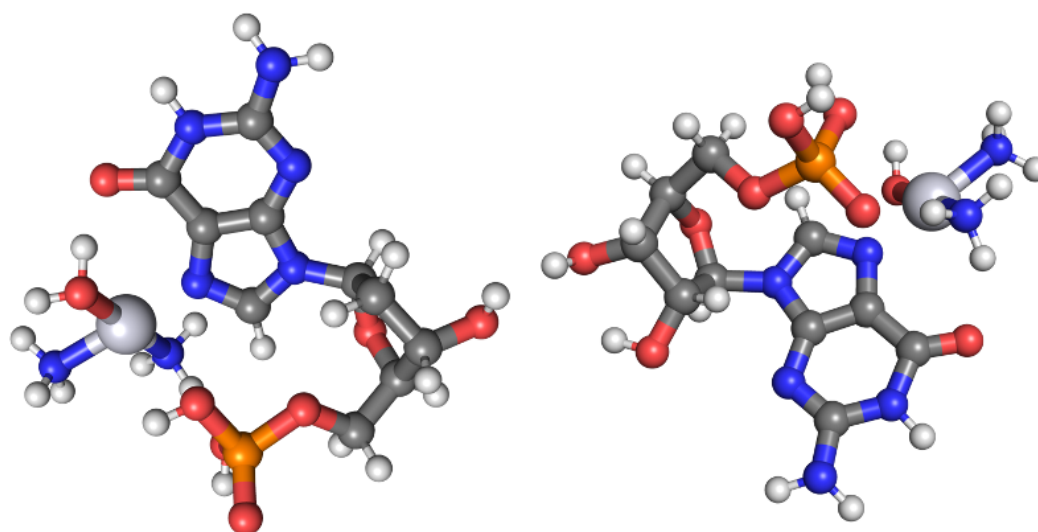


Figure 5.13: Optimised structures of activated mono-aquated complex of cisplatin with dGMP (left) and GMP (right).

CPPT-2 is able to form the similar in length Pt-N7 to both dGMP and GMP (see Figure 5.13), forming Pt-N7 bond distances of 2.002 and 1.993 Å for dGMP and GMP, respectively. The deviation from the previously published Pt-N7 bond distance of 1.992 Å could be due to the formation of additional hydrogen bonds between *CPPT-2* and the building blocks with the C=O on guanine and the phosphate group.⁸⁶ *CPPT-2* has demonstrated to form a 1.615 Å bond between the H₂O and the C=O and a 2.254 Å bond between the NH₃ and the phosphate group of dGMP. For GMP, hydrogen bond distances of 2.063 and 1.851 Å were found between NH₃ and both C=O and the phosphate group, respectively.

The importance of hydrogen bonding between cisplatin and DNA is well established.^{4,69,95–99} Evident in a crystal structure solved by Lippard *et al.* between cisplatin and double-stranded deoxyoligonucleotide, hydrogen bonds between the NH₃ group on cisplatin and the O on the phosphate group was determined, forming a bond distance of 3.1 Å.^{7,10} The hydrogen bond distance determined in this study is significantly shorter than that determined in experiments as the models used were smaller and allows for higher flexibility between the interactions between the Pt complexes and the building blocks.

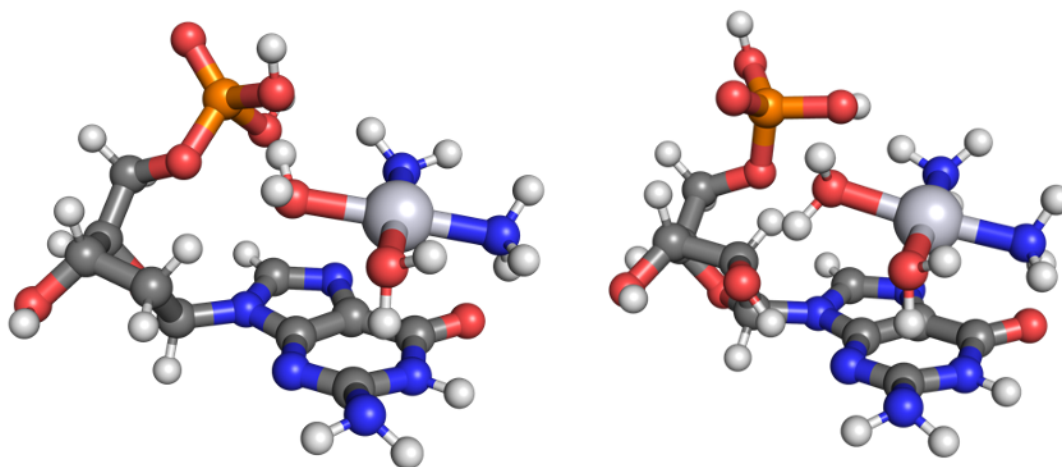


Figure 5.14: Optimised strcutures of activated di-aquated complex of cisplatin with dGMP (left) and GMP (right).

The explanation of the preferential binding of *CPPT*-3 to GMP over dGMP was further investigated. *CPPT*-3 does not form the Pt-N7 bond required to alter the geometries of DNA and RNA. From Figure 5.14, it can be seen that the addition of two water molecules results in the formation of hydrogen bonding between the dGMP or GMP building block and the Pt complex. While a hydrogen bond forms between the water and NH₂ on guanine and the phosphate group for dGMP, a hydrogen bond also forms between the water and NH₂ and the hydroxyl group of GMP. It is suggested that the hydrogen bond increases the Pt-N7 distance by 1.4 and 1.5 Å to 3.4 and 3.5 Å for dGMP and GMP, respectively, indicating that the presence of water molecules on the Pt centre plays an adverse role in coordination to the N7 position on guanine. While *CPPT*-2 is still able to form a strong Pt-N7 bond, the presence of two bound water molecules in *CPPT*-3 preferentially forms hydrogen bonds with functional groups present in the building block instead of a strong Pt-N7 bond.

Figure 5.10 also presents interaction energies between the Pt complexes and DNA building blocks calculated using the ω B97X-D3 functional. In general, a good agreement was found when compared to interaction energies calculated with the SRS-MP2 method, excluding Conf3 of *CPPT*-1, for which the deviations were found to fall in the range of 1.4 to 57.4 kJ mol⁻¹. Conf3 of *CPPT*-1 gives rise to differences of 83.8 and 80.9 kJ mol⁻¹ for dGMP and GMP, respectively. The absolute errors in interaction energies decrease with increasing number of water molecules

bound to the Pt metal centre, decreasing from 83.8 to 4.5 kJ mol⁻¹ for dGMP and 80.9 to 1.4 kJ mol⁻¹ for GMP.

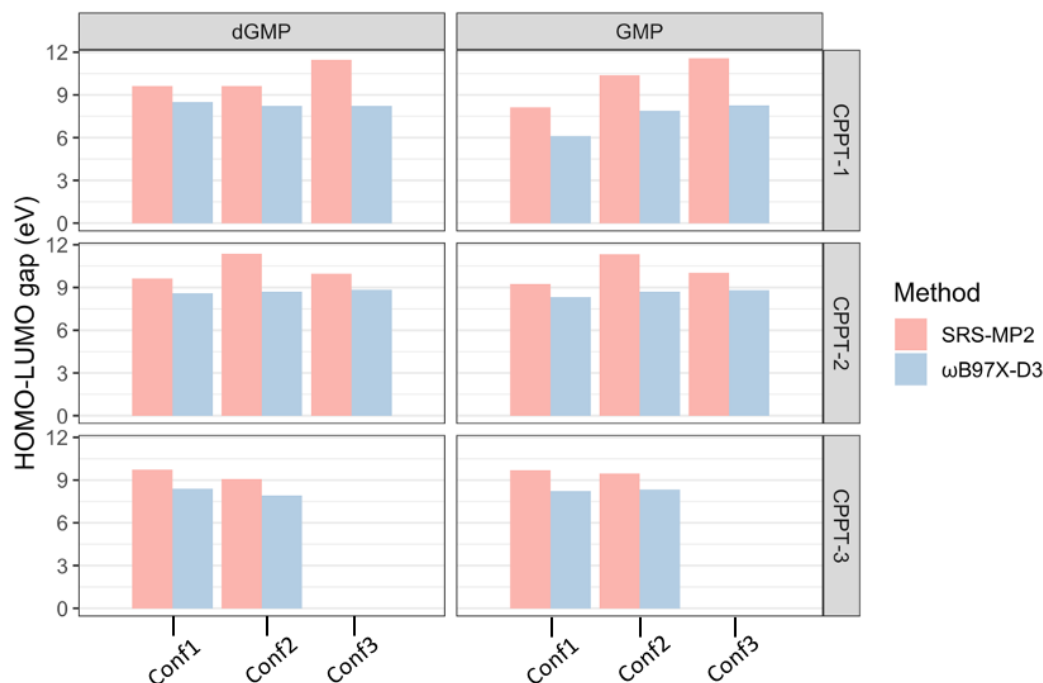


Figure 5.15: HOMO-LUMO gaps (eV) of the Pt-building blocks as calculated with SRS-MP2 and ω B97X-D3.

Table 5.2: Differences in predicted HOMO-LUMO gaps (eV) between SRS-MP2 and ω B97X-D3.

Activated Cisplatin	Configuration	dGMP	GMP
CPPT-1	1	1.110	2.010
	2	1.393	2.489
	3	3.232	3.305
CPPT-2	1	1.029	0.909
	2	2.685	2.647
	3	1.099	1.222
CPPT-3	1	1.322	1.473
	2	1.161	1.126

In an attempt to explain the trends in errors, the energy differences between the highest occupied molecular orbital (HOMO) and the lowest unoccupied molecular orbital were calculated by both SRS-MP2 and ω B97X-D3 and compared in Figure 5.15. Analysis of the HOMO-LUMO gap revealed that ω B97X-D3 predicted smaller HOMO-LUMO gaps compared to those of

SRS-MP2 by an average of 1.4 and 1.8 eV for dGMP and GMP, respectively. The smaller HOMO-LUMO gap predicted by ω B97X-D3 is not unexpected as DFT functionals have been known to underestimate HOMO-LUMO gaps due to the inability to describe excited states using ground state densities.^{100–103} As the number of Pt-bound water molecules increases, the HOMO-LUMO gap for dGMP predicted with SRS-MP2 decreases, with an average of 10.2, 9.8 and 9.4 eV for *CPPT*-1, *CPPT*-2 and *CPPT*-3, respectively. On the other hand, ω B97X-D3 predicts that *CPPT*-2 results in the largest HOMO-LUMO gap, averaging 8.7 eV. ω B97X-D3 predicts an average HOMO-LUMO gap of 8.3 and 8.2 eV for the *CPPT*-1 and *CPPT*-3 for dGMP. The same trend was observed for GMP. It is suggested that lower band gaps in *CPPT*-1 and *CPPT*-2 may be responsible for larger deviations between SRS-MP2 and ω B97X-D3.

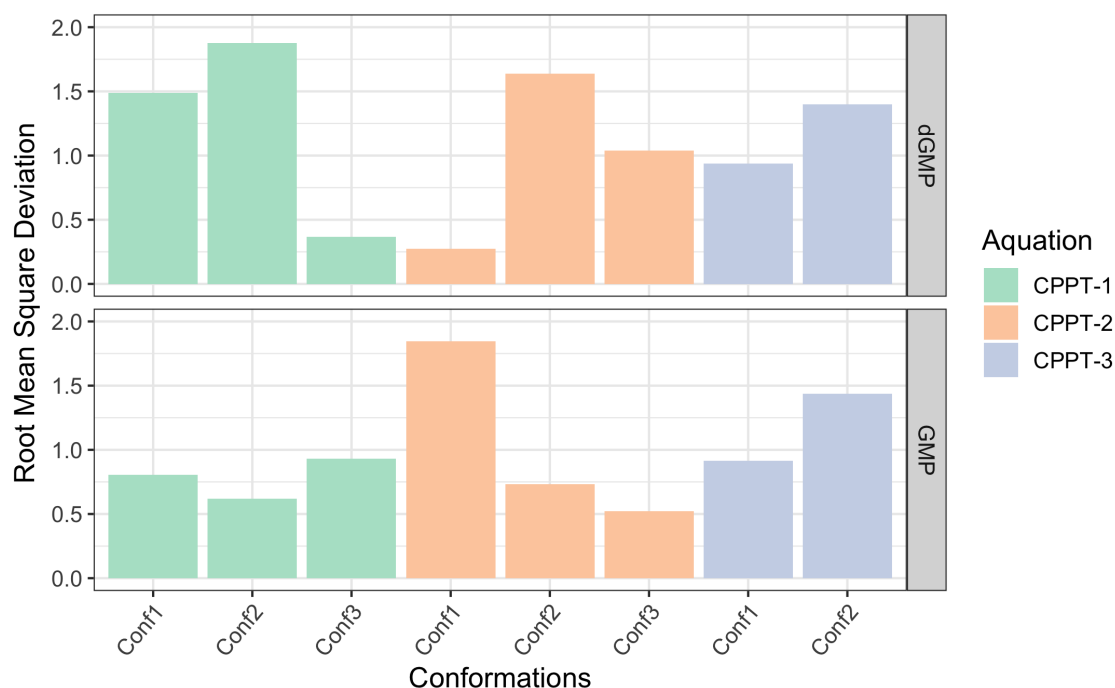


Figure 5.16: Root mean square deviation of either dGMP or GMP before and after binding event.

The RMSD values of optimised structures of dGMP and GMP before and after binding with the Pt complexes were compared in Figure 5.16. With an average RMSD of 1.2 and 0.8 Å for dGMP and GMP, respectively, the binding of *CPPT*-1 has a more significant effect on dGMP than GMP. An example of a significant geometry change in the building block is given in Figure 5.17. In the case of dGMP, the folding of the phosphate group is observed upon binding to the Pt centre in *CPPT*-1. As a result, the dihedral angle between the sugar and the phosphate group

decreases from 52° to 45° . The binding with *CPPT*-1 also altered the dihedral angle between the sugar and guanine from 62° to 89° . On the other hand, the geometry of GMP is influenced to a lesser extent by the binding event as demonstrated in Figure 5.17. This could be due to the formation of hydrogen bond between *CPPT*-1 and the hydroxyl group on the sugar. The binding of *CPPT*-1 in the Conf3 configuration with GMP resulted in the largest deviation of RMSD of 0.9 \AA , demonstrated by the displacement of the phosphate group, thus giving rise to a change in dihedral angle between the phosphate group to the sugar from 54° to 69° . In a previously published study conducted by Neidle, the dihedral angle between the sugar and phosphate group of canonical B-DNA was determined to be 133° .¹⁰⁴ The significantly smaller dihedral angles obtained in the studied models could be due to the lack of steric hindrance and further interactions between explicit solvation and π - π stacking in larger models.

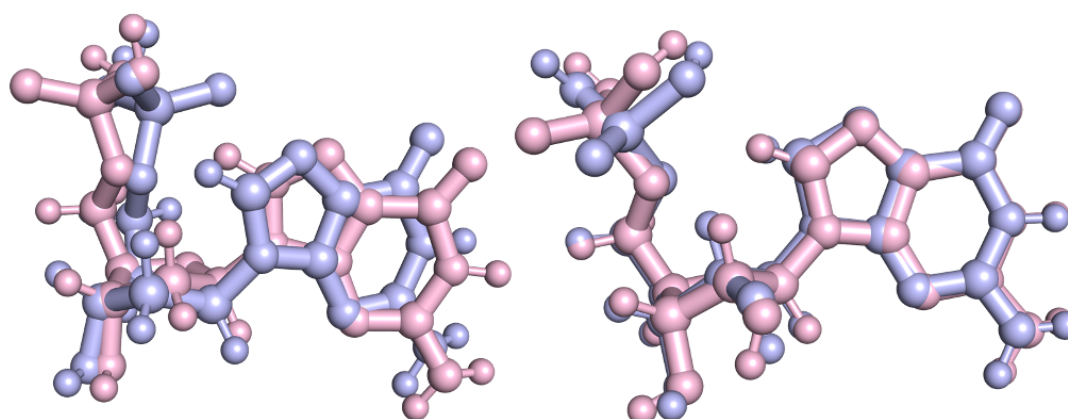


Figure 5.17: Difference in geometries of *dGMP* (left) and *GMP* (right) before (pink) and after (blue) binding to *CPPT*-1.

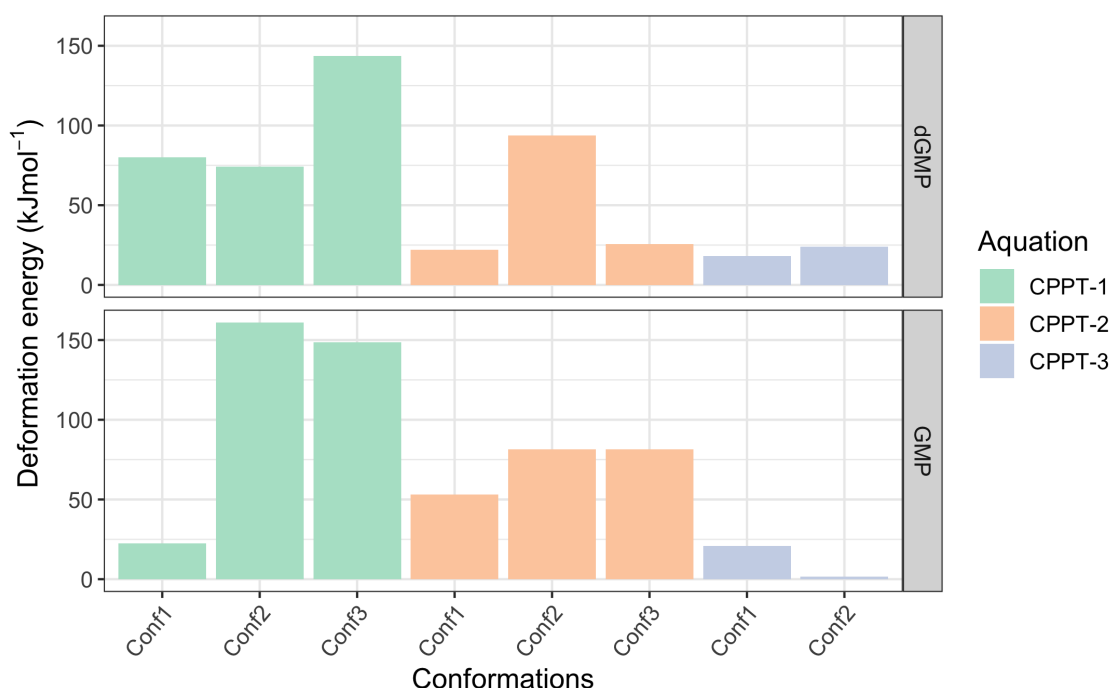


Figure 5.18: Deformation energy (kJ mol⁻¹) of either dGMP or GMP due to the binding of Pt complex.

Figure 5.18 shows differences in electronic energies, also known as deformation energies, of dGMP and GMP, before and after interacting with Pt complexes. The changes in geometry due to binding with *CPPT*-1 resulted in the largest deformation energy with both dGMP and GMP, averaging 99.3 and 110.7 kJ mol⁻¹, respectively. The deformation energies resulting from interacting with the mono- and di-aquated species of cisplatin are significantly lower for both dGMP and GMP, ranging from 21.9 to 81.3 kJ mol⁻¹ for the former and 1.9 to 23.9 kJ mol⁻¹ for the latter.

Upon comparison with RMSD values, no direct relationship between deformation energy and RMSD values was determined (see Figures 5.16 and 5.18). Whilst Conf 3 of *CPPT*-1 binding to dGMP resulted in the largest deformation energy, it did not produce the largest RMSD value.

The same analysis as shown above was applied to studying binding to dAMP and AMP. Figure 5.10 displays the interaction energies between the activated forms of cisplatin with dAMP and AMP at two levels of theory. Similar to the trend observed for dGMP and GMP, the interaction strength decreases from *CPPT*-1 to *CPPT*-3. According to the SRS-MP2 method, the mean interaction energies between *CPPT*-1 with dAMP and AMP are -708.1 and -665.9 kJ mol⁻¹,

respectively. *CPPT*-3 gives rise to mean interaction energies of -353.0 and -330.3 kJ mol^{-1} for dAMP and AMP, respectively. Interestingly, *CPPT*-3 interacts more strongly with AMP over dAMP by 22.7 kJ mol^{-1} , which is in agreement with the previously established trends for dGMP and GMP.

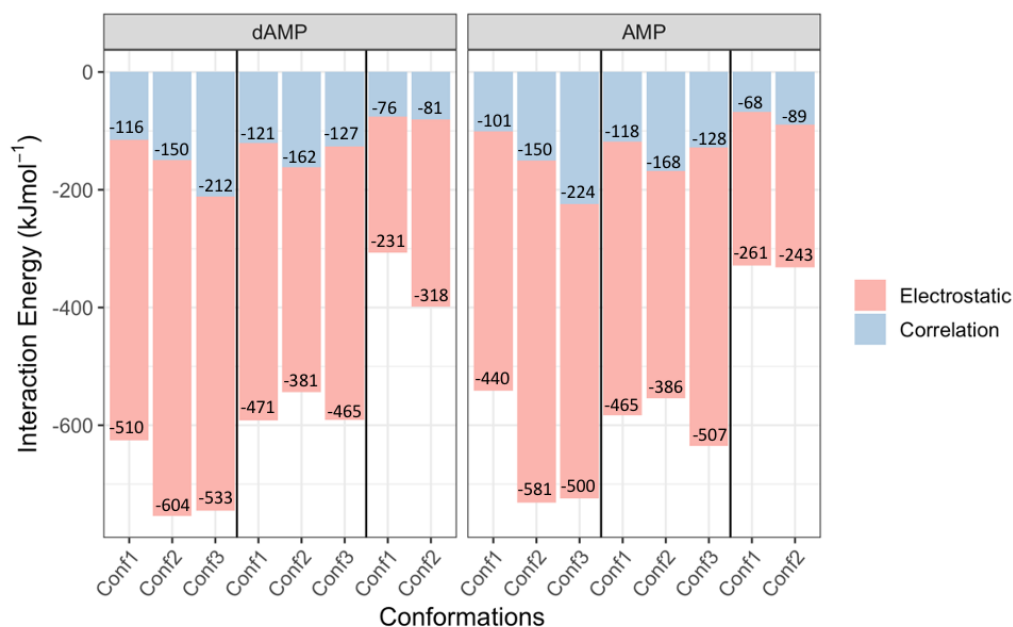


Figure 5.19: *Electrostatic and correlation components to interaction energy in complexes between activated forms of cisplatin and dAMP/AMP.*

Similar to dGMP and GMP (Figure: 5.11), electrostatics again plays a bigger part in determining the nature of the interaction between dAMP/AMP and cisplatin (Figure: 5.19). The average electrostatic contributions of *CPPT*-1, *CPPT*-2 and *CPPT*-3 with dAMP decrease from -549.2 , -439.1 to -274.9 kJ mol^{-1} , respectively. The average correlation contribution changes significantly less from -158.9 kJ mol^{-1} in *CPPT*-1 to -136.5 kJ mol^{-1} in *CPPT*-2 and -78.2 kJ mol^{-1} in *CPPT*-3. On the other hand, the average electrostatic contributions of *CPPT*-1, *CPPT*-2 and *CPPT*-3 with AMP are slightly smaller of -507.1 , -452.9 and -251.6 kJ mol^{-1} , respectively. The correlation components are practically identical to those in dAMP of -158.5 , -138.2 and -78.7 kJ mol^{-1} for *CPPT*-1, *CPPT*-2 and *CPPT*-3, respectively. Again, the decrease in electrostatics is found to be more significant than the decrease in correlation as the number of water molecules increased.

Table 5.3: *Pt-N7 distances (in Å) between the activated forms of cisplatin and dAMP/AMP building block. Values in brackets indicate the absolute deviation from the previously published Pt-N7 distance of 2.010 Å.^{61,105}*

Activated Cisplatin	Configuration	dAMP	AMP
CPPT-1	1	1.996 (0.014)	1.989 (0.021)
	2	1.993 (0.017)	1.992 (0.018)
	3	2.053 (0.043)	2.054 (0.044)
CPPT-2	1	2.006 (0.004)	1.998 (0.012)
	2	2.939 (0.929)	2.926 (0.916)
	3	1.998 (0.012)	1.996 (0.014)
CPPT-3	1	3.493 (1.483)	4.995 (2.985)
	2	3.562 (1.552)	3.314 (1.304)

Table 5.3 shows the Pt-N7 distances in complexes between the activated forms of cisplatin, CPPT-1, CPPT-2 and CPPT-3, and dAMP/AMP. Similar to dGMP and GMP, CPPT-3 results in larger variations in the Pt-N7 distance with dAMP and AMP, ranging from 3.314 to 4.995 Å, suggesting that the Pt-N7 bond is not formed. Both CPPT-1 and CPPT-2 were able to optimise to the Pt-N7 distances close to the previously reported distance of 2.010 Å,^{61,105} ranging from 1.992 to 2.053 Å.^{61,105} CPPT-2 is able to form a dative Pt-N7 bond with both dAMP and AMP, similar to both dGMP and GMP. Two types of hydrogen bonding were again observed for dAMP - 1) between the Pt-bound H₂O in CPPT-2 (1.8 Å) and 2) between the NH₃ of CPPT-2 and the NH₂ on adenine (2.1 Å). For AMP, however, hydrogen bonding was formed between different groups. For example, the Pt-bound water formed hydrogen bonding with the NH₂ on adenine (1.8 Å), while the NH₃ on CPPT-2 also interacted with the phosphate group (1.9 Å). Again, two outliers were found for Conf2 of the building blocks of AMP and dAMP when coupled with CPPT-2, with the Pt-N7 distance lengthening to 2.939 and 2.926 Å for dAMP and AMP, respectively. For CPPT-1 and CPPT-2, the Pt-N7 distance does not vary significantly between binding to guanine and adenine. Some variations in the Pt-N7 distances occur in the case of CPPT-3, for which the binding becomes non-covalent, thus resulting in broader fluctuations due to the presence of functional groups in the building block that can provide additional non-covalent bonding to the activated form of cisplatin. Similar to the trends observed in dGMP and GMP, the presence of two water molecules prevented the formation of a dative bond between the Pt metal centre and N7 of dAMP and AMP (Figure: 5.20), resulting in lengthening of the Pt-N7 distance to 3.6 and 3.3 Å, respectively. For dAMP, CPPT-3 formed four hydrogen bonds

with the phosphate and adenine with an average distance of 2.05 Å. The additional hydroxyl of AMP was found to interact with H₂O through a hydrogen bond of 1.7 Å. The geometry adopted by AMP resulted in the formation of five hydrogen bonds ranging from 1.7 to 2.5 Å. The presence of additional hydrogen bonding can explain the preferential interaction, by 22.7 kJ mol⁻¹, with AMP over dAMP.

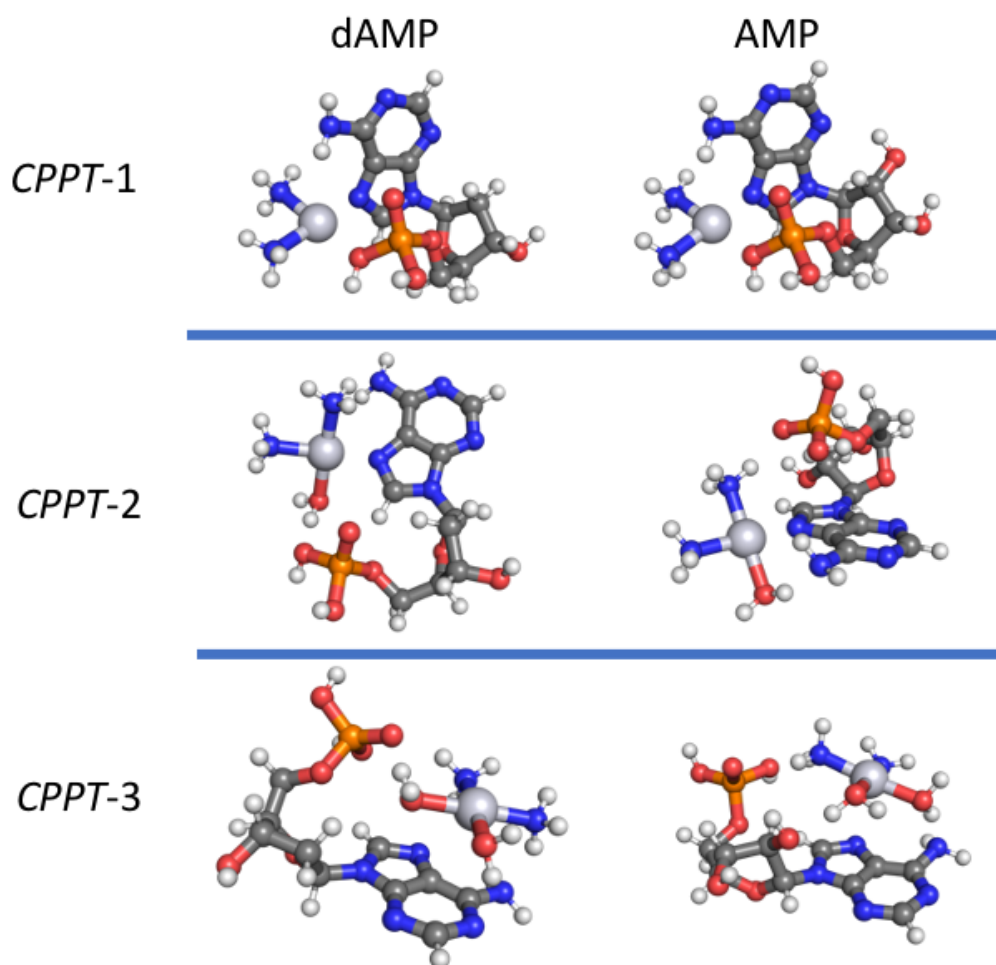


Figure 5.20: Optimised structures of complexes between CPPT-1, CPPT-2 and CPPT-3 and dAMP or AMP.

The E_{INT} calculated with both SRS-MP2 and ω B97X-D3 are compared in Figure 5.10. Similar to dGMP and GMP, the energy difference between SRS-MP2 and ω B97X-D3 was found to be the largest for conf3 of CPPT-1 for both dAMP and AMP, 62.8 and 67.3 kJ mol⁻¹, respectively. The energy difference between SRS-MP2 and ω B97X-D3 decreases with inclusion of water molecules on the Pt centre. The absolute differences for dAMP decrease from 62.8 to 2.2 kJ

mol^{-1} going from *CPPT-1* to *CPPT-3*. AMP produced a similar range, with the energy difference decreasing from 67.3 to 1.3 kJ mol^{-1} .

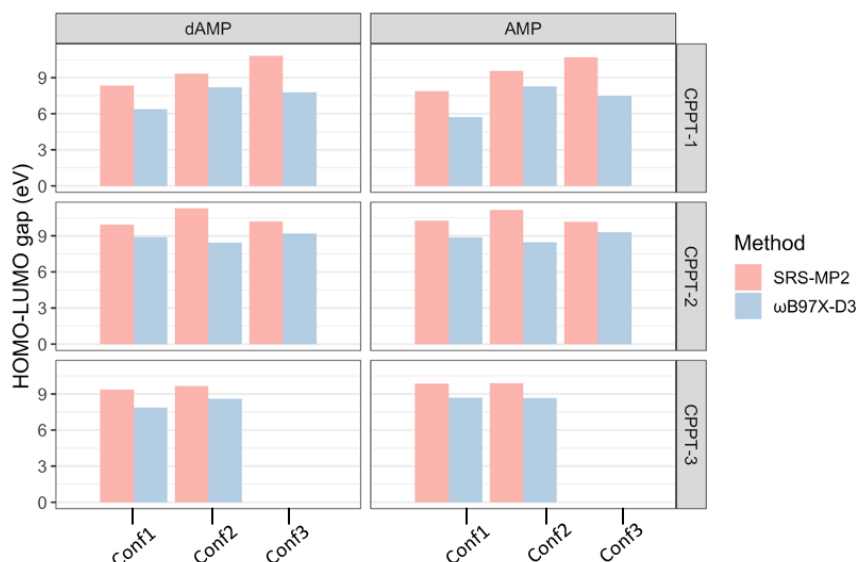


Figure 5.21: HOMO-LUMO (eV) gap of dAMP and AMP calculated with SRS-MP2 and ω B97X-D3.

Table 5.4: Difference in predicted HOMO-LUMO gap (eV) between SRS-MP2 and ω B97X-D3

Activated Cisplatin	Configuration	dAMP	AMP
CPPT-1	1	1.933	2.155
	2	1.147	1.280
	3	3.067	3.221
CPPT-2	1	1.038	1.396
	2	2.818	2.677
	3	1.001	0.848
CPPT-3	1	1.490	1.174
	2	1.064	1.209

Figure 5.21 presents predicted HOMO-LUMO gaps for dAMP and AMP calculated with both methods to explain this phenomenon. SRS-MP2 consistently predicts a larger HOMO-LUMO gap as compared to ω B97X-D3, with an average difference of 1.7 eV (Figure 5.21 and Table 5.4). The largest HOMO-LUMO gap predicted by SRS-MP2 is Conf2 of *CPPT-2*, with a gap of 11.3 and 11.2 eV for dAMP and AMP, respectively. This is contrary to the gaps found for dGMP and GMP, for which the largest HOMO-LUMO gap was found in *CPPT-1*. Average differences between

the two methods were found to be 2.1, 1.6 and 1.3 eV for *CPPT-1*, *CPPT-2* and *CPPT-3* upon binding with dAMP. A similar trend is observed for AMP, with average differences of 2.2, 1.6 and 1.2 eV, for *CPPT-1*, *CPPT-2* and *CPPT-3*, respectively. As one can see there is a correlation between the decreasing difference between the predicted HOMO-LUMO gap and the closeness of the calculated interaction energies. For *CPPT-3* the ω B97X-D3 interaction energies are reproduced within chemical accuracy when compared to SRS-MP2. These difference clearly highlight the changing nature of the Pt-N7 bond from dative in *CPPT-2* to non-covalent in *CPPT-3*.

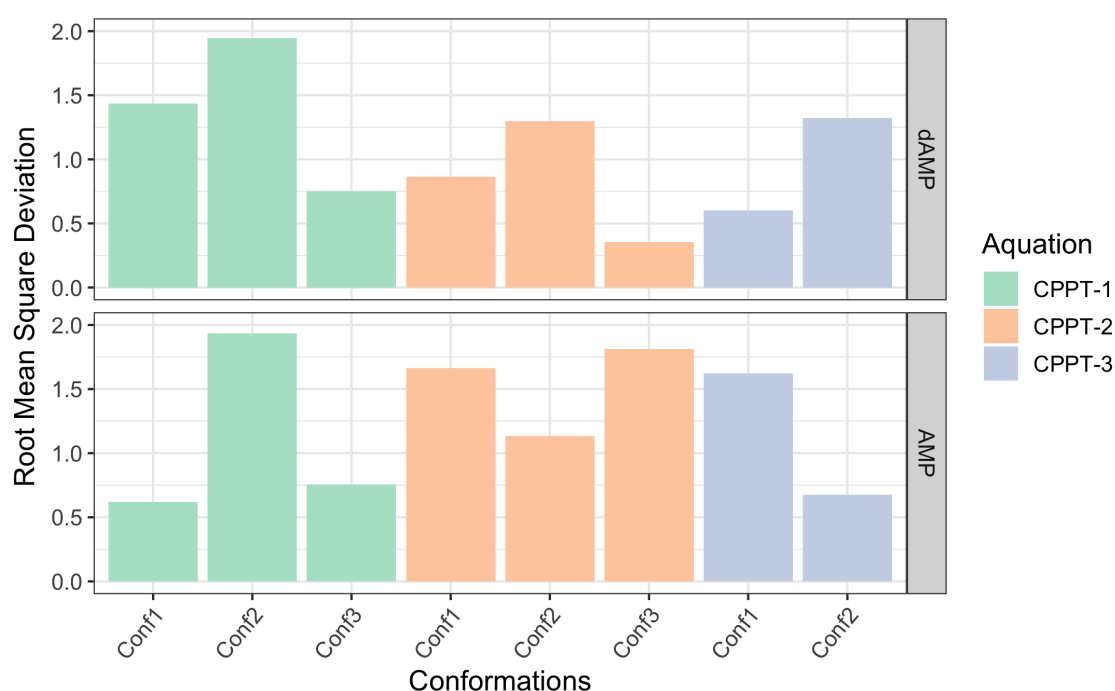


Figure 5.22: Root mean square deviation of either dAMP or AMP before and after binding event.

Unsurprisingly, the RMSD values for the building blocks of dAMP and AMP shown in Figure 5.22 are larger after interacting with *CPPT-1*, averaging 1.4 and 1.1 Å, respectively. In general, the differences in geometry in AMP are more prevalent than in dAMP, regardless of the aquation extent of the Pt complex, with an average RMSD of 1.3 and 1.1 Å. For AMP, the differences in geometry due to interaction with *CPPT-2* resulted in higher RMSD values when compared to those of *CPPT-1*, with an average of 1.5 and 1.1, respectively. This, however, was not also reflected in the calculated deformation energy of AMP (see Figure 5.23) for which the average deformation energy was found to be large for *CPPT-1* (58.5 kJ mol⁻¹) and *CPPT-2* (54.6 kJ

mol^{-1}). The highest deformation energy arises of $107.4 \text{ kJ mol}^{-1}$ for Conf3 of AMP when bound to CPPT-1 (see Figures 5.23 and 5.24).

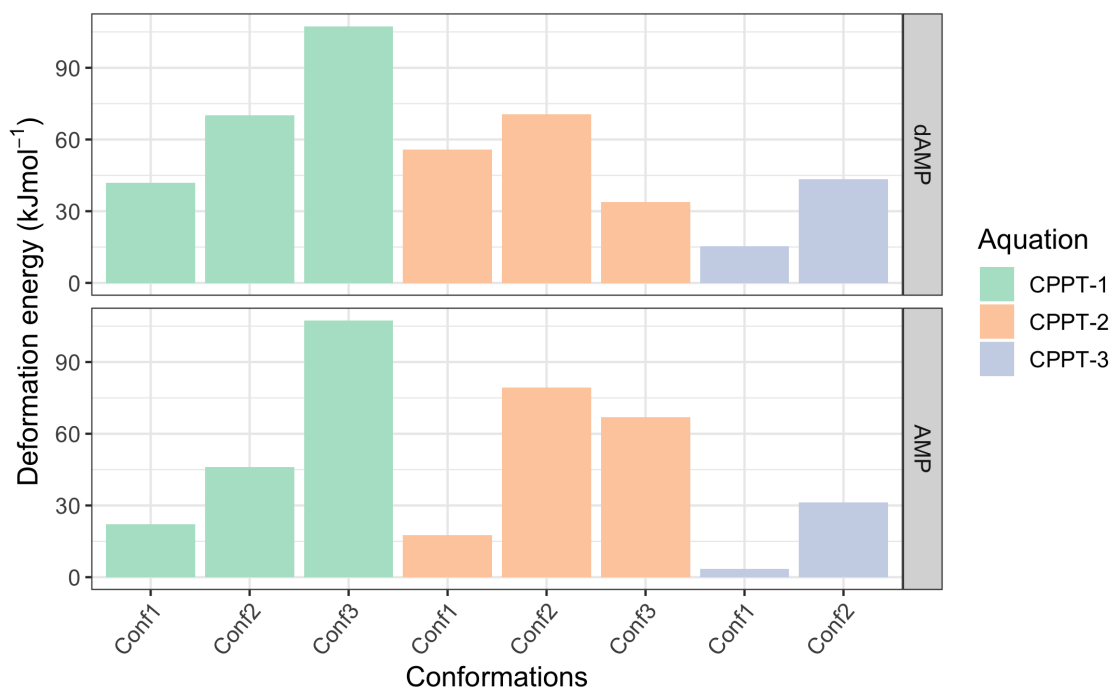


Figure 5.23: Deformation energy (kJ mol^{-1}) of dAMP and AMP upon binding to the activated forms of cisplatin.

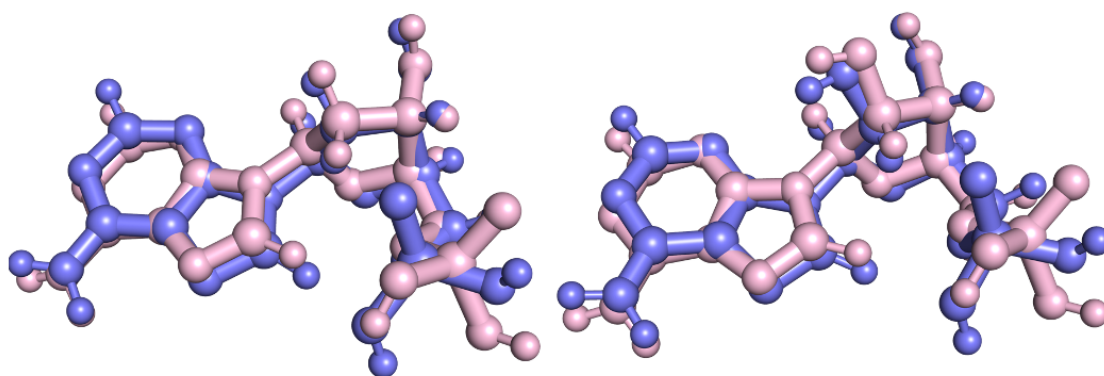


Figure 5.24: Difference in geometry of dAMP (left) and AMP (right) before (pink) and after (blue) binding of CPPT-1 with Conf3 of AMP/dAMP.

Figure 5.24 shows the displacement of the phosphate group and the hydroxyl groups of the sugar from the initial conformation of the building block due to the interaction with *CPPT*-1. Whilst the interaction with *CCPT*-1 resulted in a displacement in both the hydroxyl group and phosphate for AMP, the displacement in dAMP is only present in the phosphate group. Overall, RMSD values and deformation energies differ only slightly between dAMP and AMP, namely by 0.003 Å and 0.003 kJ mol⁻¹ on average, respectively.

Overall, comparing the extent of aquation in activated forms of cisplatin, it was determined that the presence of water molecules coordinated to the Pt metal centre has an adverse effect on the formation of a dative Pt-N7 bond, evident from the increased Pt-N7 distance reported above. The reduction of effective charge on the Pt centre coupled with the competitive formation of hydrogen bonding between the water molecules and the nucleobases shifts the nature of the Pt - N7 bond into the non-covalent range. The presence of Pt bound water molecules also decreased the SRS-MP2 interaction energy, from an average of -708.1, -575.6 and -353.0 kJ mol⁻¹ for *CPPT*-1, *CPPT*-2 and *CPPT*-3, respectively, with dAMP. The same trend was observed for AMP, where the average SRS-MP2 interaction energies also decreased, from an average of -665.6, -591.1 and -330.3 kJ mol⁻¹ for *CPPT*-1, *CPPT*-2 and *CPPT*-3, respectively.

Figure 5.25 shows the strongest interacting structures of the DNA and RNA building blocks with *CPPT*-1, *CPPT*-2 and *CPPT*-3. Figure 5.25 displays a clear trend where a decrease in interaction energies between the Pt complex and nucleobases can be seen with an increase in number of water molecules bound to the Pt metal centre. The comparison of interaction energy between dGMP and dAMP also reveals a preference for binding to the former, by 162.4 kJ mol⁻¹ for *CPPT*-1. It is similar with GMP and AMP, where *CPPT*-1 preferentially binds to GMP by 161.6 kJ mol⁻¹. This finding is in agreement to previously published studies where activated cisplatin is found to bind and form adducts between two neighbouring guanine 65% of the time, and between a neighbouring guanine and adenine 25% of the time^{4,106–111}

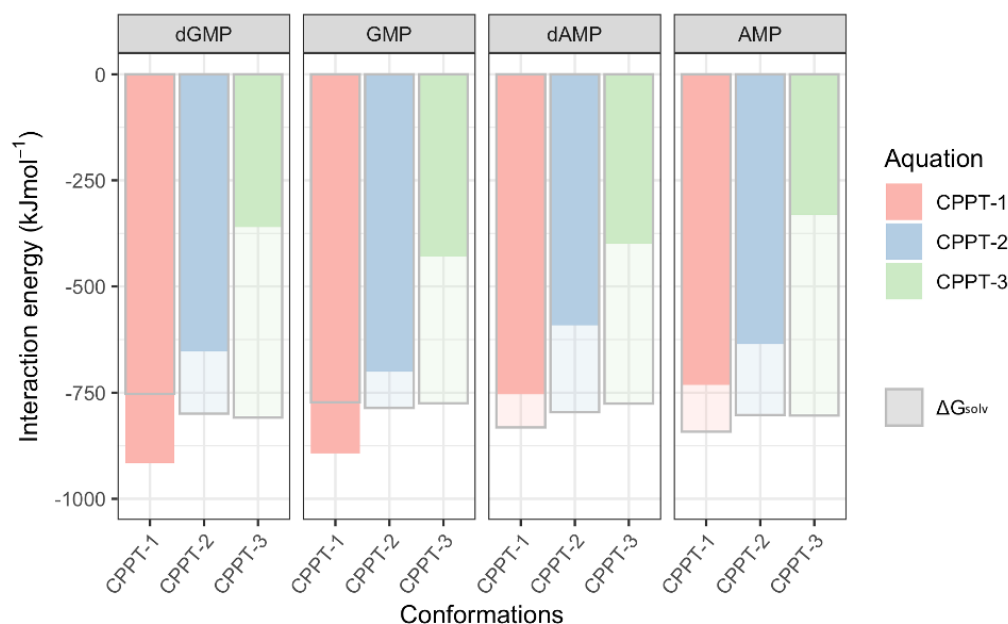


Figure 5.25: Comparison of interaction energies and Gibbs free energies of solvation (ΔG_{solv} (kJ mol⁻¹)) of activated forms of cisplatin (CPPT-1, CPPT-2 and CPPT-3) with dGMP, GMP, dAMP and AMP.

Analysis of Gibbs free energies of solvation, ΔG_{solv} showed smaller differences among the building blocks as well as activated forms of cisplatin ranging from -841.8 to -753.2 kJ mol⁻¹. This demonstrates that the solvation of the building block significantly outweighs the solvation of the activated forms of cisplatin. Therefore, the presence of explicit water molecules is important in locating the most stable configuration of the building blocks.

5.3.2 Interaction between DNA/RNA building blocks and activated forms of oxaliplatin

As determined in the previous section, the fully dissociated and mono-aquated forms of cisplatin, CPPT-1 and CPPT-2, were found to interact with the DNA/RNA building blocks and form a strong dative Pt-N7 bond. In this section the comparison of binding is made to activated forms of oxaliplatin.

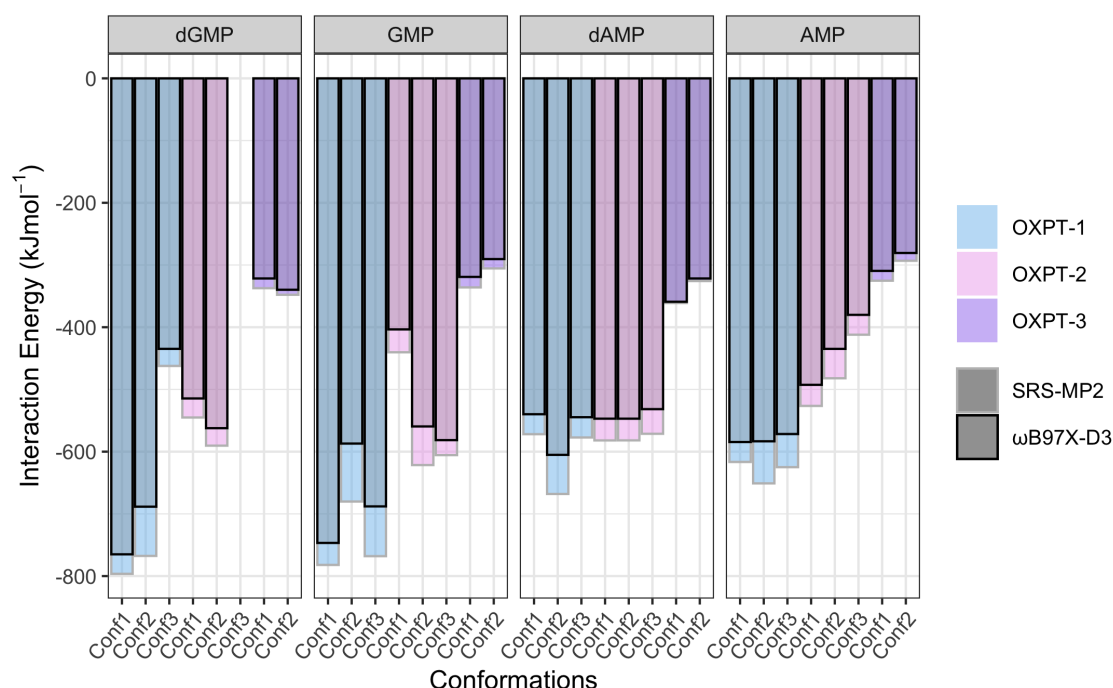


Figure 5.26: Interaction energies of activated forms of oxaliplatin with dGMP, GMP, dAMP and AMP

Figure 5.26 shows the interaction energies of the activated forms of oxaliplatin - the non-, mono- and di-aquated complexes - with dGMP, GMP, dAMP and AMP. Analysis of SRS-MP2 interaction energies demonstrates a preference for OXPT-1 to bind to dGMP over the other building blocks, with interaction energies ranging between -462.3 to $-796.4 \text{ kJ mol}^{-1}$. The surprisingly low interaction energy of Conf3 of OXPT-1 to dGMP is discussed later. The average interaction energies between OXPT-1 and GMP, dAMP and AMP were determined to be -743.4 , -605.7 and $-630.8 \text{ kJ mol}^{-1}$, respectively. Similar to aquated cisplatin, the interaction energies between the mono- (OXPT-2) and di-aquated (OXPT-3) oxaliplatin and building blocks decreases. For example, the average interaction energies between OXPT-2 and OXPT-3 with dGMP decreased by 107.7 and $332.8 \text{ kJ mol}^{-1}$, respectively, when compared to OXPT-1. Subsequently, a closer investigation was conducted to study the effects of aquation on geometries to explain the preferential binding of oxaliplatin to dGMP over the other building blocks. Similar to cisplatin, the strong interaction energies are a result of the overall $2+$ charge of the systems.

The interaction energy of activated oxaliplatin, regardless of number of water molecules, and dGMP and GMP ranges from -305.5 to $-796.4 \text{ kJ mol}^{-1}$. Comparing the SRS-MP2 interaction

energies, *OXPT*-3 interacts the weakest out of the three different activated forms of oxaliplatin, with an average interaction energy of -342.6 and -320.7 kJ mol⁻¹ for dGMP and GMP, respectively. *OXPT*-1 interacts significantly stronger than its aquated counterparts, resulting in an average interaction energy of -675.4 and -743.4 kJ mol⁻¹ for dGMP and GMP, respectively. These trends are similar to that of cisplatin and supports previously published crystal structure where *OXPT*-1 was the species determined to bind to DNA.¹⁰

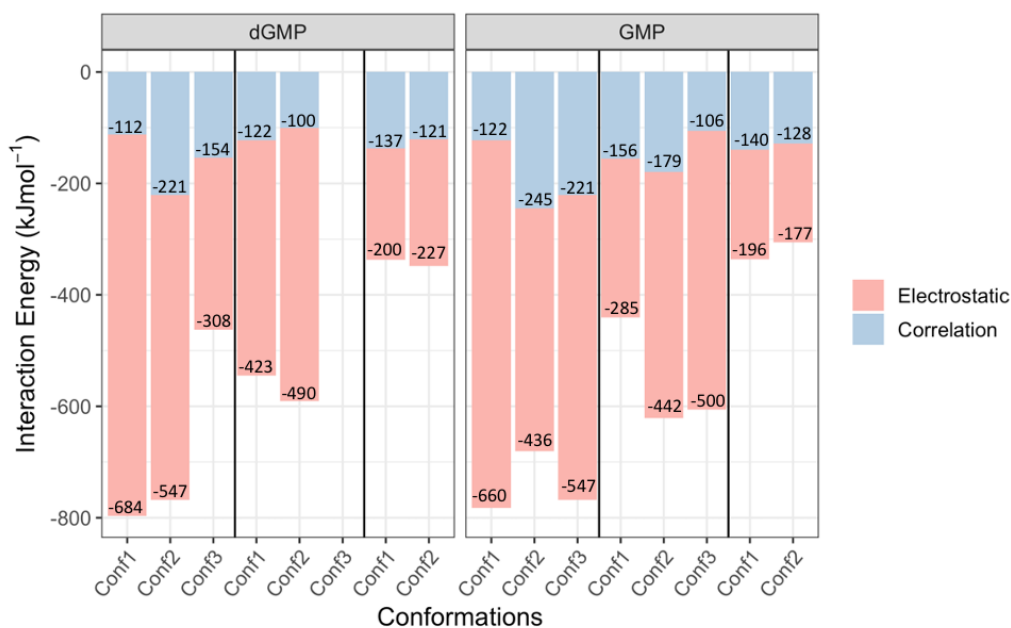


Figure 5.27: *Electrostatic and correlation components to the interaction between activated oxaliplatin with either dGMP or GMP.*

Similar to cisplatin (Figure: 5.11), the electrostatics dominate over correlation in determining the interactions between dGMP or GMP and *OXPT*-1, *OXPT*-2 and *OXPT*-3 (Figure 5.27). Where the average electrostatic component for *OXPT*-1, *OXPT*-2 and *OXPT*-3 with dGMP is -513.1, -456.3 and -213.6 kJ mol⁻¹, the average correlation component is -162.3, -111.4 and -129.0 kJ mol⁻¹, respectively. For GMP, on the other hand, the average electrostatic component for *OXPT*-1, *OXPT*-2 and *OXPT*-3 -547.3, -408.8 and -186.7 kJ mol⁻¹, respectively. The average correlation component are -196.1, -147.0 and -134.0 kJ mol⁻¹ for GMP with *OXPT*-1, *OXPT*-2 and *OXPT*-3, respectively. Similar to the trend observed with cisplatin (Figure: 5.11), the decrease in the electrostatic component is more significant than the decrease in the correlation component with an increase of Pt bound water molecules.

Table 5.5: *Pt-N7 distances (Å) between activated forms of oxaliplatin and dGMP/GMP building block. Values in brackets indicate the absolute deviation from the previously reported Pt-N7 distance (1.992 Å).⁸⁶*

Activated Oxaliplatin	Configuration	dGMP	GMP
OXPT-1	1	2.024 (0.032)	2.002 (0.010)
	2	2.037 (0.045)	2.804 (0.812)
	3	3.818 (1.824)	2.036 (0.044)
OXPT-2	1	2.016 (0.024)	3.890 (1.898)
	2	1.992 (0.000)	2.840 (0.848)
	3		2.004 (0.012)
OXPT-3	1	3.692 (1.700)	3.705 (1.713)
	2	3.319 (1.327)	3.350 (1.358)

Table 5.5 shows the Pt-N7 distances between activated forms of oxaliplatin and dGMP and GMP building blocks. Similar to the calculations reported for cisplatin above, OXPT-3 resulted in the largest Pt-N7 deviation from the experimental value, ranging between 3.350 to 3.705 Å. This range clearly suggests that the Pt-N7 bond is not formed. Both OXPT-1 and OXPT-2 have demonstrated their ability to form the dative Pt-N7 bond, with the distances ranging from 1.929 to 2.037 Å. There are two configurations that did not result in the formation of the Pt-N7 bond, Conf3 of OXPT-1 with dGMP (the Pt-N7 bond of 3.818 Å). The other geometry that did not form the Pt-N7 bond were Conf1 of OXPT-2 with GMP, resulting in Pt-N7 distance of 3.890 Å.

Similar to cisplatin, the non-aquated form of oxaliplatin, OXPT-1 interacts the strongest with both dGMP and GMP, with an average interaction energy of -675.4 and -743.4 kJ mol⁻¹, respectively (see Figure: 5.28). Though it may appear that OXPT-1 preferentially binds to GMP, the lower average interaction energy with dGMP is due to a weaker interaction energy of -462.3 kJ mol⁻¹ observed for Conf3. The significantly lower interaction between Conf3 of OXPT-1 with dGMP could be explained by the formation of a dative bond between the Pt metal ion with the O on the phosphate group, with a bond distance of 2.1 Å (Figure: 5.29). The formation of the Pt-O dative bond with the phosphate group resulted in an increase in Pt-N7 distance to 3.8 Å, preventing the formation of the Pt-N7 bond (Figure: 5.29).

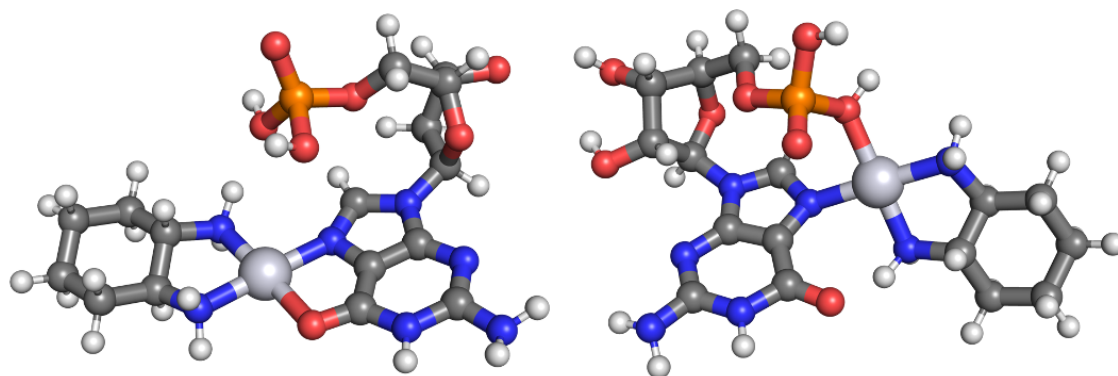


Figure 5.28: Optimised structures of OXPT-1 with dGMP (left) and GMP (right).

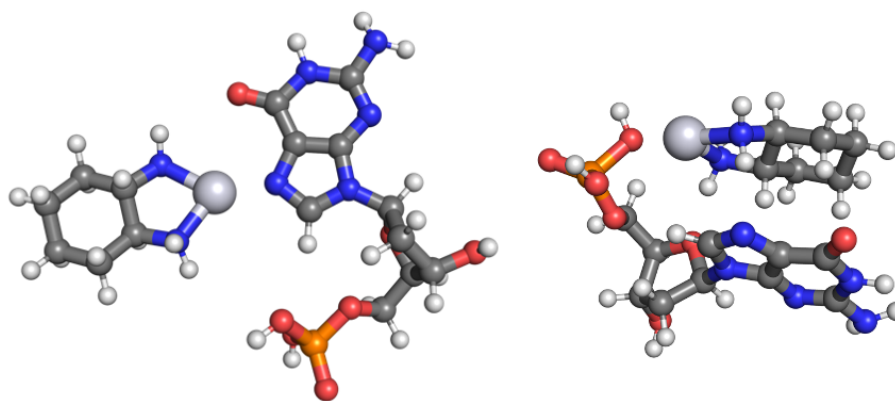


Figure 5.29: Optimised structures of OXPT-1 and dGMP building block. Conf1 (left) and Conf3 (right)

On average, OXPT-1 preferentially interacts with GMP over dGMP, giving rise to an average E_{INT} of -743.4 and -675.4 kJ mol^{-1} , respectively. However, upon comparing the strongest interaction configurations, OXPT-1 interacts more strongly with dGMP, by 14.3 kJ mol^{-1} . The preferential binding of OXPT-1 of dGMP over GMP could be seen in Figure 5.29, where different

binding modes between this active form of oxaliplatin with the nucleobase is observed. While the Pt metal ion coordinates to the N7 in both dGMP and GMP, forming the Pt-N7 bond of 2.0 Å, the metal ion also coordinates to the carbonyl group on dGMP at a relatively short distance of 2.1 Å or the phosphate group at a similar distance of 2.1 Å on GMP. The binding event resulted in a difference in building block geometries, giving rise to RMSD values of 1.488 and 1.852 Å for dGMP and GMP, respectively (Figure 5.28). The most significant difference in geometries were due to the displacement of the phosphate group, likely to accommodate the formation of hydrogen bonding with *OXPT*-1. The formation of the Pt-O dative bond with either the base or the phosphate group could result in the slightly stronger interaction between the building block and the Pt complexes, which was not observed in the case of cisplatin (see Figures 5.12 and 5.13).

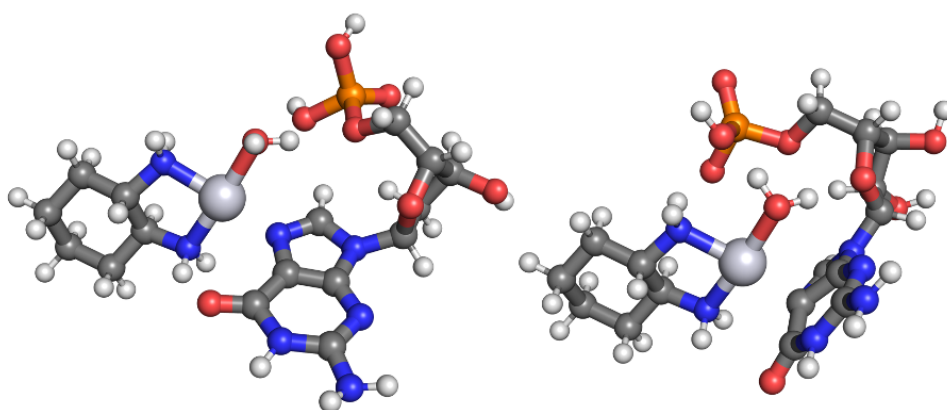


Figure 5.30: Optimised structures of dGMP or GMP with *OXPT*-2.

As seen in Figure 5.26, the interaction energy of *OXPT*-2 is significantly lower than that of *OXPT*-1, an average of 107.7 and 187.6 kJ mol⁻¹ lower for dGMP and GMP, respectively. For dGMP, *OXPT*-2 is able to form the Pt-N7 bond at 2.0 Å and two additional hydrogen bonds between the Pt-bound water molecule and the phosphate group and between the NH₂ group to the C=O on guanine (Figure: 5.30). For GMP, the conformation that resulted in the strongest interaction was accompanied by the formation of a Pt-N7 bond of 2.8 Å, 0.8 Å longer than

the experimental value.⁸⁶ This could be due to the formation of hydrogen bonding between the NH_2 group and the phosphate group. In addition, *OXPT-2* was able to interact with the oxygen atom on the sugar, forming a hydrogen bond with the Pt-bound water molecule at a distance of 1.9 Å. The inability to form the second Pt-O dative bond between the building blocks and the Pt centre due to the presence of an explicit water molecule could explain the weaker interaction when compared to *OXPT-1*.

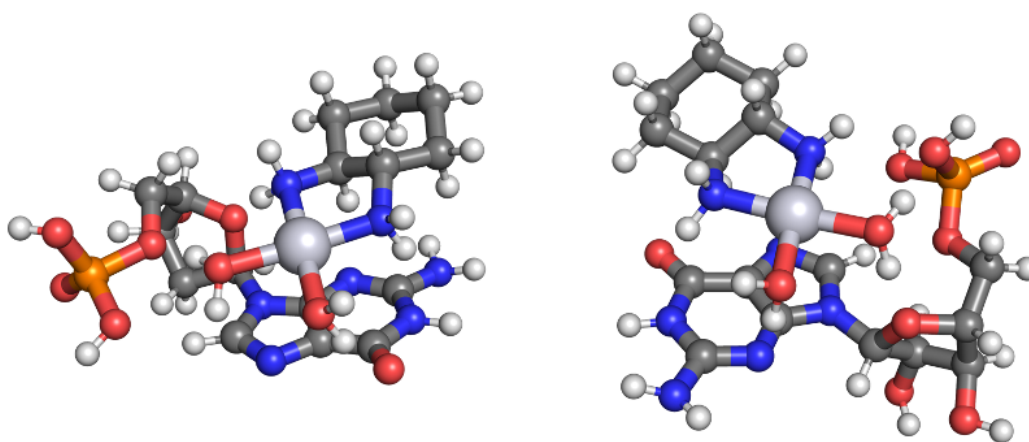


Figure 5.31: Optimised structures of dGMP or GMP with *OXPT-3*.

The presence of two Pt bound water molecules deters the formation of the Pt-N7 bond and, expectedly, interacts the weakest with dGMP and GMP when compared to *OXPT-1* and *OXPT-2*. The lack of the Pt-N7 dative bond formation between *OXPT-3* and dGMP or GMP is evident with lengthening of the Pt-N7 distance to 3.3 and 3.7 Å for dGMP and GMP, respectively (see Figure 5.31). While *OXPT-3* is still able to form hydrogen bonds and interact with dGMP and GMP, it has been shown to be unable to form the vital Pt-N7 that is required to disrupt the structure of DNA and RNA.

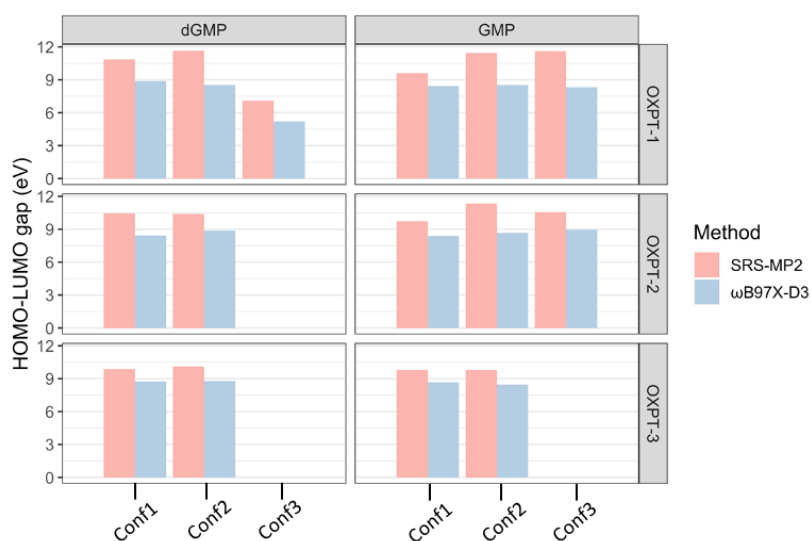


Figure 5.32: HOMO-LUMO (eV) gap of dGMP and GMP calculated with SRS-MP2 and ω B97X-D3.

Table 5.6: Difference in the predicted HOMO-LUMO gaps (eV) between SRS-MP2 and ω B97X-D3

Activated Oxaliplatin	Configuration	dGMP	GMP
OXPT-1	1	2.002	1.179
	2	3.123	2.898
	3	1.876	3.293
OXPT-2	1	2.008	1.349
	2	1.483	2.671
	3		1.629
OXPT-3	1	1.115	1.128
	2	1.329	1.355

Figure 5.32 presents the predicted HOMO-LUMO gaps for dGMP and GMP calculated using both SRS-MP2 and ω B97X-D3. Similar to cisplatin, SRS-MP2 predicts a larger HOMO-LUMO gap than ω B97X-D3 when the dGMP and GMP interacts with the activated forms of oxaliplatin, averaging 1.8 and 1.9 eV for dGMP and GMP, respectively (Table 5.6, Figure 5.32). The largest HOMO-LUMO gap predicted by SRS-MP2 is Conf2 of OXPT-1 for dGMP (11.7 eV) and Conf3 of OXPT-1 for GMP (11.6 eV). With an average HOMO-LUMO gap of 2.3, 1.7 and 1.2 eV for OXPT-1, OXPT-2 and OXPT-3 for dGMP, respectively, the decrease in energy gap is associated with the increasing number of Pt bound water molecules. The same trend can be observed for

GMP, giving rise to an average HOMO-LUMO gap of 2.5, 1.9 and 1.2 eV for *OXPT*-1, *OXPT*-2 and *OXPT*-3, respectively. With the increase of Pt bound water molecules, there is a decrease in the difference in HOMO-LUMO gap. Similar to that discovered for cisplatin, the changing nature of the Pt-N7 bond could result in the difference in closeness in the HOMO-LUMO gap of the two different methods from *OXPT*-1 and *OXPT*-2 to *OXPT*-3.

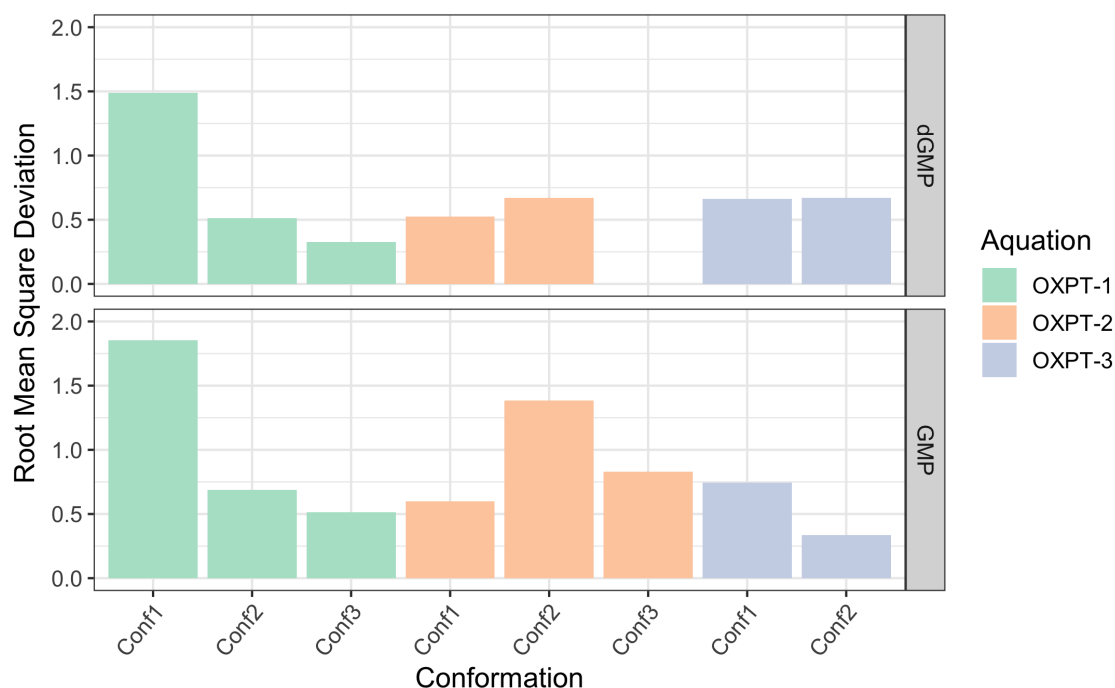


Figure 5.33: RMSD values of dGMP and GMP building blocks after binding to either *OXPT*-1, *OXPT*-2 or *OXPT*-3.

Again, the geometries of the GMP block were found to undergo significant changes compared to the dGMP building block upon binding to the activated forms of oxaliplatin, with an average RMSD of 1.0, 0.9 and 0.5 Å for *OXPT*-1, *OXPT*-2 and *OXPT*-3, respectively. dGMP is significantly less affected by the binding event, resulting with an average RMSD of 0.8, 0.6 and 0.7 Å for *OXPT*-1, *OXPT*-2 and *OXPT*-3, respectively. This suggests that oxaliplatin is able to disrupt the structural integrity of GMP more than that of dGMP. The largest RMSD values of 1.5 and 1.9 Å were observed due to the interaction between *OXPT*-1 and the dGMP and GMP building blocks, respectively, suggesting that *OXPT*-1 is able to distort the geometry of the DNA/RNA building blocks to a greater extent.

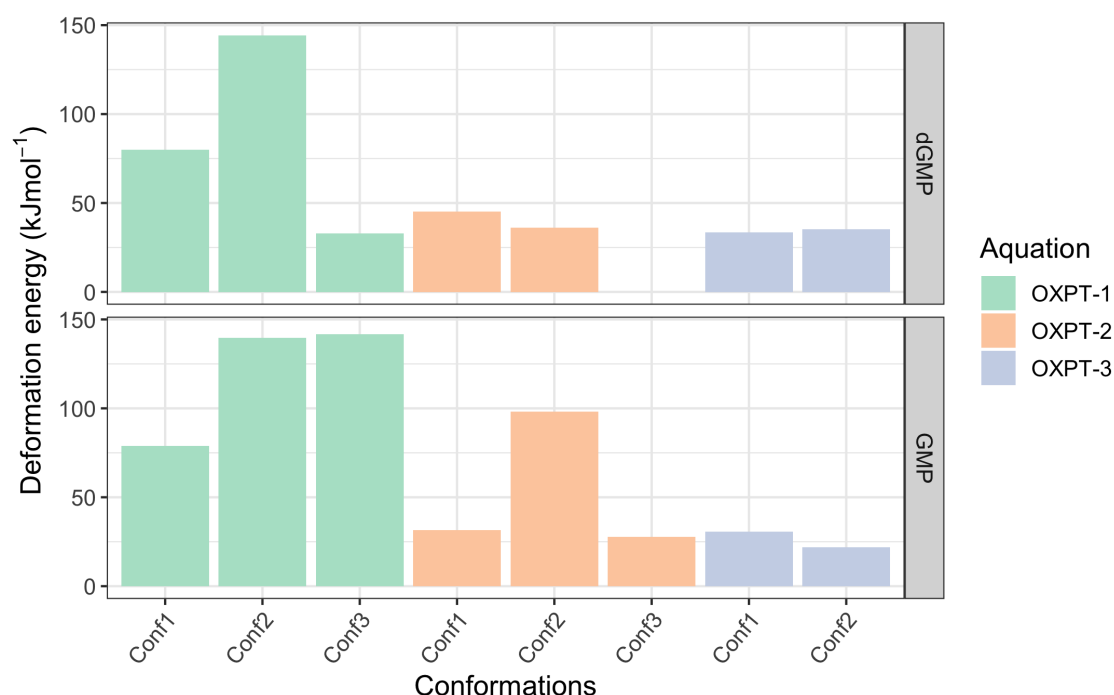


Figure 5.34: Deformation energies (kJ mol^{-1}) of the dGMP and GMP building after binding to either OXPT-1, OXPT-2 or OXPT-3.

However, after investigating the deformation energies of dGMP and GMP, there does not seem to be a direct relationship between deformation energy and RMSD (Figures 5.33 and 5.34). For example, while Conf2 of OXPT-1 resulted in the highest deformation energy of $144.4 \text{ kJ mol}^{-1}$ for dGMP, it did not result in the largest geometric change, resulting in a RMSD of 0.5 \AA . The same phenomenon was observed for GMP, where Conf2 and Conf3 of OXPT-1 resulted in the largest deformation energies of 139.8 and $141.8 \text{ kJ mol}^{-1}$, respectively. Yet it did not result in the largest RMSD values that were found to be below 0.7 \AA for both configurations. When comparing the geometries of GMP before and after binding to OXPT-1, Conf2 and Conf3 of OXPT-1 resulted in different geometries of the base. The resultant geometry of GMP after interacting with Conf2 of OXPT-2 resulted in a tilt in the guanine base, resulting in a dihedral angle of -165° between the C=O and C-H groups, and differing by 15° when compared to the original geometry of the building block (Figure: 5.35). The resultant bend in the guanine in Conf2 of OXPT-1 was to accommodate the Pt complex. For Conf3 of OXPT-1, the interaction with the Pt complex resulted in the displacement of the phosphate group, resulting in a dihedral angle of 61° between the phosphate and the sugar, differing by 7° when compared to the optimised structure of GMP before interacting with OXPT-1 (Figure: 5.35).

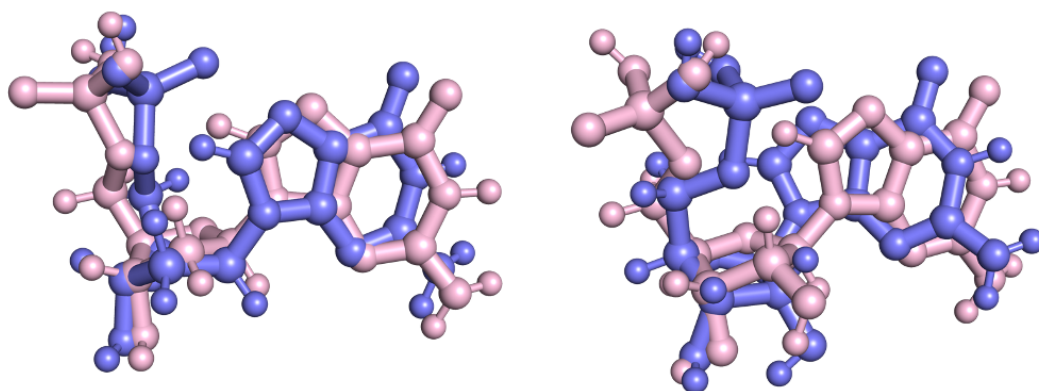


Figure 5.35: *Geometric changes of dGMP (left) and GMP (right) before (pink) and after (blue) binding to OXPT-1.*

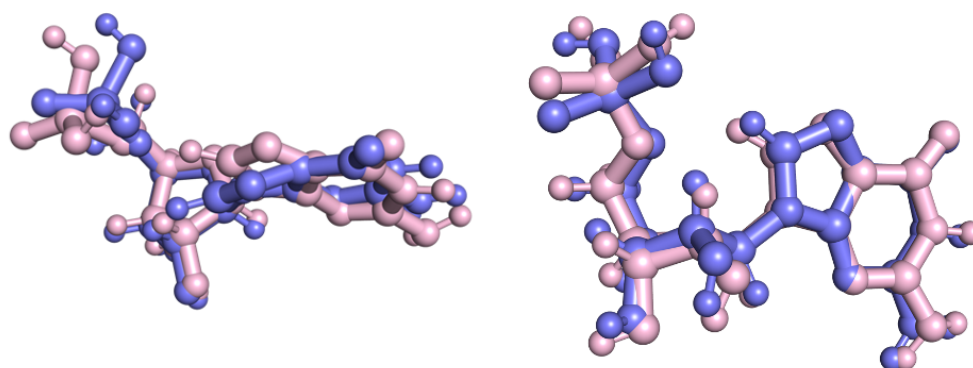


Figure 5.36: *Geometric changes of GMP after interacting with Conf2 (left) and Conf3 (right) of OXPT-1. The structure in pink and blue are before and after binding to OXPT-1, respectively.*

The effects of building blocks interacting with OXPT-1 can be seen in Figure 5.36. Before OXPT-1 binding, the dihedral angles between the sugar and the phosphate group was 52° and 54° for dGMP and GMP, respectively. After the binding to OXPT-1, the dihedral angle

changed to 52° and 48° for dGMP and GMP, respectively. This suggests that GMP might be more receptive to geometric changes than dGMP when interacting with *OXPT*-1. Interestingly, the dihedral angles between the sugar and the phosphate group was measured to be 45° and 66° after binding to *CPPT*-1 for dGMP and GMP, respectively. For dGMP, there is a difference of dihedral angle of 7° and no changes after binding to *CPPT*-1 and *OXPT*-1, respectively. The displacement of the phosphate group for GMP is more significant due to binding, with a difference of dihedral angle of 12° and 6° .

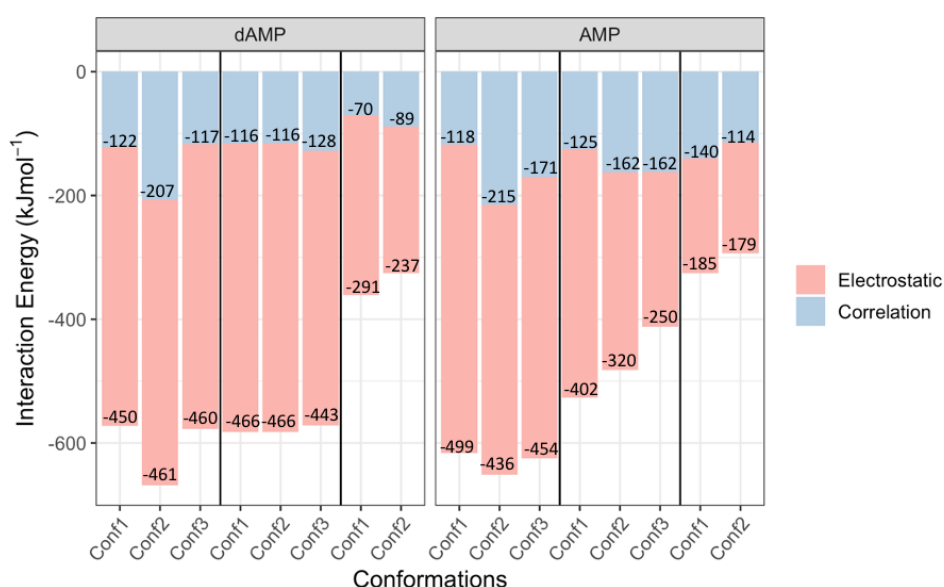


Figure 5.37: *Electrostatic and correlation components to the interaction between oxaliplatin with either dAMP or AMP.*

Similar to dGMP and GMP, the electrostatics continue to dominate over correlation in determining the interactions between building blocks and the Pt complex. Figure 5.37 displays the electrostatic and correlation components between dAMP or AMP and *OXPT*-1, *OXPT*-2 or *OXPT*-3. While the average electrostatic component for *OXPT*-1, *OXPT*-2 and *OXPT*-3 with dAMP are -457.0 , -458.3 and -264.0 kJ mol^{-1} , the average correlation is -148.7 , -120.0 and -79.4 kJ mol^{-1} , respectively. On the other hand, the average electrostatic component for *OXPT*-1, *OXPT*-2 and *OXPT*-3 with AMP is -462.9 , -323.9 and -182.0 kJ mol^{-1} , respectively. The average correlation component for *OXPT*-1, *OXPT*-2 and *OXPT*-3 with AMP are -168.0 , -150.0 and -127.2 kJ mol^{-1} , respectively. This is in agreement with the previously studied systems (Figures

5.11, 5.19, 5.27) where the decrease in electrostatic is more significant than the decrease in correlation with the increase of Pt bound water molecules.

Table 5.7: *Pt-N7 distance (\AA) between activated oxaliplatin and dAMP or AMP building blocks. Values in brackets indicate the absolute deviation from the experimental value of 2.010 \AA .^{61,105}*

Activated for of Oxaliplatin	Configuration	dAMP	AMP
OXPT-1	1	1.994 (0.016)	1.995 (0.015)
	2	2.059 (0.049)	2.042 (0.032)
	3	1.995 (0.015)	2.885 (0.875)
OXPT-2	1	1.996 (0.014)	2.002 (0.008)
	2	1.996 (0.014)	2.894 (0.884)
	3	1.995 (0.015)	3.179 (1.169)
OXPT-3	1	5.176 (3.166)	3.807 (1.797)
	2	4.474 (2.464)	3.357 (1.347)

A similar analysis was performed for the dAMP and AMP building blocks. Table 5.7 displays the Pt-N7 distances between the activated forms of oxaliplatin and dAMP or AMP building blocks. Again, the inability of the di-aquated form of oxaliplatin, OXPT-3, to form the vital Pt-N7 bond was demonstrated, with the optimised structures yielding a Pt-N7 distance between 3.357 to 4.474 \AA . Both OXPT-1 and OXPT-2 have demonstrated their ability to interact with both dAMP and AMP, forming the dative Pt-N7 bond ranging between 1.994 to 2.059 \AA . Again, the formation of this Pt-N7 bond is configuration-dependent, where Conf3 of AMP with OXPT-1 and Conf2 and Conf3 of OXPT-2 with AMP did not result in the formation of the dative bond.

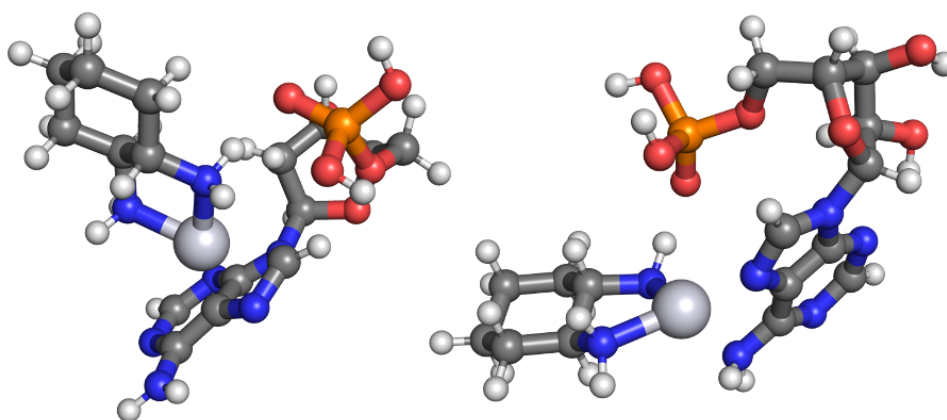


Figure 5.38: Optimised structures between *OXPT-1* and dAMP (left) and AMP (right).

OXPT-1 was also found to preferentially bind to AMP over dAMP with an average E_{INT} of -630.8 and -605.7 kJ mol^{-1} , respectively. The extent of preferential binding of AMP over dAMP is less significant as in the case of GMP over dGMP, with an average difference in 25.1 kJ mol^{-1} for the AMP/dAMP pair and 68.0 kJ mol^{-1} for the GMP/dGMP pair. Figure 5.38 shows the formation of different hydrogen bonds between *OXPT-1* and dAMP or AMP. Whereas hydrogen bonds form between NH_2 of *OXPT-1* and the phosphate group of dAMP at 1.9 Å, hydrogen bonds form between *OXPT-1* with both the phosphate group at 1.7 Å and the NH_2 group at 2.2 Å. The binding event resulted in geometrical changes of the building blocks. Whereas binding of *OXPT-1* resulted in a RMSD value of 0.781 Å for dAMP, it resulted in a RMSD value of 1.717 Å for AMP, demonstrating its ability to influence the geometry of AMP more than dAMP (for more detail see Figure 5.39).

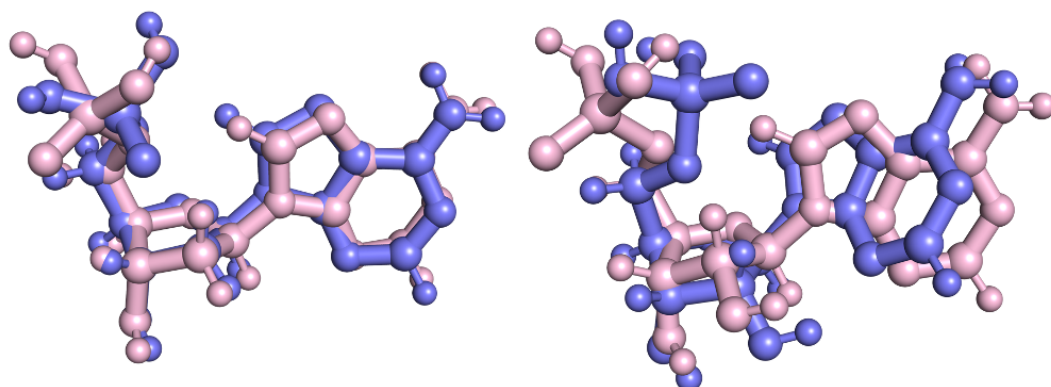


Figure 5.39: Visual geometric changes in dAMP (left) and AMP (right) before (pink) and after (blue) binding to OXPT-1

The effects of OXPT-1 binding to the AMP/dAMP building block can be visually seen in Figure 5.39. Before OXPT-1 binding, the dihedral angles between the sugar and the phosphate group was 53° and 53° for dAMP and AMP, respectively. After binding to OXPT-1, both dihedral angles increased significantly to 69° and 66° for dAMP and AMP, respectively. This suggests that both dAMP and AMP are equally susceptible to geometric changes when interacting with OXPT-1.

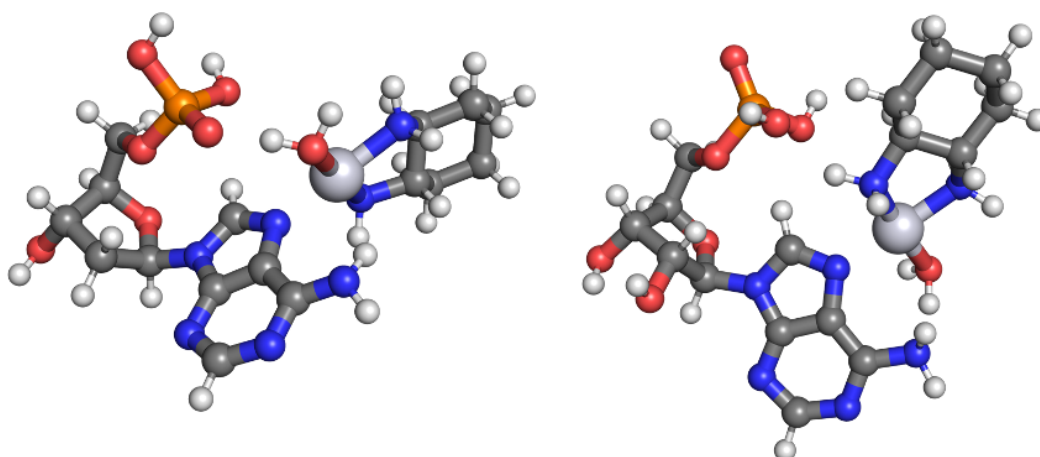


Figure 5.40: Optimised structures of dAMP and AMP with OXPT-2

The configurations that resulted in the strongest interaction energy between *OXPT-2* and dAMP and AMP appear to be rather similar (see Figure 5.40), with a flip about the Pt centre resulting in the bound water molecule to be opposite sides of the adenine base. This difference in orientation results in different hydrogen bonding. While both dAMP and AMP formed the Pt-N7 dative bonds, both at around 2.0 Å, the interaction between dAMP and *OXPT-2* was found to form a hydrogen bond between the Pt bound water molecule and the O on the phosphate group at 1.6 Å. On the other hand, AMP resulted in the formation of hydrogen bonds between the NH₂ and the O atom on the phosphate at 2.1 Å and between the Pt bound water molecule and the NH₂ group on the adenine base at 1.8 Å. This difference in the interaction resulted in a preferential binding of *OXPT-2* to dAMP over AMP by 104.8 kJ mol⁻¹.

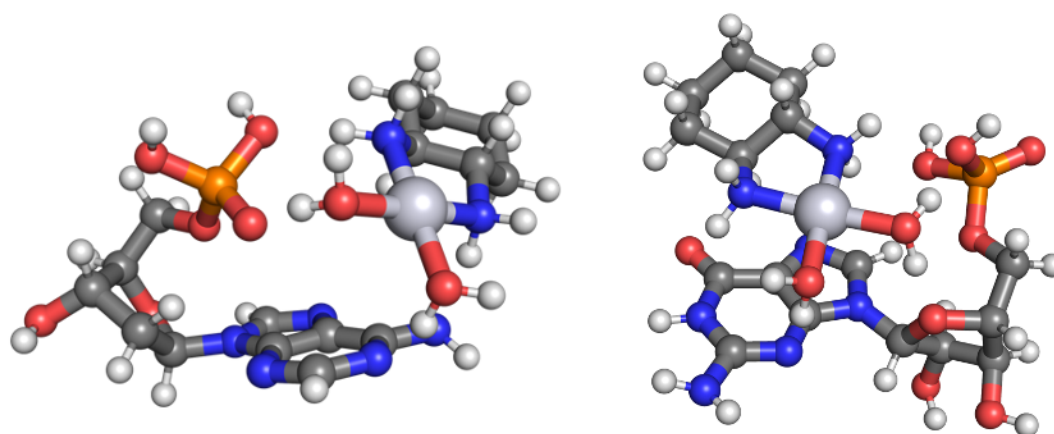


Figure 5.41: Optimised structures of dAMP and AMP with *OXPT-3*

Similar to *CPPT-3*, *OXPT-3* was unable to form a dative Pt-N7 bond, resulting in the weakest interaction energy when compared to *OXPT-1* and *OXPT-2* (see Figure 5.41). The Pt-N7 distance again is increased to 5.2 and 3.8 Å for dAMP and AMP, respectively, which is a result of hydrogen bonds between the Pt bound water molecules and NH₂ on *OXPT-3*. The presence of the two Pt bound water molecules, again, prevented the formation of the Pt-N7 dative bond. For dAMP, *OXPT-3* was still able to form hydrogen bonds with the N atom on the 4-pyrimidinamine of adenine and the phosphate group, with distances ranging from 1.6 to 2.0 Å. On the other hand, *OXPT-3* was able to form hydrogen bonds with the 4-pyrimidinamine ring

of adenine, the phosphate group and the imidazoline ring, with distances ranging from 1.7 to 2.3 Å.

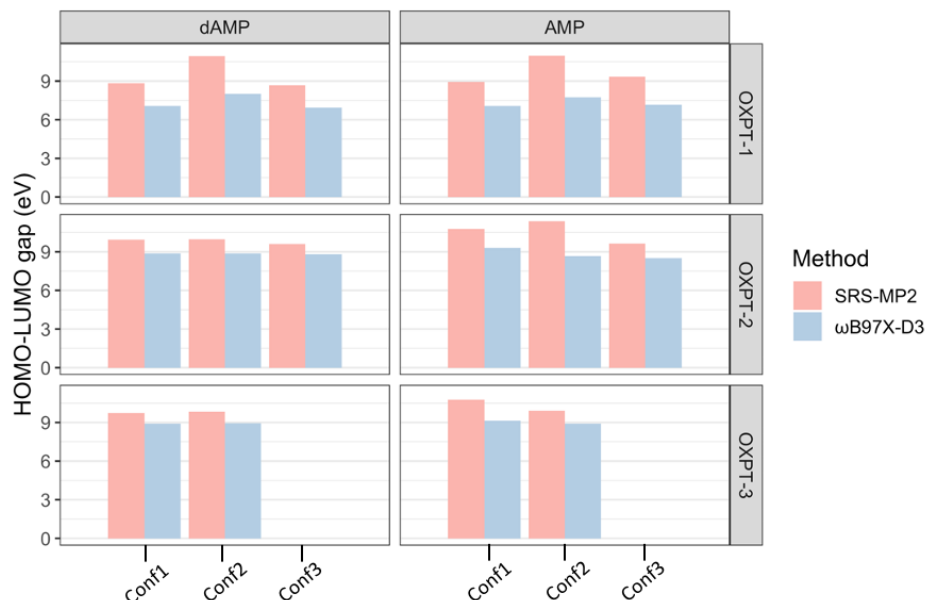


Figure 5.42: HOMO-LUMO (eV) gaps of dAMP and AMP calculated with SRS-MP2 and ω B97X-D3.

Table 5.8: Differences in predicted HOMO-LUMO gap (eV) as calculated with SRS-MP2 and ω B97X-D3

Activated Oxaliplatin	Configuration	dAMP	AMP
OXPT-1	1	1.780	1.892
	2	2.930	3.260
	3	1.759	2.160
OXPT-2	1	1.086	1.463
	2	1.094	2.701
	3	0.790	1.121
OXPT-3	1	0.827	1.643
	2	0.920	1.014

Figure 5.42 shows the predicted HOMO-LUMO gaps for dAMP and AMP with activated oxaliplatin using both SRS-MP2 and ω B97X-D3 to explain the difference in predicted interaction energies. Similar to the previous complexes, SRS-MP2 consistently predicts a larger HOMO-LUMO gap than ω B97X-D3, averaging 1.3 and 1.8 eV for dAMP and AMP, regardless of the activation state of oxaliplatin (see Figure 5.42 and Table 5.8). For dAMP, the largest HOMO-LUMO energy gap predicted by SRS-MP2 was found to be 10.9 eV when interacting with

OXPT-1, whereas for AMP the largest HOMO-LUMO energy gap was calculated to be 11.4 eV when interacting with *OXPT*-2. The average differences in the HOMO-LUMO gap were calculated to be 2.2, 1.0 and 0.9 eV for *OXPT*-1, *OXPT*-2 and *OXPT*-3, respectively, when bound to dAMP, and 2.4, 1.8 and 1.3 eV, respectively, when bound to AMP. The decrease in orbital energy differences is coupled with the increase in number of Pt bound water molecules. There is a correlation between the decrease in difference in predicted HOMO-LUMO gap and the closeness in predicted interaction energies. This could be seen with the difference between ω B97X-D3 and SRS-MP2 interaction energies decreasing from 42.5 to 3.1 kJ mol⁻¹ for dAMP with increasing water molecules, indicating a different type of interaction.

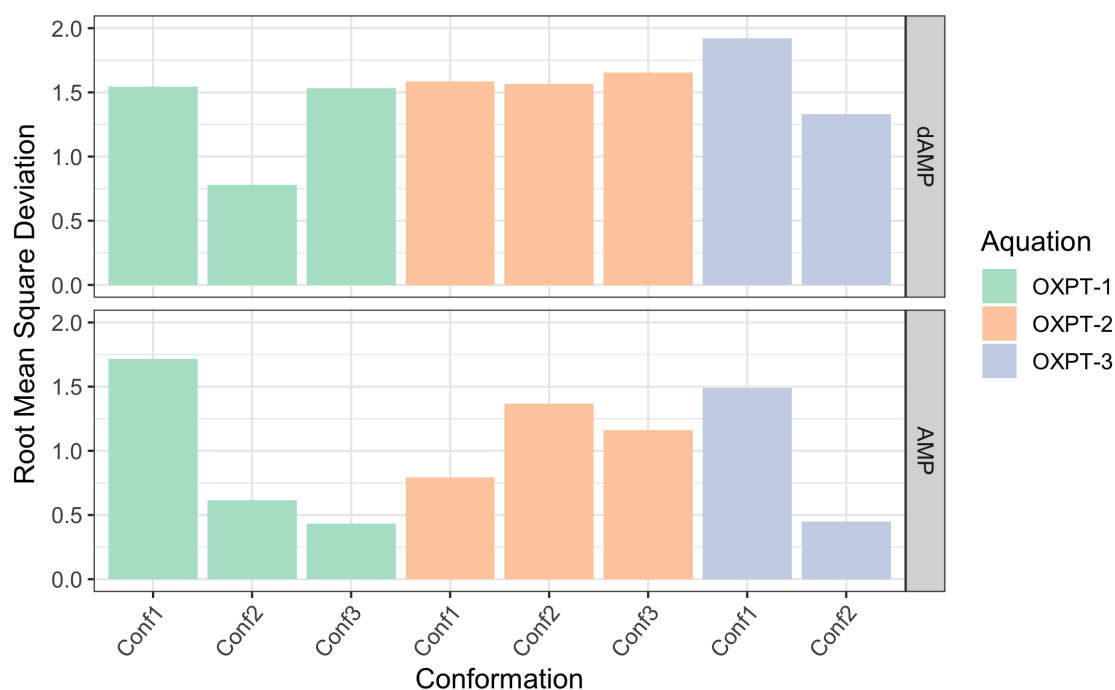


Figure 5.43: RMSD values of dAMP and AMP building blocks after binding to *OXPT*-1, *OXPT*-2 and *OXPT*-3.

Overall, oxaliplatin affects the geometry of the dAMP building block more than that of AMP, with RMSD values averaging 1.4 and 1.1 Å, respectively (see Figure 5.43). While the largest RMSD value for dAMP was calculated to be 1.9 Å when interacting with *OXPT*-3, the largest RMSD value for AMP was found to be 1.7 Å when interacting with *OXPT*-1. On average, *OXPT*-1, *OXPT*-2 and *OXPT*-3 resulted in average RMSD values of 1.3, 1.6 and 1.6 Å, respectively, for dAMP and 0.9, 1.1 and 1.0 Å, respectively, for AMP. Contrasting the observed trends in dGMP and GMP, when *OXPT*-1 resulted in the largest average RMSD value for dGMP and GMP,

OXPT-2 produced the largest geometric difference in the dAMP and AMP building blocks after binding.

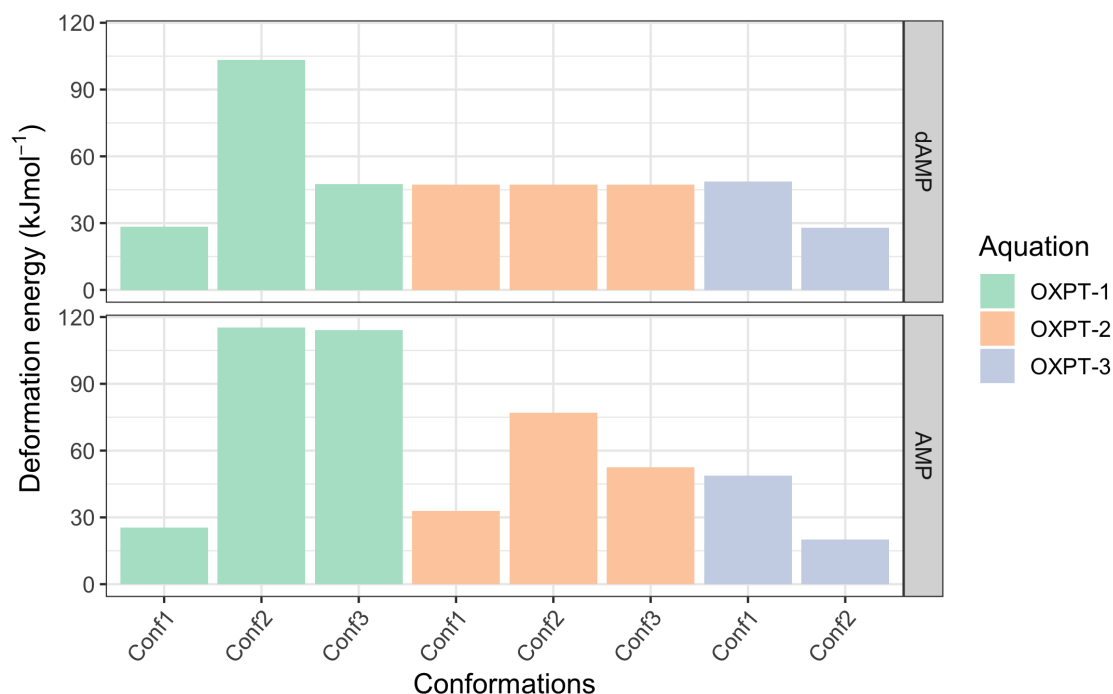


Figure 5.44: Deformation energies (kJ mol^{-1}) of the dAMP and AMP building block after binding to either *OXPT-1*, *OXPT-2* or *OXPT-3*.

From Figure 5.44, the largest deformation energies of 103.4 for dAMP kJ mol^{-1} and 115.3 kJ mol^{-1} for AMP were observed due to interaction with *OXPT-1*. Again, the largest deformation energies, both observed in Conf2 of optimised structures with *OXPT-1*, were not accompanied with the largest RMSD values (Figures 5.43), averaging 0.8 and 0.6 Å for dAMP and AMP, respectively.

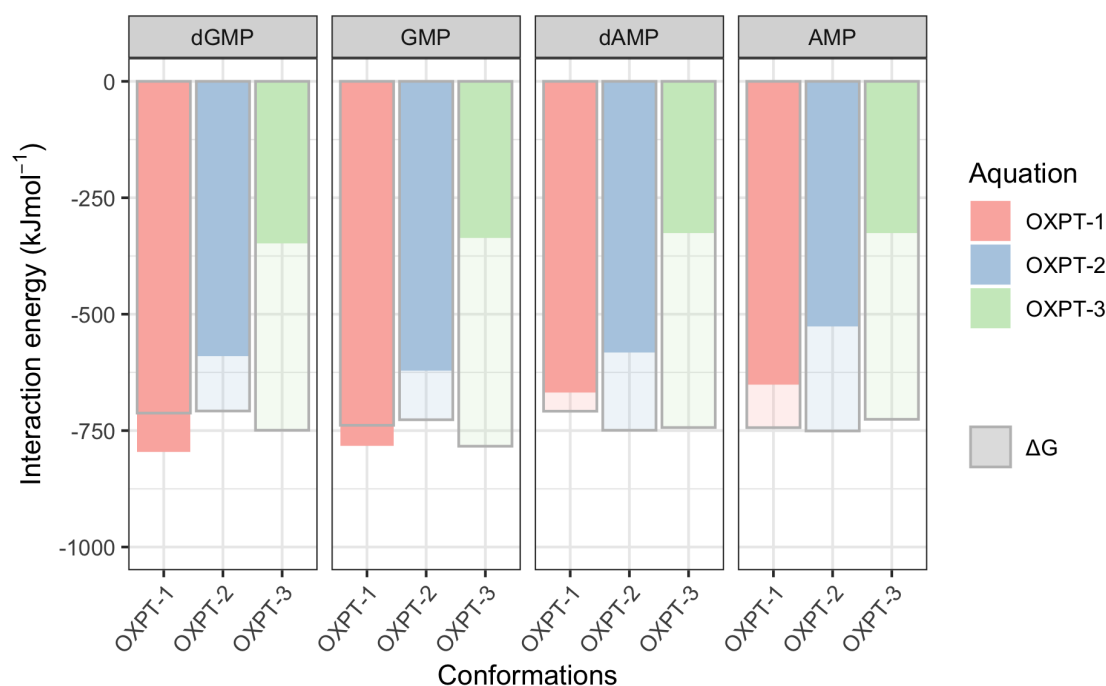


Figure 5.45: Interaction energies and Gibbs free energies of solvation (ΔG_{solv} , kJ mol^{-1}) of complexes between activated forms of oxaliplatin (OXPT-1, OXPT-2 and OXPT-3) and dGMP, GMP, dAMP or AMP.

Figure 5.45 displays the strongest interacting configuration of each building block, dGMP, GMP, dAMP and AMP with oxaliplatin of various aquation states, OXPT-1, OXPT-2 and OXPT-3. Figure 5.45 displays a similar trend to cisplatin, where there is a decrease in interaction energy between the Pt complex and DNA/RNA building blocks with increasing number of Pt bound water molecules. OXPT-1 gives rise to the largest interaction energy, ranging from -651.0 to $-796.4 \text{ kJ mol}^{-1}$ across all four building blocks. The largest interaction energy was obtained to be $-796.4 \text{ kJ mol}^{-1}$, a result of OXPT-1 interacting with dGMP. The comparison of interaction energy of between dGMP and dAMP also revealed that OXPT-1 preferentially binds with dGMP over dAMP by $128.3 \text{ kJ mol}^{-1}$, similar to that of CPPT-1. OXPT-1 also preferentially binds to GMP over AMP, by $131.1 \text{ kJ mol}^{-1}$.

Analysis of Gibbs free energies of solvation, ΔG_{solv} , again produced similar values ranging from -707.9 to $-783.5 \text{ kJ mol}^{-1}$, with the former corresponding to dGMP interacting with OXPT-2 and the latter to GMP interacting with OXPT-3. Similar to cisplatin, this is a small variation in the solvation energies across building blocks and activated forms of oxaliplatin. This clearly

indicates that the solvation of the building block strongly influences the overall solvation rather than the activated form itself.

5.3.3 Comparison of binding between cisplatin and oxaliplatin with DNA and RNA building blocks

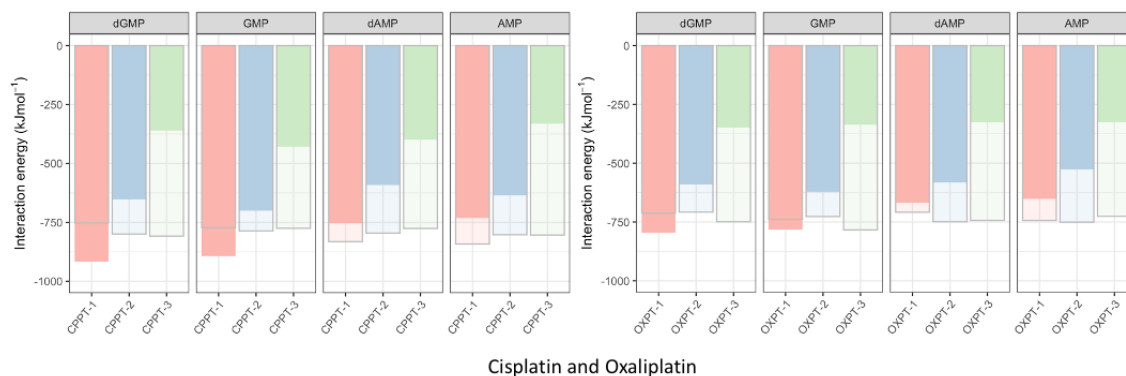


Figure 5.46: Strongest interaction energies calculated between DNA/RNA building blocks and activated forms of cisplatin and oxaliplatin.

Overall, SRS-MP2 calculations indicates that cisplatin results in stronger interactions with both DNA and RNA building blocks, averaging -823.6 , -645.1 and -380.0 kJ mol^{-1} for *CPPT*-1, *CPPT*-2 and *CPPT*-3, respectively, regardless of building block. The average interaction energies for *OXPT*-1, *OXPT*-2 and *OXPT*-3 were calculated to be -724.4 , -580.1 and -333.7 kJ mol^{-1} , respectively, regardless of building block. Among the activated forms, *CPPT*-1 and *OXPT*-1 were found to form the strongest bound complexes with both RNA and DNA building blocks, further highlighting that the non-aquated form is the most likely candidate to bind with DNA or RNA. This is consistent with the already established consensus that the fully dissociated equivalent of Pt complexes are likely to bind to DNA or RNA.

The mono-aquated form, either *CPPT*-2 or *OXPT*-2, does not interact as strongly to the building blocks as compared to *CPPT*-1 and *OXPT*-1, by an average of 178.5 and 144.3 kJ mol^{-1} , respectively. This form is still able to form the dative Pt-N7 bond (see Figures 5.13, 5.20, 5.30 and 5.40) falling in the range between 1.9 and 2.0 Å. It is suggested that this form is equally

capable of disrupting the structural integrity of DNA and RNA, potentially serving as a precursor complex before the water molecule is liberated and a stronger bond interaction is formed between the non-aquated form and DNA/RNA building blocks.

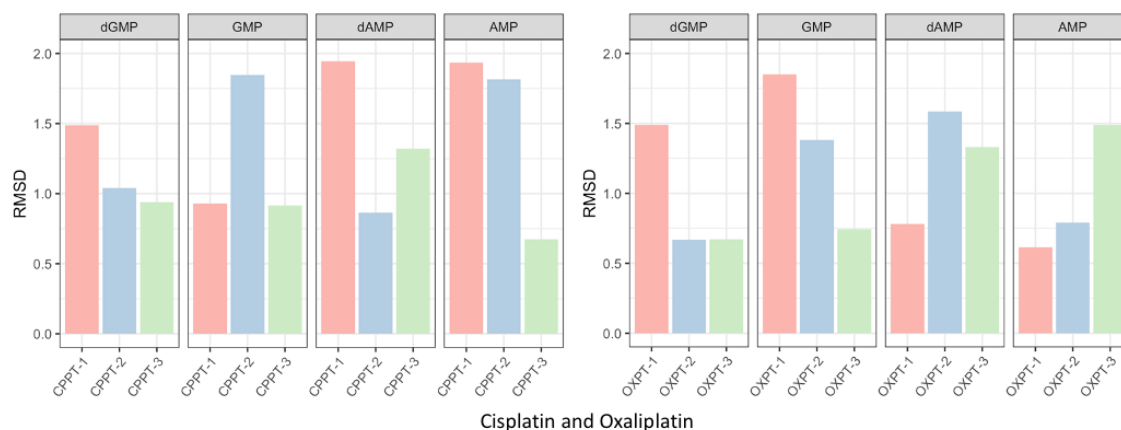


Figure 5.47: *RMSD values of DNA/RNA building blocks after interacting with activated forms of cisplatin and oxaliplatin.*

As shown in Figure 5.47, the RMSD values corresponding to geometric changes of building blocks do not exhibit a trend with respect to the formation of the dative Pt-N7 bond. The di-aquated forms of CPPT-3 and OXPT-3 have been demonstrated to be able to significantly alter the geometry of DNA or RNA building blocks. For example, CPPT-3 resulted in a large RMSD value of 1.3 Å after interacting with dAMP, compared to that of 0.9 Å observed for CPPT-2. Similarly, OXPT-3 was able to alter the geometries of building blocks to a larger extent (an RMSD value of 1.5 Å) than OXPT-1 (an RMSD value of 0.8 Å) and OXPT-2 (an RMSD value of 0.6 Å). The larger RMSD values could be attributed to the formation of hydrogen bonds between the Pt bound water molecules and the building blocks. These types of hydrogen bonding may not be available in the actual models of RNA and DNA as the phosphate groups become less flexible due to the presence of a long backbone and explicit water molecules.

This raises the question about the identity of the Pt complexes that are more likely to bind to DNA or RNA. The present results clearly indicate that the mono-aquated form cannot be excluded as a potential candidate to bind to the building blocks. The mono-aquated form may serve as a pre-cursor complex, before the water molecule dissociates and a stronger dative bond is formed between the Pt metal centre and DNA/RNA building blocks. Single nucleobase

models are used in this work to study the strength and mode of binding between activated forms of cisplatin and oxaliplatin. This is a simplified model of real-sized DNA and RNA that are less flexible and more limited in terms of potential binding modes due to steric hindrance. As seen in the previous sections, the phosphate group was found to actively participate in the binding event of the Pt complexes studied, which reveals another limitation of a small model as phosphate groups are less accessible due to their strong affinity for water. It has been previously established that water molecules surround the phosphate group of DNA, forming a network of water molecules via hydrogen bonding.¹¹² The presence of explicit water molecules around the phosphate group could prevent the interaction between the phosphate group and the Pt complex. In Chapter 3, the presence of explicit solvation has been shown to be vital to stabilise the 2+ charge of the Pt complexes and plays a role in determining the hydrolysis rate of the Pt complexes. This leads to the need to investigate interactions between Pt complexes and realistic DNA/RNA models in the presence of explicit water solvation.

5.4 Conclusion

In this chapter, a comprehensive study was conducted to analyse the strength and mode of interactions between activated forms of Pt complexes, cisplatin and oxaliplatin, and DNA or RNA building blocks. The DNA building blocks utilised for this study were dGMP and dAMP, whereas the RNA building blocks utilised were GMP and AMP. These models were selected as it was previously established that the fully dissociated Pt complexes were likely species to bind to nucleobases.^[4, 7, 28] Activated forms of cisplatin and oxaliplatin in their non- ($[\text{PtL}]^{2+}$), mono- ($[\text{PtL}(\text{H}_2\text{O})]^{2+}$) and di-aquated equivalents ($[\text{PtL}(\text{H}_2\text{O})_2]^{2+}$) were selected to study the role of water molecules coordinated to the Pt centre on the binding event. Complexes between activated forms of cisplatin and oxaliplatin and DNA and RNA building block models were constructed to promote the formation of the dative Pt-N7 bond. Optimised with SRS-MP2 and implicit solvation model, SMD, the interaction energies between the Pt complexes and building blocks were calculated to identify which activated form of the Pt complexes is most likely to bind to DNA/RNA building block. It was determined that the non-aquated form, *CPPT*-1 and *OXPT*-1, consistently resulted in the strongest interaction, with an average of -764.9 and -663.9 kJ mol⁻¹, regardless of building blocks. Unsurprisingly, the strongest interaction occurred

between the non-aquated equivalent and dGMP, -916.2 and -796.4 kJ mol^{-1} for *CPPT*-1 and *OXPT*-1, respectively. This is in agreement with the previously published crystal structure where the non-aquated Pt complexes were determined to form the adducts with DNA and RNA.

Though the non-aquated form of cisplatin and oxaliplatin was known to form the dative Pt-N7 bond with the nucleobases, this study has clearly demonstrated that the mono-aquated form, *CPPT*-2 and *OXPT*-2, is also capable of forming the dative Pt-N7 bond. With an average interaction energy of -620.8 and -544.3 kJ mol^{-1} for *CPPT*-2 and *OXPT*-2, respectively, the mono-aquated Pt complexes could potentially play a role of a precursor that binds to DNA or RNA before the water molecule dissociates, thus disrupting the structural integrity of the building blocks.

The di-aquated form of cisplatin and oxaliplatin was unable to form the Pt-N7 bond due to the presence of two Pt bound water molecules. These water molecules prevent the Pt complexes from forming dative bonds with the nucleobase, resulting in a lower interaction energy than its non- and mono-aquated counterparts. *CPPT*-3 and *OXPT*-3 resulted in an average interaction energy of -345.5 and -324.6 kJ mol^{-1} , respectively. This suggests that *CPPT*-3 and *OXPT*-3 are unlikely candidates to bind to DNA or RNA.

RMSD and deformation energies were employed as a measure of how the binding of Pt complexes alters the geometries of the various building blocks. Upon comparison, there is no direct relationship between RMSD and deformation energies. This is a result of the formation of different building block geometries to accommodate the Pt complexes. An example of this is the resultant dGMP geometry after interacting with Conf3 of *CPPT*-1. Whereas it resulted in the largest deformation energy when compared to the other configurations, 143.8 kJ mol^{-1} , it resulted in a small RMSD of 0.4 Å when compared to the geometry of dGMP before binding. This phenomenon was explained by the changes in dihedral angles between the sugar and phosphate group as well as the dihedral angles between the sugar and the guanine. After binding to *CPPT*-1, the dihedral angle changed from 54° to 69° .

Upon comparison of the strongest interacting configurations of the activated forms of cisplatin and oxaliplatin with the various different building blocks, it is suggested that different aquated

states of the Pt complexes would preferentially bind to either DNA or RNA building blocks. This could be due to the additional hydrogen bonds being formed between the Pt complex and the building blocks. For example, while *CPPT*-1 preferentially binds to DNA over RNA building blocks, by an average of 22.7 kJ mol^{-1} , *CPPT*-2 preferentially binds to RNA building blocks, by an average of 45.8 kJ mol^{-1} . The preferential binding of Pt complexes to either DNA or RNA could facilitate binding to either building blocks and cannot be excluded as a potential candidate to bind to DNA or RNA building blocks.

The comparison of predicted interaction energies using the two methods, ω B97X-D3 and SRS-MP2, was also investigated. The interaction energies predicted by ω B97X-D3 were consistently underestimated when compared to those of SRS-MP2. However, the difference in predicted interaction energies decreases with the increase in Pt bound water molecules. An example of this is the decrease of absolute errors, from 83.8 to 4.5 kJ mol^{-1} , for dGMP and cisplatin. Subsequently, HOMO-LUMO energy gaps were utilised to explain this phenomenon. It was revealed that on average the HOMO-LUMO energy gap predicted by ω B97X-D3 was smaller than that of SRS-MP2. This was not surprising as it is established that DFT functionals tend to underestimate HOMO-LUMO energy gaps. It was observed that the difference in predicted HOMO-LUMO gap of the two methods decreases with increasing number of Pt bound water molecules. This emphasises the different type of bonds present between the activated form of the Pt complexes as well.

The sugar and phosphate groups of the DNA and RNA models have been demonstrated to interact with the Pt complexes, forming hydrogen bonds, thus resulting in increased stability. The chosen small DNA and RNA models prove to be less sterically hindered than a realistic model and able to provide a stronger interaction with the Pt metal centre. Since nucleobases are involved in π - π stacking in the realistic models of DNA and RNA, there will be less spatial allowance for approaching activated forms of Pt complexes. In addition, water molecules were previously established to interact with the DNA/RNA phosphate groups, thus forming an extended hydrogen bond network. This suggests that the phosphate group in the DNA/RNA backbone is unlikely to participate in strengthening the interaction between the activated form of Pt complexes and RNA/DNA nucleobases. Therefore, more studies must be performed utilising realistic RNA and DNA building blocks and explicit water molecules to confirm that

the mono aquated form of cisplatin and oxaliplatin act as precursors before the water molecule dissociates from the Pt metal centre, exposing it for stronger interaction with nucleobases.

5.5 References

- [1] Barnett Rosenberg, Loretta Van Camp, and Thomas Krigas. Inhibition of cell division in *Escherichia coli* by electrolysis products from a platinum electrode. *Nature* **205**(4972) (1965), 698–699.
- [2] Barnett Rosenberg, Loretta Vancamp, James E Trosko, and Virginia H Mansour. Platinum compounds: a new class of potent antitumour agents. *Nature* **222**(5191) (1969), 385–386.
- [3] Markus Galanski and Bernhard K Keppler. Searching for the magic bullet: anticancer platinum drugs which can be accumulated or activated in the tumor tissue. *Anti-Cancer Agents in Medicinal Chemistry (Formerly Current Medicinal Chemistry-Anti-Cancer Agents)* **7**(1) (2007), 55–73.
- [4] Johan Raber, Chuanbao Zhu, and Leif A Eriksson. Theoretical study of cisplatin binding to DNA: the importance of initial complex stabilization. *The Journal of Physical Chemistry B* **109**(21) (2005), 11006–11015.
- [5] Alice V Klein and Trevor W Hambley. Platinum drug distribution in cancer cells and tumors. *Chemical Reviews* **109**(10) (2009), 4911–4920.
- [6] Zahid H Siddik. Cisplatin: mode of cytotoxic action and molecular basis of resistance. *Oncogene* **22**(47) (2003), 7265–7279.
- [7] Patricia M Takahara, Amy C Rosenzweig, Christin A Frederick, and Stephen J Lippard. Crystal structure of double-stranded DNA containing the major adduct of the anticancer drug cisplatin. *Nature* **377**(6550) (1995), 649–652.
- [8] Seifollah Jalili, Mina Maddah, and Jeremy Schofield. Molecular dynamics simulation and free energy analysis of the interaction of platinum-based anti-cancer drugs with DNA. *Journal of Theoretical and Computational Chemistry* **15**(06) (2016), 1650054.
- [9] Sang Soo Hah, Rhoda A Sumbad, Ralph W de Vere White, Kenneth W Turteltaub, and Paul T Henderson. Characterization of oxaliplatin- DNA adduct formation in DNA and differentiation of cancer cell drug sensitivity at microdose concentrations. *Chemical Research in Toxicology* **20**(12) (2007), 1745–1751.

- [10] Bernhard Spingler, Douglas A Whittington, and Stephen J Lippard. 2.4 Å crystal structure of an oxaliplatin 1, 2-d (GpG) intrastrand cross-link in a DNA dodecamer duplex. *Inorganic Chemistry* **40**(22) (2001), 5596–5602.
- [11] Stephen G Chaney, Sharon L Campbell, Ekaterina Bassett, and Yibing Wu. Recognition and processing of cisplatin-and oxaliplatin-DNA adducts. *Critical Reviews in Oncology/Hematology* **53**(1) (2005), 3–11.
- [12] Eslam M Moustafa, Claire L Camp, Ahmed S Youssef, Asma Amleh, Helen J Reid, Barry L Sharp, and Tamer Shoeib. Oxaliplatin complexes with carnosine and its derivatives: in vitro cytotoxicity, mass spectrometric and computational studies with a focus on complex fragmentation. *Metallomics* **5**(11) (2013), 1537–1546.
- [13] Thierry André, Corrado Boni, Lamia Mounedji-Boudiaf, Matilde Navarro, Josep Tabernero, Tamas Hickish, Clare Topham, Marta Zaninelli, Philip Clingan, John Bridge-water, et al. Oxaliplatin, fluorouracil, and leucovorin as adjuvant treatment for colon cancer. *New England Journal of Medicine* **350**(23) (2004), 2343–2351.
- [14] AM Burger, JA Double, and DR Newell. Inhibition of telomerase activity by cisplatin in human testicular cancer cells. *European Journal of Cancer* **33**(4) (1997), 638–644.
- [15] Jan Oldenburg, Sigrid M Kraggerud, Milada Cvancarova, Ragnhild A Lothe, and Sophie D Fossa. Cisplatin-induced long-term hearing impairment is associated with specific glutathione s-transferase genotypes in testicular cancer survivors. *Journal of Clinical Oncology* **25**(6) (2007), 708–714.
- [16] Murray S Davies, Susan J Berners-Price, and Trevor W Hambley. Slowing of cisplatin aquation in the presence of DNA but not in the presence of phosphate: improved understanding of sequence selectivity and the roles of monoaquated and diaquated species in the binding of cisplatin to DNA. *Inorganic Chemistry* **39**(25) (2000), 5603–5613.
- [17] CP Saris, PJ M van de Vaart, RC Rietbroek, and FA Blorumaert. In vitro formation of DNA adducts by cisplatin, lobaplatin and oxaliplatin in calf thymus DNA in solution and in cultured human cells. *Carcinogenesis* **17**(12) (1996), 2763–2769.

- [18] David H Phillips and Volker M Arlt. The ^{32}P -postlabeling assay for DNA adducts. *Nature Protocols* **2**(11) (2007), 2772.
- [19] Ewelina Lipiec, Joanna Czapla, Jakub Szlachetko, Yves Kayser, Wojciech Kwiatek, Bayden Wood, Glen B Deacon, and Jacinto Sá. Novel in situ methodology to observe the interactions of chemotherapeutical Pt drugs with DNA under physiological conditions. *Dalton Transactions* **43**(37) (2014), 13839–13844.
- [20] Luuk JP Ament, Michel Van Veenendaal, Thomas P Devereaux, John P Hill, and Jeroen Van Den Brink. Resonant inelastic x-ray scattering studies of elementary excitations. *Reviews of Modern Physics* **83**(2) (2011), 705.
- [21] Florence Gonnet, Jiří Kozelka, and Jean-Claude Chottard. Crosslinking of Adjacent Guanine Residues in an Oligonucleotide by $\text{cis-[Pt (NH}_3)_2 (\text{H}_2\text{O})_2]^{2+}$: Kinetic Analysis of the Two-Step Reaction. *Angewandte Chemie International Edition in English* **31**(11) (1992), 1483–1485.
- [22] JL Van der Veer. Investigating antitumor drug mechanisms. *Chem. Br.* **24** (1988), 775–780.
- [23] Peter M Bruno, Yunpeng Liu, Ga Young Park, Junko Murai, Catherine E Koch, Timothy J Eisen, Justin R Pritchard, Yves Pommier, Stephen J Lippard, and Michael T Hemann. A subset of platinum-containing chemotherapeutic agents kills cells by inducing ribosome biogenesis stress. *Nature Medicine* **23**(4) (2017), 461–471.
- [24] Qingfei Zhang, Gaizhen Kuang, Shasha He, Hongtong Lu, Yilong Cheng, Dongfang Zhou, and Yubin Huang. Photoactivatable Prodrug-Backboned Polymeric Nanoparticles for Efficient Light-Controlled Gene Delivery and Synergistic Treatment of Platinum-Resistant Ovarian Cancer. *Nano Letters* **20**(5) (2020), 3039–3049.
- [25] Erich G Chapman and Victoria J DeRose. Enzymatic processing of platinated RNAs. *Journal of the American Chemical Society* **132**(6) (2010), 1946–1952.
- [26] Mitsuhiro Akaboshi, Kenichi Kawai, Hirotohi Maki, Keizo Akuta, Yowri Ujeno, and Tokiharu Miyahara. The number of platinum atoms binding to DNA, RNA and protein molecules of HeLa cells treated with cisplatin at its mean lethal concentration. *Japanese Journal of Cancer Research* **83**(5) (1992), 522–526.

- [27] Mitsuhiro Akaboshi, Kenichi Kawai, Yowri Ujeno, Syotaro Takada, and Tokiharu Miyahara. Binding Characteristics of (–)-(R)-2-Aminomethylpyrrolidine (1, 1-cyclobutanedicarboxylato)-2-platinum (II) to DNA, RNA and Protein Molecules in HeLa Cells and Its Lethal Effect: Comparison with cis- and trans-Diamminedichloroplatinums (II). *Japanese Journal of Cancer Research* **85**(1) (1994), 106–111.
- [28] Alethia A Hostetter, Maire F Osborn, and Victoria J DeRose. RNA-Pt adducts following cisplatin treatment of *Saccharomyces cerevisiae*. *ACS Chemical Biology* **7**(1) (2012), 218–225.
- [29] Phillip A Sharp. The centrality of RNA. *Cell* **136**(4) (2009), 577–580.
- [30] Yitzhak Tor. Targeting RNA with small molecules. *ChemBioChem* **4**(10) (2003), 998–1007.
- [31] Ignacio Tinoco Jr and Carlos Bustamante. How RNA folds. *Journal of Molecular Biology* **293**(2) (1999), 271–281.
- [32] Harvey Lodish, Arnold Berk, S Lawrence Zipursky, Paul Matsudaira, David Baltimore, and James Darnell. Molecular cell biology 4th edition. *National Center for Biotechnology Information, Bookshelf* (2000).
- [33] Stephen Jefferson Sharp, Jerone Schaack, Lyan Cooley, Debroh Johnson Burke, and Dieter Soil. Structure and transcription of eukaryotic tRNA gene. *Critical Reviews in Biochemistry* **19**(2) (1985), 107–144.
- [34] Geoffrey M Cooper and Robert E Hausman. *The cell: Molecular approach*. 2004.
- [35] Jason R Thomas and Paul J Hergenrother. Targeting RNA with small molecules. *Chemical Reviews* **108**(4) (2008), 1171–1224.
- [36] C Frank Bennett and Eric E Swayze. RNA targeting therapeutics: molecular mechanisms of antisense oligonucleotides as a therapeutic platform. *Annual Review of Pharmacology and Toxicology* **50** (2010), 259–293.
- [37] José Gallego and Gabriele Varani. Targeting RNA with small-molecule drugs: therapeutic promise and chemical challenges. *Accounts of Chemical Research* **34**(10) (2001), 836–843.

- [38] Katherine Deigan Warner, Christine E Hajdin, and Kevin M Weeks. Principles for targeting RNA with drug-like small molecules. *Nature Reviews Drug Discovery* **17**(8) (2018), 547–558.
- [39] Xiao Li, Hilal Kazan, Howard D Lipshitz, and Quaid D Morris. Finding the target sites of RNA-binding proteins. *Wiley Interdisciplinary Reviews: RNA* **5**(1) (2014), 111–130.
- [40] Cinzia Seignani, George A Calin, Linda D Siracusa, and Carlo M Croce. Mammalian microRNAs: a small world for fine-tuning gene expression. *Mammalian Genome* **17**(3) (2006), 189–202.
- [41] K Hoogsteen. The structure of crystals containing a hydrogen-bonded complex of 1-methylthymine and 9-methyladenine. *Acta Crystallographica* **12**(10) (1959), 822–823.
- [42] Thomas Hermann and Eric Westhof. Non-Watson-Crick base pairs in RNA-protein recognition. *Chemistry & Biology* **6**(12) (1999), R335–R343.
- [43] Brenda F Baker, Sidney S Lot, Thomas P Condon, Shin Cheng-Flournoy, Elena A Lesnik, Henri M Sasmor, and C Frank Bennett. 2'-O-(2-Methoxy) ethyl-modified anti-intercellular adhesion molecule 1 (ICAM-1) oligonucleotides selectively increase the ICAM-1 mRNA level and inhibit formation of the ICAM-1 translation initiation complex in human umbilical vein endothelial cells. *Journal of Biological Chemistry* **272**(18) (1997), 11994–12000.
- [44] R.N. Shukla. *Analysis Of Chromosome*. 2014.
- [45] John A Means and Jennifer V Hines. Fluorescence resonance energy transfer studies of aminoglycoside binding to a T box antiterminator RNA. *Bioorganic & Medicinal Chemistry Letters* **15**(8) (2005), 2169–2172.
- [46] Chi-Huey Wong, Martin Hendrix, E Scott Priestley, and William A Greenberg. Specificity of aminoglycoside antibiotics for the A-site of the decoding region of ribosomal RNA. *Chemistry & Biology* **5**(7) (1998), 397–406.
- [47] Peter Jordan and Maria Carmo-Fonseca. Cisplatin inhibits synthesis of ribosomal RNA in vivo. *Nucleic Acids Research* **26**(12) (1998), 2831–2836.
- [48] Deborah B Zamble and Stephen J Lippard. Cisplatin and DNA repair in cancer chemotherapy. *Trends in Biochemical Sciences* **20**(10) (1995), 435–439.

- [49] Takuya Kumazawa, Kazuho Nishimura, Naohiro Katagiri, Sayaka Hashimoto, Yuki Hayashi, and Keiji Kimura. Gradual reduction in rRNA transcription triggers p53 acetylation and apoptosis via MYBBP1A. *Scientific Reports* **5**(1) (2015), 1–13.
- [50] Takao Kuroda, Akiko Murayama, Naohiro Katagiri, Yu-mi Ohta, Etsuko Fujita, Hiroshi Masumoto, Masatsugu Ema, Satoru Takahashi, Keiji Kimura, and Junn Yanagisawa. RNA content in the nucleolus alters p53 acetylation via MYBBP1A. *The EMBO Journal* **30**(6) (2011), 1054–1066.
- [51] Wakana Ono, Kensuke Akaogi, Tsuyoshi Waku, Takao Kuroda, Wataru Yokoyama, Yuki Hayashi, Keiji Kimura, Hiroyuki Kishimoto, and Junn Yanagisawa. Nucleolar protein, Myb-binding protein 1A, specifically binds to nonacetylated p53 and efficiently promotes transcriptional activation. *Biochemical and Biophysical Research Communications* **434**(3) (2013), 659–663.
- [52] Wakana Ono, Yuki Hayashi, Wataru Yokoyama, Takao Kuroda, Hiroyuki Kishimoto, Ichiaki Ito, Keiji Kimura, Kensuke Akaogi, Tsuyoshi Waku, and Junn Yanagisawa. The nucleolar protein Myb-binding protein 1A (MYBBP1A) enhances p53 tetramerization and acetylation in response to nucleolar disruption. *Journal of Biological Chemistry* **289**(8) (2014), 4928–4940.
- [53] Roman Mezencev. Interactions of cisplatin with non-DNA targets and their influence on anticancer activity and drug toxicity: the complex world of the platinum complex. *Current Cancer Drug Targets* **14**(9) (2014), 794–816.
- [54] Janet M Pascoe and John J Roberts. Interactions between mammalian cell DNA and inorganic platinum compounds—I: DNA interstrand cross-linking and cytotoxic properties of platinum (II) compounds. *Biochemical Pharmacology* **23**(9) (1974), 1345–1357.
- [55] Alethia A Hostetter, Erich G Chapman, and Victoria J DeRose. Rapid cross-linking of an RNA internal loop by the anticancer drug cisplatin. *Journal of the American Chemical Society* **131**(26) (2009), 9250–9257.
- [56] Sergey V Melnikov, Dieter Söll, Thomas A Steitz, and Yury S Polikanov. Insights into RNA binding by the anticancer drug cisplatin from the crystal structure of cisplatin-modified ribosome. *Nucleic Acids Research* **44**(10) (2016), 4978–4987.

- [57] Pierre Hohenberg and Walter Kohn. Inhomogeneous electron gas. *Physical Review* **136**(3B) (1964), B864.
- [58] Piotr Cysewski and Żaneta Czyżnikowska-Balcerak. The MP2 quantum chemistry study on the local minima of guanine stacked with all four nucleic acid bases in conformations corresponding to mean B-DNA. *Journal of Molecular Structure: THEOCHEM* **757**(1-3) (2005), 29–36.
- [59] Paolo Carloni, Michiel Sprik, and Wanda Andreoni. Key steps of the cis-platin-DNA interaction: density functional theory-based molecular dynamics simulations. *The Journal of Physical Chemistry B* **104**(4) (2000), 823–835.
- [60] Victor I Danilov, Victor M Anisimov, Noriyuki Kurita, and Dmytro Hovorun. MP2 and DFT studies of the DNA rare base pairs: the molecular mechanism of the spontaneous substitution mutations conditioned by tautomerism of bases. *Chemical Physics Letters* **412**(4-6) (2005), 285–293.
- [61] Jaroslav V Burda and Jerzy Leszczynski. How strong can the bend be on a DNA helix from cisplatin? DFT and MP2 quantum chemical calculations of cisplatin-bridged DNA purine bases. *Inorganic Chemistry* **42**(22) (2003), 7162–7172.
- [62] Chengteh Lee, Weitao Yang, and Robert G Parr. Development of the Colle-Salvetti correlation-energy formula into a functional of the electron density. *Physical Review B* **37**(2) (1988), 785.
- [63] Chr. Møller and M. S. Plesset. Note on an Approximation Treatment for Many-Electron Systems. In: vol. 46. 1934, pp.618–622. DOI: [10.1103/PhysRev.46.618](https://doi.org/10.1103/PhysRev.46.618).
- [64] Murray S Davies, Susan J Berners-Price, and Trevor W Hambley. Rates of platination of AG and GA containing double-stranded oligonucleotides: Insights into why cisplatin binds to GG and AG but not GA sequences in DNA. *Journal of the American Chemical Society* **120**(44) (1998), 11380–11390.
- [65] Sherif Ashraf Fahmy, Fortuna Ponte, Mohamed K Abd El-Rahman, Nino Russo, Emilia Sicilia, and Tamer Shoeib. Investigation of the host-guest complexation between 4-sulfocalix [4] arene and nedaplatin for potential use in drug delivery. *Spectrochimica Acta Part A: Molecular and Biomolecular Spectroscopy* **193** (2018), 528–536.

- [66] Eslam M Moustafa, Mohamed Korany, Noura A Mohamed, and Tamer Shoeib. Carnosine complexes and binding energies to some biologically relevant metals and platinum containing anticancer drugs. *Inorganica Chimica Acta* **421** (2014), 123–135.
- [67] Armida Torreggiani, Paola Taddei, Anna Tinti, and Giancarlo Fini. Vibrational study on the cobalt binding mode of Carnosine. *Journal of Molecular Structure* **641**(1) (2002), 61–70. DOI: [https://doi.org/10.1016/S0022-2860\(02\)00314-9](https://doi.org/10.1016/S0022-2860(02)00314-9).
- [68] Michael Lee Branham, Parvesh Singh, Krishna Bisetty, Myalo Sabela, and Thirumala Govender. Preparation, spectrochemical, and computational analysis of L-carnosine (2-[(3-aminopropanoyl) amino]-3-(1H-imidazol-5-yl) propanoic acid) and its ruthenium (II) coordination complexes in aqueous solution. *Molecules* **16**(12) (2011), 10269–10291.
- [69] Arturo Robertazzi and James A Platts. A QM/MM study of cisplatin–DNA oligonucleotides: from simple models to realistic systems. *Chemistry–A European Journal* **12**(22) (2006), 5747–5756.
- [70] Hatice Arı and Zeki Büyükmumcu. Comparison of DFT functionals for prediction of band gap of conjugated polymers and effect of HF exchange term percentage and basis set on the performance. *Computational Materials Science* **138** (2017), 70–76.
- [71] Mu-Hyun Baik, Richard A Friesner, and Stephen J Lippard. Theoretical study of cisplatin binding to purine bases: why does cisplatin prefer guanine over adenine? *Journal of the American Chemical Society* **125**(46) (2003), 14082–14092.
- [72] Bayden R Wood. The importance of hydration and DNA conformation in interpreting infrared spectra of cells and tissues. *Chemical Society Reviews* **45**(7) (2016), 1980–1998.
- [73] M. J. Frisch, G. W. Trucks, H. B. Schlegel, G. E. Scuseria, M. A. Robb, J. R. Cheeseman, G. Scalmani, V. Barone, G. A. Petersson, H. Nakatsuji, X. Li, M. Caricato, A. V. Marenich, J. Bloino, B. G. Janesko, R. Gomperts, B. Mennucci, H. P. Hratchian, J. V. Ortiz, A. F. Izmaylov, J. L. Sonnenberg, D. Williams-Young, F. Ding, F. Lipparini, F. Egidi, J. Goings, B. Peng, A. Petrone, T. Henderson, D. Ranasinghe, V. G. Zakrzewski, J. Gao, N. Rega, G. Zheng, W. Liang, M. Hada, M. Ehara, K. Toyota, R. Fukuda, J. Hasegawa, M. Ishida, T. Nakajima, Y. Honda, O. Kitao, H. Nakai, T. Vreven, K. Throssell, J. A. Montgomery Jr., J. E. Peralta, F. Ogliaro, M. J. Bearpark, J. J. Heyd, E. N. Brothers, K. N. Kudin, V. N. Staroverov, T. A. Keith, R. Kobayashi, J. Normand, K. Raghavachari, A. P. Rendell, J. C. Burant, S. S. Iyengar,

- J. Tomasi, M. Cossi, J. M. Millam, M. Klene, C. Adamo, R. Cammi, J. W. Ochterski, R. L. Martin, K. Morokuma, O. Farkas, J. B. Foresman, and D. J. Fox. *Gaussian~16 Revision C.01*. Gaussian Inc. Wallingford CT. 2016.
- [74] Frank Neese. Software update: the ORCA program system, version 4.0. *Wiley Interdisciplinary Reviews: Computational Molecular Science* **8**(1) (2018), e1327.
- [75] Michael W Schmidt, Kim K Baldridge, Jerry A Boatz, Steven T Elbert, Mark S Gordon, Jan H Jensen, Shiro Koseki, Nikita Matsunaga, Kiet A Nguyen, Shujun Su, et al. General atomic and molecular electronic structure system. *Journal of Computational Chemistry* **14**(11) (1993), 1347–1363.
- [76] Yan Zhao and Donald G Truhlar. A new local density functional for main-group thermochemistry, transition metal bonding, thermochemical kinetics, and noncovalent interactions. *The Journal of Chemical Physics* **125**(19) (2006), 194101.
- [77] David E Woon and Thom H Dunning Jr. Gaussian basis sets for use in correlated molecular calculations. IV. Calculation of static electrical response properties. *The Journal of Chemical Physics* **100**(4) (1994), 2975–2988.
- [78] Nicholas P Labello, Antonio M Ferreira, and Henry A Kurtz. Correlated, relativistic, and basis set limit molecular polarizability calculations to evaluate an augmented effective core potential basis set. *International Journal of Quantum Chemistry* **106**(15) (2006), 3140–3148.
- [79] Detlev Figgen, Kirk A Peterson, Michael Dolg, and Hermann Stoll. Energy-consistent pseudopotentials and correlation consistent basis sets for the 5 d elements Hf–Pt. *The Journal of Chemical Physics* **130**(16) (2009), 164108.
- [80] Kirk A Peterson, Detlev Figgen, Erich Goll, Hermann Stoll, and Michael Dolg. Systematically convergent basis sets with relativistic pseudopotentials. II. Small-core pseudopotentials and correlation consistent basis sets for the post-d group 16–18 elements. *The Journal of Chemical Physics* **119**(21) (2003), 11113–11123.
- [81] Kirk A Peterson, Detlev Figgen, Michael Dolg, and Hermann Stoll. Energy-consistent relativistic pseudopotentials and correlation consistent basis sets for the 4 d elements Y–Pd. *The Journal of Chemical Physics* **126**(12) (2007), 124101.

- [82] Eunice SH Gwee, Zoe L Seeger, Dominique RT Appadoo, Bayden R Wood, and Ekaterina I Izgorodina. Influence of DFT Functionals and Solvation Models on the Prediction of Far-Infrared Spectra of Pt-Based Anticancer Drugs: Why Do Different Complexes Require Different Levels of Theory? *ACS Omega* **4**(3) (2019), 5254–5269.
- [83] Aleksandr V Marenich, Christopher J Cramer, and Donald G Truhlar. Universal solvation model based on solute electron density and on a continuum model of the solvent defined by the bulk dielectric constant and atomic surface tensions. *The Journal of Physical Chemistry B* **113**(18) (2009), 6378–6396.
- [84] Minsun Hong, Mayuree Fuangthong, John D Helmann, and Richard G Brennan. Structure of an OhrR- ohrA Operator Complex Reveals the DNA Binding Mechanism of the MarR Family. *Molecular Cell* **20**(1) (2005), 131–141.
- [85] Christoph Engel, Sarah Sainsbury, Alan C. Cheung, Dirk Kostrewa, and Patrick Cramer. RNA polymerase I structure and transcription regulation. *Nature* **502**(7473) (2013), 650.
- [86] Konstantinos Gkionis, Shaun T Mutter, and James A Platts. QM/MM description of platinum–DNA interactions: comparison of binding and DNA distortion of five drugs. *RSC Advances* **3**(12) (2013), 4066–4073.
- [87] Thomas Weymuth, Erik PA Couzijn, Peter Chen, and Markus Reiher. New benchmark set of transition-metal coordination reactions for the assessment of density functionals. *Journal of Chemical Theory and Computation* **10**(8) (2014), 3092–3103.
- [88] Samuel YS Tan, Luke Wylie, Ivan Begic, Dennis Tran, and Ekaterina I Izgorodina. Application of spin-ratio scaled MP2 for the prediction of intermolecular interactions in chemical systems. *Physical Chemistry Chemical Physics* **19**(42) (2017), 28936–28942.
- [89] Samuel Tan, Santiago Barrera Acevedo, and Ekaterina I Izgorodina. Generalized spin-ratio scaled MP2 method for accurate prediction of intermolecular interactions for neutral and ionic species. *The Journal of Chemical Physics* **146**(6) (2017), 064108.
- [90] Jeng-Da Chai and Martin Head-Gordon. Long-range corrected hybrid density functionals with damped atom–atom dispersion corrections. *Physical Chemistry Chemical Physics* **10**(44) (2008), 6615–6620.

- [91] Narbe Mardirossian and Martin Head-Gordon. Thirty years of density functional theory in computational chemistry: an overview and extensive assessment of 200 density functionals. *Molecular Physics* **115**(19) (2017), 2315–2372.
- [92] Stefan Grimme. Accurate description of van der Waals complexes by density functional theory including empirical corrections. *Journal of Computational Chemistry* **25**(12) (2004), 1463–1473.
- [93] Junming Ho and Michelle L Coote. A universal approach for continuum solvent pK_a calculations: are we there yet? *Theoretical Chemistry Accounts* **125**(1-2) (2010), 3.
- [94] S F Boys and FJMP Bernardi. The calculation of small molecular interactions by the differences of separate total energies. Some procedures with reduced errors. *Molecular Physics* **19**(4) (1970), 553–566.
- [95] Arturo Robertazzi and James A Platts. Hydrogen bonding and covalent effects in binding of cisplatin to purine bases: ab initio and atoms in molecules studies. *Inorganic Chemistry* **44**(2) (2005), 267–274.
- [96] Yogita Mantri, Stephen J Lippard, and Mu-Hyun Baik. Bifunctional binding of cisplatin to DNA: why does cisplatin form 1, 2-intrastrand cross-links with AG but not with GA? *Journal of the American Chemical Society* **129**(16) (2007), 5023–5030.
- [97] Elizabeth R Jamieson and Stephen J Lippard. Structure, recognition, and processing of cisplatin- DNA adducts. *Chemical Reviews* **99**(9) (1999), 2467–2498.
- [98] Franck Legendre, Véronique Bas, Jiří Kozelka, and Jean-Claude Chottard. A complete kinetic study of GG versus AG platination suggests that the doubly aquated derivatives of cisplatin are the actual DNA binding species. *Chemistry—A European Journal* **6**(11) (2000), 2002–2010.
- [99] Truong Ba Tai and Pham Vu Nhat. A DFT investigation on interactions between asymmetric derivatives of cisplatin and nucleobase guanine. *Chemical Physics Letters* **680** (2017), 44–50.
- [100] Marek Gajdoš and Jürgen Hafner. CO adsorption on Cu (1 1 1) and Cu (0 0 1) surfaces: Improving site preference in DFT calculations. *Surface Science* **590**(2-3) (2005), 117–126.

- [101] U Salzner, JB Lagowski, PG Pickup, and RA Poirier. Design of low band gap polymers employing density functional theory—hybrid functionals ameliorate band gap problem. *Journal of computational chemistry* **18**(15) (1997), 1943–1953.
- [102] Sivan Refaely-Abramson, Roi Baer, and Leeor Kronik. Fundamental and excitation gaps in molecules of relevance for organic photovoltaics from an optimally tuned range-separated hybrid functional. *Physical Review B* **84**(7) (2011), 075144.
- [103] Stephan Kümmel and Leeor Kronik. Orbital-dependent density functionals: Theory and applications. *Reviews of Modern Physics* **80**(1) (2008), 3.
- [104] Stephen Neidle et al. *Nucleic acid structure and recognition*. 2002.
- [105] Pavel Štarha, Ján Vančo, and Zdeněk Trávníček. Platinum complexes containing adenine-based ligands: An overview of selected structural features. *Coordination Chemistry Reviews* **332** (2017), 1–29.
- [106] Johannis L Van der Veer, Hans Van den Elst, Jeroen HJ Den Hartog, Anne Marie J Fichtinger-Schepman, and Jan Reedijk. Reaction of the antitumor drug cis-diamminedichloroplatinum (II) with the trinucleotide d (GpApG): identification of the two main products and kinetic aspects of their formation. *Inorganic Chemistry* **25**(26) (1986), 4657–4663.
- [107] Amrit Sarmah and Ram Kinkar Roy. Understanding the preferential binding interaction of aqua-cisplatin with nucleobase guanine over adenine: a density functional reactivity theory based approach. *RSC advances* **3**(8) (2013), 2822–2830.
- [108] Alan Eastman. The mechanism of action of cisplatin: from adducts to apoptosis. *Cisplatin. Chemistry and Biochemistry of a Leading Anticancer Drug* (1999), 111–134.
- [109] Anne Marie J Fichtinger-Schepman, Johannis L Van der Veer, Jeroen HJ Den Hartog, Paul HM Lohman, and Jan Reedijk. Adducts of the antitumor drug cis-diamminedichloroplatinum (II) with DNA: formation, identification, and quantitation. *Biochemistry* **24**(3) (1985), 707–713.
- [110] áP Umapathy. The chemical and biochemical consequences of the binding of the antitumour drug cisplatin and other platinum group metal complexes to DNA. *Coordination Chemistry Reviews* **95**(2) (1989), 129–181.

- [111] Bruno Van Hemelryck, Jean Pierre Girault, Genevieve Chottard, Philippe Valadon, Abdelazize Laoui, and Jean Claude Chottard. Sequence-dependent platinum chelation by adenylyl (3'-5') guanosine and guanylyl (3'-5') adenosine reacting with cis-diamminedichloroplatinum (II) and its diaqua derivative. *Inorganic Chemistry* **26**(6) (1987), 787–795.
- [112] Bohdan Schneider, Ketan Patel, and Helen M Berman. Hydration of the Phosphate Group in Double-Helical DNA. *Biophysical Journal* **75**(5) (1998), 2422–2434.

Chapter 6

Conclusions

The aim of this thesis was to better understand the hydrolysis mechanism of several Pt-based anti-cancer drugs and their mode and strength of interaction with DNA and RNA building blocks.

Chapter 2 presented a step-by-step approach to investigate the effects of 4 factors - density functional theory (DFT) functionals, basis sets on the non-Pt atoms, effective core potentials (ECPs) and solvation models on the prediction of characteristic bands of cisplatin and carboplatin in the far infrared (FIR) region, 0 - 600 cm^{-1} . With the presence of different types of ligands, it was determined that two different levels of theory were optimal for the two Pt complexes. For cisplatin, the combination of PBE and SMD was optimal to predict the characteristic FIR bands with a mean absolute deviation and standard deviation of $5.7 \pm 8.5 \text{ cm}^{-1}$. For carboplatin, the combination of M06-L and either IEFPCM or CPCM was optimal with a mean absolute deviation and standard deviation of 6.8 ± 9.2 and $6.8 \pm 9.1 \text{ cm}^{-1}$, respectively. This was the result of the different nature of Pt-ligand bonds present in the two complexes. This was determined by analysing the charge transfer between charge transfer between the Pt ion and ligands using ChelpG partial atomic charge scheme. When calculated using PBE in gas phase, a charge transfer of 0.293 e was recorded from Cl^- to Pt in cisplatin, decreasing the charge on Pt to 1.786 e , below its nominal +2.0 e charge. The Pt-O bond on carboplatin, on the other hand, exhibited more ionic characteristics evident from the charge transfer of 0.036 and 0.013 e to the cyclobutanedicarboxylate and NH_3 groups, respectively, thus increasing the charge on

Pt to 2.118 e . When calculations were performed in gas phase, the stretching vibrations were usually overestimated for both cisplatin and carboplatin, up to 33 and 25 cm^{-1} , respectively. It is more challenging to predict the characteristic bands of carboplatin due to the mixing of stretching and bending vibrations. It was also determined that while the Pt-O stretching vibrations were either under- or overestimated, Pt-N vibrations were mostly overestimated. This finding suggests that different scaling factors are required for different types of vibrations instead of a universal scaling factor across the spectra.

Chapter 3 investigated the role of explicit solvation on the thermodynamic properties, such as dissociation energies, of four commonly used Pt-based anti-cancer drugs - cisplatin, carboplatin, oxaliplatin and nedaplatin. By comparing the relative energies, it was determined that the Cl^- and di-anions were energetically preferred leaving groups over the NH_3 group. The ChelpG analysis revealed the importance of explicit solvation in stabilising the overall charge of the system during the hydrolysis process. ΔG_{solv} , calculated using the thermodynamic cycle with implicit solvation, was employed to better understand the Gibbs free energy of hydrolysis, whereas ΔE_{solv} , calculated using the structures from the relaxed scans, was employed to predict the activation barriers of hydrolysis. Analysis of ΔG_{solv} and ΔE_{solv} data suggested that the Pt-complexes were more likely to be activated via a stepwise mechanism instead of a one-step reaction. The Gibbs free energy decreased significantly, by a minimum of 14.1 kJ mol^{-1} , from the first to the second step of hydrolysis for all Pt complexes except for cisplatin. This suggests that the mechanism of hydrolysis was not thermodynamically demanding. However, the thermodynamic cycle did not take into consideration the formation of a contact ion pair between the dissociated Pt-complex and the leaving dianion and therefore did not properly describe the mechanism of hydrolysis. ΔE_{solv} , on the other hand, revealed that the activation barrier of the first step was similar for all four Pt complexes, ranging from 87.3 to 125.4 kJ mol^{-1} . The activation barrier of the second step was found to be similar for cisplatin, carboplatin and oxaliplatin, with the highest barrier of 98.0 kJ mol^{-1} . Nedaplatin produced a higher activation barrier of the second step than the first step, 136.8 kJ mol^{-1} compared to 125.4 kJ mol^{-1} , respectively. The higher activation barrier was explained by analysing the charge of the 2-oxidoacetate anion. With a charge of -3.180 e , the 2-oxidoacetate anion still interacts strongly with the Pt metal ion, resulting in the higher activation barrier. The use of explicit

solvation was also employed to study the hydrolysis mechanism of cisplatin. The use of explicit solvation resulted in an energy barrier of 78.7 kJ mol^{-1} for the first step of hydrolysis, closer to previously published experimental data of 81.6 to 90.0 kJ mol^{-1} . This finding emphasised the importance of including explicit solvation when studying such reactions.

Chapter 4 explored the viability of the fragment molecular orbital (FMO) approach as a cost saving alternative to study large biomolecules. The effects of different fragmentation schemes, methods (PBE, PBE-D3 and SRS-MP2) and solvation models (CPCM and SMD) were investigated on single stranded (dGMP and dAMP), stacked (d(GpG)) and double stranded (dGMP-dCMP) DNA models. Two types of fragmentation of the DNA model were considered: 1) Fragmentation I scheme, in which the bond between the sugar and the base units is broken and 2) Fragmentation II scheme, in which two covalent bonds are broken - between the sugar and the base units and between the sugar and the phosphate units. Upon comparison to full system calculations, Fragmentation scheme I was found to outperform Fragmentation scheme II for the single base systems, producing an average energy difference of 0.02 and 3.2 kJ mol^{-1} , respectively, in the gas phase. Larger errors were incurred with the inclusion of solvation models, ranging between -0.6 to 3.6 kJ mol^{-1} for CPCM and -18.1 to 39.1 kJ mol^{-1} for SMD. The inclusion of solvation model allows for higher degree of flexibility for the phosphate and sugar backbone, evident from the higher root mean square deviation (RMSD) values when comparing the optimised geometries to full system optimisations performed without any fragmentation. This suggests that the FMO optimisations located different local minima that were usually higher in energy. The same approach was used to study the stacked and double-stranded systems. The larger-sized systems, unsurprisingly, incurred larger energy differences due to the ability of these molecular systems to adopt many more local minima on the potential energy surface as compared to the single base systems. The FMO-optimised geometries were re-optimised again using full system optimisations to determine if the local minima determined from these optimisations could be located for both the stacked and double-stranded models. Once again, different local minima of higher electronic energy were located. While the re-optimisations performed in gas phase resulted in similar local minima, resulting in energy differences of $-0.08 \text{ kJ mol}^{-1}$ for the stacked system with the use of Fragmentation scheme II, the use of CPCM and SMD solvation model resulted in larger energy difference of -0.3 and 33.4

kJ mol^{-1} , respectively. The re-optimisation of the stacked system using Fragmentation scheme I resulted in lower energy differences as compared to Fragmentation scheme II, resulting in differences of -0.003 , 0.3 and -4.9 kJ mol^{-1} for gas, CPCM and SMD, respectively. The large errors incurred by Fragmentation scheme II suggests FMO2 might not be sufficient for geometry optimisations and that FMO3, which includes three-body correction, should be used. It is not surprising that CPCM solvation model outperformed SMD as it was improved upon to work with FMO, improving how the solvation model is interfaced within the FMO approach.

Chapter 5 studies the interaction, specifically the strength and mode, between Pt-complexes (cisplatin and oxaliplatin) and DNA (dGMP and dAMP) or RNA (GMP and AMP) building blocks. Activated forms of cisplatin and oxaliplatin in their non- ($[\text{PtL}]^{2+}$), mono- ($[\text{PtL}(\text{H}_2\text{O})]^{2+}$) and di-aquated equivalents ($[\text{PtL}(\text{H}_2\text{O})_2]^{2+}$) (where L is either two ammonia for cisplatin or 1,2-diaminocyclohexane for oxaliplatin) were selected to study the role of water molecules coordinated to the Pt centre on the binding event. Complexes were constructed to encourage the formation of the Pt-N7 bond and the interaction energies were analysed to determine the likely species to bind to DNA/RNA building block. The non-aquated form of both cisplatin and oxaliplatin resulted in the strongest interaction energy, resulting in an average of -764.9 and $-663.9 \text{ kJ mol}^{-1}$, respectively. The ability of the mono-aquated form of cisplatin and oxaliplatin were also able to form the Pt-N7 bond, with an average interaction energy of -620.8 and $-544.3 \text{ kJ mol}^{-1}$, respectively. The formation of the Pt-N7 bond between two neighbouring nucleobases in DNA/RNA is crucial as it has been established that it disrupts the structural integrity of DNA and leads to cell death. The ability of mono-aquated complexes to form the Pt-N7 bond suggests that it could be a precursor complex before liberating the water molecule and forming a stronger interaction with DNA/RNA building blocks. The di-aquated form of the two Pt complexes were unable to form the Pt-N7 bond due to the presence of two Pt-bound water molecules. RMSD and deformation energies of the building blocks were also used to study the effect of binding. No direct relationship could be observed between the RMSD values and deformation energies. The highest deformation energies resulted from the interaction with the non-aquated form of the complexes, with an average of 85.4 and 87.6 kJ mol^{-1} for cisplatin and oxaliplatin, respectively. The mono- and di-aquated form of the two Pt complexes produced smaller deformation energies. For example, the deformation energies resulted from

the interaction between mono- and di-aquated cisplatin and the building blocks resulted in an average of 54.8 and 19.7 kJ mol⁻¹, respectively. This suggests that the non-aquated form of the Pt complexes are able to influence the DNA/RNA geometries stronger than the mono- and di-aquated forms. Upon analysing the two components of the interaction energy, it was determined that electrostatics play a more significant role between the interaction of the Pt complexes and building blocks than correlation. For example, the average electrostatic and correlation components in the complex between the non-aquated form of cisplatin and dGMP were calculated to be -706.3 and -160.9 kJ mol⁻¹, respectively. It was also observed that the increasing number of Pt-bound water molecules had a stronger influence on the electrostatic component than the correlation component. A direct correlation was observed between the decrease of charge on the Pt ion with the increase of explicit water molecules in the system. The predicted strongest interacting configurations of the Pt complexes with each building block, dGMP, GMP, dAMP and AMP, support previously published studies that showed the preferential binding of the Pt complexes preferentially the guanine unit (dGMP and GMP) over the adenine unit (dAMP and AMP). For example, the non-aquated form of cisplatin and oxaliplatin preferred to bind to dGMP over dAMP by 162.4 and 128.3 kJ mol⁻¹, respectively. The same trend could be seen for GMP and AMP, where the non-aquated form of cisplatin and oxaliplatin was found to preferentially bind to GMP over AMP by 161.6 and 131.1 kJ mol⁻¹, respectively.

6.1 Future Works

As demonstrated in *Chapter 3*, the importance of explicit solvation to model biochemical reactions, especially the hydrolysis reactions of Pt complexes, cannot be ignored. The inclusion of explicit solvation to study the hydrolysis reaction of the other three Pt-complexes, carboplatin, oxaliplatin and nedaplatin, should be explored.

The inclusion of explicit solvation in quantum chemical calculations is accompanied by high computational costs. This motivates the need to identify a suitable approach that is able to accurately locate the minima on the potential energy surface. As demonstrated in *Chapter 4*, the combination of FMO and implicit solvation models resulted in the location of different local minima when compared to full system calculations. This suggests that more work needs

to be done in refining solute-solvent interactions interfaced between implicit solvation models to be able to treat varying intermolecular interactions with similar accuracy. The location of different local minima could be due to the lack of steric hindrance present in larger models. The lack of explicit solvation, especially around the phosphate groups, allows for higher degree of flexibility of the sugar-phosphate motif. This suggest that explicit solvation and larger models need to be considered to better describe such systems.

Lastly, more studies need to be conducted to investigate the binding of Pt-complexes and larger models of DNA/RNA building blocks. The work reported in *Chapter 5* reports the interaction between activated Pt complexes in their non-, mono- and di-aquated forms. Again, the inclusion of explicit solvation around the system as the explicit H₂O molecules could play a role in binding event, thus affecting its kinetics. The presence of the leaving groups of Pt-based anticancer drugs (Cl⁻ for cisplatin and 1,2-diaminocyclohexane for oxaliplatin) could also play a role in the binding process. Larger DNA/RNA building block model should also be studied to investigate the binding thermodynamics of Pt-based complexes.

Appendices

Appendix A

Additional stuff

A.1 Selecting the appropriate level of theory to study the Infrared Spectra of Pt complexes - Supporting Information

./cisplatin-M06L-H2O-ApVTZ-pVTZ-2_eGeom.xyz

11

Pt	0.000035771	0.174764009	0.000188207
Cl	-1.723249004	-1.413112301	-0.001380125
Cl	1.721768212	-1.414793479	0.002759738
N	1.500351688	1.606561003	0.012137274
H	1.440076526	2.261780161	-0.757703943
H	1.515330552	2.148956975	0.867463719
N	-1.498881701	1.608017884	-0.012662907
H	-1.437942165	2.263700695	0.756730958
H	-1.513360571	2.149847293	-0.868357146
H	2.396122331	1.134726636	-0.059773030
H	-2.395109639	1.137106124	0.059595255

./cisplatin-H2O-2_eGeom.xyz

11

Pt	0.529056274	0.798174860	0.000000000
Cl	0.434968073	-1.540054934	-0.006652756
Cl	2.867286071	0.892262978	0.006652756
N	0.584422177	2.861710576	-0.008385470
H	0.178580669	3.277474059	-0.861667195
H	0.106718286	3.298320023	0.795650869
N	-1.534479444	0.742809030	0.008385470
H	-1.950242913	1.148650553	0.861667195
H	-1.971088874	1.220512937	-0.795650869
H	1.573833960	3.162669596	0.028913689
H	-1.835438500	-0.246602742	-0.028913689

./cisplatin-CPCM-pVTZ-pp-2_eGeom.xyz

11

Pt	0.000037604	0.183554403	0.000166098
Cl	-1.720625446	-1.399746995	0.004085088
Cl	1.719191457	-1.401401291	-0.002621127
N	1.492001813	1.599227184	0.005612562
H	1.458786277	2.242624243	-0.799933917
H	1.496541078	2.180153420	0.858162205
N	-1.490540468	1.600672851	-0.006138290
H	-1.456730293	2.244595388	0.798963649
H	-1.494526379	2.181015043	-0.859090968
H	2.403594490	1.112270135	-0.031873420
H	-2.402588133	1.114590618	0.031666121

./cisplatin-PBE0-SMD-ApVTZ-pVTZ-pp-3_eGeom.xyz

11

Pt	-0.001457501	0.167417542	0.002956743
Cl	1.687446971	-1.410238736	-0.006157703
Cl	-1.680743484	-1.420375113	-0.016890751
N	-1.449450838	1.601221341	0.011392265
H	-1.327837991	2.269081470	0.767600614
H	-1.461753306	2.127199596	-0.858408971
N	1.437795708	1.609911496	0.020595299
H	1.452470655	2.135981556	-0.849113543
H	1.307349509	2.277002991	0.776009302


```
H      -2.365659031      1.174822299      0.121623831
H      2.355834308      1.189033558      0.136662913
./cisplatin-M06L-SMD-TZ-aug-pVDZ-2_eGeom.xyz
11
```

```
Pt      0.000025681      0.150940916      0.000183231
Cl     -1.710503371     -1.447101340     -0.009055840
Cl      1.709001784     -1.448756634      0.010390033
N      1.471130317      1.607447034      0.018067473
H      1.359652395      2.282705476     -0.729922689
H      1.475233648      2.124567605      0.890442099
N     -1.469662841      1.608864610     -0.018581259
H     -1.357529529      2.284464305      0.729002459
H     -1.473261534      2.125463584     -0.891267158
H      2.386653496      1.183294494     -0.086332333
H     -2.385598046      1.185664951      0.086071982
./cisplatin-M062X-ApVDZ-aug-pVTZ_eGeom.xyz
11
```

```
Pt      0.493030185      0.834200950      0.000000000
Cl      0.386145829     -1.462917886      0.000002430
Cl      2.790149025      0.941085225     -0.000002430
N      0.627736725      2.920363431      0.000016893
H      0.239990966      3.371851887     -0.825310002
H      0.239969828      3.371843394      0.825338521
N     -1.593132301      0.699494484     -0.000016893
H     -2.044620742      1.087240260      0.825310002
H     -2.044612250      1.087261397     -0.825338521
H      1.640071945      3.078344520      0.000031209
H     -1.751113425     -0.312840730     -0.000031209
./cisplatin-M062X-SMD-ApVDZ-pVTZ-4_eGeom.xyz
11
```

```
Pt     -0.128718798     -0.000172377      0.195685482
Cl     -0.417637209     -1.719326252     -1.392547557
Cl     -0.296214623      1.718292590     -1.410636809
N      0.136761223      1.431729811      1.627387533
H     -0.521733303      1.335252828      2.401580709
H      1.075545386      1.391272888      2.027280428
N      0.017424557     -1.431456312      1.645052132
H     -0.771836443     -1.390785897      2.291798368
H      0.024863914     -2.367095832      1.237602109
H      0.015485315      2.367199866      1.237925213
H      0.866349677     -1.334684313      2.203853942
./cisplatin-M06L-H2O-TZ-pVTZ-2_eGeom.xyz
11
```

```
Pt      0.000036642      0.176980747      0.000192180
Cl     -1.727480342     -1.409816635      0.000146830
Cl      1.726003002     -1.411502538      0.001257538
N      1.504873327      1.607166107      0.010960003
H      1.451345183      2.257532373     -0.763612531
H      1.518830341      2.154559191      0.863212888
N     -1.503403093      1.608627543     -0.011493431
```

H	-1.449232708	2.259449625	0.762651374
H	-1.516834399	2.155474329	-0.864105444
H	2.397578810	1.128354271	-0.054170750
H	-2.396574764	1.130729986	0.053959344

./cisplatin-H20-ApVTZ-ApVDZ-pp-2_eGeom.xyz

11

Pt	0.527885539	0.799345595	0.000000000
Cl	0.438946516	-1.528620811	-0.005349190
Cl	2.855851948	0.888284535	0.005349190
N	0.576761829	2.858979302	-0.013645024
H	0.190039372	3.251770829	-0.876642925
H	0.074717193	3.281346956	0.772244892
N	-1.531748170	0.750469378	0.013645024
H	-1.924539683	1.137191849	0.876642925
H	-1.954115806	1.252514029	-0.772244892
H	1.557646043	3.155060086	0.047260398
H	-1.827828989	-0.230414825	-0.047260398

./cisplatin-M06L-aug-pVTZ-SMD-2_eGeom.xyz

11

Pt	0.000024679	0.148349602	0.000182895
Cl	-1.716229769	-1.453810748	-0.009634833
Cl	1.714720947	-1.455471588	0.010965486
N	1.462262044	1.600867085	0.018892796
H	1.357080628	2.290738371	-0.727348240
H	1.478021265	2.126011364	0.895556679
N	-1.460800588	1.602276487	-0.019401003
H	-1.354948320	2.292493816	0.726425179
H	-1.476049664	2.126908771	-0.896380597
H	2.390704278	1.188407278	-0.089347252
H	-2.389643500	1.190784562	0.089086890

./cisplatin-TZ-pVTZ-pp_eGeom.xyz

11

Pt	0.473934692	0.853296444	0.000000000
Cl	0.358010761	-1.439947061	0.000002324
Cl	2.767178201	0.969220293	-0.000002324
N	0.642580150	2.932144747	-0.000008316
H	0.262611029	3.390094219	-0.831649432
H	0.262741952	3.390103665	0.831687161
N	-1.604913617	0.684651060	0.000008316
H	-2.062863076	1.064620197	0.831649432
H	-2.062872522	1.064489274	-0.831687161
H	1.669994992	3.050017870	-0.000082433
H	-1.722786777	-0.342763777	0.000082433

./cisplatin-ApVTZ-ApVTZ-pp_eGeom.xyz

11

Pt	0.475203680	0.852027456	0.000000000
Cl	0.360673697	-1.439416178	0.000001812
Cl	2.766647318	0.966557357	-0.000001812
N	0.641235343	2.929148790	-0.000008155
H	0.258823239	3.386032122	-0.831451520

H	0.258930050	3.386042079	0.831478673
N	-1.601917660	0.685995867	0.000008155
H	-2.058800978	1.068407987	0.831451520
H	-2.058810935	1.068301176	-0.831478673
H	1.667950084	3.053549147	-0.000070025
H	-1.726318053	-0.340718870	0.000070025

./cisplatin-PBE0-CPCM-ApVDZ_eGeom.xyz

11

Pt	0.530719919	0.796511215	0.000000000
Cl	0.450213441	-1.525397296	0.000592935
Cl	2.852628433	0.877017610	-0.000592935
N	0.566208707	2.839667788	0.000056740
H	0.119674301	3.252357512	-0.821949555
H	0.119330707	3.252227417	0.821944011
N	-1.512436656	0.761022500	-0.000056740
H	-1.925126364	1.207556920	0.821949555
H	-1.924996268	1.207900514	-0.821944011
H	1.539060589	3.158892123	0.000291554
H	-1.831661025	-0.211829371	-0.000291554

./cisplatin-M06L-SMD-ApVTZ-pVDZ-2_eGeom.xyz

11

Pt	0.000047211	0.151079488	0.000184631
Cl	-1.709451315	-1.447981879	-0.008852136
Cl	1.708065302	-1.449557156	0.010192375
N	1.468821476	1.606912537	0.017470341
H	1.358342623	2.280155409	-0.732169266
H	1.470936790	2.126964317	0.887830177
N	-1.467379486	1.608259929	-0.017985116
H	-1.356269191	2.281863645	0.731236817
H	-1.469024648	2.127775127	-0.888666243
H	2.385515217	1.184912474	-0.083939652
H	-2.384461978	1.187171109	0.083696069

./cisplatin-M06L-ApVTZ-ApVDZ_eGeom.xyz

11

Pt	0.486074367	0.841156769	0.000000000
Cl	0.371017428	-1.456078828	-0.000198563
Cl	2.783309968	0.956213626	0.000198563
N	0.650017359	2.944215510	-0.000104801
H	0.274342860	3.403979276	-0.819514837
H	0.274158271	3.404070489	0.819171027
N	-1.616984381	0.677213851	0.000104801
H	-2.076748133	1.052888366	0.819514837
H	-2.076839346	1.053072955	-0.819171027
H	1.662296033	3.074259735	0.000016166
H	-1.747028642	-0.335064818	-0.000016166

./cisplatin-M06L-aug-pVTZ-H2O_eGeom.xyz

11

Pt	0.535585489	0.791645644	0.000000000
Cl	0.442908896	-1.560438757	-0.004300360
Cl	2.887669894	0.884322154	0.004300360

N	0.579410547	2.859682821	-0.013542304
H	0.199653433	3.265092736	-0.870100044
H	0.075316571	3.293701733	0.760703473
N	-1.532451688	0.747820660	0.013542304
H	-1.937861590	1.127577789	0.870100044
H	-1.966470583	1.251914652	-0.760703473
H	1.549147716	3.176523994	0.052377186
H	-1.849292896	-0.221916498	-0.052377186

./cisplatin-CPCM_eGeom.xyz

11

Pt	0.530628301	0.796602833	0.000000000
Cl	0.435887144	-1.542036756	-0.000089019
Cl	2.869267893	0.891343907	0.000089019
N	0.582777280	2.859865114	0.000064404
H	0.138345210	3.284046776	-0.829396708
H	0.138663688	3.284147737	0.829642941
N	-1.532633982	0.744453927	-0.000064404
H	-1.956815628	1.188886012	0.829396708
H	-1.956916589	1.188567534	-0.829642941
H	1.571742613	3.164561241	-0.000136724
H	-1.837330145	-0.244511395	0.000136724

./cisplatin-M06L-CPCM-ApVTZ-ApVTZ-2_eGeom.xyz

11

Pt	0.533853667	0.793377467	0.000000000
Cl	0.439867761	-1.546614241	-0.003205311
Cl	2.873845378	0.887363289	0.003205311
N	0.580444434	2.866735371	-0.011865059
H	0.190869922	3.261234798	-0.859622023
H	0.088415719	3.285852352	0.767876605
N	-1.539504239	0.746786774	0.011865059
H	-1.934003652	1.136361299	0.859622023
H	-1.958621202	1.238815504	-0.767876605
H	1.548446365	3.167229451	0.042718099
H	-1.839998353	-0.221215146	-0.042718099

./cisplatin-M062X-SMD-aug-pVTZ-4_eGeom.xyz

11

Pt	-0.065634074	-0.000542361	0.192193509
Cl	-0.153139849	-1.717942842	-1.413042869
Cl	-0.198595948	1.715293755	-1.411591299
N	0.015605373	1.441943962	1.633465474
H	-0.676623506	1.304133278	2.374966622
H	0.932329301	1.480505596	2.088177274
N	0.053783574	-1.441592212	1.632242424
H	0.971199531	-1.456235458	2.086957879
H	-0.641867661	-1.322793355	2.373830668
H	-0.154242403	2.367261550	1.230668666
H	-0.091479488	-2.370745492	1.228659582

./cisplatin-SMD-TZ-aug-pVTZ-pp-2_eGeom.xyz

11

Pt	0.543700538	0.783530596	0.000000000
----	-------------	-------------	-------------

Cl	0.466852999	-1.539752036	-0.004790641
Cl	2.866983173	0.860378051	0.004790641
N	0.558145944	2.839318776	0.017713982
H	0.016202182	3.241304247	-0.753664125
H	0.171679755	3.209529995	0.892234274
N	-1.512087643	0.769085263	-0.017713982
H	-1.914073094	1.311029039	0.753664125
H	-1.882298848	1.155551465	-0.892234274
H	1.522109287	3.180829609	-0.064288375
H	-1.853598511	-0.194878068	0.064288375

./cisplatin-M062X-H2O-ApVDZ-pVTZ_eGeom.xyz

11

Pt	0.534726588	0.792504545	0.000000000
Cl	0.442449754	-1.569889805	0.012595231
Cl	2.897120942	0.884781296	-0.012595231
N	0.558765231	2.843015473	-0.027019517
H	0.214891712	3.221582703	-0.909260721
H	0.007848964	3.268273332	0.717834063
N	-1.515784341	0.768465976	0.027019517
H	-1.894351558	1.112339508	0.909260721
H	-1.941042179	1.319382257	-0.717834063
H	1.519993181	3.168233601	0.082186741
H	-1.841002503	-0.192761962	-0.082186741

./cisplatin-M06L-aug-pVTZ_eGeom.xyz

11

Pt	0.488118497	0.839112638	0.000000000
Cl	0.376805585	-1.463376948	-0.000149566
Cl	2.790608088	0.950425469	0.000149566
N	0.647598989	2.936965069	-0.000140858
H	0.273961478	3.410938850	-0.822264827
H	0.273355185	3.411074425	0.821631861
N	-1.609733939	0.679632221	0.000140858
H	-2.083707707	1.053269749	0.822264827
H	-2.083843282	1.053876042	-0.821631861
H	1.664916216	3.081694418	0.000235322
H	-1.754463325	-0.337685001	-0.000235322

./cisplatin-PBE0-pVTZ-pp_eGeom.xyz

11

Pt	0.477695708	0.849535427	0.000000000
Cl	0.368790110	-1.435286867	-0.000141229
Cl	2.762518007	0.958440944	0.000141229
N	0.628717049	2.911573799	-0.000007311
H	0.250555297	3.375283241	-0.827187235
H	0.250781643	3.375289748	0.827272690
N	-1.584342668	0.698514160	0.000007311
H	-2.048052097	1.076675929	0.827187235
H	-2.048058604	1.076449582	-0.827272690
H	1.649187599	3.051407355	-0.000125992
H	-1.724176260	-0.321956385	0.000125992

./cisplatin-PBE0-ApVDZ-aug-pVDZ-pp_eGeom.xyz

11

Pt	0.477610269	0.849620867	0.000000000
Cl	0.367499906	-1.436960092	-0.000034565
Cl	2.764191231	0.959731148	0.000034565
N	0.627513984	2.911816682	0.000279235
H	0.246202932	3.367536481	-0.825704802
H	0.246253881	3.367294515	0.826421131
N	-1.584585552	0.699717225	-0.000279235
H	-2.040305337	1.081028293	0.825704802
H	-2.040063371	1.080977345	-0.826421131
H	1.644500888	3.052434140	0.000286502
H	-1.725203046	-0.317269674	-0.000286502

./cisplatin-M06L-CPCM-ApVTZ-pVDZ-4_eGeom.xyz

11

Pt	-0.089124558	0.001045571	0.188281030
Cl	-0.341706868	-1.721396422	-1.383002230
Cl	-0.173668494	1.720838447	-1.403795006
N	0.127255489	1.499446846	1.605407428
H	-0.655963658	1.549144877	2.245583698
H	0.966231278	1.406998521	2.164865455
N	-0.001724400	-1.494964080	1.621666025
H	-0.703984663	-1.401434695	2.345200787
H	-0.154122273	-2.388285305	1.164882885
H	0.179816255	2.391979959	1.125280947
H	0.898818021	-1.543734992	2.082503920

./cisplatin-H20-pVTZ-pp-2_eGeom.xyz

11

Pt	0.525851917	0.801379217	0.000000000
Cl	0.430214788	-1.534434668	0.006234242
Cl	2.861665805	0.897016263	-0.006234242
N	0.581603289	2.857542612	0.009487087
H	0.100941895	3.293471403	-0.792358891
H	0.179695235	3.270551412	0.865233403
N	-1.530311480	0.745627918	-0.009487087
H	-1.966240254	1.226289327	0.792358891
H	-1.943320266	1.147535987	-0.865233403
H	1.571248320	3.154964572	-0.031346359
H	-1.827733476	-0.244017102	0.031346359

./cisplatin-SMD-3_eGeom.xyz

11

Pt	0.000000000	0.000000000	0.178408224
Cl	-0.002203494	-1.708830784	-1.416114776
Cl	0.002203494	1.708830784	-1.416114776
N	-0.015531485	1.471525009	1.620112404
H	-0.888329526	1.469596842	2.173489493
H	0.763873475	1.394091770	2.293697339
N	0.015531485	-1.471525009	1.620112404
H	0.888329526	-1.469596842	2.173489493
H	-0.763873475	-1.394091770	2.293697339
H	0.056148618	2.404469263	1.179491426
H	-0.056148618	-2.404469263	1.179491426

./cisplatin-CPCM-ApVTZ-pVTZ-pp-2_eGeom.xyz
11

Pt	0.000038513	0.181471074	0.000189198
Cl	-1.709386714	-1.400020919	0.000909794
Cl	1.707898175	-1.401717678	0.000137888
N	1.490605352	1.603119675	0.009149558
H	1.434146082	2.250485334	-0.781953250
H	1.492181264	2.161672483	0.867416382
N	-1.489125240	1.604584109	-0.009575767
H	-1.431763928	2.252790152	0.780770469
H	-1.490490418	2.162173222	-0.868472285
H	2.394750826	1.120302702	-0.046806718
H	-2.393711911	1.122694844	0.047232732

./cisplatin-PBE0-H2O-ApVDZ-2_eGeom.xyz
11

Pt	0.000034474	0.179181496	0.000187440
Cl	-1.699577867	-1.404710923	-0.001998246
Cl	1.698088447	-1.406379059	0.003370192
N	1.470764243	1.597720335	0.012592598
H	1.409210068	2.263642098	-0.760674738
H	1.489115232	2.143657244	0.877068083
N	-1.469298921	1.599158927	-0.013111026
H	-1.407063690	2.265551185	0.759696183
H	-1.487145013	2.144520249	-0.877960582
H	2.381661264	1.136413747	-0.063000726
H	-2.380646238	1.138799702	0.062828821

./cisplatin-PBE0-H2O-ApVDZ-pVDZ-pp_eGeom.xyz
11

Pt	0.531688263	0.795542871	0.000000000
Cl	0.445353553	-1.531355993	-0.001737761
Cl	2.858587130	0.881877498	0.001737761
N	0.564741326	2.841637875	-0.016786466
H	0.197290846	3.229944968	-0.884543080
H	0.041632675	3.265189467	0.748239896
N	-1.514406743	0.762489881	0.016786466
H	-1.902713822	1.129940374	0.884543080
H	-1.937958316	1.285598546	-0.748239896
H	1.531153956	3.158984174	0.065501425
H	-1.831753076	-0.203922738	-0.065501425

./cisplatin-M06L-TZ-aug-pVDZ_eGeom.xyz
11

Pt	0.486239091	0.840992045	0.000000000
Cl	0.371784577	-1.456039131	-0.000115490
Cl	2.783270271	0.955446477	0.000115490
N	0.651734877	2.947539854	-0.000105950
H	0.277491986	3.407821164	-0.819921285
H	0.277150304	3.407917707	0.819500188
N	-1.620308724	0.675496333	0.000105950
H	-2.080590021	1.049739240	0.819921285
H	-2.080686564	1.050080923	-0.819500188

```
H      1.664335903      3.074037008      0.000110622
H      -1.746805915     -0.337104688     -0.000110622
./cisplatin-PBE0-SMD-ApVDZ-aug-pVTZ-pp-2_eGeom.xyz
11
```

```
Pt      0.000015782      0.158993717      0.000186031
Cl      -1.689565653     -1.429331143     -0.006283746
Cl      1.688004999     -1.431018884      0.007635602
N       1.433672868      1.597781817      0.010163864
H       1.332655184      2.250609115     -0.766805992
H       1.410693349      2.146907802      0.869573516
N      -1.432198314      1.599211778     -0.010678624
H      -1.330550356      2.252388843      0.765914955
H      -1.408640966      2.147815492     -0.870405808
H       2.361995919      1.180897914     -0.058673430
H      -2.360940812      1.183298549      0.058371632
./cisplatin-ApVDZ-aug-pVDZ-pp_eGeom.xyz
11
```

```
Pt      0.474091466      0.853139670      0.000000000
Cl      0.358909296     -1.449895375      0.000007966
Cl      2.777126515      0.968321758     -0.000007966
N       0.641059206      2.928968066     -0.000001538
H       0.260572048      3.391734621     -0.833897350
H       0.260740901      3.391739501      0.833968662
N      -1.601736936      0.686172004      0.000001538
H      -2.064503477      1.066659178      0.833897350
H      -2.064508358      1.066490325     -0.833968662
H       1.671194667      3.056560637     -0.000098371
H      -1.729329544     -0.343963453      0.000098371
./cisplatin-M062X-SMD-TZ-pVDZ_eGeom.xyz
11
```

```
Pt      0.554393365      0.772837768      0.000000000
Cl      0.477358961     -1.573826889     -0.000258130
Cl      2.901058025      0.849872088      0.000258130
N       0.537127430      2.823007818     -0.000032786
H       0.061119584      3.192732620     -0.819458068
H       0.061188579      3.192791974      0.819404694
N      -1.495776684      0.790103776      0.000032786
H      -1.865501469      1.266111635      0.819458068
H      -1.865560823      1.266042640     -0.819404694
H       1.484425282      3.193447565     -0.000090422
H      -1.866216465     -0.157194063      0.000090422
./cisplatin-M06L-CPCM-ApVDZ-pVTZ-2_eGeom.xyz
11
```

```
Pt      0.537608329      0.789622804      0.000000000
Cl      0.442929186     -1.566231429     -0.002498408
Cl      2.893462566      0.884301864      0.002498408
N       0.575181300      2.859291658      0.016372173
H       0.056627302      3.288067542     -0.748292442
H       0.207660455      3.255857263      0.879807433
N      -1.532060525      0.752049908     -0.016372173
```


H	-1.960836392	1.270603920	0.748292442
H	-1.928626118	1.119570766	-0.879807433
H	1.541141967	3.176703383	-0.063921146
H	-1.849472285	-0.213910748	0.063921146

./cisplatin-M06L-H2O-TZ-aug-pVTZ-2_eGeom.xyz

11

Pt	0.000036275	0.176043703	0.000191043
Cl	-1.724984642	-1.409903045	-0.000521105
Cl	1.723507111	-1.411586262	0.001916396
N	1.502983872	1.606780420	0.011249894
H	1.447303407	2.258453877	-0.762159249
H	1.516974581	2.152866426	0.864422040
N	-1.501513869	1.608240050	-0.011780386
H	-1.445183432	2.260373978	0.761193324
H	-1.514987932	2.153770987	-0.865315941
H	2.396640195	1.130069236	-0.055755660
H	-2.395633566	1.132445630	0.055557646

./cisplatin-PBE0-SMD-ApVTZ-2_eGeom.xyz

11

Pt	0.000038519	0.160722081	0.000178741
Cl	-1.691463883	-1.423261113	-0.007433943
Cl	1.690022390	-1.424875919	0.008740098
N	1.439331803	1.594543259	0.014187743
H	1.341444454	2.266683477	-0.750320784
H	1.437427257	2.133910868	0.883500079
N	-1.437883371	1.595909699	-0.014688675
H	-1.339299675	2.268478665	0.749353085
H	-1.435530303	2.134679811	-0.884370677
H	2.367770662	1.174226971	-0.072044480
H	-2.366715854	1.176537201	0.071896814

./cisplatin-M06L-H2O-ApVDZ-pVDZ-2_eGeom.xyz

11

Pt	0.000031816	0.167504292	0.000184957
Cl	-1.738422280	-1.433057763	-0.004553744
Cl	1.736921088	-1.434752007	0.005913383
N	1.497433620	1.606359846	0.014506697
H	1.432409565	2.277517985	-0.748913383
H	1.523410340	2.145361332	0.878600437
N	-1.495963699	1.607813724	-0.015024598
H	-1.430239097	2.279439588	0.747923872
H	-1.521464877	2.146238904	-0.879491890
H	2.403805421	1.146364771	-0.070597977
H	-2.402779897	1.148764328	0.070450246

./cisplatin-PBE0-H2O-TZ-pVTZ-pp-2_eGeom.xyz

11

Pt	0.000040447	0.185160779	0.000191794
Cl	-1.697826181	-1.389347381	0.000279788
Cl	1.696365991	-1.391007395	0.001119675
N	1.475859920	1.600638732	0.012010205
H	1.412087446	2.254985068	-0.761092992

H	1.486449477	2.141555738	0.870918008
N	-1.474395244	1.602072573	-0.012540352
H	-1.409970211	2.256877577	0.760120100
H	-1.484472430	2.142420491	-0.871812597
H	2.372134341	1.125920704	-0.059215534
H	-2.371131557	1.128278115	0.059019904

./cisplatin-PBE0-TZ-aug-pVDZ_eGeom.xyz

11

Pt	0.477613459	0.849617677	0.000000000
Cl	0.368893798	-1.428279017	0.000004854
Cl	2.755510157	0.958337257	-0.000004854
N	0.628053116	2.914537889	0.000044887
H	0.246909992	3.364849915	-0.824113879
H	0.246932848	3.364814110	0.824233960
N	-1.587306759	0.699178093	-0.000044887
H	-2.037618771	1.080321233	0.824113879
H	-2.037582967	1.080298377	-0.824233960
H	1.642202165	3.047222350	0.000038707
H	-1.719991255	-0.314970951	-0.000038707

./cisplatin-PBE0-CPCM-ApVTZ-ApVDZ-pp-2_eGeom.xyz

11

Pt	0.527398018	0.799833116	0.000000000
Cl	0.446253032	-1.513786758	-0.002769057
Cl	2.841017895	0.880978020	0.002769057
N	0.565382078	2.843225382	-0.012701384
H	0.175626310	3.232013328	-0.865614973
H	0.066690536	3.258101040	0.767861625
N	-1.515994250	0.761849129	0.012701384
H	-1.904782182	1.151604910	0.865614973
H	-1.930869890	1.260540686	-0.767861625
H	1.533636398	3.147973258	0.045033171
H	-1.820742159	-0.206405180	-0.045033171

./cisplatin-M06L-SMD-ApVDZ-pVTZ-2_eGeom.xyz

11

Pt	0.000026928	0.145551804	0.000183777
Cl	-1.718586509	-1.461157459	-0.010401290
Cl	1.717085452	-1.462811990	0.011731209
N	1.459813323	1.604510158	0.021071985
H	1.340630836	2.298674755	-0.716166467
H	1.474825749	2.115267632	0.903668736
N	-1.458350472	1.605906088	-0.021579685
H	-1.338484999	2.300419811	0.715219162
H	-1.472891574	2.116122316	-0.904497310
H	2.386316298	1.196354627	-0.098680286
H	-2.385243032	1.198717257	0.098448170

./cisplatin-PBE0-H2O-ApVDZ_eGeom.xyz

11

Pt	0.529706319	0.797524815	0.000000000
Cl	0.448686184	-1.524378714	-0.001010269
Cl	2.851609851	0.878544867	0.001010269

```

N      0.567282207      2.840934150      -0.000336652
H      0.123114331      3.255015778      -0.822908143
H      0.121831752      3.255516367      0.821284872
N     -1.513703017      0.759949000      0.000336652
H     -1.927784629      1.204116890      0.822908143
H     -1.928285219      1.205399469      -0.821284872
H      1.541159592      3.157232684      0.000290694
H     -1.830001586     -0.213928374     -0.000290694

```

./cisplatin-M062X-H2O-TZ-pVDZ-3_eGeom.xyz

11

```

Pt      0.000000000      0.000000000      0.181114075
Cl      0.004215717     -1.725359711     -1.419869611
Cl     -0.004215717      1.725359711     -1.419869611
N      0.013328498      1.478464357      1.618025597
H     -0.747421892      1.396481626      2.286002270
H      0.881755967      1.493212066      2.145054518
N     -0.013328498     -1.478464357      1.618025597
H      0.747421892     -1.396481626      2.286002270
H     -0.881755967     -1.493212066      2.145054518
H     -0.077243896      2.381384782      1.158363189
H      0.077243896     -2.381384782      1.158363189

```

./cisplatin-M062X-CPCM-ApVTZ-pVTZ_eGeom.xyz

11

```

Pt      0.534649346      0.792581788      0.000000000
Cl      0.446267451     -1.557789317      0.001180598
Cl      2.885020454      0.880963599     -0.001180598
N      0.561865423      2.847565455      0.018543972
H      0.035998485      3.262832526     -0.744706084
H      0.191283661      3.228081278      0.884586795
N     -1.520334322      0.765365783     -0.018543972
H     -1.935601374      1.291232736      0.744706084
H     -1.900850132      1.135947559     -0.884586795
H      1.524344618      3.166258911     -0.063941517
H     -1.839027813     -0.197113400      0.063941517

```

./cisplatin-M06L-H2O-ApVDZ-pVTZ_eGeom.xyz

11

```

Pt      0.537201573      0.790029560      0.000000000
Cl      0.444298829     -1.567486658      0.001745848
Cl      2.894717795      0.882932221     -0.001745848
N      0.575890775      2.860631632     -0.018936484
H      0.219440723      3.254475280     -0.888429080
H      0.046859650      3.291591722      0.737281860
N     -1.533400500      0.751340432      0.018936484
H     -1.927244136      1.107790498      0.888429080
H     -1.964360571      1.280371573     -0.737281860
H      1.540968937      3.177988391      0.072828935
H     -1.850757293     -0.213737719     -0.072828935

```

./cisplatin-M062X-H2O-ApVDZ-aug-pVDZ_eGeom.xyz

11

```

Pt      0.534872444      0.792358689      0.000000000

```

Cl	0.444757324	-1.570035949	0.008013516
Cl	2.897267086	0.882473725	-0.008013516
N	0.560578827	2.846690558	-0.020848864
H	0.207042309	3.230042611	-0.896910893
H	0.019290630	3.267429610	0.733322583
N	-1.519459425	0.766652379	0.020848864
H	-1.902811466	1.120188911	0.896910893
H	-1.940198458	1.307940592	-0.733322583
H	1.523680850	3.168635438	0.079585983
H	-1.841404340	-0.196449631	-0.079585983

./cisplatin-PBE0-H2O-ApVDZ-aug-pVTZ-pp_eGeom.xyz

11

Pt	0.526285045	0.800946089	0.000000000
Cl	0.443935961	-1.519896444	-0.005875892
Cl	2.847127581	0.883295091	0.005875892
N	0.562675400	2.838040938	-0.016593635
H	0.189621070	3.226071651	-0.881671973
H	0.047244817	3.261592388	0.753149483
N	-1.510809805	0.764555807	0.016593635
H	-1.898840505	1.137610151	0.881671973
H	-1.934361237	1.279986405	-0.753149483
H	1.531759534	3.148253179	0.058148627
H	-1.821022080	-0.204528316	-0.058148627

./cisplatin-M062X-CPCM-ApVDZ-pVTZ-2_eGeom.xyz

11

Pt	0.000000000	0.000000000	0.187748560
Cl	0.005408602	-1.735898561	-1.417877871
Cl	-0.005408602	1.735898561	-1.417877871
N	-0.019722618	1.466964555	1.620501425
H	-0.896831042	1.488917401	2.140140227
H	0.732211678	1.380527963	2.303326418
N	0.019722618	-1.466964555	1.620501425
H	0.896831042	-1.488917401	2.140140227
H	-0.732211678	-1.380527963	2.303326418
H	0.082597788	2.376883355	1.169675521
H	-0.082597788	-2.376883355	1.169675521

./cisplatin-M062X-H2O-TZ-aug-pVTZ-2_eGeom.xyz

11

Pt	0.534204738	0.793026396	0.000000000
Cl	0.446440563	-1.557373314	0.001154059
Cl	2.884604450	0.880790487	-0.001154059
N	0.563607223	2.850449026	-0.018649600
H	0.198406128	3.231417045	-0.887031907
H	0.034778917	3.266810671	0.742312195
N	-1.523217894	0.763623984	0.018649600
H	-1.904185899	1.128825092	0.887031907
H	-1.939579519	1.292452305	-0.742312195
H	1.526977336	3.165651358	0.068447934
H	-1.838420259	-0.199746118	-0.068447934

./cisplatin-CPCM-TZ-pVTZ-pp-2_eGeom.xyz

11

Pt	0.000038381	0.183698690	0.000177314
Cl	-1.713480454	-1.395826223	0.002565088
Cl	1.711996187	-1.397521622	-0.001335765
N	1.494614191	1.603601239	0.008267230
H	1.443595206	2.247162952	-0.786101196
H	1.495774419	2.165256046	0.864312349
N	-1.493136794	1.605071007	-0.008742155
H	-1.441335954	2.249323150	0.785013891
H	-1.493939348	2.165933478	-0.865308879
H	2.395490271	1.114235271	-0.042690031
H	-2.394474104	1.116621011	0.042840156

./cisplatin_eGeom.xyz

11

Pt	0.473754488	0.853476648	0.000000000
Cl	0.359392710	-1.450255700	0.000020290
Cl	2.777486840	0.967838343	-0.000020290
N	0.646893421	2.934837659	-0.000001568
H	0.274976232	3.412537432	-0.834691136
H	0.274993868	3.412540853	0.834693870
N	-1.607606529	0.680337789	0.000001568
H	-2.085306289	1.052254995	0.834691136
H	-2.085309710	1.052237359	-0.834693870
H	1.682697894	3.055588234	-0.000013062
H	-1.728357141	-0.355466680	0.000013062

./cisplatin-M062X-aug-pVTZ_eGeom.xyz

11

Pt	0.495778580	0.831452555	0.000000000
Cl	0.392258888	-1.463881524	0.000007374
Cl	2.791112662	0.934972165	-0.000007374
N	0.627086300	2.918563972	0.000014738
H	0.240035968	3.375434312	-0.826720424
H	0.240011200	3.375427418	0.826742154
N	-1.591332842	0.700144910	-0.000014738
H	-2.048203167	1.087195257	0.826720424
H	-2.048196274	1.087220025	-0.826742154
H	1.641211461	3.083378088	0.000031229
H	-1.756146993	-0.313980246	-0.000031229

./cisplatin-PBE0-SMD-ApVDZ-pVTZ-pp-2_eGeom.xyz

11

Pt	0.000015138	0.155725237	0.000179826
Cl	-1.691727469	-1.432992657	-0.011530356
Cl	1.690164321	-1.434680185	0.012839997
N	1.434815176	1.597727283	0.018081124
H	1.315517365	2.281009578	-0.730093597
H	1.436346912	2.115207732	0.897715599
N	-1.433340191	1.599152347	-0.018584873
H	-1.313349501	2.282775285	0.729167807
H	-1.434366556	2.116092673	-0.898537681
H	2.362619607	1.187559230	-0.089697386
H	-2.361552803	1.189978477	0.089457541

./cisplatin-H2O-ApVTZ-pVTZ-pp-2_eGeom.xyz
11

Pt	0.527903884	0.799327250	0.000000000
Cl	0.438256704	-1.527332032	-0.006284253
Cl	2.854563170	0.888974347	0.006284253
N	0.577187884	2.858562544	-0.013396393
H	0.189413483	3.251881419	-0.875708374
H	0.075955645	3.281317414	0.772831297
N	-1.531331412	0.750043323	0.013396393
H	-1.924650273	1.137817738	0.875708374
H	-1.954086264	1.251275577	-0.772831297
H	1.558139444	3.154967578	0.046392420
H	-1.827736481	-0.230908226	-0.046392420

./cisplatin-M062X-H2O-ApVTZ-ApVDZ-3_eGeom.xyz
11

Pt	0.000000000	0.000000000	0.185901256
Cl	0.011745742	-1.724111503	-1.416228036
Cl	-0.011745742	1.724111503	-1.416228036
N	0.006411916	1.474588700	1.620680333
H	-0.752712520	1.386589713	2.289749107
H	0.875210360	1.493743483	2.146980138
N	-0.006411916	-1.474588700	1.620680333
H	0.752712520	-1.386589713	2.289749107
H	-0.875210360	-1.493743483	2.146980138
H	-0.090417897	2.378488662	1.164246330
H	0.090417897	-2.378488662	1.164246330

./cisplatin-PBE0-SMD-ApVDZ_eGeom.xyz
11

Pt	0.549605172	0.777625961	0.000000000
Cl	0.477519997	-1.542104805	-0.000411321
Cl	2.869335941	0.849711054	0.000411321
N	0.543084972	2.814323317	-0.000047089
H	0.071047325	3.201044649	-0.821897998
H	0.071178764	3.201142595	0.821831353
N	-1.487092183	0.784146234	0.000047089
H	-1.873813498	1.256183895	0.821897998
H	-1.873911445	1.256052456	-0.821831353
H	1.496433128	3.187003486	-0.000154338
H	-1.859772387	-0.169201909	0.000154338

./cisplatin-M06L-aug-pVDZ-SMD-2_eGeom.xyz
11

Pt	0.000024189	0.144168354	0.000178210
Cl	-1.716620178	-1.463557831	-0.010392814
Cl	1.715107983	-1.465215859	0.011696355
N	1.464425789	1.602572415	0.019640457
H	1.355122813	2.294601600	-0.725074845
H	1.480146744	2.125405408	0.898561493
N	-1.462963103	1.603979469	-0.020141577
H	-1.352965108	2.296370474	0.724134905
H	-1.478210175	2.126275060	-0.899390376

H 2.395564523 1.195288782 -0.091969362
H -2.394491478 1.197667129 0.091755559
./cisplatin-M06L-CPCM-ApVDZ-aug-pVDZ-2_eGeom.xyz
11

Pt 0.537026151 0.790204982 0.000000000
Cl 0.443772883 -1.564730339 -0.001147990
Cl 2.891961476 0.883458167 0.001147990
N 0.577162037 2.861930932 0.013675048
H 0.072717879 3.288242599 -0.761540363
H 0.195702244 3.261789326 0.869304177
N -1.534699800 0.750069170 -0.013675048
H -1.961011449 1.254513343 0.761540363
H -1.934558180 1.131528978 -0.869304177
H 1.545002886 3.176691440 -0.051926112
H -1.849460342 -0.217771667 0.051926112
./cisplatin-ApVDZ-pVTZ-pp_eGeom.xyz
11

Pt 0.474320799 0.852910336 0.000000000
Cl 0.357183092 -1.448752244 0.000014043
Cl 2.775983384 0.970047962 -0.000014043
N 0.639935089 2.926766584 -0.000004514
H 0.260311932 3.391283772 -0.833542385
H 0.260452417 3.391289960 0.833593921
N -1.599535454 0.687296120 0.000004514
H -2.064052628 1.066919294 0.833542385
H -2.064058816 1.066778809 -0.833593921
H 1.670301027 3.054456151 -0.000085593
H -1.727225057 -0.343069813 0.000085593
./cisplatin-M06L-ApVDZ-aug-pVTZ_eGeom.xyz
11

Pt 0.485966278 0.841264858 0.000000000
Cl 0.371497602 -1.462264883 -0.000126191
Cl 2.789496022 0.955733452 0.000126191
N 0.646857525 2.937966517 -0.000172742
H 0.271720399 3.405303275 -0.822241680
H 0.270911810 3.405477974 0.821430806
N -1.610735387 0.680373685 0.000172742
H -2.078072132 1.055510828 0.822241680
H -2.078246831 1.056319416 -0.821430806
H 1.662631592 3.075642187 0.000333526
H -1.748411093 -0.335400378 -0.000333526
./cisplatin-PBE0-ApVTZ-pVTZ-pp_eGeom.xyz
11

Pt 0.478102033 0.849129102 0.000000000
Cl 0.368975397 -1.427507009 -0.000374487
Cl 2.754738148 0.958255657 0.000374487
N 0.627658098 2.912081239 -0.000025984
H 0.244916535 3.362912678 -0.823345983
H 0.245249812 3.362938503 0.823434424
N -1.584850109 0.699573111 0.000025984

H	-2.035681534	1.082314690	0.823345983
H	-2.035707359	1.081981413	-0.823434424
H	1.641637025	3.048653356	-0.000207705
H	-1.721422262	-0.314405811	0.000207705

./cisplatin-TZ-aug-pVDZ-pp_eGeom.xyz

11

Pt	0.474802229	0.852428907	0.000000000
Cl	0.360906968	-1.441222017	0.000013826
Cl	2.768453157	0.966324086	-0.000013826
N	0.641335967	2.931620116	-0.000005700
H	0.260864210	3.388643280	-0.831999073
H	0.260962312	3.388651797	0.832027680
N	-1.604388986	0.685895242	0.000005700
H	-2.061412137	1.066367016	0.831999073
H	-2.061420654	1.066268914	-0.832027680
H	1.668237972	3.051956348	-0.000062489
H	-1.724725255	-0.341006758	0.000062489

./cisplatin-PBE0-H2O-ApVTZ-ApVDZ-pp-2_eGeom.xyz

11

Pt	0.000039635	0.183248640	0.000188991
Cl	-1.694622746	-1.393966901	-0.001813718
Cl	1.693158022	-1.395622448	0.003193985
N	1.472522365	1.600600866	0.013138657
H	1.402696395	2.259242662	-0.755884625
H	1.484571227	2.136992252	0.874953824
N	-1.471057542	1.602030996	-0.013663081
H	-1.400561215	2.261135557	0.754902296
H	-1.482614612	2.137838562	-0.875848290
H	2.371376184	1.131846666	-0.064582542
H	-2.370365713	1.134208146	0.064412505

./cisplatin-SMD-TZ-pVDZ-pp-2_eGeom.xyz

11

Pt	0.543587103	0.783644030	0.000000000
Cl	0.464444923	-1.543520413	-0.002651182
Cl	2.870751549	0.862786128	0.002651182
N	0.559536174	2.842491979	0.017496383
H	0.019287824	3.244260404	-0.754814798
H	0.172522686	3.212182480	0.891674712
N	-1.515260846	0.767695033	-0.017496383
H	-1.917029252	1.307943397	0.754814798
H	-1.884951334	1.154708534	-0.891674712
H	1.524486381	3.180990516	-0.063169834
H	-1.853759417	-0.197255162	0.063169834

./cisplatin-M062X-pVTZ_eGeom.xyz

11

Pt	0.497406980	0.829824155	0.000000000
Cl	0.393092818	-1.466645142	0.000007991
Cl	2.793876281	0.934138236	-0.000007991
N	0.632161189	2.925112920	0.000015030
H	0.246304405	3.384060003	-0.826892815

H	0.246285708	3.384052297	0.826918442
N	-1.597881790	0.695070020	-0.000015030
H	-2.056828859	1.080926821	0.826892815
H	-2.056821153	1.080945518	-0.826918442
H	1.647113627	3.088324515	0.000027695
H	-1.761093421	-0.319882412	-0.000027695

./cisplatin-H20-TZ-aug-pVTZ-pp-2_eGeom.xyz

11

Pt	0.526768961	0.800462173	0.000000000
Cl	0.435053309	-1.525483068	-0.006932158
Cl	2.852714205	0.892177742	0.006932158
N	0.578595001	2.860067394	-0.012138349
H	0.186313953	3.255131366	-0.871587128
H	0.084054636	3.282738531	0.778357976
N	-1.532836261	0.748636206	0.012138349
H	-1.927900219	1.140917269	0.871587128
H	-1.955507382	1.243176586	-0.778357976
H	1.561215058	3.152086575	0.041625979
H	-1.824855478	-0.233983841	-0.041625979

./cisplatin-M062X-H20-aug-pVDZ_eGeom.xyz

11

Pt	0.536009492	0.791221641	0.000000000
Cl	0.445962906	-1.567655814	0.003322301
Cl	2.894886951	0.881268144	-0.003322301
N	0.563586699	2.845955132	-0.018270970
H	0.198464617	3.237967069	-0.890283239
H	0.033991152	3.272778849	0.745908639
N	-1.518724000	0.763644508	0.018270970
H	-1.910735924	1.128766604	0.890283239
H	-1.945547698	1.293240069	-0.745908639
H	1.530564932	3.172074440	0.069185232
H	-1.844843342	-0.203333714	-0.069185232

./cisplatin-M062X-H20-ApVTZ-pVTZ-3_eGeom.xyz

11

Pt	0.000000000	0.000000000	0.184555237
Cl	0.006257126	-1.724341884	-1.416393692
Cl	-0.006257126	1.724341884	-1.416393692
N	0.012017061	1.473976291	1.618681473
H	-0.747044728	1.389048983	2.288234388
H	0.880776225	1.489636639	2.145196506
N	-0.012017061	-1.473976291	1.618681473
H	0.747044728	-1.389048983	2.288234388
H	-0.880776225	-1.489636639	2.145196506
H	-0.081131057	2.378671669	1.162967706
H	0.081131057	-2.378671669	1.162967706

./cisplatin-PBE0-ApVTZ-ApVTZ-pp_eGeom.xyz

11

Pt	0.477695014	0.849536122	0.000000000
Cl	0.368190949	-1.426097850	0.000010079
Cl	2.753328989	0.959040106	-0.000010079

N	0.627889465	2.912083762	0.000183770
H	0.245195683	3.362442428	-0.823419051
H	0.245234720	3.362285587	0.823891338
N	-1.584852631	0.699341744	-0.000183770
H	-2.035211284	1.082035542	0.823419051
H	-2.035054443	1.081996505	-0.823891338
H	1.641905528	3.047937299	0.000184189
H	-1.720706205	-0.314674314	-0.000184189

./cisplatin-M06L-H2O-ApVTZ-ApVDZ-2_eGeom.xyz
11

Pt	0.000035949	0.175243574	0.000188149
Cl	-1.723066934	-1.413720391	-0.001507661
Cl	1.721585318	-1.415401421	0.002887826
N	1.500805512	1.606938541	0.012316084
H	1.440857165	2.262407524	-0.757293942
H	1.516794308	2.148850547	0.867894428
N	-1.499335118	1.608395928	-0.012841980
H	-1.438722031	2.264328948	0.756320371
H	-1.514824233	2.149741960	-0.868787917
H	2.395983794	1.134194821	-0.060244129
H	-2.394971729	1.136574971	0.060066771

./cisplatin-M062X-CPCM-aug-pVTZ-2_eGeom.xyz
11

Pt	0.000000000	0.000000000	0.185907775
Cl	-0.006297575	-1.732056482	-1.415448591
Cl	0.006297575	1.732056482	-1.415448591
N	-0.015516933	1.468702834	1.613408740
H	-0.883989118	1.483985474	2.153068349
H	0.752467802	1.400186097	2.284552094
N	0.015516933	-1.468702834	1.613408740
H	0.883989118	-1.483985474	2.153068349
H	-0.752467802	-1.400186097	2.284552094
H	0.065588146	2.380785889	1.156416020
H	-0.065588146	-2.380785889	1.156416020

./cisplatin-M06L-TZ-pVTZ_eGeom.xyz
11

Pt	0.486022018	0.841209117	0.000000000
Cl	0.369898629	-1.455212164	-0.000049127
Cl	2.782443303	0.957332424	0.000049127
N	0.652230208	2.947596113	-0.000090418
H	0.278386934	3.408550671	-0.819696276
H	0.278096853	3.408629081	0.819340180
N	-1.620364983	0.675001002	0.000090418
H	-2.081319528	1.048844293	0.819696276
H	-2.081397938	1.049134374	-0.819340180
H	1.665130461	3.072741267	0.000097096
H	-1.745510173	-0.337899246	-0.000097096

./cisplatin-M062X-H2O_eGeom.xyz
11

Pt	0.537253590	0.789977544	0.000000000
----	-------------	-------------	-------------

Cl	0.445221690	-1.567774920	-0.002444424
Cl	2.895006057	0.882009360	0.002444424
N	0.570153982	2.853525310	-0.014788891
H	0.191770068	3.252609078	-0.878330386
H	0.057489813	3.283245032	0.759955200
N	-1.526294177	0.757077225	0.014788891
H	-1.925377932	1.135461154	0.878330386
H	-1.956013881	1.269741409	-0.759955200
H	1.541129299	3.173953818	0.056077975
H	-1.846722720	-0.213898081	-0.056077975

./cisplatin-H2O-TZ-pVTZ-pp-2_eGeom.xyz
11

Pt	0.525931451	0.801299683	0.000000000
Cl	0.431652160	-1.526952193	-0.006905677
Cl	2.854183330	0.895578891	0.006905677
N	0.580176614	2.862198986	-0.011429318
H	0.186069081	3.259000140	-0.869068323
H	0.089685003	3.285364271	0.781151648
N	-1.534967853	0.747054593	0.011429318
H	-1.931768994	1.141162141	0.869068323
H	-1.958133122	1.237546219	-0.781151648
H	1.564055055	3.150498042	0.039219553
H	-1.823266945	-0.236823838	-0.039219553

./cisplatin-SMD-aug-pVTZ-2_eGeom.xyz
11

Pt	0.544015679	0.783215454	0.000000000
Cl	0.465356337	-1.546964604	-0.003632128
Cl	2.874195740	0.861874713	0.003632128
N	0.557406221	2.830756208	0.017714942
H	0.013777040	3.248030572	-0.753739226
H	0.173392011	3.214616449	0.895735357
N	-1.503525076	0.769824985	-0.017714942
H	-1.920799419	1.313454181	0.753739226
H	-1.887385303	1.153839209	-0.895735357
H	1.524175654	3.184224199	-0.065605967
H	-1.856993101	-0.196944435	0.065605967

./cisplatin-H2O-ApVDZ-pVTZ-pp-2_eGeom.xyz
11

Pt	0.530334190	0.796896944	0.000000000
Cl	0.440635742	-1.539927797	-0.001737468
Cl	2.867158934	0.886595309	0.001737468
N	0.573211711	2.852709408	-0.017136363
H	0.204931290	3.245629348	-0.892991824
H	0.049602015	3.283292568	0.755493862
N	-1.525478276	0.754019496	0.017136363
H	-1.918398202	1.122299931	0.892991824
H	-1.956061417	1.277629207	-0.755493862
H	1.552495549	3.162046846	0.064466673
H	-1.834815748	-0.225264331	-0.064466673

./cisplatin-M06L-CPCM-2_eGeom.xyz
11

```
Pt      0.000031918      0.166812920      0.000195581
Cl      -1.737235413     -1.432935956     0.000987164
Cl      1.735738114     -1.434629924     0.000431769
N       1.502292978     1.604199336     0.008019330
H       1.462909142     2.255441744    -0.778680477
H       1.515905466     2.175493635     0.855529208
N      -1.500826318     1.605658728    -0.008551609
H      -1.460807044     2.257367193     0.777730085
H      -1.513881845     2.176421995    -0.856427990
H       2.413529390     1.140672213    -0.042578612
H      -2.412514387     1.143053118     0.042343568
```

./cisplatin-M06L-SMD-ApVDZ-aug-pVDZ-2_eGeom.xyz

11

```
Pt      0.000024578      0.146136350      0.000179950
Cl      -1.717245600     -1.461098558    -0.009572381
Cl      1.715734268     -1.462758136     0.010887268
N       1.462651801     1.605093704     0.019417080
H       1.348732615     2.291515388    -0.725615987
H       1.472660171     2.124123910     0.897073674
N      -1.461186949     1.606500062    -0.019923105
H      -1.346592070     2.293264548     0.724690253
H      -1.470704965     2.125005025    -0.897895484
H       2.388766152     1.193700529    -0.091005164
H      -2.387698003     1.196072178     0.090761897
```

./cisplatin-CPCM-ApVTZ-ApVDZ-pp-2_eGeom.xyz

11

```
Pt      0.000039146      0.181534019      0.000197555
Cl      -1.709839105     -1.401348325     0.000624663
Cl      1.708350719     -1.403045252     0.000428994
N       1.490623551     1.603709004     0.009241851
H       1.433697119     2.250979832    -0.781870415
H       1.492272071     2.161596846     0.867908352
N      -1.489143262     1.605172694    -0.009670400
H      -1.431326791     2.253277406     0.780691100
H      -1.490569455     2.162103270    -0.868961309
H       2.394468458     1.120591928    -0.047222995
H      -2.393430452     1.122983576     0.047630606
```

./cisplatin-aug-pVDZ_eGeom.xyz

11

```
Pt      0.475789677      0.851441459      0.000000000
Cl      0.363117330     -1.449983791     0.000017554
Cl      2.777214931      0.964113724    -0.000017554
N       0.639966094     2.927281316    -0.000001135
H       0.264126418     3.399651282    -0.835565292
H       0.264130998     3.399655239     0.835562808
N      -1.600050186     0.687265115     0.000001135
H      -2.072420139     1.063104808     0.835565292
H      -2.072424095     1.063100228    -0.835562808
H       1.673832881     3.056899218    -0.000004736
H      -1.729668124     -0.346601666     0.000004736
```

./cisplatin-M062X-SMD-3_eGeom.xyz

11

Pt	0.551470278	0.775760855	0.000000000
Cl	0.471538862	-1.576771926	-0.000944582
Cl	2.904003062	0.855692188	0.000944582
N	0.550190120	2.830228190	0.017825891
H	0.007116360	3.238712232	-0.749336254
H	0.159615111	3.207527848	0.887382110
N	-1.502997057	0.777041087	-0.017825891
H	-1.911481079	1.320114861	0.749336254
H	-1.880296700	1.167616109	-0.887382110
H	1.504011287	3.196785554	-0.061390122
H	-1.869554455	-0.176780068	0.061390122

./cisplatin-PBE0-CPCM-pVTZ-pp-2_eGeom.xyz

11

Pt	0.527226570	0.800004564	0.000000000
Cl	0.440428554	-1.521617527	-0.004122438
Cl	2.848848664	0.886802497	0.004122438
N	0.568646141	2.841470949	-0.009973164
H	0.169170797	3.245752476	-0.859773525
H	0.082454549	3.268101390	0.781506623
N	-1.514239816	0.758585066	0.009973164
H	-1.918521329	1.158060424	0.859773525
H	-1.940870241	1.244776673	-0.781506623
H	1.543681396	3.150440594	0.035382559
H	-1.823209496	-0.216450178	-0.035382559

./cisplatin-M062X-CPCM-ApVTZ-ApVTZ_eGeom.xyz

11

Pt	0.534368460	0.792862674	0.000000000
Cl	0.445652743	-1.556815241	0.002529955
Cl	2.884046378	0.881578307	-0.002529955
N	0.561892067	2.847698600	0.018533916
H	0.035611631	3.263076730	-0.744532718
H	0.192337749	3.228167069	0.885155060
N	-1.520467467	0.765339140	-0.018533916
H	-1.935845579	1.291619591	0.744532718
H	-1.900935923	1.134893471	-0.885155060
H	1.524830176	3.165105535	-0.064877430
H	-1.837874437	-0.197598958	0.064877430

./cisplatin-M062X-TZ-pVDZ_eGeom.xyz

11

Pt	0.496820175	0.830410960	0.000000000
Cl	0.393405327	-1.459307375	-0.000008900
Cl	2.786538514	0.933825726	0.000008900
N	0.634741573	2.934230941	0.000024360
H	0.250423234	3.384386555	-0.823122103
H	0.250403236	3.384373397	0.823168717
N	-1.606999810	0.692489636	-0.000024360
H	-2.057155411	1.076807992	0.823122103
H	-2.057142254	1.076827990	-0.823168717

```
H      1.645570723      3.080220618      0.000037092
H      -1.752989524     -0.318339508     -0.000037092
./cisplatin-PBE0_eGeom.xyz
11
```

```
Pt      0.479253325      0.847977811      0.000000000
Cl      0.372907242     -1.438547159     -0.000116720
Cl      2.765778299      0.954323812      0.000116720
N       0.633214173      2.918513267      0.000008894
H       0.258050098      3.386556660     -0.826804485
H       0.258397264      3.386543887      0.826987184
N      -1.591282137      0.694017037     -0.000008894
H      -2.059325516      1.069181128      0.826804485
H      -2.059312743      1.068833962     -0.826987184
H       1.654732476      3.056027789     -0.000181131
H      -1.728796695     -0.327501261      0.000181131
./cisplatin-M062X-SMD-ApVDZ-aug-pVDZ-2_eGeom.xyz
11
```

```
Pt      0.554425850      0.772805283      0.000000000
Cl      0.480098140     -1.585037280      0.000021348
Cl      2.912268416      0.847132909     -0.000021348
N       0.533900575      2.818461398     -0.000045641
H       0.055906666      3.191689901     -0.821119905
H       0.055494569      3.191733922      0.820766389
N      -1.491230265      0.793330631      0.000045641
H      -1.864458750      1.271324553      0.821119905
H      -1.864502771      1.271736650     -0.820766389
H       1.481436002      3.196953748      0.000170322
H      -1.869722647     -0.154204783     -0.000170322
./cisplatin-PBE0-aug-pVTZ_eGeom.xyz
11
```

```
Pt      0.477233077      0.849998059      0.000000000
Cl      0.368436454     -1.432577429     -0.000172409
Cl      2.759808568      0.958794601      0.000172409
N       0.624668110      2.906010068     -0.000013964
H       0.245324450      3.368119809     -0.826847527
H       0.245547291      3.368133853      0.826914277
N      -1.578778937      0.702563099      0.000013964
H      -2.040888665      1.081906775      0.826847527
H      -2.040902709      1.081683935     -0.826914277
H       1.644238755      3.048301704     -0.000132027
H      -1.721070610     -0.317007541      0.000132027
./cisplatin-PBE0-SMD-ApVTZ-ApVDZ-pp-3_eGeom.xyz
11
```

```
Pt      -0.000036033      0.182686953     -0.008656538
Cl       1.685144748     -1.401117756     -0.027144231
Cl      -1.684655050     -1.401791985     -0.018640274
N      -1.444009686      1.621090633      0.007897322
H      -1.315692430      2.288558376      0.763318225
H      -1.459934916      2.146437262     -0.862207292
N       1.443425797      1.621670088      0.000617555
```

H	1.454741579	2.147043433	-0.869542966
H	1.318655379	2.289067627	0.756694713
H	-2.360533789	1.197077008	0.123970164
H	2.360696401	1.198025361	0.112048323

./cisplatin-M062X-SMD-ApVTZ-pVTZ_eGeom.xyz

11

Pt	0.553941880	0.773289253	0.000000000
Cl	0.479235308	-1.571460762	-0.000328985
Cl	2.898691898	0.847995742	0.000328985
N	0.534858693	2.818376996	-0.000038463
H	0.057349650	3.187375131	-0.818989128
H	0.057462660	3.187450871	0.818942507
N	-1.491145862	0.792372512	0.000038463
H	-1.860143980	1.269881569	0.818989128
H	-1.860219720	1.269768558	-0.818942507
H	1.480205614	3.193851457	-0.000127048
H	-1.866620357	-0.152974395	0.000127048

./cisplatin-M062X-H2O-pVTZ-2_eGeom.xyz

11

Pt	0.533354326	0.793876808	0.000000000
Cl	0.440305945	-1.563975023	-0.000929535
Cl	2.891206160	0.886925105	0.000929535
N	0.566402253	2.848580865	-0.015617694
H	0.191858908	3.244455225	-0.881669167
H	0.050146309	3.276695035	0.756909729
N	-1.521349732	0.760828953	0.015617694
H	-1.917224079	1.135372312	0.881669167
H	-1.949463884	1.277084913	-0.756909729
H	1.537313656	3.166165180	0.059179857
H	-1.838934082	-0.210082438	-0.059179857

./cisplatin-M06L-ApVTZ-pVTZ_eGeom.xyz

11

Pt	0.486541517	0.840689619	0.000000000
Cl	0.370902086	-1.455084882	-0.000190415
Cl	2.782316021	0.956328967	0.000190415
N	0.650273202	2.943915138	-0.000103477
H	0.274127763	3.403488138	-0.819448278
H	0.273917684	3.403576180	0.819096902
N	-1.616684009	0.676958009	0.000103477
H	-2.076256995	1.053103464	0.819448278
H	-2.076345037	1.053313543	-0.819096902
H	1.662475913	3.074883455	0.000030639
H	-1.747652361	-0.335244698	-0.000030639

./cisplatin-PBE0-CPCM-ApVDZ-pVTZ-pp-2_eGeom.xyz

11

Pt	0.529612473	0.797618661	0.000000000
Cl	0.446993921	-1.524837974	-0.000317892
Cl	2.852069111	0.880237131	0.000317892
N	0.562260076	2.837713776	-0.016112270
H	0.190278523	3.226647766	-0.881659522

H	0.043298583	3.260776011	0.752019207
N	-1.510482643	0.764971130	0.016112270
H	-1.899416619	1.136952697	0.881659522
H	-1.933544860	1.283932639	-0.752019207
H	1.529366669	3.154050546	0.061296974
H	-1.826819448	-0.202135451	-0.061296974

./cisplatin-CPCM-ApVDZ-aug-pVTZ-pp-2_eGeom.xyz

11

Pt	0.000040395	0.184063789	0.000151365
Cl	-1.715294398	-1.404005806	0.000370789
Cl	1.713822677	-1.405703055	0.000860384
N	1.484807099	1.601942364	0.009193355
H	1.430083544	2.253522708	-0.783407147
H	1.489593767	2.162568788	0.870515370
N	-1.483333043	1.603395951	-0.009657955
H	-1.427814898	2.255683443	0.782302514
H	-1.487796070	2.163205283	-0.871514560
H	2.393477025	1.120258072	-0.047902416
H	-2.392444097	1.122623462	0.048086301

./cisplatin-PBE0-SMD-TZ-pVDZ-pp-2_eGeom.xyz

11

Pt	0.000039416	0.159058117	0.000194289
Cl	-1.689042633	-1.422501798	-0.004850849
Cl	1.687620627	-1.424100100	0.006240867
N	1.444639740	1.600521367	0.010400263
H	1.344456976	2.249135188	-0.765122326
H	1.421736003	2.145173716	0.868098964
N	-1.443191486	1.601885350	-0.010925770
H	-1.342426958	2.250857768	0.764221033
H	-1.419731307	2.146013493	-0.868941593
H	2.364908492	1.174616771	-0.058582688
H	-2.363866868	1.176895128	0.058265809

./cisplatin-M06L-SMD-ApVTZ-ApVTZ-2_eGeom.xyz

11

Pt	0.000026795	0.151362247	0.000179389
Cl	-1.707182881	-1.444935429	-0.009960361
Cl	1.705682590	-1.446588740	0.011271357
N	1.469668532	1.606530914	0.018684477
H	1.356414632	2.284167523	-0.726775343
H	1.475809732	2.121327428	0.892346289
N	-1.468200590	1.607946815	-0.019192211
H	-1.354267972	2.285942940	0.725837211
H	-1.473870404	2.122198566	-0.893178055
H	2.385430213	1.183615385	-0.089052972
H	-2.384368645	1.185987352	0.088838219

./cisplatin-M062X-SMD_eGeom.xyz

11

Pt	0.554438255	0.772792878	0.000000000
Cl	0.471119859	-1.579562799	-0.000308485
Cl	2.906793935	0.856111190	0.000308485

N	0.545691806	2.824691715	-0.000055429
H	0.073035527	3.213745892	-0.822081922
H	0.073017429	3.213825126	0.821922157
N	-1.497460582	0.781539400	0.000055429
H	-1.886514742	1.254195693	0.822081922
H	-1.886593976	1.254213790	-0.821922157
H	1.500392281	3.197535108	-0.000068202
H	-1.870304009	-0.173161061	0.000068202

./cisplatin-M062X-H2O-TZ-pVTZ_eGeom.xyz

11

Pt	0.534503774	0.792727360	0.000000000
Cl	0.443618068	-1.558011206	0.013075472
Cl	2.885242343	0.883612983	-0.013075472
N	0.563680909	2.850404128	-0.033180267
H	0.201427980	3.224283122	-0.905749938
H	0.033190351	3.273709251	0.722563535
N	-1.523172995	0.763550298	0.033180267
H	-1.897051977	1.125803240	0.905749938
H	-1.946478100	1.294040871	-0.722563535
H	1.526987587	3.165563255	0.053661468
H	-1.838332156	-0.199756369	-0.053661468

./cisplatin-M06L-ApVDZ-pVDZ_eGeom.xyz

11

Pt	0.488716981	0.838514154	0.000000000
Cl	0.371105919	-1.473887575	-0.000145907
Cl	2.801118714	0.956125134	0.000145907
N	0.652361158	2.946709054	-0.000128108
H	0.278246586	3.415616639	-0.822055208
H	0.277666476	3.415746395	0.821462046
N	-1.619477924	0.674870052	0.000128108
H	-2.088385496	1.048984641	0.822055208
H	-2.088515252	1.049564751	-0.821462046
H	1.668247133	3.084699605	0.000228503
H	-1.757468512	-0.341015918	-0.000228503

./cisplatin-H2O-ApVDZ-aug-pVDZ-pp-2_eGeom.xyz

11

Pt	0.529493169	0.797737965	0.000000000
Cl	0.441351363	-1.539743749	-0.002613014
Cl	2.866974886	0.885879687	0.002613014
N	0.574850138	2.855975299	-0.015055018
H	0.195487044	3.251241568	-0.884832092
H	0.062792475	3.283560729	0.766665807
N	-1.528744167	0.752381069	0.015055018
H	-1.924010422	1.131744177	0.884832092
H	-1.956329578	1.264438747	-0.766665807
H	1.556038724	3.161518945	0.054937981
H	-1.834287847	-0.228807506	-0.054937981

./cisplatin-SMD-ApVDZ-pVTZ-pp-2_eGeom.xyz

11

Pt	0.000038236	0.153410092	0.000074448
----	-------------	-------------	-------------

Cl	-1.705549036	-1.442840671	-0.008178986
Cl	1.704006025	-1.444560373	0.009108897
N	1.453236090	1.601294059	0.018868904
H	1.336786172	2.290262695	-0.736528857
H	1.456362311	2.122328666	0.906598496
N	-1.451744151	1.602709393	-0.019258504
H	-1.334190383	2.292490814	0.735228176
H	-1.454985097	2.122685248	-0.907610437
H	2.385787237	1.178694209	-0.088985573
H	-2.384605404	1.181080868	0.089681436

./cisplatin-PBE0-ApVDZ-pVDZ-pp_eGeom.xyz

11

Pt	0.478694248	0.848536888	0.000000000
Cl	0.365494241	-1.440257889	-0.000128521
Cl	2.767489028	0.961736813	0.000128521
N	0.630619240	2.915286452	-0.000006632
H	0.250252611	3.372733189	-0.825713396
H	0.250419716	3.372710244	0.825790773
N	-1.588055322	0.696611969	0.000006632
H	-2.045502045	1.076978614	0.825713396
H	-2.045479100	1.076811509	-0.825790773
H	1.647923470	3.055471398	-0.000085511
H	-1.728240304	-0.320692256	0.000085511

./cisplatin-M062X-CPCM-TZ-aug-pVTZ_eGeom.xyz

11

Pt	0.534482924	0.792748210	0.000000000
Cl	0.445846379	-1.556644275	0.002308548
Cl	2.883875412	0.881384671	-0.002308548
N	0.562782123	2.848890097	0.017403022
H	0.040826581	3.263949108	-0.748926959
H	0.188855615	3.230419368	0.881790624
N	-1.521658964	0.764449084	-0.017403022
H	-1.936717956	1.286404641	0.748926959
H	-1.903188222	1.138375606	-0.881790624
H	1.526489686	3.165208890	-0.061194540
H	-1.837977792	-0.199258468	0.061194540

./cisplatin-ApVTZ-pVDZ-pp_eGeom.xyz

11

Pt	0.475554929	0.851676207	0.000000000
Cl	0.360247044	-1.442415708	0.000009210
Cl	2.769646848	0.966984010	-0.000009210
N	0.640746020	2.929214171	-0.000007345
H	0.258810983	3.386541017	-0.831200508
H	0.258891226	3.386550531	0.831217258
N	-1.601983041	0.686485190	0.000007345
H	-2.059309874	1.068420243	0.831200508
H	-2.059319387	1.068340000	-0.831217258
H	1.667131570	3.054031626	-0.000054448
H	-1.726800532	-0.339900356	0.000054448

./cisplatin-PBE0-TZ-pVDZ-pp_eGeom.xyz

11

Pt	0.476897332	0.850333804	0.000000000
Cl	0.367451260	-1.427552494	0.000010903
Cl	2.754783634	0.959779795	-0.000010903
N	0.629580487	2.917121322	0.000206795
H	0.250230748	3.368674530	-0.823858363
H	0.250248270	3.368500460	0.824376375
N	-1.589890192	0.697650722	-0.000206795
H	-2.041443386	1.077000477	0.823858363
H	-2.041269316	1.076982956	-0.824376375
H	1.644445415	3.044649561	0.000221235
H	-1.717418467	-0.317214202	-0.000221235

./cisplatin-PBE0-CPCM-ApVTZ-pVTZ-pp-3_eGeom.xyz

11

Pt	0.000039475	0.183133512	0.000193858
Cl	-1.693491450	-1.393314742	-0.001094299
Cl	1.692030743	-1.394966066	0.002507824
N	1.472411308	1.600015907	0.009958692
H	1.410160914	2.247320812	-0.769308728
H	1.475857736	2.149851967	0.863318609
N	-1.470948278	1.601446155	-0.010492696
H	-1.408064348	2.249197765	0.768352556
H	-1.473859802	2.150728946	-0.864210828
H	2.372352969	1.130895631	-0.052219068
H	-2.371347268	1.133245114	0.051992079

./cisplatin-PBE0-CPCM-ApVDZ-2_eGeom.xyz

11

Pt	0.530279531	0.796951603	0.000000000
Cl	0.450541860	-1.524839552	-0.001232928
Cl	2.852070689	0.876689191	0.001232928
N	0.566169944	2.839950898	-0.011933707
H	0.174776574	3.240229273	-0.867639786
H	0.067494064	3.265475497	0.772578549
N	-1.512719765	0.761061262	0.011933707
H	-1.912998126	1.152454646	0.867639786
H	-1.938244346	1.259737158	-0.772578549
H	1.537539481	3.158525221	0.044652536
H	-1.831294123	-0.210308264	-0.044652536

./cisplatin-PBE0-SMD-TZ-aug-pVTZ-2_eGeom.xyz

11

Pt	0.000029464	0.158660517	0.000296697
Cl	-1.685636902	-1.421670847	-0.004702492
Cl	1.684218546	-1.423242376	0.006679033
N	1.441425679	1.599289618	0.008365445
H	1.344244460	2.242107185	-0.772648430
H	1.413278580	2.151550740	0.861272902
N	-1.439989481	1.600662870	-0.009035165
H	-1.342895191	2.243270316	0.772161906
H	-1.410498629	2.153032339	-0.861823396
H	2.363573323	1.175812852	-0.052593519
H	-2.362607849	1.178081786	0.051025018

./cisplatin-SMD-ApVDZ-aug-pVDZ-pp-2_eGeom.xyz
11

Pt	0.000036125	0.154436304	0.000107941
Cl	-1.705226867	-1.443198344	-0.006230966
Cl	1.703700623	-1.444886575	0.007159412
N	1.456237317	1.602442575	0.016756013
H	1.346377388	2.282229851	-0.747606437
H	1.452877963	2.132297860	0.899026014
N	-1.454753350	1.603858455	-0.017159633
H	-1.343779737	2.284452791	0.746325019
H	-1.451470567	2.132675837	-0.900053613
H	2.387883776	1.175416586	-0.079773383
H	-2.386740670	1.177829659	0.080447633

./cisplatin-CPCM-aug-pVTZ-3_eGeom.xyz
11

Pt	0.079902569	-0.000111402	0.187996948
Cl	0.312646646	-1.715859586	-1.378366220
Cl	0.117742105	1.709030874	-1.402261270
N	-0.118111448	1.485008512	1.589683484
H	-0.970080528	1.403037282	2.164354353
H	0.680703247	1.538743514	2.239458148
N	0.035947043	-1.479293268	1.609115338
H	0.777747489	-1.394612159	2.320015215
H	-0.861797430	-1.530572382	2.113718256
H	-0.168821914	2.393982844	1.100835814
H	0.168756932	-2.390295178	1.139846264

./cisplatin-M06L-H2O-ApVDZ-aug-pVDZ-2_eGeom.xyz
11

Pt	0.000033454	0.170155858	0.000181945
Cl	-1.732071665	-1.427908905	-0.003876718
Cl	1.730575749	-1.429597378	0.005223517
N	1.494924049	1.605484680	0.013932600
H	1.431600872	2.273839765	-0.751870785
H	1.518813385	2.146490964	0.876651995
N	-1.493454678	1.606936498	-0.014446600
H	-1.429421036	2.275778980	0.750871864
H	-1.516882551	2.147347191	-0.877552119
H	2.400348641	1.143316048	-0.067898981
H	-2.399324218	1.145711299	0.067781282

./cisplatin-M06L-SMD-TZ-pVTZ-2_eGeom.xyz
11

Pt	0.000025068	0.153192680	0.000183515
Cl	-1.713399400	-1.442572957	-0.007904911
Cl	1.711892169	-1.444237846	0.009244897
N	1.473587979	1.607088558	0.017820271
H	1.365796248	2.281605465	-0.731286283
H	1.478911157	2.125578393	0.889295962
N	-1.472118403	1.608514354	-0.018335786
H	-1.363664267	2.283383591	0.730357155
H	-1.476940370	2.126476056	-0.890128440

```
H      2.387172277      1.178072954      -0.084739964
H      -2.386120457      1.180453751      0.084491585
./cisplatin-M062X-TZ-aug-pVDZ_eGeom.xyz
11
```

```
Pt      0.496810545      0.830420591      0.000000000
Cl      0.392912110     -1.460220294     -0.000006414
Cl      2.787451432      0.934318944      0.000006414
N       0.632617788      2.930622195      0.000024694
H       0.246186813      3.378966416     -0.823260804
H       0.246171928      3.378952929      0.823310621
N      -1.603391065      0.694613422     -0.000024694
H      -2.051735272      1.081044412      0.823260804
H      -2.051721785      1.081059298     -0.823310621
H       1.642681692      3.081599497      0.000034444
H      -1.754368403     -0.315450477     -0.000034444
./cisplatin-M062X-CPCM-ApVTZ-ApVDZ-2_eGeom.xyz
11
```

```
Pt      0.000000000      0.000000000      0.182599127
Cl     -0.008484149     -1.724375793     -1.418146227
Cl      0.008484149      1.724375793     -1.418146227
N      -0.011091119      1.472854929      1.616994198
H      -0.876319813      1.483431963      2.149324864
H       0.753322661      1.391613905      2.280784224
N       0.011091119     -1.472854929      1.616994198
H       0.876319813     -1.483431963      2.149324864
H      -0.753322661     -1.391613905      2.280784224
H       0.074387023      2.378025011      1.160899377
H      -0.074387023     -2.378025011      1.160899377
./cisplatin-CPCM-ApVDZ-pVTZ-pp-2_eGeom.xyz
11
```

```
Pt      0.000038899      0.178178847      0.000222333
Cl     -1.717060761     -1.410035386     -0.000172995
Cl      1.715578089     -1.411714451      0.001503628
N       1.483996787      1.601695420      0.011853793
H       1.421241855      2.265635194     -0.770294767
H       1.495602520      2.151795375      0.880356640
N      -1.482528979      1.603136943     -0.012358618
H      -1.419083985      2.267631751      0.769262418
H      -1.493656999      2.152564937     -0.881293332
H       2.396181917      1.128143415     -0.059156994
H      -2.395167342      1.130522955      0.059075895
./cisplatin-SMD-ApVTZ-pVTZ-pp-3_eGeom.xyz
11
```

```
Pt      0.000000000      0.000000000      0.179063522
Cl     -0.042006084     -1.696081920     -1.411647466
Cl      0.042006084      1.696081920     -1.411647466
N       0.021990865      1.460660764      1.624649614
H      -0.853927655      1.471810767      2.157474060
H       0.787723748      1.336911677      2.294491401
N      -0.021990865     -1.460660764      1.624649614
```

H	0.853927655	-1.471810767	2.157474060
H	-0.787723748	-1.336911677	2.294491401
H	0.131854708	2.383562141	1.190138629
H	-0.131854708	-2.383562141	1.190138629

./cisplatin-SMD-ApVTZ-ApVDZ-pp-3_eGeom.xyz

11

Pt	0.000000000	0.000000000	0.180053356
Cl	0.012748992	-1.697349732	-1.412128186
Cl	-0.012748992	1.697349732	-1.412128186
N	0.002579869	1.460322425	1.626733480
H	-0.766018983	1.347650767	2.295273861
H	0.878329038	1.456369796	2.159926657
N	-0.002579869	-1.460322425	1.626733480
H	0.766018983	-1.347650767	2.295273861
H	-0.878329038	-1.456369796	2.159926657
H	-0.092183249	2.385160114	1.192994511
H	0.092183249	-2.385160114	1.192994511

./cisplatin-M062X-SMD-ApVTZ-ApVDZ_eGeom.xyz

11

Pt	0.553911850	0.773319283	0.000000000
Cl	0.479545353	-1.573019807	-0.000371553
Cl	2.900250943	0.847685697	0.000371553
N	0.534782854	2.819320792	-0.000042991
H	0.057540819	3.188095824	-0.819227655
H	0.057674173	3.188181693	0.819179028
N	-1.492089658	0.792448352	0.000042991
H	-1.860864674	1.269690400	0.819227655
H	-1.860950543	1.269557046	-0.819179028
H	1.480450203	3.193866637	-0.000146379
H	-1.866635537	-0.153218984	0.000146379

./cisplatin-M06L-aug-pVDZ-H20-2_eGeom.xyz

11

Pt	0.000028458	0.167258637	0.000180115
Cl	-1.730376585	-1.432428823	-0.003439234
Cl	1.728857467	-1.434128071	0.004772871
N	1.495500276	1.603539726	0.012727168
H	1.439415444	2.272146825	-0.757480698
H	1.520304421	2.153417258	0.873454927
N	-1.494028719	1.605004749	-0.013236319
H	-1.437217440	2.274115625	0.756480370
H	-1.518369162	2.154281867	-0.874360926
H	2.407097704	1.145964255	-0.063373427
H	-2.406069865	1.148382953	0.063273152

./cisplatin-CPCM-TZ-aug-pVTZ-pp-2_eGeom.xyz

11

Pt	0.000040267	0.182777415	0.000228575
Cl	-1.710216259	-1.396813028	0.001039426
Cl	1.708732934	-1.398511712	-0.000006961
N	1.492295276	1.603185923	0.008424148
H	1.438867647	2.247879040	-0.785057042

H	1.493125062	2.163847145	0.865300205
N	-1.490815228	1.604651268	-0.008847048
H	-1.436518677	2.250200506	0.783875707
H	-1.491402343	2.164339024	-0.866362574
H	2.394719852	1.116806627	-0.044222602
H	-2.393686531	1.119192792	0.044626167

./cisplatin-M062X-ApVTZ-pVTZ_eGeom.xyz

11

Pt	0.496401064	0.830830071	0.000000000
Cl	0.391420421	-1.457602621	-0.000003130
Cl	2.784833760	0.935810632	0.000003130
N	0.631897667	2.927092528	0.000022417
H	0.244051335	3.375364068	-0.822601070
H	0.244028587	3.375352442	0.822641519
N	-1.599861398	0.695333543	-0.000022417
H	-2.048132924	1.083179891	0.822601070
H	-2.048121298	1.083202639	-0.822641519
H	1.641555278	3.081687803	0.000036858
H	-1.754456708	-0.314324063	-0.000036858

./cisplatin-M06L-aug-pVTZ-CPCM-2_eGeom.xyz

11

Pt	0.000030959	0.170898535	0.000192903
Cl	-1.730732574	-1.423265057	-0.001081558
Cl	1.729227866	-1.424963012	0.002486291
N	1.491630146	1.601600108	0.009417040
H	1.444958284	2.257173052	-0.771593591
H	1.507080613	2.165431279	0.860380721
N	-1.490162241	1.603058489	-0.009945521
H	-1.442840588	2.259091935	0.770639209
H	-1.505065910	2.166352297	-0.861274810
H	2.401662751	1.139893588	-0.049152812
H	-2.400647319	1.142283786	0.048930137

./cisplatin-PBE0-CPCM-TZ-aug-pVTZ-2_eGeom.xyz

11

Pt	0.526674829	0.800556305	0.000000000
Cl	0.443378635	-1.511391834	-0.004188669
Cl	2.838622971	0.883852417	0.004188669
N	0.566665911	2.844001509	-0.011576310
H	0.172569823	3.234242368	-0.861871017
H	0.073426673	3.258971276	0.772447930
N	-1.516770376	0.760565295	0.011576310
H	-1.907011222	1.154661398	0.861871017
H	-1.931740126	1.253804548	-0.772447930
H	1.536249451	3.145681837	0.040761574
H	-1.818450738	-0.209018233	-0.040761574

./cisplatin-PBE0-SMD-ApVDZ-pVTZ-pp_eGeom.xyz

11

Pt	0.550615318	0.776615815	0.000000000
Cl	0.477760296	-1.543368702	0.000005188
Cl	2.870599838	0.849470754	-0.000005188

N	0.536814866	2.810353100	0.000001326
H	0.061941374	3.188127235	-0.820235488
H	0.061905772	3.188128491	0.820216868
N	-1.483121966	0.790416340	-0.000001326
H	-1.860896085	1.265289845	0.820235488
H	-1.860897340	1.265325447	-0.820216868
H	1.485961595	3.184298984	0.000020941
H	-1.857067884	-0.158730376	-0.000020941

./cisplatin-H20-aug-pVDZ-2_eGeom.xyz
11

Pt	0.530321289	0.796909845	0.000000000
Cl	0.443464670	-1.538907781	-0.003506626
Cl	2.866138917	0.883766381	0.003506626
N	0.577371546	2.854772479	-0.012733084
H	0.186895242	3.261037128	-0.877290519
H	0.078587328	3.289312270	0.778991140
N	-1.527541346	0.749859661	0.012733084
H	-1.933805982	1.140335980	0.877290519
H	-1.962081120	1.248643894	-0.778991140
H	1.562125717	3.165091574	0.043921240
H	-1.837860477	-0.234894499	-0.043921240

./cisplatin-SMD-pVTZ-pp-2_eGeom.xyz
11

Pt	0.000036233	0.162495715	0.000126897
Cl	-1.710121672	-1.427538071	-0.001319735
Cl	1.708625179	-1.429210846	0.002429302
N	1.466964463	1.598287300	0.014010503
H	1.382135703	2.275280365	-0.760845785
H	1.470802056	2.144236994	0.890717694
N	-1.465492999	1.599716334	-0.014453792
H	-1.379696978	2.277427873	0.759667213
H	-1.469191325	2.144782985	-0.891713530
H	2.396968517	1.154835771	-0.068139341
H	-2.395887177	1.157240580	0.068518574

./cisplatin-PBE0-CPCM-ApVDZ-aug-pVDZ-pp-2_eGeom.xyz
11

Pt	0.529232198	0.797998936	0.000000000
Cl	0.447936945	-1.525119539	-0.000798425
Cl	2.852350676	0.879294106	0.000798425
N	0.563706910	2.840575705	-0.014221981
H	0.181393409	3.231653872	-0.874036678
H	0.055059105	3.260752299	0.762107318
N	-1.513344572	0.763524297	0.014221981
H	-1.904422726	1.145837812	0.874036678
H	-1.933521148	1.272172117	-0.762107318
H	1.532291395	3.154297504	0.052606998
H	-1.827066406	-0.205060178	-0.052606998

./cisplatin-M062X-ApVTZ-ApVDZ_eGeom.xyz
11

Pt	0.496231958	0.830999177	0.000000000
----	-------------	-------------	-------------

Cl	0.391397481	-1.459679783	-0.000004075
Cl	2.786910922	0.935833573	0.000004075
N	0.631574223	2.927662058	0.000022583
H	0.243905922	3.375645239	-0.822849893
H	0.243886532	3.375633377	0.822892392
N	-1.600430928	0.695656987	-0.000022583
H	-2.048414095	1.083325304	0.822849893
H	-2.048402233	1.083344694	-0.822892392
H	1.641308820	3.081583912	0.000034936
H	-1.754352817	-0.314077605	-0.000034936

./cisplatin-PBE0-H2O-TZ-aug-pVDZ-2_eGeom.xyz

11

Pt	0.000039545	0.183177389	0.000189103
Cl	-1.694931057	-1.393822327	-0.001409649
Cl	1.693466694	-1.395478243	0.002790883
N	1.474124195	1.601101410	0.012773483
H	1.405485069	2.258472109	-0.757437062
H	1.485315537	2.138133981	0.874201018
N	-1.472658902	1.602533354	-0.013298156
H	-1.403351962	2.260368426	0.756455753
H	-1.483356320	2.138982072	-0.875095908
H	2.372274249	1.130862610	-0.063280802
H	-2.371265048	1.133224220	0.063109337

./cisplatin-M06L-CPCM-TZ-pVDZ-2_eGeom.xyz

11

Pt	0.533158441	0.794072693	0.000000000
Cl	0.437180216	-1.550495725	0.002689639
Cl	2.877726862	0.890050835	-0.002689639
N	0.582150260	2.870242112	0.010917874
H	0.094598768	3.289684611	-0.771518476
H	0.190962845	3.266444587	0.857172767
N	-1.543010980	0.745080947	-0.010917874
H	-1.962453461	1.232632455	0.771518476
H	-1.939213441	1.136268376	-0.857172767
H	1.551664103	3.166378926	-0.040529265
H	-1.839147828	-0.224432885	0.040529265

./cisplatin-PBE0-H2O-ApVTZ-pVTZ-pp_eGeom.xyz

11

Pt	0.527833396	0.799397738	0.000000000
Cl	0.445560393	-1.513115245	-0.009022939
Cl	2.840346382	0.881670659	0.009022939
N	0.565217188	2.842422096	-0.016452236
H	0.190020357	3.226503752	-0.877990194
H	0.052535981	3.261252585	0.752791888
N	-1.515190964	0.762014018	0.016452236
H	-1.899272606	1.137210863	0.877990194
H	-1.934021434	1.274695240	-0.752791888
H	1.532022299	3.148666295	0.056220461
H	-1.821435197	-0.204791081	-0.056220461

./cisplatin-M062X-ApVDZ-pVDZ_eGeom.xyz

11

```

Pt      0.497429561      0.829801574      0.000000000
Cl      0.388294819     -1.472575225      0.000003726
Cl      2.799806365      0.938936234     -0.000003726
N       0.633831473      2.929853437      0.000018774
H       0.246452181      3.382378197     -0.825181154
H       0.246409056      3.382370618      0.825202677
N      -1.602622307      0.693399737     -0.000018774
H      -2.055147053      1.080779045      0.825181154
H      -2.055139474      1.080822170     -0.825202677
H       1.646171079      3.089101009      0.000047162
H      -1.761869915     -0.318939864     -0.000047162

```

./cisplatin-M062X-CPCM-ApVDZ-aug-pVTZ-2_eGeom.xyz

11

```

Pt      0.000000000      0.000000000      0.188205063
Cl      0.001849985     -1.733839354     -1.417255098
Cl     -0.001849985      1.733839354     -1.417255098
N      -0.016424814      1.467316759      1.615161227
H      -0.883097342      1.477984745      2.151579281
H       0.751025765      1.392945494      2.281421565
N       0.016424814     -1.467316759      1.615161227
H       0.883097342     -1.477984745      2.151579281
H      -0.751025765     -1.392945494      2.281421565
H       0.064674724      2.375231874      1.156516494
H      -0.064674724     -2.375231874      1.156516494

```

./cisplatin-PBE0-CPCM-TZ-pVTZ-pp-3_eGeom.xyz

11

```

Pt      0.000000000      0.000000000      0.183205165
Cl      0.014348196     -1.696419830     -1.392957396
Cl     -0.014348196      1.696419830     -1.392957396
N       0.003115808      1.474737796      1.599957356
H      -0.779408292      1.414028793      2.243312735
H       0.854226182      1.479140957      2.153018826
N      -0.003115808     -1.474737796      1.599957356
H       0.779408292     -1.414028793      2.243312735
H      -0.854226182     -1.479140957      2.153018826
H      -0.056852425      2.372483449      1.126417395
H       0.056852425     -2.372483449      1.126417395

```

./cisplatin-M062X-SMD-TZ-aug-pVDZ_eGeom.xyz

11

```

Pt      0.554682812      0.772548321      0.000000000
Cl      0.480025257     -1.574228649     -0.000291561
Cl      2.901459785      0.847205792      0.000291561
N       0.535290331      2.820834528     -0.000035223
H       0.057999239      3.189176624     -0.819527643
H       0.058091012      3.189242832      0.819479634
N      -1.493603394      0.791940875      0.000035223
H      -1.861945474      1.269231980      0.819527643
H      -1.862011681      1.269140206     -0.819479634
H       1.481225045      3.194828248     -0.000108427
H      -1.867597148     -0.153993826      0.000108427

```

./cisplatin-M06L-H2O-2_eGeom.xyz

11

Pt	0.000032023	0.167708689	0.000194929
Cl	-1.737108477	-1.431884537	0.000658497
Cl	1.735610045	-1.433579669	0.000756897
N	1.503626980	1.604279980	0.009982345
H	1.460349345	2.263215820	-0.770058012
H	1.523660255	2.167052993	0.863061996
N	-1.502159746	1.605740673	-0.010513804
H	-1.458236599	2.265136946	0.769101261
H	-1.521646201	2.167982652	-0.863956209
H	2.413753656	1.139756452	-0.050636649
H	-2.412739273	1.142145002	0.050406749

./cisplatin-M062X-ApVTZ-ApVTZ_eGeom.xyz

11

Pt	0.496153104	0.831078031	0.000000000
Cl	0.391608133	-1.456296283	-0.000004986
Cl	2.783527422	0.935622921	0.000004986
N	0.631797319	2.926915278	0.000022320
H	0.243838799	3.374884344	-0.822840394
H	0.243813905	3.374872846	0.822879518
N	-1.599684148	0.695433891	-0.000022320
H	-2.047653200	1.083392427	0.822840394
H	-2.047641701	1.083417320	-0.822879518
H	1.641612809	3.080987752	0.000038058
H	-1.753756658	-0.314381594	-0.000038058

./cisplatin-M062X-H2O-aug-pVTZ-2_eGeom.xyz

11

Pt	0.000000000	0.000000000	0.183590886
Cl	0.010901070	-1.732475488	-1.417123991
Cl	-0.010901070	1.732475488	-1.417123991
N	0.008321012	1.468234167	1.611371680
H	-0.758867983	1.394585332	2.282974811
H	0.876381845	1.489289844	2.151519919
N	-0.008321012	-1.468234167	1.611371680
H	0.758867983	-1.394585332	2.282974811
H	-0.876381845	-1.489289844	2.151519919
H	-0.078226081	2.380291691	1.155144138
H	0.078226081	-2.380291691	1.155144138

./cisplatin-M06L-SMD-ApVTZ-pVTZ-2_eGeom.xyz

11

Pt	0.000049605	0.150967797	0.000185036
Cl	-1.708196587	-1.446457565	-0.009337969
Cl	1.706824587	-1.448022716	0.010681821
N	1.468842018	1.606598032	0.018147327
H	1.356183531	2.282484666	-0.728917022
H	1.472755296	2.123426575	0.890546722
N	-1.467403013	1.607937636	-0.018662904
H	-1.354112310	2.284184798	0.727979471
H	-1.470853983	2.124226958	-0.891383610

```

H      2.385455382      1.184980033      -0.086943363
H      -2.384402526      1.187228788      0.086702490
./cisplatin-M062X-ApVTZ-pVDZ_eGeom.xyz
11

```

```

Pt      0.496577069      0.830654066      0.000000000
Cl      0.391929215     -1.459617254     -0.000004278
Cl      2.786848393      0.935301839      0.000004278
N       0.631987444      2.927937697      0.000021209
H       0.244517284      3.376550574     -0.822428385
H       0.244498745      3.376539652      0.822468059
N      -1.600706566      0.695243766     -0.000021209
H      -2.049319430      1.082713942      0.822428385
H      -2.049308508      1.082732480     -0.822468059
H       1.641515910      3.082154865      0.000033017
H      -1.754923771     -0.314284695     -0.000033017
./cisplatin-pVTZ-pp_eGeom.xyz
11

```

```

Pt      0.472455177      0.854775959      0.000000000
Cl      0.356034911     -1.446764472      0.000017817
Cl      2.773995612      0.971196143     -0.000017817
N       0.642291127      2.927592771     -0.000004694
H       0.267008067      3.400830731     -0.835061661
H       0.267023340      3.400836672      0.835055747
N      -1.600361641      0.684940082      0.000004694
H      -2.073599588      1.060223159      0.835061661
H      -2.073605529      1.060207887     -0.835055747
H       1.676961193      3.051817978     -0.000014647
H      -1.724586885     -0.349729978      0.000014647
./cisplatin-PBE0-H2O-2_eGeom.xyz
11

```

```

Pt      0.000038233      0.178803107      0.000195603
Cl     -1.705146318     -1.402391919      0.002357846
Cl      1.703676042     -1.404059344     -0.000936886
N       1.477925852      1.597831122      0.010531038
H       1.427599716      2.256424556     -0.770406444
H       1.493282135      2.154805949      0.868506426
N      -1.476464738      1.599265132     -0.011064023
H      -1.425494153      2.258318691      0.769443340
H      -1.491279956      2.155694524     -0.869402707
H       2.387381631      1.130249891     -0.052427134
H      -2.386376445      1.132613290      0.052200932
./cisplatin-M062X-CPCM-TZ-pVDZ_eGeom.xyz
11

```

```

Pt      0.535468824      0.791762310      0.000000000
Cl      0.446531445     -1.559549572      0.000379763
Cl      2.886780709      0.880699605     -0.000379763
N       0.563607126      2.851620231      0.017707398
H       0.041564912      3.266727676     -0.748264328
H       0.191118361      3.233086446      0.882480146
N      -1.524389099      0.763624081     -0.017707398

```

H	-1.939496525	1.285666310	0.748264328
H	-1.905855300	1.136112859	-0.882480146
H	1.527564291	3.166510058	-0.061805309
H	-1.839278959	-0.200333073	0.061805309

./cisplatin-M062X-CPCM-TZ-pVTZ-3_eGeom.xyz

11

Pt	-0.000227684	0.179118685	0.039191551
Cl	1.704790320	-1.428576102	0.262577253
Cl	-1.735537934	-1.409950914	-0.032807612
N	-1.459340875	1.620304678	-0.145484400
H	-1.536257460	2.200416125	0.685086368
H	-1.312002005	2.240017474	-0.936772301
N	1.486065314	1.603435348	0.088163212
H	1.573205020	2.100916270	-0.793432554
H	1.351204291	2.297814512	0.817230697
H	-2.357340784	1.161127737	-0.278541767
H	2.375327958	1.141958986	0.264808042

./cisplatin-CPCM-TZ-aug-pVDZ-pp-2_eGeom.xyz

11

Pt	0.000040328	0.181520980	0.000200728
Cl	-1.710058646	-1.400908977	0.000735227
Cl	1.708575540	-1.402605470	0.000286918
N	1.492201599	1.604177158	0.008856937
H	1.436555517	2.250056048	-0.783425504
H	1.493163980	2.162712591	0.867051695
N	-1.490721427	1.605642487	-0.009276850
H	-1.434165981	2.252390215	0.782228839
H	-1.491487635	2.163185615	-0.868119862
H	2.395210551	1.119497035	-0.045965181
H	-2.394171829	1.121887317	0.046425052

./cisplatin-M062X-SMD-TZ-aug-pVTZ_eGeom.xyz

11

Pt	0.553487245	0.773743888	0.000000000
Cl	0.478579836	-1.569679576	-0.000370860
Cl	2.896910712	0.848651214	0.000370860
N	0.536245981	2.820188574	-0.000043735
H	0.059668142	3.190123303	-0.819334921
H	0.059797558	3.190208792	0.819282463
N	-1.492957440	0.790985225	0.000043735
H	-1.862892152	1.267563077	0.819334921
H	-1.862977641	1.267433661	-0.819282463
H	1.482990080	3.192467635	-0.000144729
H	-1.865236535	-0.155758861	0.000144729

./cisplatin-M06L-H2O-ApVTZ-pVDZ-2_eGeom.xyz

11

Pt	0.000035977	0.175078280	0.000187728
Cl	-1.724254378	-1.414266884	-0.001293428
Cl	1.722772570	-1.415949050	0.002670962
N	1.500532484	1.606877190	0.011774966
H	1.441874135	2.260533537	-0.759385222

H	1.515024642	2.151051571	0.865843339
N	-1.499062185	1.608334412	-0.012300046
H	-1.439739219	2.262458837	0.758412103
H	-1.513054784	2.151940479	-0.866738748
H	2.396050600	1.134559219	-0.058128746
H	-2.395037843	1.136937409	0.057955093

./cisplatin-M062X-ApVDZ-pVTZ_eGeom.xyz

11

Pt	0.495888793	0.831342342	0.000000000
Cl	0.387325474	-1.467330344	0.000000351
Cl	2.794561483	0.939905580	-0.000000351
N	0.629243109	2.923184518	0.000022302
H	0.241721544	3.375591740	-0.825232401
H	0.241691115	3.375580652	0.825268824
N	-1.595953388	0.697988100	-0.000022302
H	-2.048360596	1.085509682	0.825232401
H	-2.048349508	1.085540110	-0.825268824
H	1.641542406	3.082925743	0.000042809
H	-1.755694649	-0.314311191	-0.000042809

./cisplatin-PBE0-CPCM-ApVDZ-aug-pVTZ-pp-2_eGeom.xyz

11

Pt	0.525941605	0.801289529	0.000000000
Cl	0.444610228	-1.519481829	-0.003080156
Cl	2.846712966	0.882620823	0.003080156
N	0.562857105	2.838204683	-0.013658242
H	0.177391612	3.230154226	-0.871479171
H	0.059067428	3.258970082	0.765303819
N	-1.510973550	0.764374101	0.013658242
H	-1.902923079	1.149839608	0.871479171
H	-1.931738932	1.268163794	-0.765303819
H	1.533052682	3.147613378	0.048644652
H	-1.820382280	-0.205821464	-0.048644652

./cisplatin-M06L-SMD-TZ-aug-pVTZ-2_eGeom.xyz

11

Pt	0.000025250	0.152180244	0.000181650
Cl	-1.710004837	-1.443090329	-0.008923326
Cl	1.708499399	-1.444750118	0.010248723
N	1.471542363	1.606727316	0.017843537
H	1.362068302	2.281567452	-0.730835961
H	1.476258491	2.124866729	0.889624722
N	-1.470073314	1.608149946	-0.018355488
H	-1.359929925	2.283345437	0.729905125
H	-1.474299129	2.125755116	-0.890456470
H	2.386192170	1.180212288	-0.085466743
H	-2.385136769	1.182590919	0.085232231

./cisplatin-M062X-H2O-ApVTZ-pVDZ-2_eGeom.xyz

11

Pt	0.534700701	0.792530433	0.000000000
Cl	0.448613791	-1.559688343	0.003358782
Cl	2.886919479	0.878617259	-0.003358782

N	0.562712453	2.849843632	-0.019219220
H	0.195474492	3.231084072	-0.886195865
H	0.035033644	3.265710387	0.742349466
N	-1.522612500	0.764518754	0.019219220
H	-1.903852927	1.131756728	0.886195865
H	-1.938479236	1.292197577	-0.742349466
H	1.525189989	3.167315204	0.066172124
H	-1.840084105	-0.197958771	-0.066172124

./cisplatin-PBE0-H20-pVTZ-pp-2_eGeom.xyz
11

Pt	0.000038202	0.183677438	0.000193679
Cl	-1.704492869	-1.395077857	0.001148886
Cl	1.703017096	-1.396752190	0.000262971
N	1.473783095	1.597056105	0.010765980
H	1.421798643	2.255680290	-0.769175588
H	1.489628960	2.150894645	0.869981425
N	-1.472319837	1.598494006	-0.011296610
H	-1.419683124	2.257583449	0.768207989
H	-1.487630111	2.151778608	-0.870878600
H	2.380444104	1.125924800	-0.054205504
H	-2.379442158	1.128295706	0.053993371

./cisplatin-M06L-H20-TZ-pVDZ-2_eGeom.xyz
11

Pt	0.000036147	0.175971374	0.000191391
Cl	-1.726825446	-1.412743614	-0.000217213
Cl	1.725344948	-1.414428925	0.001616153
N	1.504775114	1.607818944	0.011190023
H	1.449645716	2.258839674	-0.762730459
H	1.518598719	2.153912615	0.864288248
N	-1.503304119	1.609280393	-0.011721857
H	-1.447528580	2.260758194	0.761767489
H	-1.516607082	2.154823549	-0.865180557
H	2.398103687	1.130472686	-0.055310494
H	-2.397097103	1.132850111	0.055105277

./cisplatin-M062X-TZ-aug-pVTZ_eGeom.xyz
11

Pt	0.496509776	0.830721359	0.000000000
Cl	0.393499962	-1.456194858	-0.000005263
Cl	2.783425997	0.933731092	0.000005263
N	0.632235299	2.928286842	0.000022049
H	0.244620871	3.376223970	-0.823082103
H	0.244599041	3.376212145	0.823122357
N	-1.601055711	0.694995911	-0.000022049
H	-2.048992826	1.082610355	0.823082103
H	-2.048981001	1.082632184	-0.823122357
H	1.642023377	3.081500094	0.000036022
H	-1.754268999	-0.314792162	-0.000036022

./cisplatin-M06L-pVTZ-SMD-2_eGeom.xyz
11

Pt	0.000022931	0.149238554	0.000184781
----	-------------	-------------	-------------

Cl	-1.722350182	-1.454355252	-0.006818794
Cl	1.720829617	-1.456031552	0.008160874
N	1.469141245	1.602194054	0.017695335
H	1.370105259	2.288093847	-0.733842182
H	1.482756579	2.132163010	0.892133167
N	-1.467676013	1.603616650	-0.018206759
H	-1.367966133	2.289878605	0.732910671
H	-1.480779016	2.133063910	-0.892968189
H	2.396545713	1.183651211	-0.083845533
H	-2.395487999	1.186041962	0.083594630

./cisplatin-CPCM-ApVDZ-pVDZ-pp-2_eGeom.xyz
11

Pt	0.000035461	0.176328961	0.000022075
Cl	-1.721615834	-1.413505192	-0.000692654
Cl	1.720147836	-1.415204473	0.001927546
N	1.488626085	1.602771873	0.009966512
H	1.430853590	2.258713435	-0.779242467
H	1.495417204	2.161597400	0.872826823
N	-1.487154688	1.604233350	-0.010439965
H	-1.428416798	2.260885115	0.778103421
H	-1.493804091	2.162229911	-0.873839143
H	2.401113091	1.128563094	-0.051406330
H	-2.400059857	1.130941526	0.051772180

./cisplatin-M06L-pVTZ-CPCM-2_eGeom.xyz
11

Pt	0.535609441	0.791621692	0.000000000
Cl	0.437892398	-1.564490167	0.001808813
Cl	2.891721304	0.889338652	-0.001808813
N	0.582158428	2.863394251	0.010154890
H	0.095606440	3.296074110	-0.776788452
H	0.186849647	3.274365512	0.857697299
N	-1.536163119	0.745072779	-0.010154890
H	-1.968842961	1.231624783	0.776788452
H	-1.947134365	1.140381575	-0.857697299
H	1.554910386	3.176222911	-0.038203189
H	-1.848991813	-0.227679167	0.038203189

./cisplatin-PBE0-H2O-ApVTZ-2_eGeom.xyz
11

Pt	0.000036591	0.183300072	0.000189120
Cl	-1.701632991	-1.394783878	-0.000710080
Cl	1.700153209	-1.396455154	0.002093573
N	1.467757520	1.596034079	0.011739548
H	1.410110267	2.258489786	-0.763708233
H	1.484814169	2.145266043	0.873169275
N	-1.466293895	1.597469856	-0.012261091
H	-1.407974941	2.260398865	0.762731685
H	-1.482835593	2.146129698	-0.874065621
H	2.375574665	1.129664528	-0.059158770
H	-2.374567002	1.132041106	0.058978594

./cisplatin-SMD-ApVTZ-pVDZ-pp-3_eGeom.xyz
11

Pt	0.000000000	0.000000000	0.175396530
Cl	0.016788947	-1.698057855	-1.416610922
Cl	-0.016788947	1.698057855	-1.416610922
N	-0.001210679	1.460661916	1.621905817
H	-0.772051909	1.349335545	2.287892275
H	0.872173346	1.456659644	2.158695421
N	0.001210679	-1.460661916	1.621905817
H	0.772051909	-1.349335545	2.287892275
H	-0.872173346	-1.456659644	2.158695421
H	-0.093532791	2.385403475	1.187691644
H	0.093532791	-2.385403475	1.187691644

./cisplatin-SMD-ApVTZ-ApVTZ-pp-3_eGeom.xyz

11

Pt	0.000000000	0.000000000	0.180506562
Cl	-0.003074335	-1.696025294	-1.409653489
Cl	0.003074335	1.696025294	-1.409653489
N	-0.011333614	1.461135705	1.625987451
H	-0.887604510	1.453299586	2.158469970
H	0.757148709	1.353945573	2.295689032
N	0.011333614	-1.461135705	1.625987451
H	0.887604510	-1.453299586	2.158469970
H	-0.757148709	-1.353945573	2.295689032
H	0.078617565	2.385762298	1.190463254
H	-0.078617565	-2.385762298	1.190463254

./cisplatin-M06L-H2O-TZ-aug-pVDZ-2_eGeom.xyz

11

Pt	0.000035807	0.175025288	0.000189535
Cl	-1.724684500	-1.413717485	-0.000885973
Cl	1.723203061	-1.415400309	0.002272829
N	1.502963930	1.607482196	0.011675457
H	1.445099230	2.260669960	-0.760262503
H	1.517346692	2.151494827	0.866143988
N	-1.501493118	1.608941827	-0.012203452
H	-1.442971205	2.262592355	0.759292982
H	-1.515367970	2.152393001	-0.867037694
H	2.397436342	1.132847095	-0.057689224
H	-2.396426268	1.135226245	0.057502054

./cisplatin-M06L-CPCM-ApVDZ-pVDZ-2_eGeom.xyz

11

Pt	0.538886977	0.788344156	0.000000000
Cl	0.442602763	-1.572920054	-0.002128856
Cl	2.900151191	0.884628286	0.002128856
N	0.578342650	2.864321600	0.014008749
H	0.069231605	3.291432359	-0.757918745
H	0.201484586	3.264345483	0.871782429
N	-1.537090467	0.748888558	-0.014008749
H	-1.964201209	1.257999618	0.757918745
H	-1.937114338	1.125746636	-0.871782429
H	1.545270694	3.181179766	-0.056736385
H	-1.853948668	-0.218039476	0.056736385

./cisplatin-M062X-SMD-ApVTZ-ApVTZ_eGeom.xyz

11

Pt	0.553591867	0.773639266	0.000000000
Cl	0.478927884	-1.570265003	-0.000330220
Cl	2.897496139	0.848303165	0.000330220
N	0.534984759	2.818667744	-0.000037985
H	0.057866290	3.187897840	-0.819245728
H	0.057982280	3.187974433	0.819201296
N	-1.491436611	0.792246446	0.000037985
H	-1.860666690	1.269364928	0.819245728
H	-1.860743283	1.269248939	-0.819201296
H	1.481010706	3.192628658	-0.000128651
H	-1.865397558	-0.153779487	0.000128651

./cisplatin-PBE0-CPCM-2_eGeom.xyz

11

Pt	0.000032545	0.178073940	0.000253602
Cl	-1.705139869	-1.403309531	0.002173939
Cl	1.703642228	-1.405016592	-0.000964144
N	1.477190941	1.597826663	0.007894502
H	1.431793266	2.246059798	-0.781952320
H	1.484067195	2.165830049	0.858675205
N	-1.475718200	1.599279197	-0.008351963
H	-1.429651296	2.248178566	0.780906248
H	-1.482106816	2.166521352	-0.859644291
H	2.387789278	1.130874383	-0.042084349
H	-2.386757273	1.133237176	0.042091572

./cisplatin-SMD-ApVDZ-aug-pVTZ-pp-2_eGeom.xyz

11

Pt	0.544042302	0.783188831	0.000000000
Cl	0.470886917	-1.549359827	-0.005778607
Cl	2.876590963	0.856344134	0.005778607
N	0.552188418	2.831469150	0.018923978
H	0.001204788	3.236328294	-0.749567124
H	0.168983752	3.202420529	0.898939006
N	-1.504238017	0.775042788	-0.018923978
H	-1.909097141	1.326026433	0.749567124
H	-1.875189382	1.158247467	-0.898939006
H	1.515265135	3.184253032	-0.068985437
H	-1.857021933	-0.188033917	0.068985437

./cisplatin-PBE0-SMD-TZ-pVTZ-pp-2_eGeom.xyz

11

Pt	0.000042542	0.161302886	0.000199529
Cl	-1.688610314	-1.419071136	-0.005447897
Cl	1.687205678	-1.420657542	0.006870399
N	1.445541998	1.599743178	0.012100453
H	1.344159839	2.255236057	-0.757581413
H	1.429822826	2.138333633	0.873919463
N	-1.444098020	1.601099798	-0.012633881
H	-1.342160040	2.256923219	0.756692848
H	-1.427794928	2.139198623	-0.874748820

H 2.364257296 1.171588520 -0.064878736
H -2.363224876 1.173857764 0.064506054
./cisplatin-M06L-SMD-ApVDZ-pVDZ-2_eGeom.xyz
11

Pt 0.000022848 0.143882485 0.000178535
Cl -1.723605146 -1.465845467 -0.009664047
Cl 1.722084338 -1.467514914 0.010968478
N 1.465127634 1.605856641 0.020309039
H 1.349615281 2.295886413 -0.721390900
H 1.478323957 2.122059084 0.899770897
N -1.463660618 1.607267697 -0.020812319
H -1.347462612 2.297640407 0.720461418
H -1.476376215 2.122942890 -0.900590523
H 2.391820229 1.196499266 -0.094209031
H -2.390747695 1.198880498 0.093976453
./cisplatin-CPCM-ApVDZ-aug-pVDZ-pp-2_eGeom.xyz
11

Pt 0.000037833 0.179303456 0.000045850
Cl -1.716773934 -1.410482572 -0.000335457
Cl 1.715306959 -1.412177921 0.001566335
N 1.486990808 1.603019726 0.009592413
H 1.429736780 2.256155564 -0.781713270
H 1.491751583 2.162475587 0.871823654
N -1.485517949 1.604478314 -0.010060700
H -1.427337806 2.258335072 0.780578490
H -1.490101942 2.163095592 -0.872837996
H 2.397692613 1.125491534 -0.049593237
H -2.396642943 1.127860647 0.049931920
./cisplatin-PBE0-ApVDZ-pVTZ-pp_eGeom.xyz
11

Pt 0.477958923 0.849272212 0.000000000
Cl 0.366161149 -1.435922878 -0.000140526
Cl 2.763154018 0.961069906 0.000140526
N 0.626056797 2.909468643 0.000009956
H 0.245171790 3.366386345 -0.825797419
H 0.245384134 3.366340631 0.825941770
N -1.582237512 0.701174412 -0.000009956
H -2.039155201 1.082059435 0.825797419
H -2.039109487 1.081847092 -0.825941770
H 1.643262564 3.050262484 -0.000092293
H -1.723031390 -0.316031350 0.000092293
./cisplatin-M06L-ApVTZ-pVDZ_eGeom.xyz
11

Pt 0.486290790 0.840940346 0.000000000
Cl 0.370566432 -1.456710209 -0.000192209
Cl 2.783941348 0.956664622 0.000192209
N 0.649991793 2.944081467 -0.000099455
H 0.274339794 3.404076675 -0.819300512
H 0.274179615 3.404163277 0.818980911
N -1.616850338 0.677239417 0.000099455

H	-2.076845532	1.052891433	0.819300512
H	-2.076932134	1.053051611	-0.818980911
H	1.662163132	3.074460210	0.000004412
H	-1.747229116	-0.334931917	-0.000004412

./cisplatin-H2O-ApVDZ-aug-pVTZ-pp-2_eGeom.xyz

11

Pt	0.526044374	0.801186760	0.000000000
Cl	0.437532164	-1.534108056	0.004701182
Cl	2.861339194	0.889698887	-0.004701182
N	0.574126080	2.853781006	0.014542902
H	0.066718715	3.282090333	-0.769642005
H	0.192148778	3.249922604	0.882619893
N	-1.526549873	0.753105127	-0.014542902
H	-1.954859182	1.260512507	0.769642005
H	-1.922691458	1.135082443	-0.882619893
H	1.557089224	3.154513333	-0.051325319
H	-1.827282236	-0.229858006	0.051325319

./cisplatin-PBE0-H2O-ApVTZ-pVDZ-pp-2_eGeom.xyz

11

Pt	0.000039506	0.182951042	0.000189249
Cl	-1.695367583	-1.393881842	-0.001320078
Cl	1.693903458	-1.395538007	0.002702112
N	1.472616760	1.600336789	0.012563768
H	1.404632012	2.257134826	-0.758048972
H	1.483345197	2.139421047	0.872561791
N	-1.471152289	1.601767094	-0.013088284
H	-1.402501763	2.259028457	0.757070060
H	-1.481383377	2.140270197	-0.873456581
H	2.371737992	1.131852942	-0.062151682
H	-2.370727912	1.134212455	0.061976617

./cisplatin-ApVTZ-pVTZ-pp_eGeom.xyz

11

Pt	0.475364933	0.851866203	0.000000000
Cl	0.360442855	-1.440357911	0.000004623
Cl	2.767589051	0.966788200	-0.000004623
N	0.641052866	2.928926264	-0.000008035
H	0.258909321	3.386299854	-0.831231743
H	0.259003439	3.386309748	0.831253327
N	-1.601695134	0.686178343	0.000008035
H	-2.059068711	1.068321905	0.831231743
H	-2.059078604	1.068227787	-0.831253327
H	1.667661948	3.053797272	-0.000062880
H	-1.726566179	-0.340430734	0.000062880

./cisplatin-PBE0-TZ-pVTZ-pp_eGeom.xyz

11

Pt	0.476809368	0.850421767	0.000000000
Cl	0.366187029	-1.426810117	0.000001653
Cl	2.754041257	0.961044026	-0.000001653
N	0.628930754	2.914810869	0.000204365
H	0.248493095	3.366140345	-0.823625101

H	0.248498611	3.365968588	0.824131387
N	-1.587579738	0.698300455	-0.000204365
H	-2.038909201	1.078738131	0.823625101
H	-2.038737444	1.078732615	-0.824131387
H	1.643554239	3.044903278	0.000225945
H	-1.717672184	-0.316323025	-0.000225945

./cisplatin-SMD-ApVDZ-pVDZ-pp-2_eGeom.xyz

11

Pt	0.549613302	0.777617831	0.000000000
Cl	0.473713916	-1.561003199	-0.005761751
Cl	2.888234335	0.853517134	0.005761751
N	0.553945240	2.834302920	0.020177916
H	-0.007555664	3.241408511	-0.739948986
H	0.180354397	3.205613091	0.904571011
N	-1.507071787	0.773285966	-0.020177916
H	-1.914177358	1.334786885	0.739948986
H	-1.878381944	1.146876823	-0.904571011
H	1.513056107	3.195345842	-0.078486395
H	-1.868114743	-0.185824888	0.078486395

./cisplatin-M062X-H2O-TZ-aug-pVDZ-2_eGeom.xyz

11

Pt	0.535278384	0.791952749	0.000000000
Cl	0.449263073	-1.560339243	0.003263690
Cl	2.887570380	0.877967977	-0.003263690
N	0.563139444	2.851525697	-0.019071160
H	0.201091451	3.231213019	-0.889224992
H	0.030643759	3.266843720	0.739790857
N	-1.524294564	0.764091763	0.019071160
H	-1.903981873	1.126139769	0.889224992
H	-1.939612568	1.296587463	-0.739790857
H	1.525535339	3.168248139	0.071893903
H	-1.841017040	-0.198304120	-0.071893903

./cisplatin-M062X-SMD-ApVTZ-pVDZ_eGeom.xyz

11

Pt	0.554052937	0.773178196	0.000000000
Cl	0.479636176	-1.573369275	-0.000418361
Cl	2.900600411	0.847594874	0.000418361
N	0.535015623	2.819229035	-0.000049035
H	0.057862578	3.188725953	-0.818779155
H	0.058013105	3.188822679	0.818723245
N	-1.491997901	0.792215583	0.000049035
H	-1.861494802	1.269368641	0.818779155
H	-1.861591529	1.269218114	-0.818723245
H	1.480389884	3.194101798	-0.000165687
H	-1.866870698	-0.153158665	0.000165687

./cisplatin-PBE0-aug-pVDZ_eGeom.xyz

11

Pt	0.480211461	0.847019675	0.000000000
Cl	0.374321293	-1.438235695	-0.000079751
Cl	2.765466835	0.952909762	0.000079751

N	0.627030564	2.911369267	0.000008147
H	0.248375044	3.374466458	-0.827476257
H	0.248643941	3.374460384	0.827619266
N	-1.584138137	0.700200646	-0.000008147
H	-2.047235314	1.078856181	0.827476257
H	-2.047229240	1.078587285	-0.827619266
H	1.646843749	3.055905505	-0.000141466
H	-1.728674410	-0.319612535	0.000141466

./cisplatin-CPCM-ApVDZ-pVTZ-pp_eGeom.xyz
11

Pt	0.531061826	0.796169308	0.000000000
Cl	0.440917865	-1.540910659	-0.000545746
Cl	2.868141796	0.886313186	0.000545746
N	0.573003291	2.852057822	-0.000095488
H	0.123816693	3.263480708	-0.828203231
H	0.123756568	3.263653004	0.827891987
N	-1.524826689	0.754227916	0.000095488
H	-1.936249560	1.203414529	0.828203231
H	-1.936421856	1.203474653	-0.827891987
H	1.555491566	3.162306812	-0.000101994
H	-1.835075714	-0.228260348	0.000101994

./cisplatin-M062X-CPCM-TZ-aug-pVDZ_eGeom.xyz
11

Pt	0.535284223	0.791946911	0.000000000
Cl	0.448209229	-1.559600171	0.000486826
Cl	2.886831307	0.879021821	-0.000486826
N	0.562318106	2.850057411	0.017562287
H	0.035258827	3.264290090	-0.745496261
H	0.193806107	3.230297742	0.884659890
N	-1.522826278	0.764913101	-0.017562287
H	-1.937058938	1.291972395	0.745496261
H	-1.903066597	1.133425113	-0.884659890
H	1.525004142	3.167375443	-0.066645679
H	-1.840144344	-0.197772924	0.066645679

./cisplatin-PBE0-SMD-ApVDZ-2_eGeom.xyz
11

Pt	0.000030820	0.156526586	0.000174171
Cl	-1.690711460	-1.432800019	-0.008153585
Cl	1.689228357	-1.434435928	0.009432333
N	1.441643239	1.596092995	0.015220429
H	1.339100879	2.271615491	-0.746847462
H	1.440480427	2.131836894	0.887781275
N	-1.440185978	1.597479856	-0.015714836
H	-1.336916232	2.273434848	0.745871166
H	-1.438594333	2.132611853	-0.888650762
H	2.373091136	1.181420887	-0.075736424
H	-2.372024855	1.183771536	0.075621695

./cisplatin-M06L-ApVDZ-pVTZ_eGeom.xyz
11

Pt	0.488285673	0.838945463	0.000000000
----	-------------	-------------	-------------

```
Cl      0.371670642      -1.468201893      -0.000176746
Cl      2.795433033      0.955560412      0.000176746
N       0.648126671      2.940817089      -0.000174710
H       0.273503256      3.409210395      -0.822164331
H       0.272699304      3.409385500      0.821351122
N      -1.613585960      0.679104539      0.000174710
H      -2.081979252      1.053727971      0.822164331
H      -2.082154357      1.054531923      -0.821351122
H       1.663932099      3.079546417      0.000326859
H      -1.752315324      -0.336700884      -0.000326859
./cisplatin-CPCM-aug-pVDZ-2_eGeom.xyz
11
```

```
Pt      0.000041708      0.177708597      0.000196247
Cl     -1.714501893     -1.411689083      0.001144388
Cl      1.713034157     -1.413372613      0.000059988
N       1.487581307      1.600237982      0.007765924
H       1.442740698      2.251757643     -0.790934108
H       1.494093824      2.172408760      0.866518897
N      -1.486116106      1.601681012     -0.008232576
H      -1.440473824      2.253923407      0.789828809
H      -1.492285347      2.173032247     -0.867534067
H       2.404467901      1.124754610     -0.041655398
H      -2.403440426      1.127112439      0.041839897
./cisplatin-PBE0-SMD-TZ-aug-pVDZ-3_eGeom.xyz
11
```

```
Pt      0.007835984      0.162061009      0.013372564
Cl      1.652275146     -1.464265392     -0.002945127
Cl     -1.717565973     -1.377739956      0.050675995
N      -1.400214558      1.637919171      0.026958394
H      -1.388379888      2.158914515      0.899727612
H      -1.267995369      2.305351485     -0.727801699
N       1.489469071      1.563724685     -0.019032152
H       1.367706802      2.237668576     -0.769754555
H       1.532151926      2.083933256      0.853242049
H      -2.328354507      1.236377399     -0.075343446
H       2.392063367      1.115185250     -0.150483635
./cisplatin-PBE0-CPCM-ApVDZ-pVDZ-pp-2_eGeom.xyz
11
```

```
Pt      0.531464658      0.795766475      0.000000000
Cl      0.446431803     -1.530842198     -0.000248827
Cl      2.858073335      0.880799248      0.000248827
N       0.564871211      2.841719990     -0.014796306
H       0.185647865      3.233140488     -0.876045253
H       0.052603377      3.263226069      0.758686411
N      -1.514488857      0.762359996      0.014796306
H      -1.905909342      1.141583355      0.876045253
H      -1.935994918      1.274627845     -0.758686411
H       1.532356743      3.158671187      0.055541202
H      -1.831440089     -0.205125526     -0.055541202
./cisplatin-M062X-SMD-aug-pVDZ-2_eGeom.xyz
11
```

Pt	0.552165480	0.775065653	0.000000000
Cl	0.477669158	-1.579375893	0.005794521
Cl	2.906607028	0.849561892	-0.005794521
N	0.541854510	2.822065264	-0.015842720
H	0.139389359	3.194900244	-0.881455450
H	0.000581489	3.220078161	0.757585126
N	-1.494834130	0.785376696	0.015842720
H	-1.867669096	1.187841860	0.881455450
H	-1.892847008	1.326649731	-0.757585126
H	1.491736254	3.198268351	0.056746754
H	-1.871037252	-0.164505035	-0.056746754

./cisplatin-CPCM-ApVTZ-ApVTZ-pp-2_eGeom.xyz

11

Pt	0.000038318	0.181678565	0.000214940
Cl	-1.709144310	-1.399124883	0.000750748
Cl	1.707654926	-1.400821434	0.000284045
N	1.490950872	1.603198983	0.009246825
H	1.434169829	2.250749039	-0.781796716
H	1.492758502	2.161183233	0.867994509
N	-1.489470287	1.604663502	-0.009671023
H	-1.431803332	2.253058654	0.780612700
H	-1.491049363	2.161678591	-0.869051171
H	2.394639731	1.119448458	-0.047259433
H	-2.393602885	1.121842292	0.047672577

./cisplatin-M06L-TZ-CPCM-aug-pVDZ-2_eGeom.xyz

11

Pt	0.000035704	0.174197989	0.000188949
Cl	-1.724361489	-1.415002286	-0.000351291
Cl	1.722880092	-1.416684409	0.001734559
N	1.501709177	1.607472321	0.009603071
H	1.448057485	2.252620308	-0.769384856
H	1.509389870	2.160430490	0.858374992
N	-1.500238516	1.608931383	-0.010130443
H	-1.445932828	2.254553831	0.768418794
H	-1.507408845	2.161322222	-0.859276308
H	2.397366105	1.133670694	-0.049186847
H	-2.396354755	1.136042457	0.049007379

./cisplatin-M06L-TZ-pVDZ_eGeom.xyz

11

Pt	0.485926261	0.841304875	0.000000000
Cl	0.372306276	-1.455818505	-0.000052647
Cl	2.783049645	0.954924778	0.000052647
N	0.652804419	2.949704304	-0.000100888
H	0.280266974	3.411316241	-0.819931814
H	0.279906936	3.411406697	0.819516578
N	-1.622473175	0.674426792	0.000100888
H	-2.084085098	1.046964253	0.819931814
H	-2.084175555	1.047324291	-0.819516578
H	1.665882270	3.073024261	0.000129242
H	-1.745793167	-0.338651055	-0.000129242

./cisplatin-M06L-CPCM-ApVTZ-pVTZ-2_eGeom.xyz
11

Pt	0.533943498	0.793287635	0.000000000
Cl	0.440021970	-1.548119032	-0.002907859
Cl	2.875350169	0.887209081	0.002907859
N	0.580015615	2.866335160	-0.011763637
H	0.189675748	3.260822122	-0.859095966
H	0.088262578	3.285147940	0.768232919
N	-1.539104028	0.747215592	0.011763637
H	-1.933590976	1.137555473	0.859095966
H	-1.957916790	1.238968645	-0.768232919
H	1.547652273	3.167925375	0.042246735
H	-1.840694277	-0.220421055	-0.042246735

./cisplatin-M062X-TZ-pVTZ_eGeom.xyz
11

Pt	0.496571268	0.830659867	0.000000000
Cl	0.391796378	-1.457727854	-0.000007557
Cl	2.784958993	0.935434676	0.000007557
N	0.633957540	2.931248020	0.000023049
H	0.247956428	3.380349317	-0.823046824
H	0.247935250	3.380336915	0.823089761
N	-1.604016890	0.693273670	-0.000023049
H	-2.053118173	1.079274798	0.823046824
H	-2.053105771	1.079295976	-0.823089761
H	1.644297778	3.080848111	0.000036564
H	-1.753617017	-0.317066563	-0.000036564

./cisplatin-M062X-SMD-pVTZ-3_eGeom.xyz
11

Pt	0.000000000	0.000000000	0.182355000
Cl	-0.016660000	-1.719569000	-1.424356000
Cl	0.016660000	1.719569000	-1.424356000
N	0.000000000	1.444678000	1.630632000
H	-0.868408000	1.441569000	2.174466000
H	0.768709000	1.338854000	2.299282000
N	0.000000000	-1.444678000	1.630632000
H	0.868408000	-1.441569000	2.174466000
H	-0.768709000	-1.338854000	2.299282000
H	0.087659000	2.376251000	1.214055000
H	-0.087659000	-2.376251000	1.214055000

./cisplatin-aug-pVTZ_eGeom.xyz
11

Pt	0.473125225	0.854105911	0.000000000
Cl	0.357254162	-1.444454834	0.000013358
Cl	2.771685974	0.969976892	-0.000013358
N	0.637455137	2.921479775	-0.000005537
H	0.260728896	3.392866592	-0.834807865
H	0.260736051	3.392873779	0.834795920
N	-1.594248645	0.689776073	0.000005537
H	-2.065635449	1.066502330	0.834807865
H	-2.065642636	1.066495175	-0.834795920

```
H      1.670928803      3.050002826      -0.000010846
H      -1.722771733      -0.343697589      0.000010846
./cisplatin-M062X-H2O-ApVTZ-ApVTZ-3_eGeom.xyz
11
```

```
Pt      0.000000000      0.000000000      0.184544066
Cl      0.006707602      -1.724161462      -1.415713070
Cl      -0.006707602      1.724161462      -1.415713070
N       0.012183190      1.474192454      1.618270504
H       -0.746441694      1.389030607      2.288450124
H       0.881685234      1.490660930      2.143751040
N       -0.012183190      -1.474192454      1.618270504
H       0.746441694      -1.389030607      2.288450124
H       -0.881685234      -1.490660930      2.143751040
H       -0.082035607      2.378188770      1.161236369
H       0.082035607      -2.378188770      1.161236369
./cisplatin-PBE0-ApVTZ-ApVDZ-pp_eGeom.xyz
11
```

```
Pt      0.478079584      0.849151552      0.000000000
Cl      0.369172014      -1.429322285      -0.000388765
Cl      2.756553424      0.958059041      0.000388765
N       0.627167456      2.912415061      -0.000027210
H       0.244459810      3.362735359      -0.823617900
H       0.244807554      3.362761184      0.823710451
N       -1.585183930      0.700063753      0.000027210
H       -2.035504215      1.082771415      0.823617900
H       -2.035530040      1.082423671      -0.823710451
H       1.641098589      3.048735557      -0.000217646
H       -1.721504463      -0.313867375      0.000217646
./cisplatin-H2O-TZ-pVDZ-pp-2_eGeom.xyz
11
```

```
Pt      0.526773206      0.800457928      0.000000000
Cl      0.433741426      -1.528713178      -0.006005421
Cl      2.855944315      0.893489625      0.006005421
N       0.579679136      2.862856292      -0.011790505
H       0.187140346      3.257822536      -0.870867847
H       0.086456680      3.284821530      0.779592261
N       -1.535625160      0.747552072      0.011790505
H       -1.930591390      1.140090875      0.870867847
H       -1.957590380      1.240774542      -0.779592261
H       1.562900946      3.152444446      0.041224943
H       -1.825213349      -0.235669728      -0.041224943
./cisplatin-H2O-ApVDZ-pVDZ-pp-2_eGeom.xyz
11
```

```
Pt      0.531660034      0.795571100      0.000000000
Cl      0.440379809      -1.545225296      -0.001654544
Cl      2.872456433      0.886851241      0.001654544
N       0.576073640      2.856899036      -0.015605117
H       0.199661645      3.252871342      -0.886562044
H       0.060561891      3.286069190      0.763222223
N       -1.529667904      0.751157567      0.015605117
```

H	-1.925640196	1.127569576	0.886562044
H	-1.958838039	1.266669331	-0.763222223
H	1.555998280	3.166260923	0.057744084
H	-1.839029825	-0.228767062	-0.057744084

./cisplatin-PBE0-CPCM-TZ-pVDZ-pp-2_eGeom.xyz

11

Pt	0.527027782	0.800203352	0.000000000
Cl	0.442637997	-1.514529570	-0.003064428
Cl	2.841760707	0.884593055	0.003064428
N	0.567275456	2.846232199	-0.011669082
H	0.174381033	3.235945147	-0.862508469
H	0.073736360	3.260739631	0.772139787
N	-1.519001066	0.759955751	0.011669082
H	-1.908714001	1.152850188	0.862508469
H	-1.933508481	1.253494861	-0.772139787
H	1.537130720	3.146341825	0.041548585
H	-1.819110727	-0.209899503	-0.041548585

./cisplatin-M06L-SMD-ApVDZ-aug-pVTZ-2_eGeom.xyz

11

Pt	0.000059330	0.150626306	0.000185231
Cl	-1.714733698	-1.454021090	-0.009234645
Cl	1.713411073	-1.455553959	0.010581652
N	1.460346944	1.603941568	0.018834122
H	1.348712774	2.288553171	-0.727940942
H	1.469464495	2.124093936	0.895623952
N	-1.458922859	1.605240411	-0.019347746
H	-1.346667867	2.290210885	0.727005070
H	-1.467580513	2.124861056	-0.896457479
H	2.384942653	1.188703261	-0.089272426
H	-2.383890331	1.190899455	0.089021209

./cisplatin-PBE0-SMD-ApVTZ_eGeom.xyz

11

Pt	0.546698869	0.780532265	0.000000000
Cl	0.470705154	-1.535963248	-0.000328752
Cl	2.863194384	0.856525897	0.000328752
N	0.542592712	2.811658318	-0.000034704
H	0.072148751	3.199931309	-0.821007466
H	0.072264044	3.200009348	0.820965617
N	-1.484427185	0.784638493	0.000034704
H	-1.872700159	1.255082468	0.821007466
H	-1.872778197	1.254967175	-0.820965617
H	1.497255047	3.178568735	-0.000126221
H	-1.851337636	-0.170023829	0.000126221

./cisplatin-ApVDZ-pVDZ-pp_eGeom.xyz

11

Pt	0.475011920	0.852219215	0.000000000
Cl	0.356497250	-1.453108145	0.000023337
Cl	2.780339285	0.970733804	-0.000023337
N	0.644094219	2.931860113	-0.000006741
H	0.264613001	3.396624406	-0.833409945

H	0.264695367	3.396633663	0.833428754
N	-1.604628983	0.683136991	0.000006741
H	-2.069393263	1.062618226	0.833409945
H	-2.069402520	1.062535859	-0.833428754
H	1.674368434	3.059810019	-0.000055714
H	-1.732578926	-0.347137219	0.000055714

./cisplatin-SMD-TZ-pVTZ-pp-2_eGeom.xyz

11

Pt	0.542554468	0.784676666	0.000000000
Cl	0.462541135	-1.541176537	-0.002790787
Cl	2.868407673	0.864689916	0.002790787
N	0.560278500	2.842038111	0.017651686
H	0.020510232	3.245948148	-0.754023993
H	0.174713217	3.213481517	0.891856014
N	-1.514806978	0.766952707	-0.017651686
H	-1.918716996	1.306720989	0.754023993
H	-1.886250371	1.152518003	-0.891856014
H	1.525952517	3.178798711	-0.063531858
H	-1.851567612	-0.198721299	0.063531858

./cisplatin-M062X-aug-pVDZ_eGeom.xyz

11

Pt	0.498930166	0.828300969	0.000000000
Cl	0.395319163	-1.470463278	0.000023605
Cl	2.797694417	0.931911890	-0.000023605
N	0.631179971	2.926030786	0.000017089
H	0.246214530	3.385410165	-0.827153482
H	0.246177643	3.385401880	0.827175221
N	-1.598799655	0.696051239	-0.000017089
H	-2.058179020	1.081016696	0.827153482
H	-2.058170737	1.081053583	-0.827175221
H	1.646139869	3.090121656	0.000041210
H	-1.762890562	-0.318908653	-0.000041210

./cisplatin-M06L_eGeom.xyz

11

Pt	0.490912958	0.836318177	0.000000000
Cl	0.381820533	-1.473133474	-0.000076768
Cl	2.800364613	0.945410520	0.000076768
N	0.655737586	2.950009276	-0.000048966
H	0.285865819	3.429375237	-0.822158317
H	0.285635464	3.429419784	0.821931280
N	-1.622778146	0.671493624	0.000048966
H	-2.102144095	1.041365408	0.822158317
H	-2.102188641	1.041595763	-0.821931280
H	1.674739222	3.091580622	0.000091553
H	-1.764349529	-0.347508007	-0.000091553

./cisplatin-H20-TZ-aug-pVDZ-pp-2_eGeom.xyz

11

Pt	0.527804403	0.799426731	0.000000000
Cl	0.438300733	-1.528407714	-0.005504718
Cl	2.855638851	0.888930318	0.005504718

N	0.577687314	2.860563177	-0.012778212
H	0.189122676	3.253807379	-0.874695594
H	0.078514774	3.282581761	0.775082281
N	-1.533332044	0.749543893	0.012778212
H	-1.926576233	1.138108545	0.874695594
H	-1.955350611	1.248716448	-0.775082281
H	1.559244736	3.154669911	0.045555183
H	-1.827438814	-0.232013519	-0.045555183

./cisplatin-PBE0-ApVTZ-pVDZ-pp_eGeom.xyz
11

Pt	0.478332604	0.848898532	0.000000000
Cl	0.368860968	-1.429380907	-0.000325731
Cl	2.756612046	0.958370086	0.000325731
N	0.627465946	2.912400085	-0.000019796
H	0.244933317	3.363264479	-0.823255337
H	0.245272671	3.363285575	0.823361269
N	-1.585168954	0.699765263	0.000019796
H	-2.036033335	1.082297908	0.823255337
H	-2.036054431	1.081958554	-0.823361269
H	1.641217712	3.049053854	-0.000205281
H	-1.721822760	-0.313986498	0.000205281

./cisplatin-TZ-aug-pVTZ-pp_eGeom.xyz
11

Pt	0.474793476	0.852437660	0.000000000
Cl	0.360102523	-1.438876217	0.000002212
Cl	2.766107357	0.967128532	-0.000002212
N	0.641011072	2.929593557	-0.000009547
H	0.259526916	3.386506609	-0.831710213
H	0.259632604	3.386517822	0.831733249
N	-1.602362427	0.686220138	0.000009547
H	-2.059275466	1.067704310	0.831710213
H	-2.059286678	1.067598622	-0.831733249
H	1.667821999	3.051686684	-0.000070165
H	-1.724455591	-0.340590784	0.000070165

./cisplatin-M06L-CPCM-TZ-aug-pVTZ-2_eGeom.xyz
11

Pt	0.533105621	0.794125513	0.000000000
Cl	0.436519168	-1.547155240	-0.003557631
Cl	2.874386378	0.890711883	0.003557631
N	0.581642571	2.868264640	-0.010895274
H	0.188836501	3.264606237	-0.856406793
H	0.094836426	3.287752165	0.772057151
N	-1.541033508	0.745588636	0.010895274
H	-1.937375091	1.138394721	0.856406793
H	-1.960521015	1.232394797	-0.772057151
H	1.551052501	3.165064876	0.039143364
H	-1.837833779	-0.223821283	-0.039143364

./cisplatin-M06L-H2O-ApVTZ-ApVTZ-2_eGeom.xyz
11

Pt	0.000035693	0.174878020	0.000188509
----	-------------	-------------	-------------

Cl	-1.722320434	-1.411958443	-0.001578816
Cl	1.720840455	-1.413638591	0.002960111
N	1.500906320	1.606538184	0.012276547
H	1.440515418	2.262174870	-0.757277616
H	1.516491530	2.148367889	0.868031687
N	-1.499436305	1.607995637	-0.012802850
H	-1.438381077	2.264095050	0.756304064
H	-1.514521272	2.149259687	-0.868924836
H	2.396163986	1.133731142	-0.060340807
H	-2.395152314	1.136111555	0.060162008

./cisplatin-CPCM-TZ-pVDZ-pp-2_eGeom.xyz

11

Pt	0.000038449	0.182595611	0.000173968
Cl	-1.713317557	-1.398379712	0.002178658
Cl	1.711834934	-1.400071081	-0.000960031
N	1.494811759	1.604399614	0.008365915
H	1.441973939	2.247839795	-0.785843113
H	1.494958968	2.164971147	0.864992374
N	-1.493334324	1.605868282	-0.008837928
H	-1.439704058	2.250008638	0.784748232
H	-1.493139378	2.165633567	-0.865993311
H	2.396091140	1.116152210	-0.043292831
H	-2.395071873	1.118536929	0.043466066

./cisplatin-M062X-CPCM-aug-pVDZ-2_eGeom.xyz

11

Pt	-0.003766760	0.003769385	0.192006999
Cl	-0.013948671	-1.734244216	-1.407413604
Cl	0.011456399	1.725733804	-1.421878701
N	0.006078835	1.485636480	1.617365835
H	-0.807342664	1.457077445	2.237752164
H	0.838551393	1.465737064	2.212373471
N	-0.017833673	-1.474766776	1.624236409
H	0.793515043	-2.088558110	1.512664872
H	-0.010712064	-1.148859263	2.593386069
H	-0.005416395	2.399549170	1.154684130
H	-0.845046593	-2.067956844	1.517768295

./cisplatin-PBE0-SMD-ApVDZ-pVDZ-pp-2_eGeom.xyz

11

Pt	0.000048776	0.152814033	0.000188933
Cl	-1.695783205	-1.437912683	-0.009566202
Cl	1.694412623	-1.439470073	0.010926183
N	1.438726267	1.598925141	0.015992188
H	1.325591117	2.273529625	-0.740970717
H	1.433699097	2.126973825	0.889295565
N	-1.437293409	1.600242427	-0.016507672
H	-1.323550604	2.275193892	0.740054737
H	-1.431761280	2.127765379	-0.890125614
H	2.367819601	1.188630549	-0.080083036
H	-2.366766983	1.190862885	0.079793633

./cisplatin-M06L-pVTZ-H20-2_eGeom.xyz

11

Pt	0.000034442	0.172474957	0.000192778
Cl	-1.735879781	-1.423401109	-0.000129847
Cl	1.734388957	-1.425094880	0.001535699
N	1.499867965	1.603029209	0.010402103
H	1.454968655	2.262578476	-0.768165486
H	1.520977674	2.162614844	0.864771042
N	-1.498401658	1.604486371	-0.010930526
H	-1.452845043	2.264510042	0.767196617
H	-1.518980261	2.163523184	-0.865671717
H	2.407416221	1.135224131	-0.052650646
H	-2.406405175	1.137609776	0.052447980

./cisplatin-M06L-ApVDZ-aug-pVDZ_eGeom.xyz

11

Pt	0.488012308	0.839218827	0.000000000
Cl	0.373298816	-1.468584739	-0.000169416
Cl	2.795815879	0.953932238	0.000169416
N	0.649001094	2.942045629	-0.000167869
H	0.273803067	3.409489116	-0.822303073
H	0.273044716	3.409664154	0.821524341
N	-1.614814499	0.678230116	0.000167869
H	-2.082257973	1.053428159	0.822303073
H	-2.082433011	1.054186511	-0.821524341
H	1.664567431	3.081653137	0.000305137
H	-1.754422044	-0.337336216	-0.000305137

./cisplatin-H20-ApVTZ-pVDZ-pp-2_eGeom.xyz

11

Pt	0.527990144	0.799240990	0.000000000
Cl	0.438257674	-1.529187449	-0.005336166
Cl	2.856418586	0.888973378	0.005336166
N	0.577065034	2.858966535	-0.013168547
H	0.187781854	3.252759060	-0.874408394
H	0.077527096	3.281309883	0.774187792
N	-1.531735403	0.750166174	0.013168547
H	-1.925527914	1.139449367	0.874408394
H	-1.954078734	1.249704126	-0.774187792
H	1.557937709	3.155251358	0.044973455
H	-1.828020261	-0.230706491	-0.044973455

./cisplatin-SMD-aug-pVDZ-2_eGeom.xyz

11

Pt	0.547075541	0.780155592	0.000000000
Cl	0.473572411	-1.553412741	-0.004265777
Cl	2.880643877	0.853658639	0.004265777
N	0.557839768	2.833754132	0.018794594
H	0.009048217	3.249523597	-0.750975535
H	0.175472197	3.214978372	0.899689133
N	-1.506522999	0.769391438	-0.018794594
H	-1.922292444	1.318183004	0.750975535
H	-1.887747226	1.151759023	-0.899689133
H	1.522793847	3.193498506	-0.068084426
H	-1.866267407	-0.195562628	0.068084426

./cisplatin-PBE0-H20-ApVDZ-aug-pVDZ-pp_eGeom.xyz
11

Pt	0.529557850	0.797673284	0.000000000
Cl	0.446949254	-1.525681985	-0.003174777
Cl	2.852913122	0.880281798	0.003174777
N	0.563478209	2.840398486	-0.016901104
H	0.193298738	3.227943769	-0.883629421
H	0.043586753	3.262937035	0.750614286
N	-1.513167353	0.763752997	0.016901104
H	-1.900712623	1.133932482	0.883629421
H	-1.935705884	1.283644468	-0.750614286
H	1.530943184	3.154756578	0.062188928
H	-1.827525480	-0.203711966	-0.062188928

./cisplatin-M06L-SMD-ApVTZ-ApVDZ-2_eGeom.xyz
11

Pt	0.000026313	0.151443792	0.000182127
Cl	-1.708422308	-1.447054865	-0.009485238
Cl	1.706921139	-1.448707039	0.010813239
N	1.469378210	1.606942170	0.018437182
H	1.356815103	2.283334555	-0.728141731
H	1.474575923	2.123065612	0.891211155
N	-1.467911037	1.608357587	-0.018949535
H	-1.354687919	2.285091520	0.727219698
H	-1.472610863	2.123958014	-0.892035186
H	2.385362457	1.184376678	-0.087727170
H	-2.384305018	1.186746977	0.087473459

./cisplatin-M062X_eGeom.xyz
11

Pt	0.499023610	0.828207525	0.000000000
Cl	0.396407945	-1.469554805	0.000010094
Cl	2.796785944	0.930823108	-0.000010094
N	0.638074237	2.933886365	0.000017148
H	0.256546241	3.398585195	-0.826259068
H	0.256515487	3.398576764	0.826283950
N	-1.606655235	0.689156973	-0.000017148
H	-2.071354051	1.070684986	0.826259068
H	-2.071345620	1.070715740	-0.826283950
H	1.654505927	3.092119792	0.000037641
H	-1.764888698	-0.327274711	-0.000037641

./cisplatin-PBE0-TZ-aug-pVTZ_eGeom.xyz
11

Pt	0.477389639	0.849841496	0.000000000
Cl	0.368046758	-1.425832111	0.000004790
Cl	2.753063250	0.959184297	-0.000004790
N	0.627843400	2.912785315	0.000048421
H	0.245903705	3.363060045	-0.823866229
H	0.245928563	3.363019859	0.823996747
N	-1.585554185	0.699387809	-0.000048421
H	-2.035828901	1.081327520	0.823866229
H	-2.035788715	1.081302662	-0.823996747

H 1.641961415 3.046580239 0.000041929
H -1.719349145 -0.314730201 -0.000041929
./cisplatin-M062X-SMD-ApVDZ-aug-pVTZ-2_eGeom.xyz
11

Pt 0.549941301 0.777289832 0.000000000
Cl 0.475836221 -1.578157294 0.000048246
Cl 2.905388430 0.851394828 -0.000048246
N 0.533131764 2.815605723 -0.000064965
H 0.056340791 3.189311084 -0.821410161
H 0.055734587 3.189374398 0.820895983
N -1.488374589 0.794099442 0.000064965
H -1.862079934 1.270890428 0.821410161
H -1.862143248 1.271496632 -0.820895983
H 1.482349352 3.189739990 0.000253966
H -1.862508890 -0.155118133 -0.000253966
./cisplatin-M06L-aug-pVDZ-CPCM-2_eGeom.xyz
11

Pt 0.000029572 0.166687271 0.000185135
Cl -1.730204448 -1.433359941 -0.002183012
Cl 1.728690246 -1.435057499 0.003543252
N 1.494571459 1.603500182 0.010293093
H 1.444119290 2.262734239 -0.768353389
H 1.511549733 2.163884408 0.864382212
N -1.493101151 1.604960993 -0.010809668
H -1.441956829 2.264686513 0.767374959
H -1.509582157 2.164767437 -0.865287501
H 2.407257662 1.146175786 -0.053152780
H -2.406231378 1.148575613 0.053005701
./cisplatin-M06L-SMD-2_eGeom.xyz
11

Pt 0.000020546 0.144147737 0.000185540
Cl -1.723684479 -1.462919283 -0.004760360
Cl 1.722155685 -1.464598101 0.006103508
N 1.472321667 1.603203194 0.017102290
H 1.374824547 2.287587441 -0.736936582
H 1.483200930 2.137578884 0.889682449
N -1.470855470 1.604629265 -0.017613473
H -1.372685602 2.289377712 0.736007206
H -1.481218488 2.138482982 -0.890519256
H 2.402767821 1.188835259 -0.080462094
H -2.401705156 1.191229910 0.080208770
./cisplatin-PBE0-H2O-TZ-pVDZ-pp-2_eGeom.xyz
11

Pt 0.000039695 0.183895313 0.000191050
Cl -1.697777327 -1.391760310 -0.000219274
Cl 1.696314703 -1.393419708 0.001613565
N 1.476157019 1.601381474 0.012314699
H 1.410112528 2.256422453 -0.759882817
H 1.486419210 2.140389522 0.872314742
N -1.474691562 1.602815778 -0.012843645

H	-1.407991475	2.258313943	0.758909263
H	-1.484445826	2.141252247	-0.873207746
H	2.372844320	1.127952314	-0.060686860
H	-2.371839284	1.130311974	0.060495022

./cisplatin-PBE0-CPCM-ApVTZ-ApVTZ-pp-2_eGeom.xyz

11

Pt	0.527284666	0.799946468	0.000000000
Cl	0.445432543	-1.511717866	-0.004262056
Cl	2.838949003	0.881798509	0.004262056
N	0.565871434	2.843137193	-0.012642083
H	0.175121677	3.232002288	-0.865194971
H	0.068060502	3.258317787	0.768447606
N	-1.515906061	0.761359772	0.012642083
H	-1.904771141	1.152109543	0.865194971
H	-1.931086636	1.259170719	-0.768447606
H	1.534553314	3.147124581	0.043932103
H	-1.819893483	-0.207322097	-0.043932103

./cisplatin-PBE0-H2O-ApVTZ_eGeom.xyz

11

Pt	0.526878632	0.800352502	0.000000000
Cl	0.440285374	-1.519061734	-0.000734051
Cl	2.846292871	0.886945678	0.000734051
N	0.566251636	2.837640684	-0.000181145
H	0.123133857	3.252229148	-0.822036671
H	0.121952354	3.252992583	0.820639291
N	-1.510409551	0.760979570	0.000181145
H	-1.924997999	1.204097364	0.822036671
H	-1.925761434	1.205278868	-0.820639291
H	1.541113834	3.148354888	0.000341148
H	-1.821123790	-0.213882617	-0.000341148

./cisplatin-PBE0-CPCM-ApVTZ-pVDZ-pp-2_eGeom.xyz

11

Pt	0.527622699	0.799608435	0.000000000
Cl	0.445697226	-1.514264371	-0.002896620
Cl	2.841495508	0.881533826	0.002896620
N	0.565632750	2.843097156	-0.011924728
H	0.172394009	3.233076014	-0.862537788
H	0.070148170	3.257700692	0.770674796
N	-1.515866023	0.761598456	0.011924728
H	-1.905844868	1.154837211	0.862537788
H	-1.930469541	1.257083051	-0.770674796
H	1.533841377	3.148266626	0.042196504
H	-1.821035528	-0.206610160	-0.042196504

./cisplatin-M062X-CPCM-ApVTZ-pVDZ_eGeom.xyz

11

Pt	0.534823619	0.792407515	0.000000000
Cl	0.447216749	-1.559156836	-0.002365533
Cl	2.886387973	0.880014301	0.002365533
N	0.562283767	2.848568793	0.015976621
H	0.042715571	3.261922994	-0.752216166

H	0.185616982	3.232650597	0.877522431
N	-1.521337660	0.764947439	-0.015976621
H	-1.934691843	1.284515651	0.752216166
H	-1.905419450	1.141614239	-0.877522431
H	1.525208713	3.166419734	-0.060804492
H	-1.839188636	-0.197977494	0.060804492

./cisplatin-M06L-CPCM-ApVTZ-ApVDZ-3_eGeom.xyz

11

Pt	0.000000000	0.000000000	0.181508142
Cl	-0.014330842	-1.721790847	-1.408794958
Cl	0.014330842	1.721790847	-1.408794958
N	-0.001614384	1.498956714	1.614679856
H	-0.849791679	1.509614040	2.168194950
H	0.776988720	1.441608692	2.259690343
N	0.001614384	-1.498956714	1.614679856
H	0.849791679	-1.509614040	2.168194950
H	-0.776988720	-1.441608692	2.259690343
H	0.060596222	2.395371511	1.142814238
H	-0.060596222	-2.395371511	1.142814238

./cisplatin-PBE0-SMD-2_eGeom.xyz

11

Pt	0.000027290	0.157463270	0.000185814
Cl	-1.695622300	-1.429363970	-0.002215527
Cl	1.694123976	-1.431019594	0.003559468
N	1.450855439	1.596286767	0.014665329
H	1.357734904	2.271272729	-0.749627330
H	1.452362299	2.136181721	0.885099775
N	-1.449394497	1.597694316	-0.015174774
H	-1.355592266	2.273090366	0.748672051
H	-1.450405030	2.137019673	-0.885963153
H	2.379775801	1.173280389	-0.071468320
H	-2.378723617	1.175649332	0.071264667

./cisplatin-CPCM-ApVTZ-pVDZ-pp-2_eGeom.xyz

11

Pt	0.000039404	0.181314736	0.000197852
Cl	-1.710741626	-1.401316411	0.000869464
Cl	1.709254389	-1.403014485	0.000182453
N	1.490725500	1.603485415	0.008750582
H	1.435297583	2.249291651	-0.783512729
H	1.491350049	2.163502158	0.865877383
N	-1.489245584	1.604949329	-0.009178628
H	-1.432927584	2.251593404	0.782334972
H	-1.489648338	2.164007585	-0.866933781
H	2.394742540	1.120677027	-0.045312168
H	-2.393704332	1.123064592	0.045722600

./cisplatin-M06L-aug-pVDZ_eGeom.xyz

11

Pt	0.491464891	0.835766244	0.000000000
Cl	0.382108054	-1.470417722	-0.000071376
Cl	2.797648861	0.945122999	0.000071376

N	0.650068172	2.942631275	-0.000067384
H	0.277031407	3.417820469	-0.822554926
H	0.276722888	3.417883109	0.822245102
N	-1.615400146	0.677163038	0.000067384
H	-2.090589326	1.050199820	0.822554926
H	-2.090651966	1.050508339	-0.822245102
H	1.667618030	3.089636174	0.000121994
H	-1.762405081	-0.340386815	-0.000121994

./cisplatin-ApVDZ-aug-pVTZ-pp_eGeom.xyz

11

Pt	0.472151521	0.855079615	0.000000000
Cl	0.357058519	-1.444926576	0.000012161
Cl	2.772157716	0.970172535	-0.000012161
N	0.638882653	2.925241780	-0.000008117
H	0.258673727	3.388265689	-0.833786967
H	0.258773778	3.388273882	0.833811837
N	-1.598010650	0.688348556	0.000008117
H	-2.061034546	1.068557499	0.833786967
H	-2.061042738	1.068457448	-0.833811837
H	1.669314334	3.050539622	-0.000066661
H	-1.723308529	-0.342083120	0.000066661

./cisplatin-M062X-CPCM-ApVDZ-pVDZ-3_eGeom.xyz

11

Pt	0.003622299	0.179752067	-0.049887842
Cl	1.729872241	-1.434120962	-0.196028272
Cl	-1.741609854	-1.419705757	-0.092740836
N	-1.461371462	1.622778006	0.069862935
H	-1.349368553	2.249016413	0.866509145
H	-1.504593055	2.204104246	-0.766732305
N	1.485559126	1.609535534	-0.000667671
H	2.390027594	1.160695033	-0.149759554
H	1.381473897	2.326109233	-0.718339774
H	-2.371145394	1.170198698	0.165948735
H	1.535015271	2.088244850	0.898271970

./cisplatin-M062X-SMD-ApVDZ-pVDZ-3_eGeom.xyz

11

Pt	-0.103676309	0.001417973	0.195850537
Cl	-0.337373355	-1.717861086	-1.406267741
Cl	-0.229245184	1.725307979	-1.413417763
N	0.104510143	1.441060676	1.640421318
H	-0.568523076	1.332195804	2.400341760
H	1.035016583	1.423622614	2.060620254
N	0.013965285	-1.442443138	1.646411727
H	-0.650793941	-1.288398331	2.405798879
H	-0.177963236	-2.366259128	1.257297898
H	-0.029103163	2.373477353	1.247447914
H	0.943794322	-1.481693076	2.066639566

./cisplatin-M062X-H2O-ApVDZ-pVDZ_eGeom.xyz

11

Pt	0.537178327	0.790052806	0.000000000
----	-------------	-------------	-------------

Cl	0.444944473	-1.575310082	0.005789281
Cl	2.902541219	0.882286577	-0.005789281
N	0.561416334	2.847828423	-0.018245464
H	0.216143408	3.231613297	-0.897640112
H	0.011762131	3.268856637	0.729975680
N	-1.520597290	0.765814872	0.018245464
H	-1.904382152	1.111087813	0.897640112
H	-1.941625484	1.315469090	-0.729975680
H	1.522489136	3.173485414	0.091669229
H	-1.846254316	-0.195257918	-0.091669229

./cisplatin-PBE0-SMD-ApVDZ-aug-pVDZ-pp-2_eGeom.xyz

11

Pt	0.000033292	0.154470647	0.000188189
Cl	-1.691590736	-1.435718873	-0.007288297
Cl	1.690132979	-1.437334006	0.008647726
N	1.435767787	1.598883744	0.011961698
H	1.330077604	2.257817644	-0.759455250
H	1.416911439	2.142096522	0.875456757
N	-1.434315753	1.600252092	-0.012477942
H	-1.328012540	2.259538597	0.758553507
H	-1.414916625	2.142938386	-0.876291860
H	2.365388523	1.186152401	-0.064690294
H	-2.364333970	1.188457846	0.064393766

./cisplatin-PBE0-H2O-ApVDZ-pVTZ-pp_eGeom.xyz

11

Pt	0.529972341	0.797258793	0.000000000
Cl	0.446228477	-1.525318823	-0.002790211
Cl	2.852549960	0.881002574	0.002790211
N	0.561981199	2.837437917	-0.018626530
H	0.199027214	3.223174809	-0.889456357
H	0.034508946	3.262593623	0.742496937
N	-1.510206784	0.765250007	0.018626530
H	-1.895943663	1.128204006	0.889456357
H	-1.935362471	1.292722276	-0.742496937
H	1.528120335	3.154490871	0.067695491
H	-1.827259773	-0.200889118	-0.067695491

./cisplatin-M062X-SMD-TZ-pVTZ_eGeom.xyz

11

Pt	0.553385867	0.773845266	0.000000000
Cl	0.475892576	-1.571636204	-0.000262174
Cl	2.898867340	0.851338474	0.000262174
N	0.537286043	2.821822399	-0.000035171
H	0.061624353	3.192620564	-0.819315945
H	0.061685873	3.192680439	0.819253170
N	-1.494591265	0.789945162	0.000035171
H	-1.865389413	1.265606866	0.819315945
H	-1.865449288	1.265545346	-0.819253170
H	1.484875350	3.191802751	-0.000088525
H	-1.864571651	-0.157644131	0.000088525

./cisplatin-PBE0-H2O-ApVTZ-ApVTZ-pp_eGeom.xyz

11

Pt	0.527342639	0.799888495	0.000000000
Cl	0.445361710	-1.511789361	-0.007604620
Cl	2.839020498	0.881869341	0.007604620
N	0.565759453	2.843218340	-0.018216042
H	0.190655020	3.226842712	-0.880117231
H	0.053884176	3.262798460	0.751254334
N	-1.515987208	0.761471754	0.018216042
H	-1.899611566	1.136576201	0.880117231
H	-1.935567309	1.273347046	-0.751254334
H	1.533252360	3.147725090	0.053723811
H	-1.820493992	-0.206021142	-0.053723811

./cisplatin-PBE0-ApVDZ-aug-pVTZ-pp_eGeom.xyz

11

Pt	0.475569680	0.851661456	0.000000000
Cl	0.365638364	-1.431866048	-0.000006932
Cl	2.759097188	0.961592691	0.000006932
N	0.625396252	2.907958377	0.000208912
H	0.244246636	3.363932329	-0.825603511
H	0.244283646	3.363750671	0.826139601
N	-1.580727246	0.701834957	-0.000208912
H	-2.036701185	1.082984589	0.825603511
H	-2.036519526	1.082947580	-0.826139601
H	1.642620179	3.046519295	0.000215848
H	-1.719288201	-0.315388965	-0.000215848

./cisplatin-M06L-TZ-aug-pVTZ_eGeom.xyz

11

Pt	0.486030308	0.841200827	0.000000000
Cl	0.370584267	-1.453386542	-0.000084220
Cl	2.780617682	0.956646787	0.000084220
N	0.651493937	2.945947458	-0.000092863
H	0.276615091	3.406160328	-0.819735805
H	0.276373720	3.406241866	0.819395310
N	-1.618716329	0.675737273	0.000092863
H	-2.078929185	1.050616136	0.819735805
H	-2.079010723	1.050857506	-0.819395310
H	1.664132918	3.072806996	0.000064504
H	-1.745575902	-0.336901703	-0.000064504

./cisplatin-PBE0-CPCM-ApVTZ-2_eGeom.xyz

11

Pt	0.527363767	0.799867367	0.000000000
Cl	0.442112642	-1.519263863	-0.003771571
Cl	2.846495000	0.885118410	0.003771571
N	0.565288759	2.836669400	-0.011224353
H	0.169886308	3.238219878	-0.863499301
H	0.072559369	3.262604133	0.775742641
N	-1.509438268	0.761942447	0.011224353
H	-1.910988732	1.157344912	0.863499301
H	-1.935372983	1.254671853	-0.775742641
H	1.538004519	3.149525700	0.039753420
H	-1.822294602	-0.210773301	-0.039753420

./cisplatin-SMD-TZ-aug-pVDZ-pp-2_eGeom.xyz
11

Pt	0.545276576	0.781954557	0.000000000
Cl	0.469955683	-1.543763516	-0.004576520
Cl	2.870994652	0.857275367	0.004576520
N	0.556674557	2.839299760	0.017891866
H	0.012324272	3.239492009	-0.752672283
H	0.170426063	3.207580744	0.893281365
N	-1.512068627	0.770556649	-0.017891866
H	-1.912260856	1.314906949	0.752672283
H	-1.880349597	1.156805157	-0.893281365
H	1.519261994	3.183850032	-0.065468734
H	-1.856618934	-0.192030776	0.065468734

./cisplatin-M06L-H2O-ApVDZ-aug-pVTZ-2_eGeom.xyz
11

Pt	0.000000000	0.000000000	0.185479037
Cl	0.006824812	-1.728791363	-1.413228317
Cl	-0.006824812	1.728791363	-1.413228317
N	0.011637134	1.493276364	1.615629559
H	-0.757990570	1.434439007	2.279722740
H	0.871578004	1.513258300	2.160982027
N	-0.011637134	-1.493276364	1.615629559
H	0.757990570	-1.434439007	2.279722740
H	-0.871578004	-1.513258300	2.160982027
H	-0.063411881	2.397049585	1.148856972
H	0.063411881	-2.397049585	1.148856972

./cisplatin-M06L-SMD-TZ-pVDZ-2_eGeom.xyz
11

Pt	0.000025243	0.152209999	0.000182109
Cl	-1.713110925	-1.445466406	-0.007959379
Cl	1.711601528	-1.447131700	0.009286921
N	1.473301450	1.607694391	0.017595540
H	1.364768584	2.280979100	-0.732526794
H	1.476763933	2.126858417	0.888688600
N	-1.471830925	1.609120063	-0.018108111
H	-1.362629319	2.282764079	0.731594644
H	-1.474803169	2.127746940	-0.889523133
H	2.387669841	1.180199748	-0.083881669
H	-2.386614242	1.182580370	0.083649274

./cisplatin-PBE0-SMD-pVTZ-pp-2_eGeom.xyz
11

Pt	0.000029943	0.162519553	0.000183551
Cl	-1.694903336	-1.421791503	-0.004886895
Cl	1.693412709	-1.423445065	0.006220422
N	1.446842434	1.595612182	0.014766085
H	1.352525406	2.269967346	-0.749032635
H	1.448841384	2.132904833	0.886026535
N	-1.445382317	1.597015268	-0.015274213
H	-1.350376640	2.271783717	0.748073954
H	-1.446895730	2.133732427	-0.886890420

```
H      2.372909391      1.168446322      -0.072907376
H      -2.371861243      1.170809922      0.072718992
./cisplatin-PBE0-SMD-ApVTZ-ApVTZ-pp-2_eGeom.xyz
11
```

```
Pt      0.000030000      0.156579969      0.000218597
Cl      -1.684341636     -1.424851730     -0.004059712
Cl      1.682884868     -1.426462619      0.005595421
N       1.438637196      1.599292613      0.006648103
H       1.343137924      2.235466203     -0.780100831
H       1.403202001      2.158609543      0.854742018
N      -1.437185292      1.600675722     -0.007209655
H      -1.341283216      2.237058968      0.779320751
H      -1.400970197      2.159633891     -0.855506001
H       2.363102276      1.179625600     -0.045799904
H      -2.362071925      1.181926841      0.045149213
./cisplatin-PBE0-H2O-TZ-aug-pVTZ-2_eGeom.xyz
11
```

```
Pt      0.000040220      0.184340508      0.000189886
Cl      -1.694961522     -1.390177190     -0.000984308
Cl      1.693500631     -1.391833675      0.002370223
N       1.474042101      1.600252485      0.012342716
H       1.407562842      2.256220350     -0.759311415
H       1.484802967      2.139586740      0.872380545
N      -1.472577628      1.601684413     -0.012868584
H      -1.405434372      2.258118524      0.758331269
H      -1.482839638      2.140436745     -0.873277373
H       2.371622715      1.128283450     -0.061324146
H      -2.370616317      1.130642651      0.061149188
./cisplatin-M06L-CPCM-TZ-pVTZ-2_eGeom.xyz
11
```

```
Pt      0.000036521      0.176098885      0.000191737
Cl      -1.727255179     -1.411093424      0.000469767
Cl      1.725778052     -1.412778307      0.000930546
N       1.503553257      1.607145035      0.009054175
H       1.453689372      2.250120862     -0.771924104
H       1.511337254      2.162737256      0.856045086
N      -1.502083253      1.608605760     -0.009586480
H      -1.451580290      2.252049045      0.770965491
H      -1.509339167      2.163645022     -0.856944671
H       2.397424306      1.129327842     -0.046450361
H      -2.396418872      1.131697023      0.046246815
./cisplatin-M062X-CPCM-pVTZ-3_eGeom.xyz
11
```

```
Pt      -0.015022128      0.001079016      0.183019553
Cl      -0.030746842     -1.730856804     -1.420049814
Cl       0.157671537      1.730462276     -1.413597687
N       0.003880798      1.475534242      1.614102070
H      -0.811272787      1.459481905      2.232079100
H       0.833370903      1.439858114      2.212152043
N      -0.174024339     -1.471026844      1.607770535
```



```
H      0.576508983      -1.453750737      2.302771575
H     -1.058232151      -1.434483471      2.121421901
H      0.011413871       2.389032516      1.150872353
H     -0.136038244      -2.385336252      1.147651089
```

```
./cisplatin-M062X-ApVDZ-aug-pVDZ_eGeom.xyz
```

```
11
```

```
Pt      0.495951998      0.831279137      0.000000000
Cl      0.388616428     -1.469544322     -0.000000220
Cl      2.796775461      0.938614626      0.000000220
N       0.630659336      2.925896142      0.000020022
H       0.242826092      3.377312074     -0.825410154
H       0.242794454      3.377302338      0.825440695
N      -1.598665012      0.696571874     -0.000020022
H      -2.050080930      1.084405134      0.825410154
H      -2.050071194      1.084436771     -0.825440695
H       1.642812588      3.085234533      0.000041335
H      -1.758003438     -0.315581373     -0.000041335
```

```
./cisplatin-TZ-pVDZ-pp_eGeom.xyz
```

```
11
```

```
Pt      0.473884192      0.853346944      0.000000000
Cl      0.358938080     -1.440794842      0.000013419
Cl      2.768025982      0.968292975     -0.000013419
N       0.643179364      2.934439528     -0.000007034
H       0.264334198      3.392571851     -0.831908550
H       0.264472690      3.392582017      0.831951630
N      -1.607208398      0.684051846      0.000007034
H      -2.065340707      1.062897028      0.831908550
H      -2.065350874      1.062758536     -0.831951630
H       1.670851859      3.049401695     -0.000084704
H      -1.722170602     -0.343620646      0.000084704
```

```
./cisplatin-M06L-pVTZ_eGeom.xyz
```

```
11
```

```
Pt      0.488956590      0.838274545      0.000000000
Cl      0.376720883     -1.468249316     -0.000087038
Cl      2.795480455      0.950510170      0.000087038
N       0.652178752      2.943403574     -0.000090025
H       0.279690474      3.419083405     -0.822463858
H       0.279269321      3.419167706      0.822045398
N      -1.616172445      0.675052458      0.000090025
H      -2.091852263      1.047540753      0.822463858
H      -2.091936563      1.047961907     -0.822045398
H       1.670399017      3.086349531      0.000170060
H      -1.759118438     -0.343167802     -0.000170060
```

```
./cisplatin-M06L-CPCM-ApVDZ-aug-pVTZ_eGeom.xyz
```

```
11
```

```
Pt      0.533487068      0.793744066      0.000000000
Cl      0.441758184     -1.559344637      0.002526224
Cl      2.886575774      0.885472866     -0.002526224
N       0.576924850      2.860618942      0.013427855
H       0.076661159      3.287364810     -0.764047561
```

H	0.192091438	3.260537422	0.867331775
N	-1.533387810	0.750306358	-0.013427855
H	-1.960133660	1.250570063	0.764047561
H	-1.933306276	1.135139784	-0.867331775
H	1.546612419	3.170898455	-0.047950634
H	-1.843667357	-0.219381200	0.047950634

./cisplatin-M062X-CPCM-ApVDZ-aug-pVDZ-2_eGeom.xyz

11

Pt	-0.003797065	0.005130266	0.196400318
Cl	-0.013342108	-1.740576602	-1.398409542
Cl	0.010130900	1.726678394	-1.422657873
N	0.005279180	1.487370321	1.620519804
H	-0.807885169	1.454541206	2.234561607
H	0.835009802	1.461678683	2.212395739
N	-0.016737361	-1.474566331	1.625741275
H	0.791503920	-2.084076579	1.503977149
H	-0.005776201	-1.148920793	2.590821421
H	-0.004575504	2.395563051	1.155142647
H	-0.844275544	-2.059703476	1.514453394

./cisplatin-M062X-H2O-ApVDZ-aug-pVTZ-2_eGeom.xyz

11

Pt	0.530505941	0.796725193	0.000000000
Cl	0.441854383	-1.564437883	0.005342888
Cl	2.891669020	0.885376667	-0.005342888
N	0.559864178	2.844725657	-0.019623150
H	0.198908804	3.229152814	-0.891970685
H	0.027599320	3.265769497	0.740662816
N	-1.517494524	0.767367029	0.019623150
H	-1.901921668	1.128322416	0.891970685
H	-1.938538346	1.299631902	-0.740662816
H	1.525539372	3.161601792	0.071441416
H	-1.834370694	-0.198308154	-0.071441416

./cisplatin-ApVTZ-ApVDZ-pp_eGeom.xyz

11

Pt	0.475353478	0.851877658	0.000000000
Cl	0.360701569	-1.442149891	0.000008177
Cl	2.769381031	0.966529485	-0.000008177
N	0.640487326	2.929200054	-0.000006441
H	0.258374579	3.386032058	-0.831515035
H	0.258474105	3.386040848	0.831542864
N	-1.601968924	0.686743884	0.000006441
H	-2.058800914	1.068856647	0.831515035
H	-2.058809704	1.068757121	-0.831542864
H	1.667012436	3.053820290	-0.000064517
H	-1.726589197	-0.339781222	0.000064517

./cisplatin-M062X-CPCM-2_eGeom.xyz

11

Pt	0.082972247	0.000850822	0.189464609
Cl	0.320280703	-1.733254165	-1.392844415
Cl	0.161636906	1.730550452	-1.413416674

N	-0.117306124	1.481791832	1.609850789
H	-0.958351197	1.390884681	2.186060457
H	0.677894907	1.531790731	2.252626119
N	-0.000211698	-1.476083584	1.625614577
H	0.147255604	-2.386977088	1.179344854
H	0.711834701	-1.383590141	2.355059499
H	-0.174592912	2.391335191	1.140735309
H	-0.905878287	-1.524180592	2.100450816

./cisplatin-M06L-ApVTZ-ApVTZ_eGeom.xyz

11

Pt	0.486370161	0.840860974	0.000000000
Cl	0.371644658	-1.453397062	-0.000179406
Cl	2.780628201	0.955586396	0.000179406
N	0.650691309	2.944285477	-0.000100020
H	0.274438840	3.403655645	-0.819561682
H	0.274260972	3.403740670	0.819233778
N	-1.617054347	0.676539902	0.000100020
H	-2.076424502	1.052792386	0.819561682
H	-2.076509527	1.052970255	-0.819233778
H	1.663009722	3.074670797	0.000016533
H	-1.747439704	-0.335778508	-0.000016533

./cisplatin-PBE0-CPCM-TZ-aug-pVDZ-2_eGeom.xyz

11

Pt	0.527478963	0.799752171	0.000000000
Cl	0.445984658	-1.513923571	-0.002392612
Cl	2.841154708	0.881246394	0.002392612
N	0.566125276	2.844666572	-0.012188871
H	0.175210869	3.233553706	-0.864526205
H	0.069207193	3.259179615	0.769693385
N	-1.517435440	0.761105930	0.012188871
H	-1.906322560	1.152020352	0.864526205
H	-1.931948465	1.258024028	-0.769693385
H	1.534874964	3.147945476	0.043925074
H	-1.820714378	-0.207643746	-0.043925074

./cisplatin-PBE0-SMD-ApVTZ-pVDZ-pp-3_eGeom.xyz

11

Pt	-0.001099238	0.170469517	-0.006428817
Cl	1.689235863	-1.408306822	0.008160559
Cl	-1.681747208	-1.418674080	-0.000717542
N	-1.449298265	1.604715608	-0.019447976
H	-1.326542029	2.285094857	0.725141380
H	-1.463353908	2.116077389	-0.897735756
N	1.438289619	1.613603626	-0.011845496
H	1.453832920	2.125011351	-0.890081528
H	1.307399680	2.293235337	0.732040555
H	-2.365198115	1.180420869	0.099478750
H	2.356149680	1.194975347	0.111945871

./cisplatin-H20-aug-pVTZ-2_eGeom.xyz

11

Pt	0.527416354	0.799814780	0.000000000
----	-------------	-------------	-------------

```

Cl      0.434110896      -1.533162787      -0.006662622
Cl      2.860393924      0.893120155      0.006662622
N       0.576501093      2.851117968      -0.010963411
H       0.182656820      3.259571726      -0.871957217
H       0.083386434      3.285846763      0.783124686
N      -1.523886836      0.750730113      0.010963411
H      -1.932340579      1.144574401      0.871957217
H      -1.958615613      1.243844788      -0.783124686
H       1.562561890      3.155799696      0.040823884
H      -1.828568599      -0.235330672      -0.040823884
./cisplatin-PBE0-CPCM-ApVTZ_eGeom.xyz
11

```

```

Pt      0.527908211      0.799322923      0.000000000
Cl      0.442195744      -1.519947933      0.000478225
Cl      2.847179070      0.885035307      -0.000478225
N       0.565154947      2.836270460      0.000041477
H       0.119636175      3.249607468      -0.821157463
H       0.119324679      3.249503821      0.821125621
N      -1.509039327      0.762076260      -0.000041477
H      -1.922376320      1.207595046      0.821157463
H      -1.922272673      1.207906542      -0.821125621
H       1.538895427      3.150221248      0.000250081
H      -1.822990150      -0.211664210      -0.000250081
./cisplatin-H20-ApVTZ-ApVTZ-pp-2_eGeom.xyz
11

```

```

Pt      0.527721788      0.799509346      0.000000000
Cl      0.437797110      -1.526468805      0.006773350
Cl      2.853699942      0.889433941      -0.006773350
N       0.577394213      2.858895961      0.013492195
H       0.076246517      3.281609887      -0.772907789
H       0.189763655      3.251934564      0.876095867
N      -1.531664828      0.749836994      -0.013492195
H      -1.954378737      1.250984705      0.772907789
H      -1.924703418      1.137467566      -0.876095867
H       1.558733416      3.154224985      -0.046337747
H      -1.826993887      -0.231502199      0.046337747

```

```

./carboplatin-CPCM-aug-pVDZ_eGeom.xyz
25

```

```

Pt      -0.205020661      -0.362170927      -0.367715543
N       0.527822752      1.307200723      0.579355293
H       0.168641897      1.442948536      1.537313698
H       1.557391692      1.332786563      0.643890476
N       0.474299132      -1.682181052      1.054211157
H       1.502437256      -1.720255269      1.134952309
H       0.110183015      -1.503427104      2.003059064
H       0.247479924      2.143081987      0.039780173
H       0.165489527      -2.634288447      0.796034645
O      -0.963766248      0.913740345      -1.731877938
O      -0.989944466      -1.975406071      -1.286651983
C      -1.175365912      0.534459132      -2.986970000

```

C	-1.159217903	-2.012180374	-2.602367306
O	-1.758888408	1.285750727	-3.779587071
O	-1.701651789	-2.988985942	-3.136627422
C	-0.627042458	-0.828767370	-3.439246279
C	0.949982176	-0.896147397	-3.569760074
C	-0.709591529	-1.107611951	-4.965035452
C	0.769762449	-1.574629425	-4.953436888
H	1.488782661	-1.447262796	-2.774603687
H	1.379511491	0.122379441	-3.649975259
H	-1.473811532	-1.847775543	-5.264413059
H	-0.859817521	-0.158340151	-5.511265012
H	0.857129258	-2.676624507	-4.883108156
H	1.422512208	-1.216645897	-5.773084695

./carboplatin-M06L-H2O-TZ-aug-pVDZ_eGeom.xyz

25

Pt	0.206835847	-0.361103427	-0.411600221
N	-0.557791508	1.312662549	0.543907427
H	-1.569639245	1.323938006	0.588011110
H	-0.219079613	1.430531087	1.491410335
N	-0.481459814	-1.702188506	1.015888682
H	-0.124805961	-1.522491235	1.946815128
H	-1.491534035	-1.731788172	1.086883847
H	-0.275894947	2.137361293	0.025028760
H	-0.175578239	-2.633946473	0.756625760
O	0.974802291	0.918986680	-1.783479005
O	1.023251899	-1.964724559	-1.344439311
C	1.211271218	0.530806971	-3.004466810
C	1.200188630	-1.989445972	-2.634317253
O	1.824116546	1.243500400	-3.789984541
O	1.751793113	-2.935755209	-3.181657702
C	0.649675178	-0.814057039	-3.444900216
C	0.654187551	-1.079934289	-4.954557569
C	-0.909847121	-0.893478895	-3.496437861
C	-0.782842634	-1.603047759	-4.849766041
H	1.418457199	-1.760005960	-5.322186128
H	0.715543320	-0.139248201	-5.497040344
H	-1.401789530	-1.414360731	-2.675968504
H	-1.346212543	0.101266031	-3.583668601
H	-0.811916090	-2.685523519	-4.736221018
H	-1.484424502	-1.318305841	-5.631008931

./carboplatin-M06L-CPCM-TZ-aug-pVDZ_eGeom.xyz

25

Pt	0.208201873	-0.364285725	-0.411200304
N	-0.548931728	1.311899410	0.545721295
H	-1.560978540	1.330163605	0.583067840
H	-0.215949163	1.424082307	1.495933214
N	-0.488448428	-1.703630998	1.013489734
H	-0.131774269	-1.527521734	1.945083260
H	-1.498776962	-1.727091224	1.083105135
H	-0.257813347	2.136297098	0.031488104
H	-0.188093194	-2.636778073	0.752883365
O	0.984343536	0.913502694	-1.781204784

O	1.017273192	-1.971019068	-1.345463670
C	1.220012852	0.524743271	-3.002054432
C	1.193974547	-1.995315082	-2.635331385
O	1.839382043	1.233633034	-3.786030755
O	1.740541194	-2.944002194	-3.183758855
C	0.650013017	-0.815905270	-3.444480797
C	0.653073825	-1.079858805	-4.954529337
C	-0.909931962	-0.886211177	-3.496129918
C	-0.787089461	-1.594413526	-4.850532435
H	1.413181018	-1.764187125	-5.322950591
H	0.720180411	-0.138948775	-5.495935986
H	-1.405003429	-1.405521425	-2.676576396
H	-1.340422546	0.111217527	-3.581739504
H	-0.822748848	-2.676862424	-4.738594197
H	-1.486908621	-1.304339090	-5.631387610

./carboplatin-M062X-CPCM-TZ-pVTZ-2_eGeom.xyz

25

Pt	0.207038292	-0.363440414	-0.397575980
N	-0.550235309	1.286836955	0.554069195
H	-1.563748677	1.280501669	0.621706284
H	-0.187163194	1.413910504	1.494390869
N	-0.476105518	-1.690660052	1.009908845
H	-0.088457696	-1.530602852	1.935113759
H	-1.487574509	-1.691967113	1.104045958
H	-0.290353570	2.111564714	0.017881571
H	-0.198869828	-2.627219517	0.724924550
O	0.963673172	0.911856101	-1.773812683
O	1.010913176	-1.959436728	-1.344453754
C	1.221438459	0.527543761	-2.986069306
C	1.176009645	-1.998555277	-2.630454818
O	1.861289438	1.219021010	-3.763522822
O	1.694009745	-2.953875299	-3.187587022
C	0.646421247	-0.810923359	-3.443732179
C	0.662903116	-1.071738480	-4.958226194
C	-0.916679050	-0.877945801	-3.503347918
C	-0.785340348	-1.593104882	-4.863455801
H	1.425148423	-1.755006442	-5.319708668
H	0.720160989	-0.127458966	-5.493352445
H	-1.416479847	-1.399994958	-2.690274247
H	-1.338341016	0.121772072	-3.600617031
H	-0.814807339	-2.674505178	-4.745498705
H	-1.477542793	-1.296924238	-5.647480469

./carboplatin-CPCM-TZ-pVTZ-pp_eGeom.xyz

25

Pt	0.198638517	-0.362543308	-0.381339621
N	-0.537550006	1.309847091	0.558441758
H	-1.559664594	1.321272333	0.617568071
H	-0.176713887	1.438001647	1.508246782
N	-0.485663022	-1.682768316	1.038846049
H	-0.116333912	-1.499368937	1.976108195
H	-1.506751801	-1.703467601	1.112823344
H	-0.256249628	2.132216819	0.013860648

H	-0.181801053	-2.625494965	0.772240455
O	0.966085178	0.905029448	-1.747381841
O	0.989376750	-1.972672900	-1.298198292
C	1.201468361	0.518834925	-2.986323721
C	1.178979659	-2.009127717	-2.602145525
O	1.819870898	1.247460041	-3.768915053
O	1.743808585	-2.971845921	-3.130836162
C	0.639552718	-0.833958038	-3.438122933
C	0.689792030	-1.106895047	-4.962052707
C	-0.937089970	-0.896893134	-3.534302373
C	-0.789968970	-1.563259588	-4.924687044
H	1.436394244	-1.840617219	-5.284863421
H	0.830525521	-0.166567540	-5.507330018
H	-1.449021940	-1.451828129	-2.739022562
H	-1.366312730	0.111971225	-3.592980196
H	-0.886181487	-2.655059024	-4.866277523
H	-1.447882451	-1.192618914	-5.720485323

./carboplatin-M062X-SMD-ApVTZ-ApVDZ-pp-2_eGeom.xyz

25

Pt	-1.122022000	0.010809000	-0.045820000
N	-2.360802000	1.581325000	0.302728000
H	-3.257652000	1.476210000	-0.166575000
H	-2.554140000	1.703973000	1.294065000
N	-2.511481000	-1.289341000	0.663586000
H	-2.709842000	-1.133786000	1.649420000
H	-3.396470000	-1.216544000	0.166126000
H	-1.944697000	2.447205000	-0.034304000
H	-2.190178000	-2.250449000	0.568910000
O	0.254441000	1.307924000	-0.809395000
O	0.111579000	-1.558354000	-0.460352000
C	1.526137000	1.096574000	-0.745796000
C	1.394585000	-1.422115000	-0.514843000
O	2.333924000	1.875428000	-1.249841000
O	2.120397000	-2.318687000	-0.944010000
C	2.006961000	-0.135933000	0.020046000
C	1.810754000	0.104852000	1.555405000
C	3.522715000	-0.138910000	0.274010000
C	3.273022000	0.587324000	1.610426000
H	1.672206000	-0.846998000	2.066339000
H	1.022403000	0.796053000	1.845107000
H	3.866016000	-1.157047000	0.439442000
H	4.148005000	0.346918000	-0.469227000
H	3.865796000	0.277983000	2.467105000
H	3.334473000	1.668225000	1.496693000

./carboplatin-M062X-ApVTZ-pVDZ-2_eGeom.xyz

25

Pt	-0.111143784	-0.360122322	-0.354707873
N	0.497223149	1.416917516	0.548042511
H	0.073898592	1.619783276	1.446811632
H	1.499660956	1.540643276	0.636304162
N	0.456614956	-1.811614902	1.030674845
H	1.455074861	-1.919638163	1.169509251

H	0.017562332	-1.740687847	1.941969627
H	0.151878283	2.103477124	-0.125657996
H	0.106219454	-2.657933999	0.577393820
O	-0.761313101	0.930822642	-1.701146162
O	-0.795257748	-1.973573555	-1.270775208
C	-1.086573061	0.567208937	-2.927261182
C	-1.063396136	-2.005227358	-2.561057300
O	-1.659319831	1.322143258	-3.673405875
O	-1.570610417	-2.973972951	-3.071071608
C	-0.609207234	-0.804485541	-3.399596617
C	0.944710848	-0.892414583	-3.586650851
C	-0.752343209	-1.074370554	-4.906367138
C	0.693362941	-1.611700249	-4.927221066
H	1.503352771	-1.417303733	-2.812775813
H	1.366033579	0.102999237	-3.724163328
H	-1.544920199	-1.759786870	-5.187171026
H	-0.854495277	-0.132151765	-5.437477043
H	0.715171379	-2.692520647	-4.806256396
H	1.325122906	-1.326843000	-5.765072375

./carboplatin-PBE0-CPCM-aug-pVTZ_eGeom.xyz

25

Pt	0.195722172	-0.369389497	-0.387658975
N	-0.539155957	1.274267120	0.553852106
H	-1.559240515	1.298745385	0.603122895
H	-0.196884164	1.398117604	1.508454940
N	-0.497427499	-1.676685471	1.006179854
H	-0.151487248	-1.499146482	1.950783997
H	-1.516571654	-1.710818569	1.069324026
H	-0.251881339	2.104578735	0.029933540
H	-0.188356575	-2.618450607	0.753341677
O	0.956171630	0.894694873	-1.725807395
O	0.978951500	-1.957583278	-1.299566297
C	1.180475102	0.531818971	-2.961550882
C	1.158989405	-1.996586099	-2.593182560
O	1.770006441	1.268661093	-3.742967980
O	1.695018727	-2.958616436	-3.130260250
C	0.635957905	-0.818363578	-3.423404761
C	0.715818411	-1.087451841	-4.938382286
C	-0.927250745	-0.891891971	-3.547851034
C	-0.747184364	-1.571410536	-4.919645700
H	1.484020959	-1.805859450	-5.249924043
H	0.841985316	-0.140365284	-5.477968317
H	-1.459976549	-1.437840269	-2.756335600
H	-1.359385146	0.116416771	-3.632535340
H	-0.817310581	-2.666068682	-4.842153552
H	-1.403698225	-1.231125271	-5.732927074

./carboplatin-M062X-SMD-ApVDZ-ApVTZ_eGeom.xyz

25

Pt	-0.233773202	-0.365479471	-0.406305861
N	0.533926949	1.226578314	0.583422695
H	0.200422154	1.282972422	1.546733541
H	1.553523101	1.200406086	0.623378534

N	0.499873659	-1.638282804	0.988535816
H	1.520149405	-1.638059549	1.013664397
H	0.178690549	-1.411367546	1.930469995
H	0.274998015	2.101194843	0.124888383
H	0.203731562	-2.596172065	0.794728772
O	-1.030005170	0.905163948	-1.785279401
O	-1.056763299	-1.960461571	-1.374230846
C	-1.245240090	0.525975664	-3.006530757
C	-1.209718985	-1.982425585	-2.661177356
O	-1.875029712	1.234788754	-3.799823947
O	-1.750126830	-2.937782361	-3.228745978
C	-0.657691890	-0.803473281	-3.467659073
C	0.909094500	-0.875971332	-3.485337553
C	-0.632205749	-1.064669335	-4.985087726
C	0.804900015	-1.612433051	-4.839299110
H	1.383391167	-1.392836890	-2.645216848
H	1.330224240	0.129811301	-3.590895096
H	-1.403918129	-1.727832517	-5.384035382
H	-0.639566573	-0.112443590	-5.523112510
H	0.810007872	-2.698486300	-4.697678602
H	1.528413453	-1.339066854	-5.612535099

./carboplatin-PBE0-H2O-TZ-pVTZ-pp_eGeom.xyz

25

Pt	0.195992373	-0.366338319	-0.399291804
N	-0.532052918	1.290122887	0.535336321
H	-1.545198042	1.304503576	0.594930867
H	-0.173751169	1.414895776	1.476961869
N	-0.507084462	-1.668989100	1.001183184
H	-0.146524044	-1.492296428	1.933419988
H	-1.519946256	-1.679780671	1.067713590
H	-0.252006549	2.106125153	-0.002298491
H	-0.213757189	-2.606308070	0.738935113
O	0.969664348	0.883314045	-1.749975746
O	0.976803460	-1.960764246	-1.311091758
C	1.208455492	0.508415314	-2.971342735
C	1.171492762	-2.001933435	-2.594951562
O	1.828920561	1.220202362	-3.746561444
O	1.725881788	-2.953206396	-3.123879160
C	0.643659558	-0.831474044	-3.426765949
C	0.689381709	-1.101028326	-4.938972170
C	-0.919059986	-0.889093599	-3.516601360
C	-0.777486376	-1.563814842	-4.892249097
H	1.434455790	-1.821887213	-5.268619453
H	0.814558856	-0.164869022	-5.480406159
H	-1.431131472	-1.431611125	-2.722697392
H	-1.342555970	0.113805295	-3.585331225
H	-0.863614321	-2.648428019	-4.820935696
H	-1.437790935	-1.209914322	-5.683638742

./carboplatin-M06L-SMD_eGeom.xyz

25

Pt	0.257925275	-0.366761069	-0.417635898
N	-0.499131442	1.272187193	0.581923227

H	-1.521767803	1.304394129	0.592960920
H	-0.204652786	1.317672418	1.561086976
N	-0.523436693	-1.654231707	0.995600752
H	-0.413512174	-1.328443387	1.959385823
H	-1.524436076	-1.824337273	0.868443035
H	-0.194081502	2.149432064	0.152107037
H	-0.073012830	-2.571862906	0.951768515
O	1.093044299	0.896963218	-1.792099371
O	1.072531945	-1.980851349	-1.377673051
C	1.253102046	0.518066791	-3.036195682
C	1.211901098	-1.995462961	-2.679444189
O	1.840279952	1.243809511	-3.845100385
O	1.743280436	-2.955577134	-3.245984483
C	0.657029130	-0.811785198	-3.469900512
C	0.614410035	-1.077816563	-4.980889630
C	-0.904516022	-0.880252417	-3.478705906
C	-0.813060713	-1.614431608	-4.822852401
H	1.382424447	-1.746782580	-5.389988602
H	0.634794094	-0.127363690	-5.529081806
H	-1.384427299	-1.386524466	-2.628099749
H	-1.333801758	0.127418747	-3.577892778
H	-0.824688293	-2.704831333	-4.683838731
H	-1.548890357	-1.352981198	-5.595022124

./carboplatin-M062X-SMD-pVTZ-2_eGeom.xyz

25

Pt	-1.120283367	-0.010784593	0.050083011
N	-2.492463657	1.295795158	-0.683323423
H	-2.665523361	1.166054396	-1.684682892
H	-3.401601076	1.220027233	-0.216551076
N	-2.339321341	-1.592156403	-0.330605623
H	-3.312085747	-1.433498616	-0.051096167
H	-2.356860964	-1.838768022	-1.325004071
H	-2.178973689	2.263747895	-0.562225003
H	-2.019707510	-2.425908754	0.171967144
O	0.089390638	1.562066184	0.491803899
O	0.236306985	-1.306289170	0.838751491
C	1.386978180	1.434229329	0.511426526
C	1.519782372	-1.100409157	0.749439383
O	2.115354883	2.344210545	0.901490833
O	2.330585717	-1.891257295	1.227121539
C	1.992960768	0.138039659	-0.017854535
C	3.514369941	0.139298008	-0.250091308
C	1.814772699	-0.109488553	-1.555639509
C	3.283043749	-0.586024014	-1.592697984
H	4.124914138	-0.360958042	0.510137939
H	3.863927743	1.167032213	-0.402572576
H	1.026598496	-0.812905623	-1.855998426
H	1.675492704	0.847008348	-2.078648642
H	3.346742072	-1.676088399	-1.475661541
H	3.890662628	-0.273073325	-2.450415990

./carboplatin-M062X-H2O-TZ-pVTZ-2_eGeom.xyz

25

Pt	0.203555230	-0.363585545	-0.396976407
N	-0.535978811	1.297839844	0.549215216
H	-1.549595279	1.304366726	0.614787304
H	-0.173017492	1.422625134	1.489889127
N	-0.501887021	-1.679675669	1.010244804
H	-0.112403990	-1.525355920	1.935666654
H	-1.513309749	-1.665591210	1.103876102
H	-0.264639624	2.117922471	0.011559618
H	-0.238708794	-2.620434876	0.725710273
O	0.980916589	0.900076500	-1.771761811
O	0.990305658	-1.971042341	-1.338161568
C	1.239162588	0.511288629	-2.982578124
C	1.160917506	-2.014164225	-2.623400043
O	1.889604566	1.194653070	-3.758276854
O	1.668601177	-2.977095941	-3.176736837
C	0.650522046	-0.821020320	-3.440924294
C	0.671152737	-1.084414620	-4.954925584
C	-0.913001309	-0.868901511	-3.508165140
C	-0.783814709	-1.587868440	-4.866457830
H	1.426716702	-1.777560015	-5.311540243
H	0.742662052	-0.141733204	-5.491139531
H	-1.423106901	-1.383305377	-2.696577222
H	-1.321815947	0.135780411	-3.609207726
H	-0.826985537	-2.668621001	-4.746938052
H	-1.468544676	-1.284535340	-5.654310842

./carboplatin-ApVDZ-ApVDZ-pp_eGeom.xyz

25

Pt	-0.101589509	-0.342118478	-0.327651574
N	0.576667194	1.476889776	0.411576944
H	0.147658560	1.783264007	1.293084646
H	1.595024735	1.570103005	0.503980133
N	0.399986355	-1.702202757	1.159152204
H	1.406469825	-1.862582766	1.284191741
H	-0.012359538	-1.527652709	2.083434659
H	0.265087286	2.126179481	-0.332095434
H	-0.014918057	-2.574903501	0.787869346
O	-0.706855884	0.878219859	-1.783677270
O	-0.881295276	-2.005437986	-1.099374787
C	-1.004250362	0.421368891	-3.009586270
C	-1.168195732	-2.106171819	-2.407084088
O	-1.508172453	1.179774607	-3.835366246
O	-1.787521755	-3.083741875	-2.821080456
C	-0.614017366	-1.029851898	-3.352722148
C	0.954993596	-1.129736318	-3.563575560
C	-0.783253214	-1.331636140	-4.868242721
C	0.721671865	-1.017917697	-5.093915448
H	1.325418116	-2.125385224	-3.259699369
H	1.564563214	-0.355090083	-3.064976614
H	-1.034734814	-2.395398150	-5.012111041
H	-1.514877519	-0.692528699	-5.387588545
H	1.292410493	-1.715775072	-5.732037480
H	0.879397249	0.011978777	-5.459633632

./carboplatin-M06L-H20_eGeom.xyz

25

Pt	0.217262602	-0.368125762	-0.406093490
N	-0.542270609	1.311981450	0.557924437
H	-1.562156594	1.341543275	0.616707865
H	-0.200102135	1.444535928	1.512026872
N	-0.492314804	-1.717107526	1.015007406
H	-0.125628853	-1.569695652	1.957600500
H	-1.510059181	-1.738315619	1.107338047
H	-0.265840490	2.149371335	0.039246935
H	-0.213010066	-2.663955613	0.746079195
O	1.003750906	0.918685466	-1.769067533
O	1.027150667	-1.978136600	-1.345652087
C	1.219313889	0.536056334	-3.006464360
C	1.191214898	-1.998197069	-2.647440615
O	1.818966964	1.260016194	-3.797703350
O	1.721042682	-2.956742096	-3.203947966
C	0.650021191	-0.808432640	-3.448160030
C	0.657865684	-1.071091497	-4.960131651
C	-0.909956534	-0.884577497	-3.502824475
C	-0.780390007	-1.595023569	-4.857834295
H	1.430973662	-1.755930273	-5.330868319
H	0.719675178	-0.119938723	-5.504126199
H	-1.412598460	-1.407749546	-2.675625401
H	-1.348376527	0.120596927	-3.593650704
H	-0.807734082	-2.687780154	-4.741269859
H	-1.489492970	-1.312339844	-5.648199935

./carboplatin-M06L-CPCM-ApVTZ-ApVDZ_eGeom.xyz

25

Pt	0.205056740	-0.364061197	-0.410843482
N	-0.540812053	1.313334044	0.548813712
H	-1.552653992	1.337140752	0.586490216
H	-0.207246543	1.421210070	1.499265641
N	-0.492298494	-1.696913373	1.016729761
H	-0.131312323	-1.520482387	1.946555204
H	-1.502361596	-1.715216787	1.090490194
H	-0.245213344	2.137836921	0.037353908
H	-0.197414149	-2.632266827	0.757845929
O	0.983617800	0.907861363	-1.784305474
O	1.004349162	-1.973135304	-1.348278339
C	1.223457432	0.518705322	-3.002138144
C	1.188769035	-1.998077481	-2.635231264
O	1.850799900	1.225644560	-3.784197896
O	1.739985945	-2.947655951	-3.180648810
C	0.649943605	-0.819164361	-3.448345056
C	0.651186542	-1.083276104	-4.958313191
C	-0.910337175	-0.884423104	-3.499897638
C	-0.788953428	-1.597366207	-4.851743957
H	1.411290748	-1.765656161	-5.330589241
H	0.713681962	-0.141511126	-5.498942599
H	-1.406815566	-1.399506276	-2.678568312
H	-1.335889809	0.114745534	-3.590043385
H	-0.824637802	-2.679388145	-4.735392395

H -1.488885586 -1.308730544 -5.633194393
./carboplatin-M062X-H2O-TZ-aug-pVTZ-2_eGeom.xyz
25

Pt 0.202045054 -0.361570921 -0.397186384
N -0.544555154 1.294223805 0.551208387
H -1.558378380 1.295863222 0.615508598
H -0.183597539 1.417973118 1.492889437
N -0.491302806 -1.679638428 1.012642319
H -0.100350776 -1.521162410 1.936842582
H -1.502615625 -1.670833092 1.109046117
H -0.276304437 2.117167233 0.016216345
H -0.223655676 -2.619569854 0.729284281
O 0.968081185 0.906126966 -1.774454419
O 0.995315557 -1.964539918 -1.339580327
C 1.230793058 0.517570944 -2.983929014
C 1.166492701 -2.007087072 -2.624329366
O 1.880554606 1.202734882 -3.759123764
O 1.680559070 -2.966932669 -3.177754624
C 0.648787661 -0.817553864 -3.442862497
C 0.670464939 -1.081611022 -4.956820306
C -0.914395334 -0.874246005 -3.509873993
C -0.781094095 -1.594599290 -4.866989495
H 1.430558845 -1.769652612 -5.313658516
H 0.735080637 -0.138564358 -5.493302869
H -1.421814102 -1.389896584 -2.697431107
H -1.328395475 0.128103963 -3.612952496
H -0.816782386 -2.675409582 -4.745465009
H -1.468184519 -1.297249221 -5.655052891
./carboplatin-M06L-SMD-ApVDZ-ApVDZ_eGeom.xyz
25

Pt -0.248222461 -0.379066863 -0.422819751
N 0.481726197 1.272886299 0.558529606
H 0.333776961 1.239362118 1.566932987
H 1.483538637 1.399568382 0.417899170
N 0.591173449 -1.636274006 0.972432257
H 1.583174989 -1.797695887 0.800396946
H 0.517335360 -1.290839336 1.929075526
H 0.033448101 2.126582485 0.226514245
H 0.141590787 -2.551207636 0.957991422
O -1.144637060 0.861249216 -1.782389575
O -1.042890621 -2.013207950 -1.370753656
C -1.314094802 0.473251208 -3.016097185
C -1.210263247 -2.020212017 -2.663923963
O -1.955234122 1.171007946 -3.816581805
O -1.762225977 -2.976991108 -3.226725170
C -0.674589420 -0.832402881 -3.460658382
C 0.889175165 -0.855855853 -3.458029254
C -0.614994271 -1.091241620 -4.973342591
C 0.830492258 -1.579380652 -4.810617484
H 1.371435440 -1.360920851 -2.612409980
H 1.288110846 0.162553260 -3.541175301
H -1.355788198 -1.781961458 -5.389750222

```
H      -0.662595253      -0.141373136      -5.516535446
H      0.880124022       -2.667603893      -4.681285651
H      1.557740231       -1.280578536      -5.573805753
./carboplatin-M06L-H2O-ApVTZ-ApVDZ_eGeom.xyz
25
```

```
Pt      0.202572671      -0.365302467      -0.410133021
N      -0.541786473       1.313057637       0.549230473
H      -1.553518202       1.337192075       0.589178248
H      -0.205710060       1.423017201       1.498545068
N      -0.496930390      -1.698474892       1.016344265
H      -0.137259604      -1.522332142       1.946736037
H      -1.507105169      -1.716585885       1.088796723
H      -0.247127309       2.136222608       0.035092757
H      -0.202032195      -2.633963653       0.757833145
O      0.982490698       0.907246809      -1.781931956
O      1.001155982      -1.974468772      -1.347348559
C      1.223761837       0.518980997      -2.999865464
C      1.187850418      -1.998612737      -2.634103146
O      1.850941282       1.227089641      -3.780844580
O      1.739013715      -2.948340664      -3.179110332
C      0.651255878      -0.818842978      -3.447552883
C      0.655142500      -1.082472710      -4.957603788
C      -0.908931945      -0.883477218      -3.502040336
C      -0.785265698      -1.596385159      -4.853664801
H      1.415805408      -1.764897269      -5.328604506
H      0.718838058      -0.140535499      -5.497770928
H      -1.407243730      -1.398148365      -2.681529198
H      -1.333716195       0.115952477      -3.593227683
H      -0.821011766      -2.678381751      -4.737202287
H      -1.483882699      -1.307890055      -5.636352259
./carboplatin-ApVTZ-ApVDZ-pp_eGeom.xyz
25
```

```
Pt      -0.101555510      -0.359429516      -0.325745277
N      0.482421018       1.426665033       0.559356209
H      0.058345972       1.626150604       1.468827289
H      1.493541831       1.558453186       0.641098193
N      0.471488098      -1.801953002       1.055918491
H      1.479349497      -1.897795359       1.201921726
H      0.020688060      -1.728736888       1.971576844
H      0.124180458       2.116731864      -0.118192780
H      0.129912216      -2.662406862       0.601437649
O      -0.781455500       0.929473110      -1.677321688
O      -0.778101295      -1.994734308      -1.233401977
C      -1.079140645       0.555737597      -2.926994870
C      -1.062077348      -2.018787092      -2.539485084
O      -1.641094269       1.338140058      -3.679471313
O      -1.606448274      -2.999489562      -3.025728928
C      -0.602178612      -0.824548721      -3.395320235
C      0.962980114      -0.901663837      -3.618748909
C      -0.774837305      -1.103014678      -4.910956511
C      0.698870427      -1.575826512      -4.986319716
H      1.536760649      -1.454196131      -2.863354823
```

H	1.388331565	0.105888742	-3.720231521
H	-1.549043222	-1.835009438	-5.162148568
H	-0.954682058	-0.162602163	-5.444157574
H	0.782778036	-2.668363388	-4.926066196
H	1.298273107	-1.219035506	-5.833619443

./carboplatin-SMD-TZ-pVDZ-pp_eGeom.xyz
25

Pt	-0.228573447	-0.351361432	-0.394189589
N	0.549067884	1.268908356	0.582391034
H	0.198951209	1.350042833	1.542807531
H	1.572223542	1.231225017	0.634753850
N	0.490124375	-1.627159615	1.033735437
H	1.514183468	-1.623179869	1.079146802
H	0.142613244	-1.396514262	1.970316863
H	0.301394129	2.134892046	0.092312423
H	0.196588416	-2.588093968	0.827956980
O	-1.011910723	0.910537928	-1.774956604
O	-1.050851540	-1.952262436	-1.328922110
C	-1.217036825	0.522253279	-3.015261991
C	-1.210192255	-1.987286031	-2.633483798
O	-1.825839785	1.257146576	-3.810774446
O	-1.774571426	-2.954712966	-3.170262132
C	-0.651893699	-0.823741586	-3.462759871
C	0.926035831	-0.904573569	-3.521984395
C	-0.661940977	-1.101804402	-4.986281192
C	0.794606786	-1.616516311	-4.889892860
H	1.417208828	-1.434565066	-2.697433765
H	1.355800343	0.101369838	-3.613265028
H	-1.429755836	-1.794046489	-5.349237330
H	-0.726307619	-0.157564521	-5.539366943
H	0.838123508	-2.708079359	-4.783204698
H	1.489259580	-1.305266759	-5.679273178

./carboplatin-M06L-aug-pVDZ_eGeom.xyz
25

Pt	0.127753728	-0.365492068	-0.357369613
N	-0.529719938	1.435429399	0.519622969
H	-1.538690119	1.576035157	0.577388306
H	-0.140644005	1.678523233	1.431202018
N	-0.451128688	-1.866444239	1.006540346
H	-0.036319995	-1.824096072	1.938085342
H	-1.451944791	-2.020166393	1.132036003
H	-0.169846038	2.123279158	-0.153397788
H	-0.073568979	-2.705606791	0.549823124
O	0.814918269	0.957237273	-1.687895034
O	0.875087988	-1.984108770	-1.264451890
C	1.088430548	0.588464092	-2.937103288
C	1.116232465	-1.987267687	-2.571589090
O	1.618402188	1.369326017	-3.704251869
O	1.648330956	-2.948638127	-3.093956504
C	0.616115520	-0.790650746	-3.388729708
C	0.727776142	-1.059216509	-4.896644073
C	-0.936776458	-0.898445482	-3.547495529

C	-0.704238548	-1.611077151	-4.886480235
H	1.533351038	-1.737736077	-5.200298939
H	0.816634722	-0.108259085	-5.435922541
H	-1.487855325	-1.423468386	-2.751234314
H	-1.381870558	0.100127801	-3.675830995
H	-0.715385662	-2.703612124	-4.767907192
H	-1.367737451	-1.344489194	-5.721268515

./carboplatin-PBE0-H20-TZ-aug-pVTZ-pp_eGeom.xyz

25

Pt	0.196046818	-0.367233814	-0.399620144
N	-0.521450567	1.291962284	0.537007751
H	-1.534648629	1.312201898	0.595690494
H	-0.163592221	1.412119662	1.479499427
N	-0.511479895	-1.665294280	1.001983543
H	-0.149677750	-1.488891749	1.933890364
H	-1.524428209	-1.671079850	1.069177704
H	-0.236019939	2.107923816	0.001941737
H	-0.222570127	-2.604387368	0.740858186
O	0.974176712	0.878590188	-1.750597945
O	0.965993557	-1.965818268	-1.311923965
C	1.214246199	0.502079546	-2.970706697
C	1.163604258	-2.007109239	-2.594838677
O	1.841668091	1.209567614	-3.744834190
O	1.715630187	-2.960239109	-3.123652638
C	0.642374106	-0.834279455	-3.427819827
C	0.687634741	-1.104550740	-4.940028028
C	-0.920508232	-0.883725541	-3.519001783
C	-0.780934247	-1.561916585	-4.893079339
H	1.430324967	-1.827903990	-5.269527875
H	0.815801709	-0.168839220	-5.481572018
H	-1.436494186	-1.421398633	-2.724372518
H	-1.337995686	0.121478505	-3.590809765
H	-0.870726816	-2.646075732	-4.819243437
H	-1.439667831	-1.207532710	-5.685549368

./carboplatin-M06L-TZ-aug-pVTZ-2_eGeom.xyz

25

Pt	0.099879481	-0.369694495	-0.356997919
N	-0.483242404	1.452747160	0.515852053
H	-1.479842641	1.615047644	0.582095033
H	-0.075431716	1.664954479	1.417499177
N	-0.526710522	-1.853266077	0.997853343
H	-0.114344653	-1.813997833	1.921299607
H	-1.526503360	-1.960559208	1.111114183
H	-0.103681407	2.114148787	-0.161053661
H	-0.173278000	-2.690057279	0.534608601
O	0.826327077	0.923535061	-1.682557791
O	0.784585335	-2.007543507	-1.258333236
C	1.130978811	0.546835796	-2.914502612
C	1.064787992	-2.023087635	-2.550634570
O	1.710982037	1.302533063	-3.661058199
O	1.576535471	-2.997083351	-3.055713698
C	0.626426168	-0.813519687	-3.378358705

C	0.756741433	-1.081626002	-4.882478337
C	-0.925832098	-0.868477956	-3.564855962
C	-0.694067276	-1.577949323	-4.903753599
H	1.532567971	-1.785451210	-5.168823912
H	0.893905229	-0.142914909	-5.413335613
H	-1.497128543	-1.381051152	-2.789856292
H	-1.334537743	0.134633761	-3.687115962
H	-0.749214369	-2.659875556	-4.797762899
H	-1.322595264	-1.278633339	-5.740258038

./carboplatin-M062X-CPCM-TZ-pVDZ_eGeom.xyz

25

Pt	0.206714826	-0.362384321	-0.398200355
N	-0.549832506	1.290028502	0.552896671
H	-1.564084734	1.291361514	0.606784546
H	-0.198508676	1.411176165	1.498269347
N	-0.481995249	-1.688047461	1.009877831
H	-0.114039274	-1.516175366	1.940800448
H	-1.494839352	-1.703570658	1.085021921
H	-0.276240424	2.113989851	0.022540208
H	-0.186264081	-2.622468302	0.736859431
O	0.968120269	0.911321246	-1.774988806
O	1.009431624	-1.961373527	-1.344714788
C	1.223426669	0.526689094	-2.987420435
C	1.176679402	-1.999280666	-2.630213523
O	1.860865725	1.218850219	-3.766325565
O	1.695902241	-2.954452740	-3.186735753
C	0.648491018	-0.811637808	-3.443955606
C	0.663284215	-1.073716707	-4.957910890
C	-0.914634597	-0.877373338	-3.502702406
C	-0.783366355	-1.598626129	-4.859517988
H	1.426834029	-1.754957749	-5.320648941
H	0.716557931	-0.129737145	-5.494241691
H	-1.414959006	-1.393755884	-2.686245141
H	-1.334033732	0.122797659	-3.606113180
H	-0.808470850	-2.679672242	-4.735910060
H	-1.477732103	-1.309336975	-5.644334286

./carboplatin-M06L-TZ-aug-pVTZ_eGeom.xyz

25

Pt	-0.000342916	-0.321895795	-0.112353067
N	0.001185299	1.533506802	0.884086205
H	-0.816058403	1.741848674	1.443399402
H	0.818550546	1.740286545	1.443801020
N	-0.001955538	-1.764486926	1.421873109
H	0.815083398	-1.782760183	2.018823964
H	-0.819378682	-1.781435707	2.018337675
H	0.001990021	2.165570859	0.083018593
H	-0.002486122	-2.620102221	0.866313946
O	0.001220761	0.934645977	-1.636503706
O	-0.001664992	-1.995738233	-1.163515374
C	0.001340858	0.598493404	-2.910886369
C	-0.000919001	-2.083088657	-2.478709381
O	0.002401060	1.479803335	-3.747453583

O	-0.001312318	-3.185902618	-2.989208347
C	0.000205890	-0.854717476	-3.388069717
C	1.071107119	-1.071862607	-4.513945205
C	-1.070963786	-1.070114323	-4.514052107
C	-0.000316820	-1.608886841	-5.463394333
H	1.884703802	-1.745051991	-4.252852413
H	1.465965010	-0.109731697	-4.828643966
H	-1.885702634	-1.741959842	-4.253051101
H	-1.464224215	-0.107336441	-4.828772131
H	-0.001176908	-2.693307941	-5.510481384
H	0.000055583	-1.206128866	-6.474890741

./carboplatin-TZ-pVDZ-pp_eGeom.xyz

25

Pt	-0.106952483	-0.358051630	-0.322872115
N	0.486905807	1.432179459	0.555856315
H	0.060359118	1.642551430	1.461383343
H	1.497853076	1.562286038	0.637794977
N	0.471279287	-1.809567017	1.052904510
H	1.478778119	-1.908443609	1.196878637
H	0.019846904	-1.746818512	1.968685868
H	0.131535602	2.114145161	-0.131168427
H	0.128470634	-2.663130697	0.586854492
O	-0.789824786	0.933411354	-1.671756216
O	-0.791579680	-1.992251491	-1.228720007
C	-1.073748446	0.561903985	-2.926137992
C	-1.062696303	-2.017313525	-2.538222076
O	-1.620390214	1.348552213	-3.683726125
O	-1.596431653	-3.000663182	-3.028589314
C	-0.601219527	-0.821181764	-3.390186043
C	0.963006189	-0.904225061	-3.616143803
C	-0.777123018	-1.099441053	-4.905266298
C	0.693980905	-1.579631903	-4.982385552
H	1.536014219	-1.457048218	-2.860493664
H	1.392171585	0.101395639	-3.720125256
H	-1.554374259	-1.829175752	-5.153380662
H	-0.954239052	-0.158227100	-5.437782307
H	0.771079626	-2.672406486	-4.919084497
H	1.294605361	-1.229201050	-5.831446796

./carboplatin-PBE0-SMD-TZ-aug-pVTZ-pp_eGeom.xyz

25

Pt	-0.226153246	-0.355799865	-0.408372434
N	0.535844668	1.246889214	0.567678172
H	0.187396079	1.321888879	1.520038253
H	1.550413086	1.213396328	0.623147512
N	0.485344032	-1.616576837	1.007582144
H	1.500151079	-1.600625319	1.064147052
H	0.130330386	-1.395653577	1.934324321
H	0.290120139	2.109249711	0.088403987
H	0.209869319	-2.573255750	0.800467882
O	-0.994798805	0.889782995	-1.779498327
O	-1.028789688	-1.938651067	-1.343385371
C	-1.210892334	0.512913795	-2.999991612

C	-1.188045071	-1.981591180	-2.627518943
O	-1.824646241	1.231942633	-3.785613724
O	-1.733091118	-2.942739296	-3.165027334
C	-0.645981610	-0.821040523	-3.454654589
C	0.918026103	-0.894590414	-3.516987448
C	-0.659392431	-1.095064327	-4.966856746
C	0.785520544	-1.612177020	-4.870230278
H	1.415450890	-1.413037145	-2.698368572
H	1.340389269	0.105762399	-3.618782940
H	-1.425417778	-1.776120209	-5.332311951
H	-0.714102111	-0.155304732	-5.514104650
H	0.823074840	-2.695777368	-4.753467233
H	1.476687009	-1.314174095	-5.657746179

./carboplatin-PBE0-H2O-pVTZ-pp-2_eGeom.xyz

25

Pt	-1.001980728	-0.013618567	-0.205569492
N	-2.251643669	1.405616970	0.546973811
H	-3.204440831	1.362613335	0.178824012
H	-2.329665488	1.388937846	1.565997421
N	-2.122778833	-1.588195584	0.435980643
H	-2.201355539	-1.654291867	1.453052843
H	-3.075741526	-1.599241784	0.066409878
H	-1.882009098	2.326661393	0.296720525
H	-1.675288587	-2.452701749	0.119777496
O	0.078641633	1.503889447	-0.917302215
O	0.212893110	-1.378094746	-1.005745964
C	1.365436762	1.393848031	-1.131855507
C	1.492715409	-1.161792431	-1.171332200
O	1.993802593	2.284949493	-1.687970493
O	2.208664467	-1.990462077	-1.718303836
C	2.073591991	0.143380338	-0.614556449
C	2.199322219	0.057854535	0.947656127
C	3.612124372	0.173819237	-0.684161553
C	3.678292642	-0.337902241	0.768025355
H	1.525498159	-0.644365841	1.458917781
H	2.083065610	1.052140614	1.404160163
H	4.060598837	-0.453873409	-1.464080355
H	3.958776791	1.210009466	-0.785806025
H	3.814698899	-1.428070971	0.813890706
H	4.405822806	0.138316563	1.440614330

./carboplatin-M062X-SMD-TZ-pVDZ_eGeom.xyz

25

Pt	-0.228863687	-0.359144602	-0.403233816
N	0.531830945	1.247116253	0.586139083
H	0.188319715	1.308699686	1.542205198
H	1.547756224	1.218393726	0.635151795
N	0.511060441	-1.625919438	1.005456079
H	1.527620674	-1.607593158	1.042611713
H	0.172772525	-1.403850238	1.939147519
H	0.277281435	2.113583445	0.116803018
H	0.232519145	-2.584090422	0.803905022
O	-1.028115314	0.897480120	-1.796039840

O	-1.037537251	-1.962388986	-1.372904797
C	-1.250283326	0.513213664	-3.010697425
C	-1.185334216	-1.997429692	-2.656367992
O	-1.881684705	1.211606313	-3.800737235
O	-1.694694530	-2.964281561	-3.217966842
C	-0.661236889	-0.812943160	-3.467261873
C	0.903574540	-0.870850119	-3.503329350
C	-0.647110897	-1.079894586	-4.980623527
C	0.789884175	-1.620730999	-4.844938121
H	1.394052458	-1.366971506	-2.668648014
H	1.311317821	0.131673045	-3.626191183
H	-1.413581248	-1.743383904	-5.370337148
H	-0.662167028	-0.136957269	-5.521466857
H	0.799071936	-2.698840586	-4.694454975
H	1.500854068	-1.356848797	-5.623349443

./carboplatin-M06L-H2O-ApVTZ-pVTZ_eGeom.xyz

25

Pt	0.207166002	-0.366782115	-0.410493463
N	-0.545121781	1.304749686	0.553611943
H	-1.556853649	1.321549756	0.597082214
H	-0.207071271	1.415297926	1.502215395
N	-0.479029118	-1.706722352	1.015524536
H	-0.117553269	-1.530531093	1.945231868
H	-1.488829876	-1.730946014	1.091356338
H	-0.258160221	2.131265903	0.040376493
H	-0.179433156	-2.639857714	0.753858414
O	0.973636906	0.912371118	-1.782217273
O	1.011576884	-1.969080854	-1.352505453
C	1.214293726	0.527368209	-3.001218479
C	1.193040629	-1.991035082	-2.639917554
O	1.836211306	1.239611938	-3.782782346
O	1.746142063	-2.937554212	-3.188699440
C	0.647450277	-0.812696458	-3.449544046
C	0.647542209	-1.073479009	-4.960084143
C	-0.912574803	-0.885996890	-3.498814351
C	-0.789632264	-1.595563380	-4.852244625
H	1.410688984	-1.750886155	-5.335158092
H	0.704084435	-0.130146377	-5.498640348
H	-1.405204992	-1.405223474	-2.677765855
H	-1.343422460	0.111145771	-3.586437094
H	-0.819136514	-2.677980811	-4.737934473
H	-1.492503036	-1.309231087	-5.631929174

./carboplatin-SMD-ApVTZ-pVDZ-pp_eGeom.xyz

25

Pt	-0.221132805	-0.360908037	-0.396532837
N	0.528193146	1.265443763	0.585937320
H	0.187759508	1.328530486	1.551333990
H	1.552605283	1.251320354	0.627451165
N	0.512634573	-1.624985232	1.029800729
H	1.537071986	-1.615043229	1.068569861
H	0.171327373	-1.391639506	1.968125344
H	0.255606218	2.132013150	0.109871198

H	0.223617613	-2.589445353	0.833164174
O	-1.024529428	0.891704684	-1.772675355
O	-1.020930111	-1.970290021	-1.333280679
C	-1.241028548	0.502090882	-3.007951539
C	-1.198807199	-2.001374838	-2.633160632
O	-1.877618832	1.226762684	-3.795281305
O	-1.770746219	-2.969192793	-3.167047533
C	-0.655980590	-0.832340587	-3.465891745
C	0.923347452	-0.886866401	-3.522785366
C	-0.659685934	-1.105910686	-4.990506772
C	0.806080149	-1.594073491	-4.894097587
H	1.421104351	-1.412905433	-2.699650092
H	1.335745209	0.126843383	-3.608029542
H	-1.414542580	-1.809516531	-5.358707866
H	-0.738994759	-0.161351305	-5.541247244
H	0.871147993	-2.685234846	-4.793714959
H	1.495063161	-1.263983867	-5.680821738

./carboplatin-M062X-SMD-TZ-aug-pVTZ_eGeom.xyz

25

Pt	-0.224322067	-0.358405196	-0.402408181
N	0.537855937	1.239951764	0.593344013
H	0.194013626	1.297921692	1.549725804
H	1.553775351	1.207443860	0.643883605
N	0.492235418	-1.629336397	1.010588968
H	1.509061940	-1.625096423	1.050228925
H	0.155920388	-1.399008861	1.943173886
H	0.287384129	2.110733206	0.129444038
H	0.200838196	-2.584776926	0.813205929
O	-1.002227928	0.903880814	-1.797324709
O	-1.034116825	-1.954445046	-1.374976399
C	-1.235715596	0.520959274	-3.010137307
C	-1.185053258	-1.989382934	-2.657978624
O	-1.869316972	1.222116283	-3.796212877
O	-1.700995934	-2.953415705	-3.218634005
C	-0.655908967	-0.808021907	-3.470441332
C	0.908385159	-0.874430422	-3.511462810
C	-0.647846691	-1.074444458	-4.984022677
C	0.786114406	-1.624356289	-4.852230417
H	1.399799417	-1.372297031	-2.678365747
H	1.320470806	0.126023643	-3.636957587
H	-1.419640078	-1.732994888	-5.371549142
H	-0.658548815	-0.131093148	-5.524267574
H	0.788575972	-2.702404663	-4.700988292
H	1.496569397	-1.365473010	-5.632766497

./carboplatin-M06L-H2O-TZ-pVDZ_eGeom.xyz

25

Pt	0.198683091	-0.373946489	-0.406976754
N	-0.554390950	1.305005259	0.550389107
H	-1.566109041	1.326090090	0.592279977
H	-0.216453824	1.419021540	1.498600253
N	-0.515690645	-1.718219668	1.005678308
H	-0.159123116	-1.553516468	1.939389817

H	-1.526233333	-1.734599361	1.073398061
H	-0.263192342	2.126778033	0.032056910
H	-0.221817292	-2.651057948	0.736611927
O	0.991523541	0.905792375	-1.765457317
O	1.003407959	-1.981887390	-1.343296340
C	1.230999867	0.522381618	-2.987318785
C	1.188287772	-2.001122022	-2.632248209
O	1.855132957	1.234117352	-3.764712509
O	1.730269851	-2.951982947	-3.181165085
C	0.658584117	-0.813980951	-3.439249779
C	0.671710611	-1.070084158	-4.950479885
C	-0.901461985	-0.875424287	-3.502744267
C	-0.773126672	-1.574311310	-4.861524045
H	1.429401113	-1.758562529	-5.316116200
H	0.750886447	-0.127021590	-5.486445728
H	-1.404303015	-1.398702111	-2.690418949
H	-1.326740528	0.124680328	-3.583207764
H	-0.818478514	-2.657267455	-4.758609393
H	-1.464459056	-1.272532682	-5.645562364

./carboplatin-TZ-aug-pVTZ-pp_eGeom.xyz

25

Pt	-0.105965989	-0.357046704	-0.324369351
N	0.492455519	1.425641284	0.557898895
H	0.065081744	1.634258968	1.463657851
H	1.504320613	1.546963014	0.644748156
N	0.453195084	-1.805378490	1.056845827
H	1.459344201	-1.905626874	1.210592394
H	-0.004833576	-1.733382250	1.968913491
H	0.145185648	2.114976998	-0.126046822
H	0.111688539	-2.662519417	0.596255592
O	-0.771445550	0.936410134	-1.675380480
O	-0.792993955	-1.985709841	-1.231317581
C	-1.062450965	0.566653175	-2.928644439
C	-1.066992349	-2.010310341	-2.540125126
O	-1.609229647	1.354504208	-3.685060862
O	-1.610292027	-2.988861745	-3.029959100
C	-0.597010298	-0.818497901	-3.393670354
C	0.966797883	-0.910079130	-3.619276048
C	-0.773743535	-1.096590101	-4.908815328
C	0.694155171	-1.586953461	-4.983980020
H	1.537958183	-1.463994344	-2.862944289
H	1.400438978	0.093357862	-3.725985481
H	-1.556032160	-1.820747993	-5.157273833
H	-0.943467344	-0.154425297	-5.442033267
H	0.763469397	-2.680077910	-4.917618061
H	1.297673443	-1.242916615	-5.833540770

./carboplatin-M06L-TZ-pVDZ_eGeom.xyz

25

Pt	-0.111760964	-0.365896845	-0.356541611
N	0.514546073	1.447168980	0.517320835
H	0.111440033	1.671367137	1.418059211
H	1.514644356	1.586275832	0.581800567

N	0.466595364	-1.868155948	1.005870215
H	1.461454757	-2.002911830	1.131269548
H	0.042085916	-1.821227072	1.923418423
H	0.150551264	2.114992807	-0.161775220
H	0.096720950	-2.693256440	0.534566995
O	-0.799734801	0.943098443	-1.690135468
O	-0.832524025	-1.988451972	-1.262971043
C	-1.093037870	0.573517761	-2.927209619
C	-1.092301550	-1.999157257	-2.559543364
O	-1.637808255	1.345832128	-3.683273037
O	-1.616223144	-2.963529104	-3.070384528
C	-0.617913294	-0.800193404	-3.382622658
C	0.934470541	-0.890251802	-3.555018129
C	-0.740333056	-1.067748038	-4.887793470
C	0.700385597	-1.593995712	-4.896286505
H	1.486088898	-1.414057776	-2.773364159
H	1.366452500	0.103550630	-3.673820935
H	-1.527696650	-1.757013361	-5.178771570
H	-0.854045177	-0.127145876	-5.420970611
H	0.732691662	-2.677030432	-4.792322758
H	1.342557883	-1.306133619	-5.726630118

./carboplatin-M062X-H20-aug-pVTZ_eGeom.xyz

25

Pt	0.212887634	-0.363430080	-0.394927856
N	-0.542399585	1.276048409	0.565043033
H	-1.563696604	1.293692982	0.604049572
H	-0.209256153	1.388846895	1.524982278
N	-0.459844409	-1.693115777	1.007412896
H	-0.105544656	-1.517508957	1.949948883
H	-1.478781808	-1.734363432	1.079261406
H	-0.253642551	2.113991180	0.052743989
H	-0.145059067	-2.630829408	0.743506094
O	0.953865678	0.924922193	-1.754931645
O	1.015271602	-1.954357921	-1.336282052
C	1.185994961	0.555761407	-2.985209533
C	1.171691274	-1.987436499	-2.630734753
O	1.779077754	1.277043017	-3.775614369
O	1.683819776	-2.944844494	-3.195264605
C	0.634209894	-0.796975992	-3.441588093
C	0.672738051	-1.063294186	-4.957149520
C	-0.928834963	-0.887055481	-3.519659517
C	-0.767166309	-1.614385825	-4.872947042
H	1.459840654	-1.742000492	-5.303674767
H	0.719730779	-0.110222111	-5.496868621
H	-1.437644836	-1.408892949	-2.697758575
H	-1.364264872	0.115700293	-3.637761054
H	-0.770253413	-2.704401611	-4.738966351
H	-1.465431822	-1.343243932	-5.674738804

./carboplatin-M062X-SMD_eGeom.xyz

25

Pt	0.246135542	-0.359405971	-0.400323969
N	-0.525744712	1.247782087	0.589152886

H	-1.549163185	1.225426406	0.645605132
H	-0.184332515	1.326034442	1.553041413
N	-0.494126007	-1.641613317	1.001699268
H	-0.152974065	-1.441691493	1.947712568
H	-1.517857661	-1.629940979	1.053458312
H	-0.279957334	2.125529584	0.119511154
H	-0.222807299	-2.608027713	0.791565675
O	1.040555862	0.907533750	-1.780382218
O	1.060976166	-1.956915242	-1.366960092
C	1.228983397	0.536660359	-3.015810705
C	1.188480434	-1.990334702	-2.662546604
O	1.815187050	1.259660126	-3.818989301
O	1.682796579	-2.961400809	-3.232255170
C	0.651774206	-0.801550755	-3.465582178
C	0.647312682	-1.071941876	-4.980368903
C	-0.913538251	-0.878979593	-3.505076247
C	-0.785916603	-1.628810590	-4.848786342
H	1.429995453	-1.738338265	-5.360904885
H	0.660168446	-0.120665097	-5.525459999
H	-1.405067813	-1.385633667	-2.663504037
H	-1.338219836	0.126905440	-3.631027862
H	-0.779999708	-2.716204654	-4.694200891
H	-1.505353820	-1.374430242	-5.636696017

./carboplatin-M062X-H2O-ApVTZ-ApVDZ-pp-2_eGeom.xyz

25

Pt	-1.119730730	-0.012474995	0.039558246
N	-2.476275392	1.357761263	-0.647847319
H	-2.677132977	1.256447802	-1.638384315
H	-3.365246805	1.330912329	-0.156887320
N	-2.341595022	-1.621911269	-0.298232689
H	-3.220358589	-1.574085502	0.208956909
H	-2.568308030	-1.753367399	-1.279681525
H	-2.087832976	2.288560096	-0.513936756
H	-1.859718214	-2.461725901	0.014390315
O	0.094514378	1.552470545	0.459829655
O	0.230630227	-1.330243387	0.772018144
C	1.380256814	1.415353256	0.538812885
C	1.508182046	-1.121708116	0.729902259
O	2.100490276	2.293353363	0.993715228
O	2.308879898	-1.903094183	1.223552971
C	1.993111431	0.129981342	-0.012598799
C	3.512723789	0.142531106	-0.241025419
C	1.817869321	-0.078773403	-1.554679041
C	3.290895214	-0.530615975	-1.610450876
H	4.115158227	-0.383799570	0.492820107
H	3.860139248	1.167136727	-0.345752552
H	1.047764112	-0.779328459	-1.870129931
H	1.660137901	0.877698903	-2.051677344
H	3.374510793	-1.613605123	-1.542620597
H	3.886844058	-0.174686449	-2.446994237

./carboplatin-PBE0-CPCM-TZ-pVDZ-pp_eGeom.xyz

25

Pt	0.202555016	-0.364837015	-0.400662373
N	-0.535249280	1.289170455	0.533238021
H	-1.548305832	1.296983988	0.594434207
H	-0.175600868	1.418009287	1.473702399
N	-0.492987110	-1.671835429	1.001133741
H	-0.128710735	-1.496186243	1.932036177
H	-1.505462115	-1.685668016	1.071136775
H	-0.261311006	2.105187774	-0.007333432
H	-0.197467312	-2.606985873	0.734231642
O	0.970124517	0.889133525	-1.754858758
O	0.992126713	-1.957534360	-1.314520392
C	1.203237225	0.513543321	-2.976940163
C	1.180914024	-1.996046247	-2.599276419
O	1.816995074	1.227074120	-3.755938726
O	1.739775494	-2.943193548	-3.130985233
C	0.641355321	-0.828922693	-3.428195104
C	0.678608373	-1.098367213	-4.940584939
C	-0.921537155	-0.894351645	-3.507284453
C	-0.786181479	-1.566670360	-4.884828820
H	1.424271246	-1.816459115	-5.274966970
H	0.796925311	-0.161848909	-5.482958466
H	-1.424694089	-1.441153761	-2.710681863
H	-1.351152009	0.106236570	-3.570969034
H	-0.868177229	-2.651669451	-4.814576721
H	-1.452745085	-1.213961931	-5.671480106

./carboplatin-PBE0-SMD-ApVDZ-ApVDZ-pp_eGeom.xyz

25

Pt	-0.216859529	-0.360768770	-0.407860563
N	0.549534226	1.243658899	0.559487481
H	0.219343432	1.314960124	1.522619447
H	1.568999541	1.223107025	0.597556675
N	0.531541813	-1.610500804	0.997183372
H	1.550946207	-1.591974166	1.034601942
H	0.196320364	-1.389542588	1.935393438
H	0.287728331	2.111303002	0.090743291
H	0.257308271	-2.574315266	0.804246941
O	-1.024847317	0.883595826	-1.769211795
O	-1.027794683	-1.955457414	-1.332574656
C	-1.245412819	0.498768419	-2.990914775
C	-1.201653269	-1.991651969	-2.619546668
O	-1.882612781	1.213512287	-3.774199310
O	-1.763002702	-2.955098243	-3.153988844
C	-0.664593182	-0.829394809	-3.451631801
C	0.904071734	-0.886597173	-3.510735906
C	-0.675703436	-1.101938518	-4.968349865
C	0.782814421	-1.592984166	-4.875577877
H	1.403786000	-1.414041035	-2.690667895
H	1.318602071	0.124950387	-3.597992829
H	-1.434911189	-1.800905948	-5.333547835
H	-0.751225328	-0.157203588	-5.516931174
H	0.843538416	-2.683282094	-4.771172452
H	1.471388417	-1.268552187	-5.664057350

./carboplatin-M062X-H2O-ApVDZ-pVDZ_eGeom.xyz

25

Pt	0.206626290	-0.365686666	-0.402035072
N	-0.538539587	1.295148357	0.542981435
H	-1.557174060	1.320351482	0.572679432
H	-0.210569605	1.406031844	1.501861852
N	-0.511424803	-1.678234437	1.003249854
H	-0.135188048	-1.522001814	1.937617388
H	-1.527405660	-1.671092828	1.087020706
H	-0.237332217	2.124321074	0.029315444
H	-0.242588135	-2.624371956	0.729773999
O	1.001200524	0.904109962	-1.774432720
O	0.998795463	-1.985216930	-1.337667640
C	1.260055751	0.502865361	-2.984339959
C	1.177502747	-2.017008428	-2.625396302
O	1.930516519	1.177616018	-3.762476636
O	1.708053802	-2.975291019	-3.181558730
C	0.655007923	-0.825484363	-3.442675285
C	0.661825798	-1.087707728	-4.960019985
C	-0.911423784	-0.864812268	-3.492292901
C	-0.801578833	-1.575094279	-4.860960595
H	1.412657016	-1.794003071	-5.322239064
H	0.741823541	-0.138699042	-5.497631123
H	-1.414691090	-1.389442968	-2.673917649
H	-1.317521152	0.149239779	-3.580193847
H	-0.857988993	-2.662942026	-4.748659294
H	-1.493332396	-1.252946824	-5.645132319

./carboplatin-M06L-CPCM-ApVDZ-ApVDZ_eGeom.xyz

25

Pt	0.214062577	-0.364894236	-0.414014971
N	-0.555885372	1.305601168	0.538919628
H	-1.573747725	1.331386524	0.562142766
H	-0.241268289	1.419743787	1.501033738
N	-0.497623307	-1.699410651	1.005587439
H	-0.141325530	-1.533956721	1.945348115
H	-1.513321023	-1.718101347	1.079792437
H	-0.258264601	2.141474675	0.036815509
H	-0.208711082	-2.642690153	0.748269569
O	1.007932975	0.916874683	-1.781692942
O	1.037322368	-1.975874712	-1.344367001
C	1.240385447	0.519608003	-3.005632645
C	1.214997372	-1.992830447	-2.639512827
O	1.877312846	1.223849989	-3.793156095
O	1.781904388	-2.938063599	-3.191849989
C	0.656521352	-0.817650675	-3.447842185
C	0.643109877	-1.082255027	-4.960497205
C	-0.905336383	-0.886155470	-3.479400133
C	-0.801810226	-1.587951977	-4.842113808
H	1.401700826	-1.774534797	-5.340309777
H	0.707844938	-0.134866367	-5.506248793
H	-1.392688789	-1.415974673	-2.651551693
H	-1.337819450	0.119788123	-3.553499493
H	-0.844849301	-2.678735885	-4.734102935

H -1.513136879 -1.284732986 -5.619245720
./carboplatin-M06L-H2O-ApVDZ-pVDZ_eGeom.xyz
25

Pt 0.214619534 -0.364636790 -0.414760250
N -0.555366302 1.310765416 0.538176182
H -1.573185159 1.335466712 0.570429696
H -0.233895876 1.431330314 1.497364092
N -0.498638246 -1.700779934 1.008733418
H -0.125585088 -1.548076906 1.944286342
H -1.513271429 -1.706184405 1.100321025
H -0.264847899 2.146099049 0.030797689
H -0.228505860 -2.647077956 0.741797330
O 1.009842453 0.917305674 -1.784870914
O 1.036702857 -1.979134153 -1.345290975
C 1.242948412 0.517311049 -3.007770580
C 1.215066634 -1.995157308 -2.640392799
O 1.882037717 1.219296061 -3.795558819
O 1.781818791 -2.940483176 -3.192726785
C 0.657026525 -0.819612581 -3.448661174
C 0.642544602 -1.084330876 -4.961276214
C -0.904832474 -0.886418238 -3.478808445
C -0.803715243 -1.586178991 -4.842826946
H 1.399233553 -1.778836133 -5.340779258
H 0.710229368 -0.137299162 -5.507273997
H -1.391688674 -1.417490606 -2.651401716
H -1.336619775 0.119996739 -3.550516699
H -0.850107934 -2.677037717 -4.737108807
H -1.514503477 -1.279188849 -5.619010407
./carboplatin-H2O-ApVDZ-pVDZ-pp_eGeom.xyz
25

Pt 0.192800204 -0.348615603 -0.391309059
N -0.607293909 1.358335201 0.431567364
H -1.633508821 1.343296795 0.494038056
H -0.253794933 1.568895088 1.373726390
N -0.464383771 -1.584599258 1.113828602
H -0.121997776 -1.321386478 2.046981094
H -1.488736624 -1.644652032 1.177608876
H -0.357509858 2.159828768 -0.164608824
H -0.121746811 -2.538083600 0.930557103
O 0.913282421 0.852872206 -1.851864360
O 1.076459874 -1.990502885 -1.181272760
C 1.132627429 0.397136614 -3.072470120
C 1.313684011 -2.073430102 -2.478804314
O 1.675908683 1.118656621 -3.927916967
O 2.012851292 -2.995257536 -2.936970775
C 0.662575031 -1.033485899 -3.402414606
C 0.696767147 -1.358263063 -4.920874866
C -0.918350631 -1.106020922 -3.471949229
C -0.819464990 -1.035382681 -5.020556791
H 0.918931822 -2.427315728 -5.075165678
H 1.388329442 -0.743186054 -5.519803270
H -1.285166069 -2.082567134 -3.109417929

H -1.461288701 -0.304052983 -2.943160645
H -1.445358508 -1.747112531 -5.586826366
H -1.008308945 -0.015459576 -5.400049935
./carboplatin-PBE0-SMD-ApVTZ-ApVDZ-pp_eGeom.xyz
25

Pt -0.211411176 -0.369412342 -0.405936599
N 0.525209021 1.244530551 0.569904108
H 0.190665860 1.303026511 1.528421914
H 1.541120646 1.236652445 0.608446767
N 0.545821260 -1.617636636 0.996508820
H 1.560966544 -1.582658190 1.036949443
H 0.201273568 -1.404224261 1.929042486
H 0.249614164 2.104344419 0.102340857
H 0.284685111 -2.579182321 0.793316960
O -1.027468263 0.864069949 -1.763877070
O -0.991855649 -1.966294426 -1.340528412
C -1.251587980 0.487466006 -2.981327076
C -1.173237547 -2.003754510 -2.620425110
O -1.894685493 1.196013015 -3.755600719
O -1.717068060 -2.969732620 -3.154002216
C -0.661745850 -0.831039991 -3.450557815
C 0.903263992 -0.869101708 -3.523646389
C -0.679916414 -1.098107831 -4.964097380
C 0.778017278 -1.580136631 -4.880905816
H 1.416288207 -1.382481938 -2.711548256
H 1.302320915 0.141212728 -3.620260445
H -1.431960996 -1.795042958 -5.328562797
H -0.760746898 -0.157554873 -5.506710600
H 0.844456744 -2.663287854 -4.773103279
H 1.455288026 -1.258019304 -5.670970386
./carboplatin-M06L-H2O-ApVDZ-ApVDZ_eGeom.xyz
25

Pt 0.209935714 -0.365964421 -0.413054494
N -0.562721901 1.303380287 0.539860340
H -1.580573565 1.327515326 0.564575071
H -0.246716092 1.418842201 1.501358524
N -0.502690769 -1.702303222 1.004608843
H -0.149351974 -1.536608255 1.945444170
H -1.518531189 -1.723518668 1.076057405
H -0.267229662 2.139440154 0.036791895
H -0.210747396 -2.644716401 0.747545588
O 1.004114760 0.917781936 -1.778163121
O 1.035743826 -1.975513606 -1.343076109
C 1.239877454 0.521942678 -3.001994771
C 1.216106158 -1.991530517 -2.637942382
O 1.876929016 1.228120654 -3.787555910
O 1.783641425 -2.936587697 -3.189746541
C 0.659078138 -0.815867797 -3.446630840
C 0.650009463 -1.079163645 -4.959540373
C -0.902626612 -0.886463004 -3.482416103
C -0.794485389 -1.587049482 -4.845417121
H 1.410634484 -1.770007104 -5.337824369

H	0.714966435	-0.131199325	-5.504241353
H	-1.391383020	-1.417657997	-2.656250383
H	-1.336317767	0.118932004	-3.556935041
H	-0.836129624	-2.677963449	-4.738421948
H	-1.504224901	-1.284193419	-5.624159986

./carboplatin-M06L-SMD-ApVTZ-ApVDZ_eGeom.xyz

25

Pt	-0.224342860	-0.365873432	-0.418690172
N	0.500176980	1.283831094	0.572570514
H	0.206036686	1.310655552	1.542883853
H	1.513472876	1.320713745	0.569843029
N	0.573398974	-1.625920509	0.998804006
H	1.568064409	-1.769437044	0.863076067
H	0.451165799	-1.284549383	1.945930684
H	0.171321628	2.139700983	0.138751835
H	0.133457335	-2.538557918	0.953280129
O	-1.080725330	0.872265503	-1.793669227
O	-1.008541797	-1.992307974	-1.368034255
C	-1.276559315	0.486181024	-3.016253180
C	-1.189060627	-2.012725018	-2.651533252
O	-1.904102989	1.192160708	-3.809799551
O	-1.733326215	-2.973929911	-3.199128056
C	-0.670287440	-0.830761119	-3.463672743
C	0.891690038	-0.866767415	-3.497355430
C	-0.643910818	-1.100462233	-4.972391851
C	0.793403570	-1.612044097	-4.832254886
H	1.386926862	-1.352443194	-2.657550843
H	1.291679982	0.140090209	-3.610732487
H	-1.398674216	-1.776676626	-5.366572521
H	-0.683910549	-0.160486079	-5.518145930
H	0.825555411	-2.690773972	-4.686864194
H	1.504398614	-1.342235664	-5.609620551

./carboplatin-PBE0-H2O-ApVDZ-ApVDZ-pp_eGeom.xyz

25

Pt	0.196665916	-0.364069989	-0.402338674
N	-0.553199591	1.281285411	0.530935873
H	-1.571031958	1.293398976	0.576270767
H	-0.211210646	1.405291750	1.482865789
N	-0.497519086	-1.667963745	0.998670890
H	-0.153364001	-1.479909617	1.939084733
H	-1.514453009	-1.701045690	1.054766154
H	-0.270453932	2.108831317	0.005390445
H	-0.183262732	-2.606522673	0.751148525
O	0.965805760	0.897623753	-1.756055705
O	1.002906059	-1.957620102	-1.309985175
C	1.211504058	0.513370339	-2.976703279
C	1.202256897	-1.990275343	-2.597033125
O	1.842988266	1.226423842	-3.755032306
O	1.787193202	-2.933272684	-3.126731225
C	0.649133501	-0.830728933	-3.431389932
C	0.680762711	-1.100399697	-4.948289623
C	-0.917949439	-0.900376086	-3.500386610

C	-0.790882478	-1.560175526	-4.889318699
H	1.426507411	-1.827175783	-5.285111945
H	0.806136454	-0.159198686	-5.493651998
H	-1.413874901	-1.462113879	-2.700741202
H	-1.353151159	0.105372822	-3.548328023
H	-0.882777807	-2.651713442	-4.831639334
H	-1.461422485	-1.189389105	-5.673525331

./carboplatin-PBE0-ApVDZ-pVTZ-pp_eGeom.xyz

25

Pt	-0.105380738	-0.360088360	-0.343670189
N	0.489395665	1.399711726	0.539054921
H	0.077711802	1.605617598	1.446761381
H	1.495663312	1.532762901	0.612920750
N	0.452400915	-1.787519679	1.029057162
H	1.453863941	-1.902063058	1.168916424
H	0.014199611	-1.713723038	1.944767043
H	0.132550855	2.090660105	-0.129630787
H	0.099313662	-2.641380758	0.583947884
O	-0.758334812	0.922987324	-1.681871364
O	-0.782719642	-1.973854707	-1.241680951
C	-1.062134524	0.558834107	-2.918376622
C	-1.066212224	-2.000548265	-2.534141974
O	-1.618841919	1.333536955	-3.670183874
O	-1.614417984	-2.967421584	-3.024425272
C	-0.597290513	-0.817778809	-3.387378301
C	0.957567202	-0.909277983	-3.599583169
C	-0.767520692	-1.092703376	-4.895048912
C	0.694910437	-1.580997512	-4.962575402
H	1.523268926	-1.467382882	-2.842916290
H	1.393578696	0.092749590	-3.701441416
H	-1.549549711	-1.813973601	-5.148659498
H	-0.931836277	-0.150002063	-5.426674120
H	0.763907331	-2.673511632	-4.897109510
H	1.303213692	-1.234985768	-5.807186924

./carboplatin-PBE0-TZ-pVDZ-pp_eGeom.xyz

25

Pt	-0.105682053	-0.365452298	-0.340660262
N	0.480127017	1.397562399	0.552041444
H	0.046506107	1.599699485	1.445670040
H	1.481216821	1.523578032	0.647289028
N	0.460859285	-1.798617475	1.029478868
H	1.458636869	-1.894727219	1.178609181
H	0.007948903	-1.735019107	1.934168167
H	0.138119914	2.080090170	-0.126779595
H	0.125460083	-2.646195177	0.568268939
O	-0.762505594	0.916202865	-1.677315386
O	-0.770542350	-1.977318408	-1.249922442
C	-1.059377100	0.559957635	-2.913364675
C	-1.045721443	-2.005417739	-2.539663600
O	-1.606787269	1.333749931	-3.661237020
O	-1.568845835	-2.974961524	-3.034518127
C	-0.594321948	-0.813045875	-3.385216432

C	0.955130982	-0.898279047	-3.612348130
C	-0.774016141	-1.083273889	-4.888599328
C	0.681759688	-1.576872751	-4.964975186
H	1.529790109	-1.444427340	-2.863322553
H	1.382518870	0.099307193	-3.725836452
H	-1.554861371	-1.796323555	-5.140686998
H	-0.934341233	-0.144258549	-5.414916468
H	0.744266426	-2.662667832	-4.891436057
H	1.281968271	-1.243642693	-5.811855967

./carboplatin-ApVDZ-pVDZ-pp_eGeom.xyz
25

Pt	-0.100545075	-0.344560792	-0.327993723
N	0.567818590	1.482756358	0.410068388
H	0.130423958	1.792244863	1.286470090
H	1.584734080	1.583182379	0.511664334
N	0.413774459	-1.706062554	1.158221436
H	1.421040393	-1.858031895	1.288440030
H	-0.003521520	-1.540123334	2.081982773
H	0.260105678	2.129469939	-0.337541058
H	0.009840513	-2.583004333	0.784474215
O	-0.719383635	0.873720236	-1.782397225
O	-0.871726456	-2.014079693	-1.099314952
C	-1.015731084	0.414412714	-3.007345673
C	-1.160445803	-2.114213433	-2.406438218
O	-1.527702455	1.169136013	-3.831745838
O	-1.775378440	-3.094791848	-2.820259195
C	-0.614574528	-1.033518910	-3.351822928
C	0.954846842	-1.120649331	-3.564333527
C	-0.783256641	-1.335596360	-4.867312293
C	0.719022921	-1.010400434	-5.094433594
H	1.333898163	-2.113193139	-3.260888341
H	1.558400692	-0.340981035	-3.066232642
H	-1.026994945	-2.401111282	-5.011534952
H	-1.520318897	-0.701668201	-5.385360772
H	1.294300448	-1.703950602	-5.733199766
H	0.868679753	0.020661903	-5.460295578

./carboplatin-M062X-CPCM-ApVTZ-pVDZ-2_eGeom.xyz
25

Pt	-1.113306104	0.069692964	0.075813838
N	-2.427435472	1.479425077	-0.613835870
H	-2.621877036	1.390639665	-1.606783748
H	-3.321613305	1.472357075	-0.131975334
N	-2.370501655	-1.506157837	-0.288455175
H	-3.253734165	-1.441195544	0.208754883
H	-2.589337164	-1.624237679	-1.273243710
H	-2.016741887	2.398944751	-0.469876734
H	-1.913226738	-2.360155932	0.022195481
O	0.136079743	1.600372566	0.523609020
O	0.196481663	-1.287772046	0.812028226
C	1.416758338	1.429346707	0.613904974
C	1.478932231	-1.110851871	0.784050282
O	2.155053401	2.283589589	1.085136327

O	2.255422194	-1.914959598	1.280127435
C	2.001380939	0.133864913	0.055661664
C	3.522584977	0.110210742	-0.160661010
C	1.833133540	-0.056962923	-1.489364361
C	3.294923206	-0.544719105	-1.537931749
H	4.105801673	-0.437772835	0.572890263
H	3.896590895	1.126591915	-0.253226491
H	1.048773839	-0.735603437	-1.817191355
H	1.702874079	0.907388165	-1.979021790
H	3.351066053	-1.630056684	-1.479704422
H	3.906151755	-0.196103637	-2.366474646

./carboplatin-PBE0-SMD-ApVTZ-pVTZ-pp_eGeom.xyz

25

Pt	-0.222712455	-0.376483201	-0.406381735
N	0.534566761	1.216428562	0.587072102
H	0.189785956	1.277330228	1.541859394
H	1.549537957	1.187400776	0.638222891
N	0.493768744	-1.648532024	0.995368310
H	1.508761786	-1.632247272	1.048900043
H	0.141891996	-1.435792274	1.925319503
H	0.282835163	2.084285354	0.120815118
H	0.218384591	-2.603926898	0.781911221
O	-0.998917590	0.881199697	-1.763893973
O	-1.023647783	-1.951130695	-1.358951922
C	-1.218747095	0.517126863	-2.985812113
C	-1.192840245	-1.977191007	-2.640692267
O	-1.840502357	1.242872221	-3.761710437
O	-1.750106016	-2.928844035	-3.186188888
C	-0.649887739	-0.809533176	-3.457947485
C	0.914766506	-0.877381879	-3.514922556
C	-0.657213503	-1.066460890	-4.973355374
C	0.790248330	-1.576977646	-4.878179903
H	1.409254871	-1.405841875	-2.701001631
H	1.334242210	0.125629257	-3.600622860
H	-1.418525774	-1.746535753	-5.350236595
H	-0.714336802	-0.121129673	-5.510671843
H	0.834818478	-2.661896591	-4.777107500
H	1.481881022	-1.262720836	-5.658920508

./carboplatin-M062X-H2O-ApVDZ-ApVTZ_eGeom.xyz

25

Pt	0.201321625	-0.360995206	-0.398644195
N	-0.549977443	1.285892516	0.546081707
H	-1.568164493	1.300861111	0.583321703
H	-0.214160140	1.398410443	1.501688504
N	-0.486569796	-1.680927542	1.001770499
H	-0.129954549	-1.503419057	1.939555908
H	-1.503118047	-1.707258655	1.068728818
H	-0.258359450	2.115435307	0.027882572
H	-0.179757443	-2.617866125	0.737588344
O	0.967109816	0.915380819	-1.770153977
O	1.006587033	-1.963816593	-1.334973228
C	1.227327340	0.525020841	-2.983093548

C	1.185596930	-1.997725135	-2.622319721
O	1.877176313	1.217408311	-3.763206842
O	1.726286659	-2.951421440	-3.176611201
C	0.648547939	-0.814669184	-3.442413758
C	0.663893141	-1.078732999	-4.959388888
C	-0.917247141	-0.880767225	-3.497556340
C	-0.789768025	-1.594672167	-4.862739005
H	1.429416522	-1.770219507	-5.319306547
H	0.725882021	-0.128755416	-5.497627096
H	-1.415071218	-1.410007404	-2.678813108
H	-1.339597371	0.126048530	-3.591701882
H	-0.824197872	-2.682843647	-4.744953374
H	-1.485895338	-1.290713345	-5.650244354

./carboplatin-M06L-ApVDZ-pVDZ_eGeom.xyz

25

Pt	-0.128237023	-0.364994046	-0.365112602
N	0.525582648	1.445581468	0.499814722
H	0.152927794	1.676240386	1.418141721
H	1.532274958	1.588322634	0.536068657
N	0.475100751	-1.863094946	0.994324282
H	1.476677225	-2.003387422	1.104454497
H	0.071390344	-1.815214791	1.927245691
H	0.146692852	2.128883633	-0.162338785
H	0.097842497	-2.702344344	0.544809603
O	-0.841329344	0.949218684	-1.693995653
O	-0.878032627	-1.990839156	-1.262935887
C	-1.119033759	0.570412029	-2.936906429
C	-1.129187789	-1.993666790	-2.566419661
O	-1.674240496	1.338653239	-3.702369265
O	-1.674746818	-2.952361989	-3.083888940
C	-0.626801979	-0.801602726	-3.386473966
C	0.929820548	-0.895816060	-3.522042666
C	-0.718582510	-1.070434618	-4.895775987
C	0.725381036	-1.594544031	-4.874559571
H	1.464596388	-1.431955073	-2.726020881
H	1.370378505	0.104597872	-3.626442579
H	-1.506112622	-1.764013305	-5.204404352
H	-0.822488415	-0.123005355	-5.434309585
H	0.757691017	-2.686008443	-4.772197186
H	1.389743828	-1.298979619	-5.695794188

./carboplatin-M06L-ApVDZ-ApVTZ_eGeom.xyz

25

Pt	-0.122815400	-0.368325041	-0.363525097
N	0.494539592	1.443080987	0.502655500
H	0.123563567	1.658557544	1.425070761
H	1.498418292	1.604369719	0.533476967
N	0.505236183	-1.846853907	0.990907118
H	1.509535763	-1.973087132	1.091036057
H	0.111080210	-1.796161160	1.927489263
H	0.097177913	2.121492125	-0.153433701
H	0.133164008	-2.692483673	0.549449851
O	-0.856961611	0.930021500	-1.684144163

O	-0.840766660	-2.000980198	-1.257241339
C	-1.135982052	0.553005632	-2.927456275
C	-1.100246347	-2.012156995	-2.559193251
O	-1.704570933	1.315750890	-3.688187693
O	-1.628688223	-2.982325563	-3.072561449
C	-0.627379609	-0.811019132	-3.383376211
C	0.929429165	-0.879605935	-3.534994962
C	-0.729276353	-1.080586637	-4.892044320
C	0.722632012	-1.582539006	-4.884810505
H	1.481493604	-1.406658661	-2.744736217
H	1.352147149	0.127887224	-3.644575865
H	-1.508849036	-1.786009215	-5.193851901
H	-0.852436078	-0.134545047	-5.428873908
H	0.772361512	-2.673195289	-4.781479752
H	1.374500342	-1.277985800	-5.712727916

./carboplatin-M06L-CPCM-aug-pVTZ_eGeom.xyz

25

Pt	0.219545169	-0.362578336	-0.411216937
N	-0.540675065	1.307140179	0.546314048
H	-1.560466421	1.341052964	0.575581709
H	-0.224801114	1.423997115	1.510069473
N	-0.480119396	-1.698322951	1.010077912
H	-0.129407505	-1.529779535	1.953783950
H	-1.497593954	-1.731175732	1.086547389
H	-0.243407654	2.146573022	0.045199022
H	-0.182225546	-2.642763411	0.758265048
O	0.995621306	0.921399896	-1.770638583
O	1.028586811	-1.970318062	-1.338195375
C	1.213528668	0.535135242	-3.004828028
C	1.191796541	-1.994744882	-2.638502890
O	1.816344184	1.254817903	-3.799178555
O	1.727306950	-2.951707879	-3.194437544
C	0.645010200	-0.810696832	-3.444027632
C	0.652725199	-1.078176504	-4.955671017
C	-0.915059660	-0.889847115	-3.499358382
C	-0.783419483	-1.606974326	-4.850476513
H	1.428095042	-1.760599927	-5.325867237
H	0.709108809	-0.128540854	-5.502673718
H	-1.419401752	-1.408865946	-2.671070092
H	-1.353371697	0.114648762	-3.597081864
H	-0.806782699	-2.699131159	-4.727765973
H	-1.493629920	-1.330894404	-5.641977219

./carboplatin-ApVDZ-pVTZ-pp-2_eGeom.xyz

25

Pt	0.103805497	-0.356969996	-0.325516509
N	-0.494367298	1.428170750	0.548321623
H	-1.509911402	1.566221280	0.613594535
H	-0.086302983	1.639604804	1.466839550
N	-0.464958580	-1.803616697	1.051353663
H	-0.028067023	-1.731406166	1.978171765
H	-1.476092861	-1.920955704	1.186871789
H	-0.126283980	2.121209167	-0.127112484

H	-0.105115387	-2.664007814	0.601637807
O	0.782780329	0.937382181	-1.673441413
O	0.796819288	-1.991803378	-1.223421698
C	1.078667801	0.559625855	-2.927458885
C	1.079688783	-2.013742985	-2.534735950
O	1.640088071	1.347647024	-3.685295063
O	1.638407734	-2.994806853	-3.020854774
C	0.604303056	-0.825120033	-3.393291490
C	0.771938171	-1.104802851	-4.913172783
C	-0.965295003	-0.910093137	-3.606148108
C	-0.707502954	-1.574232314	-4.985004831
H	1.548392664	-1.844948048	-5.163767124
H	0.957486524	-0.159484090	-5.449319741
H	-1.530994542	-1.476989040	-2.845258205
H	-1.400996908	0.101505212	-3.694319380
H	-0.795571067	-2.673789153	-4.934506773
H	-1.313610922	-1.204950784	-5.831294530

./carboplatin-M06L_eGeom.xyz

25

Pt	0.121954584	-0.363368001	-0.350682444
N	-0.506480193	1.460728593	0.516913043
H	-1.512174697	1.625328611	0.576645675
H	-0.109915568	1.710075560	1.424176883
N	-0.480093761	-1.866893161	1.011268178
H	-0.067368860	-1.839650062	1.944859582
H	-1.482553293	-2.014704269	1.134720878
H	-0.134451724	2.132458224	-0.166598703
H	-0.109807784	-2.706066781	0.547252960
O	0.832199047	0.945521983	-1.685409387
O	0.847382375	-1.994473517	-1.256798248
C	1.103045590	0.573070934	-2.934824704
C	1.093686941	-2.006108314	-2.563718159
O	1.637875142	1.350681210	-3.701458828
O	1.606274553	-2.981060348	-3.079827465
C	0.619408227	-0.802555509	-3.385436267
C	0.739057504	-1.074164038	-4.892164731
C	-0.933750610	-0.890758470	-3.554463237
C	-0.702438415	-1.601155390	-4.894911883
H	1.534670676	-1.768184420	-5.187356047
H	0.850976769	-0.125610242	-5.431398190
H	-1.494034628	-1.413623961	-2.763108597
H	-1.367695515	0.113089177	-3.679082937
H	-0.733686626	-2.693871292	-4.782226885
H	-1.354772723	-1.319059287	-5.733499495

./carboplatin-M062X-H2O_eGeom.xyz

25

Pt	-0.203228668	-0.362307000	-0.389426608
N	0.566875376	1.285622644	0.568790193
H	0.203556833	1.429618559	1.514910896
H	1.587522862	1.288327668	0.644126065
N	0.463359928	-1.712152052	1.013724511
H	1.482035421	-1.753360509	1.104784799

H	0.091953742	-1.557740652	1.954846668
H	0.312511080	2.118610578	0.028285345
H	0.157928443	-2.648087335	0.728039578
O	-0.939325653	0.933402854	-1.752536539
O	-1.021317787	-1.948984549	-1.336903617
C	-1.172668536	0.570549367	-2.985999108
C	-1.184829281	-1.977780409	-2.631984792
O	-1.748677990	1.304651709	-3.775737643
O	-1.705483588	-2.930882646	-3.194136466
C	-0.640822742	-0.790070370	-3.442706300
C	0.920597789	-0.898066385	-3.524869707
C	-0.687420010	-1.055205163	-4.957826098
C	0.747035828	-1.621331718	-4.878992421
H	1.423750250	-1.428276556	-2.704625684
H	1.369536730	0.098821265	-3.641522981
H	-1.482645759	-1.726199699	-5.301084102
H	-0.727718612	-0.101322640	-5.496804059
H	0.738901895	-2.711530251	-4.746814986
H	1.445879461	-1.356659476	-5.682665954

./carboplatin-PBE0-CPCM-ApVTZ-pVDZ-pp_eGeom.xyz

25

Pt	0.195867916	-0.367372025	-0.402871798
N	-0.519442438	1.293084923	0.531019458
H	-1.533078880	1.320684559	0.577545330
H	-0.172875721	1.407047367	1.478402508
N	-0.519932098	-1.659324317	0.998881145
H	-0.165263990	-1.479285848	1.932773147
H	-1.533254445	-1.664410635	1.058918953
H	-0.222124467	2.109947354	0.004024858
H	-0.230277718	-2.600139648	0.745198632
O	0.984680874	0.873380144	-1.756905255
O	0.968050207	-1.969191320	-1.313861595
C	1.228160566	0.492095230	-2.972960972
C	1.171902894	-2.010353995	-2.594142035
O	1.867852746	1.192776988	-3.746130431
O	1.735291166	-2.960770978	-3.119732893
C	0.647379324	-0.840889754	-3.429922054
C	0.680329019	-1.111013337	-4.942637806
C	-0.916568981	-0.882574194	-3.508207420
C	-0.792451603	-1.553818150	-4.887130488
H	1.413842407	-1.840528800	-5.279067180
H	0.813520339	-0.176943355	-5.485801380
H	-1.427062918	-1.423950650	-2.712704881
H	-1.330522407	0.124690826	-3.568832472
H	-0.894637803	-2.637330370	-4.820305535
H	-1.452076979	-1.186162785	-5.672678846

./carboplatin-CPCM-ApVDZ-pVTZ-pp_eGeom.xyz

25

Pt	-0.196266842	-0.361890439	-0.388893371
N	0.554197605	1.303500827	0.544414018
H	0.214152046	1.430260692	1.506412933
H	1.581294043	1.320469762	0.585555507

N	0.494701781	-1.675697677	1.029029382
H	1.520446692	-1.709972506	1.090653713
H	0.144204613	-1.484651389	1.976373824
H	0.263519600	2.136588885	0.013847137
H	0.179182734	-2.623819565	0.780742970
O	-0.974593542	0.908839234	-1.751540010
O	-1.007649658	-1.972700237	-1.294265068
C	-1.220384093	0.513336070	-2.988370658
C	-1.210620170	-2.003788347	-2.599341711
O	-1.860250019	1.238891151	-3.771181737
O	-1.808852201	-2.959917781	-3.124372666
C	-0.652029426	-0.839380948	-3.441118016
C	0.929327092	-0.903312080	-3.511835168
C	-0.683230971	-1.113360620	-4.969544314
C	0.805892712	-1.552671218	-4.917449173
H	1.425367453	-1.475964725	-2.709609392
H	1.363868417	0.111439705	-3.545384455
H	-1.423129580	-1.860414622	-5.300865632
H	-0.832612972	-0.169981080	-5.520727400
H	0.919143505	-2.650559746	-4.876058188
H	1.471628192	-1.155596117	-5.703601535

./carboplatin-PBE0-H2O-ApVDZ-pVTZ-pp_eGeom.xyz

25

Pt	0.193576208	-0.363413775	-0.402909278
N	-0.545601087	1.287510988	0.526399200
H	-1.563532444	1.308837586	0.569176450
H	-0.206643780	1.410076575	1.479728240
N	-0.511145532	-1.660058488	0.998184365
H	-0.166715608	-1.474961113	1.939197558
H	-1.528397420	-1.685662587	1.055091141
H	-0.255221991	2.113411131	0.002259165
H	-0.205394827	-2.602142667	0.752630873
O	0.972524878	0.889107898	-1.754061861
O	0.989847073	-1.960350046	-1.305155397
C	1.219426122	0.504485572	-2.974265259
C	1.194232216	-1.998204736	-2.591068324
O	1.855688724	1.214806116	-3.751291170
O	1.775390030	-2.946081949	-3.116435306
C	0.651417304	-0.836935031	-3.429676752
C	0.686657193	-1.109034873	-4.946006127
C	-0.915774814	-0.896305959	-3.504026433
C	-0.788313754	-1.558791634	-4.891627391
H	1.428602497	-1.841404346	-5.279116118
H	0.820434441	-0.169491557	-5.492240882
H	-1.418371792	-1.453726532	-2.705496479
H	-1.344097909	0.112274088	-3.554957878
H	-0.887676419	-2.649637989	-4.832756212
H	-1.453602301	-1.184659443	-5.678705135

./carboplatin-M06L-ApVTZ-pVTZ_eGeom.xyz

25

Pt	-0.103480769	-0.365827903	-0.358166444
N	0.506073826	1.444258846	0.523483986

H	0.104742586	1.657389271	1.427773120
H	1.505725583	1.587396983	0.588090622
N	0.472176626	-1.858523181	1.009380918
H	1.467661024	-1.988899048	1.135429217
H	0.049681892	-1.803879185	1.927490509
H	0.138001019	2.118195470	-0.147416547
H	0.104421690	-2.689808262	0.547267001
O	-0.789031155	0.938766356	-1.693287784
O	-0.809181935	-1.990240941	-1.267167946
C	-1.095225770	0.569022549	-2.926503392
C	-1.083768176	-2.001221588	-2.560035871
O	-1.652959489	1.338364441	-3.676804441
O	-1.614519789	-2.964789350	-3.066049378
C	-0.617329287	-0.801862514	-3.387019472
C	0.934509835	-0.886556461	-3.565368378
C	-0.743448652	-1.070479718	-4.891610065
C	0.696099781	-1.599992352	-4.900470259
H	1.492136098	-1.402407589	-2.782638576
H	1.359390611	0.109027729	-3.694810290
H	-1.533558761	-1.756720607	-5.182412730
H	-0.852346082	-0.129306201	-5.424926214
H	0.724771490	-2.682184081	-4.786489692
H	1.336764814	-1.320075437	-5.734866904

./carboplatin-M06L-SMD-TZ-aug-pVDZ_eGeom.xyz

25

Pt	-0.234955323	-0.377252699	-0.417871679
N	0.482526076	1.274112115	0.579022197
H	0.187718357	1.296670418	1.549306614
H	1.495745436	1.315334045	0.576808467
N	0.580639209	-1.639947001	0.989531634
H	1.577943499	-1.765698530	0.854640069
H	0.450716388	-1.309965056	1.939715003
H	0.150167207	2.129735837	0.147206482
H	0.155875331	-2.559282681	0.933410061
O	-1.106749451	0.861930440	-1.783896944
O	-1.010067554	-2.005884990	-1.373411806
C	-1.290691111	0.480356050	-3.011848072
C	-1.180071557	-2.021780227	-2.660222224
O	-1.919402084	1.183638114	-3.804272375
O	-1.706877781	-2.985793085	-3.216678202
C	-0.668924203	-0.828809807	-3.461280887
C	0.893307262	-0.850827413	-3.490992689
C	-0.636828916	-1.090208540	-4.971521268
C	0.806039955	-1.586016296	-4.832426840
H	1.390823034	-1.339266214	-2.654130578
H	1.286725294	0.159728505	-3.593400784
H	-1.382665704	-1.774485647	-5.368522519
H	-0.690235541	-0.148846893	-5.513620015
H	0.850911577	-2.665489830	-4.696784418
H	1.515637611	-1.302303385	-5.605888238

./carboplatin-M062X-CPCM-ApVTZ-ApVTZ-pp-2_eGeom.xyz

25

Pt	-0.987162929	-0.009472390	0.191397026
N	-2.247181549	1.427473314	-0.540479797
H	-2.300281710	1.430901001	-1.554957326
H	-3.198054497	1.350674991	-0.191006229
N	-2.120657090	-1.573047103	-0.490855415
H	-3.066869182	-1.577169288	-0.121334845
H	-2.194393819	-1.601110317	-1.503706831
H	-1.895608813	2.338751533	-0.255325557
H	-1.679525493	-2.441712342	-0.197305343
O	0.128054263	1.499865609	0.949877637
O	0.258929477	-1.398396391	0.972635339
C	1.389490178	1.353791748	1.204921736
C	1.525376848	-1.188795659	1.142921673
O	2.021157854	2.176880109	1.853489585
O	2.255644820	-2.019800509	1.664520849
C	2.096965956	0.134413924	0.617911155
C	3.633306646	0.169749207	0.622085004
C	2.156487338	0.092287775	-0.946426059
C	3.628050038	-0.352428059	-0.828794903
H	4.127631930	-0.432953675	1.377676869
H	3.977108500	1.199289200	0.679963140
H	1.452700146	-0.569665385	-1.446269896
H	2.060174535	1.096669793	-1.357142617
H	3.717010523	-1.436525036	-0.864749508
H	4.336411028	0.090750952	-1.524101687

./carboplatin-M062X-CPCM-TZ-aug-pVTZ-2_eGeom.xyz

25

Pt	0.204156263	-0.359322627	-0.397996179
N	-0.553673940	1.290646125	0.551644537
H	-1.567365419	1.283723165	0.618065266
H	-0.192012584	1.417632275	1.492622700
N	-0.475625082	-1.682766307	1.013159154
H	-0.088055136	-1.518509686	1.937760739
H	-1.487147768	-1.684922139	1.107710967
H	-0.293558826	2.115752627	0.015991812
H	-0.197233837	-2.620131955	0.731711548
O	0.957732747	0.913900429	-1.777665794
O	1.008543204	-1.956235772	-1.341935475
C	1.220028090	0.526597808	-2.987534618
C	1.176391799	-1.997739518	-2.627069271
O	1.863459260	1.215647029	-3.764706410
O	1.697473355	-2.953192970	-3.181712104
C	0.646338028	-0.812831069	-3.444361866
C	0.665223643	-1.077109431	-4.958312491
C	-0.916541411	-0.881651405	-3.506271727
C	-0.782022643	-1.601276797	-4.863670021
H	1.429479370	-1.759297569	-5.317549680
H	0.720709171	-0.133742989	-5.495269893
H	-1.417376977	-1.401165010	-2.692252997
H	-1.338668630	0.117414261	-3.608111953
H	-0.809062002	-2.682311874	-4.741761468
H	-1.473883664	-1.309459369	-5.649613784

./carboplatin-SMD-ApVDZ-pVTZ-pp_eGeom.xyz

25

Pt	-0.221030246	-0.364005897	-0.396254906
N	0.525684305	1.266211079	0.578278303
H	0.193979863	1.332957413	1.550728776
H	1.554412452	1.262298834	0.615219852
N	0.543631028	-1.614719920	1.023225739
H	1.572271131	-1.596099689	1.054344668
H	0.212457568	-1.386720076	1.970849978
H	0.247252604	2.137786111	0.106601460
H	0.265950584	-2.588483373	0.836862921
O	-1.053738379	0.881416679	-1.762498589
O	-1.017211738	-1.983870533	-1.320044937
C	-1.268318422	0.485646108	-3.002357458
C	-1.199038113	-2.016277958	-2.625421333
O	-1.921518351	1.206573996	-3.789673081
O	-1.770421881	-2.994362213	-3.156372470
C	-0.666043454	-0.843429807	-3.462548809
C	0.917466294	-0.877929461	-3.520123523
C	-0.670552626	-1.117369755	-4.991258539
C	0.810054610	-1.574436395	-4.902625129
H	1.421831231	-1.411653260	-2.696860763
H	1.320019663	0.147624725	-3.592042902
H	-1.416711250	-1.843383916	-5.354018757
H	-0.777673990	-0.169467728	-5.544464301
H	0.901442829	-2.671485069	-4.814375711
H	1.493111299	-1.217172665	-5.692299501

./carboplatin-CPCM-ApVTZ-ApVDZ-pp_eGeom.xyz

25

Pt	0.194933736	-0.364107824	-0.387968270
N	-0.533801672	1.310967851	0.548880307
H	-1.556614524	1.331748153	0.595372073
H	-0.183518965	1.429626182	1.504030993
N	-0.509537028	-1.672599569	1.030460140
H	-0.149013687	-1.484764546	1.970421879
H	-1.531652336	-1.686807871	1.093706046
H	-0.238037741	2.134638579	0.013781028
H	-0.208351621	-2.619189370	0.774381489
O	0.985570907	0.894787145	-1.753096540
O	0.983485912	-1.981001326	-1.300191369
C	1.228056274	0.502336066	-2.985873933
C	1.188070374	-2.015175279	-2.599482001
O	1.869517352	1.219133648	-3.765178861
O	1.769083080	-2.973911624	-3.123700274
C	0.649482770	-0.842849845	-3.440243780
C	0.683213982	-1.116610752	-4.964557573
C	-0.928457759	-0.891022536	-3.520058236
C	-0.802316329	-1.553308633	-4.914440289
H	1.417641150	-1.858466118	-5.296769553
H	0.829875835	-0.178835493	-5.512873307
H	-1.435081110	-1.445136009	-2.720849086
H	-1.349333305	0.121806311	-3.569099683
H	-0.914709720	-2.643909746	-4.861528073

H -1.461198568 -1.167700165 -5.702252138
./carboplatin-H2O_eGeom.xyz
25

Pt 0.199753285 -0.358861763 -0.360390434
N -0.515243862 1.327839216 0.580862263
H -1.542878872 1.356709893 0.674042179
H -0.131037989 1.484418317 1.526436888
N -0.484173191 -1.679424568 1.066638192
H -0.107482788 -1.514368680 2.013617119
H -1.511846713 -1.707273306 1.160924773
H -0.250015686 2.153100118 0.017129697
H -0.190163010 -2.633426293 0.796729825
O 0.962486070 0.906817342 -1.733420289
O 0.966120135 -1.981570189 -1.281887517
C 1.172882113 0.527729841 -2.989501439
C 1.142972864 -2.024103127 -2.597254758
O 1.749866009 1.282635960 -3.782830994
O 1.673715350 -3.010528528 -3.124473999
C 0.627263581 -0.837464446 -3.439548527
C 0.720600880 -1.118934620 -4.963857855
C -0.949181313 -0.899962249 -3.580073651
C -0.763499148 -1.570995781 -4.966713554
H 1.479117930 -1.868892087 -5.253582376
H 0.888314278 -0.172479077 -5.509975572
H -1.491939021 -1.457197756 -2.791890636
H -1.378980733 0.118795664 -3.653157065
H -0.863439856 -2.672459113 -4.905769711
H -1.405903304 -1.200457538 -5.789181569

./carboplatin-CPCM-ApVDZ-ApVDZ-pp_eGeom.xyz
25

Pt 0.195780854 -0.361625074 -0.388190670
N -0.551190867 1.308087535 0.542734627
H -1.578234786 1.327906351 0.580051793
H -0.212272336 1.432350943 1.505346089
N -0.506970396 -1.671527672 1.028987708
H -0.158888668 -1.479603422 1.976942396
H -1.533054234 -1.700982500 1.084840831
H -0.254663368 2.138982401 0.012134492
H -0.192835647 -2.620300203 0.781852753
O 0.986141453 0.906174579 -1.752199070
O 1.003693002 -1.979453452 -1.292303300
C 1.229956875 0.506582550 -2.988216355
C 1.206622054 -2.010320410 -2.597553980
O 1.874511586 1.227251119 -3.771568995
O 1.801128603 -2.968839683 -3.122287852
C 0.654095963 -0.843410214 -3.439799974
C 0.685002442 -1.118571876 -4.968053593
C -0.927469624 -0.898988527 -3.511604170
C -0.806428566 -1.550016882 -4.916725745
H 1.421210253 -1.869721784 -5.298289399
H 0.839777743 -0.176404189 -5.519803753
H -1.426858761 -1.468496563 -2.709242457

H -1.356792518 0.117928990 -3.545975841
H -0.925438480 -2.647260990 -4.874540952
H -1.469515568 -1.150093798 -5.703663593
./carboplatin-M062X-CPCM-aug-pVDZ_eGeom.xyz
25

Pt 0.212187733 -0.360976217 -0.395288927
N -0.564423570 1.275006894 0.565386255
H -1.586481495 1.280561561 0.609442324
H -0.228103920 1.397131438 1.523945090
N -0.447558287 -1.703657653 1.008837299
H -0.087153231 -1.532342970 1.950726101
H -1.466388535 -1.752512716 1.088039070
H -0.289518369 2.115848369 0.048439814
H -0.129303555 -2.639058273 0.737480736
O 0.941627959 0.939086038 -1.760828499
O 1.036051040 -1.946963003 -1.341692537
C 1.179721376 0.567233336 -2.990143669
C 1.188995541 -1.975428405 -2.637379667
O 1.772643362 1.288381704 -3.779888522
O 1.711191623 -2.925293355 -3.204307411
C 0.635565816 -0.789233654 -3.444459968
C 0.668366759 -1.055422973 -4.959964608
C -0.926456393 -0.893123870 -3.514250830
C -0.764006015 -1.624236399 -4.865437113
H 1.461917910 -1.723886451 -5.311745401
H 0.699401232 -0.101592869 -5.499775540
H -1.427560450 -1.415318111 -2.687698640
H -1.371163073 0.105189158 -3.636160001
H -0.751733411 -2.713558883 -4.726041631
H -1.470513033 -1.366185469 -5.664362733
./carboplatin-M06L-ApVTZ-ApVDZ-2_eGeom.xyz
25

Pt -0.999842955 -0.010600638 -0.098579957
N -2.226306311 1.592059779 0.496299559
H -3.143143597 1.632339379 0.069745676
H -2.344167117 1.709952078 1.494352502
N -2.070675773 -1.741354489 0.438976466
H -2.192718846 -1.900651214 1.430728136
H -2.971934742 -1.859445856 -0.006163297
H -1.686885580 2.385233673 0.150546552
H -1.449822345 -2.466357749 0.080334744
O 0.077513869 1.531339731 -0.747333693
O 0.219739309 -1.426084012 -0.788704362
C 1.365082875 1.406140322 -1.025925762
C 1.496328036 -1.186952375 -1.033946660
O 1.966616584 2.309429111 -1.562727292
O 2.188399452 -2.031314441 -1.557624292
C 2.068482217 0.144300709 -0.543580258
C 2.226427751 0.081937699 1.011513389
C 3.599061335 0.169054187 -0.636705008
C 3.678054202 -0.361443425 0.800356291
H 1.544823566 -0.578486285 1.549027056

H	2.154165223	1.080264026	1.443439198
H	4.032484134	-0.442202077	-1.423017532
H	3.944929886	1.195629267	-0.729346178
H	3.772332459	-1.445702289	0.821655949
H	4.429710370	0.067050889	1.460971775

./carboplatin-H20-ApVDZ-ApVDZ-pp_eGeom.xyz

25

Pt	0.193050499	-0.356762124	-0.388386535
N	-0.551415664	1.316794384	0.537803229
H	-1.578331335	1.337634534	0.577393187
H	-0.210003428	1.444334960	1.499114636
N	-0.512823855	-1.661791209	1.031922571
H	-0.165315296	-1.467492219	1.979606404
H	-1.538966878	-1.690492616	1.087028709
H	-0.255328799	2.145448872	0.003459947
H	-0.198983384	-2.611421883	0.787661946
O	0.985863222	0.906111481	-1.755198526
O	0.998772950	-1.978348689	-1.287171286
C	1.230929059	0.503164221	-2.989951787
C	1.204335815	-2.013253853	-2.591949272
O	1.875944969	1.221992546	-3.774509011
O	1.797779732	-2.974514267	-3.112688087
C	0.655418302	-0.847924815	-3.438729502
C	0.689672342	-1.127636262	-4.966108170
C	-0.926090710	-0.902323520	-3.514244772
C	-0.802238968	-1.557702647	-4.917070103
H	1.426006508	-1.880452384	-5.292208449
H	0.846656513	-0.187231672	-5.520214527
H	-1.427903060	-1.468934115	-2.711316454
H	-1.354401623	0.114883340	-3.552771810
H	-0.922136115	-2.654721858	-4.871803433
H	-1.463183787	-1.159712973	-5.706797917

./carboplatin-PBE0-CPCM_eGeom.xyz

25

Pt	0.204813006	-0.360285653	-0.380578070
N	-0.526184623	1.295925603	0.562736500
H	-1.545056787	1.312113524	0.651565492
H	-0.149957966	1.446177915	1.502208655
N	-0.463459085	-1.679085152	1.028816738
H	-0.087844552	-1.518050931	1.966579940
H	-1.481433800	-1.710577664	1.124634626
H	-0.269975800	2.120531936	0.011653898
H	-0.168622603	-2.621176381	0.755062757
O	0.942679153	0.903636869	-1.743038345
O	0.984670683	-1.952473385	-1.305912557
C	1.157769433	0.538139278	-2.981476238
C	1.154476896	-1.995271329	-2.602453496
O	1.727404697	1.281195444	-3.770126518
O	1.684149358	-2.960491996	-3.137934072
C	0.624350302	-0.820221646	-3.432899042
C	0.701096581	-1.094224092	-4.946855439
C	-0.938593448	-0.905129381	-3.551065760

C	-0.759391178	-1.585626795	-4.922490288
H	1.471772107	-1.810612766	-5.257235678
H	0.822311421	-0.148295093	-5.489739954
H	-1.463587137	-1.454818345	-2.756813633
H	-1.380066887	0.099192769	-3.634326133
H	-0.823416848	-2.680528888	-4.843148377
H	-1.420595913	-1.250396610	-5.734294015

./carboplatin-PBE0-SMD-TZ-pVDZ-pp_eGeom.xyz

25

Pt	-0.230983587	-0.361912195	-0.406564147
N	0.532360127	1.241162022	0.571047441
H	0.181477760	1.317100884	1.522261335
H	1.546651667	1.206887401	0.627983146
N	0.493522532	-1.626881870	1.001319719
H	1.508059592	-1.603371171	1.056802365
H	0.136755811	-1.415646646	1.929496857
H	0.287647702	2.102107164	0.089188627
H	0.224877289	-2.583412168	0.785890515
O	-1.012027068	0.886352326	-1.773965010
O	-1.034753569	-1.945761878	-1.347358060
C	-1.218728195	0.512663730	-2.997460548
C	-1.189079010	-1.983820672	-2.632646447
O	-1.829016770	1.233349059	-3.783737578
O	-1.729077507	-2.944823354	-3.174768882
C	-0.648240162	-0.818393304	-3.453396784
C	0.916150758	-0.887565728	-3.511360771
C	-0.656666001	-1.087432629	-4.966450928
C	0.789738838	-1.599954718	-4.867978357
H	1.411735721	-1.408550568	-2.693243079
H	1.336718655	0.114135104	-3.607041412
H	-1.419247987	-1.770123767	-5.336065881
H	-0.713480168	-0.146272689	-5.511055056
H	0.830917087	-2.683889491	-4.755645145
H	1.481993496	-1.296297613	-5.652380929

./carboplatin-H20-ApVTZ-pVTZ-pp_eGeom.xyz

25

Pt	-0.193918119	-0.362704265	-0.387765946
N	0.530302361	1.315405321	0.546108553
H	0.175011582	1.438508131	1.498912575
H	1.552820811	1.336729734	0.598304575
N	0.512165332	-1.668877869	1.031492943
H	1.534275567	-1.681471089	1.095519083
H	0.151108509	-1.482044117	1.971497738
H	0.237609993	2.137016614	0.005971382
H	0.212871010	-2.616128140	0.775263868
O	-0.985876241	0.892761767	-1.753351235
O	-0.977919368	-1.981663594	-1.297296231
C	-1.229944728	0.499026244	-2.985315120
C	-1.183905975	-2.018611602	-2.596180020
O	-1.873382105	1.214089354	-3.764624789
O	-1.761931332	-2.980097420	-3.118720185
C	-0.649834005	-0.845752568	-3.439223139

C	0.928077884	-0.890282612	-3.521778906
C	-0.685517002	-1.121226019	-4.963219530
C	0.801232421	-1.554151282	-4.915296750
H	1.437528265	-1.442309573	-2.722892472
H	1.346470522	0.123507289	-3.572725134
H	-1.418509769	-1.865526753	-5.293095834
H	-0.835776664	-0.184546766	-5.512401368
H	0.916478645	-2.644430054	-4.861773261
H	1.457869415	-1.167573501	-5.704539807

./carboplatin-SMD-ApVTZ-ApVDZ-pp_eGeom.xyz

25

Pt	-0.211246416	-0.358451411	-0.395589084
N	0.501683022	1.294922957	0.569004813
H	0.169160568	1.354636281	1.537475722
H	1.526570978	1.309339110	0.599648105
N	0.578929509	-1.591578914	1.027822505
H	1.603087791	-1.549557308	1.053356219
H	0.242005103	-1.362987010	1.969025039
H	0.199860113	2.150193657	0.089946167
H	0.317303808	-2.565685238	0.840103693
O	-1.069053931	0.861861517	-1.767341620
O	-0.973760418	-1.996018392	-1.313790357
C	-1.287054219	0.459805351	-2.998465817
C	-1.165656892	-2.039387854	-2.611458860
O	-1.953182702	1.161540849	-3.782107802
O	-1.714351987	-3.026853160	-3.133538887
C	-0.668164117	-0.859204339	-3.456779552
C	0.911336814	-0.867043394	-3.533275560
C	-0.682397118	-1.141175195	-4.979832804
C	0.798204769	-1.585395467	-4.899149045
H	1.434798645	-1.373079511	-2.713542516
H	1.292085926	0.158015714	-3.629393329
H	-1.420707188	-1.868623624	-5.335061050
H	-0.796256398	-0.202348754	-5.534308443
H	0.896700120	-2.673566104	-4.793687617
H	1.467411228	-1.239712530	-5.696188929

./carboplatin-M06L-H2O-aug-pVDZ_eGeom.xyz

25

Pt	0.223086979	-0.362646354	-0.411263316
N	-0.554064390	1.301926332	0.553426058
H	-1.574566312	1.324546835	0.592227968
H	-0.230298331	1.424556770	1.514609379
N	-0.463444745	-1.711780204	1.012397856
H	-0.110362333	-1.544877513	1.956301706
H	-1.480976323	-1.754547255	1.092840492
H	-0.271906831	2.145611226	0.049142438
H	-0.158926015	-2.653815275	0.756401470
O	0.986682849	0.933670519	-1.776278241
O	1.050121555	-1.963628580	-1.348240465
C	1.202555716	0.549293787	-3.012352587
C	1.207663051	-1.981322081	-2.650105570
O	1.795953969	1.274489973	-3.807718479

O	1.752470388	-2.929798483	-3.210153209
C	0.643636868	-0.801006092	-3.449551122
C	0.643318792	-1.067404727	-4.961217702
C	-0.915618076	-0.895134673	-3.494442088
C	-0.784916261	-1.614902314	-4.844217208
H	1.424954461	-1.738811590	-5.338333469
H	0.682168189	-0.116423707	-5.507585588
H	-1.409736871	-1.415058608	-2.660188933
H	-1.363697033	0.104981882	-3.593958883
H	-0.792155458	-2.706837355	-4.717401094
H	-1.504636827	-1.351435282	-5.631468423

./carboplatin-M062X-TZ-pVTZ_eGeom.xyz
25

Pt	-0.109134410	-0.360407207	-0.350085717
N	0.496296819	1.416629108	0.556149613
H	0.071349463	1.620334789	1.453980746
H	1.498893743	1.538565523	0.645926875
N	0.442694116	-1.817468146	1.037364216
H	1.439601424	-1.934463857	1.180584792
H	-0.000723390	-1.745335417	1.946485625
H	0.153134191	2.103105894	-0.118853937
H	0.087515427	-2.659212190	0.579044778
O	-0.746582082	0.933096593	-1.696894434
O	-0.785760190	-1.972595689	-1.270844855
C	-1.071458892	0.573128631	-2.925428634
C	-1.051723140	-2.003125105	-2.562327701
O	-1.636405371	1.333085545	-3.671144608
O	-1.552680768	-2.973590546	-3.074283633
C	-0.601598672	-0.800027795	-3.399075512
C	0.950064314	-0.892771363	-3.599303060
C	-0.757146878	-1.069361010	-4.904818036
C	0.685319903	-1.615450426	-4.935472042
H	1.513879239	-1.415336859	-2.827365500
H	1.372485780	0.101234375	-3.744661886
H	-1.556100969	-1.749941596	-5.179697239
H	-0.857053435	-0.126494106	-5.435487225
H	0.700325498	-2.696167202	-4.811317205
H	1.312115292	-1.337784714	-5.779604431

./carboplatin-SMD-ApVDZ-ApVDZ-pp_eGeom.xyz
25

Pt	-0.222194315	-0.362546856	-0.396027040
N	0.527833978	1.269163414	0.575957032
H	0.196283391	1.335962440	1.548326040
H	1.556478500	1.263248906	0.610416231
N	0.547468790	-1.611818619	1.023616463
H	1.576107569	-1.594055404	1.048875109
H	0.219395736	-1.379737182	1.971225351
H	0.248270013	2.139303517	0.102475915
H	0.266007877	-2.584861329	0.839594743
O	-1.060178381	0.882853065	-1.764596829
O	-1.021152062	-1.985919823	-1.319151973
C	-1.271689846	0.484309786	-3.004187915

C	-1.201317892	-2.017356378	-2.624919617
O	-1.924500999	1.203239213	-3.793559138
O	-1.772814831	-2.994988452	-3.156411232
C	-0.667339565	-0.844770552	-3.461851231
C	0.916280340	-0.878658031	-3.517482250
C	-0.669865135	-1.120202293	-4.990359851
C	0.810844428	-1.576435225	-4.899535717
H	1.419520890	-1.411465871	-2.692978209
H	1.318537977	0.146972200	-3.589649547
H	-1.415224517	-1.846949393	-5.353246317
H	-0.776859274	-0.172940140	-5.544683021
H	0.902797747	-2.673341384	-4.810300955
H	1.494616592	-1.219358377	-5.688675050

./carboplatin-PBE0-ApVDZ-ApVDZ-pp_eGeom.xyz

25

Pt	-0.095537035	-0.363085021	-0.342096139
N	0.503678068	1.396730611	0.539873224
H	0.092789111	1.600409930	1.448364626
H	1.510257518	1.527442174	0.611778627
N	0.476110503	-1.791434573	1.025252524
H	1.478988468	-1.900955354	1.157942787
H	0.042509277	-1.718539159	1.943151456
H	0.145455243	2.088023947	-0.127525757
H	0.123137163	-2.645757519	0.581204134
O	-0.762270921	0.923304747	-1.676523283
O	-0.777747707	-1.979961950	-1.239797925
C	-1.073374548	0.557118082	-2.910687311
C	-1.067407487	-2.003151331	-2.530963285
O	-1.639216323	1.329285935	-3.658223623
O	-1.615974025	-2.969968362	-3.020892106
C	-0.605864879	-0.817199253	-3.383984321
C	0.948090976	-0.904060311	-3.604758150
C	-0.783429929	-1.090121067	-4.891265948
C	0.679911199	-1.574246231	-4.967416816
H	1.519201551	-1.461888843	-2.852020499
H	1.380874461	0.099296535	-3.707072243
H	-1.564847434	-1.813061774	-5.141865662
H	-0.953109481	-0.147024210	-5.420523041
H	0.752523201	-2.666665093	-4.904400185
H	1.282560042	-1.224844679	-5.814680095

./carboplatin-H20-ApVTZ-ApVDZ-pp_eGeom.xyz

25

Pt	-0.193189939	-0.364812088	-0.387252888
N	0.533007510	1.311133816	0.550175910
H	0.179070959	1.430903860	1.503847490
H	1.555611894	1.332539614	0.600304411
N	0.513348435	-1.672924381	1.030655126
H	1.535532913	-1.686328344	1.093076929
H	0.153328456	-1.485752433	1.970946027
H	0.238647070	2.133836582	0.012802939
H	0.212708886	-2.619715067	0.774568981
O	-0.984949875	0.893908148	-1.751636950

O	-0.979982003	-1.982231755	-1.299518503
C	-1.229248558	0.501485579	-2.984167311
C	-1.185703853	-2.016791155	-2.598663991
O	-1.872091903	1.218228814	-3.762282880
O	-1.764494632	-2.977033647	-3.122381620
C	-0.650516981	-0.843186356	-3.439847964
C	0.927407489	-0.889697469	-3.522636132
C	-0.686674852	-1.116578073	-4.964179444
C	0.799352187	-1.551863607	-4.916887108
H	1.436079075	-1.443358820	-2.724391320
H	1.347034645	0.123624422	-3.572354191
H	-1.420992682	-1.859086576	-5.295131298
H	-0.835321109	-0.178811125	-5.511957782
H	0.912877762	-2.642361645	-4.864401239
H	1.456466116	-1.165481064	-5.705816201

./carboplatin-M062X-H2O-ApVTZ-pVDZ-2_eGeom.xyz

25

Pt	-1.119476000	-0.012283000	0.039422000
N	-2.475904000	1.357799000	-0.648291000
H	-2.676600000	1.257224000	-1.638843000
H	-3.365276000	1.330523000	-0.158302000
N	-2.341303000	-1.621871000	-0.297707000
H	-3.219783000	-1.574591000	0.209810000
H	-2.569116000	-1.753922000	-1.278688000
H	-2.088435000	2.288813000	-0.514068000
H	-1.859182000	-2.461556000	0.014475000
O	0.095598000	1.552671000	0.460415000
O	0.231126000	-1.330087000	0.772996000
C	1.381091000	1.414899000	0.539362000
C	1.508531000	-1.121895000	0.730402000
O	2.102003000	2.292130000	0.994787000
O	2.309519000	-1.902824000	1.224382000
C	1.992759000	0.129394000	-0.013014000
C	3.511985000	0.141848000	-0.243762000
C	1.814833000	-0.078761000	-1.554724000
C	3.287879000	-0.530140000	-1.613389000
H	4.115423000	-0.385307000	0.488662000
H	3.859561000	1.166424000	-0.348145000
H	1.044609000	-0.779595000	-1.869221000
H	1.655753000	0.877800000	-2.051125000
H	3.371876000	-1.613171000	-1.546756000
H	3.882305000	-0.173282000	-2.450617000

./carboplatin-H2O-TZ-pVTZ-pp_eGeom.xyz

25

Pt	0.197002517	-0.360607767	-0.380696677
N	-0.545501811	1.308452558	0.560159953
H	-1.567191604	1.312496222	0.626683119
H	-0.178517512	1.441243387	1.506985169
N	-0.478125676	-1.683822591	1.041119377
H	-0.107728662	-1.498965961	1.977677154
H	-1.498932331	-1.710266063	1.117241883
H	-0.274266725	2.131835905	0.011995466

H	-0.169537134	-2.624646081	0.773290112
O	0.955047378	0.910411461	-1.748402418
O	0.993477919	-1.967344463	-1.298243007
C	1.191513974	0.525849452	-2.987625773
C	1.184343198	-2.002647103	-2.602084467
O	1.803440264	1.259021127	-3.770987582
O	1.754703755	-2.962347407	-3.130164560
C	0.638608317	-0.830906045	-3.438825337
C	0.691693720	-1.104331096	-4.962614080
C	-0.937577700	-0.903617323	-3.536280379
C	-0.785429040	-1.569400576	-4.926355875
H	1.442857382	-1.833887459	-5.284225955
H	0.827460606	-0.163494050	-5.508233524
H	-1.446732426	-1.461589375	-2.741312192
H	-1.373078708	0.102532268	-3.595509407
H	-0.875403158	-2.661725865	-4.867998040
H	-1.444819531	-1.202595923	-5.722721971

./carboplatin-PBE0-CPCM-ApVTZ-ApVTZ-pp_eGeom.xyz

25

Pt	0.196428038	-0.367293557	-0.402250513
N	-0.524530920	1.289731738	0.533213270
H	-1.538251728	1.310359244	0.584874801
H	-0.173518985	1.406376555	1.478822714
N	-0.510648337	-1.662941563	1.000235216
H	-0.154709655	-1.480552942	1.933373093
H	-1.524032818	-1.672295577	1.062138865
H	-0.235158743	2.108068825	0.003736869
H	-0.217122065	-2.602647162	0.746130301
O	0.976937461	0.877061321	-1.755964623
O	0.972576638	-1.964817529	-1.314480064
C	1.220110426	0.498231841	-2.972749175
C	1.174765622	-2.004962806	-2.594973508
O	1.855181226	1.202738088	-3.746503030
O	1.740433697	-2.953558157	-3.121731172
C	0.645407046	-0.837242429	-3.430621264
C	0.680071943	-1.106806471	-4.943437120
C	-0.918468791	-0.886095318	-3.509788591
C	-0.790657875	-1.556520660	-4.888757470
H	1.417109471	-1.832810322	-5.279791709
H	0.809095433	-0.171941784	-5.486271774
H	-1.427081261	-1.429739331	-2.714589162
H	-1.336988558	0.119288027	-3.570774578
H	-0.888047717	-2.640506388	-4.822511159
H	-1.451592536	-1.191476413	-5.674459224

./carboplatin-PBE0-aug-pVDZ_eGeom.xyz

25

Pt	-0.105286839	-0.363209636	-0.333651713
N	0.467378740	1.405436034	0.550847056
H	0.030633382	1.622717088	1.447906236
H	1.472668651	1.554425530	0.648386833
N	0.478929800	-1.792251971	1.029649241
H	1.482522344	-1.888473237	1.190096588

H	0.019622983	-1.752726851	1.940871856
H	0.118032945	2.087908841	-0.136241487
H	0.155212607	-2.648662725	0.558863756
O	-0.779924293	0.918369288	-1.666583840
O	-0.759087866	-1.987185733	-1.236705284
C	-1.068548395	0.556687550	-2.910320062
C	-1.032348314	-2.016168099	-2.533608321
O	-1.617396446	1.330607637	-3.664035891
O	-1.545817541	-2.995197365	-3.031124278
C	-0.592239620	-0.816638643	-3.381600629
C	0.958000398	-0.890122077	-3.622674763
C	-0.783853406	-1.093786979	-4.885872338
C	0.676126359	-1.581060909	-4.970806478
H	1.552516014	-1.426965451	-2.868139215
H	1.376844394	0.119710711	-3.749870275
H	-1.570070334	-1.818578641	-5.127167477
H	-0.955786248	-0.148674210	-5.415820705
H	0.744625146	-2.675122332	-4.887089280
H	1.274552550	-1.251390590	-5.832438539

./carboplatin-PBE0-SMD-ApVDZ-pVDZ-pp_eGeom.xyz

25

Pt	-0.226973716	-0.359523991	-0.410662772
N	0.548283323	1.239867586	0.563577564
H	0.211182776	1.317990781	1.524008546
H	1.567324016	1.210665955	0.612645221
N	0.503806287	-1.617935308	0.999802397
H	1.522675138	-1.599809735	1.054688085
H	0.155649506	-1.404436270	1.935299184
H	0.301619529	2.111028492	0.092753018
H	0.235129691	-2.581945434	0.799421087
O	-1.016563038	0.893821556	-1.778054037
O	-1.046410130	-1.948772506	-1.342373656
C	-1.230845836	0.510018993	-3.001206640
C	-1.213342131	-1.980542447	-2.630315471
O	-1.856528023	1.229479745	-3.789467587
O	-1.782932087	-2.936400036	-3.169754179
C	-0.657424583	-0.823190050	-3.456950532
C	0.911002201	-0.894959719	-3.501958285
C	-0.657645205	-1.094946812	-4.973881840
C	0.795494439	-1.599104511	-4.868469451
H	1.398415095	-1.427928497	-2.678067568
H	1.335698881	0.112761926	-3.584501150
H	-1.419862758	-1.786857620	-5.346187437
H	-0.719884213	-0.149283504	-5.522569971
H	0.845470940	-2.689999271	-4.764348871
H	1.493966907	-1.280352094	-5.650554664

./carboplatin-ApVTZ-pVTZ-pp_eGeom.xyz

25

Pt	-0.100511872	-0.357625337	-0.325811828
N	0.492411670	1.426098252	0.556914936
H	0.069277012	1.630443456	1.465789162
H	1.504144166	1.552883873	0.639260716

N	0.460225364	-1.803648190	1.056407432
H	1.467195117	-1.907450303	1.203320856
H	0.009901430	-1.727559025	1.972108238
H	0.138443500	2.116658182	-0.122607897
H	0.112463910	-2.661569872	0.601538438
O	-0.769446864	0.934165800	-1.678007216
O	-0.785212594	-1.988487987	-1.232247766
C	-1.069159173	0.562283397	-2.927777283
C	-1.068849319	-2.012244622	-2.538458871
O	-1.625103968	1.348076275	-3.681162755
O	-1.618851634	-2.989968559	-3.024353363
C	-0.601148692	-0.821496754	-3.395005187
C	0.963586629	-0.908721972	-3.617804339
C	-0.774940125	-1.099951697	-4.910523103
C	0.695698018	-1.582379199	-4.984870595
H	1.533692967	-1.464329387	-2.861859116
H	1.395388732	0.096011504	-3.720098825
H	-1.553730983	-1.827130101	-5.161521373
H	-0.948454372	-0.158805455	-5.444527448
H	0.772508862	-2.675384140	-4.923622040
H	1.297779228	-1.230220909	-5.832209783

./carboplatin-PBE0-CPCM-ApVDZ-ApVTZ-pp_eGeom.xyz

25

Pt	0.198803901	-0.362205006	-0.402814514
N	-0.540328468	1.285765081	0.525222428
H	-1.557903791	1.302514985	0.571662783
H	-0.197086932	1.409313043	1.476502575
N	-0.496396705	-1.660917284	0.996535587
H	-0.149120296	-1.474004309	1.935749638
H	-1.513200529	-1.688114541	1.055277590
H	-0.253913983	2.110565906	-0.002424895
H	-0.187963300	-2.601065752	0.748064971
O	0.969625536	0.891519632	-1.754718934
O	0.996285306	-1.955674249	-1.306003101
C	1.211554392	0.508644850	-2.976087298
C	1.194945288	-1.994160936	-2.592508873
O	1.842206085	1.220763197	-3.756227305
O	1.776047603	-2.940841157	-3.120350709
C	0.645852377	-0.834601019	-3.429592154
C	0.677347444	-1.106580355	-4.946099616
C	-0.921516591	-0.899837941	-3.499374372
C	-0.795585693	-1.562205405	-4.887206333
H	1.421138996	-1.835908308	-5.281760386
H	0.805423675	-0.166499845	-5.492739610
H	-1.419545109	-1.459424638	-2.699501017
H	-1.354034508	0.106978418	-3.548849243
H	-0.890548404	-2.653356881	-4.827516312
H	-1.464779282	-1.191020256	-5.672369909

./carboplatin-PBE0-ApVTZ-pVDZ-pp_eGeom.xyz

25

Pt	-0.100977214	-0.354939595	-0.345348720
N	0.486853531	1.406691166	0.541143380

H	0.058506648	1.608257352	1.437627182
H	1.488780817	1.529764935	0.633830382
N	0.451941421	-1.776000376	1.037890174
H	1.449256619	-1.875869928	1.189014710
H	0.001092130	-1.696465589	1.942550285
H	0.145290568	2.093899616	-0.133217018
H	0.111906157	-2.629619117	0.591336171
O	-0.746845997	0.919731443	-1.692880298
O	-0.768875597	-1.968969268	-1.246647207
C	-1.056530190	0.556039552	-2.922745057
C	-1.053533874	-2.003101194	-2.533464432
O	-1.611983418	1.324653383	-3.671340629
O	-1.591207583	-2.970115783	-3.019194167
C	-0.595176797	-0.820321271	-3.389031055
C	0.954857845	-0.910860443	-3.610916992
C	-0.771514823	-1.098884806	-4.891462925
C	0.683921973	-1.594852916	-4.961149404
H	1.525632125	-1.455500036	-2.857839182
H	1.385022805	0.085163827	-3.727504396
H	-1.553301240	-1.811244881	-5.142561670
H	-0.928288747	-0.162777813	-5.424044239
H	0.746015378	-2.680409955	-4.883683205
H	1.286464470	-1.264621073	-5.807490698

./carboplatin-M062X-TZ-aug-pVDZ_eGeom.xyz

25

Pt	-0.100567583	-0.364649758	-0.349940318
N	0.507039836	1.410072519	0.557720234
H	0.080649318	1.612666879	1.455163388
H	1.509516007	1.532311812	0.648624870
N	0.466084502	-1.820313321	1.031741779
H	1.463681178	-1.927167724	1.178025313
H	0.018318006	-1.756921042	1.939447517
H	0.164145438	2.097248166	-0.116795546
H	0.121188858	-2.663987836	0.569006347
O	-0.751529126	0.931744940	-1.692160274
O	-0.779920708	-1.979162932	-1.271166479
C	-1.084899821	0.570343213	-2.917875262
C	-1.053989469	-2.005476812	-2.560903595
O	-1.661677130	1.326644639	-3.658329254
O	-1.558224151	-2.974218435	-3.073073953
C	-0.609788728	-0.799304456	-3.396797997
C	0.941287230	-0.885108175	-3.602154428
C	-0.769212788	-1.066091868	-4.902594126
C	0.674939558	-1.607597869	-4.938095436
H	1.510454949	-1.405336987	-2.832657043
H	1.358608132	0.110920669	-3.748491935
H	-1.567008507	-1.748454881	-5.176360483
H	-0.873509727	-0.122420616	-5.431023284
H	0.693359594	-2.688355384	-4.814462010
H	1.298362142	-1.327737509	-5.783977036

./carboplatin-M062X-SMD-ApVTZ-pVTZ-2_eGeom.xyz

25

Pt	-1.121864377	-0.010904887	-0.045742654
N	-2.510135169	1.289435840	0.663363982
H	-3.395235507	1.218240554	0.165767237
H	-2.709549528	1.132912482	1.648865052
N	-2.359225281	-1.581460859	0.303462379
H	-2.553743494	-1.703132613	1.294726030
H	-3.256041862	-1.478250555	-0.166426479
H	-2.188445180	2.250645652	0.570502693
H	-1.942381069	-2.447809810	-0.031601993
O	0.110697868	1.557296390	-0.461090900
O	0.253658621	-1.307441474	-0.808898495
C	1.393739408	1.421995640	-0.514979939
C	1.525334310	-1.096530301	-0.745587707
O	2.119448227	2.318968446	-0.943713477
O	2.333075649	-1.875766055	-1.249296244
C	2.006445234	0.135998240	0.019965531
C	1.810551444	-0.104122611	1.555424753
C	3.522242359	0.138912296	0.273674774
C	3.272633879	-0.587158822	1.610221138
H	1.021989305	-0.794898749	1.845654860
H	1.672575197	0.847977083	2.066061614
H	4.147294657	-0.347174541	-0.469601162
H	3.865762485	1.157015781	0.438882691
H	3.333698698	-1.668102649	1.496653962
H	3.865663125	-0.277850480	2.466733353

./carboplatin-M06L-SMD-aug-pVTZ_eGeom.xyz

25

Pt	0.261436275	-0.366971520	-0.422034381
N	-0.505431960	1.259948087	0.569069563
H	-1.512012027	1.368877422	0.430356838
H	-0.361273626	1.229170365	1.580303737
N	-0.502994561	-1.654904898	0.985706311
H	-0.443258998	-1.303795763	1.943543849
H	-1.488655932	-1.872718718	0.825622371
H	-0.079407607	2.130411560	0.244609279
H	-0.009071165	-2.549279243	0.976713532
O	1.080717988	0.904263146	-1.786179260
O	1.084638243	-1.971356510	-1.373880283
C	1.239894335	0.528266056	-3.029907110
C	1.222183654	-1.983123365	-2.674684619
O	1.820897561	1.257592639	-3.841373421
O	1.765866160	-2.934848316	-3.245470263
C	0.651838972	-0.805487477	-3.463854480
C	0.606012044	-1.071072226	-4.975295375
C	-0.909240400	-0.886292088	-3.468681554
C	-0.815450661	-1.621603958	-4.811852264
H	1.378919594	-1.731507014	-5.388671376
H	0.613605497	-0.119930355	-5.522424833
H	-1.384664985	-1.394211405	-2.616936347
H	-1.345159235	0.118315498	-3.569398322
H	-0.815762225	-2.711770793	-4.670684891
H	-1.556319932	-1.368323892	-5.581725712

./carboplatin-SMD_eGeom.xyz

25

Pt	-0.233627096	-0.361254944	-0.375199553
N	0.500954519	1.283236188	0.601379152
H	0.147863758	1.375671114	1.568743905
H	1.532443503	1.286455102	0.667417963
N	0.514938988	-1.629099463	1.049623171
H	1.546660331	-1.613184974	1.108651087
H	0.165330460	-1.424283871	2.000653761
H	0.238312990	2.153541266	0.109165152
H	0.248566644	-2.606929812	0.844975373
O	-1.040532344	0.888480658	-1.751809289
O	-1.010022968	-1.982473308	-1.312654727
C	-1.220021846	0.508119780	-3.010417821
C	-1.163196840	-2.022649887	-2.629009341
O	-1.806590997	1.258513189	-3.810872955
O	-1.684404179	-3.017321394	-3.164817216
C	-0.644909375	-0.837750894	-3.460867906
C	0.935439587	-0.886716991	-3.558599950
C	-0.689774401	-1.116097664	-4.987139848
C	0.787090157	-1.584800696	-4.935477745
H	1.462664744	-1.422865057	-2.746195136
H	1.348205912	0.137589931	-3.644759325
H	-1.450798469	-1.845632231	-5.320113472
H	-0.813094645	-0.165886097	-5.538537761
H	0.868423872	-2.685726915	-4.845575240
H	1.457384707	-1.239285801	-5.745691289

./carboplatin-M062X-ApVDZ-ApVDZ-2_eGeom.xyz

25

Pt	0.120514383	-0.361799867	-0.357263687
N	-0.501120297	1.414396448	0.536956592
H	-1.508222991	1.543481728	0.602641916
H	-0.096051726	1.620314082	1.447378713
N	-0.468036799	-1.815164068	1.016526611
H	-0.048816825	-1.747413199	1.941241583
H	-1.472001206	-1.931888750	1.133225282
H	-0.139795162	2.104306003	-0.129896410
H	-0.103343982	-2.662834317	0.569579235
O	0.791835083	0.937464780	-1.694396043
O	0.818995443	-1.981868104	-1.263900380
C	1.106146990	0.565366928	-2.926005041
C	1.081511564	-2.005714405	-2.560507430
O	1.686199309	1.317826460	-3.678461342
O	1.598923730	-2.973602911	-3.075792398
C	0.613090221	-0.804930751	-3.396016321
C	0.743379339	-1.074976808	-4.906998066
C	-0.944836457	-0.889581645	-3.565602608
C	-0.710372529	-1.601351421	-4.917719134
H	1.533667991	-1.772561341	-5.190965819
H	0.852256314	-0.126869040	-5.439966467
H	-1.495488967	-1.425451222	-2.783914923
H	-1.369805669	0.113170301	-3.690408237
H	-0.740192932	-2.689654689	-4.804303680

H -1.351127813 -1.301016960 -5.752560955
./carboplatin-PBE0-H2O-ApVTZ-pVDZ-pp_eGeom.xyz
25

Pt	0.195279421	-0.367020480	-0.402737746
N	-0.527910973	1.288155291	0.534644791
H	-1.541368326	1.308893130	0.587301812
H	-0.176155047	1.404406040	1.479844897
N	-0.509120756	-1.664647260	0.999544771
H	-0.153462467	-1.483138622	1.932773528
H	-1.522257991	-1.676748743	1.061909001
H	-0.239185353	2.106905325	0.005801332
H	-0.213463059	-2.603183922	0.744282410
O	0.972681340	0.880053914	-1.757295761
O	0.975602124	-1.963223681	-1.316315336
C	1.216763149	0.502026521	-2.974285468
C	1.179458207	-2.001446373	-2.596693080
O	1.848871874	1.208840118	-3.747997031
O	1.749412995	-2.947219031	-3.123451525
C	0.645841817	-0.835243727	-3.431338968
C	0.679603333	-1.104641905	-4.944155264
C	-0.917854102	-0.888820431	-3.508384879
C	-0.789714893	-1.558724762	-4.887578770
H	1.418517162	-1.828340533	-5.281339811
H	0.805178629	-0.169431936	-5.487165609
H	-1.423295787	-1.434341313	-2.712437567
H	-1.339599894	0.115221166	-3.568452994
H	-0.883779857	-2.642984224	-4.821147429
H	-1.452734538	-1.195697332	-5.672454315

./carboplatin-CPCM-ApVTZ-pVDZ-pp_eGeom.xyz
25

Pt	0.193584498	-0.362571446	-0.388638868
N	-0.537946710	1.312136459	0.546384848
H	-1.560724539	1.332593260	0.591767197
H	-0.189345265	1.431824140	1.501918730
N	-0.508406852	-1.671533729	1.030538998
H	-0.148835321	-1.482837586	1.970596001
H	-1.530369594	-1.688062609	1.093853136
H	-0.242242428	2.135812620	0.011447307
H	-0.205370090	-2.617579804	0.775090431
O	0.982282723	0.896798274	-1.754932725
O	0.985692208	-1.978885673	-1.299518934
C	1.227015252	0.503367249	-2.986842700
C	1.191309414	-2.013626694	-2.598510222
O	1.868672381	1.219917785	-3.766210927
O	1.774867406	-2.971330416	-3.121815917
C	0.650392620	-0.843021529	-3.440009614
C	0.683794848	-1.117651645	-4.964119676
C	-0.927426202	-0.893647659	-3.518588033
C	-0.801370970	-1.555577632	-4.913164744
H	1.418628623	-1.859231258	-5.296059978
H	0.829590401	-0.180225842	-5.513247666
H	-1.432409948	-1.448894281	-2.719135007

```
H      -1.350131462      0.118440620      -3.566900670
H      -0.912987697      -2.646270336      -4.860483835
H      -1.460956286      -1.170295040      -5.700546142
./carboplatin-PBE0-CPCM-ApVDZ-pVTZ-pp_eGeom.xyz
25
```

```
Pt      0.203683712      -0.359919628      -0.404912220
N      -0.556254643      1.278401247      0.529798316
H      -1.574158230      1.282172007      0.578691555
H      -0.213892198      1.407062705      1.481086061
N      -0.466701051      -1.667738651      1.002350284
H      -0.118096658      -1.476079451      1.940521684
H      -1.482890971      -1.710443947      1.067428342
H      -0.283470314      2.109079372      0.003784082
H      -0.147150799      -2.604715696      0.755121073
O      0.950137226      0.905187887      -1.762981561
O      1.019194061      -1.943596529      -1.313879107
C      1.192590303      0.524056932      -2.985026953
C      1.212231928      -1.978088086      -2.601577366
O      1.811304624      1.243754626      -3.767708619
O      1.804739597      -2.915981389      -3.132348473
C      0.642090409      -0.826390697      -3.435176867
C      0.667473747      -1.097858549      -4.951805453
C      -0.924566986      -0.911800910      -3.494661392
C      -0.799248256      -1.571966055      -4.883547785
H      1.418187986      -1.817915000      -5.292082371
H      0.780503142      -0.156264143      -5.499192173
H      -1.410325621      -1.477640338      -2.691672553
H      -1.370059555      0.089509121      -3.541189106
H      -0.879957084      -2.664307663      -4.823937286
H      -1.478057356      -1.208869935      -5.664211121
./carboplatin-M062X-SMD-ApVDZ-pVTZ_eGeom.xyz
25
```

```
Pt      -0.229223524      -0.364636132      -0.407431287
N      0.513749170      1.246887384      0.575937299
H      0.185049920      1.301466918      1.541427246
H      1.534160321      1.240603424      0.612466003
N      0.541810594      -1.614315458      0.992572934
H      1.562283189      -1.592407415      1.013201380
H      0.222429657      -1.390975744      1.936407423
H      0.238669575      2.117145578      0.118110370
H      0.267211251      -2.580504410      0.807574085
O      -1.062223534      0.884361291      -1.788246984
O      -1.024700365      -1.982699132      -1.365546136
C      -1.281262719      0.493297083      -3.005250025
C      -1.187008519      -2.011686784      -2.651379179
O      -1.936460277      1.182457636      -3.795211490
O      -1.711442730      -2.980125124      -3.211703790
C      -0.666304214      -0.823826079      -3.465564340
C      0.901377027      -0.859969379      -3.492545140
C      -0.644200924      -1.089715372      -4.982211677
C      0.806325601      -1.603074624      -4.843520158
H      1.392814342      -1.362285503      -2.653424882
```


H	1.298080169	0.155063556	-3.604374812
H	-1.402540638	-1.772311133	-5.374037320
H	-0.677432024	-0.139779115	-5.523372753
H	0.837779799	-2.688342802	-4.698956809
H	1.518365863	-1.314981434	-5.622048968

./carboplatin-PBE0-CPCM-TZ-aug-pVDZ-pp_eGeom.xyz

25

Pt	0.201970874	-0.362657160	-0.402107973
N	-0.530108610	1.292039705	0.532710246
H	-1.543553368	1.304563743	0.589357495
H	-0.174661173	1.415120869	1.475677205
N	-0.494774793	-1.663324603	1.003363911
H	-0.136704805	-1.479879937	1.935302516
H	-1.507754056	-1.679587414	1.067928772
H	-0.250112819	2.110010716	-0.001994567
H	-0.195598475	-2.600238727	0.746364171
O	0.971005136	0.887538597	-1.758262764
O	0.987305653	-1.957631079	-1.313897007
C	1.206162899	0.509258996	-2.979245600
C	1.177660261	-1.998370514	-2.598401893
O	1.825022042	1.218774026	-3.757970705
O	1.736872090	-2.946325820	-3.128429121
C	0.640184124	-0.831786737	-3.429827885
C	0.677213391	-1.104419926	-4.941759514
C	-0.922702325	-0.893085081	-3.509954135
C	-0.787514252	-1.572640100	-4.883879068
H	1.423108674	-1.822679474	-5.275177034
H	0.794666089	-0.168708892	-5.485770708
H	-1.429196770	-1.433128109	-2.710889077
H	-1.348255101	0.108798729	-3.580436599
H	-0.868661510	-2.657294764	-4.807380318
H	-1.454266162	-1.224699816	-5.672449357

./carboplatin-M06L-SMD-ApVDZ-pVTZ_eGeom.xyz

25

Pt	0.249035231	-0.371361368	-0.425725817
N	-0.504646224	1.258927878	0.571483081
H	-1.523987111	1.287329059	0.571537787
H	-0.215481492	1.291860310	1.549104173
N	-0.540697474	-1.644876759	0.982166537
H	-0.439442270	-1.306626335	1.938931240
H	-1.536904638	-1.810821948	0.840524435
H	-0.191549324	2.131690880	0.146894454
H	-0.087540913	-2.557539466	0.947493868
O	1.097061371	0.888684102	-1.794237262
O	1.069742275	-1.985120466	-1.380727823
C	1.271239246	0.505527859	-3.028567683
C	1.231412706	-1.990162236	-2.674406434
O	1.889050869	1.220403030	-3.832452614
O	1.802293391	-2.934992036	-3.238780836
C	0.664211482	-0.816407035	-3.469861111
C	0.604449345	-1.078123299	-4.981941276
C	-0.898484604	-0.878527484	-3.460444479

C	-0.827404498	-1.602854981	-4.812019136
H	1.360804952	-1.750041674	-5.401155872
H	0.625220478	-0.127843564	-5.526103945
H	-1.364614032	-1.393214223	-2.611545026
H	-1.322507636	0.129655978	-3.544293597
H	-0.848458930	-2.691763146	-4.680603656
H	-1.565495190	-1.324155845	-5.572398019

./carboplatin-M06L-SMD-TZ-pVTZ_eGeom.xyz

25

Pt	-0.239836200	-0.364651040	-0.420679397
N	0.513927055	1.268835127	0.579000521
H	0.208425617	1.304407074	1.545587855
H	1.527813098	1.280527308	0.589124029
N	0.519431060	-1.648300145	0.999345067
H	1.514076493	-1.804662887	0.878104548
H	0.386755126	-1.313682988	1.947512354
H	0.212114392	2.132004683	0.139858804
H	0.067891069	-2.554453408	0.937940165
O	-1.056312447	0.895402619	-1.798797592
O	-1.050361256	-1.972119713	-1.378496738
C	-1.242944318	0.515731501	-3.026909592
C	-1.209674865	-1.988454949	-2.666676935
O	-1.842682196	1.235947897	-3.826585224
O	-1.757668073	-2.940026702	-3.224120838
C	-0.658479702	-0.813389815	-3.467134201
C	0.902667656	-0.881681071	-3.484776095
C	-0.622538089	-1.080320471	-4.976292353
C	0.804117046	-1.617776183	-4.824884286
H	1.379122257	-1.382181834	-2.642855401
H	1.326532539	0.116548725	-3.586822696
H	-1.384980760	-1.743665629	-5.377305400
H	-0.644045437	-0.139480219	-5.521485254
H	0.816374056	-2.697718046	-4.686130134
H	1.527582889	-1.357192606	-5.593650215

./carboplatin-M062X-aug-pVDZ-2_eGeom.xyz

25

Pt	-0.120405578	-0.361364970	-0.349890751
N	0.508173161	1.410600030	0.553873142
H	0.070080534	1.640963317	1.447339431
H	1.516391682	1.534204992	0.659181373
N	0.439339365	-1.828146027	1.026090275
H	1.441331055	-1.952573811	1.178954120
H	-0.012227391	-1.781835246	1.941086917
H	0.181001766	2.100238505	-0.136847978
H	0.089493310	-2.672585718	0.552531874
O	-0.761198108	0.949671124	-1.686936197
O	-0.820563838	-1.973210698	-1.264885151
C	-1.071527028	0.587994679	-2.925320337
C	-1.071201840	-1.994997940	-2.565716567
O	-1.626498779	1.352403237	-3.679852068
O	-1.576804276	-2.961982759	-3.088556801
C	-0.599435568	-0.790322969	-3.396474412

C	0.953870913	-0.895569849	-3.588167825
C	-0.751358204	-1.060202256	-4.905018254
C	0.687840586	-1.620302460	-4.926185575
H	1.518195114	-1.423824959	-2.805706880
H	1.387845719	0.103872763	-3.737652287
H	-1.561664800	-1.742780137	-5.180287771
H	-0.843099234	-0.108167480	-5.439853340
H	0.689997249	-2.709981161	-4.793651635
H	1.329731200	-1.352452978	-5.775182313

./carboplatin-M062X-CPCM-2_eGeom.xyz

25

Pt	0.214331188	-0.359722918	-0.393066425
N	-0.546959068	1.297477499	0.558837216
H	-1.566768193	1.300355600	0.645165021
H	-0.173972709	1.448121648	1.500139943
N	-0.465769349	-1.700705582	1.013498776
H	-0.083473807	-1.554904153	1.951639038
H	-1.484180279	-1.723310187	1.113605931
H	-0.298603982	2.126706780	0.009902345
H	-0.180042822	-2.641420462	0.723358307
O	0.962872663	0.925437587	-1.761735028
O	1.022651978	-1.956095930	-1.333844764
C	1.195072643	0.550593221	-2.991805013
C	1.174426789	-1.994386033	-2.630333804
O	1.789409071	1.268081590	-3.783393824
O	1.678322516	-2.956923367	-3.191471676
C	0.639818544	-0.803197447	-3.442304204
C	0.673978432	-1.071725145	-4.957391605
C	-0.923416439	-0.889360107	-3.513382812
C	-0.771595041	-1.608269782	-4.872527192
H	1.453082510	-1.759988534	-5.303079862
H	0.732382371	-0.120368913	-5.498925994
H	-1.426663586	-1.418695959	-2.692803051
H	-1.361278505	0.113558104	-3.618688882
H	-0.787792888	-2.699145514	-4.748078438
H	-1.468525025	-1.322464764	-5.670443013

./carboplatin-H20-aug-pVTZ_eGeom.xyz

25

Pt	-0.208134443	-0.358807346	-0.370408269
N	0.527725673	1.303043002	0.576051349
H	0.172827259	1.436757404	1.534919751
H	1.556739866	1.324112889	0.636683612
N	0.457338621	-1.675317433	1.053613736
H	1.484450414	-1.721732268	1.131672405
H	0.097360994	-1.487679165	2.001332845
H	0.247720417	2.139770786	0.039408646
H	0.138417091	-2.624262646	0.800017265
O	-0.951008864	0.916290071	-1.732920059
O	-0.994063048	-1.965708479	-1.283873784
C	-1.161315751	0.539587969	-2.987868885
C	-1.162327323	-2.006420772	-2.598712735
O	-1.735309615	1.295533270	-3.784080128

O	-1.707983205	-2.982524413	-3.132350999
C	-0.622553903	-0.828383705	-3.437813289
C	0.954622066	-0.906878257	-3.566980982
C	-0.706133124	-1.107984514	-4.963583093
C	0.772280608	-1.578022242	-4.953879506
H	1.487461814	-1.466956484	-2.774164942
H	1.392458142	0.108561724	-3.639885719
H	-1.471512299	-1.847546092	-5.261370657
H	-0.855756612	-0.159418952	-5.510997785
H	0.858699716	-2.680488852	-4.890500141
H	1.425302517	-1.215878263	-5.771437647

./carboplatin-pVTZ-pp_eGeom.xyz

25

Pt	-0.112026450	-0.354746403	-0.314180378
N	0.494040407	1.427388362	0.558870967
H	0.068214159	1.660283584	1.468305419
H	1.512098776	1.561458699	0.645625741
N	0.442953745	-1.810765297	1.057351537
H	1.453809305	-1.930829526	1.217508375
H	-0.016083441	-1.758548487	1.978960883
H	0.146645984	2.118935156	-0.134716879
H	0.096160107	-2.669711565	0.586485808
O	-0.773938764	0.946344316	-1.661098580
O	-0.806134471	-1.983772845	-1.217465750
C	-1.043184096	0.581242141	-2.929105307
C	-1.066023612	-2.009562269	-2.537148860
O	-1.558032724	1.386126344	-3.696992815
O	-1.599010441	-2.997103419	-3.031751740
C	-0.591420460	-0.814381041	-3.389496579
C	0.972708297	-0.918426200	-3.625522368
C	-0.782820284	-1.094182100	-4.905850018
C	0.685005958	-1.590475998	-4.993448320
H	1.549613496	-1.482850729	-2.866047288
H	1.417957689	0.090942940	-3.731648370
H	-1.575650104	-1.826031897	-5.142139089
H	-0.959223141	-0.142718249	-5.440008584
H	0.751132162	-2.694009224	-4.929354659
H	1.290514914	-1.244959063	-5.854262156

./carboplatin-PBE0-H2O_eGeom.xyz

25

Pt	0.201062117	-0.359688456	-0.380026732
N	-0.530860447	1.296638506	0.562445335
H	-1.549280001	1.310880829	0.656329731
H	-0.150027426	1.450418332	1.499500798
N	-0.467188113	-1.678851504	1.029175967
H	-0.091334414	-1.518197264	1.966919336
H	-1.485131036	-1.710775837	1.125202693
H	-0.279109521	2.120157634	0.007672072
H	-0.172026549	-2.620732970	0.754897032
O	0.938057844	0.904841185	-1.742121488
O	0.982259629	-1.951671952	-1.304322576
C	1.156465115	0.539295899	-2.980022935

C	1.155446239	-1.994381890	-2.600439702
O	1.726431244	1.283082630	-3.767682118
O	1.687039522	-2.959212278	-3.134571654
C	0.625987010	-0.819948188	-3.432215479
C	0.706167207	-1.094173113	-4.945915392
C	-0.936621570	-0.906876672	-3.553538114
C	-0.753742312	-1.587411887	-4.924455680
H	1.478355098	-1.809691243	-5.254485721
H	0.827336573	-0.148188406	-5.488716446
H	-1.462452366	-1.457125383	-2.760207655
H	-1.379296286	0.096845818	-3.637844539
H	-0.816487382	-2.682368439	-4.845034451
H	-1.413743164	-1.253218120	-5.737671292

./carboplatin-M06L-CPCM-ApVDZ-pVDZ_eGeom.xyz

25

Pt	0.214695800	-0.360364069	-0.415930864
N	-0.572193189	1.306941701	0.537282984
H	-1.590356779	1.322622446	0.564572750
H	-0.256712339	1.427382609	1.498485371
N	-0.482679952	-1.702667756	1.009436572
H	-0.113129985	-1.543153762	1.945236785
H	-1.497302122	-1.720772036	1.099513745
H	-0.286674124	2.146459421	0.033972576
H	-0.200083684	-2.645978064	0.744846593
O	0.995427771	0.928061551	-1.788831956
O	1.052987032	-1.966912739	-1.346300869
C	1.230050607	0.528892930	-3.011648847
C	1.228910268	-1.982458381	-2.641651321
O	1.861495737	1.235720392	-3.801382320
O	1.805803181	-2.921669485	-3.194072170
C	0.656067978	-0.814077960	-3.449906265
C	0.640449231	-1.080747585	-4.962191644
C	-0.905072053	-0.896805587	-3.475790095
C	-0.800593595	-1.596483733	-4.839589353
H	1.402794067	-1.768587086	-5.342573320
H	0.697706090	-0.133929514	-5.509759557
H	-1.384156404	-1.432391323	-2.646782040
H	-1.347455490	0.105031377	-3.546740931
H	-0.836457000	-2.687690896	-4.733157719
H	-1.516214039	-1.296775222	-5.614167114

./carboplatin-PBE0-H20-aug-pVDZ_eGeom.xyz

25

Pt	0.207808391	-0.362291077	-0.388397647
N	-0.523349926	1.287612231	0.555672339
H	-1.543302649	1.309311708	0.622913189
H	-0.164346975	1.420781802	1.503818011
N	-0.472693535	-1.672085451	1.016570916
H	-0.112374810	-1.498850548	1.957516195
H	-1.491636774	-1.706134968	1.094761451
H	-0.249297528	2.116822551	0.021150576
H	-0.168769488	-2.614684387	0.756681249
O	0.957155130	0.902056006	-1.742837660

O	0.989433085	-1.956063676	-1.306899991
C	1.173359165	0.532623269	-2.979247887
C	1.158900774	-1.995802351	-2.602882966
O	1.756491014	1.266390858	-3.767162820
O	1.692920348	-2.957170405	-3.141581523
C	0.626543921	-0.819985938	-3.431130507
C	0.692557853	-1.095186207	-4.945502671
C	-0.937152913	-0.896013435	-3.541114948
C	-0.767262253	-1.587672280	-4.908095308
H	1.462055628	-1.809895583	-5.262292259
H	0.806686726	-0.149178861	-5.489835213
H	-1.463328068	-1.433807493	-2.739561663
H	-1.370286336	0.111326079	-3.633311745
H	-0.828504546	-2.681932810	-4.818099076
H	-1.434299225	-1.260521806	-5.718259053

./carboplatin-M06L-CPCM-ApVTZ-pVTZ_eGeom.xyz

25

Pt	0.204184243	-0.365874069	-0.410432700
N	-0.555369822	1.303195094	0.552122699
H	-1.567444213	1.318407082	0.588044461
H	-0.224790850	1.412010262	1.503553317
N	-0.479826890	-1.707958799	1.014253600
H	-0.120487360	-1.530575871	1.944556729
H	-1.489681639	-1.735115524	1.088318195
H	-0.265824618	2.131347805	0.042999820
H	-0.177027416	-2.640209648	0.753152852
O	0.969614693	0.915225321	-1.781366508
O	1.015323619	-1.965911172	-1.350889375
C	1.212860219	0.530283683	-2.999767438
C	1.198298589	-1.987470296	-2.638029341
O	1.834658874	1.243401148	-3.780754076
O	1.755731160	-2.932057077	-3.185952529
C	0.649691241	-0.811218280	-3.448442567
C	0.651873595	-1.072138413	-4.958980064
C	-0.910051032	-0.888278761	-3.499097519
C	-0.784264769	-1.597342803	-4.852554829
H	1.416795236	-1.748029330	-5.333247973
H	0.707054408	-0.128822390	-5.497699640
H	-1.402289455	-1.408819711	-2.678687308
H	-1.343130735	0.107859306	-3.586957485
H	-0.811580156	-2.679847887	-4.738419168
H	-1.487009911	-1.312412440	-5.632852163

./carboplatin-M06L-CPCM-ApVTZ-ApVTZ-3_eGeom.xyz

25

Pt	-1.113061201	-0.012138176	0.039985497
N	-2.476203262	1.390276725	-0.638148363
H	-2.683561826	1.303636580	-1.625785462
H	-3.362373944	1.366509925	-0.147854274
N	-2.349130847	-1.636637171	-0.315685057
H	-3.218442892	-1.603367731	0.203177590
H	-2.592694712	-1.752224994	-1.292101309
H	-2.086652288	2.316324080	-0.498533587

H	-1.865559746	-2.480969085	-0.029284210
O	0.095955169	1.551276746	0.489905209
O	0.225499585	-1.346668969	0.770344025
C	1.387447599	1.406370131	0.543960178
C	1.506369625	-1.126640482	0.728955623
O	2.109943278	2.293477152	0.986561078
O	2.303032807	-1.908845398	1.235886673
C	1.984675557	0.121796739	-0.014858889
C	3.498638960	0.132201179	-0.255258697
C	1.801872823	-0.073943741	-1.554272616
C	3.269350193	-0.511279879	-1.627559369
H	4.105101144	-0.409017760	0.466470605
H	3.855193525	1.156717049	-0.332868582
H	1.031652135	-0.775304036	-1.872066535
H	1.623162757	0.881381918	-2.046878320
H	3.364900727	-1.595225894	-1.589310765
H	3.858489044	-0.141337369	-2.464064976

./carboplatin-M06L-H20-pVTZ_eGeom.xyz
25

Pt	0.216771930	-0.363445968	-0.408536548
N	-0.547342291	1.309633958	0.549519680
H	-1.567425437	1.336821032	0.591918593
H	-0.218843396	1.435888571	1.508543264
N	-0.480740041	-1.707219430	1.013177512
H	-0.119445075	-1.547581849	1.955127528
H	-1.498186162	-1.735646468	1.098934165
H	-0.261946141	2.147271426	0.037579950
H	-0.189745940	-2.651526873	0.750657866
O	0.992161526	0.923398859	-1.770525456
O	1.030085619	-1.970229479	-1.340102139
C	1.211089943	0.539253038	-3.006856031
C	1.194508296	-1.993538922	-2.641783036
O	1.808886358	1.262764075	-3.799854203
O	1.729728937	-2.950025132	-3.196625499
C	0.647174051	-0.808521476	-3.445149387
C	0.656370167	-1.075034659	-4.956584378
C	-0.912507807	-0.890538609	-3.500437762
C	-0.779549127	-1.605053364	-4.852950041
H	1.432578172	-1.757375986	-5.325336454
H	0.713854076	-0.124989461	-5.502898919
H	-1.414809208	-1.411876257	-2.672065435
H	-1.353683848	0.112976689	-3.595880418
H	-0.801963247	-2.697502415	-4.732615097
H	-1.489714347	-1.328254069	-5.644386766

./carboplatin_eGeom.xyz
25

Pt	-0.104193951	-0.352472877	-0.306489301
N	0.494692722	1.441329105	0.566291223
H	0.051184563	1.688230789	1.464240810
H	1.510054454	1.587116977	0.670716289
N	0.445191837	-1.821799741	1.065080571
H	1.453768294	-1.952777207	1.234438872

H	-0.021792093	-1.785908288	1.984146859
H	0.154946475	2.121372243	-0.143968586
H	0.098413799	-2.672053971	0.576269084
O	-0.763943566	0.949923312	-1.661097659
O	-0.797837634	-1.984293437	-1.217158554
C	-1.031324652	0.585966547	-2.929379550
C	-1.061365499	-2.008388893	-2.535807941
O	-1.535960143	1.396736061	-3.698168620
O	-1.593342214	-2.997750539	-3.028274012
C	-0.590285778	-0.813209333	-3.390312269
C	0.972177542	-0.924239653	-3.633942727
C	-0.790591072	-1.092785274	-4.905523727
C	0.675020632	-1.594291649	-5.000833388
H	1.548764490	-1.492467465	-2.877139024
H	1.422444653	0.082736613	-3.741357947
H	-1.586981877	-1.822245063	-5.137368376
H	-0.966566861	-0.140828517	-5.439017972
H	0.737491684	-2.698105700	-4.937972206
H	1.277341203	-1.250146810	-5.864500859

./carboplatin-M062X-SMD-ApVTZ-pVDZ_eGeom.xyz

25

Pt	-0.223493922	-0.359753715	-0.404408669
N	0.553535724	1.226237039	0.597519628
H	0.209913782	1.284286790	1.553710751
H	1.568868899	1.184525072	0.648456286
N	0.469780094	-1.640405640	1.010104277
H	1.486104105	-1.650558568	1.053990630
H	0.133205057	-1.405556589	1.941238525
H	0.311173713	2.100491465	0.136395659
H	0.165944858	-2.591457531	0.811685331
O	-0.981977070	0.915898131	-1.803277904
O	-1.053526112	-1.944475476	-1.385863398
C	-1.218217100	0.537643099	-3.014990784
C	-1.209003498	-1.970656085	-2.666735695
O	-1.842946503	1.248140809	-3.802299025
O	-1.751300843	-2.920174409	-3.230249297
C	-0.654426036	-0.798382744	-3.476002771
C	0.909186739	-0.885733438	-3.501738211
C	-0.635619939	-1.061346301	-4.990116858
C	0.790462518	-1.628325053	-4.846524983
H	1.384159710	-1.394277580	-2.665696914
H	1.335652753	0.109720316	-3.617691495
H	-1.411534781	-1.708981073	-5.387527694
H	-0.629571778	-0.116529969	-5.527801465
H	0.780070504	-2.706976574	-4.700016150
H	1.510866136	-1.373704746	-5.619288785

./carboplatin-M06L-SMD-ApVTZ-pVDZ_eGeom.xyz

25

Pt	-0.227324828	-0.369146391	-0.418302834
N	0.513469448	1.266437487	0.583343909
H	0.216567649	1.292205970	1.552762381
H	1.527037519	1.291755953	0.584456794

N	0.544126537	-1.645876566	0.998254391
H	1.537324674	-1.803447004	0.868189992
H	0.421119505	-1.307289233	1.946200664
H	0.196313266	2.128300693	0.152823278
H	0.091352859	-2.551754384	0.945678320
O	-1.058956525	0.885947025	-1.793403416
O	-1.028881851	-1.980859842	-1.378601785
C	-1.254617937	0.507427077	-3.018253413
C	-1.204314912	-1.993763195	-2.662779600
O	-1.868435579	1.225165425	-3.812070490
O	-1.760203448	-2.944747204	-3.216604018
C	-0.664771807	-0.816249718	-3.467790324
C	0.896606951	-0.874237008	-3.493673395
C	-0.634652426	-1.080416884	-4.977368808
C	0.794686665	-1.612518437	-4.832189375
H	1.380550509	-1.370553052	-2.653518502
H	1.311474037	0.127281406	-3.600673164
H	-1.396742162	-1.744527657	-5.377966633
H	-0.658826426	-0.137867843	-5.519622571
H	0.811124475	-2.692175322	-4.691161785
H	1.513280819	-1.349444069	-5.604858626

./carboplatin-CPCM-TZ-aug-pVTZ-pp_eGeom.xyz
25

Pt	0.195490926	-0.362864166	-0.381411612
N	-0.525778710	1.316194724	0.555997989
H	-1.548088136	1.338025382	0.610473450
H	-0.168129246	1.438988558	1.507811820
N	-0.504548120	-1.673201042	1.038853215
H	-0.136611835	-1.490568365	1.976899476
H	-1.526123169	-1.684039473	1.109674605
H	-0.233517886	2.136748037	0.014214300
H	-0.208671243	-2.619569773	0.775869338
O	0.978149189	0.895493767	-1.746342708
O	0.971551926	-1.981202506	-1.294525745
C	1.216044054	0.505625111	-2.982981655
C	1.167246860	-2.020082206	-2.596890686
O	1.847295299	1.226166719	-3.763516262
O	1.727186956	-2.987605983	-3.122981204
C	0.641659995	-0.841306043	-3.436952623
C	0.694406722	-1.116568629	-4.960565267
C	-0.935135135	-0.888603957	-3.538865987
C	-0.789464128	-1.559779684	-4.927001007
H	1.435708626	-1.856873877	-5.280456004
H	0.844600192	-0.178000246	-5.506361276
H	-1.455888291	-1.435979096	-2.744110789
H	-1.353389684	0.124587249	-3.602039636
H	-0.895261405	-2.650552870	-4.866020807
H	-1.441426745	-1.185384400	-5.725899935

./carboplatin-aug-pVTZ_eGeom.xyz
25

Pt	-0.119904106	-0.356872255	-0.322451158
N	0.493264170	1.419856427	0.546042723

H	0.085115740	1.644443464	1.464889544
H	1.512091440	1.555232671	0.613478722
N	0.464927024	-1.801458404	1.042089239
H	1.478655549	-1.912024976	1.186446089
H	0.020126127	-1.747842821	1.969904799
H	0.131563801	2.115857593	-0.134937689
H	0.118033371	-2.665394459	0.581511308
O	-0.808258004	0.938348485	-1.657265818
O	-0.819551486	-1.986242563	-1.214593254
C	-1.070829368	0.570721717	-2.924048464
C	-1.073151988	-2.014237040	-2.533728993
O	-1.599446265	1.366983676	-3.692989003
O	-1.603995445	-3.002369999	-3.031463495
C	-0.599332115	-0.818022428	-3.385431709
C	0.967424757	-0.907926154	-3.610861463
C	-0.777294849	-1.099231964	-4.903374133
C	0.695094952	-1.583414377	-4.980203130
H	1.544875168	-1.466977814	-2.847743199
H	1.403269328	0.105896896	-3.715299300
H	-1.562709113	-1.836823496	-5.146104313
H	-0.956757918	-0.149547287	-5.439491249
H	0.770451718	-2.686322783	-4.914803361
H	1.303644522	-1.232984879	-5.836701701

./carboplatin-M06L-CPCM-TZ-pVTZ_eGeom.xyz

25

Pt	0.206714998	-0.367549487	-0.409859945
N	-0.545966003	1.309890672	0.548513028
H	-1.557805453	1.329763965	0.589088711
H	-0.210095800	1.422852141	1.497612711
N	-0.490210857	-1.709404703	1.012527801
H	-0.129075668	-1.538452940	1.943357663
H	-1.500235515	-1.729985419	1.086601463
H	-0.255082650	2.133074157	0.032179090
H	-0.193807577	-2.642314077	0.746450317
O	0.982827804	0.910398042	-1.776737484
O	1.010501177	-1.973835105	-1.345427713
C	1.220192928	0.523929232	-2.998087210
C	1.188864480	-1.997911644	-2.635096664
O	1.840178178	1.234354646	-3.780146677
O	1.732014994	-2.948465203	-3.183640362
C	0.650130514	-0.815712215	-3.443317119
C	0.656301097	-1.076551113	-4.953853969
C	-0.909959473	-0.882826758	-3.498539695
C	-0.786144940	-1.585897492	-4.855576522
H	1.414645893	-1.763308292	-5.321450794
H	0.729012820	-0.134943058	-5.493296058
H	-1.407248234	-1.404974585	-2.682172620
H	-1.338907908	0.115572121	-3.580509313
H	-0.826840050	-2.668682845	-4.748761100
H	-1.482697744	-1.289372809	-5.636986549

./carboplatin-SMD-aug-pVDZ_eGeom.xyz

25

Pt	-0.231902946	-0.364012770	-0.383198094
N	0.516090717	1.261560154	0.603656569
H	0.203625946	1.314327975	1.587228139
H	1.548952582	1.281465978	0.622275555
N	0.497583892	-1.637794115	1.040079346
H	1.515737854	-1.791067268	0.951659181
H	0.332941217	-1.312398384	2.006565608
H	0.214315936	2.141126456	0.152572735
H	0.055409748	-2.568774657	0.963398963
O	-1.022747587	0.903206233	-1.751499616
O	-1.031889529	-1.972441629	-1.320793416
C	-1.210369424	0.523780350	-3.008564629
C	-1.181990287	-2.003717023	-2.636932141
O	-1.800531567	1.274488386	-3.806668812
O	-1.721378598	-2.984989329	-3.180372687
C	-0.642196225	-0.823663931	-3.462313819
C	0.937837286	-0.888478917	-3.550315683
C	-0.678651879	-1.098748874	-4.989632542
C	0.788808629	-1.594294819	-4.923143952
H	1.456882634	-1.421278907	-2.730356056
H	1.357687625	0.132375493	-3.645135948
H	-1.450555118	-1.812158842	-5.332127721
H	-0.775958050	-0.145030689	-5.540130189
H	0.847743735	-2.695797468	-4.822880138
H	1.471860417	-1.268036169	-5.730499662

./carboplatin-PBE0-SMD-aug-pVTZ_eGeom.xyz

25

Pt	-0.239326804	-0.362479643	-0.402028540
N	0.515241115	1.237302898	0.576348225
H	0.199999054	1.296358521	1.547873518
H	1.537868483	1.239710297	0.602213468
N	0.478221415	-1.626342993	1.004032079
H	1.486906978	-1.774856710	0.918059248
H	0.312013589	-1.308037565	1.961680080
H	0.233178461	2.110765493	0.124614220
H	0.041270032	-2.547750753	0.921877563
O	-1.009932474	0.890831238	-1.759942658
O	-1.038605971	-1.944777840	-1.335021822
C	-1.200023359	0.522499487	-2.997129737
C	-1.178215810	-1.986684106	-2.630593820
O	-1.785086250	1.258749923	-3.792328261
O	-1.702343387	-2.957802923	-3.177276899
C	-0.637171972	-0.816692102	-3.450504420
C	0.929349165	-0.890358998	-3.524659508
C	-0.663236296	-1.088148073	-4.966554991
C	0.787149694	-1.599393251	-4.884931326
H	1.439093645	-1.417733286	-2.706197344
H	1.353951724	0.119566007	-3.622738347
H	-1.436089915	-1.781216194	-5.322252183
H	-0.734536513	-0.139381602	-5.513404326
H	0.830375437	-2.692794728	-4.775682269
H	1.477256970	-1.291685868	-5.682580961

./carboplatin-PBE0-SMD_eGeom.xyz

25

Pt	-0.234193283	-0.363631128	-0.393104086
N	0.505134766	1.258775063	0.578068363
H	0.155258671	1.348598073	1.536964758
H	1.527393194	1.253473325	0.643627712
N	0.516313688	-1.621383717	1.012692638
H	1.538005782	-1.589434060	1.078198442
H	0.159953563	-1.430680906	1.954101291
H	0.251378524	2.124947023	0.093584095
H	0.269133658	-2.592472416	0.799768701
O	-1.037371192	0.874314081	-1.758952479
O	-1.011323270	-1.964984746	-1.330142922
C	-1.225009995	0.502362884	-2.996979410
C	-1.159038328	-2.010166966	-2.626212816
O	-1.818620606	1.232534063	-3.789959690
O	-1.665554109	-2.993052929	-3.166419786
C	-0.646784421	-0.830279223	-3.450502556
C	0.919871904	-0.878918462	-3.536210288
C	-0.680900406	-1.103584210	-4.965729416
C	0.779472702	-1.587710006	-4.896912680
H	1.442618221	-1.401032174	-2.722524888
H	1.329976819	0.136972649	-3.633750082
H	-1.443535952	-1.811964335	-5.313464083
H	-0.776368912	-0.156916276	-5.512711358
H	0.844208133	-2.680357205	-4.790895638
H	1.457287859	-1.265761170	-5.699662833

./carboplatin-M06L-SMD-aug-pVDZ-2_eGeom.xyz

25

Pt	-0.975798905	-0.010524249	-0.254299693
N	-2.270499136	1.401087886	0.499006652
H	-3.242518120	1.240018098	0.224609646
H	-2.267485422	1.446394908	1.520606773
N	-2.110689350	-1.539068538	0.532773279
H	-1.934782895	-1.689381067	1.529004467
H	-3.118789580	-1.392754360	0.442320773
H	-2.034014927	2.341222587	0.172821686
H	-1.908490861	-2.428637011	0.070782329
O	0.121187990	1.494555002	-1.096272391
O	0.273605794	-1.411991423	-1.066412791
C	1.413827007	1.361712760	-1.259522456
C	1.551893274	-1.171344475	-1.210083974
O	2.066668324	2.225534536	-1.854692017
O	2.294472785	-2.000670181	-1.745588626
C	2.098557961	0.144447693	-0.658060003
C	2.122437842	0.086678101	0.903720664
C	3.632750125	0.176171490	-0.616123806
C	3.581199159	-0.379340915	0.811845427
H	1.383841665	-0.567768467	1.389659548
H	2.031541593	1.098016009	1.326261083
H	4.164046273	-0.400775438	-1.383808106
H	3.985505965	1.215108370	-0.636409433
H	3.650888411	-1.476390486	0.823939478

H 4.290473028 0.024283166 1.546611494
./carboplatin-M062X-SMD-aug-pVDZ-2_eGeom.xyz
25

Pt 0.243206496 -0.362216265 -0.402985641
N -0.533685953 1.233378946 0.591296737
H -1.558161974 1.230260690 0.608619583
H -0.224629819 1.279743371 1.567348171
N -0.475773320 -1.650740092 0.998605293
H -0.335097734 -1.326072977 1.960209235
H -1.480630379 -1.821725363 0.892176530
H -0.251172331 2.115390853 0.152260010
H -0.015673031 -2.563692268 0.926310316
O 1.019533904 0.920595031 -1.782599003
O 1.076710755 -1.952158928 -1.371036179
C 1.222006386 0.543785522 -3.013499334
C 1.198615324 -1.980376443 -2.666930543
O 1.821390040 1.260308558 -3.813182428
O 1.704001993 -2.942647666 -3.242279322
C 0.646347057 -0.794962578 -3.465591992
C 0.637887577 -1.060946192 -4.981693054
C -0.918630264 -0.878954578 -3.499934321
C -0.792921013 -1.623741239 -4.846531200
H 1.421302457 -1.723397664 -5.366757648
H 0.645002665 -0.107835261 -5.523252236
H -1.406933447 -1.390116734 -2.659379769
H -1.347027394 0.125879952 -3.622060659
H -0.782611504 -2.711461602 -4.695349758
H -1.515749481 -1.368649845 -5.630891797
./carboplatin-PBE0-TZ-aug-pVTZ-pp_eGeom.xyz
25

Pt -0.095446605 -0.360998986 -0.341193202
N 0.466848842 1.409001460 0.545588437
H 0.035149139 1.603730058 1.441984907
H 1.466934453 1.546450691 0.637797540
N 0.490324147 -1.777258305 1.033575593
H 1.489692423 -1.855623135 1.183768254
H 0.037376662 -1.711968643 1.938335135
H 0.114266955 2.089651405 -0.129794432
H 0.168343084 -2.634804301 0.581230938
O -0.769447297 0.906017055 -1.679376609
O -0.738124683 -1.983094547 -1.242342914
C -1.077534117 0.542143972 -2.910374879
C -1.026880603 -2.019900249 -2.528841408
O -1.646327086 1.304639845 -3.654058209
O -1.544596957 -2.996703538 -3.015326446
C -0.598089615 -0.825516573 -3.383430676
C 0.950231023 -0.890666029 -3.624534168
C -0.787654601 -1.103317202 -4.884340841
C 0.673523499 -1.578805683 -4.971599679
H 1.539930939 -1.425620328 -2.879049219
H 1.362479300 0.112267213 -3.746628891
H -1.561933819 -1.826598900 -5.127281355

H -0.964047362 -0.168103730 -5.412302639
H 0.750400345 -2.663374582 -4.893663867
H 1.261888944 -1.241899737 -5.825270378
./carboplatin-M062X-ApVDZ-pVTZ_eGeom.xyz
25

Pt 0.112860119 -0.366551709 -0.353518618
N -0.508070537 1.404803811 0.545341833
H -1.515623979 1.535373424 0.602358088
H -0.112511539 1.606311994 1.460907500
N -0.464886222 -1.824767825 1.016783348
H -0.051641983 -1.752635125 1.943882756
H -1.467939383 -1.954053188 1.129342326
H -0.140715218 2.098732956 -0.114092601
H -0.089193653 -2.669201301 0.572583436
O 0.778620257 0.934793727 -1.684152080
O 0.808314618 -1.979885023 -1.265502008
C 1.093171743 0.573233431 -2.918778689
C 1.076737927 -2.000553726 -2.560459027
O 1.662197392 1.336545517 -3.668713262
O 1.596436312 -2.967143901 -3.076334158
C 0.611944606 -0.798352631 -3.395369521
C 0.754339515 -1.064513916 -4.905960166
C -0.944030773 -0.887594315 -3.578577256
C -0.695485940 -1.601426898 -4.926725045
H 1.552427823 -1.754371287 -5.187145200
H 0.858316321 -0.113419544 -5.434755139
H -1.500324561 -1.421574252 -2.799596624
H -1.368847533 0.114326738 -3.711019767
H -0.716971952 -2.689671585 -4.809897672
H -1.331816350 -1.308758141 -5.767731465
./carboplatin-H20-TZ-aug-pVTZ-pp_eGeom.xyz
25

Pt 0.193268782 -0.363257432 -0.380736016
N -0.501840998 1.329555961 0.551766776
H -1.523567489 1.367411449 0.607958836
H -0.140412011 1.450263969 1.502434253
N -0.533568127 -1.659526089 1.039166127
H -0.165058005 -1.482512059 1.978066612
H -1.555371749 -1.652832217 1.107194909
H -0.197883841 2.143522863 0.006450331
H -0.253235921 -2.611063251 0.777793836
O 1.000717975 0.879966126 -1.744737158
O 0.944732818 -1.995878525 -1.288650514
C 1.237269646 0.484802242 -2.980037095
C 1.146734211 -2.039649524 -2.589931887
O 1.881842563 1.194845141 -3.759177789
O 1.693673610 -3.016755883 -3.111782286
C 0.644138324 -0.853907677 -3.434371748
C 0.699751558 -1.132728103 -4.957210247
C -0.932682872 -0.876403592 -3.543722448
C -0.791143278 -1.552267354 -4.930014655
H 1.430737813 -1.885239712 -5.272250130

H	0.867437146	-0.197627233	-5.503865919
H	-1.465723478	-1.414133328	-2.750504825
H	-1.334652531	0.143132540	-3.610613615
H	-0.914573930	-2.641109044	-4.867714480
H	-1.433283205	-1.168962040	-5.732639875

./carboplatin-M062X-CPCM-ApVDZ-pVTZ_eGeom.xyz

25

Pt	0.206123912	-0.361937829	-0.400932099
N	-0.555804039	1.282807188	0.547136458
H	-1.574549464	1.293424743	0.580150027
H	-0.226455481	1.396805830	1.505150251
N	-0.478166546	-1.684201134	1.004288869
H	-0.119652321	-1.508115042	1.942008193
H	-1.494731577	-1.710924122	1.075176549
H	-0.267619982	2.116361009	0.033175637
H	-0.173943144	-2.622477407	0.741233485
O	0.968255318	0.918071260	-1.774908198
O	1.018017498	-1.963100600	-1.339909967
C	1.228245567	0.526290583	-2.987530864
C	1.193373878	-1.994906756	-2.627937496
O	1.878759944	1.217580132	-3.768145141
O	1.737582335	-2.945505747	-3.184258267
C	0.648908647	-0.813490141	-3.445258637
C	0.657860631	-1.076482537	-4.962447979
C	-0.916820663	-0.881150755	-3.492825488
C	-0.795654284	-1.591996039	-4.860170070
H	1.421536076	-1.768257576	-5.325899509
H	0.718245491	-0.126324593	-5.500599356
H	-1.410062780	-1.412462701	-2.672672151
H	-1.340733282	0.125396126	-3.582826086
H	-0.830497919	-2.680493311	-4.745301852
H	-1.494910805	-1.285263349	-5.643825321

./carboplatin-M062X_eGeom.xyz

25

Pt	-0.115270099	-0.363437990	-0.342024009
N	0.490050781	1.423396220	0.561909072
H	0.051202029	1.655897236	1.454939101
H	1.496417041	1.566292515	0.664940074
N	0.447316669	-1.839220432	1.032440192
H	1.449350117	-1.976426836	1.177228709
H	0.004718443	-1.798476273	1.952548031
H	0.151163563	2.103610882	-0.133271497
H	0.087133367	-2.677850831	0.555270347
O	-0.765377206	0.941106245	-1.678853848
O	-0.795764590	-1.978976718	-1.264140549
C	-1.060569855	0.589023112	-2.924309269
C	-1.054170691	-2.001237384	-2.563860143
O	-1.590563860	1.366738616	-3.682843935
O	-1.550355917	-2.974092033	-3.084463472
C	-0.597959085	-0.792058122	-3.395702819
C	0.953935185	-0.894608223	-3.599420525
C	-0.761080034	-1.061516844	-4.903178039

C	0.680415299	-1.615393190	-4.937700034
H	1.520792493	-1.425498453	-2.820776660
H	1.386701107	0.105532092	-3.746640872
H	-1.570842282	-1.747270596	-5.172630507
H	-0.861839204	-0.108841888	-5.435309652
H	0.688058210	-2.705682876	-4.810033561
H	1.313845527	-1.341361000	-5.791245144

./carboplatin-PBE0-SMD-aug-pVDZ_eGeom.xyz

25

Pt	-0.237968146	-0.366180807	-0.399205727
N	0.480239237	1.257679208	0.575484996
H	0.163206344	1.312091528	1.547697419
H	1.503350209	1.286596435	0.601104378
N	0.518702540	-1.612619125	1.008025064
H	1.531962269	-1.733305094	0.921660441
H	0.344055395	-1.299462552	1.966821340
H	0.176353440	2.123660196	0.121264738
H	0.108033563	-2.547188890	0.926578027
O	-1.049289448	0.868477751	-1.761736506
O	-1.003555923	-1.973881347	-1.332865647
C	-1.238473214	0.490205065	-2.997029883
C	-1.147662345	-2.017974614	-2.628655712
O	-1.850129965	1.207113105	-3.788915294
O	-1.649012335	-3.001927445	-3.172492841
C	-0.641382014	-0.833810174	-3.450874774
C	0.925857198	-0.865624724	-3.531209423
C	-0.665713215	-1.108787361	-4.966184060
C	0.796063676	-1.586897348	-4.886238482
H	1.453637384	-1.372617309	-2.711187025
H	1.322064715	0.154854269	-3.639326851
H	-1.423904627	-1.819437528	-5.318784327
H	-0.759089829	-0.162509857	-5.514207341
H	0.862897954	-2.678268325	-4.768463679
H	1.477064147	-1.270537830	-5.688387843

./carboplatin-PBE0-CPCM-ApVTZ-pVTZ-pp-2_eGeom.xyz

25

Pt	-1.111759480	-0.011978795	0.035754861
N	-2.447724576	1.375408054	-0.620377238
H	-2.659672087	1.289566281	-1.609470644
H	-3.331909829	1.355247487	-0.121641879
N	-2.332116461	-1.598270993	-0.337523424
H	-3.215708196	-1.553907638	0.160390817
H	-2.548504423	-1.714741258	-1.322581704
H	-2.046502667	2.298983342	-0.479784224
H	-1.858938869	-2.444840990	-0.032501890
O	0.083183886	1.522203209	0.492760276
O	0.199494060	-1.340318899	0.745564283
C	1.372810967	1.391492600	0.547997510
C	1.479452203	-1.131410616	0.728517975
O	2.086598517	2.279355613	0.995652467
O	2.260099634	-1.912297012	1.255756016
C	1.982272961	0.110868784	-0.010227340

C	3.505038877	0.119910041	-0.218945468
C	1.822726151	-0.071224374	-1.557910088
C	3.307218318	-0.469824488	-1.626570955
H	4.085747415	-0.461225086	0.494143277
H	3.872070721	1.144549710	-0.245225639
H	1.076555602	-0.793684175	-1.886268900
H	1.623396843	0.884605708	-2.044047420
H	3.435369035	-1.552531421	-1.641532707
H	3.894724397	-0.034990085	-2.434748960

./carboplatin-H2O-TZ-aug-pVDZ-pp_eGeom.xyz

25

Pt	0.193944801	-0.359848949	-0.383341306
N	-0.566455029	1.300189448	0.559163101
H	-1.588644487	1.296714654	0.619165939
H	-0.205901347	1.431754476	1.508670067
N	-0.471928142	-1.688262017	1.038034454
H	-0.108413461	-1.495831533	1.975799020
H	-1.492839446	-1.726661258	1.108659756
H	-0.297649672	2.127571809	0.015769103
H	-0.150746857	-2.626318652	0.775223189
O	0.944021837	0.920427208	-1.750155247
O	1.010979629	-1.958675028	-1.301147683
C	1.184461388	0.536915583	-2.988949509
C	1.203332691	-1.988975032	-2.604814217
O	1.792732447	1.273756083	-3.771809678
O	1.788893791	-2.938949980	-3.134005290
C	0.641445031	-0.823767807	-3.440172397
C	0.691013926	-1.096664870	-4.964132011
C	-0.934059262	-0.911262269	-3.531050853
C	-0.780655693	-1.578103738	-4.920592737
H	1.449113158	-1.817307474	-5.289481152
H	0.813412208	-0.154235942	-5.510267412
H	-1.434888548	-1.471668587	-2.732572675
H	-1.378586936	0.090875190	-3.590997491
H	-0.857651723	-2.671281172	-4.859245815
H	-1.447623295	-1.220742914	-5.714878168

./carboplatin-M06L-CPCM-TZ-pVDZ_eGeom.xyz

25

Pt	0.209456760	-0.368634290	-0.409348084
N	-0.542150365	1.310873032	0.547906349
H	-1.553954464	1.332247557	0.588210821
H	-0.205844714	1.424138129	1.496787988
N	-0.493945411	-1.710268767	1.011159623
H	-0.133195388	-1.542040970	1.942627443
H	-1.504120238	-1.728156983	1.083768247
H	-0.249973149	2.132968454	0.030620105
H	-0.199801756	-2.643390850	0.743397517
O	0.992539080	0.908415950	-1.776434546
O	1.012192784	-1.977469090	-1.346214251
C	1.224654222	0.521627990	-2.998624115
C	1.188136212	-2.000266558	-2.636269723
O	1.843642769	1.231447555	-3.781970522

O	1.728761326	-2.951485072	-3.186072861
C	0.650655762	-0.816555994	-3.443060074
C	0.653933971	-1.077071883	-4.953617764
C	-0.909643758	-0.880188698	-3.495765430
C	-0.789626242	-1.582838669	-4.853373196
H	1.409984862	-1.765733699	-5.322365225
H	0.728271312	-0.135579208	-5.493040923
H	-1.406338128	-1.401817797	-2.678641048
H	-1.336747551	0.119131293	-3.576168944
H	-0.832993988	-2.665570904	-4.747056246
H	-1.486586900	-1.284133300	-5.633584151

./carboplatin-SMD-aug-pVTZ_eGeom.xyz

25

Pt	-0.242697104	-0.356179519	-0.388658007
N	0.526144114	1.253804655	0.598466370
H	0.284144822	1.269657031	1.601744974
H	1.556143388	1.298966950	0.544672957
N	0.451021554	-1.639148994	1.037742889
H	1.459625954	-1.834729921	0.935717177
H	0.314680794	-1.297908180	2.002274586
H	0.172745863	2.136983484	0.196791300
H	-0.030527005	-2.550460908	0.977090324
O	-0.995553726	0.920584461	-1.758157064
O	-1.064040148	-1.946266706	-1.323332615
C	-1.174814630	0.546464434	-3.017012708
C	-1.204894033	-1.979325368	-2.639615701
O	-1.736980090	1.310191478	-3.823935532
O	-1.761357985	-2.950227134	-3.185759212
C	-0.631820769	-0.814108677	-3.463148578
C	0.947632553	-0.913857688	-3.535685776
C	-0.659996409	-1.090584791	-4.990470917
C	0.797716924	-1.612443229	-4.912114158
H	1.445814497	-1.461712135	-2.712822207
H	1.391584206	0.097477111	-3.621132561
H	-1.441436432	-1.790962319	-5.338158469
H	-0.736273038	-0.136537628	-5.543534879
H	0.837049708	-2.715169190	-4.816045414
H	1.493394005	-1.294859990	-5.712045790

./carboplatin-aug-pVDZ_eGeom.xyz

25

Pt	-0.117102130	-0.355615410	-0.318223962
N	0.499976321	1.425165215	0.554282688
H	0.074953354	1.661070735	1.463535961
H	1.518519554	1.558406442	0.639569898
N	0.449083021	-1.812070594	1.051199564
H	1.460286026	-1.930993853	1.211391113
H	-0.010968868	-1.765531722	1.972864746
H	0.152853117	2.116768976	-0.140334638
H	0.104292589	-2.670606000	0.576689060
O	-0.790515448	0.948225273	-1.662617118
O	-0.822301176	-1.985539776	-1.219794589
C	-1.056319653	0.579623785	-2.929202077

C	-1.076809983	-2.007011776	-2.539446228
O	-1.579245527	1.379273675	-3.697811715
O	-1.615856290	-2.989996404	-3.037728201
C	-0.594704560	-0.812742222	-3.389813355
C	0.970939374	-0.912554032	-3.615317087
C	-0.774054666	-1.093831503	-4.907579881
C	0.693278221	-1.593882117	-4.980672773
H	1.546584582	-1.468407817	-2.848483065
H	1.411192557	0.098564404	-3.727757353
H	-1.567365132	-1.822695111	-5.151063422
H	-0.941698305	-0.142335574	-5.444493143
H	0.755875407	-2.697106437	-4.907086097
H	1.306414626	-1.256530925	-5.839237336

./carboplatin-M062X-CPCM-ApVDZ-ApVDZ-2_eGeom.xyz

25

Pt	-1.101603141	0.006140734	0.102283582
N	-2.447670600	1.370741662	-0.616942057
H	-2.638152930	1.262206660	-1.612260185
H	-3.346841211	1.354012660	-0.137129214
N	-2.323463055	-1.605121079	-0.226379775
H	-3.211141657	-1.553446325	0.271618176
H	-2.541384891	-1.753563599	-1.210911018
H	-2.059686976	2.306116994	-0.488907473
H	-1.845309645	-2.444566994	0.103239658
O	0.111101000	1.580614049	0.515235226
O	0.236284930	-1.313484213	0.867914100
C	1.400931145	1.431018692	0.592805448
C	1.518713995	-1.102915614	0.819664023
O	2.130504211	2.310829342	1.044319911
O	2.321485586	-1.877557867	1.333968583
C	2.004694723	0.134571977	0.049606675
C	3.526817063	0.138055713	-0.183368441
C	1.819279896	-0.095034843	-1.490159654
C	3.297344390	-0.543735612	-1.551368911
H	4.127938429	-0.393115279	0.558474927
H	3.880391976	1.167115837	-0.293225488
H	1.046305782	-0.809853086	-1.789639801
H	1.651885429	0.859271977	-2.002180995
H	3.384036042	-1.632983717	-1.478866239
H	3.891024509	-0.186064070	-2.397990058

./carboplatin-SMD-TZ-aug-pVDZ-pp_eGeom.xyz

25

Pt	-0.218818264	-0.360155920	-0.392961433
N	0.535999759	1.266826472	0.587950332
H	0.195777102	1.331521480	1.553314446
H	1.560428725	1.249987866	0.628392831
N	0.521520885	-1.627182404	1.029892978
H	1.546186444	-1.618176956	1.063006680
H	0.184620169	-1.394320737	1.969932388
H	0.265244628	2.133248789	0.110625811
H	0.230497081	-2.591001815	0.833155061
O	-1.025525844	0.894797190	-1.764930128

O	-1.020379938	-1.970142888	-1.327216268
C	-1.239671318	0.506040165	-3.003606731
C	-1.191556106	-2.003296186	-2.630318202
O	-1.870070604	1.232155052	-3.790399239
O	-1.747724390	-2.976412508	-3.165541190
C	-0.657163393	-0.829296898	-3.460965303
C	0.921243337	-0.884868790	-3.533060710
C	-0.674781274	-1.103584108	-4.985171190
C	0.789471217	-1.598115287	-4.900209794
H	1.428403359	-1.406317128	-2.712775624
H	1.333140721	0.128161528	-3.628317646
H	-1.435762627	-1.805208746	-5.344398432
H	-0.755945528	-0.158650738	-5.534883971
H	0.848369478	-2.689013894	-4.793908317
H	1.473803393	-1.277346307	-5.694735359

./carboplatin-PBE0-TZ-aug-pVDZ-pp_eGeom.xyz

25

Pt	-0.102634244	-0.360686738	-0.342473419
N	0.478829611	1.403268221	0.546620124
H	0.045697341	1.604081283	1.440930912
H	1.480025120	1.530025758	0.641582798
N	0.465554225	-1.784910997	1.033190934
H	1.463533969	-1.875343746	1.185600017
H	0.010358918	-1.716899155	1.936588699
H	0.135918556	2.086632892	-0.130941395
H	0.135027710	-2.637624496	0.577895516
O	-0.761886641	0.915563059	-1.683072782
O	-0.763945477	-1.976485836	-1.246976607
C	-1.064696244	0.553999945	-2.916280090
C	-1.043446659	-2.008453979	-2.535783465
O	-1.621116874	1.321803228	-3.663702156
O	-1.568910086	-2.978768328	-3.026663342
C	-0.594923843	-0.818132042	-3.386066963
C	0.954437708	-0.899051972	-3.614809727
C	-0.775250219	-1.093698926	-4.888450631
C	0.681247487	-1.585378845	-4.963530465
H	1.532914407	-1.438506535	-2.863876918
H	1.377346130	0.099708876	-3.734724522
H	-1.555504286	-1.808313475	-5.137839079
H	-0.936864242	-0.156545034	-5.417710637
H	0.745322199	-2.670668617	-4.883933755
H	1.280272444	-1.255967312	-5.812702057

./carboplatin-PBE0-pVTZ-pp_eGeom.xyz

25

Pt	-0.106034646	-0.357961233	-0.331914790
N	0.481676484	1.403451225	0.553661528
H	0.044596001	1.625786628	1.449098949
H	1.488541749	1.536683351	0.655623823
N	0.437452951	-1.793319241	1.039185874
H	1.438172526	-1.906689452	1.205133014
H	-0.025365803	-1.738111778	1.947578954
H	0.145512961	2.090289335	-0.134810797

H	0.100017044	-2.645643521	0.571980732
O	-0.742773030	0.929568329	-1.671700601
O	-0.772361864	-1.970803695	-1.236983514
C	-1.029626517	0.575091806	-2.918650056
C	-1.043668483	-2.000450083	-2.535128354
O	-1.550685150	1.362835128	-3.677296453
O	-1.567775482	-2.974408506	-3.030722331
C	-0.583717656	-0.810081944	-3.384456377
C	0.965217422	-0.914721802	-3.625231268
C	-0.781444790	-1.085466505	-4.888137440
C	0.670551434	-1.595406762	-4.975944323
H	1.546706289	-1.467823366	-2.872381961
H	1.406330291	0.086114072	-3.746527689
H	-1.578713212	-1.799053915	-5.126796750
H	-0.940822713	-0.138349309	-5.418419899
H	0.722278651	-2.690730765	-4.897590133
H	1.273242552	-1.271150767	-5.836699145

./carboplatin-PBE0-ApVTZ-ApVDZ-pp-2_eGeom.xyz

25

Pt	-1.017345027	-0.016676486	-0.099271044
N	-2.238610741	1.536800157	0.475317459
H	-3.153654833	1.555706899	0.039056112
H	-2.361800358	1.641053514	1.476173565
N	-2.095946104	-1.680800101	0.453629070
H	-2.229664729	-1.804310173	1.450882448
H	-2.996080872	-1.782220516	-0.002042441
H	-1.710521991	2.342898827	0.135874705
H	-1.487991077	-2.430917597	0.119527363
O	0.055379255	1.496952714	-0.744126905
O	0.189375963	-1.423166853	-0.754186505
C	1.334897234	1.382886884	-1.045705161
C	1.459071723	-1.202986476	-1.033329109
O	1.919749245	2.283103676	-1.600031819
O	2.129011846	-2.056944672	-1.564395186
C	2.061964195	0.127348744	-0.577046646
C	2.291228625	0.087342973	0.974166414
C	3.590612411	0.150377663	-0.747087147
C	3.750816272	-0.318007096	0.710268299
H	1.658005362	-0.593220099	1.544622394
H	2.207535478	1.088224181	1.400663469
H	3.980707427	-0.500358690	-1.525604877
H	3.928472618	1.172824063	-0.905232852
H	3.888376609	-1.397392715	0.775872407
H	4.513188468	0.174025180	1.314521987

./carboplatin-M06L-SMD-ApVTZ-ApVTZ-2_eGeom.xyz

25

Pt	-1.112458000	-0.011294000	-0.049513000
N	-2.511874000	1.320403000	0.655005000
H	-3.408272000	1.218798000	0.191241000
H	-2.679830000	1.211518000	1.649103000
N	-2.362968000	-1.599247000	0.334232000
H	-2.367610000	-1.850511000	1.316756000

H	-3.325694000	-1.417627000	0.071822000
H	-2.208714000	2.277347000	0.508928000
H	-2.065118000	-2.420911000	-0.180411000
O	0.110302000	1.555275000	-0.500754000
O	0.250749000	-1.319960000	-0.815394000
C	1.400227000	1.420629000	-0.507825000
C	1.525190000	-1.090905000	-0.756406000
O	2.129870000	2.335169000	-0.899363000
O	2.331686000	-1.856499000	-1.288927000
C	1.994565000	0.130895000	0.026517000
C	1.782316000	-0.116272000	1.554906000
C	3.502477000	0.128265000	0.302188000
C	3.235678000	-0.595550000	1.625882000
H	0.985546000	-0.805452000	1.831773000
H	1.629554000	0.829053000	2.074186000
H	4.138463000	-0.356459000	-0.434622000
H	3.851962000	1.145420000	0.464263000
H	3.302075000	-1.676831000	1.515306000
H	3.819650000	-0.295752000	2.492905000

./carboplatin-M062X-CPCM-pVTZ-2_eGeom.xyz

25

Pt	-1.118582512	-0.012810935	0.041890686
N	-2.464174599	1.365695075	-0.656637476
H	-2.682904908	1.262278865	-1.650473275
H	-3.356909529	1.366995732	-0.157006879
N	-2.326748471	-1.630333615	-0.318306470
H	-3.212389598	-1.609636430	0.193005722
H	-2.559551194	-1.761176241	-1.305796589
H	-2.059553833	2.299358485	-0.539838553
H	-1.831201219	-2.474808623	-0.017547831
O	0.072095106	1.556027743	0.480852932
O	0.211889472	-1.335385664	0.785161975
C	1.371719217	1.428613120	0.536280380
C	1.500557651	-1.129553787	0.728047912
O	2.091309798	2.323823174	0.954565055
O	2.302055456	-1.926282487	1.194565571
C	1.983747183	0.133384744	-0.003354874
C	3.510554796	0.142835788	-0.197421740
C	1.839408318	-0.076484476	-1.549806022
C	3.317196061	-0.526735228	-1.575452575
H	4.091019943	-0.400782253	0.556022762
H	3.864476878	1.176692979	-0.284411429
H	1.068522416	-0.784439371	-1.883422833
H	1.688689449	0.887132154	-2.057173984
H	3.400126635	-1.619430648	-1.505651515
H	3.935457486	-0.167059102	-2.407500951

./carboplatin-M062X-CPCM-ApVDZ-pVDZ_eGeom.xyz

25

Pt	0.204900709	-0.376220431	-0.399811606
N	-0.562490128	1.266536124	0.558804994
H	-1.581283497	1.275392789	0.592819906
H	-0.232516640	1.376333510	1.517132431

N	-0.493755836	-1.710214897	0.994834425
H	-0.124662665	-1.552928527	1.931854979
H	-1.510052608	-1.722317187	1.074010372
H	-0.276597927	2.103832381	0.049586502
H	-0.206396197	-2.649519490	0.716684558
O	0.980848875	0.915172831	-1.763201942
O	1.019426207	-1.976943172	-1.349211946
C	1.242521197	0.527077608	-2.976700933
C	1.196717632	-1.995705524	-2.637317404
O	1.902553042	1.216750698	-3.750783518
O	1.741771981	-2.940999811	-3.201800098
C	0.654775672	-0.805834953	-3.444295631
C	0.661994457	-1.056074796	-4.963652088
C	-0.910985688	-0.866862831	-3.490794981
C	-0.794371015	-1.564344758	-4.865498143
H	1.421634350	-1.749162471	-5.333024016
H	0.727738219	-0.101950368	-5.494101339
H	-1.404911220	-1.405382257	-2.675786368
H	-1.331672538	0.141982305	-3.569304616
H	-0.835743025	-2.653745432	-4.762013143
H	-1.492136348	-1.245224111	-5.645559408

./carboplatin-PBE0-SMD-pVTZ-pp_eGeom.xyz

25

Pt	-0.232936574	-0.362462434	-0.397427174
N	0.530205831	1.242151752	0.572813778
H	0.188793188	1.328394885	1.534255732
H	1.552107457	1.220246861	0.627821185
N	0.499701649	-1.626476991	1.003886586
H	1.521605907	-1.611369563	1.059147913
H	0.152874740	-1.422528795	1.945233856
H	0.282375267	2.112329649	0.094327831
H	0.230906161	-2.591866471	0.795412061
O	-1.018940380	0.887019038	-1.755060634
O	-1.032679035	-1.949111757	-1.328989252
C	-1.210677269	0.519033336	-2.993906495
C	-1.178611272	-1.992385074	-2.625564576
O	-1.796698611	1.255235288	-3.786681136
O	-1.699636797	-2.966281822	-3.167806774
C	-0.646724552	-0.819586753	-3.447273727
C	0.919364710	-0.887952425	-3.528965722
C	-0.680230562	-1.091670134	-4.962779348
C	0.773186790	-1.595719298	-4.889613748
H	1.434191657	-1.415067821	-2.713471190
H	1.341417029	0.122986561	-3.626968718
H	-1.451649501	-1.789205663	-5.312944934
H	-0.760730347	-0.143431002	-5.509396804
H	0.822524785	-2.689060037	-4.782593214
H	1.457566737	-1.283574100	-5.690584504

./carboplatin-M06L-pVTZ-2_eGeom.xyz

25

Pt	-1.001887879	-0.018192403	-0.121045782
N	-2.209624513	1.586498832	0.516457365

H	-3.151150768	1.642960643	0.127010509
H	-2.293376505	1.722777737	1.524081237
N	-2.044951466	-1.752936388	0.467738657
H	-2.136252606	-1.920349779	1.469935146
H	-2.967558134	-1.895328736	0.055471649
H	-1.682803503	2.387648096	0.148174072
H	-1.433038907	-2.488414509	0.094259458
O	0.046145518	1.529359768	-0.818169696
O	0.200876412	-1.435297922	-0.851743273
C	1.343503141	1.410300771	-1.093708292
C	1.484541322	-1.190075129	-1.098635480
O	1.942688771	2.323487204	-1.627984694
O	2.181467364	-2.040216851	-1.619273167
C	2.054918063	0.147717335	-0.615662652
C	2.237791962	0.086069379	0.937281714
C	3.585743128	0.176692408	-0.734606891
C	3.690975449	-0.348284343	0.703716445
H	1.563752888	-0.583457254	1.494729092
H	2.164852502	1.092965905	1.375906644
H	4.011443380	-0.440907529	-1.533997351
H	3.929049765	1.213103766	-0.839666401
H	3.793487260	-1.442191541	0.728653145
H	4.458330357	0.088082541	1.358696546

./carboplatin-CPCM-TZ-aug-pVDZ-pp_eGeom.xyz

25

Pt	0.196227449	-0.361764043	-0.383583808
N	-0.543442849	1.309149785	0.556170586
H	-1.565939276	1.320564151	0.610096218
H	-0.186923602	1.434119526	1.508078533
N	-0.493041020	-1.679728985	1.036206713
H	-0.129237773	-1.492206867	1.974855294
H	-1.514576813	-1.703161720	1.104265503
H	-0.259442817	2.133329290	0.015674693
H	-0.184995088	-2.622472919	0.774506435
O	0.969837653	0.906291734	-1.748908789
O	0.992534061	-1.972821315	-1.298694247
C	1.206363962	0.518513470	-2.987035060
C	1.186108740	-2.006587219	-2.602027488
O	1.827961940	1.245048242	-3.769155191
O	1.758666729	-2.965218144	-3.130025566
C	0.642702883	-0.833581417	-3.438683139
C	0.690008725	-1.107918635	-4.962450797
C	-0.933727626	-0.897239274	-3.531584091
C	-0.788504943	-1.568096897	-4.920055287
H	1.438023203	-1.839417534	-5.286929410
H	0.826144295	-0.167453568	-5.508729354
H	-1.444269197	-1.448782993	-2.733091291
H	-1.362829870	0.111485220	-3.593453088
H	-0.880971619	-2.659953440	-4.856937344
H	-1.449370136	-1.202449219	-5.715639036

./carboplatin-M06L-CPCM_eGeom.xyz

25

Pt	0.218201999	-0.363290901	-0.407313074
N	-0.546014912	1.315891312	0.554359956
H	-1.566274692	1.344752894	0.607206171
H	-0.209864341	1.447055409	1.510791971
N	-0.485894773	-1.711475686	1.016929370
H	-0.119359738	-1.560324275	1.959006076
H	-1.503510167	-1.736050936	1.109810043
H	-0.267153986	2.154315629	0.038637621
H	-0.203235360	-2.657946072	0.750151517
O	1.000138712	0.922737413	-1.773907281
O	1.032513535	-1.972683400	-1.344358402
C	1.213951050	0.538664943	-3.011138346
C	1.196314618	-1.994565907	-2.646069921
O	1.808802556	1.263540675	-3.805263604
O	1.730959204	-2.951468450	-3.200876908
C	0.649012322	-0.808945950	-3.448913183
C	0.655430021	-1.075353908	-4.960190599
C	-0.910742538	-0.891087931	-3.500841384
C	-0.780543575	-1.604757331	-4.854110288
H	1.430645309	-1.758078940	-5.330483804
H	0.712440925	-0.125345667	-5.506692588
H	-1.410094729	-1.413730461	-2.671331577
H	-1.353001441	0.112201833	-3.593902143
H	-0.803349541	-2.697306993	-4.734547398
H	-1.492063448	-1.327100071	-5.644081235

./carboplatin-PBE0-CPCM-pVTZ-pp_eGeom.xyz

25

Pt	0.206419911	-0.362970661	-0.385542355
N	-0.522384912	1.287900664	0.555446106
H	-1.542032518	1.307011920	0.624487899
H	-0.161566928	1.424273791	1.502231225
N	-0.470138962	-1.673659482	1.018429689
H	-0.105581637	-1.502831296	1.957981009
H	-1.488689763	-1.704179951	1.099748983
H	-0.249988252	2.113975052	0.016039954
H	-0.169012613	-2.615281752	0.753388504
O	0.952192752	0.898460719	-1.738474025
O	0.983614254	-1.954342124	-1.303257145
C	1.167331984	0.533262718	-2.977115953
C	1.155082432	-1.997392070	-2.599711325
O	1.743768678	1.271893516	-3.764787155
O	1.686588482	-2.961077358	-3.135794164
C	0.625529770	-0.821383848	-3.428843500
C	0.698113347	-1.095098023	-4.943015255
C	-0.937963820	-0.899051488	-3.543933368
C	-0.764276566	-1.580596652	-4.915646028
H	1.465511530	-1.814184737	-5.255179316
H	0.821817954	-0.149419874	-5.485767049
H	-1.464495239	-1.445293773	-2.748392326
H	-1.374184194	0.107559347	-3.627242679
H	-0.832690129	-2.675201961	-4.836065343
H	-1.425658550	-1.242725449	-5.726115392

./carboplatin-M06L-CPCM-ApVDZ-pVTZ_eGeom.xyz

25

Pt	0.201696664	-0.351565389	-0.415797908
N	-0.671042403	1.338943930	0.408666055
H	-1.685154025	1.282503423	0.487084323
H	-0.322734773	1.575271904	1.336281707
N	-0.420042822	-1.609237221	1.107191664
H	-0.120150132	-1.320579941	2.037039998
H	-1.430547258	-1.728253667	1.154320684
H	-0.471660261	2.141357637	-0.187945300
H	-0.028565237	-2.537989614	0.953497493
O	0.882312892	0.864897595	-1.893883347
O	1.149835174	-1.964434845	-1.211087754
C	1.092149827	0.413666462	-3.102636585
C	1.375144001	-2.035700093	-2.496978482
O	1.576947390	1.135419330	-3.976833677
O	2.098793321	-2.916301721	-2.969107478
C	0.674605009	-1.029122336	-3.402996743
C	0.675614559	-1.355079471	-4.903680495
C	-0.884953657	-1.137174858	-3.438139795
C	-0.815485434	-0.994016121	-4.966163815
H	0.850349437	-2.425847261	-5.053618932
H	1.370740727	-0.781513622	-5.525616825
H	-1.213544409	-2.135241955	-3.121405617
H	-1.444465497	-0.386959606	-2.865721057
H	-1.471498504	-1.639588738	-5.561818958
H	-0.971037578	0.046193408	-5.277778168

./carboplatin-PBE0-H2O-aug-pVTZ_eGeom.xyz

25

Pt	0.210139946	-0.364616201	-0.389553076
N	-0.517312155	1.280165438	0.555935282
H	-1.536977531	1.304483822	0.613079204
H	-0.167590799	1.404914448	1.507720143
N	-0.468184102	-1.670249838	1.013312365
H	-0.114060911	-1.490614652	1.954470480
H	-1.486630113	-1.706761726	1.085567606
H	-0.234314089	2.110223034	0.029276235
H	-0.158969480	-2.611577993	0.758793642
O	0.956068260	0.897121859	-1.737698023
O	0.986313431	-1.953867095	-1.305063001
C	1.169639466	0.531901672	-2.974756905
C	1.154869634	-1.996201214	-2.600122078
O	1.749994555	1.268460776	-3.763192541
O	1.686488171	-2.959386659	-3.139335571
C	0.623798576	-0.820453217	-3.428913320
C	0.692407935	-1.093173734	-4.943809848
C	-0.940159832	-0.896547156	-3.541262363
C	-0.769636223	-1.579358615	-4.912600914
H	1.459348535	-1.811106709	-5.259445384
H	0.812890264	-0.147169079	-5.486581071
H	-1.466082271	-1.441254768	-2.744327133
H	-1.374402734	0.110928094	-3.625243535
H	-0.837379195	-2.673907410	-4.831672674

H -1.432952328 -1.242305847 -5.721706532
./carboplatin-M06L-TZ-aug-pVDZ-2_eGeom.xyz
25

Pt	-0.998628342	-0.012776251	0.109758127
N	-2.211692903	1.592240576	-0.512232989
H	-2.312438360	1.708301136	-1.512325997
H	-3.134733433	1.638614550	-0.099949273
N	-2.055168523	-1.748415879	-0.447435399
H	-2.961288815	-1.872753140	-0.014035162
H	-2.162230078	-1.908522791	-1.440740566
H	-1.672654610	2.382512373	-0.159516570
H	-1.433601886	-2.468319884	-0.080040593
O	0.065985592	1.531255436	0.778266596
O	0.209451431	-1.427222080	0.825812292
C	1.353223459	1.406897910	1.062322188
C	1.485960655	-1.187170100	1.074032282
O	1.951891489	2.310999282	1.599974076
O	2.177071512	-2.030868740	1.599415614
C	2.059455992	0.144311323	0.585416819
C	3.589237224	0.170694528	0.691420961
C	2.229571584	0.081573223	-0.968517524
C	3.682556105	-0.353005403	-0.747231881
H	4.015115087	-0.445171675	1.478181045
H	3.933537906	1.196682033	0.795050657
H	1.556196304	-0.583376730	-1.510765681
H	2.153038785	1.078100812	-1.403778208
H	3.785712094	-1.436297530	-0.773773473
H	4.436304730	0.083258021	-1.400075341

./carboplatin-H20-aug-pVDZ_eGeom.xyz
25

Pt	-0.204429698	-0.354630552	-0.368748651
N	0.542432823	1.309808847	0.576040940
H	0.181315369	1.452612545	1.532250319
H	1.571985613	1.324702874	0.644053823
N	0.457082070	-1.678085476	1.058499722
H	1.484539652	-1.727719805	1.141412748
H	0.092846738	-1.493469545	2.006163047
H	0.272906466	2.146963456	0.032886335
H	0.137764127	-2.626875393	0.801008811
O	-0.945604088	0.925409036	-1.738390946
O	-1.002639337	-1.962604920	-1.285342103
C	-1.158884221	0.545251779	-2.992895868
C	-1.170645289	-2.000937779	-2.601202383
O	-1.731772148	1.301213832	-3.788796754
O	-1.721809054	-2.973754870	-3.133733795
C	-0.625196462	-0.825267257	-3.440466629
C	0.951173327	-0.910905681	-3.568486580
C	-0.708498270	-1.107797001	-4.965522324
C	0.765057162	-1.592681616	-4.949745179
H	1.482607083	-1.464774501	-2.770272524
H	1.392133282	0.102435633	-3.652310049
H	-1.481170000	-1.839450108	-5.264080944

H -0.846062480 -0.158409711 -5.514880126
H 0.838685196 -2.695370687 -4.874837989
H 1.423489148 -1.246015872 -5.769731911
./carboplatin-M06L-SMD-TZ-pVDZ_eGeom.xyz
25

Pt -0.239065643 -0.367580260 -0.418874885
N 0.525388111 1.261813587 0.580337470
H 0.221635752 1.298484652 1.547411291
H 1.539335667 1.268321225 0.588297520
N 0.526025605 -1.656953458 0.993607527
H 1.520198285 -1.812809970 0.867797448
H 0.396592990 -1.326109410 1.943524406
H 0.226853270 2.126346676 0.141672850
H 0.073739627 -2.562527054 0.929817195
O -1.060527449 0.897672007 -1.793041815
O -1.059820612 -1.971338936 -1.379589804
C -1.243685761 0.521619671 -3.022777757
C -1.218365822 -1.983183469 -2.667882872
O -1.839175039 1.245899073 -3.821898157
O -1.770130259 -2.931077219 -3.227810260
C -0.662490794 -0.808219090 -3.465335348
C 0.898415472 -0.882135656 -3.482449244
C -0.626914344 -1.071895989 -4.975071040
C 0.797956806 -1.614179535 -4.824659856
H 1.372301415 -1.387072360 -2.641665233
H 1.326351105 0.114691091 -3.581106064
H -1.391280685 -1.732042483 -5.377700543
H -0.645427752 -0.129876132 -5.518316203
H 0.806917667 -2.694533174 -4.688966658
H 1.522479399 -1.353666556 -5.592448978
./carboplatin-M062X-SMD-ApVDZ-pVDZ_eGeom.xyz
25

Pt -0.224844712 -0.374425842 -0.406036946
N 0.505598798 1.249312047 0.577040114
H 0.201317912 1.287197855 1.551251803
H 1.526348449 1.273237591 0.585810020
N 0.577917179 -1.625059598 0.984307144
H 1.581764249 -1.754535293 0.848632398
H 0.450692889 -1.294920581 1.942225505
H 0.193221115 2.115253403 0.134956669
H 0.150538988 -2.551030961 0.930707694
O -1.087217239 0.873107299 -1.777861262
O -1.014103514 -2.002111242 -1.366500940
C -1.304757399 0.481352364 -2.995022935
C -1.183374962 -2.023189374 -2.651710912
O -1.973022850 1.162895659 -3.780596739
O -1.705892771 -2.990699374 -3.215407253
C -0.674197279 -0.826719100 -3.461173496
C 0.893588188 -0.847710056 -3.490185031
C -0.652028443 -1.084552836 -4.979304979
C 0.804358084 -1.582435947 -4.846209476
H 1.389849060 -1.352479318 -2.655407500

H	1.281733549	0.171425298	-3.594229854
H	-1.403504353	-1.773266015	-5.373613458
H	-0.696910627	-0.132142686	-5.515274877
H	0.848716261	-2.668285632	-4.709520475
H	1.511516438	-1.280570431	-5.624004224

./carboplatin-M06L-H2O-TZ-pVTZ-2_eGeom.xyz

25

Pt	-0.978468583	-0.010285469	0.225973549
N	-2.243560974	1.465052854	-0.493408338
H	-2.311495639	1.481604989	-1.503806242
H	-3.188924049	1.400662750	-0.135132355
N	-2.125003541	-1.588224279	-0.481075706
H	-2.221416945	-1.599383316	-1.489331461
H	-1.672298503	-2.456724808	-0.217414916
H	-1.880043714	2.367635108	-0.207108960
H	-3.061017110	-1.613128749	-0.094719906
O	0.126877945	1.494272048	1.013129419
O	0.253246440	-1.420722474	0.999845501
C	1.401420642	1.342545886	1.236744106
C	1.526082790	-1.200875857	1.165812216
O	2.040277558	2.177822346	1.864802424
O	2.251959600	-2.037123791	1.688630192
C	2.087860837	0.121349273	0.640008553
C	3.620451150	0.153830077	0.631265440
C	2.138386593	0.092512678	-0.921389516
C	3.607979611	-0.333182715	-0.822184928
H	4.117799473	-0.467919547	1.371186259
H	3.971526968	1.178847650	0.724662126
H	1.435444496	-0.571173469	-1.423037519
H	2.017336981	1.094268772	-1.332533341
H	3.716390113	-1.414438423	-0.889803094
H	4.308207634	0.127027865	-1.515980982

./carboplatin-M06L-SMD-ApVDZ-pVDZ_eGeom.xyz

25

Pt	0.249966989	-0.375825962	-0.425224865
N	-0.504975623	1.260009824	0.571622530
H	-1.524078564	1.296281919	0.561693220
H	-0.225759970	1.289668115	1.552235982
N	-0.555704927	-1.650329207	0.979276332
H	-0.468028643	-1.309308531	1.936465088
H	-1.549594060	-1.820115811	0.826213471
H	-0.182390589	2.132279609	0.152919614
H	-0.100103104	-2.562183563	0.954274722
O	1.112621764	0.884637774	-1.792300052
O	1.070252807	-1.995374602	-1.382867129
C	1.284987341	0.499525490	-3.026435976
C	1.232758975	-1.995707204	-2.676618718
O	1.909764933	1.209537455	-3.829180241
O	1.802646751	-2.939525508	-3.243574514
C	0.668837192	-0.817990641	-3.468782102
C	0.606085492	-1.076211658	-4.981422341
C	-0.894002034	-0.872332902	-3.457267850

C	-0.828828742	-1.592283752	-4.811514821
H	1.357767803	-1.752209324	-5.402493697
H	0.632760692	-0.125042889	-5.523796578
H	-1.361463311	-1.388367976	-2.609935333
H	-1.313511718	0.138108591	-3.536307335
H	-0.856827548	-2.681502374	-4.683977288
H	-1.565874897	-1.306089642	-5.570131127

./carboplatin-M062X-H2O-TZ-pVDZ-2_eGeom.xyz

25

Pt	0.206211548	-0.362969931	-0.398352825
N	-0.557136485	1.289391067	0.549282603
H	-1.570260275	1.280138572	0.620315987
H	-0.190450157	1.422780609	1.487214715
N	-0.484780367	-1.690654604	1.008291133
H	-0.092258042	-1.537237623	1.932485694
H	-1.495805443	-1.685887371	1.105952917
H	-0.301647074	2.111338892	0.006876458
H	-0.214500633	-2.627395893	0.717459055
O	0.969004750	0.912892749	-1.773179537
O	1.015156699	-1.960887543	-1.342437460
C	1.225925169	0.527224979	-2.985079597
C	1.180420835	-1.999199900	-2.628379637
O	1.865226487	1.218372306	-3.763244997
O	1.698528942	-2.954438214	-3.185503752
C	0.650784013	-0.811560531	-3.441660835
C	0.666464667	-1.072598217	-4.956110895
C	-0.912287161	-0.878881647	-3.500224818
C	-0.781900680	-1.593462489	-4.860726454
H	1.428314574	-1.756190204	-5.317777110
H	0.723899988	-0.128447293	-5.491432500
H	-1.410941345	-1.401743936	-2.686998160
H	-1.334567395	0.120677173	-3.596360510
H	-0.811683205	-2.674893304	-4.743251823
H	-1.474412400	-1.296720417	-5.644286661

./carboplatin-M06L-SMD-ApVTZ-pVTZ_eGeom.xyz

25

Pt	-0.248202430	-0.374664390	-0.417544617
N	0.443109026	1.282862569	0.582882721
H	0.125154484	1.312897450	1.545673341
H	1.456186417	1.323231316	0.606249030
N	0.550754985	-1.644714365	0.992126236
H	1.310966557	-2.188351515	0.598347130
H	0.915318830	-1.181113015	1.816967813
H	0.122577669	2.135771040	0.137214524
H	-0.147915050	-2.307184235	1.311419447
O	-1.110295802	0.856276135	-1.793709455
O	-0.996340411	-2.009450704	-1.381073411
C	-1.288173854	0.471642834	-3.019583882
C	-1.160377236	-2.027290677	-2.666730141
O	-1.921818786	1.169077977	-3.815896958
O	-1.679893013	-2.995688941	-3.225727191
C	-0.653483634	-0.831958629	-3.467076129

C	0.909193584	-0.839848328	-3.484053155
C	-0.605945899	-1.093149531	-4.976855054
C	0.838821576	-1.579407093	-4.823803789
H	1.404463915	-1.321126527	-2.641747751
H	1.292165640	0.174653018	-3.587714203
H	-1.343943542	-1.780939479	-5.382590255
H	-0.657214921	-0.151222785	-5.518289888
H	0.888996501	-2.658142387	-4.683705918
H	1.553202401	-1.292512510	-5.591907454

./carboplatin-M062X-H2O-TZ-aug-pVDZ-2_eGeom.xyz

25

Pt	0.203777009	-0.364379188	-0.398243292
N	-0.559828057	1.282168221	0.555376075
H	-1.573569168	1.274054278	0.619314969
H	-0.199628992	1.406432537	1.497183700
N	-0.481067057	-1.691898253	1.008493400
H	-0.095191372	-1.529977407	1.934126250
H	-1.492755317	-1.694485751	1.100485840
H	-0.299344007	2.109020353	0.022737284
H	-0.201824539	-2.628420158	0.725305024
O	0.961026296	0.915109576	-1.773099586
O	1.014354195	-1.959289647	-1.345655019
C	1.222177253	0.530834623	-2.984684976
C	1.182778676	-1.994826297	-2.631353803
O	1.863363916	1.222881311	-3.760498628
O	1.706871786	-2.946406552	-3.189122027
C	0.649430039	-0.808152914	-3.444071490
C	0.666419752	-1.068142957	-4.958732362
C	-0.913314341	-0.878877023	-3.503737681
C	-0.779807025	-1.594939021	-4.863118908
H	1.431286816	-1.748049567	-5.320906230
H	0.719583937	-0.123173037	-5.493097922
H	-1.412374274	-1.400832446	-2.690209300
H	-1.336945936	0.119853603	-3.602627399
H	-0.804675848	-2.676302565	-4.743709571
H	-1.473436733	-1.302554489	-5.647283355

./carboplatin-PBE0-CPCM-TZ-aug-pVTZ-pp_eGeom.xyz

25

Pt	0.199555166	-0.362499946	-0.401236394
N	-0.546533477	1.283243177	0.536718009
H	-1.560007872	1.285646950	0.594529539
H	-0.191755036	1.408828666	1.479640523
N	-0.476697839	-1.672607985	1.004493180
H	-0.115498231	-1.487801773	1.935008600
H	-1.489121853	-1.697957203	1.074963817
H	-0.274979533	2.104469302	0.002508316
H	-0.170554481	-2.606359141	0.743835273
O	0.948163114	0.896760866	-1.756789509
O	0.996821827	-1.946450762	-1.315998822
C	1.188947068	0.523260910	-2.977616593
C	1.186609219	-1.985560951	-2.600118258
O	1.800599903	1.240590445	-3.755419578

O	1.753159002	-2.928714292	-3.131625668
C	0.638365448	-0.823355326	-3.430669209
C	0.679413047	-1.093467524	-4.943032131
C	-0.923874128	-0.901506143	-3.512273884
C	-0.780322277	-1.577238154	-4.887170723
H	1.433074528	-1.803363592	-5.276911934
H	0.787339955	-0.155801057	-5.485630302
H	-1.425061671	-1.448581444	-2.714628297
H	-1.360175673	0.095857363	-3.581331227
H	-0.850101301	-2.662822256	-4.812675847
H	-1.450057894	-1.234922903	-5.675697890

./carboplatin-PBE0-H2O-ApVTZ-ApVDZ-pp-2_eGeom.xyz

25

Pt	-1.112116577	-0.012002399	0.035664980
N	-2.449995152	1.375335715	-0.618056736
H	-2.664215514	1.290161537	-1.606681816
H	-3.332559542	1.354662361	-0.116532772
N	-2.333134534	-1.598277910	-0.338301594
H	-3.216419293	-1.553369107	0.160035034
H	-2.549457656	-1.714379126	-1.323404331
H	-2.047929129	2.298451883	-0.477380872
H	-1.860265400	-2.445052343	-0.033278032
O	0.083322041	1.522879781	0.492293033
O	0.200028046	-1.340900497	0.744770215
C	1.373261239	1.392474414	0.546491662
C	1.480068114	-1.131057225	0.729008826
O	2.086672429	2.281908723	0.991144885
O	2.260154141	-1.911463366	1.257354806
C	1.982975626	0.111090660	-0.009889898
C	3.505893325	0.119903778	-0.217489925
C	1.824703025	-0.072534320	-1.557579316
C	3.309144682	-0.471656201	-1.624500027
H	4.085994627	-0.460194944	0.496905526
H	3.872837793	1.144538420	-0.244823886
H	1.078388934	-0.794998581	-1.885687544
H	1.626229640	0.882922921	-2.044780249
H	3.437034001	-1.554412688	-1.637849338
H	3.897452135	-0.038137487	-2.432813631

./carboplatin-M06L-CPCM-ApVTZ-pVDZ_eGeom.xyz

25

Pt	0.198795307	-0.370326392	-0.408833097
N	-0.536143254	1.310839364	0.551795554
H	-1.547782307	1.344725052	0.584699406
H	-0.206466056	1.413177993	1.504135792
N	-0.516050288	-1.701308552	1.011134584
H	-0.158251022	-1.531319059	1.943311353
H	-1.526464734	-1.711658366	1.080345560
H	-0.230085170	2.133778009	0.044117117
H	-0.227906389	-2.638197257	0.750501841
O	0.994566180	0.898602831	-1.775475457
O	0.988478926	-1.983794323	-1.347154246
C	1.238113524	0.510544848	-2.992781535

C	1.180102477	-2.006699977	-2.632992855
O	1.876174216	1.213774829	-3.769547373
O	1.726727990	-2.959112124	-3.178151304
C	0.655341544	-0.821099443	-3.445510979
C	0.661625407	-1.081074547	-4.956140666
C	-0.905134293	-0.872961579	-3.504593225
C	-0.783317688	-1.583099857	-4.857858909
H	1.417663323	-1.768872756	-5.326728411
H	0.734758791	-0.138421385	-5.493907913
H	-1.409817997	-1.386332612	-2.687222600
H	-1.321798964	0.130020760	-3.593821439
H	-0.828785304	-2.665093216	-4.744605262
H	-1.477037209	-1.286445012	-5.641844947

./carboplatin-PBE0-H2O-ApVTZ-pVTZ-pp_eGeom.xyz

25

Pt	0.193217814	-0.366248450	-0.402319463
N	-0.559805254	1.273255112	0.538586109
H	-1.573303475	1.271516678	0.596486244
H	-0.205769939	1.397822366	1.482035895
N	-0.481613381	-1.679775188	0.999377409
H	-0.126316443	-1.492819355	1.931811829
H	-1.494241750	-1.711443348	1.065108266
H	-0.292032698	2.098010891	0.007731172
H	-0.168816481	-2.612183189	0.741514090
O	0.942164227	0.897437342	-1.755734709
O	1.000790102	-1.945002973	-1.319870586
C	1.190652724	0.526676141	-2.974047914
C	1.201743260	-1.977921778	-2.600863229
O	1.807042083	1.247068486	-3.748066644
O	1.787155946	-2.912583058	-3.130634696
C	0.644768623	-0.820482160	-3.432721329
C	0.680982815	-1.086744706	-4.946074223
C	-0.917774738	-0.903665056	-3.507435313
C	-0.779218334	-1.569224652	-4.887696231
H	1.433036569	-1.795609865	-5.285688949
H	0.787581864	-0.148390609	-5.487734538
H	-1.411907543	-1.459200812	-2.711305892
H	-1.358382501	0.092391177	-3.565989979
H	-0.852112917	-2.655204685	-4.822688207
H	-1.450533564	-1.218031078	-5.670908121

./carboplatin-CPCM-ApVTZ-pVTZ-pp_eGeom.xyz

25

Pt	0.193916535	-0.363355774	-0.388146024
N	-0.536072809	1.311872473	0.546195861
H	-1.558928508	1.331884089	0.592506903
H	-0.186649739	1.432733882	1.501440533
N	-0.509199831	-1.672111420	1.030069498
H	-0.148957545	-1.484690222	1.970269474
H	-1.531297155	-1.687037641	1.093768057
H	-0.241224408	2.135322994	0.010059018
H	-0.207749822	-2.618613143	0.773688596
O	0.983475979	0.894920690	-1.752786394

O	0.983372248	-1.979445448	-1.298556880
C	1.227763660	0.502426962	-2.985040612
C	1.188689836	-2.014810621	-2.597520419
O	1.869855155	1.218968633	-3.764216983
O	1.770236236	-2.973707740	-3.121125699
C	0.650076553	-0.843203985	-3.439360000
C	0.684603410	-1.117525556	-4.963552339
C	-0.927796982	-0.891734255	-3.519891249
C	-0.800962314	-1.554243986	-4.914077047
H	1.419115812	-1.859620250	-5.295054913
H	0.831617302	-0.180007575	-5.512213175
H	-1.434761909	-1.445770270	-2.720841449
H	-1.348927243	0.120979167	-3.569396504
H	-0.913396922	-2.644840558	-4.861099063
H	-1.459490528	-1.168743218	-5.702248199

./carboplatin-PBE0-CPCM-ApVDZ-pVDZ-pp_eGeom.xyz

25

Pt	0.201464578	-0.364016396	-0.404337555
N	-0.549031251	1.285622140	0.527594786
H	-1.566828073	1.297022909	0.579062011
H	-0.203838867	1.415472085	1.477772987
N	-0.496183447	-1.667331838	1.000075874
H	-0.142336961	-1.487585472	1.938711033
H	-1.512941564	-1.690416279	1.067238768
H	-0.272340409	2.113483396	-0.000955874
H	-0.196253575	-2.609710920	0.748491484
O	0.974776056	0.896210860	-1.760598378
O	1.006589118	-1.961384865	-1.311675926
C	1.218484099	0.507830065	-2.980174561
C	1.202348437	-1.994490951	-2.599078941
O	1.854638959	1.215592219	-3.759793962
O	1.785232689	-2.938253664	-3.130109255
C	0.648858511	-0.834204297	-3.432197449
C	0.674712171	-1.104010021	-4.949164956
C	-0.918579305	-0.898276821	-3.495470198
C	-0.799307749	-1.555576714	-4.886338483
H	1.415288123	-1.835208506	-5.287880725
H	0.804273521	-0.163680834	-5.495051216
H	-1.413345580	-1.460804049	-2.695691828
H	-1.350839582	0.108927204	-3.538859155
H	-0.897539541	-2.646713408	-4.831118742
H	-1.469993349	-1.178848609	-5.667578749

./carboplatin-PBE0-aug-pVTZ_eGeom.xyz

25

Pt	-0.115471567	-0.359359690	-0.338276690
N	0.484037346	1.394323603	0.544565277
H	0.062354158	1.610862787	1.448069637
H	1.492212603	1.524570989	0.631026414
N	0.445262461	-1.786129006	1.028210401
H	1.447725073	-1.894859402	1.182947850
H	-0.006765357	-1.727060828	1.941144908
H	0.139018588	2.086758941	-0.133041281

H	0.105680142	-2.642179570	0.570624796
O	-0.766694827	0.925505856	-1.669734742
O	-0.791110539	-1.969408920	-1.235925419
C	-1.046680836	0.569921046	-2.916257998
C	-1.052397662	-2.000871415	-2.534503027
O	-1.574830328	1.352561463	-3.676551039
O	-1.574248835	-2.974958017	-3.034065024
C	-0.588137239	-0.811018066	-3.382468673
C	0.962989723	-0.909318656	-3.612603497
C	-0.773755781	-1.086745543	-4.887852466
C	0.680523381	-1.591753211	-4.964959146
H	1.542208864	-1.459910456	-2.856085909
H	1.400083614	0.093664340	-3.731813237
H	-1.567068946	-1.802411090	-5.133087873
H	-0.931635119	-0.140271645	-5.419570250
H	0.735812486	-2.686837545	-4.885633091
H	1.288195608	-1.265428734	-5.821288931

./carboplatin-M062X-H2O-pVTZ-2_eGeom.xyz

25

Pt	-1.121325165	-0.017068185	0.032411583
N	-2.470682454	1.360804281	-0.657094701
H	-2.673893071	1.273953510	-1.655766014
H	-3.370541384	1.345627593	-0.170595902
N	-2.328887599	-1.633941901	-0.328550517
H	-3.221315464	-1.606039398	0.170434981
H	-2.548552373	-1.772488989	-1.317990239
H	-2.075727211	2.295529145	-0.517480855
H	-1.840581337	-2.477684811	-0.014040603
O	0.066026585	1.552168667	0.471904620
O	0.212743302	-1.339284768	0.768204783
C	1.366612392	1.432720521	0.523343094
C	1.500522267	-1.126957343	0.721725474
O	2.082245926	2.336315966	0.929877808
O	2.302172960	-1.919878665	1.194681394
C	1.984281441	0.136998247	-0.007391242
C	3.512001172	0.147660100	-0.192381330
C	1.851396003	-0.076879652	-1.554430495
C	3.326710807	-0.535328328	-1.564798207
H	4.089132339	-0.387057095	0.570086579
H	3.863370765	1.181764090	-0.287977601
H	1.077755997	-0.779482086	-1.893334583
H	1.713814220	0.887472426	-2.064407634
H	3.402035163	-1.627678795	-1.480151501
H	3.953812720	-0.189928528	-2.396420891

./carboplatin-PBE0-SMD-ApVDZ-pVTZ-pp_eGeom.xyz

25

Pt	-0.222120086	-0.363118969	-0.409111621
N	0.525376870	1.246587741	0.561657409
H	0.191759223	1.315500127	1.523922612
H	1.544950192	1.235737756	0.604714379
N	0.527965650	-1.605665182	0.999520190
H	1.546827531	-1.575271200	1.048087049

H	0.182361822	-1.390700718	1.935548027
H	0.259107636	2.113080656	0.093216133
H	0.268677510	-2.573266897	0.804784598
O	-1.031701930	0.873618150	-1.771074106
O	-1.014426052	-1.961765009	-1.335481373
C	-1.249037416	0.489522828	-2.993450440
C	-1.188922805	-1.999906466	-2.622190994
O	-1.889204090	1.201334245	-3.777078469
O	-1.744625449	-2.967013953	-3.156162295
C	-0.659041783	-0.834438104	-3.454303759
C	0.910041342	-0.880060366	-3.511377706
C	-0.666118653	-1.107216650	-4.970914422
C	0.795728380	-1.587915225	-4.876011383
H	1.413050695	-1.403055406	-2.690462999
H	1.316844055	0.134598554	-3.599182708
H	-1.419930293	-1.811392983	-5.337297323
H	-0.747322119	-0.163015106	-5.519676529
H	0.864048477	-2.677709508	-4.771112246
H	1.483018305	-1.258821085	-5.663691033

./carboplatin-PBE0-CPCM-ApVDZ-ApVDZ-pp_eGeom.xyz

25

Pt	0.193399879	-0.364458673	-0.402119023
N	-0.537419526	1.293945758	0.523042784
H	-1.555274359	1.321331672	0.561132948
H	-0.200481374	1.414409748	1.477216311
N	-0.529837710	-1.654599047	0.996837361
H	-0.188146963	-1.470667345	1.938968949
H	-1.547488158	-1.670548653	1.047075110
H	-0.238686615	2.116348426	-0.001717981
H	-0.230109812	-2.598825321	0.752805186
O	0.991402705	0.882209991	-1.753356958
O	0.980776580	-1.971819235	-1.302295952
C	1.237087095	0.491755389	-2.971960445
C	1.185540979	-2.010102041	-2.588289667
O	1.884821628	1.192634933	-3.748101347
O	1.758691237	-2.962922999	-3.113472413
C	0.654723382	-0.843557344	-3.427308755
C	0.689107244	-1.116174690	-4.943628844
C	-0.912949242	-0.887520270	-3.503589310
C	-0.790238740	-1.551302142	-4.891011221
H	1.424153661	-1.855899484	-5.275765305
H	0.832801030	-0.178115940	-5.489900706
H	-1.421882870	-1.440020494	-2.705720442
H	-1.331364617	0.125160839	-3.554795910
H	-0.900570586	-2.641088573	-4.832260111
H	-1.450747837	-1.170527274	-5.678913268

./carboplatin-PBE0-ApVTZ-pVTZ-pp_eGeom.xyz

25

Pt	-0.098741463	-0.360378138	-0.343074067
N	0.487758454	1.398783423	0.548367729
H	0.058786867	1.598580733	1.445083976
H	1.489735242	1.521517031	0.642173178

N	0.451309690	-1.786409791	1.035464393
H	1.448663849	-1.887996515	1.186043400
H	0.000944343	-1.708845845	1.940663481
H	0.146604084	2.087254425	-0.125231869
H	0.109905746	-2.638297544	0.586198974
O	-0.741746595	0.918501215	-1.686085425
O	-0.764897887	-1.970707606	-1.249373449
C	-1.053091850	0.559803262	-2.917099811
C	-1.051357923	-2.001049120	-2.535998717
O	-1.607786967	1.331959780	-3.662611275
O	-1.589193608	-2.966793654	-3.024091131
C	-0.594450469	-0.815641856	-3.388902073
C	0.955029108	-0.907214139	-3.615151584
C	-0.774740800	-1.089534377	-4.891771028
C	0.679784361	-1.587362238	-4.966456240
H	1.527322405	-1.454572827	-2.865167126
H	1.385878567	0.088678477	-3.730326389
H	-1.558182981	-1.799962476	-5.143205720
H	-0.931399858	-0.151599352	-5.421191643
H	0.740493624	-2.673205733	-4.891907438
H	1.280681069	-1.255859906	-5.813479155

./carboplatin-H2O-TZ-pVDZ-pp_eGeom.xyz

25

Pt	0.195707529	-0.365269896	-0.380494068
N	-0.524967271	1.318379427	0.554497577
H	-1.546659859	1.340573318	0.615411966
H	-0.159826183	1.447088682	1.502476716
N	-0.516791068	-1.678065817	1.034816957
H	-0.147972553	-1.503691765	1.973900798
H	-1.538308458	-1.683507231	1.104054522
H	-0.235842076	2.134097772	0.004238539
H	-0.225752635	-2.623756588	0.764778875
O	0.989511959	0.893512896	-1.743521857
O	0.972781437	-1.987436288	-1.294023124
C	1.222932674	0.503443049	-2.981560830
C	1.168363407	-2.023982600	-2.597085793
O	1.852244736	1.224505147	-3.762335542
O	1.725107401	-2.992478084	-3.123505436
C	0.645662853	-0.842431600	-3.434511789
C	0.696569435	-1.115584486	-4.958320276
C	-0.931266770	-0.886242395	-3.534035362
C	-0.789549853	-1.551274492	-4.925716533
H	1.433693020	-1.859792604	-5.278911218
H	0.852640764	-0.177361792	-5.503059471
H	-1.450583202	-1.437498525	-2.740981689
H	-1.348996634	0.127554005	-3.590404520
H	-0.901406343	-2.641754842	-4.870486860
H	-1.439985300	-1.169378062	-5.722350593

./carboplatin-PBE0-CPCM-ApVTZ-ApVDZ-pp_eGeom.xyz

25

Pt	0.192259057	-0.350161206	-0.405536947
N	-0.646687632	1.313476861	0.416091013

H	-1.658339255	1.260624543	0.482905586
H	-0.295004838	1.525843659	1.344408390
N	-0.407677224	-1.587249262	1.094917079
H	-0.066693479	-1.309529067	2.010033100
H	-1.416946330	-1.672261159	1.163618156
H	-0.426525560	2.109564655	-0.176658864
H	-0.041017832	-2.517054359	0.908871658
O	0.852075973	0.845971429	-1.863434105
O	1.099031397	-1.942999957	-1.202360003
C	1.074174983	0.417143927	-3.067342949
C	1.331249065	-2.031113056	-2.475917325
O	1.570828768	1.140542999	-3.919957267
O	2.035378771	-2.919897010	-2.936597488
C	0.656802243	-1.018438546	-3.393918442
C	0.695340966	-1.335941569	-4.897285928
C	-0.904140438	-1.131816425	-3.462176382
C	-0.807961294	-1.021205345	-4.993809718
H	0.909618453	-2.392334499	-5.050231643
H	1.376274834	-0.731963882	-5.493078731
H	-1.237826770	-2.117025988	-3.134090432
H	-1.468881316	-0.372774877	-2.922302136
H	-1.423269863	-1.707907013	-5.574524972
H	-0.994755666	-0.003847622	-5.338750660

./carboplatin-M062X-ApVDZ-pVDZ-2_eGeom.xyz

25

Pt	0.119736001	-0.368059183	-0.358915168
N	-0.516933297	1.406943202	0.539174323
H	-1.524253580	1.526159393	0.619850293
H	-0.101309452	1.619906675	1.443353733
N	-0.469673831	-1.835423833	1.007623713
H	-0.039067391	-1.780038281	1.928048791
H	-1.472749964	-1.947806413	1.136341947
H	-0.172499730	2.100554481	-0.132878268
H	-0.115368687	-2.681618494	0.549498028
O	0.793039166	0.940684966	-1.687728333
O	0.832791841	-1.981946908	-1.268305336
C	1.106141465	0.573598066	-2.920919735
C	1.095159839	-1.997782421	-2.564891281
O	1.683024945	1.330367917	-3.671668594
O	1.620478402	-2.959179368	-3.084533764
C	0.617233922	-0.796875591	-3.394775439
C	0.744461742	-1.060486811	-4.907070678
C	-0.940610247	-0.888866317	-3.559655417
C	-0.706901566	-1.593505002	-4.915691963
H	1.537241101	-1.753255907	-5.195885627
H	0.847499942	-0.109805195	-5.436635381
H	-1.485612492	-1.431263669	-2.778480660
H	-1.371463495	0.112128043	-3.678524837
H	-0.731557817	-2.682475101	-4.807172845
H	-1.351499809	-1.292307018	-5.747286516

./carboplatin-M062X-TZ-aug-pVTZ_eGeom.xyz

25

Pt	-0.107827477	-0.364081896	-0.349545646
N	0.495985901	1.408783689	0.561461647
H	0.069539603	1.608584058	1.459591724
H	1.498620232	1.529197634	0.654112528
N	0.445965894	-1.819548134	1.035733469
H	1.442985559	-1.930125210	1.183833389
H	-0.001982236	-1.749807432	1.942959279
H	0.154890353	2.098900799	-0.110939162
H	0.097930337	-2.663633382	0.576174489
O	-0.746295818	0.930716001	-1.694332657
O	-0.782632794	-1.974709501	-1.273838890
C	-1.074373354	0.572372213	-2.922312520
C	-1.050635388	-2.003052533	-2.564756268
O	-1.644449976	1.331791506	-3.664847984
O	-1.552779571	-2.972394210	-3.077971492
C	-0.602087620	-0.798488818	-3.400279607
C	0.949433299	-0.888281195	-3.602104016
C	-0.758560357	-1.065033560	-4.906477744
C	0.684495588	-1.609590828	-4.938926199
H	1.515348641	-1.410860561	-2.831710882
H	1.369684703	0.106749694	-3.746785794
H	-1.557099043	-1.745791254	-5.182079365
H	-0.859711134	-0.121141654	-5.435101523
H	0.700413973	-2.690428821	-4.815803086
H	1.310447694	-1.330479374	-5.783182700

./carboplatin-M062X-CPCM-aug-pVTZ_eGeom.xyz

25

Pt	0.211112957	-0.364721611	-0.394625680
N	-0.539076604	1.278447986	0.562824131
H	-1.560452447	1.300675619	0.598147115
H	-0.209160990	1.389552747	1.524072434
N	-0.472089523	-1.691313517	1.005411416
H	-0.119371124	-1.518342646	1.949034634
H	-1.491428678	-1.726825090	1.074478744
H	-0.244735143	2.115227519	0.051813290
H	-0.161877160	-2.630574887	0.741612030
O	0.962854061	0.919848632	-1.752723077
O	1.008043802	-1.959838540	-1.334097881
C	1.196375370	0.548846927	-2.982124078
C	1.166941366	-1.993674626	-2.628182129
O	1.797160901	1.265670001	-3.770851877
O	1.675849848	-2.953429257	-3.191775424
C	0.637030298	-0.800351574	-3.439821188
C	0.676633960	-1.066421438	-4.955384160
C	-0.926323353	-0.881531786	-3.520313446
C	-0.766706022	-1.608874744	-4.873859401
H	1.460251237	-1.749749622	-5.300784347
H	0.730293723	-0.113499909	-5.494766089
H	-1.439314282	-1.401166666	-2.699647153
H	-1.356047612	0.123681613	-3.638254368
H	-0.776706394	-2.698953803	-4.740647029
H	-1.461951180	-1.333034100	-5.676665477

./carboplatin-PBE0-ApVDZ-ApVTZ-pp_eGeom.xyz

25

Pt	-0.104162793	-0.361566520	-0.342705601
N	0.480797596	1.397046252	0.541386372
H	0.058877022	1.599673262	1.444880743
H	1.485904306	1.530205957	0.626545613
N	0.461245427	-1.784163675	1.026951607
H	1.463167956	-1.888697975	1.169632937
H	0.019583213	-1.712093010	1.940871909
H	0.129054430	2.087183615	-0.130470087
H	0.116248292	-2.640291723	0.580440778
O	-0.763180121	0.918575109	-1.678339540
O	-0.772977942	-1.976784315	-1.240815738
C	-1.066326461	0.555289133	-2.915246587
C	-1.058435377	-2.004896025	-2.532765736
O	-1.626099579	1.328566511	-3.666041090
O	-1.602349136	-2.974244861	-3.022792815
C	-0.596961661	-0.819343827	-3.386376428
C	0.957756252	-0.904765211	-3.603524497
C	-0.770464382	-1.093937719	-4.893834376
C	0.693440945	-1.576888955	-4.965997734
H	1.528049048	-1.461472917	-2.849240463
H	1.389706542	0.098937357	-3.706115833
H	-1.550599364	-1.817771998	-5.145827225
H	-0.939555786	-0.151475232	-5.424396580
H	0.766669063	-2.669135507	-4.901073560
H	1.297919519	-1.228300498	-5.812275079

./carboplatin-SMD-ApVDZ-ApVTZ-pp_eGeom.xyz

25

Pt	-0.226486951	-0.359886314	-0.397450258
N	0.545376856	1.254701719	0.577407462
H	0.208478052	1.326750420	1.547286077
H	1.573332118	1.229664450	0.618408157
N	0.506762503	-1.628144159	1.018834436
H	1.535126737	-1.627131747	1.053410019
H	0.173564612	-1.395597619	1.964217766
H	0.284196014	2.129167116	0.101564767
H	0.210721992	-2.594941397	0.825405088
O	-1.028004876	0.901731678	-1.764106451
O	-1.049973717	-1.961381468	-1.324270140
C	-1.238187265	0.512808171	-3.006601752
C	-1.222321684	-1.990377296	-2.630713247
O	-1.868952676	1.247620856	-3.799456759
O	-1.809326315	-2.956330713	-3.166906092
C	-0.659372792	-0.828097446	-3.463164724
C	0.923575176	-0.896295742	-3.509431518
C	-0.658346153	-1.101444870	-4.992011439
C	0.810966181	-1.591284027	-4.892340372
H	1.410283258	-1.440478209	-2.682370108
H	1.348572570	0.120313637	-3.578765447
H	-1.417781493	-1.810296149	-5.361065804
H	-0.739845175	-0.151150248	-5.545475124
H	0.877161860	-2.689984190	-4.802357358

H 1.507788180 -1.250289223 -5.677176189
./carboplatin-PBE0_eGeom.xyz
25

Pt -0.100168656 -0.358717461 -0.325007757
N 0.488701428 1.409226880 0.563791192
H 0.037030041 1.645286511 1.449209661
H 1.493633589 1.548335128 0.681858438
N 0.430224587 -1.810163223 1.045306090
H 1.428321726 -1.938978581 1.219484323
H -0.039065641 -1.767571154 1.951795744
H 0.162934901 2.088819846 -0.138397069
H 0.088590743 -2.653480010 0.562633811
O -0.727753792 0.934901871 -1.670123894
O -0.771997168 -1.969405485 -1.240175854
C -1.013458959 0.584832179 -2.918559901
C -1.045385754 -1.994190112 -2.537976093
O -1.521884957 1.381026687 -3.677073542
O -1.572548804 -2.966322696 -3.034063466
C -0.581676520 -0.804391820 -3.386454348
C 0.965644798 -0.921413806 -3.631493191
C -0.785976835 -1.076304300 -4.889841344
C 0.662000286 -1.596807950 -4.982851473
H 1.543261004 -1.481590447 -2.880931198
H 1.415697539 0.075599371 -3.751369476
H -1.588968438 -1.784038623 -5.126904917
H -0.940180230 -0.127287987 -5.418283108
H 0.705728109 -2.692649489 -4.907019591
H 1.264604014 -1.275068099 -5.844682049

./carboplatin-H20-ApVTZ-ApVTZ-pp_eGeom.xyz
25

Pt 0.189928553 -0.364457190 -0.386386337
N -0.545916106 1.306542866 0.551411802
H -1.568765934 1.322073900 0.600384853
H -0.194155697 1.427489855 1.505833796
N -0.506685991 -1.678225147 1.030772972
H -0.147125603 -1.489548323 1.971016196
H -1.528766968 -1.698165390 1.094357785
H -0.255720551 2.131740339 0.015357280
H -0.200366464 -2.622973017 0.773480838
O 0.972219295 0.899361191 -1.749473789
O 0.985224156 -1.975768249 -1.298986259
C 1.219930721 0.509852149 -2.982077768
C 1.191820502 -2.009111063 -2.597842497
O 1.858306277 1.231437119 -3.759579169
O 1.776204469 -2.966047033 -3.121745947
C 0.650517807 -0.838429176 -3.439412934
C 0.691005239 -1.110703944 -4.963914241
C -0.926940602 -0.894668214 -3.525202956
C -0.792333494 -1.555368584 -4.919471234
H 1.430489931 -1.848458021 -5.294002189
H 0.834741703 -0.171708530 -5.510902683
H -1.433931970 -1.451835611 -2.728307722

```

H      -1.352782422      0.116062849      -3.575387764
H      -0.899032446      -2.646602255      -4.867682603
H      -1.450557396      -1.172843294      -5.709368440
./carboplatin-H2O-ApVDZ-ApVTZ-pp_eGeom.xyz
25

```

```

Pt      0.191587289      -0.360776369      -0.387217076
N      -0.538048527      1.314315373      0.538475285
H      -1.564591027      1.342979180      0.579063857
H      -0.194786865      1.437763019      1.499428482
N      -0.520061495      -1.664746510      1.025000893
H      -0.169671055      -1.476320625      1.972537632
H      -1.546168727      -1.685704043      1.081543063
H      -0.235399662      2.140303768      0.003832328
H      -0.213325947      -2.615264749      0.775625267
O      0.989763800      0.897713017      -1.746305724
O      0.985221421      -1.981463367      -1.285279864
C      1.234338238      0.499432522      -2.982270880
C      1.193428439      -2.018145874      -2.589182482
O      1.882688420      1.218052955      -3.764423671
O      1.780835158      -2.983079309      -3.110190007
C      0.653888775      -0.848141855      -3.435804135
C      0.691220251      -1.125169265      -4.963633422
C      -0.927825297      -0.895343420      -3.516506025
C      -0.802273873      -1.549998027      -4.919482973
H      1.425830110      -1.879710009      -5.289608274
H      0.852667438      -0.184125842      -5.515355701
H      -1.434806736      -1.460743375      -2.715930047
H      -1.351410871      0.123827541      -3.555494435
H      -0.926119895      -2.646606277      -4.875075905
H      -1.459672350      -1.149401231      -5.710875195
./carboplatin-M06L-CPCM-ApVDZ-ApVTZ-2_eGeom.xyz
25

```

```

Pt      0.245411915      -0.418324606      -0.408252646
N      -0.385554493      1.283559857      0.578110504
H      -1.398210135      1.379563124      0.625108515
H      -0.043542991      1.359732107      1.534306940
N      -0.548142964      -1.722903136      0.986232126
H      -1.561540827      -1.669374989      1.071401491
H      -0.330344812      -2.678805669      0.707387220
H      -0.039918408      2.103765489      0.081356038
H      -0.172462461      -1.602273034      1.924912356
O      1.122876022      0.825039176      -1.753293764
O      0.939216385      -2.065911851      -1.371686596
C      1.326248518      0.432025191      -2.983263831
C      1.102808250      -2.076138331      -2.668284291
O      2.021458561      1.094094427      -3.758018696
O      1.585702633      -3.055033635      -3.241888232
C      0.635809655      -0.845095421      -3.450709520
C      0.598487093      -1.073037256      -4.968959388
C      -0.926805243      -0.785868251      -3.476484118
C      -0.886617380      -1.448358846      -4.862007254
H      1.290904241      -1.823904567      -5.363240673

```

H	0.752345292	-0.124173904	-5.493701724
H	-1.453944570	-1.304626927	-2.666409476
H	-1.278084326	0.253166210	-3.511593733
H	-1.031965617	-2.533433979	-4.792139212
H	-1.566827330	-1.054033949	-5.626011044

./carboplatin-PBE0-SMD-TZ-pVTZ-pp_eGeom.xyz

25

Pt	-0.228292884	-0.361465854	-0.406741090
N	0.531915752	1.240878958	0.572009579
H	0.183367935	1.314184993	1.524387128
H	1.546454169	1.208807552	0.627298930
N	0.489778436	-1.625633988	1.003431663
H	1.504484653	-1.606297803	1.059386903
H	0.134535515	-1.410733802	1.931436946
H	0.284970617	2.103419164	0.093916797
H	0.217656497	-2.582047343	0.791471018
O	-1.003591650	0.885921322	-1.773844616
O	-1.028871306	-1.943953298	-1.346233426
C	-1.215361902	0.512466749	-2.996565762
C	-1.185870178	-1.983890291	-2.631089682
O	-1.828011567	1.233086582	-3.781125527
O	-1.726503307	-2.945543198	-3.171557571
C	-0.646801161	-0.819032498	-3.453803410
C	0.917482060	-0.888040549	-3.515570682
C	-0.659011045	-1.088215048	-4.966789627
C	0.787853363	-1.600219753	-4.872028722
H	1.415480267	-1.409123179	-2.698940890
H	1.337733180	0.113699137	-3.612238312
H	-1.422248289	-1.771370022	-5.334204690
H	-0.717701592	-0.147195501	-5.511397545
H	0.829900167	-2.684176251	-4.760280195
H	1.477959279	-1.295878850	-5.658056226

./carboplatin-H20-ApVTZ-pVDZ-pp_eGeom.xyz

25

Pt	0.184142414	-0.373224382	-0.385010796
N	-0.519557197	1.312653937	0.551493538
H	-1.541917762	1.353625486	0.591557079
H	-0.173540161	1.422565207	1.509145544
N	-0.555887851	-1.673451141	1.022987547
H	-0.199784291	-1.496324418	1.966606258
H	-1.578433222	-1.669373167	1.078381116
H	-0.204360679	2.131629846	0.020469210
H	-0.270163227	-2.624343833	0.765519946
O	1.008622545	0.875552744	-1.739500344
O	0.949907770	-2.001777052	-1.296085308
C	1.256579170	0.482653192	-2.971018478
C	1.167418880	-2.035461780	-2.593235437
O	1.917854483	1.190494597	-3.741777644
O	1.735950439	-3.002972632	-3.114831895
C	0.658659844	-0.850748780	-3.435047056
C	0.701745117	-1.120270168	-4.959869036
C	-0.919050303	-0.869859175	-3.529626374

C	-0.792001432	-1.529535092	-4.925125855
H	1.425471228	-1.874565261	-5.287489680
H	0.870974359	-0.183720342	-5.503734286
H	-1.443012063	-1.417397092	-2.737085084
H	-1.320949640	0.150645391	-3.578929697
H	-0.925098230	-2.618049544	-4.877293979
H	-1.436263180	-1.129099310	-5.717628298

./carboplatin-PBE0-ApVTZ-ApVTZ-pp_eGeom.xyz

25

Pt	-0.098990723	-0.362399761	-0.342534662
N	0.490290061	1.394485342	0.551629155
H	0.060794028	1.593595558	1.448271053
H	1.492565096	1.514064451	0.646723516
N	0.446431437	-1.790793903	1.035434326
H	1.443398764	-1.895111576	1.187016964
H	-0.004630227	-1.711137468	1.940136401
H	0.151640506	2.084896593	-0.121252139
H	0.102944075	-2.641974663	0.586407646
O	-0.738148962	0.919326365	-1.684487979
O	-0.767441132	-1.970268245	-1.251340468
C	-1.048275260	0.563089415	-2.916574622
C	-1.054293943	-1.997885662	-2.537930892
O	-1.599564976	1.337869590	-3.661857372
O	-1.595914648	-2.961034140	-3.026972395
C	-0.593136964	-0.813188250	-3.389721710
C	0.956034663	-0.908210446	-3.615891082
C	-0.773975385	-1.084625067	-4.893011792
C	0.679546535	-1.585440764	-4.968366765
H	1.527141349	-1.458208846	-2.866877651
H	1.389374328	0.086839282	-3.729226472
H	-1.558756053	-1.793304228	-5.145170908
H	-0.928867126	-0.145646347	-5.421089989
H	0.737873691	-2.671541030	-4.895710408
H	1.281267877	-1.253748971	-5.814730765

./carboplatin-SMD-ApVTZ-ApVTZ-pp_eGeom.xyz

25

Pt	-0.224437157	-0.363411943	-0.396520559
N	0.518984845	1.264888647	0.586744288
H	0.174462172	1.328534155	1.550870296
H	1.543414559	1.251252500	0.632348996
N	0.515319774	-1.624967978	1.028545806
H	1.539790474	-1.607489731	1.069065779
H	0.170510677	-1.394741462	1.966574185
H	0.247831963	2.130955327	0.108539576
H	0.233619799	-2.591461388	0.830364908
O	-1.032535836	0.886015370	-1.770005954
O	-1.016870353	-1.974170893	-1.333305079
C	-1.245607568	0.497506275	-3.006187124
C	-1.192635281	-2.005943283	-2.633448323
O	-1.884419957	1.220543958	-3.793393244
O	-1.758988717	-2.976495142	-3.168516023
C	-0.654660463	-0.833995482	-3.465555866

C	0.924950482	-0.881587701	-3.523122370
C	-0.657491537	-1.106345382	-4.990409216
C	0.810315822	-1.588506681	-4.894833977
H	1.425548157	-1.405929769	-2.700602347
H	1.332854024	0.133973902	-3.608120291
H	-1.409510607	-1.812828524	-5.358952778
H	-0.740891131	-0.161689719	-5.540394681
H	0.880059047	-2.679447501	-4.795265978
H	1.497693822	-1.255010324	-5.681549033

./carboplatin-M062X-CPCM-ApVTZ-ApVDZ-pp-2_eGeom.xyz

25

Pt	-1.119590000	0.012346000	0.039559000
N	-2.340749000	1.622128000	-0.298154000
H	-2.565436000	1.754200000	-1.279974000
H	-3.220481000	1.574162000	0.207331000
N	-2.476013000	-1.357312000	-0.648968000
H	-3.363493000	-1.333487000	-0.155149000
H	-2.680353000	-1.252540000	-1.638466000
H	-1.859151000	2.461549000	0.015859000
H	-2.086100000	-2.288170000	-0.519942000
O	0.230963000	1.329680000	0.773434000
O	0.095001000	-1.552818000	0.460053000
C	1.508380000	1.121049000	0.730673000
C	1.380628000	-1.415174000	0.538487000
O	2.309412000	1.901400000	1.225634000
O	2.101474000	-2.292492000	0.994035000
C	1.992814000	-0.129783000	-0.013530000
C	3.512179000	-0.142107000	-0.243560000
C	1.815776000	0.079639000	-1.555270000
C	3.288776000	0.531409000	-1.612573000
H	3.859688000	-1.166608000	-0.348983000
H	4.115388000	0.384143000	0.489732000
H	1.657345000	-0.876581000	-2.052510000
H	1.045482000	0.780424000	-1.869636000
H	3.883731000	0.175505000	-2.449828000
H	3.372610000	1.614392000	-1.544757000

./carboplatin-CPCM-ApVDZ-ApVTZ-pp_eGeom.xyz

25

Pt	0.194937398	-0.346906308	-0.390993074
N	-0.580749482	1.308807174	0.531881756
H	-1.607553107	1.306181083	0.576291602
H	-0.238040157	1.445881132	1.491173475
N	-0.465775898	-1.665206452	1.032437589
H	-0.114919736	-1.461390819	1.976608664
H	-1.490351040	-1.717364067	1.096273841
H	-0.305555870	2.141904906	-0.006537132
H	-0.131797423	-2.607109020	0.785376605
O	0.944659619	0.928987677	-1.761751066
O	1.032785450	-1.946472492	-1.287440534
C	1.191634714	0.532147652	-2.997605749
C	1.231803709	-1.982620968	-2.592708929
O	1.812647371	1.265657246	-3.788206125

O	1.846384892	-2.930350650	-3.114209126
C	0.648349244	-0.834447051	-3.440085763
C	0.680756311	-1.117472725	-4.966910378
C	-0.931725134	-0.930256897	-3.506114636
C	-0.798967669	-1.586513885	-4.907719865
H	1.434590021	-1.851591613	-5.295647103
H	0.809477735	-0.174840469	-5.524493410
H	-1.413975253	-1.507693287	-2.698896906
H	-1.386730665	0.075268784	-3.544985186
H	-0.889623918	-2.686149568	-4.858193130
H	-1.474954102	-1.208802154	-5.694674427

./carboplatin-M062X-CPCM-ApVTZ-pVTZ-2_eGeom.xyz

25

Pt	-1.119651899	-0.012256178	0.039014027
N	-2.475489752	1.358004799	-0.648476204
H	-2.680738332	1.253007563	-1.637765217
H	-3.362973532	1.335108247	-0.154553996
N	-2.340179919	-1.622297569	-0.297720435
H	-3.220532951	-1.574496600	0.206772298
H	-2.564570719	-1.755376658	-1.279498716
H	-2.085165022	2.288868248	-0.520372753
H	-1.858783255	-2.461591209	0.017012651
O	0.094455369	1.552075385	0.458991166
O	0.230040815	-1.329252354	0.772007042
C	1.379918791	1.414826031	0.538744105
C	1.507491073	-1.121643187	0.729570066
O	2.100368951	2.292063865	0.995300750
O	2.308128680	-1.902904165	1.223958537
C	1.992846147	0.129709810	-0.013155221
C	3.512443636	0.142225579	-0.241708135
C	1.817324192	-0.078635561	-1.555239760
C	3.290476792	-0.530024751	-1.611552688
H	4.114963643	-0.384689106	0.491683487
H	3.860098858	1.166818990	-0.345813316
H	1.047560116	-0.779450272	-1.870903891
H	1.659092586	0.877914539	-2.051933494
H	3.374470456	-1.613057079	-1.544787604
H	3.886111276	-0.173149367	-2.447913701

./carboplatin-M062X-TZ-pVDZ_eGeom.xyz

25

Pt	-0.112379354	-0.358445517	-0.352223802
N	0.499099259	1.422016147	0.549987002
H	0.070909663	1.632699711	1.444586123
H	1.501340270	1.544134547	0.642174888
N	0.447453211	-1.817285232	1.034727188
H	1.444157061	-1.932387496	1.180023051
H	0.000889530	-1.752214715	1.942763276
H	0.158504281	2.103781908	-0.131129717
H	0.095800727	-2.657255529	0.570345073
O	-0.757055646	0.935292826	-1.698876700
O	-0.795047588	-1.973064769	-1.269474903
C	-1.076784456	0.572522437	-2.927654557

C	-1.057724994	-2.003466262	-2.561365852
O	-1.639494781	1.330908564	-3.676791084
O	-1.558315744	-2.973818743	-3.074103923
C	-0.604437748	-0.801125189	-3.397467787
C	0.947884236	-0.893920735	-3.591183818
C	-0.754000935	-1.072082055	-4.903510075
C	0.688735585	-1.617894061	-4.927744109
H	1.508233164	-1.415725119	-2.816290068
H	1.371129144	0.099874031	-3.735637095
H	-1.551573894	-1.753379244	-5.180613370
H	-0.852182472	-0.129877918	-5.435675648
H	0.703241046	-2.698489074	-4.802338031
H	1.318927444	-1.341151283	-5.769655072

./carboplatin-ApVTZ-pVDZ-pp-2_eGeom.xyz

25

Pt	-1.025465030	-0.017051236	0.098454079
N	-2.243116053	1.561930680	-0.483494897
H	-2.354901240	1.672801690	-1.494166218
H	-3.171595608	1.583221068	-0.054436970
N	-2.103703792	-1.702748807	-0.462367625
H	-3.013747518	-1.807732036	-0.006689611
H	-2.233690006	-1.829807280	-1.468879315
H	-1.710187176	2.371297145	-0.130895873
H	-1.488750777	-2.456907352	-0.121049041
O	0.054532015	1.511720341	0.767210365
O	0.186164387	-1.442975106	0.773009202
C	1.354633274	1.388267552	1.057379510
C	1.473819965	-1.212397107	1.047944304
O	1.944698788	2.303231916	1.613093768
O	2.144658112	-2.078115619	1.591113800
C	2.078347594	0.123580595	0.579266283
C	3.620387988	0.145066508	0.740603416
C	2.300866820	0.086278880	-0.987407431
C	3.775232478	-0.308582833	-0.732904451
H	4.014584651	-0.521862009	1.513988700
H	3.962215245	1.171621691	0.914822793
H	1.662919676	-0.604290811	-1.554199508
H	2.201530618	1.092955480	-1.415335644
H	3.927652564	-1.392279943	-0.814628209
H	4.532658023	0.204097590	-1.339493425

./carboplatin-M06L-H20-aug-pVTZ_eGeom.xyz

25

Pt	0.219788798	-0.364955899	-0.410716982
N	-0.549320431	1.297601927	0.552423426
H	-1.569188785	1.324588144	0.585401807
H	-0.230574590	1.414732406	1.515197593
N	-0.469647489	-1.708643648	1.008322137
H	-0.119567796	-1.540265402	1.952299871
H	-1.486791102	-1.749352765	1.085391446
H	-0.259588037	2.140155478	0.052117011
H	-0.164983711	-2.650241135	0.753813607
O	0.985486959	0.926862041	-1.768210636

O	1.037449431	-1.965335878	-1.342529525
C	1.204321470	0.544824544	-3.003599205
C	1.198595644	-1.986134438	-2.643227963
O	1.801412362	1.270183151	-3.797002263
O	1.738311686	-2.938940205	-3.202092421
C	0.643737644	-0.803473648	-3.445230836
C	0.651330096	-1.067324145	-4.957512997
C	-0.915803392	-0.892270574	-3.498997449
C	-0.781276029	-1.605601607	-4.851825145
H	1.430634584	-1.743853788	-5.330181481
H	0.700978374	-0.116018431	-5.502270395
H	-1.415910864	-1.416150761	-2.671178069
H	-1.360459861	0.109707869	-3.594154967
H	-0.797405813	-2.698130665	-4.731529461
H	-1.494222140	-1.332315339	-5.641836113

./carboplatin-M062X-ApVTZ-ApVTZ-pp_eGeom.xyz

25

Pt	-0.106084819	-0.361781652	-0.350622824
N	0.495097852	1.412408275	0.556929685
H	0.075136234	1.609807461	1.458599109
H	1.497868144	1.537114799	0.642169588
N	0.449493068	-1.813613853	1.035727417
H	1.447166294	-1.927252219	1.177048680
H	0.008948654	-1.738914988	1.946145488
H	0.146427158	2.102162025	-0.112083026
H	0.095538820	-2.658730765	0.582378510
O	-0.748134317	0.930036882	-1.697390282
O	-0.780810040	-1.974440981	-1.272347754
C	-1.076671147	0.569914355	-2.923924936
C	-1.052706521	-2.004202518	-2.561842738
O	-1.647778389	1.328529476	-3.667449391
O	-1.558619845	-2.973648816	-3.072079597
C	-0.604423836	-0.801630978	-3.400766563
C	0.947814565	-0.890396859	-3.599806845
C	-0.758071068	-1.070560656	-4.906843251
C	0.685942631	-1.612480065	-4.936497244
H	1.511888559	-1.412646926	-2.827925350
H	1.367304901	0.105012782	-3.743614361
H	-1.555237670	-1.752523012	-5.183327442
H	-0.859596719	-0.127423387	-5.436690820
H	0.704344907	-2.693214634	-4.813108434
H	1.312469594	-1.331876516	-5.779806630

./carboplatin-SMD-ApVDZ-pVDZ-pp_eGeom.xyz

25

Pt	-0.228206109	-0.359791649	-0.398260293
N	0.553709934	1.254534886	0.583080644
H	0.215905977	1.331757286	1.552715404
H	1.581739319	1.225649992	0.629259212
N	0.502454212	-1.630423221	1.026718113
H	1.530960439	-1.631316189	1.068891935
H	0.166594109	-1.400086654	1.972237609
H	0.302050016	2.132976650	0.108947511

H	0.209495207	-2.598834756	0.835675040
O	-1.027219258	0.908239745	-1.772818143
O	-1.059179545	-1.964581220	-1.330837362
C	-1.238257573	0.514759673	-3.014083740
C	-1.230878769	-1.988056964	-2.637880981
O	-1.868964507	1.248595635	-3.807768268
O	-1.823753331	-2.949425408	-3.175717135
C	-0.660720031	-0.827633171	-3.468091824
C	0.921919728	-0.899398870	-3.509208336
C	-0.656275276	-1.100505607	-4.997079392
C	0.812866354	-1.590394359	-4.894402591
H	1.404405041	-1.447101924	-2.682055154
H	1.349781664	0.116327569	-3.573883241
H	-1.414690020	-1.809718891	-5.367535089
H	-0.737302917	-0.150229447	-5.550648416
H	0.879391236	-2.689376300	-4.808081689
H	1.511481107	-1.246319577	-5.676302823

./carboplatin-CPCM-ApVTZ-ApVTZ-pp_eGeom.xyz

25

Pt	0.193838316	-0.363460424	-0.387486546
N	-0.535601794	1.311393177	0.548221755
H	-1.558418429	1.330638629	0.596971233
H	-0.183779154	1.431833125	1.502678862
N	-0.507475597	-1.672846534	1.031181187
H	-0.146470604	-1.484790912	1.971000192
H	-1.529589563	-1.687985081	1.095435966
H	-0.242392697	2.135068056	0.011497145
H	-0.205720317	-2.619248744	0.774662686
O	0.981389066	0.895570932	-1.752257271
O	0.982459248	-1.979088148	-1.298557188
C	1.225909173	0.503254262	-2.984507506
C	1.186727277	-2.014664147	-2.597680371
O	1.867932729	1.220193493	-3.763461813
O	1.766597658	-2.974394841	-3.121638523
C	0.648919932	-0.842474200	-3.439566739
C	0.685312753	-1.116533405	-4.963811195
C	-0.928941423	-0.891764061	-3.522268276
C	-0.799885483	-1.554553861	-4.916089503
H	1.420976439	-1.857728971	-5.294760286
H	0.831953740	-0.178680764	-5.512013229
H	-1.436960329	-1.445757895	-2.723853633
H	-1.350300601	0.120816977	-3.572782309
H	-0.911365672	-2.645236753	-4.862853070
H	-1.457807657	-1.169912680	-5.705190578

./carboplatin-M06L-CPCM-aug-pVDZ_eGeom.xyz

25

Pt	0.218361328	-0.364792758	-0.410275508
N	-0.547263118	1.307105153	0.550886899
H	-1.567842032	1.342909045	0.576461803
H	-0.234828079	1.421845356	1.516786119
N	-0.489583653	-1.707277472	1.008806000
H	-0.140313551	-1.543598980	1.954684242

H	-1.507922579	-1.740247781	1.083417342
H	-0.247760526	2.149062730	0.053781321
H	-0.192557216	-2.652161544	0.754538202
O	1.003687115	0.923225697	-1.771296352
O	1.033974892	-1.974233082	-1.342953453
C	1.221578794	0.536069781	-3.006084690
C	1.196844662	-1.994136465	-2.644102406
O	1.827902898	1.254003533	-3.798380036
O	1.733748611	-2.948696723	-3.201547290
C	0.649501976	-0.807758271	-3.446174103
C	0.653491869	-1.074008851	-4.957873537
C	-0.910445537	-0.884583550	-3.498476950
C	-0.781333455	-1.605482571	-4.847806198
H	1.429309591	-1.754188002	-5.331316730
H	0.705603971	-0.123529121	-5.504017551
H	-1.414310851	-1.399156553	-2.666751323
H	-1.346904508	0.120469811	-3.599766785
H	-0.801362015	-2.697294647	-4.721221358
H	-1.494271577	-1.333897504	-5.638446669

./carboplatin-M06L-H2O-TZ-aug-pVTZ-2_eGeom.xyz

25

Pt	-0.978027841	-0.013876346	0.226091918
N	-2.248161882	1.455211435	-0.494861309
H	-2.315987212	1.469648855	-1.505357849
H	-3.193411868	1.387240480	-0.136826488
N	-2.122001940	-1.595128716	-0.475214407
H	-2.219540094	-1.608511409	-1.483391891
H	-1.668091257	-2.462628724	-0.210149507
H	-1.888854743	2.360018054	-0.210066762
H	-3.057678195	-1.620284446	-0.087965554
O	0.124236286	1.495214233	1.007725302
O	0.257541781	-1.419274198	1.001301791
C	1.398315156	1.346464943	1.233149622
C	1.529271658	-1.195996789	1.167408582
O	2.035172717	2.183487696	1.861542992
O	2.257656754	-2.028837202	1.692846633
C	2.088502590	0.126235058	0.638524088
C	3.621100773	0.162350644	0.629399074
C	2.138867504	0.094248346	-0.922774434
C	3.609262247	-0.328392825	-0.822800608
H	4.120083423	-0.456174815	1.370897103
H	3.969574021	1.188514152	0.719925267
H	1.437310292	-0.571925888	-1.423013801
H	2.015856604	1.094981538	-1.335780281
H	3.719554365	-1.409638873	-0.887525757
H	4.308468632	0.131304197	-1.517951205

./carboplatin-M062X-H2O-ApVDZ-ApVDZ_eGeom.xyz

25

Pt	0.192046693	-0.378954834	-0.395639046
N	-0.558951776	1.269874018	0.557679838
H	-1.577657360	1.295507668	0.574599903
H	-0.241500851	1.368951875	1.521229856

N	-0.530557145	-1.702270641	0.991584604
H	-0.179846570	-1.537839143	1.934238950
H	-1.548101471	-1.713759202	1.049080316
H	-0.249176865	2.102788407	0.055505463
H	-0.236106807	-2.642276588	0.723876623
O	0.990969277	0.902228082	-1.751676601
O	0.992150680	-1.986765700	-1.339472678
C	1.258972980	0.514229991	-2.964081808
C	1.180037071	-2.009638868	-2.626206946
O	1.929932232	1.200247313	-3.731681431
O	1.714290424	-2.964071596	-3.185193422
C	0.663320290	-0.812488906	-3.438762642
C	0.684980790	-1.063098776	-4.957947837
C	-0.902619094	-0.855570810	-3.503977482
C	-0.777199847	-1.557213549	-4.875725181
H	1.442044680	-1.763445257	-5.318715587
H	0.765719737	-0.109643764	-5.487500290
H	-1.412612790	-1.385736130	-2.693416108
H	-1.310051817	0.158066196	-3.590317471
H	-0.829671994	-2.645928726	-4.770244798
H	-1.463103457	-1.233543830	-5.664365235

./carboplatin-M06L-ApVDZ-pVTZ_eGeom.xyz

25

Pt	-0.123504519	-0.368269763	-0.363500332
N	0.494105852	1.448819547	0.500965257
H	0.134395827	1.665315753	1.427787118
H	1.497582852	1.615684675	0.518569903
N	0.508450216	-1.849438313	0.992922746
H	1.513028119	-1.978439894	1.088451947
H	0.119102019	-1.800562342	1.931821603
H	0.086498070	2.125616144	-0.150781133
H	0.133707623	-2.694883657	0.552954148
O	-0.861522678	0.929716777	-1.686379290
O	-0.841259697	-2.004015329	-1.257615275
C	-1.141300078	0.549744615	-2.928623098
C	-1.100496114	-2.014760874	-2.559628116
O	-1.713547939	1.310005124	-3.689287721
O	-1.627794751	-2.985693972	-3.072975683
C	-0.628929768	-0.813042108	-3.383595844
C	0.928138827	-0.877813916	-3.533006671
C	-0.728434817	-1.082974481	-4.892278033
C	0.725049484	-1.580398296	-4.883585147
H	1.480276165	-1.403626132	-2.742007822
H	1.348496161	0.130818567	-3.641437693
H	-1.505560868	-1.790863617	-5.194741246
H	-0.854219007	-0.137357813	-5.429299245
H	0.778239123	-2.671036402	-4.781345839
H	1.376806911	-1.272897064	-5.710513546

./carboplatin-M06L-ApVDZ-ApVDZ_eGeom.xyz

25

Pt	-0.126767092	-0.367227119	-0.363421424
N	0.518409494	1.439021692	0.504234862

H	0.151513208	1.662284018	1.426603020
H	1.524676349	1.585726876	0.532786017
N	0.479206439	-1.858368542	0.994201240
H	1.481607607	-1.998968231	1.095099667
H	0.083742618	-1.805439637	1.930296983
H	0.130669957	2.122554358	-0.152439975
H	0.096607918	-2.698044823	0.550143781
O	-0.841112121	0.944715345	-1.690555037
O	-0.867718192	-1.993688131	-1.262448719
C	-1.121268586	0.567217052	-2.933540411
C	-1.120206158	-1.998110793	-2.565849847
O	-1.679900133	1.334952321	-3.696807147
O	-1.660007184	-2.959996625	-3.083178772
C	-0.626212371	-0.802752781	-3.386157178
C	0.930399836	-0.890258351	-3.527761732
C	-0.722087191	-1.070504729	-4.895512023
C	0.723778237	-1.589538520	-4.879546515
H	1.470945092	-1.423898335	-2.734008007
H	1.365861697	0.112176782	-3.633911886
H	-1.508065028	-1.766694971	-5.202184222
H	-0.831056156	-0.122968949	-5.432807885
H	0.760068512	-2.680862582	-4.777272335
H	1.384220258	-1.291678094	-5.703091465

./carboplatin-CPCM-2_eGeom.xyz

25

Pt	-1.019097064	-0.010993087	-0.201832226
N	-2.273429426	1.446967325	0.534869134
H	-3.232478185	1.417873517	0.153320480
H	-2.367391522	1.442669998	1.562853726
N	-2.163063497	-1.595575669	0.452089234
H	-2.252384667	-1.658924374	1.478638377
H	-3.123258200	-1.611943889	0.073058471
H	-1.885558050	2.371303830	0.281215449
H	-1.711523904	-2.473310335	0.143895830
O	0.083359337	1.510509236	-0.936023098
O	0.202963221	-1.409831876	-0.989305912
C	1.390031379	1.387096765	-1.143269565
C	1.501824503	-1.191834425	-1.158735116
O	2.023350990	2.291862968	-1.702325759
O	2.212516552	-2.046344486	-1.704169696
C	2.095259263	0.126323455	-0.616791734
C	2.239358974	0.064465810	0.959281266
C	3.645554695	0.148363832	-0.704059893
C	3.730845552	-0.320399639	0.772415412
H	1.572817552	-0.645070321	1.487070250
H	2.111045262	1.070195624	1.406449550
H	4.078538816	-0.517412429	-1.472852622
H	3.997759519	1.185740598	-0.852199457
H	3.885364905	-1.414201942	0.854051446
H	4.462952996	0.192034512	1.426521452

./carboplatin-CPCM-ApVDZ-pVDZ-pp_eGeom.xyz

25

Pt	0.192801804	-0.363914405	-0.388650608
N	-0.564017433	1.304295698	0.543394888
H	-1.591063046	1.318399033	0.588273592
H	-0.221577082	1.435092759	1.504071060
N	-0.509477779	-1.680121996	1.027386175
H	-0.156818203	-1.495446872	1.975280406
H	-1.535390226	-1.707689327	1.090633998
H	-0.278665259	2.138033872	0.010861118
H	-0.201590025	-2.630063399	0.776372480
O	0.982574404	0.909760781	-1.750672970
O	1.009803011	-1.979424455	-1.293960637
C	1.229737816	0.510962487	-2.986194362
C	1.215334640	-2.005940921	-2.598787441
O	1.874495501	1.233499758	-3.767788208
O	1.816450161	-2.959920413	-3.124470607
C	0.657804121	-0.840207083	-3.439502496
C	0.689996925	-1.112598046	-4.968211639
C	-0.923422410	-0.900628611	-3.511098564
C	-0.801044841	-1.545693861	-4.918923018
H	1.427161655	-1.862628440	-5.298899641
H	0.844670140	-0.169446135	-5.518310362
H	-1.420525361	-1.475601923	-2.711215070
H	-1.356447423	0.114862089	-3.540688907
H	-0.919392818	-2.643200461	-4.881671169
H	-1.464091260	-1.142732899	-5.704357030

./carboplatin-PBE0-H2O-ApVDZ-pVDZ-pp_eGeom.xyz

25

Pt	0.201121959	-0.364421129	-0.404104509
N	-0.539620473	1.289356310	0.528451491
H	-1.557212844	1.306087506	0.582056229
H	-0.191612552	1.417796559	1.477807234
N	-0.503043452	-1.664147491	1.000484434
H	-0.147456186	-1.486679200	1.938893269
H	-1.519853379	-1.682199122	1.068495792
H	-0.259722935	2.115564414	-0.001007165
H	-0.207952524	-2.607843947	0.748169241
O	0.980190804	0.891843283	-1.760429239
O	0.997411785	-1.966233190	-1.310938898
C	1.222779534	0.502662860	-2.980034788
C	1.195755616	-1.999931792	-2.598006460
O	1.860962802	1.208536876	-3.759589558
O	1.775443966	-2.946168237	-3.127932925
C	0.648576982	-0.837403302	-3.432156055
C	0.675204904	-1.108079529	-4.948956742
C	-0.919022481	-0.894906250	-3.497417067
C	-0.800748161	-1.553602960	-4.887702832
H	1.413241974	-1.842499744	-5.286220267
H	0.809366412	-0.168574851	-5.495136341
H	-1.417108756	-1.454686219	-2.697737622
H	-1.346964324	0.114095367	-3.542171371
H	-0.903472180	-2.644289535	-4.831954992
H	-1.468959482	-1.174629448	-5.669989870

./carboplatin-M062X-CPCM-TZ-aug-pVDZ-2_eGeom.xyz

25

Pt	0.189728804	-0.361369212	-0.397329119
N	-0.641136925	1.326041945	0.422327201
H	-1.651726093	1.273628544	0.511422684
H	-0.269346617	1.551291280	1.340439986
N	-0.454643527	-1.599268947	1.104677590
H	-0.109381758	-1.334191215	2.022669813
H	-1.466738696	-1.657509209	1.169115744
H	-0.432940481	2.112728693	-0.188407776
H	-0.111587185	-2.538043792	0.914337607
O	0.885277228	0.835241199	-1.875142665
O	1.088461165	-1.985987041	-1.206855029
C	1.081375959	0.407513351	-3.083878664
C	1.345415017	-2.054960343	-2.476820482
O	1.536726409	1.127364236	-3.959059167
O	2.063520122	-2.924086155	-2.947020175
C	0.670795570	-1.037539011	-3.394252878
C	0.702019367	-1.355815125	-4.897514575
C	-0.890342068	-1.132481281	-3.461170201
C	-0.785923109	-0.961309061	-4.990323504
H	0.848781056	-2.422722935	-5.044229712
H	1.414313617	-0.793286300	-5.493083626
H	-1.224375432	-2.130167603	-3.178820826
H	-1.451814595	-0.392939613	-2.894520346
H	-1.432771325	-1.583231210	-5.603763010
H	-0.906379494	0.080746037	-5.279927877

./carboplatin-M06L-SMD-TZ-aug-pVTZ_eGeom.xyz

25

Pt	-0.240270997	-0.368393445	-0.421019958
N	0.510479776	1.262833103	0.583382406
H	0.205781788	1.294119381	1.550393855
H	1.524407301	1.276610858	0.592800090
N	0.517586443	-1.653048398	0.998119794
H	1.512826305	-1.807349740	0.878758775
H	0.382386318	-1.319748056	1.946434562
H	0.206549425	2.127197260	0.147915412
H	0.067771918	-2.559965255	0.934949324
O	-1.055632708	0.893955316	-1.796729340
O	-1.048116630	-1.974433376	-1.382205606
C	-1.243338366	0.516185145	-3.024874901
C	-1.208137513	-1.987977148	-2.669929845
O	-1.845763061	1.236468268	-3.822875490
O	-1.756537755	-2.938116960	-3.229884980
C	-0.657194466	-0.811171109	-3.468342930
C	0.903934855	-0.878171925	-3.485015078
C	-0.620029147	-1.075124167	-4.978043183
C	0.806785154	-1.612070780	-4.826418806
H	1.380050332	-1.379754792	-2.643549843
H	1.326971825	0.120584485	-3.585111268
H	-1.381953777	-1.737891245	-5.380994072
H	-0.641494957	-0.133104132	-5.521218592
H	0.819528362	-2.692244787	-4.689516688

H 1.530716585 -1.349741271 -5.594152651
./carboplatin-M062X-ApVTZ-pVTZ-3_eGeom.xyz
25

Pt	-1.009863149	-0.013227158	-0.106637819
N	-2.243669075	1.554089403	0.495274679
H	-3.160916446	1.581360147	0.063617660
H	-2.363426231	1.654947238	1.497110543
N	-2.091785410	-1.707598273	0.445334909
H	-2.212648163	-1.845188108	1.442627534
H	-2.997315500	-1.812134254	0.000841004
H	-1.711657418	2.358866321	0.157416093
H	-1.481103786	-2.448557515	0.094761689
O	0.065340180	1.514931295	-0.741627184
O	0.205431114	-1.415845586	-0.783806287
C	1.340429836	1.397742019	-1.061425536
C	1.479015030	-1.197298549	-1.045380456
O	1.928430869	2.285916675	-1.627194002
O	2.168924305	-2.048796756	-1.550201281
C	2.068187070	0.141889106	-0.586396120
C	2.265193241	0.087316363	0.968022393
C	3.599145262	0.168868146	-0.725584940
C	3.719980218	-0.358893309	0.718742795
H	1.605962522	-0.578628160	1.523458381
H	2.207063749	1.089450311	1.391828873
H	4.009132221	-0.446883936	-1.519054256
H	3.938258295	1.196327504	-0.823692524
H	3.809879467	-1.442790765	0.737240175
H	4.485535799	0.080374842	1.353748676

./carboplatin-PBE0-ApVDZ-pVDZ-pp_eGeom.xyz
25

Pt	-0.102139492	-0.360498145	-0.344385196
N	0.501782227	1.402756293	0.536686539
H	0.080509834	1.615162271	1.438555141
H	1.507925222	1.529682225	0.622095103
N	0.462666715	-1.793574678	1.026805394
H	1.463823122	-1.900919313	1.174402746
H	0.016278871	-1.727644463	1.939224196
H	0.156792363	2.094037936	-0.137853797
H	0.119520453	-2.648411027	0.575835562
O	-0.763211590	0.927501390	-1.682442930
O	-0.789432806	-1.977555047	-1.241600934
C	-1.068785208	0.559471619	-2.917196851
C	-1.073901182	-1.999736363	-2.533761489
O	-1.629343238	1.331685061	-3.668840838
O	-1.626059053	-2.963938500	-3.025065230
C	-0.602515247	-0.816944416	-3.385767288
C	0.952285452	-0.909416998	-3.597008561
C	-0.772265862	-1.091149258	-4.893680096
C	0.690100238	-1.579529178	-4.960916964
H	1.516607733	-1.469006846	-2.840471734
H	1.389370477	0.092304231	-3.697128219
H	-1.554401466	-1.812074922	-5.147842987

```
H      -0.936278809      -0.148165742      -5.424931152
H       0.759308339      -2.672140330      -4.897008271
H       1.298669918      -1.232248571      -5.804831155
./carboplatin-PBE0-TZ-pVTZ-pp_eGeom.xyz
25
```

```
Pt      -0.104451077      -0.359582150      -0.341113962
N       0.485125884       1.400305556       0.550473488
H       0.050805666       1.604484327       1.443385526
H       1.486786787       1.520070626       0.648991317
N       0.441259294      -1.789812781       1.037213957
H       1.437624656      -1.892368820       1.192173042
H      -0.014793265      -1.715804795       1.939631030
H       0.149461814       2.085926825      -0.128423941
H       0.101616216      -2.638648595       0.581487874
O      -0.741920521       0.921588582      -1.684332484
O      -0.771894914      -1.968578530      -1.248729876
C      -1.043071908       0.565226387      -2.919439697
C      -1.048956575      -1.999110534      -2.538172111
O      -1.584754471       1.341281167      -3.669084814
O      -1.579914118      -2.966004972      -3.029795857
C      -0.589276945      -0.812759547      -3.387771852
C       0.959393847      -0.910292616      -3.615953588
C      -0.772061237      -1.086141185      -4.890250110
C       0.679728059      -1.591440994      -4.965987662
H       1.531103615      -1.458014346      -2.865771161
H       1.393774915       0.083799559      -3.733525365
H      -1.558719037      -1.793686941      -5.139743109
H      -0.925174711      -0.147446214      -5.419265358
H       0.733696054      -2.677432619      -4.888682314
H       1.281918983      -1.265910159      -5.814441986
./carboplatin-M06L-ApVTZ-pVDZ_eGeom.xyz
25
```

```
Pt      -0.098250485      -0.364161883      -0.357717678
N       0.550011801       1.431158093       0.526780897
H       0.149323400       1.653615083       1.428995619
H       1.552256839       1.551660081       0.595829935
N       0.439554663      -1.868702118       1.012151265
H       1.431182833      -2.020794605       1.143523992
H       0.013276047      -1.804621632       1.927822518
H       0.200361145       2.112999159      -0.145825319
H       0.056360367      -2.692106636       0.548752750
O      -0.750414269       0.956430455      -1.695572132
O      -0.838971427      -1.972360939      -1.270077975
C      -1.062786266       0.594047440      -2.929234050
C      -1.112639754      -1.975794394      -2.563110876
O      -1.600616148       1.376552315      -3.680491637
O      -1.666272519      -2.925976974      -3.069941006
C      -0.616594129      -0.787687502      -3.389059072
C       0.933034682      -0.908550852      -3.564961364
C      -0.746841791      -1.052806883      -4.893868782
C       0.680201402      -1.615228872      -4.901060710
H       1.477111921      -1.437858569      -2.781736731
```


H	1.381325527	0.076884722	-3.693006375
H	-1.552120746	-1.720652437	-5.185905884
H	-0.833482184	-0.109243334	-5.427038240
H	0.684019940	-2.697899754	-4.788098631
H	1.328276163	-1.349252732	-5.734279523

./carboplatin-PBE0-SMD-ApVTZ-pVDZ-pp_eGeom.xyz

25

Pt	-0.221604379	-0.360464798	-0.409383055
N	0.508872254	1.256853966	0.564981868
H	0.168756687	1.318640074	1.521219626
H	1.524411334	1.250029695	0.610082610
N	0.519620641	-1.603600979	1.005749867
H	1.534340777	-1.571856561	1.054866483
H	0.168408885	-1.384598731	1.934324966
H	0.235774334	2.114992076	0.093123936
H	0.257402010	-2.565246647	0.804940463
O	-1.023117008	0.868464217	-1.780521248
O	-0.997445291	-1.960853983	-1.342349260
C	-1.242148766	0.485398422	-2.996776757
C	-1.171498166	-2.003990730	-2.622983321
O	-1.880323461	1.190392302	-3.778310876
O	-1.714703664	-2.971002708	-3.155304084
C	-0.651674131	-0.836546020	-3.455268900
C	0.913605146	-0.877813219	-3.516718223
C	-0.659573623	-1.110861485	-4.967576705
C	0.796950021	-1.594830690	-4.871605985
H	1.419727718	-1.388529488	-2.698652127
H	1.315332875	0.131285437	-3.614934059
H	-1.410090720	-1.808347950	-5.334112550
H	-0.734964428	-0.172834979	-5.515335397
H	0.860834390	-2.677576119	-4.758343237
H	1.480413574	-1.277453874	-5.658243045

./carboplatin-M06L-ApVTZ-ApVTZ-2_eGeom.xyz

25

Pt	-1.000613295	-0.009983377	-0.099324585
N	-2.221900422	1.596758481	0.494736654
H	-3.141449781	1.635976036	0.073882010
H	-2.333639629	1.718566019	1.493070764
N	-2.069273853	-1.738613536	0.448554066
H	-2.186801311	-1.894375903	1.441452404
H	-2.972944313	-1.857367159	0.008465584
H	-1.683892640	2.388230982	0.142682176
H	-1.450687983	-2.465418340	0.089365885
O	0.074747686	1.527861578	-0.757231586
O	0.214322947	-1.428287601	-0.788565487
C	1.362375750	1.401165947	-1.035375457
C	1.491356432	-1.191821577	-1.034406464
O	1.964501815	2.302014786	-1.575518618
O	2.182603637	-2.038743166	-1.555028836
C	2.064928228	0.140460967	-0.548477527
C	2.223226968	0.083208927	1.006801461
C	3.595504206	0.163643456	-0.641979480

C	3.674433374	-0.362005197	0.796838907
H	1.541442676	-0.575084888	1.546793529
H	2.151798810	1.083010286	1.435508939
H	4.028225443	-0.450699552	-1.426275946
H	3.942159219	1.189618173	-0.738349876
H	3.767781769	-1.446263008	0.821773017
H	4.426560267	0.068064666	1.455899466

./carboplatin-M062X-H20-ApVTZ-ApVTZ-pp-2_eGeom.xyz

25

Pt	-1.070139481	-0.002064476	0.136064614
N	-2.401080351	1.410126432	-0.513823279
H	-2.571409756	1.366347054	-1.514327776
H	-3.305259882	1.358854855	-0.053353058
N	-2.283337086	-1.585617956	-0.328817494
H	-3.178674318	-1.562136007	0.150445185
H	-2.477638775	-1.662774261	-1.323002829
H	-2.015160970	2.330428668	-0.315094804
H	-1.813862693	-2.443163465	-0.046689690
O	0.132674253	1.531436866	0.681008551
O	0.252785453	-1.363622258	0.833957854
C	1.414777106	1.385622146	0.794339665
C	1.531478087	-1.158902933	0.844674902
O	2.121302912	2.234057751	1.321426911
O	2.314046926	-1.971184393	1.317400749
C	2.043638106	0.131276373	0.191677795
C	3.570155078	0.151065897	0.015527344
C	1.920335812	0.011420001	-1.364935557
C	3.393587250	-0.441959503	-1.396877511
H	4.146358973	-0.418779521	0.737856159
H	3.922901727	1.178629825	-0.018469120
H	1.160044136	-0.667110681	-1.745689107
H	1.781289157	0.995266838	-1.811576060
H	3.473003978	-1.527343718	-1.388383203
H	4.018007355	-0.040890533	-2.191168239

./carboplatin-M062X-H20-aug-pVDZ_eGeom.xyz

25

Pt	0.214050295	-0.361999080	-0.395315341
N	-0.548669431	1.280265551	0.565857892
H	-1.570498998	1.293597612	0.612911555
H	-0.208448926	1.400692653	1.523262750
N	-0.455114034	-1.698975013	1.009791021
H	-0.093764039	-1.529196031	1.951595565
H	-1.474252775	-1.741411666	1.088947404
H	-0.268950284	2.118580887	0.047400038
H	-0.142691392	-2.636568048	0.739285397
O	0.952190117	0.932156025	-1.761461150
O	1.024634336	-1.954785171	-1.341244945
C	1.188124240	0.558206703	-2.990545794
C	1.178176748	-1.984773661	-2.636891516
O	1.786027202	1.275069802	-3.780331819
O	1.692748371	-2.939059267	-3.203243386
C	0.634632642	-0.794564935	-3.444644192

C	0.666390130	-1.061434885	-4.960097256
C	-0.928126670	-0.886813392	-3.515480764
C	-0.770250322	-1.619473719	-4.866355041
H	1.455062027	-1.736129197	-5.310923462
H	0.705266785	-0.108088044	-5.500213301
H	-1.433561784	-1.405109664	-2.689085074
H	-1.365300836	0.114757326	-3.637880211
H	-0.766011947	-2.708810687	-4.726652765
H	-1.474354445	-1.356486870	-5.665814616

./carboplatin-PBE0-SMD-ApVTZ-ApVTZ-pp_eGeom.xyz

25

Pt	-0.214015629	-0.368904588	-0.406213724
N	0.491805259	1.262078576	0.563444097
H	0.157008101	1.317329342	1.522160743
H	1.507777218	1.273960886	0.601396008
N	0.569713615	-1.598120355	0.998015872
H	1.584036787	-1.542510419	1.037487396
H	0.222086339	-1.389228456	1.930478131
H	0.199433691	2.114993252	0.093280635
H	0.328250868	-2.565527917	0.797616967
O	-1.056532872	0.843564987	-1.764969527
O	-0.963629065	-1.982729382	-1.333942478
C	-1.276788568	0.459213216	-2.980600386
C	-1.146022479	-2.028830949	-2.613301176
O	-1.937086389	1.151983604	-3.754835755
O	-1.669460513	-3.008304606	-3.142863767
C	-0.661356583	-0.848124169	-3.448425717
C	0.903871825	-0.854136024	-3.526755993
C	-0.678916471	-1.119611615	-4.961232066
C	0.788865426	-1.571367855	-4.881635443
H	1.430394484	-1.354480895	-2.715151216
H	1.281649900	0.163933967	-3.627647181
H	-1.417638319	-1.832825779	-5.321458040
H	-0.780797106	-0.182379636	-5.506067296
H	0.877838860	-2.652624015	-4.771069176
H	1.456818631	-1.237703942	-5.674839918

./carboplatin-H20-ApVDZ-pVTZ-pp_eGeom.xyz

25

Pt	0.193358407	-0.362755464	-0.387836964
N	-0.543754021	1.308987642	0.544878856
H	-1.570696664	1.335140465	0.584726145
H	-0.203704135	1.432409498	1.507323098
N	-0.511160591	-1.670551149	1.029079161
H	-0.162260156	-1.481671313	1.977443911
H	-1.537293755	-1.698213289	1.087593932
H	-0.244958889	2.139774274	0.015180523
H	-0.200917029	-2.620698741	0.781894446
O	0.984169312	0.901232791	-1.749210850
O	0.992101335	-1.980634822	-1.291442856
C	1.229551456	0.504438971	-2.985752750
C	1.199812862	-2.013186077	-2.595786982
O	1.874550460	1.226562093	-3.767394890

O	1.792221608	-2.974138821	-3.118465022
C	0.653548681	-0.844653150	-3.439894095
C	0.688472718	-1.119648565	-4.968060612
C	-0.927971342	-0.896801340	-3.516795994
C	-0.803803139	-1.548744642	-4.921132839
H	1.424478604	-1.871853168	-5.296337827
H	0.846218522	-0.177524536	-5.519047279
H	-1.431420781	-1.464742852	-2.715810058
H	-1.354764800	0.121145550	-3.553375007
H	-0.924483993	-2.645805764	-4.878580163
H	-1.463987660	-1.148420360	-5.710324896

./carboplatin-M06L-TZ-pVTZ_eGeom.xyz

25

Pt	0.112066424	-0.361555467	-0.357548895
N	-0.492860610	1.457908856	0.513676954
H	-1.491565231	1.605380808	0.581705642
H	-0.085423839	1.678869327	1.413309070
N	-0.473308971	-1.853107757	1.010980079
H	-0.047557318	-1.804546935	1.927890306
H	-1.469112609	-1.978516797	1.138859516
H	-0.125431509	2.122572979	-0.166683132
H	-0.111202027	-2.683955570	0.543703370
O	0.805829773	0.936769255	-1.695472830
O	0.813685166	-1.992188355	-1.259903898
C	1.100140870	0.561863857	-2.930876405
C	1.077440339	-2.009648483	-2.555708116
O	1.653072862	1.327443487	-3.687817514
O	1.594850702	-2.979654625	-3.062475583
C	0.614891307	-0.809256168	-3.383347634
C	0.737651076	-1.082357984	-4.887578744
C	-0.937941880	-0.886606446	-3.558563500
C	-0.707176536	-1.597263141	-4.896658867
H	1.519930532	-1.778802012	-5.175111532
H	0.859590572	-0.144297592	-5.423353895
H	-1.495951460	-1.402537864	-2.776230601
H	-1.360743794	0.110540854	-3.682261762
H	-0.747850118	-2.679624689	-4.788431699
H	-1.345716713	-1.307782307	-5.729229338

./carboplatin-M06L-CPCM-pVTZ_eGeom.xyz

25

Pt	0.216429728	-0.361226180	-0.409181565
N	-0.545389394	1.314646858	0.545604301
H	-1.565581907	1.345169328	0.583379347
H	-0.221044384	1.439273192	1.506255232
N	-0.486120141	-1.701217893	1.013420704
H	-0.126111656	-1.540742900	1.955724975
H	-1.503790001	-1.726721670	1.097552619
H	-0.255010678	2.151582381	0.035321130
H	-0.197318516	-2.646790934	0.753184980
O	0.996609743	0.921866296	-1.772296081
O	1.027741746	-1.971118533	-1.337601988
C	1.215498449	0.535132816	-3.007774389

C	1.193182726	-1.996492937	-2.639058820
O	1.816539386	1.255393891	-3.801374349
O	1.727805002	-2.954386680	-3.192162692
C	0.648195019	-0.811741289	-3.444448524
C	0.657263830	-1.080577052	-4.955454918
C	-0.911609612	-0.890799236	-3.499942040
C	-0.779653567	-1.607746287	-4.851274956
H	1.432269800	-1.764900543	-5.323134747
H	0.716563538	-0.131563853	-5.503394472
H	-1.415102897	-1.409892203	-2.670908548
H	-1.350787665	0.113413504	-3.597072860
H	-0.804170932	-2.699958345	-4.729150185
H	-1.489100606	-1.330954502	-5.643341163

./carboplatin-M06L-SMD-pVTZ_eGeom.xyz
25

Pt	0.248294725	-0.362482393	-0.418905856
N	-0.511507648	1.273110924	0.571699545
H	-1.533713399	1.289223542	0.591187425
H	-0.207763225	1.328570854	1.546816192
N	-0.531209300	-1.637029518	0.996977418
H	-0.254915923	-1.397886716	1.951885022
H	-1.553314039	-1.661306903	0.993030382
H	-0.221131001	2.148624047	0.130317971
H	-0.220197978	-2.598504952	0.840165589
O	1.084716972	0.895919873	-1.790522170
O	1.058112707	-1.979680692	-1.365798164
C	1.257287659	0.512145514	-3.031416591
C	1.206747803	-2.000041968	-2.666513969
O	1.853895390	1.232529353	-3.838148139
O	1.739208099	-2.963349940	-3.226464167
C	0.661219582	-0.817569837	-3.464932993
C	0.629183716	-1.089191900	-4.975275903
C	-0.900403741	-0.879575142	-3.485891115
C	-0.801108201	-1.620775078	-4.825591638
H	1.398205887	-1.762020601	-5.375966759
H	0.656353961	-0.140804941	-5.526690070
H	-1.390139184	-1.378393387	-2.636712985
H	-1.323434854	0.129743784	-3.594705632
H	-0.816813720	-2.710404394	-4.681037640
H	-1.530267278	-1.361202299	-5.604634767

./carboplatin-M062X-CPCM_eGeom.xyz
25

Pt	0.000149104	-0.315310376	-0.134174473
N	-0.001413576	1.405000062	0.992037523
H	-0.824054253	1.516277887	1.590679844
H	0.817140289	1.514055431	1.596661608
N	-0.005402537	-1.588874172	1.480252618
H	0.813358234	-1.504050423	2.088473186
H	-0.828175430	-1.503614314	2.082978239
H	0.001989378	2.203232527	0.348418753
H	-0.004467938	-2.549033785	1.120228868
O	0.005847739	0.922289141	-1.712753085

O	0.002057161	-1.995024072	-1.230297013
C	0.008664181	0.591847636	-2.971315302
C	0.006950122	-2.093074591	-2.527739179
O	0.012552321	1.460959893	-3.837162646
O	0.010963813	-3.197800831	-3.062179223
C	0.005466449	-0.868792689	-3.455484447
C	1.079435411	-1.094599485	-4.581458023
C	-1.080108384	-1.091849781	-4.571559954
C	-0.005405580	-1.620944986	-5.540729704
H	1.886264041	-1.789588002	-4.318596414
H	1.490997676	-0.131719945	-4.901846173
H	-1.886710577	-1.784361146	-4.301347215
H	-1.492258852	-0.127949331	-4.888307711
H	-0.006908158	-2.714159562	-5.599786596
H	-0.009623624	-1.193267856	-6.552122492

./carboplatin-PBE0-H2O-ApVDZ-ApVTZ-pp_eGeom.xyz

25

Pt	0.197923140	-0.367043049	-0.401565421
N	-0.528008087	1.284827636	0.530100070
H	-1.545327192	1.309359816	0.578190652
H	-0.182237068	1.403983536	1.481042463
N	-0.509118063	-1.663425147	0.994174872
H	-0.160977489	-1.481939299	1.934126675
H	-1.526141235	-1.683018944	1.052190652
H	-0.236026992	2.108388089	0.003551456
H	-0.207653241	-2.605156345	0.743105532
O	0.979646123	0.883514129	-1.749761403
O	0.983079148	-1.964949249	-1.307234833
C	1.220228981	0.502117304	-2.971939067
C	1.185171708	-2.001794478	-2.593297510
O	1.855533053	1.212436733	-3.749839353
O	1.760659017	-2.951487329	-3.121705687
C	0.646563071	-0.836468141	-3.429233543
C	0.679441620	-1.105983281	-4.946130994
C	-0.921089613	-0.890668167	-3.502647574
C	-0.796639469	-1.551808057	-4.891168116
H	1.419100035	-1.839643183	-5.281407282
H	0.814993906	-0.165770700	-5.490746804
H	-1.424751563	-1.447693292	-2.704487682
H	-1.346331499	0.119283000	-3.551842897
H	-0.899046745	-2.642402943	-4.833414013
H	-1.461684535	-1.175011407	-5.677189203

./carboplatin-M062X-SMD-TZ-aug-pVDZ_eGeom.xyz

25

Pt	-0.218283960	-0.363366066	-0.401647598
N	0.520556729	1.251350903	0.587865831
H	0.184233049	1.301357799	1.547253374
H	1.537308171	1.240360456	0.628192596
N	0.541295931	-1.617517673	1.005800557
H	1.558112033	-1.591959972	1.032912288
H	0.210650805	-1.391592921	1.941397561
H	0.246677104	2.116119622	0.126164395

H	0.267311342	-2.579051042	0.813686093
O	-1.038661354	0.883432740	-1.790476029
O	-1.006075960	-1.978105310	-1.367945507
C	-1.271254212	0.494618736	-3.001883776
C	-1.166705227	-2.014048117	-2.649956622
O	-1.924396525	1.181704539	-3.784037581
O	-1.669353551	-2.986743612	-3.207380540
C	-0.666269620	-0.822083750	-3.465218693
C	0.898659646	-0.856015903	-3.515339031
C	-0.661672759	-1.088501162	-4.978782923
C	0.783990598	-1.608886266	-4.855147310
H	1.405084256	-1.343017920	-2.684847576
H	1.289214482	0.152671770	-3.643627346
H	-1.422078894	-1.762719169	-5.361844194
H	-0.694806671	-0.145592483	-5.518905357
H	0.809299918	-2.686584587	-4.703388489
H	1.484471679	-1.336183384	-5.639973133

./carboplatin-M062X-ApVDZ-ApVTZ-2_eGeom.xyz

25

Pt	0.117193464	-0.361112610	-0.356692744
N	-0.502916284	1.409344452	0.538214595
H	-1.509568747	1.535329276	0.614127616
H	-0.090568014	1.615203026	1.445243918
N	-0.465212470	-1.812063025	1.014848761
H	-0.042390426	-1.742925384	1.937657155
H	-1.468473611	-1.928383316	1.136810496
H	-0.149404441	2.100702327	-0.131140147
H	-0.102348490	-2.659899371	0.567032669
O	0.782715774	0.935435921	-1.689987295
O	0.815874042	-1.974513902	-1.261606142
C	1.096216019	0.569738258	-2.923598307
C	1.081161354	-2.001188620	-2.557508467
O	1.668891080	1.328149373	-3.675654032
O	1.601316754	-2.968866826	-3.070284679
C	0.611514613	-0.802833004	-3.395530647
C	0.748036605	-1.072700264	-4.905989782
C	-0.945638655	-0.894251957	-3.570683354
C	-0.703253801	-1.605538366	-4.921638118
H	1.542262918	-1.766959405	-5.187060959
H	0.854519477	-0.124250890	-5.438781803
H	-1.497021390	-1.432758532	-2.791238739
H	-1.374546866	0.106572629	-3.697356847
H	-0.728498417	-2.693846211	-4.807470691
H	-1.342553478	-1.308736347	-5.758841464

./carboplatin-M062X-pVTZ_eGeom.xyz

25

Pt	-0.116403926	-0.362358411	-0.346834602
N	0.501200289	1.409731512	0.556350650
H	0.074678750	1.629945554	1.457762744
H	1.510324723	1.535949947	0.648532271
N	0.440784707	-1.826163501	1.028631204
H	1.444196424	-1.960046941	1.163025518

H	0.007562391	-1.763945537	1.951361909
H	0.162012738	2.102325342	-0.124805728
H	0.073300815	-2.670637635	0.569837379
O	-0.760411061	0.942538075	-1.680247798
O	-0.804796520	-1.973095835	-1.262477638
C	-1.061266648	0.589578020	-2.924325563
C	-1.061364549	-1.997521325	-2.562657880
O	-1.596577230	1.364732492	-3.681540631
O	-1.562391359	-2.968086894	-3.082688205
C	-0.598810877	-0.791458394	-3.395168175
C	0.953062163	-0.896882238	-3.597510829
C	-0.760938848	-1.061466827	-4.902639590
C	0.679227949	-1.618864676	-4.935120630
H	1.519809279	-1.426944692	-2.818137620
H	1.386710239	0.102727636	-3.745956523
H	-1.572276361	-1.745069163	-5.172689372
H	-0.858584057	-0.108860261	-5.435472415
H	0.684143284	-2.708998046	-4.806011608
H	1.314114696	-1.347480973	-5.788345879

./carboplatin-PBE0-H2O-ApVTZ-ApVTZ-pp_eGeom.xyz

25

Pt	0.195521110	-0.364729621	-0.402447448
N	-0.533421762	1.288426899	0.533766837
H	-1.547026466	1.302875349	0.589082846
H	-0.179556149	1.408450377	1.477896319
N	-0.500166699	-1.664271589	1.002219188
H	-0.142891012	-1.479747635	1.934427530
H	-1.513309941	-1.680092764	1.066840692
H	-0.250865573	2.107712627	0.002067429
H	-0.201326257	-2.602098354	0.747358054
O	0.964246000	0.884394458	-1.758186888
O	0.980061032	-1.957648162	-1.315042045
C	1.208737302	0.506957688	-2.975266302
C	1.182282669	-1.996784926	-2.595625189
O	1.836505361	1.216480750	-3.750240239
O	1.754215406	-2.941654231	-3.122137766
C	0.644115220	-0.833352195	-3.431663453
C	0.679868920	-1.104100712	-4.944248983
C	-0.919336520	-0.894171635	-3.509854294
C	-0.787346432	-1.565219722	-4.888093691
H	1.422370427	-1.824616860	-5.280334176
H	0.801240331	-0.168726266	-5.487954538
H	-1.423404650	-1.440410663	-2.713481967
H	-1.345428072	0.107978589	-3.571970498
H	-0.876134746	-2.649843352	-4.820524134
H	-1.451642486	-1.206160820	-5.673716291

./carboplatin-PBE0-CPCM-TZ-pVTZ-pp_eGeom.xyz

25

Pt	0.200331870	-0.363009744	-0.400817686
N	-0.545769716	1.284440463	0.535377993
H	-1.559086536	1.287285703	0.594167665
H	-0.189852248	1.411991141	1.477517082

N	-0.480383356	-1.673586207	1.003093984
H	-0.119128947	-1.491369630	1.934005764
H	-1.492785492	-1.697511287	1.073018643
H	-0.274574357	2.104327498	-0.000867853
H	-0.175662378	-2.607168898	0.740603051
O	0.953424150	0.895327875	-1.755426852
O	0.997718493	-1.948148071	-1.314938016
C	1.191272234	0.522173098	-2.977428599
C	1.186209003	-1.987690669	-2.599740854
O	1.800861587	1.240001733	-3.755801580
O	1.749946688	-2.932197984	-3.131044150
C	0.639607819	-0.824287321	-3.429373674
C	0.680395615	-1.093876893	-4.941705535
C	-0.922761705	-0.900720511	-3.510600364
C	-0.780614523	-1.573944447	-4.886943452
H	1.432122837	-1.806017764	-5.275229006
H	0.791516339	-0.156539884	-5.484184301
H	-1.423919714	-1.449314043	-2.713941139
H	-1.358696225	0.096976236	-3.577005279
H	-0.853574970	-2.659482417	-4.815055527
H	-1.449289460	-1.228010744	-5.674809327

./carboplatin-M06L-H2O-ApVTZ-pVDZ_eGeom.xyz

25

Pt	0.201241852	-0.366438619	-0.409746336
N	-0.534680662	1.315442663	0.549057318
H	-1.546194414	1.346458277	0.587682101
H	-0.199688101	1.422086818	1.499073904
N	-0.508125412	-1.695814939	1.014949889
H	-0.148693151	-1.522840583	1.945942513
H	-1.518350944	-1.708536602	1.086422518
H	-0.233972604	2.137582569	0.036862135
H	-0.218172774	-2.632563564	0.755769839
O	0.991103900	0.901323617	-1.780295244
O	0.992075306	-1.980064468	-1.346368624
C	1.232823381	0.511829312	-2.997622797
C	1.180985336	-2.005529210	-2.632636270
O	1.866348504	1.215919817	-3.777191230
O	1.727056638	-2.958626277	-3.176952462
C	0.652968832	-0.822339119	-3.446635902
C	0.657646528	-1.085361241	-4.956703765
C	-0.907457406	-0.878169761	-3.503372018
C	-0.785817032	-1.591112179	-4.855204534
H	1.415010957	-1.771798061	-5.327044781
H	0.727311683	-0.143559256	-5.496395526
H	-1.409697011	-1.390774988	-2.683970356
H	-1.326753100	0.123567433	-3.594431496
H	-0.828138257	-2.672966264	-4.739514880
H	-1.481525040	-1.298068145	-5.638803007

./carboplatin-PBE0-SMD-ApVDZ-ApVTZ-pp_eGeom.xyz

25

Pt	-0.220645705	-0.370935263	-0.406397785
N	0.525920040	1.234453231	0.566580363

H	0.193832665	1.297324863	1.529369469
H	1.545320665	1.223787308	0.605736726
N	0.535167877	-1.621876548	0.988024156
H	1.554157228	-1.594394703	1.026857034
H	0.196582946	-1.409673248	1.926742581
H	0.255602640	2.101118529	0.101142103
H	0.269267926	-2.586346081	0.787493069
O	-1.036225549	0.870149209	-1.757380325
O	-1.013528811	-1.964158757	-1.336471391
C	-1.251732854	0.493172033	-2.982074122
C	-1.186682864	-1.998554272	-2.623175799
O	-1.892527807	1.208359585	-3.762203519
O	-1.738012429	-2.965576642	-3.161833948
C	-0.660507866	-0.827820594	-3.450316058
C	0.908685063	-0.871973528	-3.510716423
C	-0.670145444	-1.093056138	-4.968313835
C	0.792241857	-1.572994554	-4.878759790
H	1.413263545	-1.399424076	-2.693570664
H	1.315021681	0.143254939	-3.593494092
H	-1.424046178	-1.796077995	-5.336719487
H	-0.753260590	-0.146287180	-5.512262137
H	0.861726401	-2.663201598	-4.779265578
H	1.477832574	-1.239621289	-5.666119555

./carboplatin-M062X-SMD-TZ-pVTZ_eGeom.xyz

25

Pt	-0.229661161	-0.363517012	-0.402024278
N	0.512960025	1.246126093	0.591180909
H	0.169885537	1.300826368	1.547919096
H	1.529251447	1.228506419	0.639685818
N	0.511206237	-1.625624543	1.007496103
H	1.527816715	-1.604347001	1.044877355
H	0.172836334	-1.402968648	1.941149544
H	0.248814113	2.112060991	0.125953649
H	0.235798377	-2.585327777	0.808836387
O	-1.030482083	0.888802072	-1.794015958
O	-1.021330921	-1.969885283	-1.374777803
C	-1.255194365	0.504388136	-3.008423948
C	-1.170131056	-2.005872795	-2.658267725
O	-1.895322317	1.198440096	-3.795066110
O	-1.671316314	-2.976685850	-3.220134628
C	-0.656973471	-0.816342649	-3.468624219
C	0.908156857	-0.861149386	-3.508537688
C	-0.644104762	-1.080956918	-4.982374572
C	0.797259219	-1.611016690	-4.850383980
H	1.405712359	-1.353312557	-2.675649075
H	1.306614950	0.145021330	-3.632289931
H	-1.406376992	-1.749674281	-5.371389862
H	-0.667370394	-0.137266086	-5.521594416
H	0.814672528	-2.689094424	-4.700499782
H	1.504586148	-1.341482375	-5.630173893

./carboplatin-M062X-H2O-ApVTZ-pVTZ-2_eGeom.xyz

25

Pt	-1.119690229	-0.012560295	0.038876039
N	-2.475570820	1.358131832	-0.647745788
H	-2.678687595	1.255444280	-1.637693244
H	-3.364001752	1.333531631	-0.155600022
N	-2.340953456	-1.622292443	-0.297752279
H	-3.220088066	-1.574681765	0.208865886
H	-2.567741099	-1.754677709	-1.279079598
H	-2.086002400	2.288896439	-0.516570976
H	-1.859069826	-2.461953104	0.015321018
O	0.094068815	1.551606857	0.458474027
O	0.229717397	-1.329835315	0.770905364
C	1.379627120	1.414857395	0.538865152
C	1.507303232	-1.122274076	0.729112072
O	2.099479728	2.292976414	0.994383369
O	2.307678379	-1.904366433	1.222416047
C	1.993146681	0.129705862	-0.012191733
C	3.512946100	0.142440518	-0.239402199
C	1.819107803	-0.077999730	-1.554553383
C	3.292302525	-0.529339283	-1.609717301
H	4.114716787	-0.384754584	0.494367938
H	3.860552645	1.167127185	-0.342716049
H	1.049432847	-0.778522155	-1.871205964
H	1.661492889	0.878832391	-2.050928756
H	3.376255539	-1.612366840	-1.543076429
H	3.888672757	-0.172177070	-2.445440188

./carboplatin-SMD-ApVTZ-pVTZ-pp_eGeom.xyz

25

Pt	-0.221149104	-0.366265165	-0.395704122
N	0.492337284	1.280214961	0.579178896
H	0.153981802	1.338631175	1.545763743
H	1.517063870	1.289529380	0.616950392
N	0.559469972	-1.608358808	1.024425686
H	1.583391258	-1.565454876	1.057794711
H	0.215924455	-1.387040417	1.965028847
H	0.198425464	2.138926492	0.101227748
H	0.300706936	-2.581622411	0.828216265
O	-1.069245039	0.861801468	-1.764842574
O	-0.983497709	-1.996355432	-1.324707741
C	-1.281074874	0.466715742	-2.999163359
C	-1.166955350	-2.034099190	-2.623647526
O	-1.941693651	1.173330617	-3.783228255
O	-1.714153508	-3.018183111	-3.153837386
C	-0.661696132	-0.851072117	-3.460441711
C	0.918135939	-0.861483926	-3.527193904
C	-0.666988753	-1.125722751	-4.984910473
C	0.812205638	-1.573335762	-4.897009858
H	1.435769962	-1.372100236	-2.706589738
H	1.301322161	0.163308405	-3.616417770
H	-1.404412763	-1.850022794	-5.348304704
H	-0.775464184	-0.184036616	-5.535622739
H	0.907741982	-2.662184504	-4.795858985
H	1.487161355	-1.225472895	-5.688234451

./carboplatin-SMD-TZ-aug-pVTZ-pp-2_eGeom.xyz

25

Pt	-1.123308694	-0.007046881	-0.037153497
N	-2.495569093	1.327173214	0.678624646
H	-3.394687687	1.262674487	0.189370543
H	-2.683867349	1.186097358	1.676642703
N	-2.369283406	-1.579701873	0.348900481
H	-2.558979304	-1.688851083	1.350536369
H	-3.274671282	-1.482646095	-0.122652052
H	-2.155907270	2.288468407	0.566697102
H	-1.948181890	-2.455586989	0.020395007
O	0.084079787	1.550499105	-0.496731901
O	0.206991666	-1.325738405	-0.803089310
C	1.391732941	1.414184771	-0.536283728
C	1.502898025	-1.110733805	-0.760830480
O	2.108128954	2.334818838	-0.964922762
O	2.289927400	-1.906086353	-1.300728689
C	2.007291065	0.123211692	-0.001425876
C	1.858751802	-0.096293737	1.557364334
C	3.541961116	0.125777434	0.207766994
C	3.341934035	-0.536718520	1.592284200
H	1.089720302	-0.808898131	1.877980244
H	1.696103380	0.864522248	2.062691840
H	4.135685584	-0.411857098	-0.539794904
H	3.906175778	1.155895849	0.296344018
H	3.440424813	-1.628804235	1.542608369
H	3.951795327	-0.158675200	2.421534348

./carboplatin-M062X-H2O-ApVDZ-pVTZ_eGeom.xyz

25

Pt	0.202996234	-0.362686099	-0.400366414
N	-0.545913513	1.289966469	0.544691962
H	-1.564767416	1.315303075	0.563466434
H	-0.228544988	1.395432976	1.507730448
N	-0.496884116	-1.676970368	1.004841287
H	-0.139876861	-1.502126248	1.943389304
H	-1.513858944	-1.695155238	1.072888709
H	-0.238693453	2.121626846	0.038659437
H	-0.199713730	-2.618411385	0.744933286
O	0.980112796	0.909109342	-1.772812966
O	1.001152169	-1.972444230	-1.335688918
C	1.240987958	0.514709549	-2.984547501
C	1.181732405	-2.006566032	-2.623079274
O	1.898676987	1.200899606	-3.763480660
O	1.718547179	-2.962870874	-3.176541221
C	0.652176974	-0.820440333	-3.443519014
C	0.665151092	-1.085209048	-4.960288186
C	-0.913860318	-0.873850421	-3.497460166
C	-0.793610830	-1.586999248	-4.863697088
H	1.423739388	-1.784911485	-5.319106215
H	0.737261324	-0.136459250	-5.499467011
H	-1.415051590	-1.399974487	-2.678746571
H	-1.328417339	0.136396091	-3.589969622
H	-0.839517186	-2.675026045	-4.748546421

H -1.486517211 -1.273695930 -5.650412629
./carboplatin-TZ-aug-pVDZ-pp_eGeom.xyz
25

Pt -0.097172350 -0.342969170 -0.327116910
N 0.603156894 1.468651740 0.415651169
H 0.158807599 1.782682249 1.282090319
H 1.616961388 1.539734758 0.530124599
N 0.381625290 -1.708336266 1.164911232
H 1.382377089 -1.867536021 1.303530956
H -0.045725024 -1.530362660 2.077174438
H 0.319230912 2.112270770 -0.338372018
H -0.029827517 -2.573322786 0.782914786
O -0.678344252 0.878871777 -1.785685068
O -0.892393140 -1.991932647 -1.102344616
C -0.974218441 0.432015001 -3.011183445
C -1.176749920 -2.094635396 -2.406615644
O -1.450768231 1.195009767 -3.837693700
O -1.797921803 -3.061634679 -2.819706270
C -0.612799127 -1.025554017 -3.350263686
C 0.948877616 -1.148375945 -3.574115892
C -0.794546270 -1.321102765 -4.861402281
C 0.705106101 -1.010040795 -5.096141856
H 1.300924403 -2.150228475 -3.293613087
H 1.574852206 -0.399815168 -3.071357800
H -1.045349727 -2.378058283 -5.005556016
H -1.523447051 -0.684087331 -5.372318235
H 1.265349929 -1.691709615 -5.748680264
H 0.859300432 0.020113188 -5.441359720

./carboplatin-M06L-H2O-ApVDZ-pVTZ_eGeom.xyz
25

Pt 0.211549353 -0.365677365 -0.413856458
N -0.547307919 1.308868748 0.539145634
H -1.565050220 1.340983090 0.564729669
H -0.231011799 1.422084281 1.500930020
N -0.506018939 -1.695234968 1.006586364
H -0.149975368 -1.530846933 1.946711416
H -1.521859591 -1.710200727 1.081349666
H -0.246433488 2.143658757 0.037018396
H -0.221169792 -2.640242527 0.750854852
O 1.010879106 0.909936773 -1.779325231
O 1.024352787 -1.979727677 -1.341705886
C 1.244635786 0.513291989 -3.003089597
C 1.205847857 -1.999630507 -2.636189937
O 1.884781423 1.216329149 -3.789083624
O 1.767561043 -2.949401317 -3.186067571
C 0.657020858 -0.821749507 -3.447214386
C 0.647792608 -1.086449976 -4.959845178
C -0.905078877 -0.882521871 -3.484442646
C -0.800266160 -1.584412071 -4.847008147
H 1.404048138 -1.782997403 -5.336473665
H 0.720143237 -0.139543748 -5.505445467
H -1.398011330 -1.410389845 -2.658639849

```
H      -1.332436475      0.125531451      -3.559849858
H      -0.849511043      -2.674988186      -4.739651554
H      -1.507174183      -1.277022379      -5.626565972
./carboplatin-M06L-H2O-ApVDZ-ApVTZ_eGeom.xyz
25
```

```
Pt      0.210816745      -0.364480629      -0.412721638
N      -0.549810610      1.305642235      0.538419768
H      -1.567238371      1.332746640      0.570352739
H      -0.226397148      1.421238070      1.497220161
N      -0.495256223      -1.697835848      1.004301744
H      -0.139444068      -1.529996940      1.943552702
H      -1.510761582      -1.719415905      1.078446996
H      -0.254392976      2.138990505      0.031032482
H      -0.202558907      -2.639875601      0.747012402
O      1.000114057      0.914715215      -1.776741634
O      1.027792386      -1.973373950      -1.340396471
C      1.233757641      0.520670486      -3.001166866
C      1.206789068      -1.993830265      -2.634985989
O      1.868172528      1.227883100      -3.788065190
O      1.769145444      -2.942604018      -3.185928926
C      0.653521519      -0.817629288      -3.445661577
C      0.646651810      -1.081801196      -4.958455400
C      -0.908351825      -0.887423862      -3.484212499
C      -0.798145228      -1.589218080      -4.846422946
H      1.407584476      -1.773082353      -5.335251054
H      0.712796010      -0.134136913      -5.503483333
H      -1.399011892      -1.418361354      -2.659067474
H      -1.341647593      0.118040051      -3.560152920
H      -0.840080427      -2.679978890      -4.738185513
H      -1.506737825      -1.287233981      -5.626568572
./carboplatin-TZ-pVTZ-pp_eGeom.xyz
25
```

```
Pt      -0.104821059      -0.356997965      -0.322878291
N      0.482957798      1.431866076      0.557108791
H      0.055541094      1.639136477      1.463052868
H      1.493814754      1.562179499      0.641345034
N      0.465989561      -1.804702588      1.056369176
H      1.473108508      -1.903146144      1.204071746
H      0.012575227      -1.736622949      1.970902205
H      0.128378571      2.116513215      -0.127714751
H      0.124104175      -2.661037346      0.594666705
O      -0.780903594      0.932475599      -1.673310228
O      -0.782986393      -1.990882736      -1.228515256
C      -1.069383676      0.561172381      -2.927015160
C      -1.057632220      -2.017954063      -2.537490193
O      -1.617910673      1.347336475      -3.683581521
O      -1.592228521      -3.001617914      -3.026087888
C      -0.598357483      -0.822330996      -3.391412085
C      0.965386863      -0.905047227      -3.621383914
C      -0.777806981      -1.101658944      -4.905909552
C      0.692935828      -1.582516744      -4.985895200
H      1.541166243      -1.456503507      -2.866790866
```

H	1.393537989	0.100706434	-3.728253673
H	-1.555996254	-1.831095652	-5.151876818
H	-0.955524491	-0.160682135	-5.438640828
H	0.769735393	-2.675220683	-4.920921001
H	1.291626350	-1.233721330	-5.836968310

./carboplatin-PBE0-SMD-TZ-aug-pVDZ-pp_eGeom.xyz

25

Pt	-0.222518286	-0.363420688	-0.406359990
N	0.511166463	1.255187097	0.566572148
H	0.170120498	1.319050975	1.522374773
H	1.526742551	1.245741992	0.611691381
N	0.532533134	-1.608673262	1.001701941
H	1.547382265	-1.571427982	1.045629758
H	0.183763456	-1.394905829	1.932453768
H	0.240087273	2.112622494	0.092283055
H	0.274484626	-2.570811084	0.797745147
O	-1.034941883	0.866425883	-1.770761430
O	-0.997863667	-1.965096464	-1.338503812
C	-1.247802954	0.485582585	-2.991060906
C	-1.164439173	-2.008477228	-2.622108603
O	-1.881537205	1.191311715	-3.772419720
O	-1.691598059	-2.980334990	-3.157604341
C	-0.654231950	-0.834293512	-3.450274762
C	0.910674061	-0.870557563	-3.521872289
C	-0.670001098	-1.107009709	-4.962651824
C	0.787011258	-1.590609149	-4.874663616
H	1.425168892	-1.376899332	-2.706248327
H	1.308261182	0.139676194	-3.625836883
H	-1.422143418	-1.805310823	-5.324343170
H	-0.749657142	-0.168238799	-5.508521718
H	0.850037425	-2.673090487	-4.758273726
H	1.466608762	-1.276794803	-5.666075863

./carboplatin-M06L-aug-pVTZ_eGeom.xyz

25

Pt	0.129263946	-0.364881274	-0.360103593
N	-0.550702708	1.420354633	0.516197002
H	-1.561556703	1.546623047	0.561947140
H	-0.176982295	1.658751425	1.434650882
N	-0.434481419	-1.866939432	0.998905690
H	-0.029539225	-1.812501218	1.933439363
H	-1.433976237	-2.031641850	1.115363719
H	-0.191411609	2.117789042	-0.145919844
H	-0.041907886	-2.702705642	0.550464000
O	0.802208983	0.961925984	-1.683007212
O	0.895726550	-1.968574292	-1.262619909
C	1.073519571	0.600735310	-2.934365749
C	1.132306878	-1.972852121	-2.570237354
O	1.590624530	1.389467287	-3.702843139
O	1.672735706	-2.929307443	-3.093787058
C	0.616133306	-0.783126602	-3.386918057
C	0.728297241	-1.048696656	-4.895425466
C	-0.935797129	-0.910469240	-3.542533160

C	-0.698023399	-1.615093443	-4.884877374
H	1.540066671	-1.718992784	-5.200755906
H	0.807269797	-0.096453453	-5.433826111
H	-1.477528686	-1.447031130	-2.747664424
H	-1.394858491	0.082501855	-3.664657535
H	-0.698522498	-2.708184346	-4.771396107
H	-1.365557885	-1.351050427	-5.717158809

./carboplatin-H20-pVTZ-pp-2_eGeom.xyz
25

Pt	-0.202773099	-0.357563737	-0.366984775
N	0.533563079	1.312924436	0.571418931
H	0.160570024	1.461584952	1.521983452
H	1.561916104	1.328868589	0.651767000
N	0.474076223	-1.679928779	1.051437022
H	1.500796797	-1.700071416	1.150596211
H	0.089052894	-1.519207019	1.995082648
H	0.268876933	2.144229266	0.017852892
H	0.186344340	-2.632625573	0.773639414
O	-0.952594265	0.915727919	-1.731641465
O	-0.994830538	-1.966778627	-1.276470238
C	-1.164803392	0.537457697	-2.988019878
C	-1.167955850	-2.010218901	-2.593007984
O	-1.736251063	1.294073181	-3.783365310
O	-1.714929658	-2.986913755	-3.121099221
C	-0.628952820	-0.833359443	-3.434051033
C	0.947986145	-0.912222680	-3.564142708
C	-0.717312978	-1.112906000	-4.959026854
C	0.766283413	-1.566356687	-4.959707800
H	1.478704038	-1.486476021	-2.779831716
H	1.390816513	0.101997384	-3.619602563
H	-1.475382507	-1.862899736	-5.249864870
H	-0.884710761	-0.166744008	-5.505699337
H	0.867170634	-2.668444537	-4.913815289
H	1.411646803	-1.184499275	-5.774575538

./carboplatin-SMD-pVTZ-pp_eGeom.xyz
25

Pt	-0.234373581	-0.363701442	-0.380398166
N	0.537358969	1.253020744	0.600447087
H	0.192757666	1.341332449	1.570487466
H	1.568474470	1.229878947	0.656508680
N	0.486099597	-1.646611025	1.036099663
H	1.517626893	-1.653428253	1.086665718
H	0.145625591	-1.429845901	1.986979822
H	0.288971872	2.131812389	0.117726799
H	0.193406451	-2.616253699	0.832631961
O	-1.013967103	0.907518632	-1.745080597
O	-1.045619076	-1.961148087	-1.317309074
C	-1.197883674	0.535989678	-3.006147026
C	-1.194230574	-1.994238399	-2.634821253
O	-1.770554355	1.297729842	-3.805548316
O	-1.737332937	-2.973130089	-3.177387099
C	-0.644478274	-0.818132453	-3.458611225

C	0.935041646	-0.897664601	-3.546528885
C	-0.685004795	-1.090259468	-4.986181982
C	0.781323022	-1.589964140	-4.925837231
H	1.447287789	-1.444590839	-2.731751965
H	1.367150534	0.118933756	-3.629037068
H	-1.459135279	-1.802327417	-5.326567951
H	-0.784086731	-0.135789509	-5.535044257
H	0.838861510	-2.692506251	-4.837570171
H	1.463987378	-1.256977632	-5.730853940

./carboplatin-CPCM-pVTZ-pp-2_eGeom.xyz
25

Pt	-0.205269930	-0.356771582	-0.367651957
N	0.531707319	1.313467558	0.570555065
H	0.163946142	1.459220908	1.523590906
H	1.560478134	1.330933113	0.645254418
N	0.470777321	-1.678485387	1.051584153
H	1.497543186	-1.699002700	1.150265494
H	0.086443221	-1.516517952	1.995289463
H	0.262669238	2.145679030	0.020470263
H	0.182474123	-2.631349064	0.774994416
O	-0.954542197	0.915904873	-1.733436972
O	-0.997677985	-1.966024101	-1.277028130
C	-1.164912550	0.536970482	-2.989902192
C	-1.168615425	-2.010129513	-2.593810370
O	-1.735921523	1.292837337	-3.786340952
O	-1.715365683	-2.986803741	-3.122275383
C	-0.627952600	-0.833851514	-3.434563451
C	0.949203552	-0.912636905	-3.562038427
C	-0.713811988	-1.114060565	-4.959568868
C	0.769834028	-1.567326048	-4.957639180
H	1.478703186	-1.486557293	-2.776681823
H	1.392030789	0.101595883	-3.617124448
H	-1.471337927	-1.864231721	-5.251423021
H	-0.880381921	-0.168141162	-5.506916138
H	0.870839562	-2.669379595	-4.911122964
H	1.416446941	-1.185693109	-5.771608911

./carboplatin-PBE0-H2O-TZ-aug-pVDZ-pp_eGeom.xyz
25

Pt	0.200667293	-0.364259453	-0.401332601
N	-0.541009679	1.283453642	0.538360444
H	-1.554314055	1.288896040	0.598075532
H	-0.183389388	1.407672870	1.480366956
N	-0.483920431	-1.673301071	1.002501475
H	-0.124757094	-1.489757057	1.933999600
H	-1.496587929	-1.697090025	1.069672696
H	-0.268171654	2.104037100	0.003919196
H	-0.178564676	-2.607367933	0.742233654
O	0.957235216	0.894649541	-1.756079754
O	0.995933528	-1.951469579	-1.317435430
C	1.193926935	0.521011761	-2.978291042
C	1.185922622	-1.988247328	-2.602144781
O	1.804745968	1.237914680	-3.756489384

O	1.751436011	-2.931136183	-3.134366679
C	0.639235590	-0.824071877	-3.430946491
C	0.677781615	-1.093746457	-4.943364439
C	-0.923160510	-0.898016750	-3.510658091
C	-0.782871369	-1.574589267	-4.885516778
H	1.429653330	-1.804968294	-5.278379944
H	0.786869000	-0.156055582	-5.485689439
H	-1.424981281	-1.443033403	-2.711991570
H	-1.356799914	0.100498805	-3.579875319
H	-0.854576455	-2.659998986	-4.810385518
H	-1.452995663	-1.231377965	-5.673311302

./carboplatin-M06L-H2O-ApVTZ-ApVTZ_eGeom.xyz

25

Pt	0.204796351	-0.366548178	-0.409915504
N	-0.541560009	1.309958269	0.550665795
H	-1.553385212	1.332408341	0.590525636
H	-0.206009300	1.418661815	1.500391613
N	-0.492550830	-1.701621803	1.015658124
H	-0.131865921	-1.526306885	1.945863195
H	-1.502710953	-1.719467760	1.089318162
H	-0.247984747	2.134572122	0.038070954
H	-0.198099394	-2.636919160	0.755766588
O	0.981511588	0.907530535	-1.780680982
O	1.003159450	-1.973938756	-1.348375063
C	1.223080093	0.519935351	-2.998683390
C	1.186666795	-1.998379981	-2.635450607
O	1.850958648	1.228022997	-3.779254708
O	1.734581962	-2.949096624	-3.182171419
C	0.650227005	-0.817484393	-3.447511149
C	0.653664878	-1.079200806	-4.957929616
C	-0.910079230	-0.882273991	-3.501796200
C	-0.786789017	-1.593038909	-4.854575146
H	1.414188806	-1.761122431	-5.330154037
H	0.717362905	-0.136511220	-5.496799887
H	-1.408290823	-1.398558465	-2.682249786
H	-1.335188333	0.117185348	-3.591134366
H	-0.822912928	-2.675228287	-4.740062110
H	-1.485464773	-1.302929899	-5.636645108

./carboplatin-M06L-SMD-ApVDZ-ApVTZ_eGeom.xyz

25

Pt	-0.234112664	-0.377661815	-0.422031793
N	0.505559483	1.261722567	0.564062036
H	0.229914282	1.286726986	1.545406952
H	1.523849692	1.306778889	0.547680101
N	0.592498612	-1.641483694	0.968339397
H	1.590635544	-1.784322663	0.817547932
H	0.489941794	-1.309876181	1.926949842
H	0.169701890	2.128402935	0.144804575
H	0.157607356	-2.562680284	0.930199691
O	-1.118681434	0.870376630	-1.774262418
O	-1.041623844	-2.000567227	-1.366870872
C	-1.299608011	0.488257815	-3.007705263

C	-1.217365254	-2.007302934	-2.658470648
O	-1.936048821	1.195706850	-3.803613297
O	-1.779299768	-2.960385732	-3.217951729
C	-0.678102330	-0.823699458	-3.458831552
C	0.885391158	-0.862690621	-3.469103687
C	-0.633260303	-1.082355315	-4.971978018
C	0.807921805	-1.586755707	-4.820502758
H	1.369429381	-1.371440455	-2.626671207
H	1.293568901	0.151651934	-3.556938277
H	-1.384982088	-1.764447930	-5.382942054
H	-0.674229439	-0.131753158	-5.514379508
H	0.845995906	-2.675298622	-4.690179676
H	1.532605160	-1.297255580	-5.589686778

./carboplatin-ApVTZ-ApVTZ-pp_eGeom.xyz
25

Pt	-0.100918746	-0.359359205	-0.325469386
N	0.494070323	1.422313055	0.560026346
H	0.070284280	1.625192204	1.468946596
H	1.506039329	1.546613750	0.643717847
N	0.456903145	-1.807620687	1.055645794
H	1.463766626	-1.913185391	1.202283198
H	0.006802788	-1.730320802	1.971368310
H	0.142166465	2.115044665	-0.118365614
H	0.107334165	-2.664791745	0.600707857
O	-0.767164900	0.934843530	-1.676357150
O	-0.787449838	-1.988101753	-1.233830091
C	-1.066476391	0.564710057	-2.926788558
C	-1.070225287	-2.010151083	-2.540258595
O	-1.621007897	1.352080056	-3.679552020
O	-1.621328673	-2.986587768	-3.027455077
C	-0.600219658	-0.819243283	-3.395568847
C	0.964360519	-0.908697874	-3.618429219
C	-0.774445647	-1.095692285	-4.911402006
C	0.695471192	-1.580217012	-4.986367845
H	1.533646482	-1.466292311	-2.863291140
H	1.397872720	0.095441895	-3.719400335
H	-1.554334965	-1.821425250	-5.163183614
H	-0.946576662	-0.153662006	-5.444312417
H	0.770683178	-2.673408546	-4.926531272
H	1.298054462	-1.227834980	-5.833261772

./carboplatin-SMD-TZ-pVTZ-pp_eGeom.xyz
25

Pt	-0.220652027	-0.357679800	-0.392491883
N	0.541501104	1.268113183	0.584542903
H	0.198243424	1.340526107	1.548224585
H	1.565518558	1.244005259	0.629448911
N	0.514269162	-1.627855224	1.030249696
H	1.538646719	-1.617981993	1.069488054
H	0.172164367	-1.398888208	1.969329047
H	0.279280988	2.133953261	0.101578774
H	0.225576518	-2.591220331	0.828388273
O	-1.020465800	0.897594246	-1.765071868

O	-1.027052636	-1.964067892	-1.324652153
C	-1.233470456	0.509893159	-3.004313523
C	-1.194490469	-2.000369029	-2.628259842
O	-1.858094737	1.238981189	-3.792885179
O	-1.749417560	-2.974397053	-3.162953233
C	-0.656702506	-0.828585764	-3.459432495
C	0.921680347	-0.890106031	-3.531681343
C	-0.675571946	-1.103391879	-4.983485551
C	0.787778098	-1.600726918	-4.899973453
H	1.426578951	-1.415526509	-2.712494623
H	1.338057389	0.121308037	-3.624656217
H	-1.437925733	-1.804008586	-5.341826233
H	-0.755692755	-0.158699998	-5.533718363
H	0.845364947	-2.691919238	-4.796270176
H	1.472183061	-1.279302759	-5.694213120

./carboplatin-M062X-aug-pVTZ-2_eGeom.xyz

25

Pt	-0.128414566	-0.359131992	-0.353813261
N	0.507156871	1.404412698	0.546172588
H	0.088403164	1.623205359	1.450873949
H	1.517087682	1.523604717	0.631931483
N	0.438504574	-1.815671681	1.019912874
H	1.442388817	-1.940461771	1.154526896
H	0.005197741	-1.753656398	1.941963478
H	0.168096679	2.101761534	-0.129254547
H	0.077299378	-2.664070327	0.564705925
O	-0.775467271	0.944524998	-1.684355290
O	-0.834702812	-1.964589892	-1.260344767
C	-1.071195139	0.587326285	-2.926655383
C	-1.076457490	-1.993503874	-2.562096224
O	-1.613917051	1.355705840	-3.686842097
O	-1.577740402	-2.963497621	-3.084465414
C	-0.600542009	-0.792441914	-3.394650144
C	0.953614566	-0.901393453	-3.581545271
C	-0.748796697	-1.063419055	-4.903413874
C	0.691218091	-1.621288805	-4.922925075
H	1.512906619	-1.435255884	-2.799338210
H	1.391498923	0.097289568	-3.724157515
H	-1.557237474	-1.747881963	-5.179450375
H	-0.841743865	-0.112203071	-5.439271050
H	0.695677459	-2.711537783	-4.795522155
H	1.334471223	-1.348178285	-5.769115552

./carboplatin-ApVDZ-ApVTZ-pp_eGeom.xyz

25

Pt	-0.103311364	-0.357841351	-0.325459024
N	0.488198993	1.425693583	0.548207955
H	0.073570361	1.634204978	1.464210752
H	1.503140861	1.563048518	0.620159939
N	0.472074817	-1.798406611	1.049590225
H	1.483588235	-1.905772688	1.188938726
H	0.030780603	-1.725283654	1.974038466
H	0.122632128	2.117104549	-0.129940107

H	0.120148111	-2.661966832	0.600268635
O	-0.787505699	0.933706778	-1.670870387
O	-0.790687647	-1.993660316	-1.222121390
C	-1.082781912	0.556470852	-2.925196652
C	-1.074620103	-2.017329872	-2.533147979
O	-1.647022225	1.342862507	-3.682422755
O	-1.629699613	-3.000403690	-3.019094536
C	-0.604586016	-0.826745207	-3.392156717
C	0.964977027	-0.907269423	-3.608302309
C	-0.774190857	-1.106388259	-4.911921566
C	0.706205718	-1.572066180	-4.986675980
H	1.533973793	-1.473110592	-2.849030380
H	1.397725823	0.105520123	-3.697090862
H	-1.549165607	-1.848388970	-5.161478993
H	-0.963042211	-0.161381678	-5.447439354
H	0.797022671	-2.671368707	-4.936020450
H	1.309881122	-1.201580628	-5.834174266

./carboplatin-PBE0-H2O-TZ-pVDZ-pp_eGeom.xyz

25

Pt	0.194979253	-0.368464817	-0.398623652
N	-0.527661495	1.294042602	0.532264226
H	-1.540739382	1.314322190	0.589581501
H	-0.169871364	1.418547677	1.474031075
N	-0.525646581	-1.668653490	0.997059329
H	-0.164596316	-1.499465748	1.930415493
H	-1.538619715	-1.669596217	1.061257438
H	-0.241485828	2.106467817	-0.007397740
H	-0.240834551	-2.607283466	0.730347244
O	0.985479828	0.877462108	-1.746724165
O	0.970854990	-1.969589861	-1.308665819
C	1.222366210	0.500051512	-2.967676617
C	1.167053184	-2.010140946	-2.592299993
O	1.848892859	1.207352661	-3.742059126
O	1.716275008	-2.964496277	-3.120951127
C	0.648206646	-0.835548060	-3.423925649
C	0.693333524	-1.104443891	-4.936229625
C	-0.914742189	-0.882096111	-3.514742078
C	-0.777231607	-1.555510551	-4.891509401
H	1.432948137	-1.831041130	-5.265570628
H	0.826660668	-0.169020738	-5.477002232
H	-1.430529854	-1.422752383	-2.722007985
H	-1.331555777	0.123718150	-3.581485689
H	-0.872383466	-2.639501868	-4.822357994
H	-1.433845172	-1.194711934	-5.682855795

./carboplatin-M062X-SMD-aug-pVTZ-2_eGeom.xyz

25

Pt	-1.118443537	-0.011165820	-0.046038153
N	-2.490901362	1.289521010	0.688195979
H	-3.408877172	1.191306986	0.245376123
H	-2.639132451	1.179653473	1.695253812
N	-2.334546289	-1.590931640	0.335136384
H	-2.329884394	-1.854998598	1.324508687

H	-3.312361517	-1.422098094	0.082826398
H	-2.195444462	2.258758702	0.539760059
H	-2.033851049	-2.417337144	-0.189451475
O	0.082662645	1.563065309	-0.486600661
O	0.233950838	-1.305338061	-0.835556599
C	1.378797290	1.438212547	-0.511770321
C	1.515506715	-1.094903484	-0.755362900
O	2.104115414	2.351801569	-0.902549807
O	2.327011074	-1.882065741	-1.240627809
C	1.991543918	0.142987076	0.011182618
C	1.823254497	-0.108924369	1.549622581
C	3.514111669	0.145291937	0.236161974
C	3.289598544	-0.591604936	1.573312445
H	1.033063468	-0.808133523	1.854613002
H	1.694683710	0.848085412	2.074775237
H	4.123555219	-0.345627163	-0.531196476
H	3.861673968	1.172405501	0.398318935
H	3.347782969	-1.680841166	1.444602762
H	3.904084295	-0.289713782	2.430080206

./carboplatin-M06L-H2O-TZ-aug-pVTZ_eGeom.xyz

25

Pt	0.203708587	-0.373017333	-0.410444669
N	-0.516112014	1.305011547	0.569927444
H	-1.523687494	1.315433909	0.673685414
H	-0.119160693	1.433761970	1.493036208
N	-0.486225129	-1.713162722	1.018317982
H	-0.371643974	-1.399582917	1.974431192
H	-1.467842913	-1.934122591	0.897851448
H	-0.266421661	2.123821381	0.025831080
H	0.019315663	-2.588436171	0.932799197
O	0.961680382	0.910727388	-1.782274451
O	0.997334369	-1.975753649	-1.358853000
C	1.195023709	0.532912502	-3.006387406
C	1.200069600	-1.985527702	-2.644033201
O	1.799763607	1.254937863	-3.790348768
O	1.778895570	-2.916801766	-3.190551855
C	0.639933910	-0.813183939	-3.452162037
C	0.645461340	-1.072625472	-4.963008483
C	-0.919192635	-0.896728280	-3.501570725
C	-0.796468127	-1.585201257	-4.866292814
H	1.405491162	-1.757835460	-5.329702210
H	0.717263140	-0.130773495	-5.502146847
H	-1.405051213	-1.433240268	-2.687671116
H	-1.361226582	0.097024692	-3.570221469
H	-0.839292092	-2.669311489	-4.774601196
H	-1.494309504	-1.278679512	-5.642738730

./carboplatin-CPCM-aug-pVTZ_eGeom.xyz

25

Pt	0.207686510	-0.358664125	-0.370604236
N	-0.523010305	1.306814901	0.573364864
H	-1.552172168	1.333105793	0.629542676
H	-0.171765057	1.438209498	1.533891500

N	-0.466379152	-1.671008704	1.053103410
H	-0.107309745	-1.483990316	2.001285972
H	-1.493838243	-1.712422817	1.129350029
H	-0.236459949	2.142408109	0.038429968
H	-0.151548461	-2.621757262	0.801168654
O	0.959262029	0.911974534	-1.732776463
O	0.988490767	-1.969525936	-1.281694266
C	1.169070223	0.533301454	-2.987177621
C	1.157486495	-2.012065857	-2.596355771
O	1.748217239	1.285539300	-3.783251226
O	1.699425454	-2.990943611	-3.128824081
C	0.623815258	-0.832212331	-3.436755301
C	0.707368851	-1.113191367	-4.962285177
C	-0.953647620	-0.903107594	-3.567271287
C	-0.773343303	-1.575900947	-4.953632586
H	1.469385123	-1.856651263	-5.259057243
H	0.862104838	-0.165703256	-5.510141755
H	-1.489949686	-1.460129058	-2.774659358
H	-1.386433237	0.114416236	-3.641100859
H	-0.865351611	-2.677889554	-4.889693297
H	-1.423797240	-1.210958595	-5.771985558

./carboplatin-M062X-ApVTZ-ApVDZ-pp-3_eGeom.xyz

25

Pt	-1.010882015	-0.016403427	-0.110559334
N	-2.245314381	1.554461194	0.481136668
H	-3.164043574	1.575257258	0.052338032
H	-2.361193833	1.664420024	1.482466141
N	-2.090440129	-1.704889988	0.463941011
H	-2.208575165	-1.830727824	1.463096763
H	-2.996873493	-1.814146795	0.022479349
H	-1.716396868	2.357033272	0.133445063
H	-1.480662134	-2.449730398	0.120198559
O	0.061545205	1.507656645	-0.765599914
O	0.204486797	-1.425877369	-0.778507376
C	1.335218277	1.387136771	-1.089691261
C	1.476552344	-1.207702115	-1.047634669
O	1.920321139	2.269197134	-1.667885094
O	2.165531976	-2.062997966	-1.547255633
C	2.065729988	0.136803644	-0.604192746
C	2.268362610	0.098190431	0.949952263
C	3.596165610	0.163941555	-0.749160598
C	3.722685718	-0.349129353	0.699954140
H	1.611747256	-0.562654397	1.514434921
H	2.210749246	1.104517947	1.363756578
H	4.004005746	-0.459249822	-1.537912608
H	3.933811359	1.190723205	-0.858741122
H	3.813689233	-1.432706347	0.729015344
H	4.490131089	0.097195721	1.327721522

./carboplatin-M06L-CPCM-TZ-aug-pVTZ_eGeom.xyz

25

Pt	0.205073437	-0.368232521	-0.409969179
N	-0.554283261	1.303487272	0.551431396

H	-1.566231465	1.317682639	0.593367133
H	-0.217981949	1.416408392	1.500435311
N	-0.482344476	-1.713231424	1.013009429
H	-0.120695696	-1.539954559	1.943240074
H	-1.492203028	-1.738400990	1.088704070
H	-0.268646032	2.129482917	0.036535424
H	-0.181885608	-2.644892132	0.747058108
O	0.972072945	0.914846400	-1.776544265
O	1.015107044	-1.969621599	-1.347651667
C	1.212558237	0.530573406	-2.997428699
C	1.195012942	-1.990969587	-2.636658517
O	1.830013850	1.244392853	-3.778901195
O	1.745151113	-2.937108538	-3.186523310
C	0.649458550	-0.811486935	-3.444530566
C	0.656610354	-1.070965038	-4.955371323
C	-0.910213591	-0.886288661	-3.499480854
C	-0.783225617	-1.587741990	-4.857043464
H	1.418453353	-1.753390564	-5.323730523
H	0.724214573	-0.128411369	-5.493836397
H	-1.404858827	-1.411734805	-2.683668144
H	-1.343997665	0.110075516	-3.580620424
H	-0.818382647	-2.670790510	-4.750944133
H	-1.481469526	-1.294080942	-5.638007296

./carboplatin-CPCM-TZ-pVDZ-pp_eGeom.xyz

25

Pt	0.198599341	-0.362502667	-0.381987451
N	-0.538100868	1.313818064	0.553555746
H	-1.560138803	1.326425091	0.611795570
H	-0.176906676	1.444240536	1.502801023
N	-0.497247363	-1.681262666	1.035984741
H	-0.128628640	-1.501447152	1.974107418
H	-1.518509560	-1.697461032	1.107085648
H	-0.255174206	2.133196999	0.005531079
H	-0.196641317	-2.624159006	0.766780602
O	0.977641480	0.902990618	-1.747612426
O	0.990309418	-1.977257875	-1.296731212
C	1.210431173	0.514344142	-2.986134252
C	1.181393118	-2.012528251	-2.600424239
O	1.831327811	1.240151642	-3.769323163
O	1.746706089	-2.975298610	-3.128442219
C	0.643512149	-0.836833395	-3.436384333
C	0.690531474	-1.110126403	-4.960241200
C	-0.933300261	-0.895502670	-3.529104819
C	-0.791173402	-1.560051785	-4.921022025
H	1.433434474	-1.847247132	-5.283891210
H	0.834987365	-0.170602314	-5.505957200
H	-1.443975477	-1.451114694	-2.733506779
H	-1.360818430	0.114262432	-3.584285217
H	-0.892363597	-2.651507682	-4.864623919
H	-1.448588284	-1.184878959	-5.715099175

./carboplatin-M062X-SMD-ApVDZ-ApVDZ_eGeom.xyz

25

Pt	-0.227831994	-0.354998261	-0.408167263
N	0.519312229	1.263401305	0.565195315
H	0.217969038	1.305928669	1.539892565
H	1.540029692	1.275865671	0.569002619
N	0.541231565	-1.605881877	0.996445244
H	1.543685053	-1.751955594	0.869321734
H	0.409564900	-1.265727739	1.950051212
H	0.212512431	2.129726515	0.120273708
H	0.097570994	-2.523979823	0.943392804
O	-1.057957687	0.892703398	-1.796015833
O	-1.034063778	-1.976247893	-1.359089544
C	-1.276170224	0.495272575	-3.011303444
C	-1.195029717	-2.008691805	-2.645199332
O	-1.927441332	1.182632700	-3.805959825
O	-1.724742171	-2.976015084	-3.202326405
C	-0.666447900	-0.827128768	-3.463712634
C	0.901136961	-0.872843931	-3.488039195
C	-0.643669117	-1.099770154	-4.979192511
C	0.803831174	-1.620352739	-4.836461741
H	1.387368476	-1.375805742	-2.646348028
H	1.304802894	0.139161669	-3.602142426
H	-1.405212809	-1.779803273	-5.369192741
H	-0.670986384	-0.151989086	-5.524453676
H	0.829513791	-2.705238664	-4.688042534
H	1.518330926	-1.338614841	-5.615057079

./carboplatin-M062X-SMD-ApVTZ-ApVTZ-pp-2_eGeom.xyz

25

Pt	-0.231400959	-0.359841922	-0.405130087
N	0.533333415	1.231878580	0.596306599
H	0.192814500	1.282483724	1.554270081
H	1.549528625	1.203587801	0.641521782
N	0.464324946	-1.640709847	1.008682125
H	1.466731855	-1.793009481	0.920382138
H	0.294480305	-1.311814250	1.956654213
H	0.276624896	2.104329242	0.138928657
H	0.013538059	-2.549157572	0.919808975
O	-0.991604935	0.912751363	-1.804106927
O	-1.057328845	-1.946041173	-1.386691987
C	-1.218154505	0.533959382	-3.017638033
C	-1.205793049	-1.973356854	-2.668509826
O	-1.840972766	1.242089700	-3.808558050
O	-1.745041148	-2.923322759	-3.234340985
C	-0.647686902	-0.800908028	-3.475941690
C	0.916377858	-0.886621709	-3.495182803
C	-0.622499908	-1.062761289	-4.990414144
C	0.805158944	-1.625029644	-4.843047238
H	1.388132797	-1.399163337	-2.659872656
H	1.343756181	0.109095933	-3.604526569
H	-1.394519269	-1.712944494	-5.390993774
H	-0.618431495	-0.117306416	-5.526673090
H	0.798640504	-2.703991606	-4.699970104
H	1.527297906	-1.364548115	-5.612085614

./carboplatin-PBE0-CPCM-aug-pVDZ_eGeom.xyz

25

Pt	0.207328320	-0.360419445	-0.389137354
N	-0.521312964	1.293273691	0.550087030
H	-1.541458021	1.318746161	0.613244154
H	-0.165746879	1.426035234	1.499578644
N	-0.481210241	-1.665325726	1.016415265
H	-0.123307448	-1.490959940	1.958068862
H	-1.500499457	-1.695719510	1.091455195
H	-0.242122546	2.120967340	0.015872560
H	-0.179681238	-2.609581367	0.759758845
O	0.964884167	0.898911285	-1.744016098
O	0.986337548	-1.958082466	-1.303375243
C	1.181422899	0.526195082	-2.979369019
C	1.155806266	-2.001138149	-2.599192845
O	1.769920532	1.255521938	-3.767519589
O	1.686115192	-2.965695569	-3.135973948
C	0.628744187	-0.824504638	-3.429661365
C	0.694514340	-1.102275821	-4.943587988
C	-0.935153529	-0.894062297	-3.540403261
C	-0.767402088	-1.588498185	-4.906277990
H	1.461232400	-1.820585014	-5.259052184
H	0.812867662	-0.157579856	-5.489315080
H	-1.463955870	-1.428552421	-2.738389855
H	-1.364026358	0.114923192	-3.634268567
H	-0.833523968	-2.682358189	-4.814730205
H	-1.432465899	-1.259588101	-5.717338975